ISSN 0021-9673

VOL. 454 NOVEMBER 11, 1988
COMPLETE IN ONE ISSUE

JOURNAL OF CHROMATOGRAPHY

INTERNATIONAL JOURNAL ON CHROMATOGRAPHY, ELECTROPHORESIS AND RELATED METHODS

ELSEVIER

JOURNAL OF CHROMATOGRAPHY

Scope. The *Journal of Chromatography* publishes papers on all aspects of chromatography, electrophoresis and related methods. Contributions consist mainly of research papers dealing with chromatographic theory, instrumental development and their applications. The section *Biomedical Applications*, which is under separate editorship, deals with the following aspects: developments in and applications of chromatographic and electrophoretic techniques related to clinical diagnosis or alterations during medical treatment; screening and profiling of body fluids or tissues with special reference to metabolic disorders; results from basic medical research with direct consequences in clinical practice; drug level monitoring and pharmacokinetic studies; clinical toxicology; analytical studies in occupational medicine.

Submission of Papers. Papers in English, French and German may be submitted, in three copies. Manuscripts should be submitted to: The Editor of *Journal of Chromatography*, P.O. Box 681, 1000 AR Amsterdam, The Netherlands, or to: The Editor of *Journal of Chromatography, Biomedical Applications*, P.O. Box 681, 1000 AR Amsterdam, The Netherlands. Review articles are invited or proposed by letter to the Editors. An outline of the proposed review should first be forwarded to the Editors for preliminary discussion prior to preparation. Submission of an article is understood to imply that the article is original and unpublished and is not being considered for publication elsewhere. For copyright regulations, see below.

Subscription Orders. Subscription orders should be sent to: Elsevier Science Publishers B.V., P.O. Box 211, 1000 AE Amsterdam, The Netherlands, Tel. 5803 911, Telex 18582 ESPA NL. The *Journal of Chromatography* and the *Biomedical Applications* section can be subscribed to separately.

Publication. The *Journal of Chromatography* (incl. *Biomedical Applications* and *Cumulative Author and Subject Indexes, Vols. 401–450*) has 37 volumes in 1988. The subscription prices for 1988 are:

J. Chromatogr. (incl. *Cum. Indexes, Vols. 401–450*) + *Biomed. Appl.* (Vols. 424–460):
Dfl. 6290.00 plus Dfl. 962.00 (p.p.h.) (total *ca.* US$ 3537.50)

J. Chromatogr. (incl. *Cum. Indexes, Vols. 401–450*) only (Vols. 435–460):
Dfl. 5070.00 plus Dfl. 676.00 (p.p.h.) (total *ca.* US$ 2803.00)

Biomed. Appl. only (Vols. 424–434):
Dfl. 2145.00 plus Dfl. 286.00 (p.p.h.) (total *ca.* US$ 1185.75).

Our p.p.h. (postage, package and handling) charge includes surface delivery of all issues, except to subscribers in Argentina, Australia, Brasil, Canada, China, Hong Kong, India, Israel, Malaysia, Mexico, New Zealand, Pakistan, Singapore, South Africa, South Korea, Taiwan, Thailand and the U.S.A. who receive all issues by air delivery (S.A.L. — Surface Air Lifted) at no extra cost. For Japan, air delivery requires 50% additional charge; for all other countries airmail and S.A.L. charges are available upon request. Back volumes of the *Journal of Chromatography* (Vols. 1 through 423) are available at Dfl. 230.00 (plus postage). Claims for missing issues will be honoured, free of charge, within three months after publication of the issue. Customers in the U.S.A. and Canada wishing information on this and other Elsevier journals, please contact Journal Information Center, Elsevier Science Publishing Co. Inc., 52 Vanderbilt Avenue, New York, NY 10017. Tel. (212) 916-1250.

Abstracts/Contents Lists published in Analytical Abstracts, ASCA, Biochemical Abstracts, Biological Abstracts, Chemical Abstracts, Chemical Titles, Chromatography Abstracts, Current Contents/Physical, Chemical & Earth Sciences, Current Contents/Life Sciences, Deep-Sea Research/Part B: Oceanographic Literature Review, Excerpta Medica, Index Medicus, Mass Spectrometry Bulletin, PASCAL-CNRS, Referativnyi Zhurnal and Science Citation Index.

See inside back cover for Publication Schedule, Information for Authors and information on Advertisements.

0021-9673/88/$03.50

Printed in The Netherlands

CONTENTS

(Abstracts/Contents Lists published in Analytical Abstracts, ASCA, Biochemical Abstracts, Biological Abstracts, Chemical Abstracts, Chemical Titles, Chromatography Abstracts, Current Contents/Physical, Chemical & Earth Sciences, Current Contents/Life Sciences, Deep Sea Research/Part B: Oceanographic Literature Review, Excerpta Medica, Index Medicus, Mass Spectrometry Bulletin, PASCAL-CNRS, Referativnyi Zhurnal and Science Citation Index)

(Continued overleaf)

(*Continued overleaf*)

In articles with more than one author, the name of the author to whom correspondence should be addressed is indicated in the article heading by a 6-pointed asterisk (*)

New Tel. No. (0 24 21) 6 98-0

JOURNAL OF CHROMATOGRAPHY

VOL. 454 (1988)

JOURNAL
of
CHROMATOGRAPHY

INTERNATIONAL JOURNAL ON CHROMATOGRAPHY,
ELECTROPHORESIS AND RELATED METHODS

ELSEVIER
AMSTERDAM — OXFORD — NEW YORK — TOKYO

0021-9673/88/$03.50

Printed in The Netherlands

Journal of Chromatography, 454 (1988) 1–21
Elsevier Science Publishers B.V., Amsterdam — Printed in The Netherlands

CHROM. 20 816

THEORETICAL OPTIMIZATION OF OPERATING PARAMETERS IN NON-IDEAL DISPLACEMENT CHROMATOGRAPHY

MICHAEL W. PHILLIPS, GUHAN SUBRAMANIAN and STEVEN M. CRAMER*
Bioseparations Research Center, Department of Chemical Engineering, Rensselaer Polytechnic Institute, Troy, NY 12180-3590 (U.S.A.)
(First received April 18th, 1988; revised manuscript received July 19th, 1988)

SUMMARY

A mathematical model was developed for the simulation of non-ideal displacement chromatography. The model incorporates finite mass transport to the solid adsorbent by using a linear driving force approximation with a coupled external film and internal pore mass transfer coefficient. Equilibrium adsorption at the fluid–solid interface is described using competitive langmuirian adsorption isotherms. A finite difference numerical technique was employed to approximate the system of coupled, non-linear partial differential equations. The model was used to simulate the effluent concentration profiles under various displacement chromatographic conditions. The effects of axial dispersion and finite mass transport were examined by varying the Peclet and Stanton numbers, respectively. Slow mass transfer rates were shown to have a dispersive effect on the shock waves generated in displacement chromatography, resulting in greater zone overlap. Constant pattern formation was observed under non-ideal conditions. The throughput obtained in displacement chromatography was examined as a function of feed load, flow velocity, and displacer concentration. For non-ideal systems, the throughput was shown to exhibit a maximum at unique values of these operating parameters. The effects of particle diameter and solute diffusivity on the throughput were also examined. Model predictions indicate that the use of large particles could be detrimental to the performance of displacement systems when high velocities are employed. For macromolecular separations by displacement chromatography, small particles are required regardless of the linear velocity. The model presented here is a useful tool for the optimization and scale-up of displacement chromatographic processes.

INTRODUCTION

Displacement chromatography is rapidly evolving into a powerful preparative bioseparation technique due to the high throughput and product purity associated with the process. The separation is based on competition of the components for adsorption sites on the stationary phase and the process takes advantage of the non-linearity of the isotherms. Although the physicochemical basis of displacement chromatography was established by Tiselius in 1943[1], the full potential of this

0021-9673/88/$03.50

technique was not fully realized until the recent work by Horváth and co-workers[2–8].

In displacement chromatography, a front of displacer solution traveling behind the feed drives the separation of the feed components into adjacent pure zones which move at the same velocity as the displacer front. The concentration of each zone is determined solely by its adsorption isotherm and the concentration and isotherm of the displacer. The displacer must have a higher affinity for the stationary phase than any of the feed components[7].

In this method, the column is first equilibrated with an inert carrier solvent. The feed mixture is then introduced into the column followed by a step-change at the column inlet to a solution containing the displacer compound. Upon completion of the displacement process, the displacer is removed from the column by the passing of a suitable regenerant solution.

Displacement chromatography offers significant advantages in preparative chromatography as compared to the conventional elution mode[7]. Since displacement chromatography takes advantage of the non-linearity of the isotherms, a larger feed can be separated on a given column with the purified components recovered at significantly higher concentrations. Furthermore, the tailing observed in preparative-scale elution chromatography is greatly reduced in displacement chromatography due to the sharp zones formed in the process. These advantages are particularly significant for the isolation of biomolecules from relatively dilute solutions such as those encountered in biotechnology processes.

While the effects of axial dispersion and mass transport have been included in models of multicomponent adsorption[9–15], work on modeling displacement chromatography has been mainly limited to ideal chromatographic systems. Helfferich and Klein[16] and Helfferich[17,18] developed a model for displacement systems assuming equilibrium adsorption, plug flow, and constant separation factors. In their treatment, a so-called "*h*-transformation" was employed to convert the system of coupled partial differential equations to a set of algebraic equations. Rhee and co-workers[19,20] used a similar approach to solve the mass balance equations. Yu and Wang[21], and Geldart *et al.*[22], have used the "*h*-transform" technique to study the dynamics of elution and displacement ion-exchange chromatography. Frenz and Horváth[5] compared experimental displacement data obtained with analytical HPLC columns to the predictions of the ideal displacement model. Guiochon and Katti[23] have compared displacement and elution profiles obtained by numerically solving the mass balance equations. Morbidelli *et al.*[24,25] have used the pore diffusion model in their studies of gas adsorption separation processes.

To date, the theory of displacement in liquid chromatography (LC) applied only to conditions of ideal chromatography, neglecting the effects of dispersion and finite mass transport. However, the scale-up of the process with respect to stationary phase particle size, column dimensions, feed load, volumetric flow-rates, and molecular dimensions of the feed and displacer components may affect the effluent displacement profiles.

We have recently shown that the preparative separation of peptides, antibiotics, and proteins can be accomplished using high-performance liquid chromatography (HPLC) columns in the displacement mode[26]. We are presently investigating the scale-up of these displacement processes to larger column systems. In order to facilitate the scale-up of the process, it is important that a model be developed to predict the

effects of scale-up on the effluent displacement profiles. In this work, we present theoretical results on the simulation of displacement chromatography under chromatographic conditions which include the effects of axial dispersion and finite mass transfer.

THEORETICAL DEVELOPMENT

Consider an isothermal chromatographic column of constant void fraction, ε, through which an inert carrier containing N adsorbable species flows with a constant interstitial velocity, u_0. The system is assumed to be one dimensional in the direction of flow with uniform cross-sectional area. Let c_i denote the molar concentration of species i in the fluid phase and $\bar{q}_i$ represent the average concentration of species i in the stationary phase material. Let D_i and k_i represent the axial dispersion coefficient and the overall mass transfer coefficient of species i, respectively. The material balance for species i in the fluid phase can then be written as

$$\frac{\partial c_i}{\partial t} + u_0 \frac{\partial c_i}{\partial z} + \frac{1 - \varepsilon}{\varepsilon} \frac{\partial \bar{q}_i}{\partial t} - D_i \frac{\partial^2 c_i}{\partial z^2} = 0 \qquad i = 1, 2, \ldots, N \tag{1}$$

$$\frac{\partial \bar{q}_i}{\partial t} = k_i (q_i^* - \bar{q}_i) \qquad i = 1, 2, \ldots, N \tag{2}$$

where q_i^* represents the stationary phase concentration in the absence of mass transport limitations. The axial dispersion coefficient for species i, D_i, includes longitudinal spreading due to both molecular diffusion and eddy dispersion[27,28]. The stationary phase accumulation term, $\partial \bar{q}_i / \partial t$, is approximated using a linear driving force model which employs an overall effective mass transfer coefficient, k_i, to describe both the film and intraparticular mass transport.

It has been established that the equilibrium adsorption of most substances in chromatographic systems can be described by the langmuir adsorption isotherm[29–31]. For a multicomponent system, the langmuir isotherm for component i is given by

$$q_i^* = \frac{a_i c_i}{1 + \sum_{j=1}^{N} b_j c_j} \tag{3}$$

where a_i and b_i are the langmuir parameters for species i and N is the number of components in the mixture[30–32]. The system of equations described by eqns. 1 and 2 are coupled through this multicomponent adsorption isotherm.

Similar systems of equations have been solved numerically for multicomponent adsorption[9,14,15,31,33]. In order to use these equations to describe non-ideal displacement chromatography, the appropriate initial and boundary conditions must be employed. Specifically, the introduction of the feed, displacer, regenerant and carrier solutions must be represented by appropriate inlet boundary conditions.

Initially, the column is equilibrated with the inert carrier fluid. This initial state of the column can be represented as

$$c_i = \bar{q}_i = 0 \qquad \text{at } t = 0,\ 0 \leqslant z \leqslant L \qquad (4)$$

$$i = 1, 2, \ldots, N$$

At $t = 0$, a feed solution containing $N - 1$ components at concentrations of c_{1F}, $c_{2F}, \ldots, c_{(N-1)F}$ is introduced into the column for a time t_{feed}. The inlet boundary conditions during the introduction of the feed are

$$u_0 c_i = u_0 c_{iF} + D_i \left.\frac{\partial c_i}{\partial z}\right|_{z=0} \qquad \text{at } z = 0,\ 0 \leqslant t \leqslant t_{feed} \qquad (5)$$

$$i = 1, 2, \ldots, N - 1$$

and

$$c_N = 0 \qquad \text{at } z = 0,\ 0 \leqslant t \leqslant t_{feed} \qquad (6)$$

Following the introduction of the feed, a solution containing only the displacer at a concentration c_{NF} is pumped into the column. The introduction of the displacer continues until time t_{displ}, the breakthrough time of the displacer at the column outlet. The inlet boundary conditions during the introduction of the displacer are

$$u_0 c_i = D_i \left.\frac{\partial c_i}{\partial z}\right|_{z=0} \qquad \text{at } z = 0,\ t_{feed} < t \leqslant t_{displ} \qquad (7)$$

$$i = 1, 2, \ldots, N - 1$$

and

$$u_0 c_N = u_0 c_{NF} + D_N \left.\frac{\partial c_N}{\partial z}\right|_{z=0} \qquad \text{at } z = 0,\ t_{feed} < t \leqslant t_{displ} \qquad (8)$$

The outlet boundary condition during the entire cycle of operation is given by

$$\left.\frac{\partial c_i}{\partial z}\right|_{z=L} = 0 \qquad \text{at } z = L,\ t \geqslant 0 \qquad (9)$$

$$i = 1, 2, \ldots, N$$

A suitable regenerant scheme was also included in the model to calculate the time required to both remove the displacer from the column and to re-equilibrate the column with the inert carrier.

It is convenient to define the following dimensionless variables and parameters in order to facilitate the study of dispersion and mass transport effects in displacement systems:

$$\tau = \frac{u_0 t}{L},\ x = \frac{z}{L},\ Pe_i = \frac{u_0 L}{D_i},\ St_i = \frac{k_i L}{u_0}$$

where τ, x, Pe, and St represent dimensionless time, dimensionless axial position, Peclet number, and Stanton number, respectively. (Note: the fluid and stationary phase concentrations were kept in dimensional form in this model.)

Eqns. 1, 2, and 4–9 become, respectively,

$$\frac{\partial c_i}{\partial \tau} + \frac{\partial c_i}{\partial x} + \frac{1-\varepsilon}{\varepsilon}\frac{\partial \bar{q}_i}{\partial \tau} - \frac{1}{Pe_i}\frac{\partial^2 c_i}{\partial x^2} = 0 \qquad i = 1, 2, \ldots, N \tag{10}$$

$$\frac{\partial \bar{q}_i}{\partial \tau} = St_i\,(q_i^* - \bar{q}_i) \qquad i = 1, 2, \ldots, N \tag{11}$$

$$c_i = \bar{q}_i = 0 \qquad \text{at } \tau = 0,\ 0 \leqslant x \leqslant 1 \qquad i = 1, 2, \ldots, N \tag{12}$$

$$c_i = c_{iF} + \frac{1}{Pe_i}\frac{\partial c_i}{\partial x}\bigg|_{x=0} \qquad \text{at } x = 0,\ 0 \leqslant \tau \leqslant \tau_{\text{feed}} \qquad i = 1, 2, \ldots, N-1 \tag{13}$$

$$c_N = 0 \qquad \text{at } x = 0,\ 0 \leqslant \tau \leqslant \tau_{\text{feed}} \tag{14}$$

$$c_i = \frac{1}{Pe_i}\frac{\partial c_i}{\partial x}\bigg|_{x=0} \qquad \text{at } x = 0,\ \tau_{\text{feed}} < \tau \leqslant \tau_{\text{displ}} \qquad i = 1, 2, \ldots, N-1 \tag{15}$$

$$c_N = c_{NF} + \frac{1}{Pe_N}\frac{\partial c_N}{\partial x}\bigg|_{x=0} \qquad \text{at } x = 0,\ \tau_{\text{feed}} < \tau \leqslant \tau_{\text{displ}} \tag{16}$$

$$\frac{\partial c_i}{\partial x}\bigg|_{x=1} = 0 \qquad \text{at } x = 1,\ \tau \geqslant 0 \qquad i = 1, 2, \ldots, N \tag{17}$$

NUMERICAL PROCEDURE

A finite difference technique was employed to approximate the system of coupled, non-linear partial differential equations. The first order spatial and temporal derivatives were approximated using forward and backward differencing, respectively, and the second order spatial derivative was approximated using central differencing. Denoting the position of the node within the computational grid along the x and τ coordinates as m and n, respectively, eqns. 10 and 11 were combined and written as the following difference equations

$$c_i(m+1, n+1) = c_i(m, n+1) - \frac{\Delta x}{\Delta \tau}[c_i(m, n+1) - c_i(m, n)] +$$

$$- \frac{1-\varepsilon}{\varepsilon} \Delta x \, St_i [q_i^*(m, n+1) - \bar{q}_i(m, n)] +$$

$$+ \frac{1}{Pe_i \Delta x}[c_i(m+2, n) - 2c_i(m+1, n) + c_i(m, n)] \quad (18)$$

$$\bar{q}_i(m, n+1) = \Delta \tau \, St_i [q_i^*(m, n+1) - \bar{q}_i(m, n)] + \bar{q}_i(m, n) \quad (19)$$

The stability of the finite difference numerical scheme was evaluated for ideal displacement chromatography. Under these conditions, the steepest concentration gradients are produced, thus making this a useful test of stability in these systems. From a von Neumann analysis[34] the stability criterion was found to be

$$\psi = \frac{\Delta x}{u_{\min} \Delta \tau} \leqslant 1 \quad (20)$$

where $u_{\min}$ is the ratio of the minimum velocity of any species moving within the column to the interstitial velocity, u_0. In this study, the value of ψ was always less than 0.8 to assure stable solutions.

A FORTRAN program was written to march through the resulting difference equations. The program was initiated with the following parameters: spatial (Δx) and temporal ($\Delta \tau$) step increments, τ_{feed}, u_0, column dimensions, ε, isotherm parameters and input concentrations of all species, and the characteristic Peclet and Stanton numbers. The isotherm parameters of the feed components and the displacer compound employed in this study are given in Table I. These parameters are representative of those obtained in experimental studies of the displacement chromatography of small biomolecules[5]. The operating parameters employed in the various simulation experiments are given in Table II. In all cases, the Peclet and Stanton numbers specified in this table represent the values for each component. The effect of increasing mass transport resistance was studied by varying the Stanton number in displacement simulations 1–3. The effect of axial dispersion was examined in simulations 4 and 5. In simulations 6–10, the column length was varied from 10 to 50 cm to examine the displacement development patterns produced in systems with axial dispersion and finite mass transport.

TABLE I

LANGMUIR PARAMETERS

Component	*a*	*b* (mM^{-1})
1	3.297	0.0905
2	4.200	0.1100
3	5.740	0.1247
4	9.203	0.1501

TABLE II

SIMULATION PARAMETERS

Unless otherwise stated, all displacement simulations used: u_0 = 1 cm/min, ε = 0.6, L = 25 cm, column inner diameter = 4.6 mm, Δx = 0.0004, $\Delta\tau$ = 0.00125; feed mixture, 10 mM each of components 1 and 3; displacer, component 4 at a concentration of 40 mM.

Displacement simulation run	τ_{feed}	*St*	*Pe*
1*	0.24	1600	1000 000
2*	0.24	800	1000 000
3*	0.24	200	1000 000
4*	0.24	1600	1000 000
5*	0.24	1600	30 000
6**,***	0.09	800	30 000
7**,***	0.09	800	30 000
8**,***	0.09	800	30 000
9**,***	0.09	800	30 000
10**,***	0.09	800	30 000
11	0.12–1.20	800	1000 000
12	0.12–1.20	300	30 000
13§	0.24	800	1000 000
14§	0.24	300	30 000
15	0.24	50–800	13 750–36 970
16	0.24	40–1600	100 000
17	0.24	5–1600	100 000

* Δx = 0.0002 and $\Delta\tau$ = 0.000625.

** Feed mixture contained 10 mM each of components 1, 2, and 3.

*** Column lengths of 10, 20, 30, 40, and 50 cm, were employed in displacement simulations 1, 2, 3, 4, and 5, respectively.

§ Displacer concentrations of 15, 30, 40, 60, 80, 100, and 140 mM were used to generate the throughput curves.

The model was used to both generate displacement effluent profiles under various conditions and to calculate the throughput obtained in these displacement systems. The throughput is defined as the mass of product isolated per unit time at a specified level of purity. The throughput for each species was calculated by numerically summing all fractions containing the component at a purity greater than 98% and dividing this by the total displacement cycle time which includes the introduction of feed, displacer, regenerant and carrier solutions.

Throughput curves were generated in simulations 11–17. The effect of increasing feed volumes at various levels of non-ideality was studied in runs 11 and 12. In simulations 13 and 14, the effect of increasing displacer concentration on product throughput was examined at various levels of chromatographic non-ideality. Simulation 15 examined the effect of increasing interstitial velocity on the throughput under both ideal and non-ideal displacement conditions. The throughput curve for the non-ideal system in simulation 15 was generated by assuming a constant mass transfer coefficient of k = 0.53 s^{-1} and an axial dispersion coefficient which varied with velocity according to the treatment of Horváth and Lin[27,28]

$$D = D_m + \frac{\lambda d_p u_0}{1 + \omega \left(\frac{d_p u_0}{D_m}\right)^{-1/3}} \tag{21}$$

where D_m is the solute molecular diffusivity, d_p is the stationary phase particle diameter, λ is a measure of the flow inequality in the bed, and ω is a function of the bed porosity. The subscript i has been omitted to simplify the expression. Values of $2 \cdot 10^{-5}$ cm^2/s, $5 \cdot 10^{-4}$ cm, 2.5, and 2.0 were used for D_m, d_p, λ, and ω, respectively.

The influence of mass transfer limitations on product throughput were investigated as a function of particle diameter, interstitial velocity, and solute diffusivity in simulation runs 16 and 17. The expression for the overall mass transfer coefficient used in this study was[31]

$$\frac{1}{kK} = \frac{d_p}{6k_f} + \frac{d_p^2}{60\ \varepsilon_p D_p} \tag{22}$$

where K is the equilibrium partition coefficient, k_f is the film mass transfer coefficient, ε_p is the intraparticular porosity, and D_p is the intraparticular diffusion coefficient.

The film mass transfer coefficient and the intraparticular diffusivity can be written using the expressions of Horváth and Lin[27,28]

$$k_f = \frac{\Omega D_m}{d_p}\left(\frac{d_p u_0}{D_m}\right)^{1/3} \tag{23}$$

$$D_p = \frac{D_m\ \varepsilon_p}{\theta} \tag{24}$$

where θ is the tortuosity factor and Ω is a function of the interparticular bed porosity.

Eqns. 22 through 24 were combined to obtain an expression for the Stanton number:

$$St = \frac{D_m L}{u_0 K d_p^2}\left[\frac{1}{\frac{1}{6\Omega}\left(\frac{D_m}{d_p u_0}\right)^{1/3} + \frac{\theta}{60\ \varepsilon_p^2}}\right] \tag{25}$$

In this study, values of 5.0, 0.5, 2.0, and 7.5 were used for K, ε_p, θ, and Ω, respectively.

RESULTS AND DISCUSSIONS

The effects of axial dispersion and finite mass transport in multicomponent adsorption systems have been studied by several authors[9–15]. In this work, we examine the effect of these non-idealities on the effluent concentration profiles obtained in simulations of displacement chromatography.

The effect of mass transfer limitations on the displacement effluent profile was investigated by varying the Stanton number. For a Stanton number of 1600, the

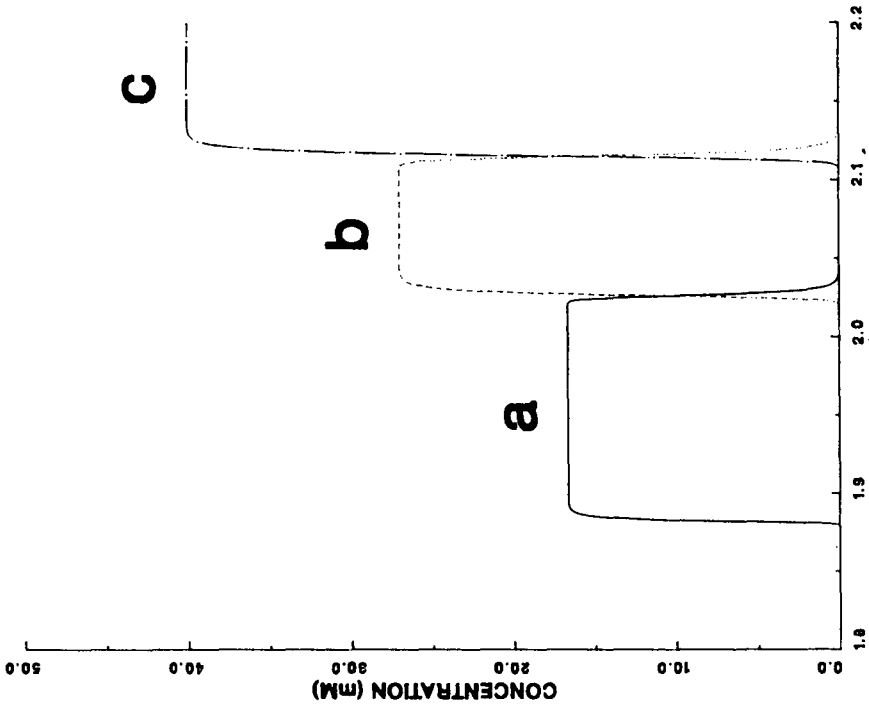

Fig. 1. Effluent displacement profile obtained with a Stanton number of 1600. Simulation conditions are described in Table II for run 1. a = Component 1; b = component 3; c = component 4 (displacer).

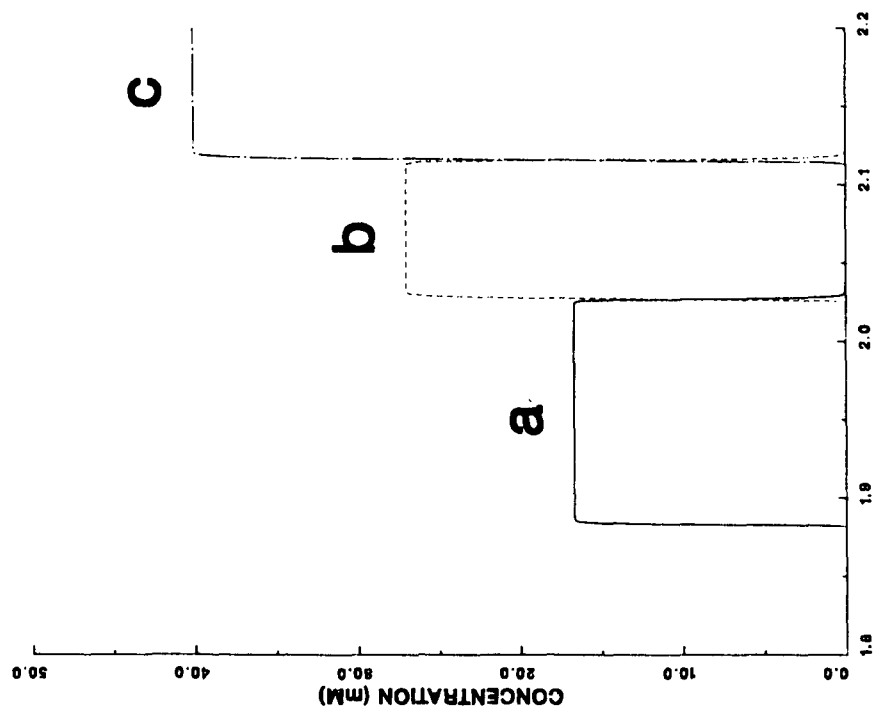

Fig. 2. Effluent displacement profile obtained with Stanton number of 800. Simulation conditions are described in Table II for run 2. Symbols as described in Fig. 1.

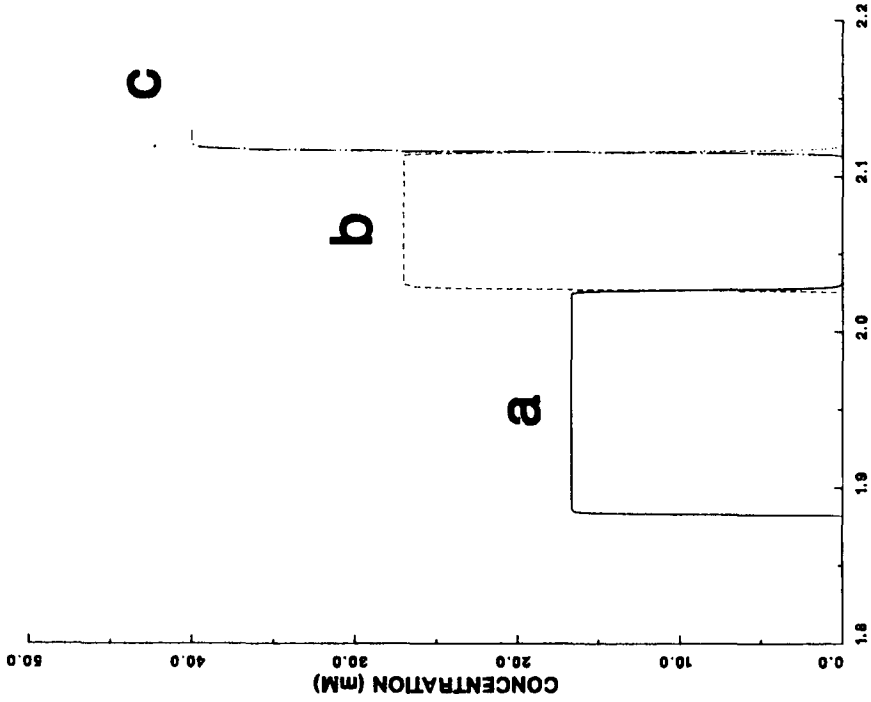

Fig. 3. Effluent displacement profile obtained with a Stanton number of 200. Simulation conditions are described in Table II for run 3. Symbols as described in Fig. 1.

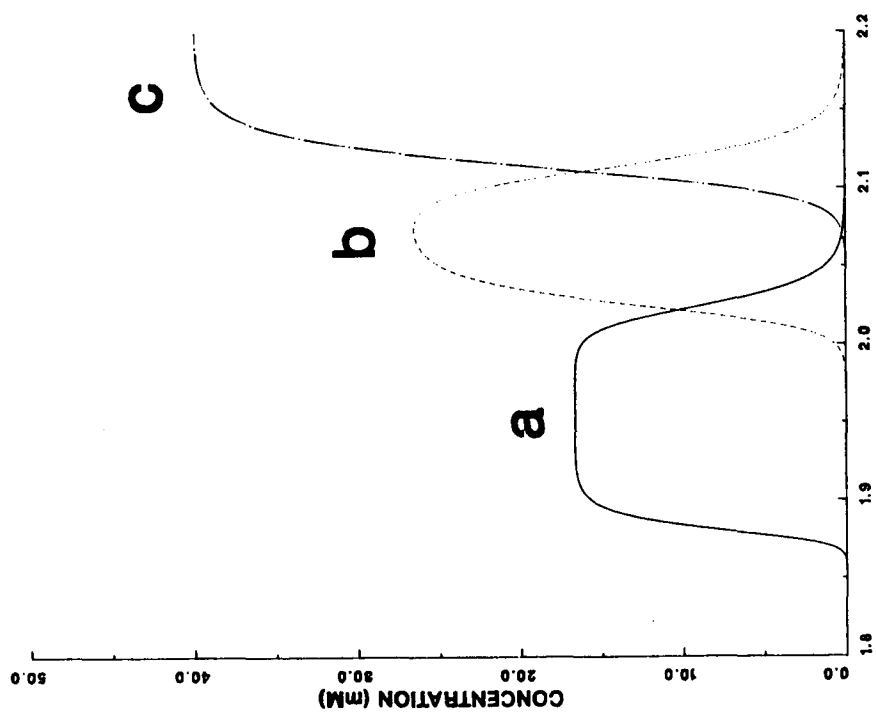

Fig. 4. Effluent displacement profile obtained with a Peclet number of 1000 000. Simulation conditions are described in Table II for run 4. Symbols as described in Fig. 1.

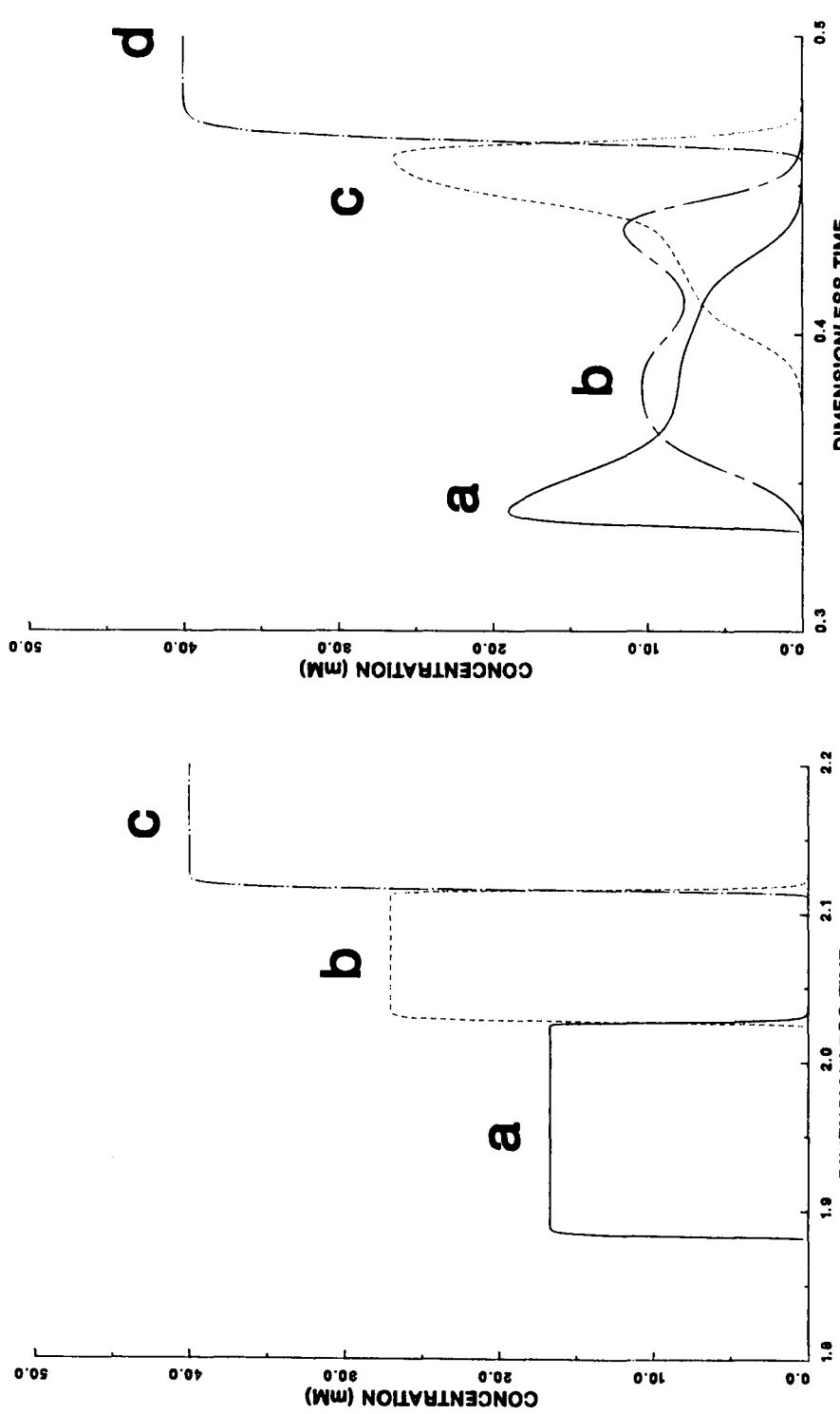

Fig. 5. Effluent displacement profile obtained with a Peclet number of 30 000. Simulation conditions are described in Table II for run 5. Symbols as described in Fig. 1.

Fig. 6. Effluent displacement profile obtained with a column length of 10 cm. Simulation conditions are described in Table II for run 6. a = Component 1; b = component 2; c = component 3; d = component 4 (displacer).

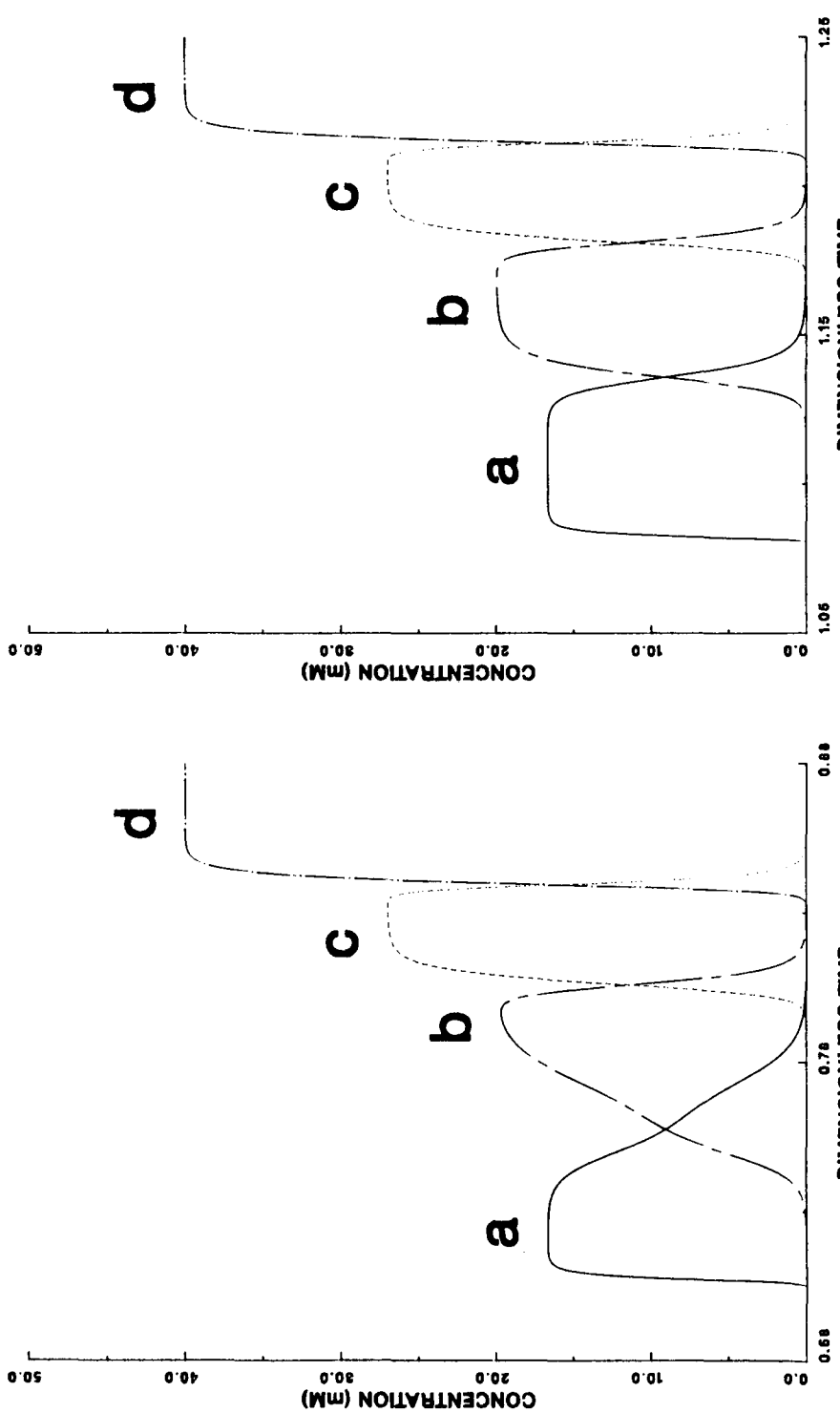

Fig. 7. Effluent displacement profile obtained with a column length of 20 cm. Simulation conditions are described in Table II for run 7. Symbols as described in Fig. 6.

Fig. 8. Effluent displacement profile obtained with a column length of 30 cm. Simulation conditions are described in Table II for run 8. Symbols as described in Fig. 6.

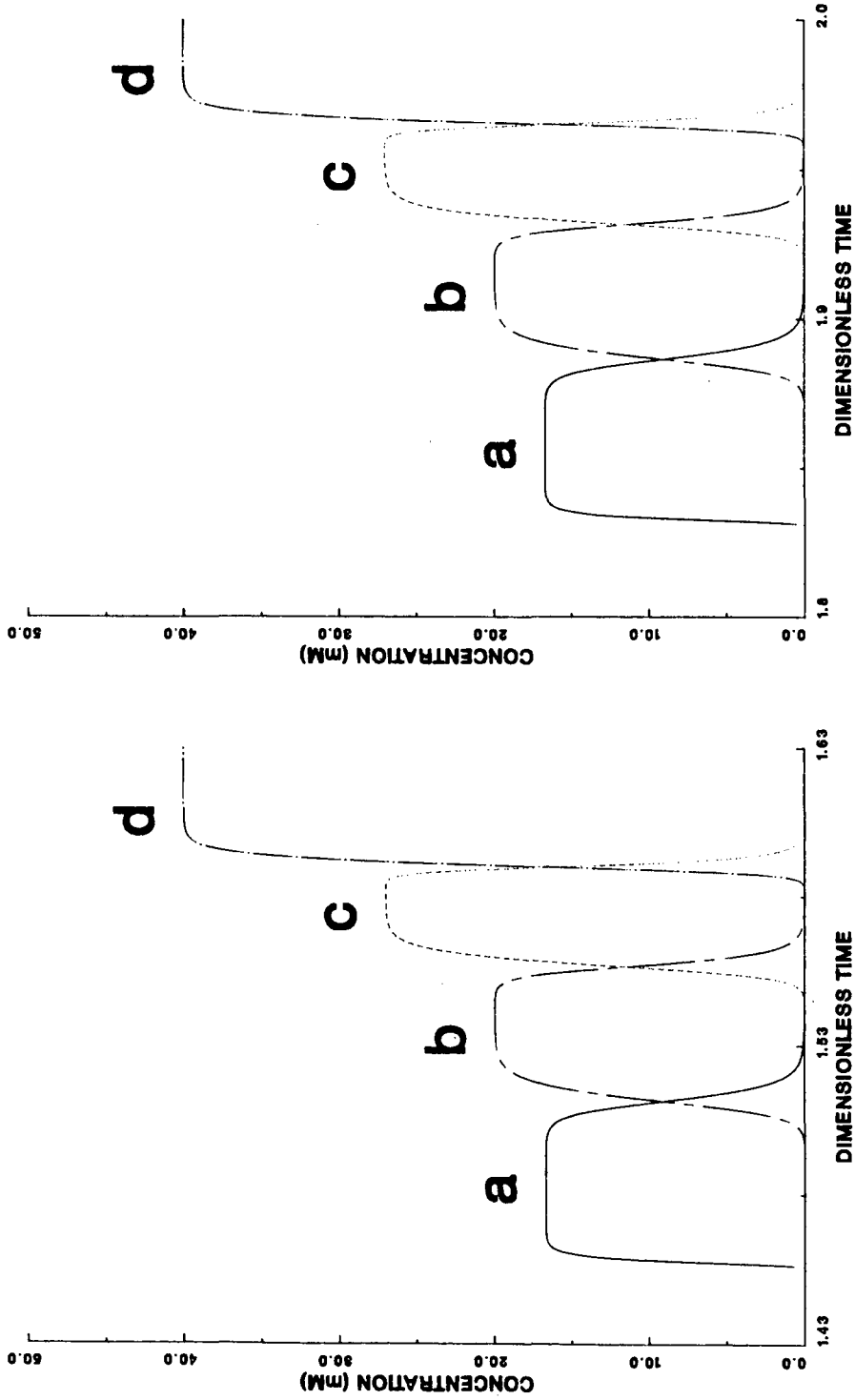

Fig. 9. Effluent displacement profile obtained with a column length of 40 cm. Simulation conditions are described in Table II for run 9. Symbols as described in Fig. 6.

Fig. 10. Effluent displacement profile obtained with a column length of 50 cm. Simulation conditions are described in Table II for run 10. Symbols as described in Fig. 6.

displacement effluent profile approached that obtained under ideal chromatographic conditions as shown in Fig. 1. When the Stanton number is decreased to 800, the concentration shock waves separating the displacement zones become more diffuse, resulting in increased zone overlap as illustrated in Fig. 2. This result is dramatically depicted in Fig. 3, which shows the effluent profile for a Stanton number of 200. Under these conditions, the mass transport limitations result in excessive zone overlap, significantly decreasing the amount of purified material obtained in the separation process. Clearly, mass transport effects can play a major role in displacement chromatography.

The column Peclet number was varied to study the effect of axial dispersion in displacement chromatography. For Peclet numbers normally encountered in analytical liquid chromatography (30 000–1000 000), the axial dispersion was found to have little effect on the profiles as illustrated in Figs. 4 and 5. For large particles, a Peclet number on the order of 5000 is obtained. Under these conditions, the model also shows little effect of axial dispersion on the displacement profiles. However, for non-uniformly packed columns or process-scale systems with pronounced entrance and exit effects, axial dispersion may indeed become a dominant dispersive force.

Figs. 6–10 simulate various stages in the development of displacement zones in the presence of axial dispersion and finite mass transfer. These patterns are similar to those obtained in ideal displacement chromatography with the concentration shock waves now replaced with dispersed shock layers. The unusual shapes of these zones can be attributed to a combination of chromatographic modes operating simultaneously within the column. Specifically, during the introduction of the feed, multicomponent frontal chromatography is occuring, resulting in the formation of concentration profiles similar to those described by Jacobson *et al.*[32]. Upon the introduction of the displacer at τ_{feed}, the frontal chromatographic patterns are disturbed by the action of the displacer resulting in a development pattern as illustrated in Fig. 6. At this column length, the displacement zone of component 3 begins to form. The displacement of the less adsorbing feed components, 1 and 2, results in the accumulation of these solutes further downstream, leading to the formation of elevated concentration peaks. Fig. 7 depicts the effluent profile for a 20-cm column. At this column length, the displacement zone of component 3 is essentially fully developed while the displacement zones of components 1 and 2 are being formed. Full displacement development is achieved at a column length of 30 cm, as shown in Fig. 8. The effect of mass transfer limitations is clearly seen by the significant amount of zone overlap at full development.

In non-ideal multicomponent adsorption systems, it has been established that constant patterns are obtained with sufficiently long columns[9,35]. These constant patterns result from a dynamic balance of the dispersive and self-sharpening forces acting on the concentration front. Figs. 9 and 10 show the effluent profiles for column lengths of 40 and 50 cm, respectively. It can be seen that the displacement profiles achieved at these two column lengths are identical. Thus, this model predicts that constant pattern formation is also achieved in non-ideal displacement chromatography.

The major goal in process-scale chromatography is to maximize the product throughput, the total mass purified per unit time at a specified purity. Frenz *et al.*[36] have experimentally investigated the optimization of flow-rate, feed load, and

displacer concentration in high-performance displacement chromatography. In our work, we examine the effects of these operating parameters on throughput maximization under conditions of ideal and non-ideal chromatography. Furthermore, we extend the treatment to include the effects of particle diameter and solute diffusivity.

Fig. 11 demonstrates the effect of increasing feed load on the throughput of components 1 and 3 under various conditions of non-ideality. All throughput curves exhibit a maximum at a unique value of the feed volume. At low feed loads, complete development is achieved but the column is "under-utilized" with only a small fraction of the column bed being employed in the separation at a given time. At high feed loads, the column length is insufficient for full development, resulting in incomplete separation of the products and a corresponding decrease in throughput at the elevated mass loadings. The effects of mass transfer are clearly seen in this figure by the reduction of the throughput values with decreasing Stanton numbers. Under non-ideal

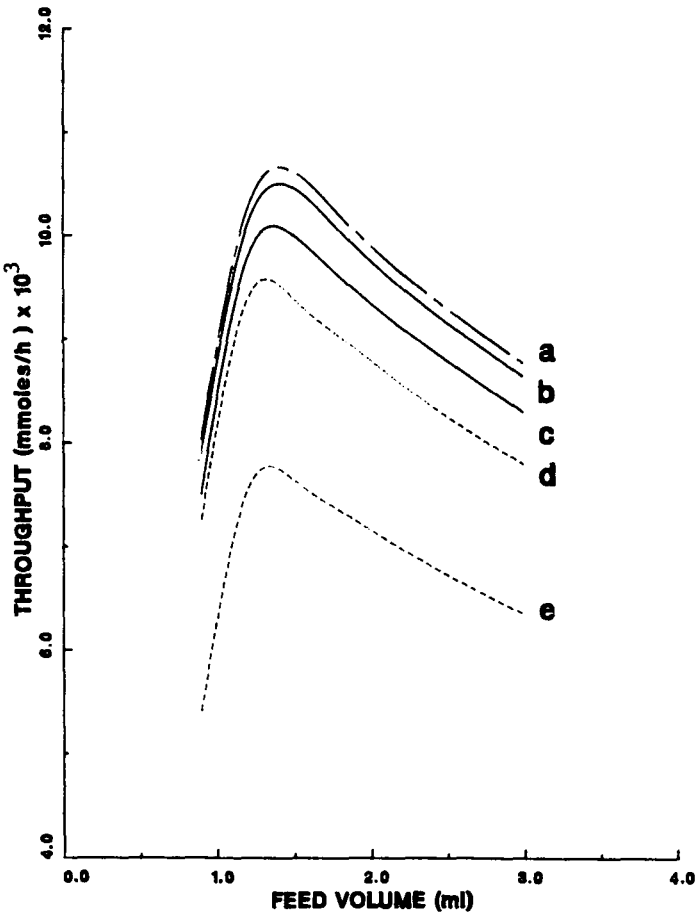

Fig. 11. The effect of feed volume on product throughput. Simulation conditions are described in Table II for runs 11 and 12. a = Components 1 and 3, ideal; b = component 1, St = 800; c = component 1, St = 300; d = component 3, St = 800; e = component 3, St = 300.

displacement conditions, component 1 has a higher throughput than component 3. This is due to the relative position of the components in the displacement train. At full development, component 1 can mix only with component 3, whereas component 3 can mix with both component 1 and the displacer. Furthermore, the equilibrium concentration of component 3 is higher, with a corresponding smaller zone width. This leads to a greater loss of pure material due to zone mixing.

The effect of displacer concentration on product throughput is illustrated in Fig. 12. All data in this figure were generated by using displacer concentrations above 12 mM, the minimum concentration required for displacement of all feed components[7]. The speed of the displacer shock wave is an increasing function of its concentration[5,20]. At low concentrations, the shock wave moves slowly through the column resulting in long separation times and accompanying low throughputs. Ideally, increasing the displacer concentration results in shorter separation times and elevated throughputs. However, this is not the case for non-ideal displacement systems as seen

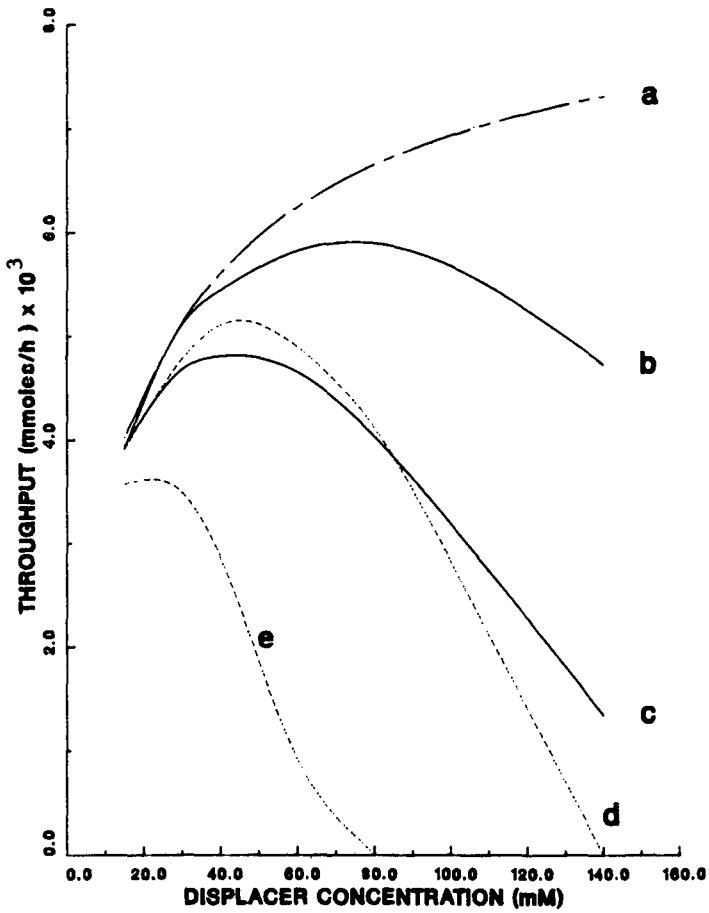

Fig. 12. The effect of displacer concentration on product throughput. Simulation conditions are described in Table II for runs 13 and 14. Symbols as described in Fig. 11.

in Fig. 12. Higher displacer concentrations result in both elevated product concentrations and narrow widths of the displacement zones. Thus, as the displacer concentration increases, mixing due to mass transfer limitations will become increasingly significant. For non-ideal displacement systems, an optimum value of the displacer concentration exists which maximizes the throughput of a given compound.

Fig. 13 illustrates the effect of increasing interstitial velocity on the throughput in both ideal and non-ideal displacement chromatography. In ideal chromatography, the throughput will continue to increase with increasing velocity. In actuality, the throughput decreases at high velocities due to the mass transport limitations and accompanying zone mixing. Thus, an optimal value of the flow-rate exists which maximizes throughput. The theoretical results presented in Figs. 11–13 are in concordance with the experimental results reported by Frenz *et al.*[36].

The influence of mass transfer limitations on product throughput were

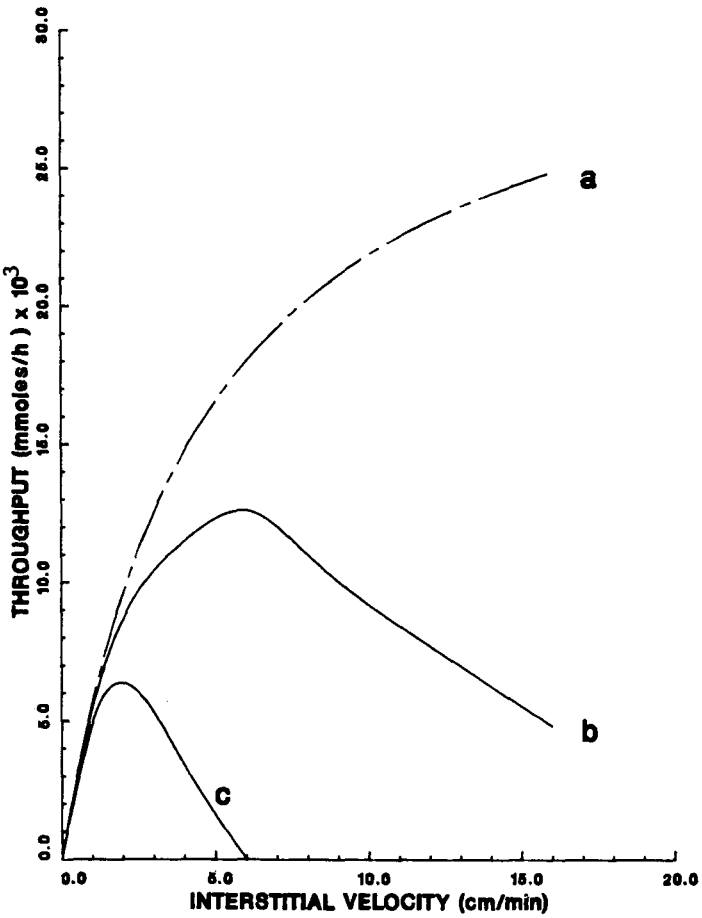

Fig. 13. The effect of interstitial velocity on product throughput. Simulation conditions are described in Table II for run 15. a = Components 1 and 3, ideal; b = component 1, non-ideal; c = component 3, non-ideal.

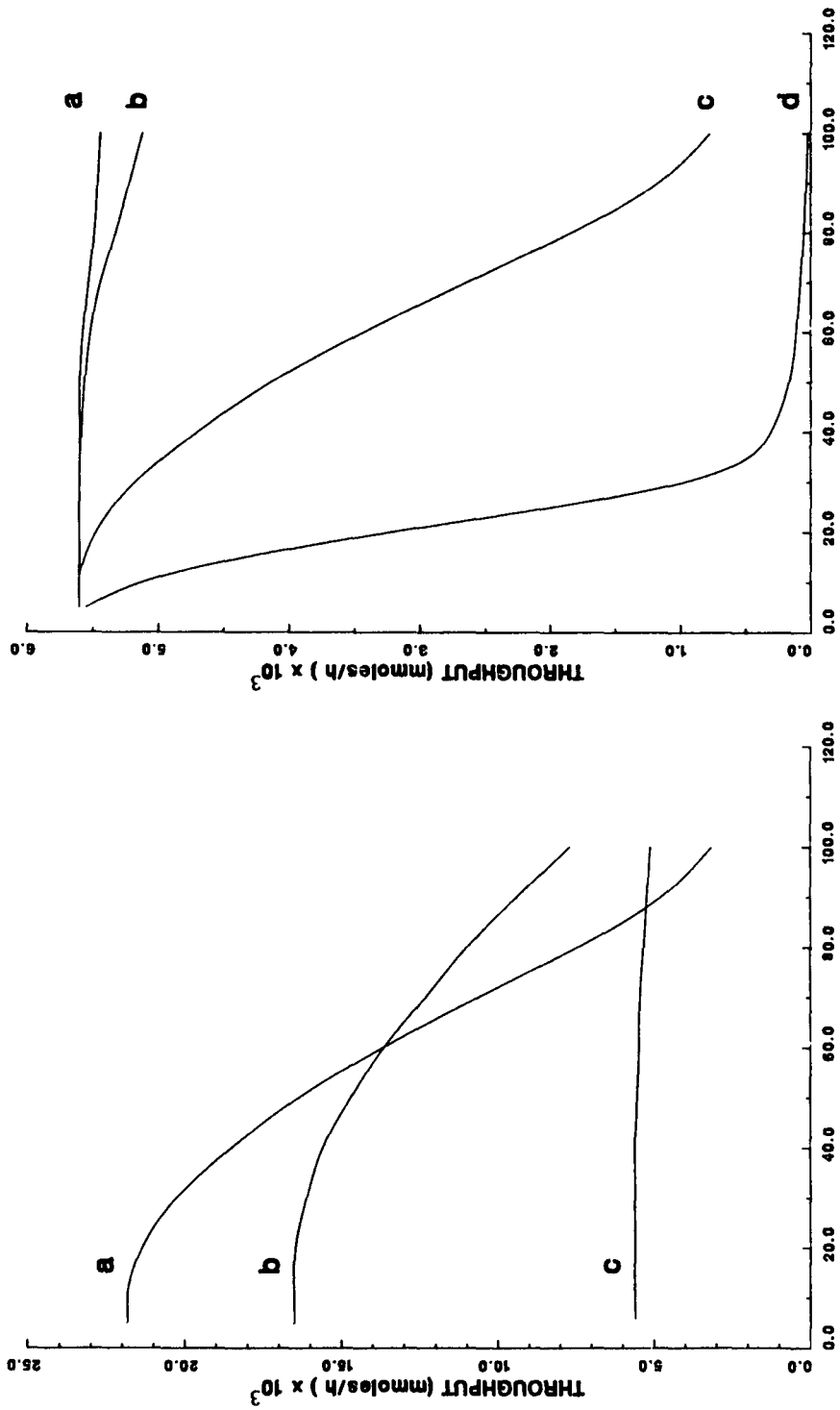

Fig. 14. The effect of particle diameter on product throughput at a constant solute diffusivity of $2 \cdot 10^{-5}$ cm^2/s. Simulation conditions are described in Table II for run 16. u_0: a = 10 cm/min; b = 5 cm/min; c = 1 cm/min.

Fig. 15. The effect of particle diameter on product throughput at a constant interstitial velocity of 1 cm/min. Simulation conditions are described in Table II for run 17. D: a = $4 \cdot 10^{-5}$ cm^2/s; b = $2 \cdot 10^{-5}$ cm^2/s; c = $2 \cdot 10^{-6}$ cm^2/s; d = $2 \cdot 10^{-7}$ cm^2/s.

investigated as a function of particle diameter, interstitial velocity and solute diffusivity. The effects of interstitial velocity and particle diameter on the throughput of component 1 are illustrated in Fig. 14. A constant solute diffusivity of $2 \cdot 10^{-5}$ cm^2/s, typical of small solutes, along with a Stanton number which varied according to eqn. 25 was used to generate this plot. At low velocities, the throughput is essentially independent of particle diameter. The throughput can be dramatically increased by operating at elevated velocities when small particle diameter adsorbents are employed. As the particle diameter increases, however, these advantages become less pronounced. In fact, at large particle diameters, the throughput obtained at high velocities can actually be lower than when operating at lower velocities.

In Fig. 15, the combined effects of solute diffusivity and particle diameter on the throughput are illustrated for a constant interstitial velocity of 1 cm/min. The throughput is insensitive to the particle diameter for small solutes. Thus, large particles can be employed for the separation of relatively small biomolecules with an accompanying reduction in capital costs. On the other hand, as the molecular dimensions of the solute increase, the throughput becomes an increasingly stronger function of the particle diameter. This effect is dramatically shown for a solute diffusivity of $2 \cdot 10^{-7}$ cm^2/s, typical of proteins. Clearly, for the separation of macromolecules by displacement chromatography, it is imperative that small particles be employed.

CONCLUSION

A mathematical model was developed to study the effects of axial dispersion and finite mass transfer in displacement chromatography. While the displacement profile was fairly insensitive to axial dispersion, slow mass transfer rates were shown to have a significant dispersive effect on the concentration shock waves generated in displacement chromatography. In addition, constant pattern formation was obtained under non-ideal conditions. The model was also employed to examine the throughput of these systems as a function of feed load, displacer concentration and interstitial velocity. Under non-ideal conditions, a unique optimum value of these operating parameters existed which maximized the throughput. In order to examine the potential scale-up of the process, the interplay of particle diameter, solute diffusivity, and interstitial velocity was investigated. The results indicated that the use of large particles are potentially detrimental to the performance of displacement systems when high velocities are employed. In fact, macromolecular separations by displacement chromatography may necessitate the use of small particle diameters. The incorporation of adsorption and desorption kinetics along with the experimental evaluation of the model predictions will be the subject of a future report.

SYMBOLS

a_i Langmuir parameter for species i (dimensionless)
b_i langmuir parameter for species i (mM^{-1})
c_{iF} feed concentration for species i (mM)
c_i mobile phase concentration of species i (mM)
D_i effective axial dispersion coefficient of species i (cm^2/s)

D_m solute molecular diffusion coefficient (cm^2/s)
D_p solute intraparticular diffusion coefficient (cm^2/s)
d_p stationary phase particle diameter (cm)
K equilibrium partition coefficient (dimensionless)
k_f film mass transfer coefficient (cm/s)
k_i overall mass transfer coefficient of species i (s^{-1})
L column length (cm)
m axial coordinate of the node within the computational grid (dimensionless)
n temporal coordinate of the node within the computational grid (dimensionless)
N number of components (dimensionless)
Pe_i $u_0 L/D_i$, column Peclet number (dimensionless)
$\bar{q}_i$ average stationary phase concentration of species i (mM)
q_i^* equilibrium stationary phase concentration of species i (mM)
St_i $k_i L/u_0$, Stanton number (dimensionless)
t time (s)
t_{displ} displacer breakthrough time (s)
t_{feed} feed introduction time (s)
u_{min} minimum velocity of any species moving within the column (dimensionless)
u_0 interstitial mobile phase velocity (cm/s)
x z/L, dimensionless axial position
z axial position (cm)
ε fractional void space of fixed bed (dimensionless)
ε_p intraparticular void space (dimensionless)
θ tortuosity factor (dimensionless)
λ parameter which measures flow inequalities in the bed (dimensionless)
τ $u_0 t/L$, dimensionless time
τ_{displ} dimensionless displacer breakthrough time
τ_{feed} dimensionless feed introduction time
ψ dimensionless stability parameter
Ω dimensionless parameter dependent only on interparticulate porosity
ω dimensionless parameter dependent on bed porosity

ACKNOWLEDGEMENT

This work was supported in part by Grant No. CBT-8708799 from the National Science Foundation.

REFERENCES

1 A. Tiselius, *Ark. Kemi, Mineral. Geol.*, 16 (A) (1943) 1.
2 S. M. Cramer and Cs. Horváth, *Prep. Chromatogr.*, 1 (1988) 29.
3 Cs. Horváth, A. Nahum and J. H. Frenz, *J. Chromatogr.*, 218 (1981) 365.
4 Cs. Horváth, J. H. Frenz and Z. El Rassi, *J. Chromatogr.*, 255 (1983) 273.
5 J. H. Frenz and Cs. Horváth, *AIChE J.*, 31 (1985) 400.
6 S. M. Cramer, Z. El Rassi and Cs. Horváth, *J. Chromatogr.*, 394 (1987) 305.
7 Cs. Horváth, in F. Bruner (Editor), *The Science of Chromatography (Journal of Chromatography Library*, Vol. 32), Elsevier, Amsterdam, 1985, pp. 179–203.
8 A. W. Liao, Z. El Rassi, D. M. LeMaster and Cs. Horváth, *Chromatographia*, 24 (1987) 881.
9 W. G. Bradley and N. H. Sweed, *AIChE Symp. Ser.*, 71, 152 (1975) 59.

10 A. I. Liapis and D. W. T. Rippin, *Chem. Eng. Sci.*, 32 (1977) 619.
11 M. W. Balzli, A. I. Liapis and D. W. T. Rippin, *Trans. Inst. Chem. Eng.*, 56 (1978) 145.
12 J. S. C. Hsieh, R. M. Turian and C. Tien, *AIChE J.*, 23 (1977) 263.
13 S.-C. Wang and C. Tien, *AIChE J.*, 28 (1982) 565.
14 M. Morbidelli, A. Servida, G. Storti and S. Carra, *Ind. Eng. Chem. Fundam.*, 21 (1982) 123.
15 E. Santacesaria, M. Morbidelli, A. Servida, G. Storti and S. Carra, *Ind. Eng. Chem. Process Des. Dev.*, 21 (1982) 446.
16 F. G. Helfferich and G. Klein, *Multicomponent Chromatography: Theory of Interference*, Marcel Dekker, New York, 1970.
17 F. G. Helfferich, *AIChE Symp. Ser.*, 80, 233 (1984) 1.
18 F. G. Helfferich, *J. Chromatogr.*, 373 (1986) 45.
19 H.-K. Rhee, R. Aris and N. R. Amundson, *Philos. Trans., R. Soc. London Ser. A*, 267 (1970) 419.
20 H.-K. Rhee and N. R. Amundson, *AIChE J.*, 28 (1982) 423.
21 Q. Yu and N.-H. L. Wang, *Sep. Purif. Methods*, 15 (2) (1986) 127.
22 R. W. Geldart, Q. Yu, P. C. Wankat and N.-H. L. Wang, *Sep. Sci. Technol.*, 21 (9) (1986) 873.
23 G. Guiochon and A. Katti, *Chromatographia*, 24 (1987) 165.
24 M. Morbidelli, G. Storti, S. Carra, G. Niederjaufner and A. Pontoglia, *Chem. Eng. Sci.*, 39 (3) (1984) 383.
25 M. Morbidelli, G. Storti, S. Carra, G. Niederjaufner and A. Pontoglia, *Chem. Eng. Sci.*, 40 (7) (1985) 1155.
26 G. Subramanian, M. W. Phillips and S. M. Cramer, *J. Chromatogr.*, 439 (1988) 341.
27 Cs. Horváth and H.-J. Lin, *J. Chromatogr.*, 126 (1976) 401.
28 Cs. Horváth and H.-J. Lin, *J. Chromatogr.*, 149 (1978) 43.
29 J. R. Condor and C. L. Young, *Physicochemical Measurements by Gas Chromatography*, Wiley, New York, 1979.
30 J. Jacobson, J. Frenz and Cs. Horváth, *J. Chromatogr.*, 316 (1984) 53.
31 D. M. Ruthven, *Principles of Adsorption and Adsorption Processes*, Wiley, New York, 1984.
32 J. Jacobson, J. H. Frenz and Cs. Horváth, *Ind. Eng. Chem. Res.*, 26 (1987) 43.
33 H.-K. Rhee and N. R. Amundson, *Chem. Eng. Sci.*, 27 (1972) 199.
34 L. Lapidus and G. F. Pinder, *Numerical Solution of Partial Differential Equations in Science and Engineering*, Wiley, New York, 1982.
35 D. O. Cooney and E. Lightfoot, *Ind. Eng. Chem. Process Des. Dev.*, 5 (1) (1966) 25.
36 J. Frenz, Ph. van der Schrieck and Cs. Horváth, *J. Chromatogr.*, 330 (1985) 1.

Journal of Chromatography, 454 (1988) 23–36
Elsevier Science Publishers B.V., Amsterdam — Printed in The Netherlands

CHROM. 20 776

STUDY OF THE INJECTION PROCESS IN A GAS CHROMATOGRAPH SPLIT INJECTION PORT

A. E. KAUFMAN* and C. E. POLYMEROPOULOS*
Department of Mechanical and Aerospace Engineering, Rutgers University, P.O. Box 909, Piscataway, NJ 08855-0909 (U.S.A.)
(First received January 4th, 1988; revised manuscript received June 22nd, 1988)

SUMMARY

Pressure and temperature variations which occur during an injection in a gas chromatograph split injection port were measured for different sample sizes, injection port temperatures, solvents, injection port inserts, and split flow-rates. A control volume analysis of the injection process was developed to predict the pressure, temperature and split ratio variations during and after the injection. Comparison of the predicted pressure and temperature results with the experimental measurements was satisfactory. An example is presented demonstrating how the model can be used to predict the quantitative error in a split injection port.

INTRODUCTION

Split injection is a convenient, widely used sample introduction technique for capillary column gas chromatography. The carrier gas entering the injection port is split into two unequal flows with the smaller flow entering the capillary column, and the ratio of these flows (split flow:column flow) defines the split ratio. Ideally, when the sample is injected, it is split at this preset ratio resulting in a known fraction of the sample passing through the column. Though split injection is based on a very simple concept many problems arise when accurate quantitative results are required. Peak areas may vary by a factor of two from one injection to the next[1] and deviations from the preset split ratio are often much greater[2,3].

Many reasons have been proposed to explain the discrimination and quantitation problems observed in split injections. Broadly these can be grouped into five categories: (a) syringe related problems, such as selective evaporation from the syringe needle[4–7] and non-reproducibility in injection technique[8]; (b) split ratio variations caused by temporal changes in pressure[9–11] or viscosity of the insert mixture[4]; (c) incomplete droplet vaporization[12–14]; (d) non-homogeneity of the resulting sample-carrier mixture[14–16]; and (e) thermal or chemical adsorption[5,6,17]. Experimental

* Present address: Continuum Dynamics, P.O. Box 3073, Princeton, NJ 08543, U.S.A.

0021-9673/88/$03.50

support for these mechanisms most often is based on the observed variations in peak areas as chromatographic conditions are changed within the experimental design matrix.

A different approach was used in the present work to improve our understanding of the operation of a split injection port: pressure and temperature measurements were made during the injection and a thermodynamic model of the injection process was developed to predict the pressure, flow and temperature variations that occur during an injection.

EXPERIMENTAL

Apparatus and procedure

A 12.5 m × 0.2 mm I.D. OV-101 column was installed in a Hewlett-Packard Model 5890 A gas chromatograph, and the Hewlett-Packard Model 7673A automated injector was used to make the injections. A Setra Model 205 pressure transducer was connected to the septum purge line six inches from the injection port. The selected transducer had a response time of less than 1 ms. Its volume was filled with an incompressible silicone oil to prevent distortion of the measured pressure pulse[18]. The pressure response was recorded using a digital oscilloscope which was triggered by the pressure increase in the injection port.

Temperature also was measured at several experimental conditions by replacing the capillary column with a thermocouple. The thermocouple response was measured with a Hewlett-Packard 3561 dynamic signal analyzer. Because of the thermal inertia of the approximately 0.3-mm diameter junction the thermocouple response was too slow to measure the temperature changes accurately[19] so the temperature data was used only qualitatively.

A full factorial experiment was designed to investigate the effects on pressure of five variables: injection sample size, injection port temperature, split ratio (or split flow-rate), insert geometry and solvent. A random number table was used to randomize the experimental order to minimize bias and guarantee inferential validity even with unknown sources of variability. Once the experimental conditions were set and the system had equilibrated an injection was made and the pressure and

TABLE I

RANGE OF VARIABLES USED IN EXPERIMENTS

Helium was the carrier gas in all experiments.

Variable	*Range*
Sample size (μl)	1, 3, 4
Initial pressure (kPa)	68.7
Split flow-rate (ml/min)	15, 100, 500
Column flow-rate (ml/min)	1
Injection port temperature (°C)	100, 200, 400
Insert type (78.5 mm length)	2 mm I.D.
	4 mm I.D.
	4 mm I.D. Jenning's cup
Solvent	Hexane, isooctane

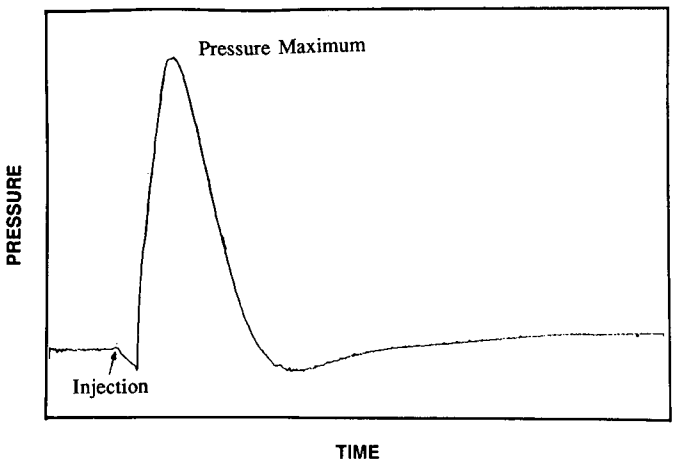

Fig. 1. Characteristic pressure response inside the injection port.

temperature responses were measured and recorded. All of the experimental conditions were replicated. Table I shows the range of experimental conditions that were investigated.

Experimental results

A typical pressure response is shown in Fig. 1. The initial pressure decrease was of the order of 0.7 kPa and was followed by a positive pressure change whose magnitude depended on the experimental conditions. The pressure returned to equilibrium after approximately 1 s from the beginning of injection. The specific effects of each variable on the pressure response are summarized as follows: (a) larger sample injections (Fig. 2), and (b) higher injection port temperatures result in larger pressure pulses (Fig. 3), (c) the lower boiling point solvent also yielded larger pressure pulses

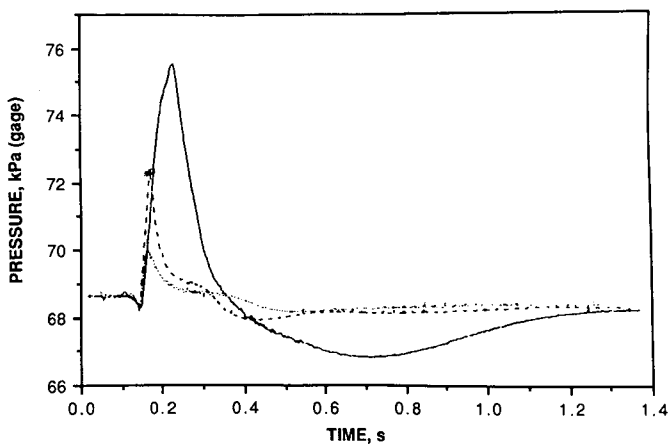

Fig. 2. Effect of sample size on pressure response. Solvent, hexane; wall temperature, 200°C; insert, 4 mm diameter; split flow-rate, 100 ml/min. · · · ·, 1 μl injection; – – –, 3 μl injection; ——, 5 μl injection.

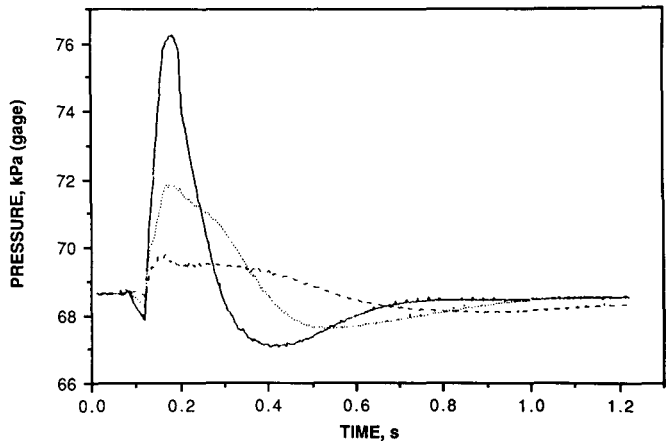

Fig. 3. Effect of wall temperature on pressure response. Solvent, hexane; insert, Jenning's 4 mm; sample size, 3 μl; split flow-rate, 100 ml/min. – – –, 100°C; · · · · ·, 200°C; ——, 400°C.

(Fig. 4), (d) the split flow-rate did not affect the magnitude of the pressure pulse, but it did have a dramatic effect on the rate at which the pressure returned to equilibrium (Fig. 5). At very low flow-rates the system appeared to be overdamped, while at high flow-rates the pressure undershoots the initial pressure significantly, (e) packed and unpacked 4-mm I.D. liners showed no significant differences in pressure response, except when both the flow-rate and the injection size were at their maximum value (Fig. 6). The similarity of the responses indicates that the packing, for these conditions, had very little impact on the vaporization rate. The pressure amplitudes were much larger in the smaller (2-mm) diameter liner because of the reduced system volume.

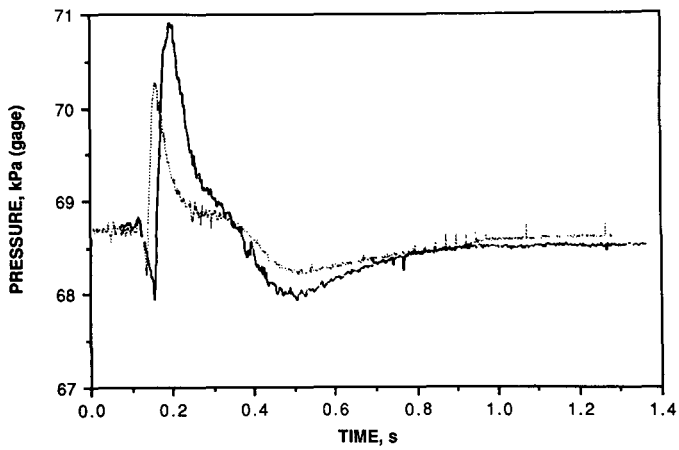

Fig. 4. Effect of solvent on pressure response. Insert, 4 mm diameter; wall temperature, 200°C; sample size, 1 μl; split flow-rate, 100 μl/min. ——, Hexane; · · · · ·, isooctane.

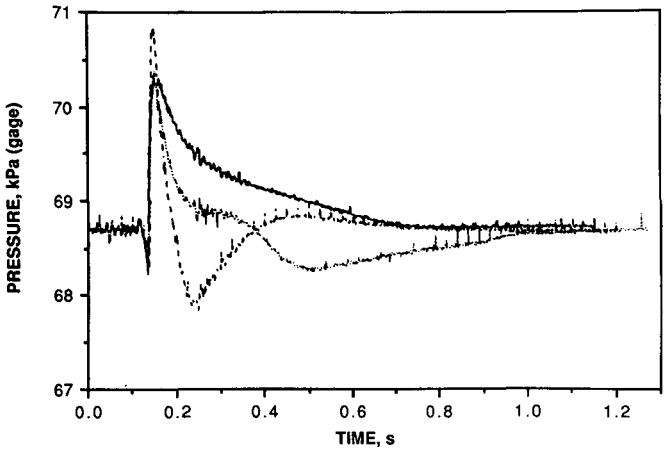

Fig. 5. Effect of split flow-rate on pressure response. Solvent, hexane; insert, 4 mm diameter; sample size, 1 μl; wall temperature, 200°C. ——, 15 ml/min; · · · · ·, 100 ml/min; – – –, 500 ml/min.

THERMODYNAMIC MODEL

Uniform property but time dependent control volume analysis of the injection port was used to model the pressure and temperature responses. For this purpose the injection port, which is represented schematically in Fig. 7, was divided into three control volumes: (a) the insert control volume for which the liquid sample represents a source of mass and a sink of energy due to the vaporization process, (b) the mass flow controller (MFC) control volumes, and (c) the back pressure regulator (BPR) control volume. The first of the three control volumes represents the temperature-controlled insert, while the last two represent the tubing and miscellaneous other volumes

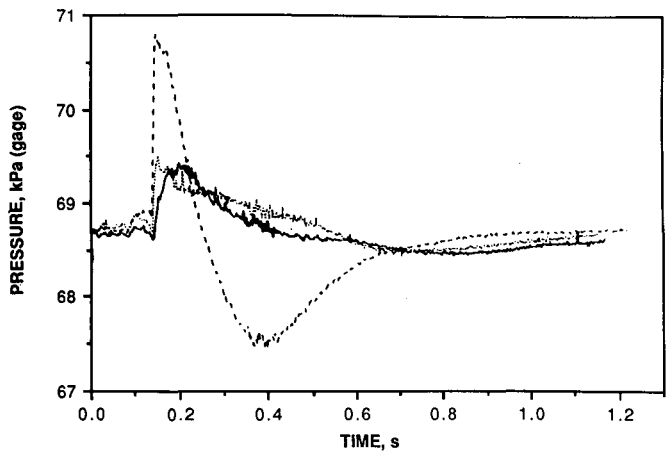

Fig. 6. Effect of different inserts on pressure response. Solvent, hexane; sample size, 1 μl; wall temperature, 100°C; split flow-rate, 100 μl/min. – – –, 2 mm insert; ——, 4 mm insert; ···· Jenning's insert, 4 mm.

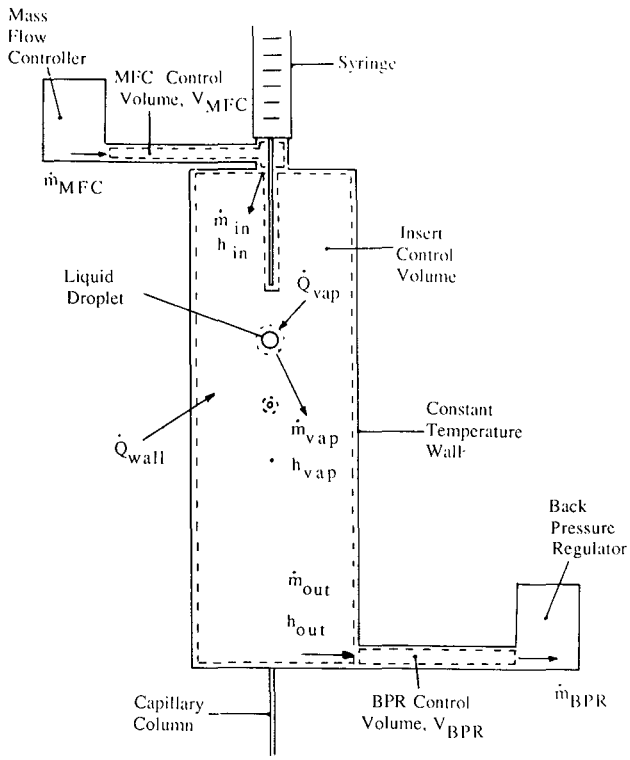

Fig. 7. Schematic representation of split injection port and associated control volumes.

associated with the MFC and BPR, respectively. A mass balance for the insert control volume can be written as follows:

$$\dot{m}_{in} + \dot{m}_{vap} - \dot{m}_{out} = \dot{m}_{cv} \tag{1}$$

where $\dot{m}_{in}$ and $\dot{m}_{out}$ are the mass flow-rates in and out of the insert control volume, respectively, $\dot{m}_{vap}$ is the sample vaporization rate, and $\dot{m}_{cv}$ is the rate of change of mass in the insert control volume. Assuming the carrier gas and sample vapor are homogeneously mixed ideal gases inside the insert volume, V, eqn. 1 can be written as

$$\dot{m}_{cv} = \frac{V}{RT}\frac{dP}{dt} - \frac{PV}{R^2T}\frac{dR}{dt} - \frac{PV}{RT^2}\frac{dT}{dt} \tag{2}$$

where P and T are the uniform insert pressure and temperature, respectively, and R is the instantaneous mixture gas constant. Similar mass balances for the BPR and MFC can be used for evaluating $\dot{m}_{in}$ and $\dot{m}_{out}$, respectively. Substituting the resulting expressions in eqn. 2, and solving for dP/dt yields

$$\frac{dP}{dt} = \frac{\frac{RT}{V}(\dot{m}_{MFC} + \dot{m}_{vap} - \dot{m}_{BPR}) + \frac{P}{T}\frac{dT}{dt} + \frac{P}{R}\frac{dR}{dt}}{\left(1 + \frac{TV_{MFC}}{T_{MFC}t} + \frac{TV_{BPR}}{T_{BPR}V}\right)} \tag{3}$$

where $\dot{m}_{MFC}$, and V_{MFC} are the inlet mass flow-rate and volume of the MFC, and $\dot{m}_{BPR}$, and V_{BPR} are the outlet mass flow-rate and volume of the BPR, respectively. In deriving eqn. 3 it was assumed that the temperatures of the gas in the MFC, T_{MFC}, and BPR, T_{BPR}, are approximately equal to the mean temperature between the insert and the ambient temperatures. This assumption was used for simplicity and does not affect the character of the predicted response by the model, but only has a small effect in the scaling of the pressure and temperature maxima and minima.

Regarding the mass flow-rates in eqn. 3 it is assumed that the mass flow controller behaves ideally, which implies that $\dot{m}_{MFC}$ remains constant regardless of downstream pressure variations. The back pressure regulator is assumed to act as a second order regulator with $\dot{m}_{BPR}$ given by the pressure and time-dependent expression shown in Appendix 1. The sample vaporization rate, $\dot{m}_{vap}$ is modeled assuming that the syringe injector produces a stream of spherical droplets which all have an initial diameter equal to the syringe inside diameter. This assumption is made in the absence of initial droplet size data for samples ejected by the syringe system used and appears to be an adequate idealization in view of the reasonable pressure and temperature responses that were computed. The droplets according to the D^2 law with the vaporization constant computed from quasi-steady theory[20] using the relations shown in Appendix 2. The time derivative of the mixture gas constant R requires knowledge of the carrier gas and sample vapor masses inside the insert volume. These are given by the following relationships:

$$\dot{m}_s = \dot{m}_{vap} - [m_s/(m_s + m_c)]\dot{m}_{out}$$

$$\dot{m}_c = \dot{m}_{in} - [m_s/(m_s + m_c)]\dot{m}_{out} \tag{4}$$

where m_s and m_c are the sample and carrier gas masses in the insert volume, and $\dot{m}_s$ and $\dot{m}_c$ are their time derivatives.

Evaluation of dT/dt in eqn. 3 requires an energy balance on the insert control volume. Using Fig. 7 this can be written as follows:

$$\dot{m}_{in}h_{in} + \dot{m}_{vap}h_{vap} - \dot{Q}_{vap} - \dot{m}_{out}h_{out} + \dot{Q}_{wall} = \dot{E}_{cv} \tag{5}$$

where h_{in} and h_{out} are the enthalpies of the entering carrier gas and exiting mixture, respectively, h_{vap} is the enthalpy of the sample vapor at the temperature of the control volume, $\dot{Q}_{vap}$ is the energy rate required to vaporize the sample, $\dot{Q}_{wall}$ is the rate of energy addition from the liner wall and $\dot{E}_{cv}$ is the rate of energy change in the insert control volume. Heat transfer to the syringe is neglected. For an ideal gas $\dot{E}_{cv} = d(m_{cv}c_vT)/dt$ where c_v is the instantaneous mixture specific heat at constant volume. Substituting this expression into eqn. 5 and solving for dT/dt yields

$$\frac{dT}{dt} = \frac{1}{m_{cv}c_v}(\dot{m}_{in}h_{in} - \dot{m}_{out}h_{out} + \dot{m}_{vap}h_{vap} - \dot{Q}_{vap} + \dot{Q}_{wall}) - \\ + \frac{T}{m_{cv}}\frac{dm_{cv}}{dt} - \frac{T}{c_v}\frac{dc_v}{dt} \quad (6)$$

The heat transfer coefficient, h, from the insert wall can be estimated using the Nusselt number for fully developed flow in an isothermal tube, $hD/k = 3.66$, where k is the temperature-dependent thermal conductivity of the gas mixture. However, the value of the resulting heat transfer coefficient was too small to provide good correlation with the peak pressure experimental values. A value of 5 h was empirically found to yield better agreement with the experimental results and was used for all calculations. This can be justified because some sample droplets may impinge on the wall producing better mixing and heat transfer than that predicted by the fully developed laminar flow relation. The pure component enthalpies in eqn. 6 are evaluated using the ideal gas assumption, and h_{out} is the resulting mixture enthalpy. c_v and its derivative are obtained for the mixture in a similar fashion.

RESULTS AND DISCUSSION

The two coupled differential equations, eqns. 3 and 6, together with the previously discussed necessary auxiliary relations were integrated numerically for the experimental conditions tested, using the constants in Table II. Physical properties were obtained from ref. 21. Typical results for the pressure and temperature responses are shown in Figs. 8 and 9, respectively, where they are also compared with experimental data. The evolution of the pressure response to an injection is described below. It appears that the initial pressure decrease was caused by the temperature reduction which occurred as a result of energy transfer from the gas to the sample. As the temperature difference between the liner wall and the gas increased more heat was convected from the wall. This energy, combined with the increased mass from the sample vaporization process caused the pressure in the insert to increase. As the pressure approached its maximum value the response of the back pressure regulator became dominant reducing the pressure in the injection port by increasing $\dot{m}_{out}$ and accounting for the return to equilibrium conditions. The return to equilibrium pressure is the portion of the response where the difference between the experimental data and the model was greatest, indicating that a better model for the back pressure regulator is needed. Comparisons for different operating conditions showed good agreement between computed and measured pressure responses for the initial pressure response with similar difficulties in estimating the response of the back pressure regulator. Regarding the temperature response in Fig. 9, although there is qualitative agreement between computed and measured results, the measured temperatures lag the computed values. The previously mentioned thermal inertia of the thermocouple junction is a probable reason for the lag.

The split ratio is defined as the ratio of split flow (through the back pressure regulator) to column flow. The column flow, Q_c, can be computed assuming

TABLE II

PARAMETER VALUES USED IN CALCULATIONS

Parameter	*Value*
Back pressure regulator control volume (V_{BPR}) (cm^3)	0.7
Mass flow controller control volume (V_{MFC}) (cm^3)	0.7
Initial sample droplet size (D_0) (μm)	150
Length of column (L) (m)	12.5
Column radius (r_c) (mm)	0.25

incompressible, laminar, constant viscosity flow with negligible mass transfer to the column liquid phase

$$\dot{Q}_c = \frac{\pi r_c^4}{8\mu}\frac{dp}{dx} \tag{7}$$

where μ is the viscosity, r_c is the column radius and dp/dx is the constant pressure gradient. Therefore, the split ratio (SR), written in terms of the mass flows is

$$SR = \frac{8\dot{m}_{out}\mu L}{\pi\rho r_c^4(P - P_{atm})} \tag{8}$$

where L is the column length, ρ is the gas density and $(P - P_{atm})$ is the instantaneous difference in pressure between the liner and the surroundings. Fig. 10 shows that the predicted split ratio using eqn. 8 differs significantly from the preset steady-state value.

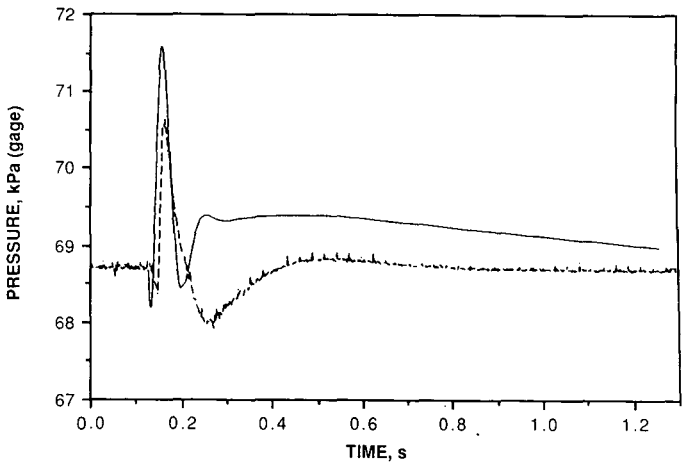

Fig. 8. Predicted (——) *vs.* experimental (– – –) pressure response. Solvent, hexane; sample size, 1 μl; insert, 4 mm diameter; wall temperature, 200°C; split flow-rate, 500 ml/min.

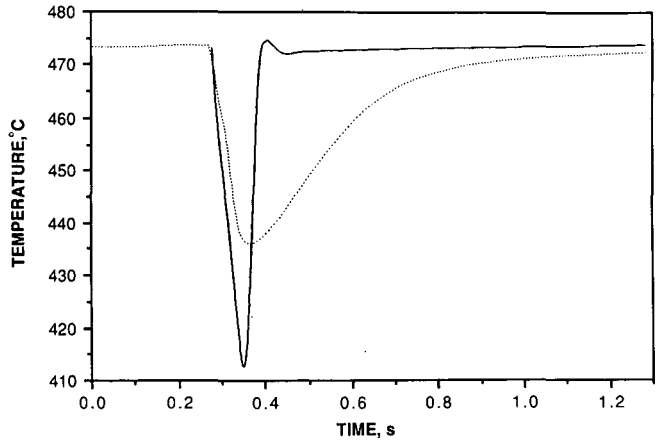

Fig. 9. Predicted (——) *vs.* experimental (· · · · ·) temperature response. Solvent, hexane; sample size, 5 μl; insert, 4 mm diameter; wall temperature, 200°C; split flow-rate, 500 ml/min.

In general, to determine the discrimination or quantitative errors associated with the variable split ratio the mass of each solute at the split point must be known as a function of time. Then integration of the split ratio weighted by the mass distribution at the split point yields the average split ratio for the solute of interest:

$$\overline{\mathrm{SR}} = \frac{1}{\Delta T} \int_0^{\Delta T} m(t)\, \mathrm{SR}(t)\, \mathrm{d}t \tag{9}$$

where ΔT is the time the solute is split, $m(t)$ is the time varying fraction of the total mass of the solute at the split point and $\mathrm{SR}(t)$ is the time varying split ratio. Accurate

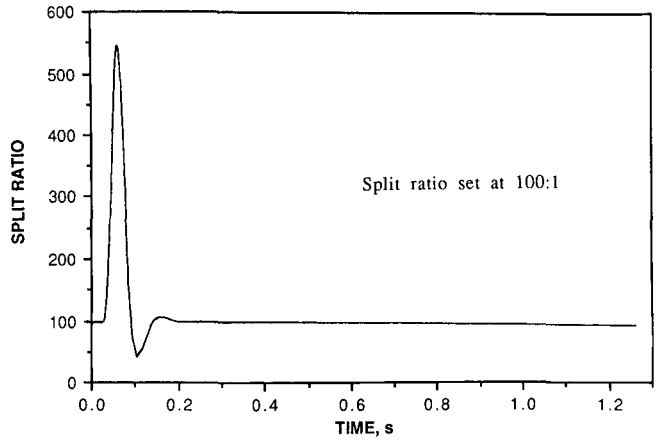

Fig. 10. Predicted split ratio response. Solvent, hexane; sample size, 1 μl; insert, 4 mm diameter; wall temperature, 200°C; split flow-rate, 100 ml/min.

estimation of $m(t)$ requires knowledge of the local vapor concentration within the insert, which is not included in the present model. However, a single component example can be used to illustrate how this model can be used to quantify split ratio errors, using the conditions for the injection depicted in Fig. 10. The hexane vapor fraction at the split point will be assumed to be normally distributed and split completely within 1 s, which is approximately the time required to purge the insert volume twice. Performing the integration indicated in eqn. 9 yields an average split ratio of 106:1 instead of the anticipated 100:1. This 6% error will vary depending on the actual $m(t)$ and $SR(t)$ for a particular injection.

An additional use of the present model is to evaluate alternate injection port designs. For example, alternate flow systems can be studied by substituting appropriate response functions for $\dot{m}_{MFC}$ and $\dot{m}_{BPR}$ in the equations. Different insert geometries can be investigated by varying the volume and heat transfer coefficient of the insert.

CONCLUSIONS

The pressure and temperature changes that occur during injection in a split injection port were measured. The experimental data was then compared to the results of a thermodynamic model which qualitatively predicted all of the important features of the pressure and temperature responses seen in the experimental data. The model was then extended to predict the variations that occur in the split ratio.

Coupling the model with a simulation of the time varying solute distribution in the insert would allow the average split ratio of each solute to be predicted. Future work to extend and improve the model should include a better response model for the back pressure regulator, improved sample vaporization modeling to handle realistic sample mixtures and a better simulation of the column flow.

ACKNOWLEDGEMENT

We gratefully acknowledge the scholarship support and the loan of laboratory equipment provided by the Avondale Division of Hewlett-Packard Company in Avondale, PA, U.S.A.

APPENDIX I

Response of the back pressure regulator

The BPR controls the upstream pressure by allowing a variable flow-rate through a nozzle flapper assembly. Masters[22] has shown that the flow response of a BPR is highly non-linear and depends on parameters which were unknown for the BPR employed in the present work. Therefore, the BPR was modeled as a second order regulator with a natural frequency (w_n = 80 radians/s) and a damping coefficient (b = 0.55) determined from experimental measurements. Further, it was assumed that the forcing function disturbing the BPR was the increase in pressure from the evaporation process and that when the pressure began to decrease the forcing function stopped and the BPR responded freely. The forcing function was approximated by a series of impulses each with an amplitude equal to a constant multiplied by the

pressure difference between the actual and set pressure. The volumetric flow response, Flow(t), of this second order regulator to an impulse of amplitude A was therefore expressed as:

$$\text{Flow}(t) = Aw_n/(1 - b^2) \exp(-bw_n t) \sin[w_n(1 - b^2)t] \tag{A1}$$

where t is the time. The total mass flow-rate out of the BPR is the initial mass flow-rate plus the gas density multiplied by the sum of the dynamic responses. Therefore

$$\dot{m}_{BPR} = \dot{m}_{in} + \rho\Sigma[\text{Flow}(t)] \tag{A2}$$

APPENDIX II

Droplet vaporization rate

The mass vaporization rate of a droplet can be related to the diameter change by

$$\dot{m}_{drop} = -\frac{\pi}{4}\rho_l D \frac{dD^2}{dt} \tag{A3}$$

where ρ_l and D are the liquid density and diameter of the droplet, respectively. Using the D^2 evaporation law [20]

$$D^2 = D_0^2 - e_{vap}t \tag{A4}$$

where D_0 is the initial sample droplet size, results in

$$\frac{dD^2}{dt} = -e_{vap} \tag{A5}$$

where e_{vap} is the vaporization constant. For small droplets in a hot ambient gas ref. 20 gives the following relation for e_{vap}

$$e_{vap} = \frac{8\rho_g\alpha_g}{\rho}\ln(B + 1) \tag{A6}$$

where ρ_g and α_g are the density and thermal diffusivity of the gas and B is defined as

$$B = c_P(T - T_S)/L = (-Y_\infty + Y_{FS})/(1 - Y_{FS}) \tag{A7}$$

where c_p is the gas specific heat at constant pressure, T_S is the saturation temperature of the sample vapor, L is the latent heat of vaporization of the droplet, Y_{FS} is the mass fraction of sample vapor at the droplet surface and Y_∞ is the sample vapor mass fraction far away from the droplet. In the present case Y_∞ was set to zero and the Clausius–Clapeyron equation was used to relate Y_{FS} and T_S

$$Y_{FS} = \frac{M_S}{M_M} \exp\left[\frac{LM_S}{R}\left(\frac{1}{T_B} - \frac{1}{T_S}\right)\right] \tag{A8}$$

where M_S is the molecular weight of the sample, M_M is the molecular weight of the mixture, T_B is the boiling point of the sample, and L is its latent heat of vaporization. By substituting eqn. A8 into eqn. A7, T_S can be found using any iterative method. Substituting this value of T_S into eqn. A7 yields the value of B from which e_{vap} and $\dot{m}_{drop}$ can be calculated. The total vaporization rate, $\dot{m}_{vap}$, is given by summing up the vaporization rate of all droplets present.

REFERENCES

1 K. Grob and S. Rennhard, *J. High Resolut. Chromatogr. Chromatogr. Commun.*, 3 (1980) 627.
2 G. Schomburg, H. Husmann and R. Rittmann, *J. Chromatogr.*, 204 (1981) 85.
3 K. Grob and K. Grob, Jr., *J. Chromatogr.*, 151 (1978) 311.
4 K. Grob, Jr., in R. E. Kaiser (Editor), *Capillary Chromatography, Fourth International Symposium, Hindelang, 1981*, Institute of Chromatography, Bad Dürkheim, 1981, p. 185.
5 G. Schomburg, in R. E. Kaiser (Editor), *Capillary Chromatography, Fourth International Symposium, Hindelang, 1981*, Institute of Chromatography, Bad Dürkheim, 1981, p. 371.
6 K. Grob, Jr. and H. P. Neukan, *J. High Resolut. Chromatogr. Chromatogr. Commun.*, 2 (1978) 15.
7 F. Poy, S. Visani and F. Terrosi, *J. Chromatogr.*, 217 (1981) 81.
8 D. W. Grant and A. Clarke, *J. Chromatogr.*, 97 (1974) 115.
9 F. Munari and S. Trestianu, in R. E. Kaiser (Editor), *Capillary Chromatography, Fourth International Symposium, Hindelang, 1981*, Institute of Chromatography, Bad Dürkheim, 1981, p. 849.
10 H. Brudereck, W. Schneider and I. Halasz, *J. Gas Chromatogr.*, 5 (1967) 217.
11 K. Grob, Jr. and H. P. Neukom, *J. High Resolut. Chromatogr. Chromatogr. Commun.*, 2 (1979) 563.
12 G. Schomburg, H. Behlau, R. Dielmann, F. Weeke and H. Husmann, *J. Chromatogr.*, 142 (1972) 87.
13 A. L. German and E. C. Horning, *Anal. Lett.*, 5 (1972) 619.
14 C. Watanabe, H. Tomita and N. Sato, in R. E. Kaiser (Editor), *Capillary Chromatography, Fourth International Symposium, Hindelang, 1981*, Institute of Chromatography, Bad Dürkheim, 1981, p. 499.
15 M. J. Hartigan and L. S. Ettre, *J. Chromatogr.*, 119 (1976) 187.
16 L. S. Ettre, *Introduction to Open Tubular Columns*, Perkin-Elmer, Norwalk, CT, 1979.
17 J. Eyem, *J. Chromatogr.*, 217 (1981) 99.
18 G. White, *Instrument Notes*, Statham Labs., Los Angeles, CA, 1949, p. 7.
19 A. Kaufman, *Masters Thesis*, Rutgers University, Piscataway, NJ, 1987.
20 M. Kanury, *Introduction to Combustion Phenomenon*, Gordon and Breach, New York, 1975.
21 R. Reid and T. Sherwood, *Properties of Gases and Vapors*, McGraw-Hill, New York, 1966.
22 C. A. Masters, *Dynamic Characteristics of a Restrictor Compensated Nozzle/Flapper Pressure Transducer*, Department of Chemical Engineering, Northwestern University, Evanston, IL, 1974.

Journal of Chromatography, 454 (1988) 37–50
Elsevier Science Publishers B.V., Amsterdam — Printed in The Netherlands

CHROM. 20 787

CORRELATIONS BETWEEN OCTANOL–WATER PARTITION COEFFICIENTS AND REVERSED-PHASE HIGH-PERFORMANCE LIQUID CHROMATOGRAPHY CAPACITY FACTORS

CHLOROBIPHENYLS AND ALKYLBENZENES

PAUL M. SHERBLOM* and ROBERT P. EGANHOUSE*

Environmental Sciences Program, University of Massachusetts at Boston, Harbor Campus, Boston, MA 02125-3393 (U.S.A.)

(First received March 15th, 1988; revised manuscript received June 15th, 1988)

SUMMARY

The capacity factors (k'_φ) of 4 chlorobiphenyls and 39 alkylbenzenes (C_1–C_{10}) were determined using reversed-phase high-performance liquid chromatography at eight different mobile phase compositions (φ = 50–90% acetonitrile in water). The predicted capacity factors in water (log k'_0) were determined by linear regression of log k'_φ and the acetonitrile concentration. Comparison of log k'_0 data from two solvent systems (acetonitrile–water, methanol–water) with published data indicates that this parameter is dependent on both the mobile phase and the chromatographic system used in determining log k'_φ.

The determined log k'_0 values and *n*-octanol–water partition coefficients (log P_{oct}) taken from the literature were analyzed by linear regression. Log P_{oct} estimates made from separate regressions using the individual and combined compound classes are presented and compared. The slopes of the lines for the two compound classes were similar, but each had distinctly different intercepts. Log P_{oct} estimates resulting from the individual compound class regressions agreed more closely with published data than did estimates derived by combining the two classes during regression. It is recommended that separate regressions be developed for each compound class of interest.

Log P_{oct} estimates for the alkylbenzenes were also made using fragment constants. The fragment constants were compared with structural group factors derived from the log k'_0 based estimates. It is noted that the substitution pattern of the benzene ring affects these group factors.

INTRODUCTION

Reversed-phase high-performance liquid chromatography (RP-HPLC) has been used to estimate *n*-octanol–water partition coefficients (log P_{oct}), and recent

* Present address: Southern California Coastal Water Research Project, 646 W. Pacific Coast Highway, Long Beach, CA 90806, U.S.A.

0021-9673/88/$03.50

reviews have discussed the merits of this method[1–4]. RP-HPLC avoids many of the potential problems associated with the traditional shake flask method for direct determination of log P_{oct}. More important, it allows the estimation of log P_{oct} values (*i.e.*, log $P_{oct} > 6$) whose direct measurement is difficult because of analytical limitations[1–4].

In this study RP-HPLC was used to estimate log P_{oct} for a variety of alkylbenzenes and selected chlorobiphenyls. Log P_{oct} values for several short chain alkylbenzenes have been determined directly[5–8] or estimated by RP-HPLC[9–13]. We wanted to extend this database in order to enhance our understanding of their environmental distributions.

The RP-HPLC estimation method is based on the linear regression of a compound's log P_{oct} and the logarithm of its RP-HPLC aqueous capacity factor (log k'_0). Others have reported good correlations using pooled data for several classes of compounds in this regression[6,9,12,14,15]. We had originally intended to extend the log P_{oct} range beyond that of the short chain alkylbenzenes for which data are available by using selected polychlorophenyls (PCBs). The latter were chosen because they span a wide range of log P_{oct} values and are relatively well characterized[16]. Recently however, Opperhuizen *et al.*[17] suggested that each compound class yields a distinct relationship between log k'_0 and log P_{oct}. Thus, greater estimation errors could result if the data are combined during linear regression. In this paper we verify this increase in estimation error by presenting log P_{oct} – log k'_0 correlations for alkylbenzenes and PCBs using both acetonitrile and methanol mobile phases. The resulting correlation lines are compared with relationships developed using published log k'_0 values[13,17].

Log P_{oct} estimates made using the acetonitrile log k'_0 data, as well as estimates made using the fragment constants of Hansch and Leo[5] (as discussed by Lyman[18]) are presented and compared with each other and available literature data.

MATERIALS AND METHODS

Chemicals

The alkylbenzenes used in this study were obtained from Aldrich Chemical, Supelco, Alfa/Morton Thiokol, Alltech Assoc. and the American Petroleum Institute. The PCBs were from Ultra Scientific. All analytes were of the highest purity available (95 to 99+%) and purity was verified by high-resolution gas chromatography prior to use. Double distilled deionized water, filtered through a 0.45-μm membrane filter (Nylon 66, Supelco), and HPLC-grade methanol or acetonitrile (J. T. Baker) were sparged with helium before use.

Apparatus

A Perkin-Elmer (PE) Series 400 liquid chromatograph and a PE LC-15B UV (254 nm) detector were used. The chromatograph was equipped with a Rheodyne 7125 injector, a 20-μl loop, and a 125 mm × 4.6 mm PE HS-5-C_{18} (5 μm silica based octadecyl) column, operated at a flow-rate of 1.5 ml/min.

Void volumes were determined using two approaches: (1) injections of a sodium nitrate solution and (2) linearization of data for an alkylbenzene homologue series. It has been suggested that the latter procedure gives a more reliable estimate of the void volume[17,19,20]. The column's solvent volume was also determined via differential

weighing[19,21] with methanol and dichloromethane as solvents. This volume is the maximum void volume ($V_{0,max}$) since it includes mobile phase in the solvation layer of the stationary phase[19,21].

Two linearization methods were used: (1) the procedure recommended by Berendsen *et al.*[19], and (2) two versions of a procedure recommended by Van Tulder *et al.*[20]. These linearization methods have been applied to the *n*-alkylbenzene series[17,19,20], and will be briefly described below. For a more thorough discussion the reader is referred to the original references[19,20]. Compounds for which retention data were available included benzene and the *n*-alkylbenzenes from toluene to *n*-pentadecylbenzene (excluding *n*-pentylbenzene and *n*-heptylbenzene). Retention times for the latter two compounds were estimated by linear interpolation of the retention times of *n*-butyl-, *n*-hexyl- and *n*-octylbenzene. To estimate the error associated with these interpolations we also interpolated values for *n*-propyl- and *n*-nonylbenzene. The interpolated retention times for these compounds exceeded the actual retention times by 0.61% and 2.67% respectively. The second linearization procedure presented by Van Tulder *et al.*[20] allowed the use of only the even numbered *n*-alkylbenzenes. Thus, these results are not dependent on interpolation.

Both linearization methods utilize the retention times of consecutive homologues n and $n+1$. The procedure of Berendsen *et al.*[19] uses linear regression of the equation

$$t_{R,n+1} = At_{R,n} - (A - 1)t_0 \tag{1}$$

Where $t_{R,n}$ and $t_{R,n+1}$ are the retention times of homologues n and $n+1$ respectively, A is a constant and t_0 is the void time.

The procedure of Van Tulder *et al.*[20] is based on the equation

$$\ln(t_{R,n} - t_0) = b^0(z^0 + n) + c \tag{2}$$

Where n is the number of additional carbons, z^0 is the number of carbons in the basic group (in this case benzene), and b^0 and c are constants. The sequence number of the homologue is i such that $i = 1,2,\ldots, N$ ($N = 16$ homologues). This then leads to derivation of the following equations:

$$\ln(t_{R,i+1} - t_{R,i}) = b^0 i + c'' \tag{3}$$

where c'' is an operational constant, and

$$t_{R,i} = t_0 + pq^i \tag{4}$$

with $q = e^{b^0}$. Linear regression of $\ln(t_{R,i+1} - t_{R,i})$ against i (eqn. 3) gives b^0 as the slope. This is then used to derive q^i which is regressed against $t_{R,i}$ (eqn. 4). The intercept of eqn. 4 yields t_0. The second linearization procedure discussed by Van Tulder *et al.* is a variation which allows the use of non-consecutive homologues as long as they are equally spaced. For example, in our work only the even numbered *n*-alkylbenzenes were used, with i being replaced by j such that $j = 2i$. Retention times are converted to retention volumes via multiplication by the flow-rate.

RESULTS AND DISCUSSION

Determination of the void volume

The capacity factor (k'_φ) at each concentration (φ) of organic modifier is dependent on the retention volumes of the solute and of an unretained compound:

$$k'_\varphi = (V_{R,\varphi} - V_{0,\varphi})/V_{0,\varphi} \quad (5)$$

where k'_φ = capacity factor, $V_{R,\varphi}$ = retention volume of the solute, $V_{0,\varphi}$ = retention volume of an unretained compound. Because of the importance of the void volume ($V_{0,\varphi}$) in determining k'_φ, we utilized and compared several methods for estimating this parameter. These methods were described briefly above. The resulting estimates of $V_{0,\varphi}$ are shown in Table I. Differential weighing indicated $V_{0,max}$ to be 1.88 ml.

The retention volumes of sodium nitrate generally decreased with increasing water content for both mobile phases. The retention volume at 90% methanol is anomalous (low) compared to the rest of the sodium nitrate data. However, multiple determinations under these conditions agreed within 0.02 ml.

The linearization methods gave inconsistent results. With the acetonitrile–water mobile phase, linearization of the data yielded void volumes that had no apparent relationship with φ. In the methanol–water mobile phase the linearization methods both produced relationships between φ and V_0. The resulting values however, differed from one another and were inversely related to those determined using sodium nitrate.

TABLE I

COMPARISON OF ESTIMATED VOID VOLUMES, V_0

$V_{0,max}$ was determined to be 1.88 ml via differential weighing, see text for details.

Mobile phase composition	$NaNO_3$ *(ml)*	*Linearization methods*								
		Van Tulder et al.[20]						*Berendsen et al.*[19]		
		V_0 *(i=1) (ml)*	R^2	*n*	V_0 *(i=2) (ml)*	R^2	*n*	V_0 *(ml)*	R^2	*n*
Acetonitrile–water										
90:10	1.35	1.56	0.9999	14	1.56	0.9999	8	1.66	0.9999	15
85:15	1.35	1.49	0.9997	14	1.52	0.9998	8	2.15	0.9999	15
80:20	1.28	1.34	0.9997	14	1.43	0.9997	8	1.93	0.9999	15
75:25	1.26	1.51	0.9999	13	1.53	1.000	8	1.90	0.9999	14
70:30	1.26	1.66	0.9999	9	1.83	0.9999	6	1.73	0.9976	10
65:35	1.23	0.97	0.9991	7	1.79	1.000	5	0.61	0.9888	8
60:40	1.22	1.06	0.9998	8	4.17	0.9956	5	0.39	0.9946	9
50:50	1.19	1.93	0.9999	5	–	–		2.11	0.9998	4
Methanol–water										
90:10	1.32	1.07	0.9989	4	–	–		1.20	0.9891	3
85:15	1.40	1.15	0.9988	4	–	–		1.30	0.9910	3
80:20	1.38	1.18	0.9987	4	–	–		1.34	0.9875	3
75:25	1.35	1.28	0.9991	4	–	–		1.50	0.9940	3
70:30	1.35	1.33	0.9992	4	–	–		1.60	0.9941	3

In RP-HPLC the alkyl chains of the stationary phase are solvated to some extent by the organic modifier[21,22]. The extent of this solvation is dependent on both the solvent strength of the modifier and the composition of the mobile phase (*i.e.* water content). Thus, at the same mobile phase composition, acetonitrile will associate with the stationary phase to a greater extent than methanol[21]. Changing the organic modifier concentration in the mobile phase will alter the amount of modifier available to partition into the stationary phase. This change may affect the degree to which water is associated with the stationary phase, since it has been shown with acetonitrile, that the amount of associated water decreases as the bulk mobile phase water content increases[22]. A decrease in the concentration of organic modifier associated with the stationary phase could increase the self-association of the (C_{18}) alkyl chains. Mobile phase access to pore spaces in the particles may be restricted if these are blocked by the collapsed alkyl chains. This would result in a shorter retention time for an unretained component (*i.e.*, smaller $V_{0,\varphi}$) given a constant flow-rate.

Except for the anomalous point for 90% methanol, the trends of the sodium nitrate V_0 data fit the processes just discussed, and are similar to those found by McCormick and Karger[21] for ^2H_2O with mobile phases of the same composition. The differences between the sodium nitrate determined void volumes in the two mobile phases is hard to explain in terms of the processes discussed above, however the difference between the hydrophobicity of these two modifiers may affect the relative amount of water associated with the stationary phase, and thus be reflected in the void volume determinations. The results obtained by linearization of the data, as previously noted, were inconsistent, and both linearization procedures gave V_0 values greater than $V_{0,max}$ at one or more acetonitrile concentrations. Therefore, we chose to utilize the V_0 values derived using sodium nitrate in our determination of k'_φ.

Determining log k'_0 from log k_φ

The capacity factor in water (log k'_0), of each compound was estimated from the capacity factors (log k'_φ) at each modifier concentration φ(φ = 90% methanol was not used) using least squares linear regression of the equation:

$$\log k_\varphi = b(\varphi) + \log k'_0 \tag{6}$$

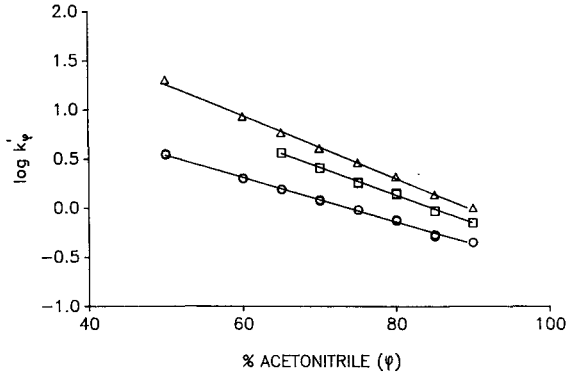

Fig. 1. Log k'_φ–φ relationships for benzene (○), biphenyl (□), and *n*-butylbenzene (△) at φ = 50–90% acetonitrile.

TABLE II

DIRECTLY DETERMINED LOG P_{oct} VALUES AND ESTIMATED AQUEOUS CAPACITY FACTORS (LOG k'_0) OF THE ALKYLBENZENES AND CHLOROBIPHENYLS WHICH WERE USED IN THE REGRESSION ANALYSIS

Compound	*Log P_{oct} values**	*Ref.*	*Log k'_0 values*			
			Acetonitrile (this report)	*Methanol*		
				This report	*Ref. 17*	*Ref. 13***
Alkylbenzenes						
Benzene	2.13, 2.15, 2.15	5	1.649	2.019	0.993	2.389
Toluene	2.65, 2.65, 2.69, 2.73	5,6,8	1.936	2.559	1.536	3.027
Ethylbenzene	3.13, 3.13, 3.15	5,6,8	2.200	3.066	2.093	3.535
n-Propylbenzene	3.68, 3.69, 3.69, 3.69	5,6,8	2.533	3.658	2.655	4.174
n-Butylbenzene	4.26, 4.28, 4.29	5,6,8	2.846		3.212	4.760
Chlorobiphenyls						
Biphenyl	3.76, 3.89, 4.09	16	2.389	3.231	2.121	4.278
4-Monochlorobiphenyl	4.49, 4.61	16	2.738	4.078	2.947	
2,4,6-Trichlorobiphenyl	5.47	16	3.190	4.875	4.110	
2,2′,4,5,5′-Pentachlorobiphenyl	5.92, 6.11, 6.50	16	3.703	5.873	4.861	
2,2′,4,4′,5,5′-Hexachlorobiphenyl	6.72, 6.90	16	4.040	6.537	5.480	

* Repetitions of log P_{oct} values were considered independent when they had different original sources.

** Transformed from ln k'_0 to log k'_0.

Estimation of log k'_0 by eqn. 6 has two potential sources of error. The first possibility is that the relationship could be non-linear. Work by Karger *et al.*[23] investigating the relationship between φ and log k_φ for alcohols, resulted in the suggestion[9] that eqn. 6 is valid only for acetonitrile concentrations below 50%. However, we found linearity over the range of 50 to 90% as demonstrated in Fig. 1 for benzene, *n*-butylbenzene, and biphenyl in acetonitrile. The squared correlation coefficient (the coefficient of determination, R^2) for all regressions using eqn. 6 with an acetonitrile mobile phase was 0.997 or greater. Consequently, we used the linear model to determine log k'_0. It is possible that the relationship is non-linear below 50% and that our extrapolated value for log k'_0 is not, in fact, the capacity factor in water. This will be discussed further below. We report the coefficient of determination rather than the correlation coefficient (r) because R^2 better measures the strength of the linear relationship between the two variables[24].

The second potential source of error to estimates of log k'_0 is interaction of the organic modifier with water or the stationary phase. Log k'_0 values derived using eqn. 6 for both acetonitrile and methanol mobile phases are shown in Table II. We found that the log k'_0 values were dependent on the mobile phase used to determine log k'_φ (and hence log k'_0). This effect has been reported before[25,26] and was suggested to result from differences in the modifier's ability to hydrogen bond with water[25], or to interact with the stationary phase[26]. The difference in the log k'_0 values we determined using acetonitrile and methanol mobile phases (Table II, log k'_0 columns 1 and 2, respectively) lead us to conclude that these log k'_0 values are not the capacity factors in water. Whether this results solely from a mobile phase interaction, or interaction and non-linearity is uncertain.

The direct measurement of log k'_0 would be impractical for most of these compounds. Since the data fit the linear model so well, we felt we could use these estimates in the correlation with log P_{oct} without pursuing the source of these differences further.

Correlation of log k'_0 and log P_{oct}

Log P_{oct} data for the alkylbenzenes were collected from the literature[5–8]. Values for the PCBs were taken from a recent compilation by Shiu and Mackay[16]. All literature values used in the regression equations were determined by either shake flask or generator column methods and are listed in Table II. The literature data for log P_{oct} and the experimentally determined log k'_0 values were fit to the equation:

$$\log P_{oct} = b \log k'_0 + a \tag{7}$$

using a geometric mean linear regression[27]. This is the appropriate regression model when measurement error is associated with both variates (log P_{oct} and log k'_0). A regression was developed for benzene and the *n*-alkylbenzenes from toluene to *n*-butylbenzene because of the quantity of log P_{oct} data available for these compounds. The value of *n*-hexylbenzene (5.52) fell outside the 95% confidence intervals[28] of this line. Since this log P_{oct} value is in the range where direct determination becomes difficult, *n*-hexylbenzene was not added to the regression. Separate regressions were performed for the alkylbenzenes and the PCBs to allow comparison of the slopes and intercepts of the lines for these two compound classes. The derived regression lines for the log P_{oct} – log k'_0 relationships are listed in Table III.

TABLE III

REGRESSION EQUATIONS FOR THE LOG P_{oct} – LOG k'_0 CORRELATIONS

Mobile phase	*Compound*	*n*	*Regression equation*	R^2
Methanol	*Alkylbenzenes*			
	This report	14	Log P_{oct} = 0.937 ± 0.045 log k'_0 + 0.265	0.999
	Opperhuizen[17]	17	Log P_{oct} = 0.947 ± 0.038 log k'_0 + 1.198	0.998
	Harnisch[13]*	17	Log P_{oct} = 0.895 ± 0.030 log k'_0 − 0.020	0.998
	Polychlorobiphenyls			
	This report	11	Log P_{oct} = 0.886 ± 0.135 log k'_0 + 1.012	0.979
	Opperhuizen[17]	11	Log P_{oct} = 0.859 ± 0.129 log k'_0 + 2.042	0.980
Acetonitrile (this report)	Alkylbenzenes	17	Log P_{oct} = 1.759 ± 0.050 log k'_0 −0.744	0.999
	PCBs	11	Log P_{oct} = 1.757 ± 0.263 log k'_0 −0.278	0.980
	Combined	28	Log P_{oct} = 1.987 ± 0.133 log k'_0 −1.159	0.979

* Data transformed from ln k'_0 to log k'_0.

Selected log P_{oct} – log k'_0 relationships are plotted in Figs. 2 and 3. The lines in Fig. 2 are for log k'_0 values from methanol–water mobile phase systems, with data from this work and that reported by Opperhuizen *et al.*[17] and Harnisch *et al.*[13]. Fig. 3 compares the log P_{oct} – log k'_0 relationships we developed using methanol–water and acetonitrile–water mobile phases to estimate log k'_0.

Initial inspection of the lines in Fig. 2 suggests that the slopes of the alkylbenzene and PCB lines are similar, but that the intercepts vary. Comparison of the lines in Fig. 2 and Table III indicate that the intercepts depend on both the chromatographic system used and the compound class investigated. Braumann[1] showed that when a methanol–water mobile phase and six different *n*-alkyl-bonded stationary phases were used the log k_φ – φ relationship for benzene exhibited similar slopes, but different intercepts. Since this intercept is usually taken to represent log k'_0, this would explain the dependence of the log P_{oct} – log k'_0 relationship on the chromatographic system.

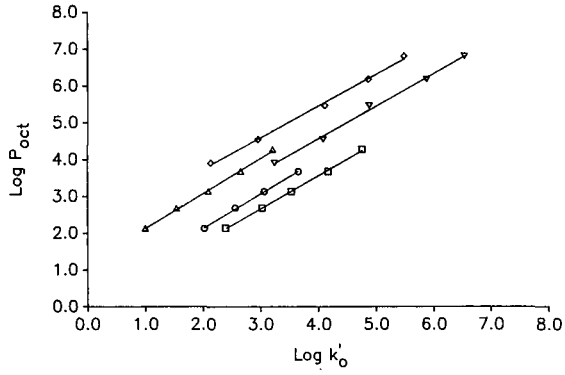

Fig. 2. Comparison of the log P_{oct} – log k'_0 relationships developed using a methanol–water mobile phase to estimate log k'_0. Alkylbenzenes: (○) this report; (△) ref. 17; (□) ref. 13. PCBs: (▽) this report; (◇) ref. 17.

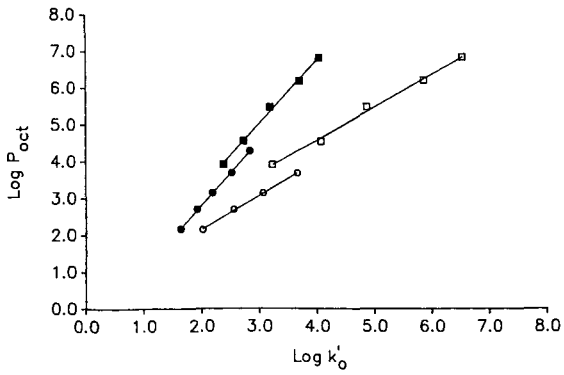

Fig. 3. Comparison of the log P_{oct} – log k'_0 relationships developed for our alkylbenzene and PCB data from the methanol–water (open symbols) and the acetonitrile–water (closed symbols) mobile phases. (○,●) Alkylbenzenes; (□,■) PCBs.

The slopes of our alkylbenzene and PCB regression lines within each organic modifier were tested for parallelism using a non-parametric procedure[29]. We also compared the slopes of our alkylbenzene log P_{oct} – log k'_0 correlation in methanol to those generated by regressing the log k'_0 data of Opperhuizen *et al.*[17] and Harnisch *et al.*[13] against the literature log P_{oct} values. We found no significant differences between the alkylbenzene and PCB slopes ($\alpha = 0.061$) for either mobile phase. Undoubtedly the variance of the PCB log P_{oct} values obscures the apparent difference in these slopes in the methanol mobile phase. The slope of our alkylbenzene line for the methanol–water system was not significantly different from the slope derived using the data of Opperhuizen *et al.*[17] ($\alpha = 0.016$). The slope resulting from the log k'_0 data of Harnisch *et al.*[13] failed the test for parallelism with both our methanol–water alkylbenzene line and that developed using the data of Opperhuizen *et al.*[17]. This may result from error associated with our transformation of their data from the natural logarithm to the base ten logarithm, or it may be from some other cause.

Estimated log P_{oct} values, comparison with the literature

Log P_{oct} estimates for benzene and 39 alkylbenzenes as well as biphenyl and 4 chlorobiphenyls were obtained using the separate acetonitrile log P_{oct} *vs.* log k'_0 regression lines. These estimates are shown in Table IV (estimate 1). Our *n*-alkylbenzene log P_{oct} estimates are in good agreement with the available literature data. There are some differences evident for the substituted benzenes, and these will be discussed below. However, our estimates for these compounds are similar to the RP-HPLC estimates of Hammers *et al.*[9] and Harnisch *et al.*[13].

Also shown in Table IV are the log P_{oct} estimates resulting from the regression line derived by combining the alkylbenzene and PCB data in the acetonitrile–water system (estimate 2). These estimates are usually higher for the alkylbenzenes and lower for the PCBs than the estimates determined from the individual compound class regressions. The combined regression estimate also usually deviates further from the available directly measured literature log P_{oct} values.

The log P_{oct} estimates made using the fragment constant approach[5,18] are also shown in Table IV. Beyond benzene these estimates were determined using our

TABLE IV

LOG k'_0 DATA, ESTIMATED LOG P_{oct} VALUES AND LITERATURE DATA FOR THE TEST COMPOUNDS

Compound	*Log* k'_0	*Log* P_{oct} *estimates**			*Literature values (ref.)***
		1	*2*	*Fragment constants*[5] *(pred. base compound)*	
Alkylbenzenes					
Benzene	1.649	2.16	2.12	2.13	2.20 (9), 2.13, 2.23 (13)
Toluene	1.936	2.66	2.69	2.82 (benzene)	2.78 (9), 2.65, 2.77 (13)
Ethylbenzene	2.200	3.13	3.21	3.20 (toluene)	3.26 (9), 3.17, 3.30 (13)
1,2-Dimethylbenzene	2.271	3.25	3.35	3.32 (toluene)	3.12 (5), 3.13 (6,8), 3.19 (9)
1,3-Dimethylbenzene	2.317	3.33	3.45	3.32 (toluene)	3.20 (5,8), 3.29 (9)
1,4-Dimethylbenzene	2.333	3.36	3.48	3.32 (toluene)	3.15 (5), 3.18 (6,8), 3.28 (9)
n-Propylbenzene	2.533	3.71	3.88	3.67 (ethyl)	3.90 (9), 3.69, 3.84 (13)
(1-Methylethyl)benzene	2.633	3.89	4.07	3.54 (ethyl)	3.66 (5)
1,2,3-Trimethylbenzene	2.526	3.70	3.86	3.91 (1,2-dimethyl	3.55 (5), 3.66 (9)
1,2,4-Trimethylbenzene	2.596	3.82	4.00	3.91 (1,2-dimethyl)	3.78 (9)
1-Ethyl-2-methylbenzene	2.571	3.78	3.95	3.79 (ethyl)	3.53 (8)
1-Ethyl-3-methylbenzene	2.630	3.88	4.07	3.79 (ethyl)	
1-Ethyl-4-methylbenzene	2.639	3.90	4.09	3.79 (ethyl)	
n-Butylbenzene	2.846	4.26	4.50	4.25 (*n*-propyl)	4.44 (9), 4.21, 4.38 (13)
(1,1-Dimethylethyl)benzene	2.840	4.25	4.49	4.19 (ethyl)	4.11 (5)
(1-Methylpropyl)benzene	2.947	4.44	4.70	4.12 (*n*-propyl)	
(2-Methylpropyl)benzene	3.006	4.54	4.82	4.12 (*n*-propyl)	
1-Methyl-2-(1-methylethyl)benzene	2.844	4.26	4.49	4.55 (1-methylethyl)	
1-Methyl-3-(1-methylethyl)benzene	2.912	4.38	4.63	4.55 (1-methylethyl)	
1-Methyl-4-(1-methylethyl)benzene	2.940	4.43	4.68	4.55 (1-methylethyl)	
1,2-Diethylbenzene	2.865	4.30	4.54	4.33 (ethyl)	
1,3-Diethylbenzene	2.947	4.44	4.70	4.33 (ethyl)	
1,4-Diethylbenzene	2.954	4.45	4.71	4.33 (ethyl)	
1-Methyl-2-propylbenzene	2.913	4.38	4.63	4.37 (*n*-propyl)	
1-Methyl-3-propylbenzene	3.000	4.53	4.80	4.37 (*n*-propyl)	
1-Methyl-4-propylbenzene	3.013	4.56	4.83	4.37 (*n*-propyl)	
1-Ethyl-2,3-dimethylbenzene	2.820	4.22	4.45	4.45 (ethyl)	
1-Ethyl-2,4-dimethylbenzene	2.895	4.35	4.59	4.45 (ethyl)	

1-Ethyl-3,5-dimethylbenzene	2.939	4.43	4.68	4.45 (ethyl)	
2-Ethyl-1,3-dimethylbenzene	2.794	4.17	4.39	4.45 (ethyl)	
2-Ethyl-1,4-dimethylbenzene	2.874	4.31	4.55	4.45 (ethyl)	
4-Ethyl-1,2-dimethylbenzene	2.913	4.38	4.63	4.45 (ethyl)	
1,2,3,4-Tetramethylbenzene	2.864	4.30	4.53	4.36 (1,2,3-trimethyl)	4.11 (9)
1,2,3,5-Tetramethylbenzene	2.842	4.26	4.49	4.36 (1,2,3-trimethyl)	4.17 (9)
1,2,4,5-Tetramethylbenzene	2.768	4.13	4.34	4.48 (1,2,4-trimethyl)	4.00 (5)
Hexamethylbenzene	3.037	4.60	4.88	5.62 (1,2,3,4-tetramethyl)	4.61 (7), 5.11 (9)
n-Hexylbenzene	3.411	5.26	5.62	5.34 (*n*-butyl)	5.52 (6,8), 5.25, 5.45 (13)
n-Octylbenzene	4.031	6.35	6.85	6.42 (*n*-butyl)	6.29, 6.52 (13)
n-Nonylbenzene	4.306	6.83	7.40	6.96 (*n*-butyl)	
n-Decylbenzene	4.613	7.37	8.01	7.50 (*n*-butyl)	7.33, 7.60 (13)
Polychlorobiphenyls					
Biphenyl	2.389	3.92	3.58		4.04, 3.70, 3.79, 4.10, 3.75 (16), 3.93, 3.78 (13)
4-Monochlorobiphenyl	2.738	4.53	4.27		4.34, 4.40, 4.69 (16)
2,4,6-Trichlorobiphenyl	3.190	5.33	5.17		
2,2',4,5,5'-Pentachlorobiphenyl	3.703	6.23	6.18		6.85, 7.64, 6.15, 6.44, 6.42 (16)
2,2',4,4',5,5'-Hexachlorobiphenyl	4.040	6.82	6.85		7.44, 6.93 (16)

* Estimate 1 results from the correlations of the individual compound classes, estimate 2 results from combining the compound classes in the regression analysis.

** See also Table II, refs. 5–8 are directly determined, others are RP-HPLC estimates.

estimate 1 as the basic fragment. These estimates also seem good for the short chain *n*-alkylbenzenes, and not as good for the poly-substituted benzenes.

The deviation of the estimated values of log P_{oct} for the substituted benzenes, relative to the directly determined values is intriguing. The magnitude of this deviation may be affected by the substitution pattern of the ring. Our RP-HPLC estimates and those using the fragment constants exceed the directly measured log P_{oct} values for most of the multi-substituted benzenes. Rapaport and Eisenreich[15] reported a similar but opposite effect for the PCBs they studied. They found the RP-HPLC method underestimated the log P_{oct} values of PCBs having chlorines *ortho* to the phenyl bridge. They proposed a correction factor which when applied to the RP-HPLC estimate brought the value in line with those measured directly. Currently the database of directly determined alkylbenzene log P_{oct} values is insufficient to permit the estimation of similar factors for the substituted benzenes. However, we feel that this matter should be investigated more thoroughly, as it may lead to insights into the interaction of the analyte with the stationary and mobile phases.

If we consider only differences between our RP-HPLC estimates for isomeric structures, trends become more apparent. For example, isomers with *ortho* substitution have log P_{oct} values about 0.1 log units lower than those having *meta* and *para* substitution. The log P_{oct} values of the trisubstituted benzenes seem to differ by this amount for each *ortho* substitution. This pattern, however, is not readily apparent for the tetramethylbenzenes.

The fragment constant method[5] adds a factor to the log P_{oct} value for each

TABLE V

COMPARISON OF GROUP FACTORS FOR LOG P_{oct}, FROM THE FRAGMENT CONSTANT METHOD[5,18] AND DERIVED FROM THE RP-HPLC ESTIMATIONS

	Group being added:			
	Methyl	*Ethyl*	*1-Methylethyl*	*Propyl*
Fragment constants	0.66	1.20	1.61	1.74
RP-HPLC factors				
ortho to:				
Methyl	0.59	1.12	1.60	1.72
Ethyl	0.65	1.17	–	–
Propyl	0.67	–	–	–
1-Methylethyl	0.37	–	–	–
meta to:				
Methyl	0.67	1.22	1.72	1.88
Ethyl	0.76	1.32	–	–
Propyl	0.82	–	–	–
1-Methylethyl	0.49	–	–	–
para to:				
Methyl	0.70	1.24	1.77	1.90
Ethyl	0.77	1.33	–	–
Propyl	0.85	–	–	–
1-Methylethyl	0.54	–	–	–

additional structural fragment added to the molecule. Since our RP-HPLC estimates were used as the basic group for the fragment constant log P_{oct} predictions, direct comparison of these results with the log k'_0 based estimates is useful only in evaluating the group factors added to the basic compounds. In Table V we make this comparison for the disubstituted benzenes. The difference between adding a group at the *ortho* position *versus* the *meta* and *para* positions is evident in this table. This comparison shows that the position of substitution can affect the log P_{oct} value added by a fragment. For example the fragment constants for the addition of a methyl or ethyl group to toluene match the group factor for *meta* substitution, whereas the 1-methylethyl and propyl group additions match *ortho* substitution more closely. Also of interest in this table is the effect of the group already on the ring, an effect is evident for all groups but particularly the 1-methylethyl group. These data suggest that the log P_{oct} value added by a structural group can be dependent on another structural group on the ring.

CONCLUSIONS

Our void volume measurements suggest that the linearization procedures investigated do not always yield a better estimate of the void volume. Both linearization procedures occasionally gave volumes greater than the maximum solvent volume of the column as determined by differential weighing. This leads us to conclude that injection of a sodium nitrate solution gave a more reliable estimate of V_0.

The difference of log k'_0 values for a given compound, in the two mobile phases indicates that the values determined using this method are not the true aqueous capacity factor. When the aqueous capacity factor is desired, it should be determined directly.

Comparison of our log k'_0 results in methanol with literature data suggest that for a given mobile phase the slopes of the log P_{oct} − log k'_0 regression lines are similar, but that the intercepts vary with chromatographic system used. This variability and the dependence on the organic modifier indicates that log k'_0 is not a good hydrophobic parameter by itself, as has been suggested[1], but is strongly correlated with log P_{oct}.

It appears that log P_{oct} − log k'_0 correlations allow us to estimate log P_{oct} of hydrophobic compounds reasonably accurately, however the correlation cannot be extended over different compound classes without some loss in predictive power. This should be of particular concern when using RP-HPLC to estimate log P_{oct} values beyond the calibration range (log $P_{oct} > 4$–6).

The fragment constant method of Hansch and Leo[5] yields log P_{oct} estimates similar to the RP-HPLC estimates. The fragment constant method needs to be adjusted to include ring substitution effects that it does not currently account for.

ACKNOWLEDGEMENTS

We would like to thank J. Teal and A. McElroy for making the UV detector available to us, and E. Gallagher and P. Gschwend for useful discussions. P. Szalay and J. Underwood assisted with preparation of the graphics and manuscript, respectively.

REFERENCES

1 T. Braumann, *J. Chromatogr.*, 373 (1986) 191.
2 H. Terada, *Quant. Struct.-Act. Relat.*, 5 (1986) 81.
3 C. F. Carney, *J. Liq. Chromatogr.*, 8 (1985) 2781.
4 T. L. Hafkenscheid and E. Tomlinson, *Adv. Chromatogr.*, 25 (1986) 1.
5 C. Hansch and A. Leo, *Substituent Constants for Correlation Analysis in Chemistry and Biology*, Wiley, New York, 1979.
6 M. M. Schantz and D. E. Martire, *J. Chromatogr.*, 391 (1987) 35.
7 M. M. Miller, S. Ghodbane, S. P. Wasik, Y. B. Tewari and D. E. Martire, *J. Chem. Eng. Data*, 29 (1984) 184.
8 Y. B. Tewari, M. M. Miller, S. P. Wasik and D. E. Martire, *J. Chem. Eng. Data*, 27 (1982) 451.
9 W. E. Hammers, G. J. Meurs and C. L. de Ligny, *J. Chromatogr.*, 247 (1982) 1.
10 R. M. Smith, *J. Chromatogr.*, 209 (1981) 1.
11 K. Jinno and K. Kawasaki, *Anal. Chim. Acta*, 152 (1983).
12 L. P. Burkhard, D. W. Kuehl and G. D. Veith, *Chemosphere*, 14 (1985) 1551.
13 M. Harnisch, H. J. Möckel and G. Schulze, *J. Chromatogr.*, 282 (1983) 315.
14 Y.-P. Chin, W. J. Weber, Jr. and T. C. Voice, *Water Res.*, 20 (1986) 1443.
15 R. A. Rapaport and S. J. Eisenreich, *Environ. Sci. Technol.*, 18 (1984) 163.
16 W. Y. Shiu and D. Mackay, *J. Phys. Chem. Ref. Data*, 15 (1986) 911.
17 A. Opperhuizen, T. L. Sinnige, J. M. D. van der Steen and O. Hutzinger, *J. Chromatogr.*, 388 (1987) 51.
18 W. J. Lyman, in W. J. Lyman, W. F. Reehl and D. H. Rosenblatt (Editors), *Handbook of Chemical Property Estimation Methods: Environmental Behavior of Organic Compounds*, McGraw-Hill, 1981, pp. 1–54.
19 G. E. Berendsen, P. J. Schoenmakers, L. de Galan, G. Vigh, Z. Varga-Puchony and J. Inczédy, *J. Liq. Chromatogr.*, 3 (1980) 1669.
20 P. J. van Tulder, J. P. Franke and R. A. de Zeeuw, *J. High Resolut. Chromatogr. Chromatogr. Commun.*, 10 (1987) 191.
21 R. M. McCormick and B. L. Karger, *Anal. Chem.*, 52 (1980) 2249.
22 D. B. Marshall and W. P. McKenna, *Anal. Chem.*, 56 (1984) 2090.
23 B. L. Karger, J. R. Gant, A. Hartkopf and P. H. Wiener, *J. Chromatogr.*, 128 (1976) 65.
24 D. G. Klienbaum and L. L. Kupper, *Applied Regression Analysis and Other Multivariable Methods*, Duxbury, North Scituate, MA 1978.
25 T. Braumann, G. Weber and L. H. Grimme, *J. Chromatogr.*, 261 (1983) 329.
26 P. J. Schoenmakers, H. A. H. Billiet and L. de Galan, *J. Chromatogr.*, 282 (1983) 107.
27 E. Halfon, *Environ. Sci. Technol.*, 19 (1985) 747.
28 R. R. Sokal and F. J. Rohlf, *Biometry*, W. H. Freeman, San Francisco, CA, 1981.
29 M. Hollander and D. A. Wolfe, *Nonparametric Statistical Methods*, Wiley, New York, 1973.

Journal of Chromatography, 454 (1988) 51–63
Elsevier Science Publishers B.V., Amsterdam — Printed in The Netherlands

CHROM. 20 791

MEASUREMENT OF THE POLARITY OF ALKYL DERIVATIVES OF DIAZAPOLYOXYETHYLENE ETHERS BY GAS CHROMATOGRAPHY

ADAM VOELKEL and JAN SZYMANOWSKI*
Institute of Chemical Technology and Engineering, Technical University of Poznań, Pl. M. Sklodowskiej-Curie 2, 60-965 Poznań (Poland)
and
JÖRG BEGER and HORST RÜSTIG
Mining Academy at Freiberg, Freiberg (G.D.R.)
(Received May 25th, 1988)

SUMMARY

The polarity of alkyl derivatives of diazapolyoxyethylene ethers determined by gas chromatography was investigated. The influence of the structure of isomeric compounds on their polarity is discussed. It was found that the polarity depends on the lengths of the alkyl and polyoxyethylene chains, on the distribution of carbon atoms in alkyl groups linked with the nitrogen and oxygen atoms and the distribution of oxyethylene groups.

INTRODUCTION

The polarities of individual compounds containing one nitrogen atom[1,2] and of α,ω-diamino oligoether derivatives were studied previously[3]. The relationships between different polarity parameters and the increments of the polarity due to characteristic structural fragments were calculated.

The aim of this work was to examine the influence of the structure of alkyl derivatives of diazapolyoxyethylene ethers, which contain two nitrogen atoms bridged by an oligooxyethylene chain or by two methylene groups. The structures of investigated compounds are as follows:

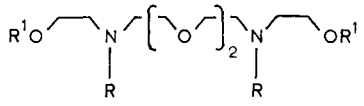

1

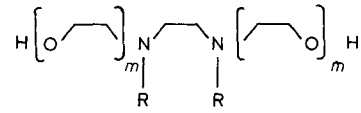

2

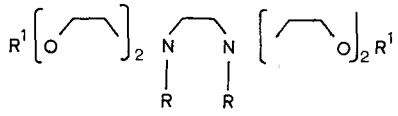

3

0021-9673/88/$03.50

where R and R^1 denote alkyl groups (CH_3–C_8H_{17}) or hydrogen (R^1) and m = 0, 1 or 2.

The polarities of some individual octylaminooligooxyethylene methyl ethers (4) and octylamino N-mono- (5) and N,N-dioligooxyethylene glycols (6):

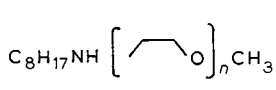

4

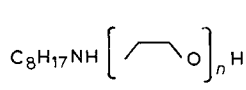

5

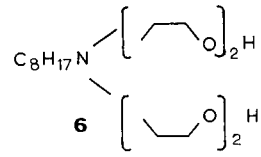

6

where n = 1, 2 or 3, were also determined.

Some of the compounds examined in this work have also been tested as crown ether analogues for the extraction of alkaline earth metals[4] and for mercury(II) chloride extraction[4–6].

EXPERIMENTAL

Eighteen pure model compounds (Table I) were used for polarity measure-

TABLE I

STRUCTURES OF AND PHYSICAL DATA FOR ALKYL DERIVATIVES OF DIAZAPOLYOXYETHYLENE ETHERS AND OF OXYETHYLENE OCTYLAMINES

Compound	*R*	*R'*	*m*	*n*	*B.p. (°C/mmHg)*	n_D^{20}
1a	C_8H_{17}	H	–	–	226–230/0.05	1.4677
1b	C_8H_{17}	CH_3	–	–	210–214/0.01	1.4578
1c	C_4H_9	C_4H_9	–	–	203/0.01	1.4524
1d	CH_3	C_8H_{17}	–	–	214/0.02	1.4548
1e	C_6H_{13}	C_2H_5	–	–	190–198/0.01	1.4533
2a	C_8H_{17}	–	0	–	150–152/0.01	–
2b	C_8H_{17}	–	1	–	196–198/0.01	1.4691
2c	C_8H_{17}	–	2	–	220–224/0.01	1.4701
3a	C_8H_{17}	CH_3	1	–	176–178/0.01	1.4551
3b	C_8H_{17}	CH_3	2	–	205–210/0.01	1.4561
3c	CH_3	C_8H_{17}	2	–	208–210/0.01	1.4560
3d	C_4H_9	C_4H_9	2	–	185–190/0.01	1.4526
4a	–	–	–	1	120/15	1.4342
4b	–	–	–	2	113–115/0.5	1.4395
5a	–	–	–	1	87–88/0.2*	1.4526
5b	–	–	–	2	108/0.05**	1.4538**
5c	–	–	–	3	170–172/0.01***	1.4568***
6	–	–	–	2*2	175–177/0.1§	1.4654§

* B.p. 85–87°C/0.09 mmHg[9].
** B.p. 130–135°C/90 Pa; n_D^{20} = 1.4540[10].
*** B.p. 190–195°C/0.06 mmHg; n_D^{20} = 1.4644[9].
§ B.p. 226–232°C/0.03 mmHg; n_D^{20} = 1.4662[9].

ments. They were obtained by treating the required amino alcohol derivatives in the presence of sodium carbonate with 1,8-dichloro-3,6-dioxaoctane for compounds 2b, 2c and 3:

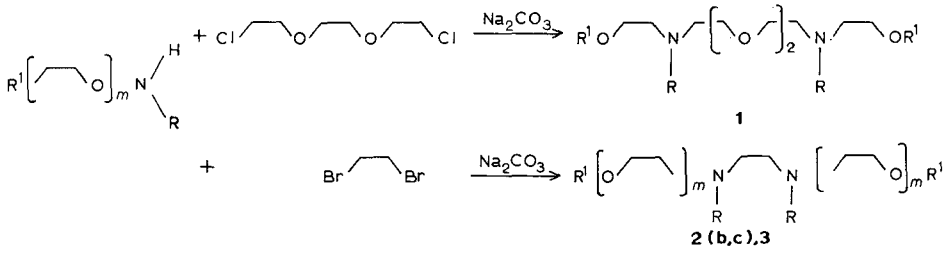

In the same way, 6 was obtained from octylamine and 2-chloroethyl-2-hydroxyethyl ether.

Compounds 4 and 5 were prepared according to known methods by reaction of the appropriate 2-chloroethyl ethers or 2-chloroethyl alcohols with an excess of octylamine:

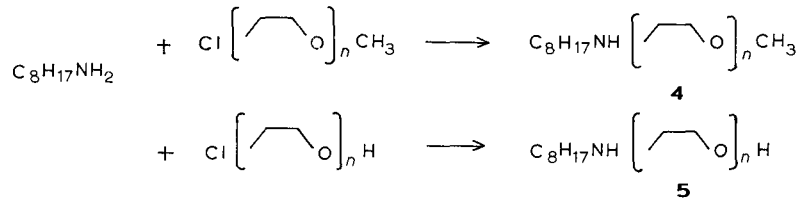

Analogous 2a was obtained by treating 1,2-dibromoethane with an excess of octylamine.

The reaction conditions were as described previously[4–6].

The purities and structures of all the compounds were confirmed by elemental analyses, ^{1}H NMR spectroscopy and gas–liquid and thin-layer chromatography. ^{1}H NMR spectra were recorded on a Tesla BS 487B 80 MHz instrument using [^{2}H]chloroform as solvent and HMDS as the internal standard. The structures and some physical data are given in Table I.

Chromatographic measurements

The conditions of the chromatographic measurements and the parameters used for the characterization of the polarities of the compounds have been reported previously[3].

RESULTS AND DISCUSSION

The values of the polarity parameters are given in Tables II–IV (compound numbering as in Table I). The precision of the determination of the polarity param-

TABLE II

EMPIRICAL POLARITY PARAMETERS

Compound	*Temperature (°C)*	I_R		*PI*		ρ	
		CH_3OH	C_2H_5OH	CH_3OH	C_2H_5OH	CH_3OH	C_2H_5OH
1a	70	700	726	96.4	101.0	2.29	2.84
	90	688	708	94.1	97.8	1.94	2.25
1b	70	716	753	99.4	105.4	2.61	3.53
	90	721	751	99.3	105.2	2.45	3.06
1c	70	710	745	98.1	104.0	2.49	3.32
	90	721	748	100.2	104.7	2.48	3.04
1d	70	605	642	73.2	83.5	1.05	1.43
	90	604	634	72.6	81.4	1.03	1.29
1e	70	729	769	101.3	107.2	2.85	3.87
	90	740	775	103.5	108.7	2.83	3.65
2a	70	619	651	77.2	85.7	1.18	1.55
	90	621	642	77.8	83.8	1.18	1.40
2b	70	688	713	94.0	98.8	2.09	2.57
	90	690	700	94.6	96.4	2.00	2.15
2c	70	709	731	97.7	101.9	2.43	3.21
	90	711	730	98.4	101.8	2.26	2.60
3a	70	683	704	92.2	98.8	2.02	2.53
	90	681	701	91.8	97.4	2.00	2.13
3b	70	709	737	98.4	103.3	2.48	3.13
	90	686	740	93.3	103.1	1.91	2.86
3c	70	703	732	96.9	101.9	2.38	3.02
	90	705	722	97.2	100.3	2.23	2.54
3d	70	631	665	80.8	89.2	1.29	1.72
	90	630	655	80.6	86.8	1.26	1.52
4a	70	698	729	96.1	102.1	2.41	3.29
	90	677	703	94.6	99.2	1.98	2.47
4b	70	714	757	99.0	106.0	2.64	3.78
	90	704	742	97.1	103.7	2.23	2.98
5a	70	710	749	98.5	105.0	2.67	3.74
	90	694	742	95.5	104.1	2.15	3.15
5b	70	749	800	106.0	112.4	3.94	5.12
	90	744	799	102.7	111.7	3.86	4.93
5c	70	803	838	112.5	116.9	5.03	6.66
	90	797	829	111.8	115.9	4.12	5.02
6	70	778	823	109.1	115.3	4.16	6.01
	90	771	809	106.7	111.8	3.99	5.83

eters is good and similar to that reported in earlier studies[2,7,8]. The relationships between polarity parameters are similar to those presented previously[2,7,8].

As previously[2,3,7,8], linear relationships were observed between the examined polarity parameters and the sum of the first five McReynolds constants (Table V). The regression coefficients are not high but are still acceptable. These relationships indicate that the polarity parameters considered adequately describe solute–solvent intermolecular interactions.

The polarities of the investigated compounds depend significantly on their

TABLE III

THERMODYNAMIC POLARITY PARAMETERS

Compound	ΔG_s^m *(OH) (kJ mol*$^{-1}$*)*		ΔG_s^m *(C=O) (kJ mol*$^{-1}$*)*	
	CH_3OH	C_2H_5OH	*2-Butanone*	*2-Pentanone*
1a	−10.9	−9.2	−9.3	−9.0
1b	−11.2	−9.7	−9.7	−9.3
1c	−11.3	−9.7	−9.2	−8.9
1d	−9.9	−8.4	−8.2	−7.8
1e	−11.9	−10.4	−9.5	−9.0
2a	−10.0	−8.2	−7.5	−7.2
2b	−10.7	−9.0	−8.9	−8.6
2c	−10.7	−9.2	−8.9	−8.6
3a	−9.8	−8.3	−8.0	−7.7
3b	−11.1	−9.5	−8.9	−8.6
3c	−11.4	−9.7	−8.8	−8.5
3d	−9.7	−8.2	−8.4	−8.1
4a	−11.0	−9.9	−9.2	−9.0
4b	−11.4	−10.1	−9.5	−9.1
5a	−11.3	−9.8	−9.5	−9.2
5b	−12.1	−11.0	−9.7	−9.4
5c	−12.6	−11.1	−10.1	−9.7
6	−12.0	−11.0	−9.7	−9.3

TABLE IV

THE SUM OF THE FIRST FIVE McREYNOLDS CONSTANTS AND THE CONTRIBUTION OF THE SUCCESSIVE TEST SOLUTES TO $\sum_{i=1}^{5} \Delta I_i$

Compound	*Benzene (%)*	*1-Butanol (%)*	*2-Pentanone (%)*	*Pyridine (%)*	*1-Nitropropane (%)*	$\sum_{i=1}^{5} \Delta I_i$
1a	9.4	31.8	15.4	20.6	22.8	1036
1b	9.6	31.6	15.2	18.9	24.6	1194
1c	9.4	33.7	14.6	17.9	24.3	1103
1d	9.5	35.0	14.3	16.9	24.3	732
1e	9.6	32.8	14.9	18.4	24.2	1223
2a	9.4	34.2	14.4	19.5	22.5	775
2b	9.4	33.1	14.2	20.9	22.4	947
2c	8.9	32.7	15.0	21.0	22.2	1084
3a	9.2	37.2	13.1	16.3	24.2	911
3b	9.0	34.1	14.4	18.7	23.8	989
3c	9.0	36.4	13.5	16.6	24.4	945
3d	9.1	34.5	14.6	17.1	24.6	808
4a	8.9	35.1	14.6	17.5	24.2	1091
4b	8.8	35.0	14.7	17.5	24.0	1152
5a	8.8	35.1	14.8	17.4	23.9	1180
5b	9.0	33.7	14.6	20.1	22.6	1316
5c	12.1	31.2	14.7	19.8	22.3	1458
6	9.2	33.5	14.0	16.9	23.4	1355

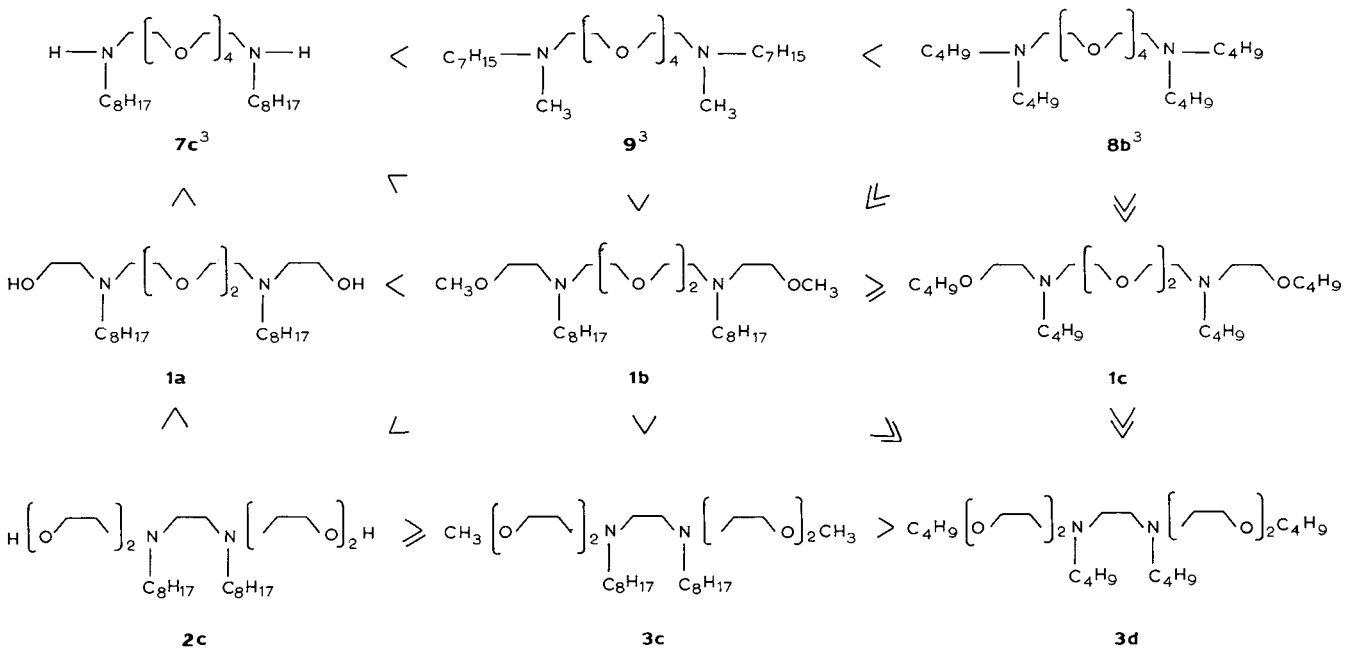

Scheme 1. Polarities of isomeric $C_{26}H_{52}N_2O_2$ and isomeric homologues $C_{28}H_{60}N_2O_4$.

TABLE V

REGRESSION AND CORRELATION COEFFICIENTS FOR THE RELATIONSHIP $PP = a + b \sum_{i=1}^{5} \Delta I_i$

PP	*Solute*	*a*	*b*	*r*
I_R	Methanol	452.1	0.234	0.9071
	Ethanol	463.7	0.255	0.9472
PI	Methanol	45.53	0.0470	0.8725
	Ethanol	56.25	0.0428	0.9165
ρ	Methanol	−2.53	$4.73 \cdot 10^{-3}$	0.8995
	Ethanol	−3.73	$6.66 \cdot 10^{-3}$	0.9186
ΔG_s^m (OH)	Methanol	−7.005	$-3.78 \cdot 10^{-3}$	0.8428
	Ethanol	−4.879	$-4.38 \cdot 10^{-3}$	0.8804
ΔG_s^m (C=O)	2-Butanone	−5.723	$-3.11 \cdot 10^{-3}$	0.8414
	2-Pentanone	−5.518	$-2.99 \cdot 10^{-3}$	0.8260

structures. The compounds examined differ rather in the position and distribution of the alkyl groups than in their length or the length of the oxyethylene chain.

The polarity of compounds 2, 4 and 5 increases as the length of the oxyethylene chains increases. This effect is stronger than that observed previously for compound 7:

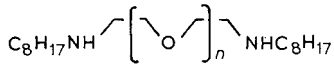

7[3]

7	*n*
a	2
b	3
c	4

but similar (not stronger) to that reported for 8:

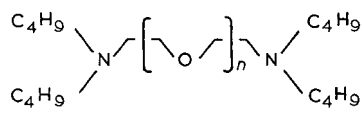

8[3]

8	*n*
a	2
b	4

The sharp polarity increase that is observed for compound 2b may be attributed to the presence of hydroxyethyl groups (absent in 2a).

The important role of the distribution of carbon atoms in both alkyl groups was discussed in recent paper[3]. There it was indicated that compounds having two alkyl groups linked with the nitrogen atom (8) are much more polar than that having one, long alkyl chain linked to each nitrogen atom (7). Different distributions of four oxyethylene units significantly change the polarities of compounds, in the order shown in Scheme 1. It can be seen that the polarity depends significantly on the distribution of oxyethylene groups and alkyl chains in the molecule.

For compounds 7c, 1a and 2c, having heteroatom-bonded protons (=N–H; –O–H) the polarity increases as the oxyethylene groups are shifted from centre of the molecule into terminal positions (left-hand column of Scheme 1). An analogous effect is observed for compounds 7a[3] and 2b:

7a[3] **2b**

Opposite effects are observed for the second and third columns of compounds in Scheme 1 (9, 1b, 3b and 8b, 1c, 3d) having four alkyl substituents. The effect is stronger for compounds having four butyl groups (8b, 1c and 3d) than for compounds having two long and two methyl groups. For α,ω-bisamino oligoethers it was demonstrated that compounds having four short butyl groups exhibit higher polarities[3] (first row in Scheme 1). As a result, compounds 2c and 3b are more polar than 3d. The decrease in the polarity of compounds 1c and 3d is probably caused by the shortening of the oligooxyethylene chain present in the centre of the molecule and by the screening of the terminal oxygens by hydrophobic alkyl groups. As a result, oxyethylene groups linked with nitrogen and butyl groups become less polar or even act rather as non-polar groups. Such a supposition is confirmed by comparison of the polarities of compounds 1b, 1d, 3b and 3c:

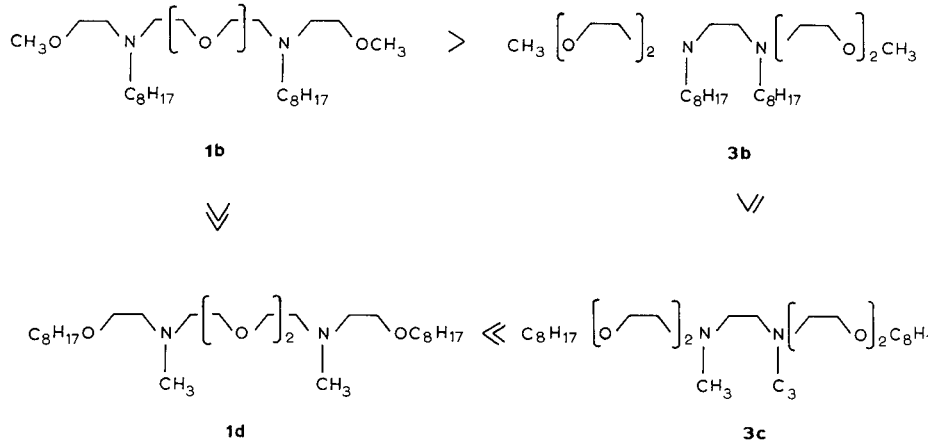

1b **3b**

1d **3c**

The lowest and highest polarities are shown by compounds 1d and 1b, respectively, having two oxyethylene groups in the centre of the molecule and two oxyethylene groups at periphery. The screening of the oxygen atom by the bulky octyl group is so effective that the polar character of this oxyethylene group disappears and compound 1d shows a low polarity. The methyl group is small and its effect is relatively weak. Compounds 3b and 3c are only slightly less polar than 1b but much more polar than 1d. This means that the presence of two oxyethylene groups on each side of the molecule significantly decreases the screening effect of the terminal alkyl groups.

Moreover, the polarities of compounds 3b and 3c, having the bulky octyl group linked with nitrogen and oxygen, respectively, are almost the same. It also means that all compounds with the ethylenediamine structure exhibit only a weak influence of the number of oxyethylene chains and the distribution of alkyl chains in the molecule on their polarity, as shown for compounds 2 and 3.

The effect of the screening of oxygen atoms by alkyl groups is clearly observed when the polarity of compound 1c is compared with those of 8a[3] and 8b[3]:

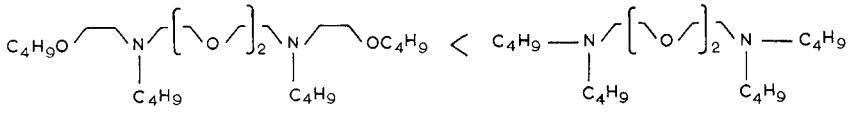

1c **8a[3]**

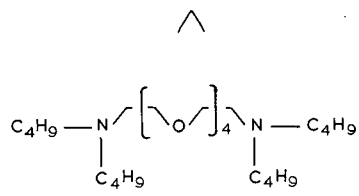

8b[3]

Compound 1c is not only less polar than 8b[3], having four oxyethylene units, but also less polar than 8a[3], having only two oxyethylene groups in the centre of the molecule. This means that the polar character of the oxygen atoms decreases so significantly that the oxyethylene groups linked with the terminal butyls become even non-polar.

Compounds 1a, 1c and 1e are isomers with different distributions of carbon atoms in their alkyl groups while the number and distribution of the oxyethylene groups are the same. Their polarities change in the following order:

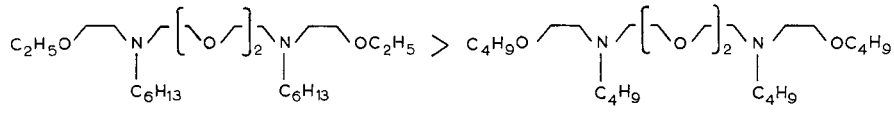

1e **1c**

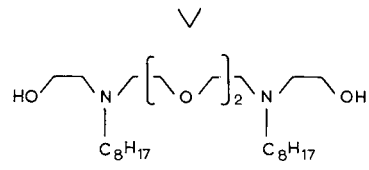

1a

In this instance, compounds having short alkyl groups linked with each nitrogen atom and each terminal oxygen are more polar than compounds having the long alkyl group linked with each nitrogen atom. The conclusion is similar to that reported previously[3], where it was demonstrated that compounds having two short alkyl groups connected with the nitrogen atom are more polar than compounds having

only one long alkyl group. This effect is even more important than the screening of the oxygen atoms by short alkyl groups. However, the polarity decreases as the length of this alkyl groups increases. As a result, compound 1c is less polar than 1e. Similarly, compound 1d is less polar than 1b:

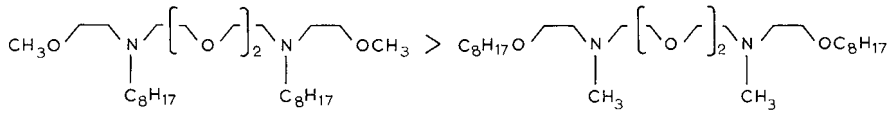

1b **1d**

These last compounds are also less polar than compounds 1a, 1c and 1e as a result of the two additional methylene groups present in their molecules.

The effect of the lengths of the alkyl groups bonded with nitrogen and oxygen atoms can be described quantitatively (Fig. 1) when the differences between the number of carbon atoms in the alkyl groups are taken under consideration; $\Delta n = m - n$ for

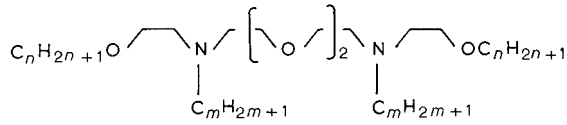

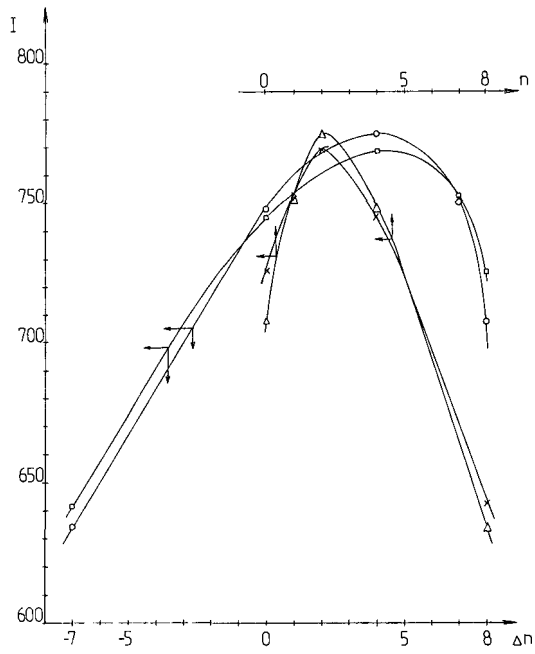

Fig. 1. Influence of the distribution of carbon atoms in alkyl chains on the retention index (I) of ethanol for compounds 1:

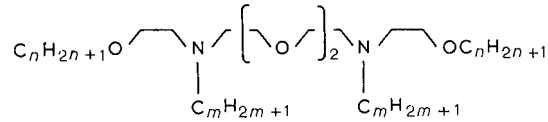

× △ = I *vs.* n; □,○ = I *vs.* Δn; ×,□ = at 70°C; △,○ = at 90°C.

For low and high Δn values low polarity is observed, and the polarity increases as the differences between the numbers of carbon atoms in the alkyl groups decrease. However, the maximal polarity is not obtained for $\Delta n = 0$ but for $\Delta n = 4$. When the relationship between I and n is considered (Fig. 1), where n denotes the number of carbon atoms in the alkyl group bonded with the oxygen atom, the maximal polarity is observed for $n = 2$. This means that the polarity increases as the alkyl chain length increases only up to ethyl. A further increase in the alkyl chain length results in a decrease in polarity.

However, the influence of the lengths of alkyl groups linked to oxygen and nitrogen atoms should be examined in detail for the different types of compounds, and this problem will be investigated in the future.

The screening effect of the small methyl group is weak and almost negligible. As a result, compounds having free hydroxyl groups exhibit a polarity similar to that observed for compounds having terminal methyl groups, *i.e.*, the polarities of compounds 2b and 2c are similar to those of 3a and 3b. The limited decrease in polarity for compound 1a may be attributed to the internal hydrogen bonding, which is much weaker for compounds 2b and 2c:

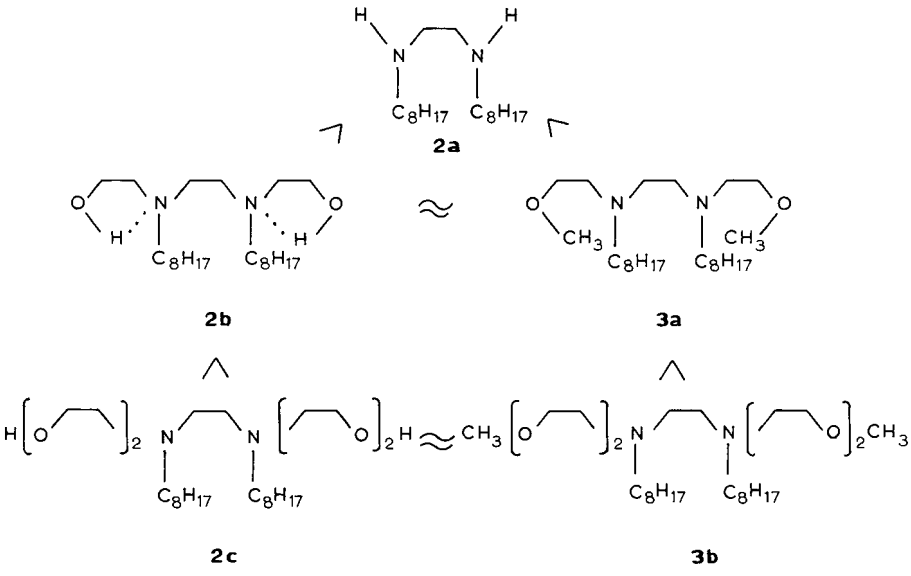

Hence the effects of methoxy and hydroxyl groups on polarity are similar. Similar relationships are observed for compounds 4a and 5a and for 4b and 5b, although the differences in their polarities are larger than those for compounds having two nitrogen atoms.

The effect of different groups and their position in the molecule can be quantitatively measured by means of the "hydrophobe effective length"[3]. As previously, $RNHCH_2(CH_2OCH_2)CH_2NHR$ (compounds 1 in ref. 3) were used as standards. The hydrophobe effective length is equal to the number of carbon atoms in both alkyl groups linked to the nitrogen atoms in a hypothetical standard which exhibits the same polarity as the compound being considered.

TABLE VI

HYDROPHOBE EFFECTIVE LENGTHS

Compound	*Actual number of carbon atoms*	*Hydrophobe effective length*				
		I_R		*PI*		$\Sigma \Delta I_i$
		CH_3OH	C_2H_5OH	CH_3OH	C_2H_5OH	
1a	16	9.6	11.1	10.3	11.4	8.9
1b	18	5.9	5.0	7.0	5.9	−0.2
1c	16	7.3	6.8	8.4	7.7	5.0
1d	18	32	30	36.3	34.1	26.5
1e	16	2.8	1.8	4.9	3.6	−1.9
2a	16	28.7	28.0	31.8	31.2	24.0
2b	16	12.5	14.0	13.0	14.4	14.1
2c	16	7.5	10.0	8.9	10.4	6.1
3a	18	13.6	16.0	15.0	14.4	16.2
3b	18	7.5	8.6	8.1	8.6	11.6
3c	18	8.9	9.8	9.8	10.4	14.2
3d	16	25.9	24.8	27.8	26.7	22.1
4a	18	10.1	10.4	10.7	10.1	5.7
4b	18	6.3	4.1	7.4	5.1	2.2
5a	16	7.3	5.9	8.0	6.4	0.6
5b	16	−1.9	−5.5	−0.4	−3.1	−7.3
5c	16	−14.6	−14.1	−7.6	−8.9	−15.5
6	16	−8.7	−10.7	−3.8	−6.8	−9.6

Much lower values were obtained (Table VI) in comparison with the actual number of carbon atoms which demonstrates the weak effect of short alkyl groups linked with nitrogen and oxygen atoms in comparison with single alkyl groups linked to the nitrogen atoms in the standard. For compounds 5 and 6 even negative values were obtained. Hence the compounds investigated here are much more polar than the compounds $RNHCH_2(CH_2OCH_2)CH_2NHR$ used as standards.

CONCLUSIONS

The polarity of alkyl derivatives of diazapolyoxyethylene ethers depends on the lengths of the alkyl and polyoxyethylene chains, on the distribution of carbon atoms in alkyl groups linked with the nitrogen and oxygen atoms and on the distrtibution of the oxyethylene groups.

Compounds having the same number of carbon atoms are more polar when the atoms are distributed among several alkyl groups. The distribution of oxyethylene groups among different oligooxyethylene chains decreases the polarity as a result of screening of the single oxygen atom by non-polar alkyl groups.

ACKNOWLEDGEMENT

This work was supported by Polish Research Programme CPBP No. 03.08.

REFERENCES

1 J. Szymanowski, A. Voelkel, J. Beger and C. Pöschmann, *Tenside Deterg.*, 20 (1983) 273.
2 A. Voelkel, J. Szymanowski, J. Beger and K. Ebert, *J. Chromatogr.*, 391 (1987) 373.
3 A. Voelkel, J. Szymanowski, J. Beger and H. Rüstig, *J. Chromatogr.*, 448 (1988) 219.
4 K. Gloe, P. Mühl, H. Rüstig and J. Beger, *Solvent Extr. Ion Exch.*, in press.
5 J. Beger, H. Rüstig, K. Gloe and P. Mühl, to be published.
6 H. Rüstig, *Doctoral Thesis*, Mining Academy, Freiberg (1985).
7 A. Voelkel, J. Szymanowski, J. Beger and K. Ebert, *J. Chromatogr.*, 398 (1987) 31.
8 A. Voelkel, J. Szymanowski, J. Beger and K. Ebert, *J. Chromatogr.*, 409 (1987) 29.
9 P. L. Kuo, M. Miki, I. Ikeda and M. Okahara, *J. Am. Oil Chem. Soc.*, 57 (1980) 227.
10 H. Merkwitz, *Doctoral Thesis*, Mining Academy, Freiberg (1985).

Journal of Chromatography, 454 (1988) 65–71
Elsevier Science Publishers B.V., Amsterdam — Printed in The Netherlands

CHROM. 20 802

PROBLEMS WITH THE REPRODUCIBILITY OF RETENTION DATA ON CAPILLARY COLUMNS WITH HYDROCARBON C_{87} AS THE STATIONARY PHASE

E. MATISOVÁ*, A. MORAVCOVÁ and J. KRUPČÍK
Department of Analytical Chemistry, Faculty of Chemical Technology, Slovak Technical University, Radlinského 9, 812 37 Bratislava (Czechoslovakia)
P. ČELLÁR
VURUP, Vlčie hrdlo, 824 17 Bratislava (Czechoslovakia)
and
P. A. LECLERCQ
Laboratory of Instrumental Analysis, Eindhoven University of Technology, 5600 MB Eindhoven (The Netherlands)
(First received March 25th, 1988; revised manuscript received June 3rd, 1988)

SUMMARY

The reproducibility of retention data on hydrocarbon C_{87} stationary phase coated on soda lime glass capillary columns was systematically studied. For mixtures of *n*-alkanes and of alkylbenzenes it was found that the selectivity of the stationary phase is higher and the retention indices of alkylbenzenes and their temperature coefficients are higher compared to those obtained on OV-101. The reproducibility of the column preparation was good, the differences in retention indices measured on several columns being of the order of several decimals of index units. The columns were stable at lower temperatures (100, 120°C) within a certain time interval (14 days). In the course of longer measurements, the stationary phase slowly increases in polarity; a rapid change in polarity was observed at elevated temperatures (180°C).

INTRODUCTION

The largest amount of retention data published for hydrocarbons was obtained on squalane which is generally accepted as the standard non-polar stationary phase[1–3]. Squalane, however, suffers from the obvious disadvantage that,due to its volatility, the temperature limit of its use in glass capillary columns is about 90°C[4,5]. At higher temperatures there is considerable column bleeding. Mixtures of diastereoisomers do not fulfil the demands concerning the purity of the stationary phase and the reproducibility of retention data[6]. Therefore the use of methylsilicones has been advanced as a standard or as one of a set of preferred phases[7,8], as they are almost non-polar and stable at higher temperatures[9]. This choice may also be criticized for several reasons, in respect of the stability and performance[10].

0021-9673/88/$03.50

The requirements of an hydrocarbon for use at high temperature have been considered by Huber and Kováts[11], who deduced that a molecular weight in excess of 1100 would allow an upper limit of 300°C. Riedo *et al.*[10] synthesized the hydrocarbon 24,24-diethyl-19,29-dioctadecylheptatetracontane of formula $C_{87}H_{176}$, and provided a possible solution to the problem of the non-polar standard stationary phase between the temperature limits of 30 to 250°C. The properties of this phase have been described in several papers[10,12–16]. Prolonged use in columns with silanized packing material at 180°C was possible without any significant increase in the phase constants or deterioration of the peak shape[13].

Comparing the Mc Reynolds constants on hydrocarbon C_{87} and on squalane, it was shown that the values for benzene, *n*-butanol, 2-pentanone, 2-nitropropane, pyridine were higher on hydrocarbon C_{87}, the largest differences being found for benzene and pyridine[14].

Some authors have accepted hydrocarbon C_{87} as a standard non-polar stationary liquid, having the commercial name Apolane-87[17]. Its use as well as retention data were reported for packed columns[10,15,16,19–22]. Only a few papers deal with the application of hydrocarbon C_{87} as a stationary phase in support-coated open-tubular (SCOT)[23] and wall-coated open-tubular (WCOT)[24,25] columns. Soják *et al.*[24] used this stationary phase with success; they prepared highly efficient capillary columns with very thin film (SLP) for the separation of isomers of linear pentadecenes and compared the results with those obtained on squalane. The retention indices of *n*-pentadecenes on C_{87} differed from those on squalane by less than ± 2 index units (i.u.). A slight difference has been found between the selectivity of C_{87} hydrocarbon and that of squalane. This selectivity, in combination with an efficient separation system, made it possible to separate *n*-pentadecene isomers more rapidly and more completely. The authors also published the retention indices of C_8 alkylbenzenes which were higher than on squalane (the difference was from 16.3 to 20.9 i.u.), but the reproducibility of retention data and the column stability was not described.

The aim of our work was to use capillary columns with hydrocarbon C_{87} as a standard non-polar stationary liquid for the identification of alkylbenzenes. In the course of long isothermal experiments under routine laboratory conditions, changes in retention data were observed. Therefore a systematic examination of the reproducibility of retention characteristics of alkylbenzenes was undertaken on several glass capillary columns with dynamically or statically coated stationary phases (with various inner surface pretreatments).

EXPERIMENTAL

Capillary columns were made of soda lime glass (Unihost, Teplice, Czechoslovakia. Surface roughening was performed by statically etching the inner surface with gaseous hydrogen chloride at 330°C for 16 h. Two columns were further deactivated with Carbowax 20M[26]. Two silanized columns (with dipentyltetramethyldisilazane) were leached with liquid hydrochloric acid (20%) at 140°C for 15 h[27]. The columns were coated dynamically (15% solutions of hydrocarbon C_{87} in toluene and OV-101 in chloroform) or statically (0.15–0.4% solutions of hydrocarbon C_{87} in pentane) with the stationary phase.

Gas chromatographic (GC) measurements were performed on a Model 2350 gas

chromatograph (Carlo Erba, Milan, Italy) equipped with a flame ionization detector and stream splitter. Glass capillary columns were coated with hydrocarbon C_{87} (I, 200 m × 0.25 mm I.D.; II, 100 m × 0.25 mm I.D., dynamically coated; 30 m × 0.25 mm I.D., statically coated) and OV-101 (278 m × 0.25 mm I.D. dynamically coated). The carrier gas was nitrogen (at a linear velocity of 10 cm/s) or hydrogen (30 cm/s) at 100 and 120°C. The nitrogen used for filament lamps and electrolytic hydrogen were of guaranteed purity of 99.998% and were not specially purified.

Mixed samples were prepared by alkylation reactions of benzene or alkylbenzenes with alkyl halogenides in the presence of aluminium chloride. Samples were injected after dilution in acetone and addition of *n*-alkanes (C_7–C_{14}) with 1- and 10-μl Hamilton syringes. Methane was used for the determination of the gas hold-up time. The elution time was measured with a digital stop-watch Time Calculator RM 4111 (Tesla, Rožnov, Czechoslovakia).

NMR measurements of pure hydrocarbon C_{87} (Supelco, Bellefonte, PA, U.S.A.) and the washed-out phase of the column were performed on a Brooker CXP 300 NMR spectrometer operated at 300 MHz for ^{13}C and ^{1}H spectra.

RESULTS AND DISCUSSION

Hydrocarbon C_{87} stationary phase was chosen to study the retention behaviour of alkylbenzenes with carbon atom numbers from C_7 to C_{15}. Squalane is not suitable for the analysis of alkylbenzenes with carbon atom numbers over 10 for long periods. Standards of higher alkylbenzenes were lacking, therefore mixed samples were prepared. No retention data for alkylbenzenes on hydrocarbon C_{87} were available, so the components were identified by comparison with data on an OV-101 capillary column and by GC–mass spectrometry (MS). In Figs. 1 and 2 chromatograms are shown illustrating the separation of mixtures of *n*-alkanes and products of alkylation of 1,2-dimethylbenzene by ethyl bromide on columns of hydrocarbon C_{87} and OV-101 at 120°C. The composition of the mixture together with the retention indices, I, at 120°C and $I/10$°C are given in Table I. The separation of alkylbenzene isomers was better on hydrocarbon C_{87} (column I; effective plate number, $N_e = 329\,000$; $k = 4.0$) than on OV-101 ($N_e = 395\,720$; $k = 4.4$). Retention indices as well as their temperature coefficients are systematically higher on hydrocarbon C_{87} in comparison with OV-101.

During work at 100 and 120°C over a long period it was observed that the retention indices of alkylbenzenes increased. Retention data (I, k) for alkylbenzenes on two new capillary columns (I, II) of differing film thicknesses (column II gave about capacity factors, *ca.* 50% lower) and their values after 8 months of use of column I are given in Table II.

The retention indices measured on the new columns were approximately the same, independent of the film thickness. The capacity factors on column I decreased within 8 months of use. The percentage degrees in capacity factors for *n*-alkanes and some alkylbenzenes are given in Table III. The largest decrease was observed for the *n*-alkanes (7–8%); for aromatic hydrocarbons the decrease was 1.5–3%, as expected from the increase in polarity. Also the values of the relative retentions, r (Table III), of *n*-alkanes and aromatics differ significantly. For *n*-alkanes the decrease in relative retention, Δr, was 4.5–6.0%, increasing with increasing carbon chain length. For alkylbenzenes, Δr slightly increased. From these results it follows that the polarity of column I has changed.

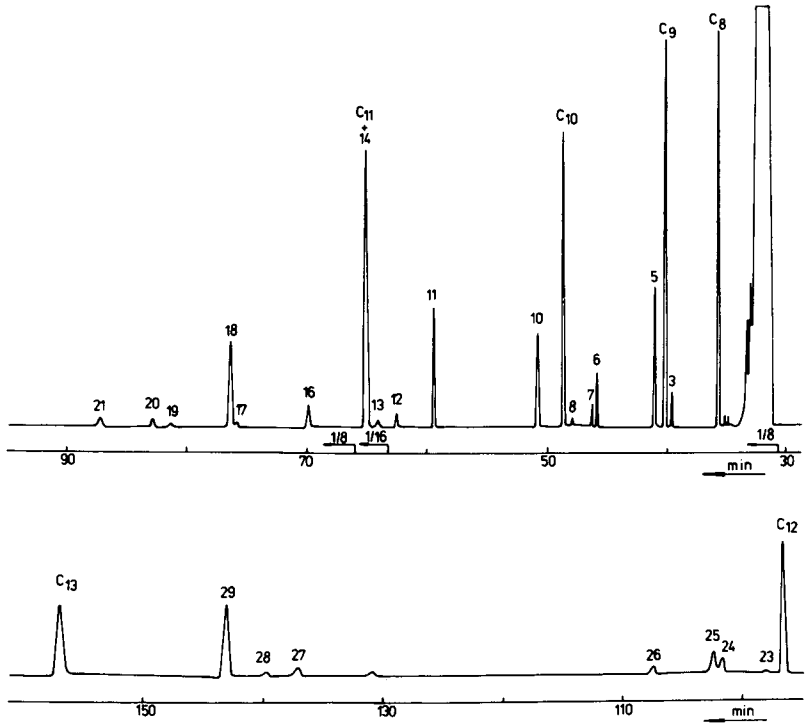

Fig. 1. Chromatogram of the separation of *n*-alkanes and products of alkylation of 1,2-dimethylbenzene by ethyl bromide on an hydrocarbon C_{87} glass capillary column I at 120°C with nitrogen as the carrier gas. For peak designation see Table I.

According to our previous experience of the reproducibility of measurement of retention data on squalane columns (below 90°C) and OV-101 columns under the same experimental conditions (purity of carrier gas, capillary inner wall quality) and the published thermal stability of hydrocarbon C_{87}, chemical changes of this stationary

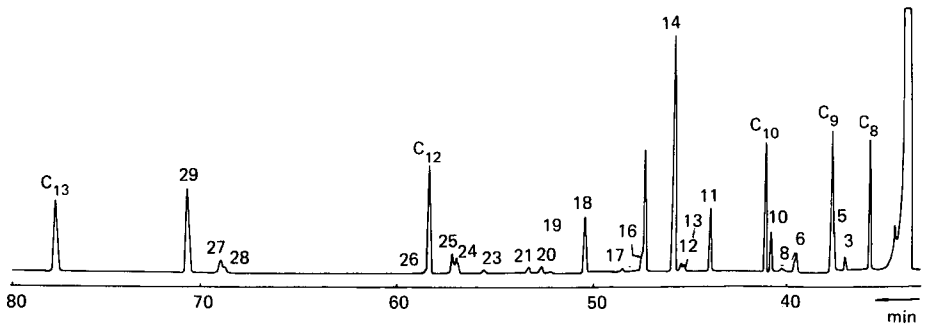

Fig. 2. Chromatogram of the separation of *n*-alkanes and products of alkylation of 1,2-dimethylbenzene by ethyl bromide on an OV-101 glass capillary column at 120°C with hydrogen as the carrier gas. For peak designation see Table I.

TABLE I

RETENTION INDICES, *I*, OF PRODUCTS OF ALKYLATION OF 1,2-DIMETHYLBENZENE BY ETHYL BROMIDE AND THEIR TEMPERATURE COEFFICIENTS, $\Delta I/10°C$, MEASURED ON HYDROCARBON C_{87} AND OV-101 CAPILLARY COLUMNS

Peak No.	*Compound**	*Hydrocarbon C_{87}*		*OV-101*	
		I_{120}	$\Delta I/10°C$	I_{120}	$\Delta I/10°C$
3	1,4-DiMeB	889.7	2.95	870.9	2.50
5	1,2-DiMeB	913.7	3.50	895.0	3.20
6	1-Me3EtB	973.4	3.15	959.6	2.70
7	1-Me4EtB	977.4	3.80	962.2	2.54
8	1-Me2EtB	993.9	4.05	976.4	3.10
10	1,2,4-TriMeB	1017.4	3.65	993.0	3.10
11	1,3-DiMe5EtB	1072.8	3.00	1052.9	2.25
12	1,4-DiMe2EtB	1088.6	3.85	1073.1	2.95
13	1,3-DiMe4EtB	1096.2	4.05	1075.2	3.10
14	1,2-DiMe4EtB	1100.0	4.00	1080.8	3.05
16	1,2-DiMe3EtB	1120.5	4.60	1101.2	3.60
17	1,2,4,5-TetraMeB	1142.1	4.50	1113.2	3.55
18	1,3-DiEt5MeB	1143.5	2.75	1134.0	2.10
19	1,2-DiEt4MeB	1159.4	3.45	1149.7	3.00
20	1,4-DiEt2MeB	1163.8	3.40	1154.9	2.90
21	1,3-DiEt4MeB	1176.5	3.60	1160.2	3.00
23	TriMeEtB	1203.8	3.85	1179.9	3.45
24	TriMeEtB	1211.6	3.80	1190.0	3.30
25	TriMeEtB	1213.2	3.85	1191.6	3.40
26	TriMeEtB	1223.6	4.05	1200.0	3.40
27	DiMeDiEtB	1273.5	3.50	1260.9	3.10
28	DiMeDiEtB	1277.7	3.80	1261.8	2.95
29	DiMeDiEtB	1281.8	3.50	1269.9	3.00

* Abbreviations: Me = methyl, Et = ethyl, B = benzene.

phase under relatively mild conditions (120°C) were not expected. Therefore we have tried to find an explanation for the polarity changes of the stationary phase in columns statically coated with the defined film thickness of SLP. We have considered the influences of column ageing, properties of the inner surface of the capillary wall, film thickness of SLP, carrier gas (nitrogen, hydrogen), temperature of column conditioning.

The reproducibility of retention index measurements on six columns conditioned at 150°C was in the range of several decimals of index units, without regard to the quality of the inner walls (non-deactivated columns; deactivated Carbowax; silanized), film thickness of hydrocarbon C_{87} (0.1–0.25 μm) and nature of the carrier gas (nitrogen hydrogen). The reproducibility on the same columns over 2 weeks was found to be of the order of 0.3 i.u. On the same columns after conditioning at higher temperature (180°C) and on the other four columns directly conditioned at 180°C, the indices measured significantly increased, but on most columns the values of the retention indices were similar to those obtained on column after 8 months used.

For the identification of the eventual chemical changes in the composition of the stationary phase, the NMR spectra of pure hydrocarbon C_{87} and of washed-out

TABLE II

RETENTION INDICES, *I*, AND CAPACITY FACTORS, *k*, OF ALKYLBENZENES MEASURED ON HYDROCARBON C_{87} COLUMNS I, II AT 120°C

*Compound**	*Column I*				*Column II*	
	I	*k*	*I***	*k***	*I*	*k*
1,2-DiMeB	913.7	0.32	924.4	0.32	913.3	0.15
1-Me3EtB	973.4	0.48	982.9	0.47	973.1	0.22
1-Me4EtB	977.4	0.49	986.7	0.48	978.1	0.23
1-Me2EtB	993.9	0.55	1003.6	0.54	993.9	0.26
1,2,4-TriMeB	1017.4	0.64	1027.1	0.63	1017.0	0.30
1,3-DiMe5EtB	1072.8	0.92	1081.6	0.90	1072.4	0.43
1,4-DiMe2EtB	1088.6	1.02	1097.3	1.00	1088.5	0.48
1,2-DiMe4EtB	1100.0	1.10	1109.3	1.08	1100.0	0.52
1,2-DiMe3EtB	1120.5	1.26	1130.4	1.24	1120.3	0.59
1,3-DiEt5MeB	1143.5	1.47	1152.1	1.43	1143.2	0.68
1,2-DiEt4MeB	1159.4	1.63	1168.1	1.59	1158.9	0.76
1,4-DiEt2MeB	1163.8	1.68	1172.6	1.64	1163.5	0.78
1,3-DiEt4MeB	1176.5	1.82	1185.6	1.78	1176.1	0.85
TriMeEtB	1203.8	2.18	1213.3	2.14		
TriMeEtB	1211.6	2.29	1220.9	2.25	1211.1	1.08
TriMeEtB	1213.2	2.32	1222.6	2.27		
TriMeEtB	1223.6	2.48	1233.2	2.43	1223.1	1.16
DiMeDiEtB	1273.5	3.45	1282.8	3.36	1273.0	1.60
DiMeDiEtB	1277.7	3.53	1286.6	3.44	1277.4	1.65
DiMeDiEtB	1281.8	3.63	1291.3	3.55	1281.3	1.69

* Abbreviations as in Table I.

** Values measured on column I after 8 months of use.

TABLE III

CAPACITY FACTORS, *k*, RELATIVE RETENTIONS, *r*, OF *n*-ALKANES AND ALKYLBENZENES MEASURED ON COLUMN I AT 120°C AND THEIR DIFFERENCES, Δk, Δr, AFTER 8 MONTHS OF COLUMN USE

*Compound**	*k*	*r*	*k***	*r***	Δk (%)	Δr (%)
n-C_9	0.29	0.20	0.27	0.19	6.89	−4.50
1-Me4EtB	0.49	0.34	0.48	0.34	2.04	+0.89
n-C_{10}	0.57	0.39	0.53	0.37	7.02	−5.14
1,2,4-TriMeB	0.64	0.44	0.63	0.44	1.56	+0.92
n-C_{11}	1.10	0.75	1.02	0.71	7.27	−5.33
1,3-DiEt5MeB	1.47	1.00	1.43	1.00	2.72	
n-C_{12}	2.13	1.45	1.96	1.37	7.98	−5.59
TriMeEtB	2.29	1.57	2.25	1.57	1.75	+0.06
n-C_{13}	4.09	2.79	3.76	2.62	8.07	−5.92

* Abbreviations as in Table I.

** Values measured on column I after 8 months of use.

stationary phase were compared. Since from one column after the change in SPL polarity it was possible to wash out 3–6 mg of stationary phase, no changes in the composition or structure of the stationary phase were determined by NMR spectroscopy.

CONCLUSIONS

According to the results obtained glass capillary columns made of soda lime glass and containing the stationary phase hydrocarbon C_{87} underwent column ageing. The stationary phase is stable at lower temperatures (100, 120°C) over a certain time interval (14 days). In the course of longer measurements, the stationary phase slowly increases in polarity, or a rapid change in polarity occurs at elevated temperatures (180°C) due to chemical changes in the thin film of the stationary phase. Since no special purification of the carrier gases was employed, this is most probably a result of oxidation caused by the catalytic activity of the glass surface and by trace oxygen impurities in the carrier gas. Under these conditions, however, OV-101 and SE-54 capillary columns are perfectly stable with respect to the reproducibility of retention index measurements.

REFERENCES

1 L. Rohrschneider, *J. Chromatogr.*, 22 (1966) 6.
2 L. Rohrschneider, *Fresenius' Z. Anal. Chem.*, 170 (1959) 256.
3 W. O. McReynolds, *J. Chromatogr. Sci.*, 8 (1970) 685.
4 W. G. Jennings, *Gas Chromatography with Glass Capillary Columns*, Academic Press, New York, 2nd ed., 1980, p. 294.
5 C. F. Chien, M. M. Lopeěni and R. J. Laub, *J. High Resolut. Chromatogr. Chromatogr. Commun.*, 4 (1981) 539.
6 F. Vernon and C. O. E. Ogundipe, *J. Chromatogr.*, 132 (1977) 181.
7 J. J. Leary, J. B. Justice, S. Tsuge, S. R. Lowry and T. L. Isenhour, *J. Chromatogr. Sci.*, 11 (1973) 201.
8 S. Howkes, D. Grossman, A. Hartkopf, T. Isenhour, J. Leary and P. Parcher, *J. Chromatogr. Sci.*, 13 (1975) 115.
9 J. K. Haken, *J. Chromatogr.*, 300 (1984) 1.
10 F. Riedo, D. Fritz, G. Tarján and E. sz. Kováts, *J. Chromatogr.*, 126 (1976) 63.
11 G. A. Huber and E. sz. Kováts, *Anal. Chem.*, 45 (1973) 1155.
12 L. Boksányi and E. sz. Kováts, *J. Chromatogr.*, 126 (1976) 87.
13 J. K. Haken and D. K. M. Ho, *J. Chromatogr.*, 142 (1977) 203.
14 J. K. Haken and F. Vernon, *J. Chromatogr.*, 186 (1979) 89.
15 A. N. Korol, *J. Chromatogr.*, 172 (1979) 77.
16 A. N. Korol and T. I. Dovbush, *J. Chromatogr.*, 209 (1981) 21.
17 *Gas Chromatogr., Newsletter*, 19, No. 4 (1978) 7.
18 J. R. Ashes, S. C. Mills and J. K. Haken, *J. Chromatogr.*, 166 (1978) 391.
19 I. Fisch, I. Olácsi, M. Richter, A. P. Sinka, E. C. Takács, J. M. Takács, J. Vörös and G. Tarján, *J. Chromatogr.*, 148 (1978) 17.
20 L. Egri, L. L. Egri, J. M. Takács and D. C. Kralik, *J. Chromatogr.*, 198 (1980) 85.
21 J. K. Haken and F. Vernon, *J. Chromatogr.*, 361 (1986) 57.
22 W. L. Zielinski, Jr., M. M. Miller, G. Ulma and S. P. Wasik, *Anal. Chem.*, 58 (1986) 2692.
23 J. A. Ballantine, K. Williams and R. J. Morris, *J. Chromatogr.*, 166 (1978) 491.
24 L. Soják, J. Krupčík and J. Janák, *J. Chromatogr.*, 191 (1980) 199.
25 F. Hoffer and J. Takács, *Magy. Kem. Fol.*, 86 (1980) 566.
26 L. Blomberg, *J. Chromatogr.*, 115 (1975) 365.
27 K. Grob, G. Grob, W. Blum and W. Walther, *J. Chromatogr.*, 244 (1982) 197.

Journal of Chromatography, 454 (1988) 73–81
Elsevier Science Publishers B.V., Amsterdam — Printed in The Netherlands

CHROM. 20 785

GAS CHROMATOGRAPHIC RETENTION ON CARBON ADSORBENTS COATED WITH MONOLAYERS OF POLYNUCLEAR AROMATIC HYDROCARBONS*

T. B. GAVRILOVA* and E. V. VLASENKO
Department of Chemistry, Lomonosov State University of Moscow, 119899 Moscow (U.S.S.R.)
and
N. PETSEV, I. TOPALOVA, Chr. DIMITROV and S. IVANOV
Department of Chemistry, Sofia University, 1126 Sofia (Bulgaria)
(Received July 8th, 1988)

SUMMARY

Monolayers of polynuclear aromatic hydrocarbons (PAHs) were used to modify carbon adsorbents (non-graphitized and graphitized thermal carbon blacks). The thermodynamic adsorption characteristics, retention volumes and initial differential heats of adsorption, of molecules belonging to different classes of organic compounds were measured by gas chromatography on these sorbents. The nature of the retention of molecules with different chemical properties on PAH-modified surfaces is determined predominantly by dispersion interaction by competing electrostatic interaction. The effect of PAH modification is the greatest on the retention of oxygen- and nitrogen-containing compounds. Exposure of thermal carbon blacks, modified with monomolecular PAH layers, to an high-frequency low-temperature plasma helps to improve the symmetry of chromatographic peaks.

INTRODUCTION

In order to extend the range of applications of gas–solid chromatography (GSC), homogeneous surface adsorbents are needed. Adsorbent surfaces can be made more homogeneous by a variety of methods, *e.g.*, by application of monomolecular layers of organic molecules[1]. Modification of carbon adsorbent surfaces with monomolecular layers of planar molecules, such as phthalocyanins of metals, 2,4,5,7-tetranitrofluorenal and pyrene and porphyrin derivatives, has demonstrated practically unlimited possibilities of producing adsorbents capable of both weak non-specific and strong specific interactions[2–5].

When non-graphitized thermal carbon black, whose surface is chemically and geometrically heterogeneous[6], is used as a support, the application of monolayers

* Presented at the *6th Danube Symposium on Chromatography, Varna, October 12–17, 1987*. The majority of papers presented at this symposium have been published in *J.Chromatogr.*, Vol. 446 (1988).

0021-9673/88/$03.50

does not always lead to the desired results. The method of sorbent treatment with an high-frequency low-temperature plasma (HLP) helps greatly to improve the surface homogeneity[7,8].

In this work we have modified carbon adsorbents with molecules of various polynuclear aromatic hydrocarbons (PAHs) to study gas chromatographic (GC) retention. Changes in the surface properties of PAH-modified adsorbents exposed to HLP were analysed as well.

EXPERIMENTAL

Geometrically and chemically heterogeneous non-graphitized (TG-10) and graphitized thermal carbon blacks (GTCBs) with specific surface areas of 10 and 8 m^2/g, respectively, were used as adsorbent supports. Planar PAH molecules, *viz.*, anthracene, pyrene, 1,2,5,6-dibenzanthracene and coronene having different electron densities, were used to modify the two adsorbents. The quantity of PAH adsorbed on the carbon black surface from a solution in benzene was calculated from the close packing of Van der Waal's radii of the modifier molecules, distributed over a planar surface, and using GC data[2]. The quantity of modifier was adjusted so as to form a monomolecular layer and was equal to 0.4 mg/m^2 for anthracene and 0.6 mg/m^2 for pyrene, 1,2,5,6-dibenzanthracene and coronene.

The thermal carbon black TG-10, modified with pyrene and 1,2,5,6-dibenzanthracene, was additionally treated with HLP, as reported in ref. 8.

The retention volumes, V_g (per gram of adsorbent), relative retention volumes, $V_{rel} = V/V_{n\text{-}C_6H_{14}}$, and initial differential heats of adsorption, $\bar{q}_1$, at low coverages of different classes of organic compounds. The initial of heats of adsorption were calculated from the slope of the linear dependence $\log V_g = f(1/T)$, where T is the column temperature.

The precision of the $\bar{q}_1$ values was evaluated statistically. The relative error was 0.5–1.0%.

Gas chromatographic measurements were made on a Tsvet-102 chromatograph equipped with a flame ionization detector and glass columns (0.5–1 m × 1–2 mm I.D.). The adsorbent particle size was 0.16–0.2 or 0.25–0.3 mm. Helium was used as the carrier gas (flow-rate 20–30 $cm^3\ min^{-1}$).

RESULTS AND DISCUSSION

The retention volumes of a variety of organic molecules, differing in both geometric and electronic structure, were determinated on all adsorbents studied. A comparative study of the surface properties of adsorbents modified with PAH monolayers was carried out (Table I and Fig. 1). The data in Fig. 1 show that the retention volumes on GTCB with PAH monolayers are lower than in the case of pure GTCB. The greatest decrease in V_g occurs when coronene is used as the modifier. The V_g values of *n*-hydrocarbons on the modified surface are smaller due to the drop in adsorption potential caused by the decrease in the number of surface centres of force. The retention of aromatic hydrocarbons (Table I) on a GTCB surface coated with PAH is, probably, decreased in comparison with GTCB, due to repulsion between the π-electrons of the modified surface and the molecules adsorbed. This is seen most clearly when the relative retention volumes of hydrocarbon pairs with the same num-

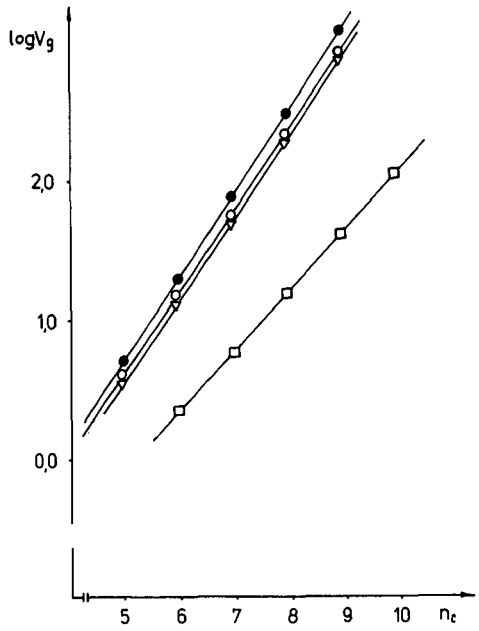

Fig. 1. Dependence of log V_g on the number of carbon atoms, n_c, of *n*-hydrocarbons on GTCB (●) and GTCB modified with monomolecular layers of anthracene (○), pyrene (▽) and coronene (□).

TABLE I

RELATIVE RETENTION VOLUMES, V_{rel} (WITH RESPECT TO *n*-HEXANE) AT 100°C ON UNMODIFIED GTCB AND ON GTCB MODIFIED WITH PAH MONOLAYER

Adsorbate	*Unmodified GTCB*	*GTCB modified with monolayer of*		
		Anthracene	*Pyrene*	*Coronene*
n-Heptane	3.9	3.7	3.6	2.5
Benzene	0.68	0.37	0.53	0.56
Toluene	4.1	1.6	2.4	1.8
p-Xylene	26	7.9	13	5.6
Propyl acetate	0.85	1.3	1.8	1.8
Di-*n*-propyl ester	1.8	–	2.1	2.0
n-Pentanol	0.89	1.3	3.1	1.9
Cyclohexane	0.04	0.45	0.69	0.65
Adamantane	2.4	7.7	8.4	9.0
Pyridazine	2.1	2.9	14	5.1
V_g of *n*-Hexane	20	15	14	2.3
$\frac{V_g \text{ of Toluene}}{V_g \text{ of } n\text{-Heptane}}$	1.0	0.43	0.66	0.69
$\frac{V_g \text{ of } p\text{-Xylene}}{V_g \text{ of } n\text{-Octane}}$	1.8	0.57	0.92	0.82

ber of carbon atoms are compared. For example, toluene and heptane, *p*-xylene and octane. The increase in relative retention volumes of adsorbates whose molecules possess polar functional groups indicates a greater contribution of specific interactions to the total adsorption energy than in the case with unmodified GTCB. There is probably a large increase in the electrostatic interactions involving the π-electron system of the modifying layer with adsorbed molecules whose electron density is localized on their periphery.

Compared with untreated carbon black, the pyrene-modified GTCB shows the most obvious increase in retention values for substances containing polar functional groups. At the same time, the retention values of *n*-alkanes are somewhat reduced (Table I). GTCB with a monomolecular coronene layer, displays the greatest decrease in retention of *n*-alkanes relative to unmodified GTCB, and the increase in the retention of polar compounds is somewhat less than in the case of GTCB with a pyrene monolayer. It is possible that the retention of molecules of different natures is affected, in this case, by competing contributions: a reduction in dispersion forces, on the one hand, and an increase in induction or electrostatic intermolecular interactions on PAH-modified adsorbents (unlike untreated GTCB) on the other hand. A significant reduction of the dispersion component may alleviate the effect of induction and electrostatic interactions.

The coefficients of $\log V_g = a + b_n$ for *n*-alkanes and *n*-alkylbenzenes were calculated for all adsorbents studied. Table II gives the values of *a* and *b* on untreated and PAH-modified carbon adsorbents and, for comparison, on a liquid phase, squalane in gas–liquid chromatography[9]. GTCB and GTCB with a monomolecular anthracene or pyrene layer have almost identical contributions to the adsorption of the methylene group (coefficient *b*) on the adsorbent surface.

Although selectivity in homologous series of normal and aromatic hydrocarbons somewhat decreases when the initial carbon black is modified with PAH, it remains quite high, much higher than on squalane which is one of the most selective liquid phases for non-polar compounds.

When the PAH-modified non-graphitized thermal carbon black TG-10 is used as the adsorbent support, the changes in the retention of molecules belonging to

TABLE II

COEFFICIENTS IN $\log V_g = a + b_n$ AT 100°C FOR THE ADSORPTION OF *n*-ALKANES AND *n*-ALKYLBENZENES ON DIFFERENT ADSORBENTS

Adsorbent	*n-Alkanes*		*n-Alkylbenzenes*	
	a	*b*	*a*	*b*
GTCB	−2.22	0.59	−3.54	0.78
GTCB + anthracene	−2.24	0.57	−3.08	0.64
GTCB + pyrene	−2.26	0.58	−3.09	0.66
GTCB + coronene	−2.10	0.41	−2.68	0.47
TG-10	−2.34	0.65	−3.21	0.78
TG-10 + pyrene	−2.03	0.50	−2.68	0.55
TG-10 + 1,2,5,6-dibenzanthracene	−2.27	0.48	−2.85	0.54
Squalane[9]	−0.35	0.32	−0.52	0.37

TABLE III

RELATIVE RETENTION VOLUMES, V_{rel} (WITH RESPECT TO *n*-HEXANE) AT 100°C ON UNMODIFIED AND MODIFIED THERMAL CARBON BLACK TG-10

Adsorbate	*Untreated TG-10*	*TG-10 treated with monolayer of*			
		Pyrene	*Pyrene and HLP*	*1,2,5,6-dibenz-anthracene*	*1,2,5,6-dibenz-anthracene and HLP*
Toluene	4.2	1.9	1.9	2.0	2.0
Diisopropyl ester	0.69	1.1	1.1	1.1	1.1
Ethyl acetate	0.61	1.1	0.90	0.95	0.92
Methyl ethyl ketone	0.50	0.96	0.67	0.70	0.67
n-Propanol	–	–	0.61	0.61	0.60
V_g of *n*-Hexane	40	9.2	4.6	4.1	3.8

different classes of organic compounds were the same as on GTCB (Tables I–III). When monomolecular PAH layers are applied, the decrease in V_{rel} is more apparent on TG-10 than on GTCB. Suerface modification of TG-10 with PAH seems not only to decrease the adsorption potential, as is the case with GTCB, but also results in the blocking of additional adsorption centres on the TG-10 surface.

Samples of TG-10 with PAH monolayers were exposed to HLP. This treatment caused the retention of molecules of different compounds to decrease somewhat (Table III). The effect of exposure of the PAH-modified TG-10 to HLP is best seen from the shapes of the chromatographic peaks of substances whose molecules have the ability to undergo specific interactions with the adsorbent surface and therefore are sensitive to chemical and geometric heterogeneities of the adsorbent surface. Asymmetry factors measured at one-tenth peak height[10] are shown in Table IV; exposure to HLP causes chromatographic peaks to become more symmetrical.

Greater symmetry of chromatographic peaks, as a result of exposure of the adsorbents investigated to HLP, indicates higher geometric and chemical surface homogeneity. A similar picture was observed earlier[8] for diatomaceous earth coated with 5% squalane and then treated with an argon plasma.

TABLE IV

ASYMMETRY FACTORS[10] OF PEAKS OBTAINED ON UNMODIFIED AND MODIFIED THERMAL CARBON BLACK AT 100°C

Adsorbate	*Untreated TG-10*	*TG-10 modified with monolayer of*			
		Pyrene	*1,2,5,6-dibenz-anthracene*	*Pyrene and HLP*	*1,2,5,6-dibenz-anthracene and HLP*
Adamantane	2.0	1.0	1.0	1.0	1.0
p-Xylene	3.6	1.5	1.0	1.0	1.0
n-Butanol	5.0	2.0	2.0	1.0	1.0
Pyridine	5.0	3.5	2.5	2.0	1.5

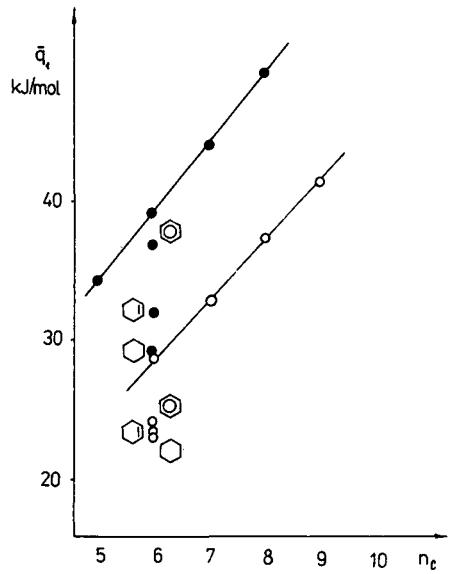

Fig. 2. Dependence of $\bar{q}_1$ on n_c in the adsorption of *n*-alkanes, cyclohexane, cyclohexene and benzene on GTCB (●)[12] and GTCB coated with a monolayer of coronene (○).

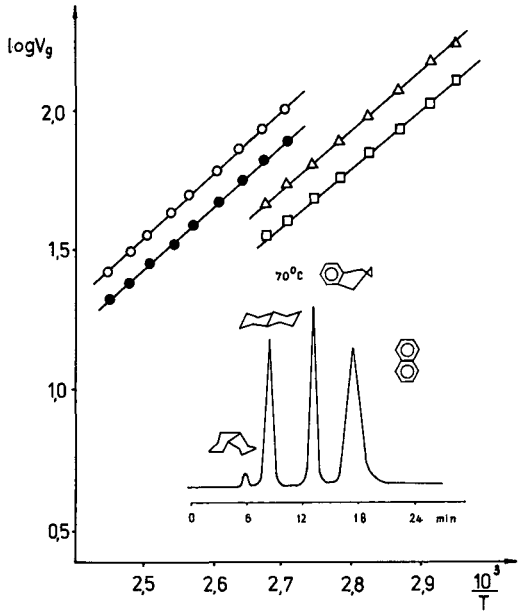

Fig. 3. Dependence of log V_g on $1/T$ for the adsorption of: □—□, *cis*-decalin; △—△, *trans*-decalin; ●—●, tetralin; ○—○, naphthalene on GTCB with a monolayer of coronene. The values of V_g are expressed in cm^3/g.

Coronene-modified GTCB was used to determine the initial heats of adsorption of some compounds. The influence of the electron density distribution in molecules adsorbing on the PAH-modified carbon black surface can be demonstrated. On the initial GTCB the $\bar{q}_1$ value for nitrobenzene is 59 kJ/mole; for aniline it is 54 kJ/mole[11]. On the coronene-modified GTCB the corresponding values are 41 and 27 kJ/mole, respectively. On the latter adsorbent a greater reduction in the $\bar{q}_1$ values (27 kJ/mole) for aniline is observed than in the case of nitrobenzene (18 kJ/mole). This is due to the different effects of the $-NO_2$ and $-NH_2$ groups on the π-electron density of the benzene ring in the adsorbate molecules.

Fig. 2 shows the initial heats of adsorption of *n*-alkanes, cyclohexane, cyclohexene, and benzene on GTCB[12] and GTCB modified with coronene. Modifications reduces the $\bar{q}_1$ values for all hydrocarbons studied. Both adsorbents show an identical elution sequence of C_6 hydrocarbons which corresponds to the increase in energy of non-specific intermolecular interaction with the surface. However, the $\bar{q}_1$ values of hexane, benzene and cyclohexane, determined on GTCB coated with a coronene monolayer, are similar to each other, unlike the corresponding values for these compounds on unmodified GTCB.

Due to changes in the electronic structure of the carbon black surface, as a result of modification with coronene, the separation of naphthalene and its hydrogenated derivatives becomes possible on a packed column without temperature programming (Fig. 3), which is necessary when a GTCB column is used[1].

On PAH-modified adsorbents, various mixtures of organic compounds were separated. Fig. 4 shows a chromatogram of the separation of aliphatic alcohol isomers. A complete separation of butyl and amyl alcohol isomers and a partial separation of hexanol isomers was obtained. A mixture of methyl derivatives of phenol, isomers of *o*- and *m*-methylphenol and dimethylphenol, was separated isothermally (Fig. 5).

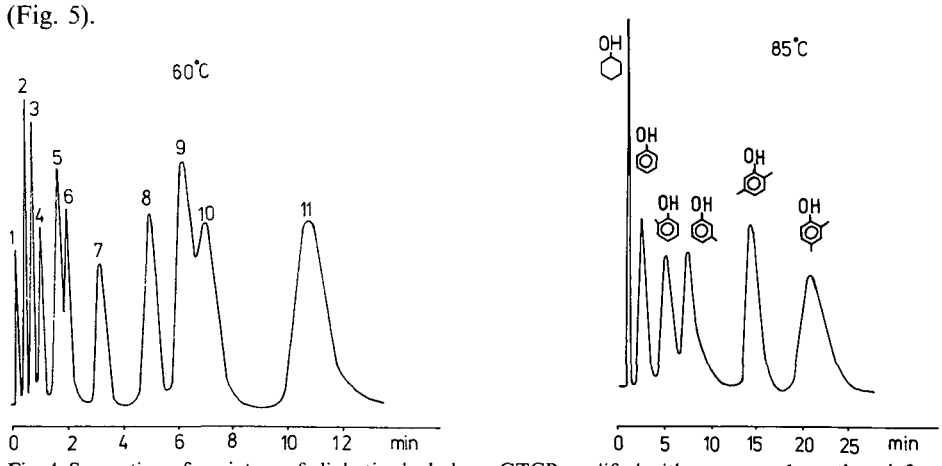

Fig. 4. Separation of a mixture of aliphatic alcohols on GTCB modified with coronene: 1 = ethanol; 2 = 2-methyl-2-propanol; 3 = 2-butanol; 4 = 1-butanol; 5 = 3-pentanol; 6 = 2-pentanol; 7 = 1-pentanol; 8 = 2-methyl-2-pentanol; 9 = 2-ethyl-1-butanol; 10 = 2-hexanol; 11 = 1-hexanol. Column: 70 cm × 0.2 cm.

Fig. 5. Separation of methylphenols on GTCB modified with coronene: 1 = cyclohexanol; 2 = phenol; 3 = 2-methylphenol; 4 = 3-methylphenol; 5 = 2,5-dimethylphenol; 6 = 2,4-dimethylphenol. Column: 70 cm × 0.2 cm.

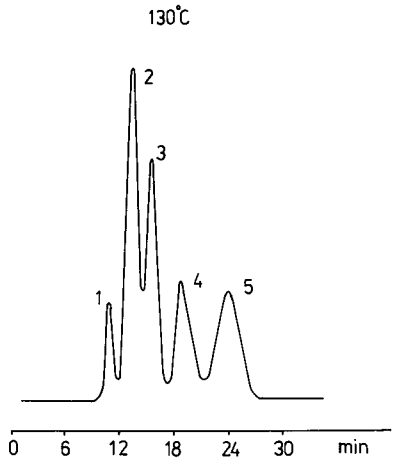

Fig. 6. Chromatograms of isomers of substituted pentanols and cyclohexanols on coronene-modified GTCB: 1 = 1-(3-methylbutyl)-1-cyclohexanol; 2 = 2-methyl-4-cyclohexyl-2-butanol; 3 = 1-cyclohexyl-2-pentanol; 4 = *cis*-2-pentyl-1-cyclohexanol; 5 = *trans*-2-pentyl-1-cyclohexanol. Column: 70 cm × 0.2 cm.

Isomers of substituted pentanols and cyclohexanols, having the general formula $C_{11}H_{21}OH$, were separated (Fig. 6). The sequence in which the isomers emerge corresponds to their number of contacts with the adsorbent surface. For example, a straight-chain hydrocarbon radical in *ortho*-position with respect to the –OH group, present in 2-pentyl-1-cyclohexanol, produces a maximum number of molecular contacts with the surface and this, therefore, results in the greatest retention; 2-pentyl-1-cyclohexanol shows two peaks, corresponding to the *cis*- and *trans*-isomers. The

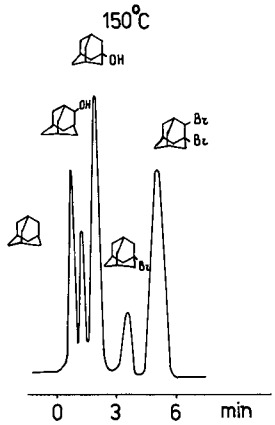

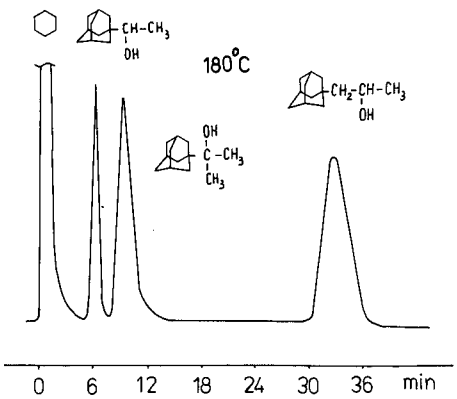

Fig. 7. Chromatogram of adamantane derivatives on GTCB modified with coronene: 1 = adamantane; 2 = 2-adamantanol; 3 = 3-adamantanol; 4 = 3-bromoadamantane; 5 = 2,3-dibromoadamantane. Column: 70 cm × 0.2 cm.

Fig. 8. Chromatogram of adamantane derivatives on GTCB modified with coronene. 1 = cyclohexane; 2 = 3-adamantane-1-ethanol; 3 = 3-adamantane-1-isopropanol; 4 = 3-adamantane-2-propanol. Column: 70 cm × 0.2 cm.

presence of a branched-chain hydrocarbon radical and an hydroxyl group on the carbon atom of 1-(3-methylbutyl)-1-cyclohexanol causes the retention of this compound to decrease considerably.

Figs. 7 and 8 show the separation of adamantane derivatives which are intermediate products in the synthesis of the biologically active, 2-adamantanamine. Both kinds of mixtures contain structural isomers that are well separated on the coronene-modified GTCB owing to differences in their geometric structures.

ACKNOWLEDGEMENTS

The authors thank Drs. E. A. Shokova and V. V. Kovaleva for kindly supplying some of the compounds.

REFERENCES

1 A. V. Kiselev, *Intermolecular Interactions in Adsorption and Chromatography*, Vyschaya Shkola, Moscow, 1986.
2 L. Ya. Gavrilina, O. A. Emelyanova, V. I. Zheivot, A. V. Kiselev and N. V. Kovaleva, *Kolloidn. Zh.*, 40 (1978) 636.
3 A. Di Gorcia, A. Liberti and R. Samperi, *J. Chromatogr.*, 122 (1976) 459.
4 T. B. Gavrilova, T. M. Roshchina, E. V. Vlasenko, Chr. Dimitrov, S. Ivanov, N. Petsev and I. Topalova, *J. Chromatogr.*, 364 (1986) 439.
5 A. V. Kiselev, N. V. Kovaleva and E. V. Zagorevskaya, *Adv. Colloid Interface Sci.*, 25 (1986) 227.
6 I. Topalova, N. Petsev, Chr. Dimitrov, T. B. Gavrilova, T. M. Roshina and E. V. Vlasenko, *J. Chromatogr.*, 364 (1986) 431.
7 S. Oka, Y. Yamamoto and K. Hayashi, *Bull. Chem. Soc. Jpn.*, 55 (1982) 3496.
8 Chr. Dimitrov, N. Petsev, M. Gigova and S. Ivanov, *C.R. Acad. Bulg. Sci.*, 31 (1978) 1429.
9 M. S. Vigdergaus and R. I. Izmailov, *Application of Gas Chromatography for Identification of Physicochemical Properties of Substances*, Nauka, Moscow, 1970.
10 L. A. Kogan, *Quantitative Gas Chromatography*, Khimiya, Moscow, 1975, pp. 22, 24.
11 A. V. Kiselev and Ya. I. Yashin, *Gas–Solid Chromatography*, Nauka, Moscow, 1967 (or *Gas-Adsorption Chromatography*, Plenum, New York, 1969).
12 E. V. Kalashnikova, A. V. Kiselev and K. D. Scherbakova, *Chromatographia*, 7 (1974) 22.

Journal of Chromatography, 454 (1988) 83–94
Elsevier Science Publishers B.V., Amsterdam — Printed in The Netherlands

CHROM. 20 806

SELECTION OF HIGH-PERFORMANCE LIQUID CHROMATOGRAPHIC METHODS IN PHARMACEUTICAL ANALYSIS

I. OPTIMIZATION FOR SELECTIVITY IN REVERSED-PHASE CHROMATOGRAPHY

M. GAZDAG, G. SZEPESI* and E. SZELECZKI
Chemical Works of Gedeon Richter, Ltd., P.O. Box 27, 1475 Budapest 10 (Hungary)
(First received November 13th, 1987; revised manuscript received June 16th, 1988)

SUMMARY

The application of solvent optimization to the development of isocratic reversed-phase liquid chromatography has been reported in several publications. Two different approaches to solvent optimization for controlling band spacing for the maximum resolution of samples are "solvent strength" and "solvent type" optimization. To improve the separation selectivity further the combination of these two approaches was examined, as a (global) optimum mobile phase composition requires the optimization of the solvent strength by varying the percentage of organic component and of the solvent selectivity of methanol, acetonitrile, tetrahydrofuran and water. It was found that the combination of "solvent strength" and "solvent type" optimization provides a markedly better separation than either procedure alone.

INTRODUCTION

When a new analytical problem has to be solved and insufficient chromatographic information is available about the separation characteristics of the sample, the analyst is working "in the dark". As we must be sure that both unknown and known sample components are separated in the final procedure, two high-performance liquid chromatographic (HPLC) systems (*e.g.*, reversed-phase and normal-phase) should be developed in order to minimize the possibility of band overlap and failure to recognize the presence of unknown species. The initial eluent compositions in both systems can be chosen either on the basis of sample characterization (our work in this field will be published elsewhere) or by the application of gradient elution using one or more gradient runs to predict isocratic conditions from the retention data obtained by gradient elution. Several such appoaches have been published by Berridge[1], Schoenmakers *et al.*[2], Quarry and co-workers[3,4] and Molnár[5].

The next step in the experiments is the optimization of the mobile phase composition in order to improve the selectivity of separations in both reversed- and normal-phase systems. In this paper the optimization of reversed-phase systems is discussed, and Part II[6] will consider normal-phase chromatography.

0021-9673/88/$03.50

Several studies have been reported on the optimization of reversed-phase systems in which the organic solvents used in the mobile phase are varied, *e.g.*, methanol, acetonitrile, tetrahydrofuran (THF) and water. The methods have been well reviewed by Berridge[1] and Schoenmakers[7].

Among the methods applicable to the optimization of reversed-phase systems, two approaches can be distinguished. The first type is the "iterative lattice method", developed by Schoenmakers *et al.*[8], in which the sample resolution is expressed as a function of the composition of the mobile phase prepared from two isoelutropic mixtures from methanol–water, acetonitrile–water and THF–water. This procedure is a typical "solvent-type optimization" introduced originally Glajch and Kirkland[9], based on the almost constant elutropic strength of the mobile phase during an experiment. However, such an approach often requires a large number of experimental runs.

An alternative approach, introduced by Quarry *et al.*[4] for optimizing band spacing, is based on the variation of the solvent strength (organic solvent concentration in the mobile phase). Although this procedure is less powerful, it is simpler and faster than the iterative lattice method, requiring fewer experimental runs, and can lead to significant changes in band spacing for many samples[10].

In this paper, the combination of "solvent type" and "solvent strength" optimization is introduced, providing better separations than either procedure alone.

EXPERIMENTAL

A liquid chromatograph (HP1090A gradient system from Hewlett-Packard, F.R.G.) equipped with an autosampler, an HP 1040A photodiode array detector, an HP 85B personal computer, a disc drive and an HP 3392A electronic integrator (all from Hewlett-Packard) was used.

The separations were performed on a prepacked 250 × 4.6 mm I.D. column of Nucleosil C_{18} (10 μm). Eluents were prepared from HPLC-grade solvents (acetonitrile, methanol, THF) and used at a flow-rate of 1 ml/min. Compounds were detected at 240 nm.

Steroids were used as models for the experiments. They are listed in Table I and were prepared at the Chemical Works of Gedeon Richter (Budapest, Hungary) to USP XXI[11] quality.

TABLE I

COMPOUNDS USED IN THE EXPERIMENTS

Compound	*Abbreviation*
Norethindrone	N
Ethinylestradiol	E
Norgestrel	NG
Estrone	EO
Norethindrone acetate	NAC
Mestranol	M

RESULTS AND DISCUSSION

Optimization criteria

Based on the results obtained in the initial isocratic runs, the strategy for further investigation can be selected. As our subsequent experiments were focused on the improvement of the selectivity of separation, the following optimization criteria were established:

(a) Minimum value of the resolution ($R_{s,min}$) obtained for the worst separated peak pairs appearing at any position on the chromatogram.

(b) Minimum value of the normalized resolution (D_{min}). The term normalized resolution (D_{min}) is similar to the meaning of "relative resolution" used by Quarry *et al.*[4] for calculating the resolution for a 10 000-plate column. Normalized resolution is calculated from the well known resolution equation:

$$R_s = 0.25 \left(\frac{k'_2}{k'_2 + 1}\right)\left(\frac{\alpha - 1}{\alpha}\right) N^{1/2} = 0.25 \cdot N^{1/2} D_{min} \tag{1}$$

$$D_{min} = \frac{k'_2}{k'_2 + 1} \cdot \frac{\alpha - 1}{\alpha} = \frac{k'_2 - k'_1}{k'_2 + 1} \tag{2}$$

The normalized resolution (D_{min}) is directly proportional to $R_{s,min}$; the only difference is its independence of the column efficiency (plate number, N). For this reason, D_{min} ignores differences between N values for different bands, and therefore $R_{s,min}$ measures the actual resolution, corrected for the variation of N from band to band. (Further symbols in eqns. 1 and 2: k' = capacity factor; α = separation factor).

For the same mobile phase composition, R_s will be proportional to the column plate number and therefore it can be increased by increasing N (*e.g.*, by increasing the column length or decreasing the flow-rate).

The use of D_{min} as an optimization criterion leads to further information: when R and D do not show the same optimum, D_{min} shows an optimum with respect to the best solvent selectivity and $R_{s,min}$ indicates where the best separation efficiency via increased column efficiency should be obtained. In this instance the next eluent composition is selected according to the optimum shown by the D value.

A knowledge of D_{min} also provides information when more optima are found, but both $R_{s,min}$ and D_{min} indicate the same optima. When the $R_{s,min}$ values are almost identical, the eluent composition for the next experiment can be selected on the basis of a higher D_{min} value. Naturally in this instance when the $R_{s,min}$ values differ from each other the next eluent composition is selected at its highest value, independent of the actual values of D at the same optima.

Assuming an average column efficiency (16 000 plates/m), the optimal value of D is about 0.080–0.150, equivalent to a range of R_s of about 1.25–2.4.

(c) R_s values measured between the main component and compounds eluting most closely to it (R_{sb} and R_{sa}).

These criteria (their calculation can be seen in Fig. 1) are significant in trace analysis, because a value of $R_{s,min}$ of 1.0 would be sufficient for the separation of two

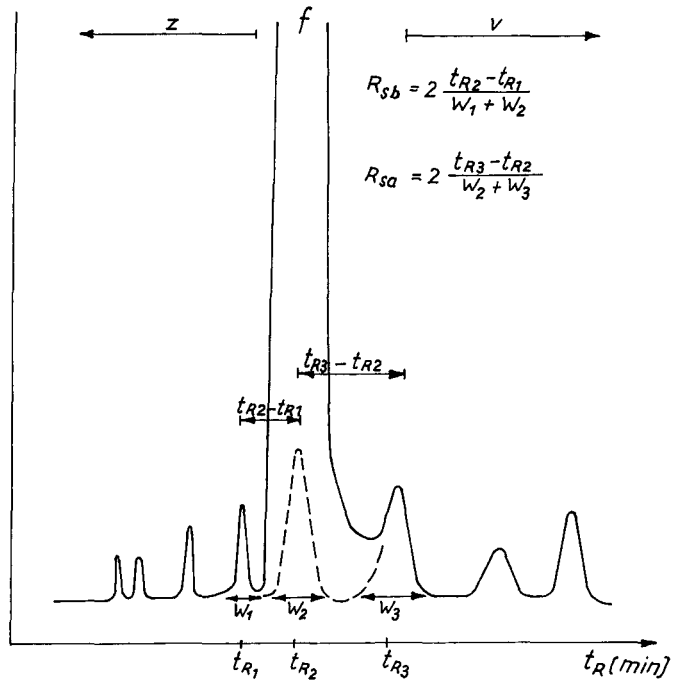

Fig. 1. Calculation of R_{sb} and R_{sa}. f = Main component; z = peaks eluting before the main component; v = peaks eluting after the main component. t_R = Retention time; W = peak width.

impurities present at similar concentrations, but would be unsuitable for separating compounds differing substantially in concentration.

R_{sb} and R_{sa} values are especially important when comparing HPLC systems with respect to their power and performance, as will be discussed in Part III[13].

Optimization for selectivity in reversed-phase systems

The combination of "solvent strength"[4] and "solvent type"[8] optimization was chosen in order to optimize the separation system using the model mixture of steroids indicated in Table I. For the calculation of R_{sb} and R_{sa}, norgestrel (NG) was selected as the main component and the others as trace components.

First, "solvent strength" optimization[4] was considered, studying the variation of resolution with percentage of organic component in methanol–water, acetonitrile–water and THF–water eluents. Retention data were plotted against volume fraction of organic solvent for the methanol–water eluent and from the window diagram its optimal composition was determined as shown in Fig. 2.

Fig. 2 also shows the chromatogram with methanol–water as eluent obtained for the model compounds. The values of R_{sb} and R_{sa} are adequate, but low values of $R_{s,min}$ and D_{min} were obtained, indicating the unsatisfactory selectivity with methanol as organic modifier in the eluent.

In the next experiment, the starting composition of acetonitrile–water was calculated according to Schoenmakers *et al.*[2] from the proportions of methanol and

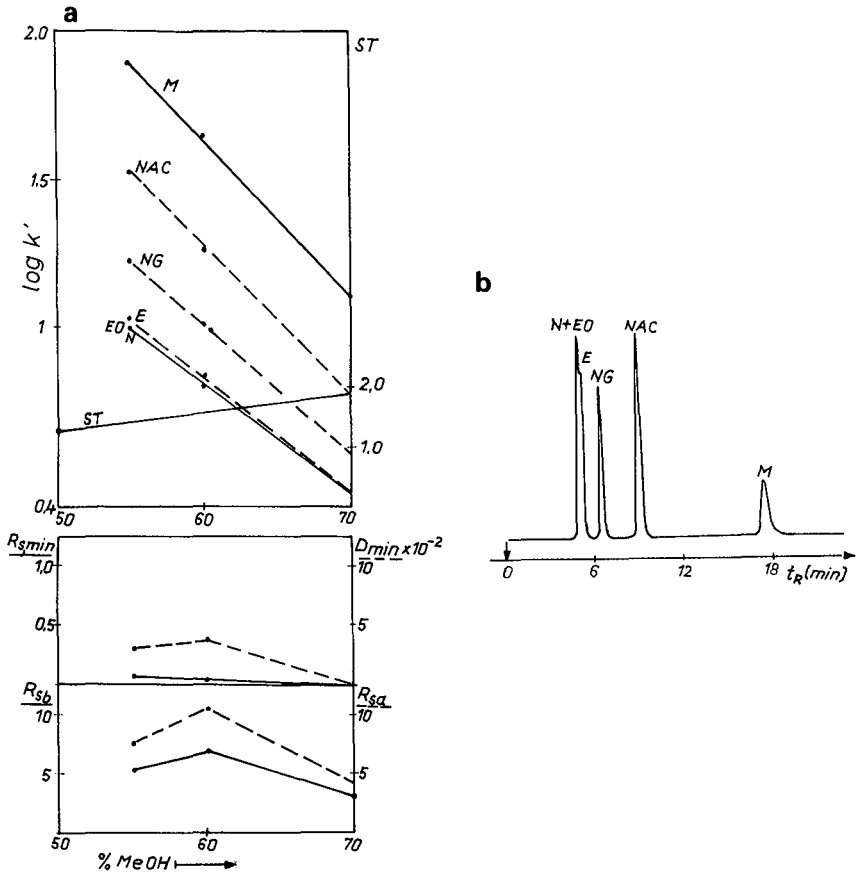

Fig. 2. Plots of log k' *vs.* volume fraction of methanol (MeOH) in water to illustrate the resolution of the steroid samples. (a) Window diagram; (b) chromatogram of model mixture (methanol–water, 7:3). Column, Nucleosil 10 C_{18} (250 × 4.6 mm I.D.); flow-rate, 1 ml/min; detection at 240 nm. Compounds as in Table I. Solid lines, $R_{s,min}/R_{sb}$; broken lines, D_{min}/R_{sa}.

water found to be optimal. (According to our findings, no significant differences in the eluent compositions were obtained when the calculations were performed using either the method published by Snyder *et al.*[12] or that of Schoenmaker *et al.*[2], but when using the iterative lattice method we wanted to follow the method described by Schoenmakers *et al.*[8] so all calculations were performed according to their procedure.)

The results of the experiments are shown in Fig. 3. The values of R_{sb} and R_{sa} are acceptable (NG is well separated from EO and NAC) and better values of $R_{s,min}$ and D_{min} were obtained than with methanol–water as the eluent, but the latter were not adequate for a perfect separation.

Similar experiments were carried out using THF–water eluents, the starting composition being calculated from the optimal acetonitrile–water ratio. The results are shown in Fig. 4.

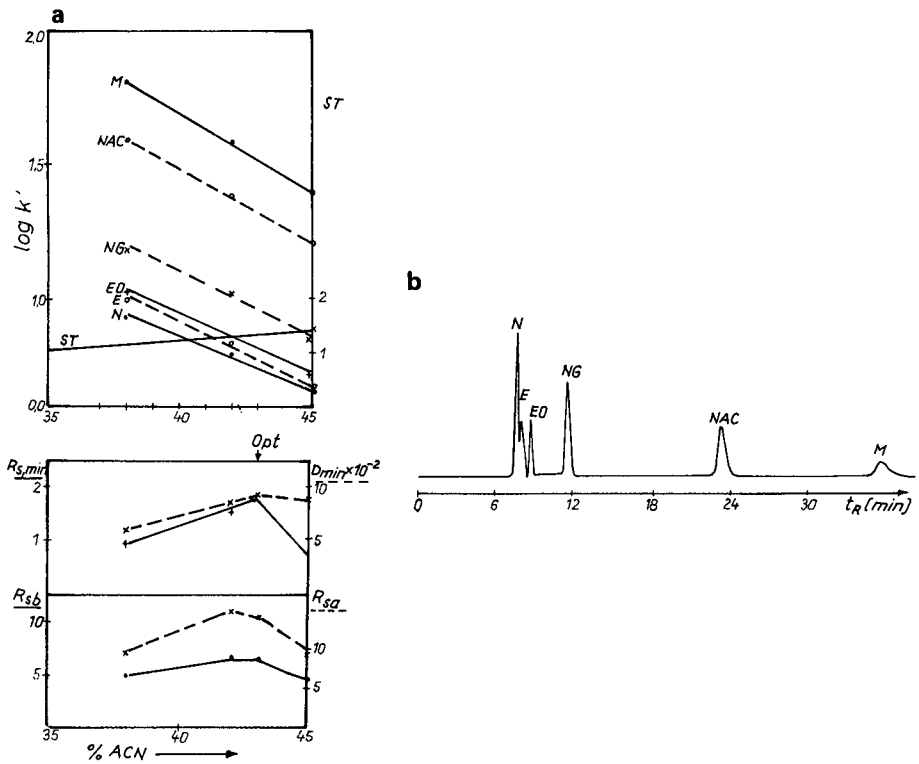

Fig. 3. Plots of log k' *vs.* volume fraction of acetonitrile (ACN) in water. (a) Window diagram; (b) chromatogram of model mixture (acetonitrile–water, 45:55). Details as in Fig. 2.

From the retention data and from the chromatogram obtained with the optimal THF–water system (Fig. 4), it can be concluded that this system provides the best separation of the steroid mixture, giving acceptable values of $R_{s,\min}$ and $D_{\min}$. However, a significant decrease in R_{sb} and R_{sa} was observed, resulting in a system suitable for the separation of steroid compounds present at similar concentrations but insufficient for trace analysis when the separation of impurities has to be performed in the presence of large amounts of the main component (NG).

From the data in Figs. 2–4 it can also be concluded that by using "solvent strength" optimization as described by Quarry *et al.*[4], variations in the solvent strength result in data points close to a straight line and, as a consequence of the different slopes obtained for the different steroid compounds, the relative band spacing can be altered and improved. The improvement in band spacing is a function of the type of solvents, and acetonitrile–water (43:57, system A) and THF–water (32:68, system B) were selected for further experiments as the best two-component eluents. With respect to suitable values of R_{sb} and R_{sa} system A and for $R_{s,\min}$ and $D_{\min}$ system B provide the best possibilities.

The experiments were continued using the iterative lattice method but, in contrast to the original work of Schoenmakers *et al.*[8], "solvent type" optimization

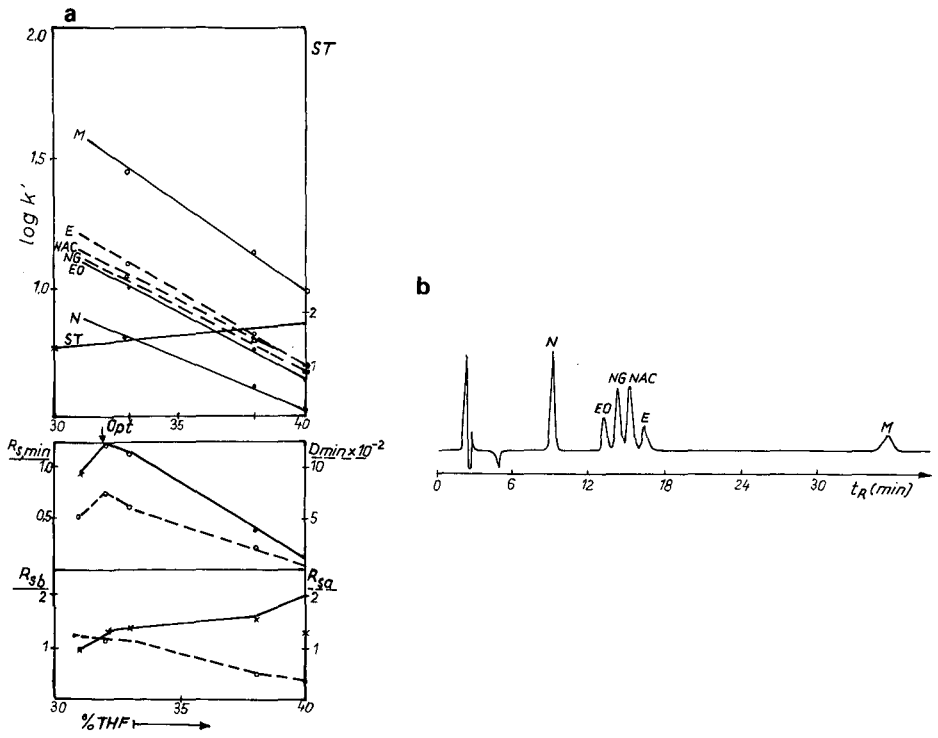

Fig. 4. Plots of log k' *vs.* volume fraction of tetrahydrofuran in water. (a) Window diagram; (b) chromatogram of model mixture (THF–water, 33:67). Details as in Fig. 2.

with mixtures of non-isoelutropic eluents was applied. The optimal composition for the initial three-component eluent mixture can be selected from the window diagram shown in Fig. 5 [A–B (45:55)].

The chromatogram obtained with this mobile phase composition is shown in Fig. 6. As can be seen, the separation is better but the R_{sa} value between NG and E is not satisfactory, that is, the predictions of Fig. 5 differ from the chromatogram shown in Fig. 6. The window diagram was corrected using the retention data obtained in this experiment and the corrected diagram is also shown in Fig. 6.

Based on the data for the corrected window diagram, the new optimum indicating the next eluent composition [A–B (25:75)] was determined. The chromatogram obtained with this eluent is shown in Fig. 7. The separation is further improved, acceptable values for R_{sb} and R_{sa} being obtained, and the system is suitable for purity testing. However, on re-correcting the window diagram a better optimum is indicated, corresponding to an eluent composition of A–B (30:70). When the separation was performed with this eluent composition an excellent separation of the Model compounds was obtained, as shown in Fig. 8. All criteria the show acceptable values, and the same optimum can be obtained again when the window diagram is re-corrected with the retention data from this experiment. The optimal composition of the mobile phase in this particular instance was found to be acetonitrile–THF–water (12.9:22.4:64.7).

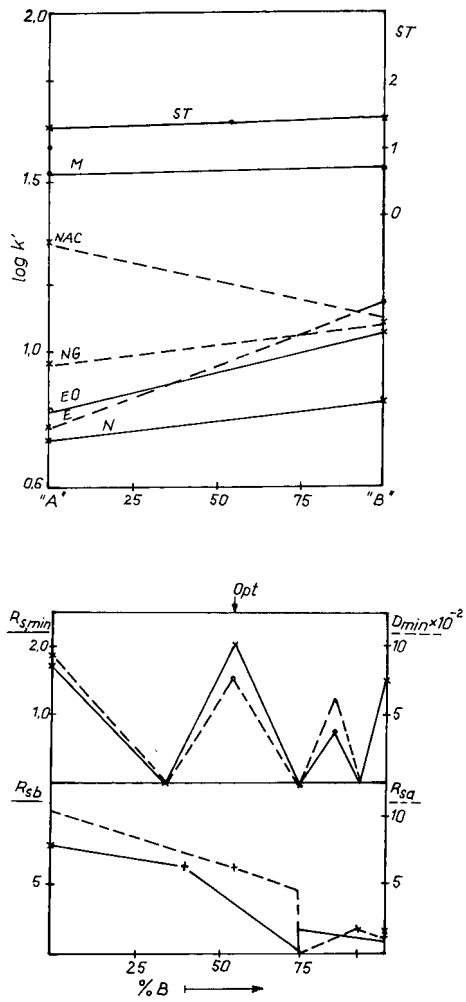

Fig. 5. Window diagram for the selection of initial three-component eluent mixture. System A, acetonitrile–water (43:57); system B, THF–water (32:68). Details as in Fig. 2.

The separation power of the combined "solvent strength"–"solvent type" optimization was compared with those of the individual optimization procedures using the conditions described in the original paper[4,8]. Figs. 2–4 show the chromatograms obtained with methanol–water, acetonitrile–water and THF–water eluents. Using "solvent strength" optimization a local optimum was obtained for the THF–water eluent (33% THF, Fig. 4b).

Initial eluent compositions for the iterative lattice method performed according to the original paper[8] were calculated according to ref. 2 [methanol–water (60:40); acetonitrile–water (45.7:54.3), system A; and THF–water (39.6:60.4), system B]. The initial optimum for three-component eluent mixture selecting system A (acetonitrile–

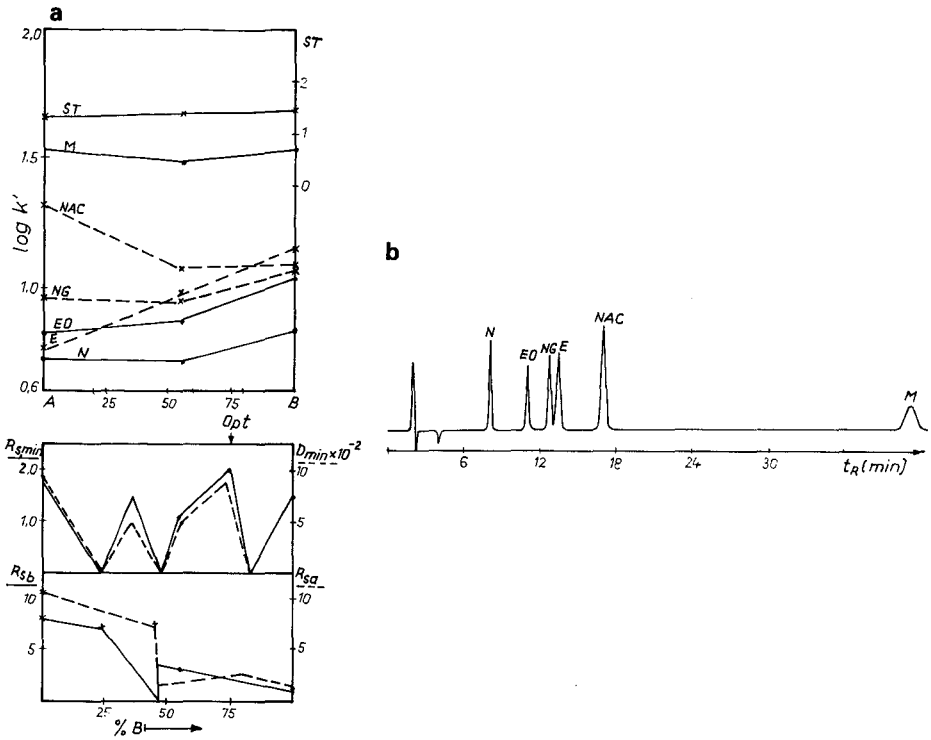

Fig. 6. First correction of window diagram (b) based on the retention data of the resulting chromatogram (a). Mobile phase composition in (a): acetonitrile–THF–water (19.4:17.6:63.0); ST (eluent strength) = 1.41. Details as in Fig. 2.

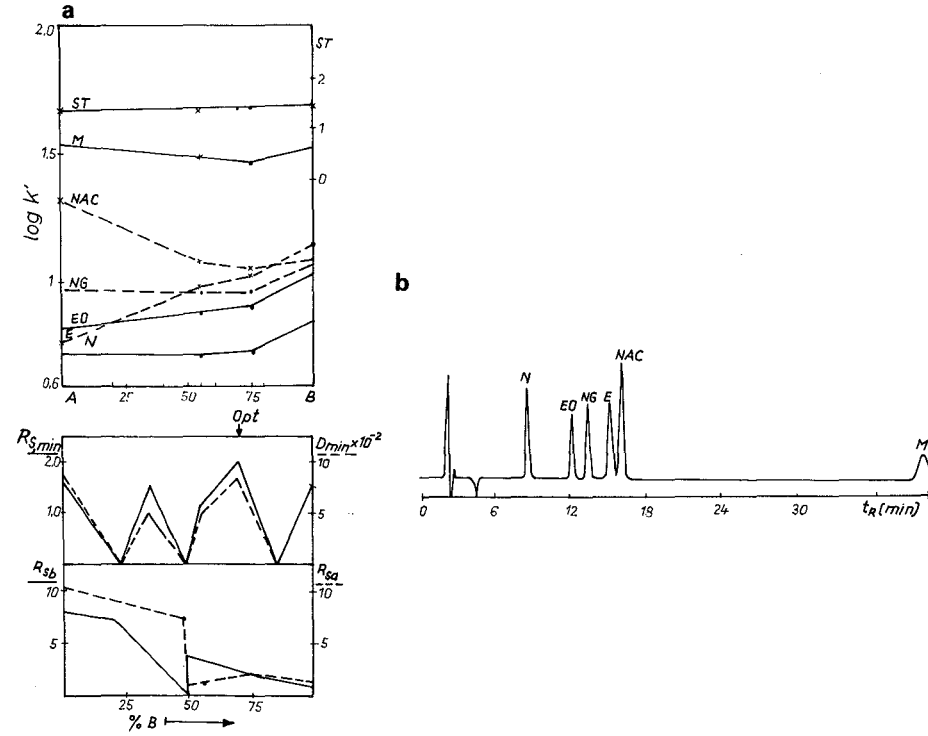

Fig. 7. Second correction of window diagram (b) based on the retention data of the resulting chromatogram (a). Mobile phase composition in (a); acetonitrile–THF–water (10.75:24.0:65.25); ST = 1.42. Details as in Fig. 2.

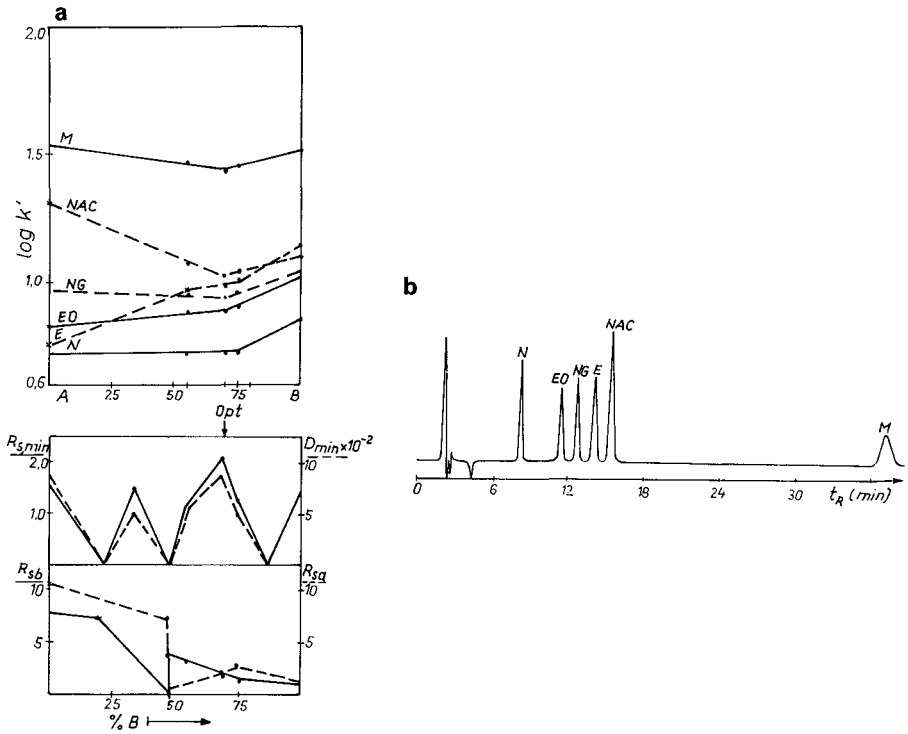

Fig. 8. Third correction of window diagram (b) based on the retention data of the resulting chromatogram (a). Mobile phase composition in (a): acetonitrile–THF–water (12.9:22.4:64.7); ST = 1.42. Details as in Fig. 2.

water) and system B (THF–water) as best two-component eluents was found to be A–B (29:71), corresponding to the eluent composition acetonitrile–THF–water (13.3:28.1:58.6). The chromatogram obtained with this eluent is shown in Fig. 9a.

The window diagram was corrected using the retention data from this experiment, indicating a new optimum of A–B (49:51) [corresponding to acetonitrile–THF–water (22.4:20.2:57.4)]. The resulting chromatogram is shown in Fig. 9b.

The experiments were not continued as the local optimum is far from the global optimum found in our experiments, and possibly cannot be reached owing to the imperfectly optimized starting conditions.

CONCLUSION

The advantages and limitations of combined "solvent strength"–"solvent type" optimization can be summarized as follows:

(a) It provides a markedly better separation (see Fig. 8) than either procedure alone (see Figs. 4 and 9b).

(b) A global optimum can be found with a significant ability to effect changes in band spacing.

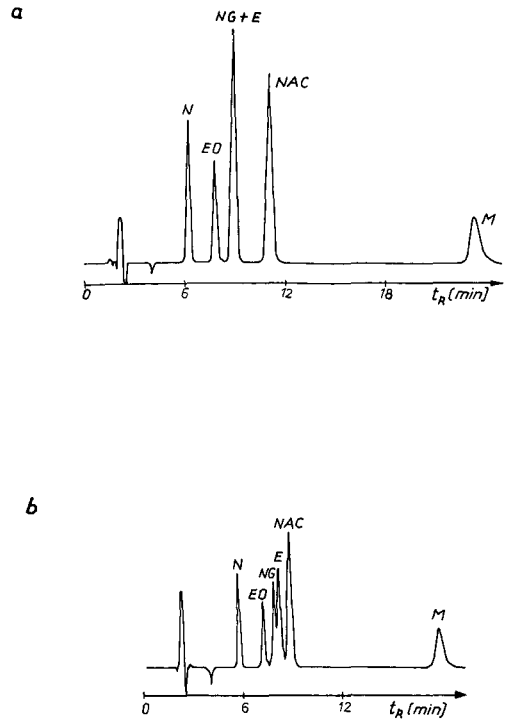

Fig. 9. Chromatograms obtained with the initial (a) and second (b) three-component eluents optimized according to the literature procedure[7]. Mobile phase compositions: (a) acetonitrile–THF–water (13.3:28.1:58.6); (b) acetonitrile–THF–water (22.4:20.2:57.6). Other conditions as in Fig. 2.

(c) The optimization procedure includes "solvent strength" optimization; when the samples do not require "solvent type" optimization, the experiments can be finished when the local optimum has been obtained. Several examples of HPLC method development based on "solvent strength" optimization were illustrated by Snyder *et al.*[10], which is a very practical approach.

(d) Large numbers of experimental runs are required to obtain the global optimum. The number of experiments can possibly be reduced (*e.g.*, only one experimental run with the solvent system resulting in a low separation efficiency, such as methanol–water here, and/or two runs with others, presuming a linear correlation between log k' and the percentage of organic component are carried out); however, there is a risk to failure to recognize the global optimum.

ACKNOWLEDGEMENT

The authors are indebted to Dr. L. R. Snyder (LC Resources, Orinda, CA, U.S.A.) for his kind help and contributions to this work.

REFERENCES

1 J. C. Berridge, *Techniques for the Automated Optimization of HPLC Separations*, Wiley-Interscience, New York, 1985, p. 41.
2 P. J. Schoenmakers, H. A. H. Billiet and L. de Galan, *J. Chromatogr.*, 205 (1981) 13.
3 M. A. Quarry, R. L. Grob and L. R. Snyder, *Anal. Chem.*, 58 (1986) 907.
4 M. A. Quarry, R. L. Grob, L. R. Snyder, J. W. Dolan and M. P. Rigney, *J. Chromatogr.*, 384 (1987) 163.
5 I. Molnár, *J. High Resolut. Chromatogr. Chromatogr. Commun.*, 4 (1981) 276.
6 M. Gazdag, G. Szepesi and K. Fábián-Varga, *J. Chromatogr.*, 454 (1988) 95.
7 P. J. Schoenmakers, *Optimization of Chromatographic Selectivity (Journal of Chromatography Library*, Vol. 35), Elsevier, Amsterdam, 1986.
8 P. J. Schoenmakers, A. C. J. H. Drouen, H. A. H. Billiet and L. de Galan, *Chromatographia*, 5 (1982) 688.
9 J. L. Glajch and J. J. Kirkland, *Anal. Chem.*, 54 (1982) 2593.
10 L. R. Snyder, M. A. Quarry and J. L. Glajch, *Chromatographia*, 24 (1987) 33.
11 *United States Pharmacopoeia XXI*, USP Convention Inc., Rockville, MD, 1984.
12 L. R. Snyder, J. W. Dolan and J. R. Gant, *J. Chromatogr.*, 165 (1979) 3.
13 G. Szepesi, M. Gazdag and K. Mihályfi, *J. Chromatogr.*, in press.

Journal of Chromatography, 454 (1988) 95–107
Elsevier Science Publishers B.V., Amsterdam — Printed in The Netherlands

CHROM. 20 807

SELECTION OF HIGH-PERFORMANCE LIQUID CHROMATOGRAPHIC METHODS IN PHARMACEUTICAL ANALYSIS

II. OPTIMIZATION FOR SELECTIVITY IN NORMAL-PHASE SYSTEMS

M. GAZDAG, G. SZEPESI* and K. FÁBIÁN-VARGA
Chemical Works of Gedeon Richter, Ltd., P.O. Box 27, 1475 Budapest 10 (Hungary)
(First received November 13th, 1987; revised manuscript received June 16th, 1988)

SUMMARY

Optimization of selectivity in normal-phase chromatography was studied. Using the same optimization criteria ($R_{s,min}$, D_{min}, R_{sb} and R_{sa}) as in Part I the possible combination of "solvent strength" optimization by variation of the percentage of polar modifier in the less polar mobile phase and "solvent type" optimization by measuring the solvent selectivity of chloroform, acetonitrile, tetrahydrofuran and dioxane was examined. From the results it can be concluded that by replacement of medium-polarity solvents (chloroform, acetonitrile, tetrahydrofuran and dioxane) in the mobile phase, the selectivity of the separation can be significantly improved as the elution order is a function of solvent type belonging to Class P. In the separation of a steroid mixture dioxane provides the best properties for improving band spacing.

INTRODUCTION

In Part I[1] we considered optimization for selectivity in reversed-phase systems. Such optimization with normal-phase systems is more complex for two main reasons, as studied extensively by Snyder and co-workers[2–7]: solvent–solute localization and its effect on solvent selectivity.

As a continuation of our work in Part I[1], the combination of "solvent strength" and "solvent type" optimization in normal-phase systems has been studied.

EXPERIMENTAL

The same instrumentation (HP 1090A) as described in Part I[1] was used. Separations were performed on a LiChrosorb Si 60 (5 μm) column (250 × 4.6 mm I.D.) (Chrompack, Middelburg, The Netherlands). The eluent flow-rate was 1 ml/min and the steroids (as listed in Table I in Part I[1]) were detected at 254 nm. Other experimental details can be found in Part I[1].

0021-9673/88/$03.50

TABLE I

ESTABLISHMENT OF ELUENT COMPOSITION FOR INITIAL ISOCRATIC SEPARATIONS

Abbreviations: B1 = phosphate buffer (pH 2.2); B2 = 10 m*M* ammonium carbonate buffer; THF = tetrahydrofuran.

Sample characterization			*Eluent selection*	
Solubility	*Polarity*	*Basicity*	C_{18}	*Si 60*
Lipophilic	Non-polar	Neutral	Acetonitrile–water (8:2)	Hexane–chloroform (98:2)
	Medium	Neutral	Methanol–water (7:3)	Hexane–isopropanol (99:1)
	Medium	Proton donor	THF–water (1:1)	Hexane–isopropanol (99:1)
	Medium	Proton acceptor	Methanol–water (6:4)	Hexane–isopropanol (99:1)
	Medium	H-bond formation	Acetonitrile–water (6:4)	Hexane–isopropanol (99:1)
	Polar	Proton donor	Methanol–water (4:6)	Hexane–isopropanol (98:2)
	Polar	Proton acceptor	THF–water (3:7)	Hexane–isopropanol (98:2)
	Polar	H-bond formation	Acetonitrile–water (4:6)	Hexane–isopropanol (98:2)
Hydrophilic	Medium	Proton donor	Acetonitrile–B1 (6:4)	Chloroform–methanol–glacial acetic acid (95:5:1)
	Medium	Proton acceptor	Acetonitrile–B2 (6:4)	Chloroform–methanol (95:5)
	Polar	Proton donor	Acetonitrile–B1 (3:7)	Chloroform–isopropanol–glacial acetic acid (9:1:1)
	Polar	Proton acceptor	Acetonitrile–B2 (3:7)	Chloroform–isopropanol–diethylamine (9:1:1)
	Polar	Neutral	Methanol–water (3:7)	Hexane–isopropanol (9:1)
	Ionic	Cationic	Special techniques	
	Ionic	Anionic	Special techniques	

RESULTS AND DISCUSSION

Optimization criteria

The same optimization criteria as discussed in Part I[1], $R_{s,min}$, R_{sb}, R_{sa} and D_{min}, were applied.

Optimization for selectivity in normal-phase systems

The importance of the contribution of solvent–solute localization to solvent selectivity effects in separations performed on silica and alumina columns using less polar eluents (liquid–solid chromatography) has been investigated in detail by Snyder and co-workers[2–7]. A quantitative model for solvent–solute localization and its effects on solvent selectivity was also established. With respect to solvent localization capability, the solvents were classified into three groups as follows[3]:

(a) Class N: less polar solvents that show no tendency for localization at low volume fractions in the mobile phase (molecules possessing no functional group).

(b) Class P: more polar solvents that cannot self-hydrogen bond and that can localize at low volume fractions in a mobile phase containing only one polar functional group or only one heteroatom, *e.g.*, alkyl ethers, ketones, nitriles (sub-class Pa); or the molecule is aromatic (*e.g.*, pyridine), multifunctional (*e.g.*, dioxane) or the polar functional group contains more than one heteroatom (sub-class Pb).

(c) Class AB: amphotheric molecules that can self-hydrogen bond and that are fairly polar (alcohols, carboxylic acids, etc.).

As a result of the comprehensive studies described in the literature[2–7], predictions of solvent strength for binary, ternary and quaternary eluent systems can be made.

Three important features of sample molecules can provide useful information for their chromatographic characterization: the lipophilic and hydrophilic character of the compounds to be tested (solubility in hexane, chloroform, chloroform–ethanol and water); polarity of the compounds (depending on the functional group attached to the basic skeleton); and basicity relating to the proton donor or acceptor properties and to hydrogen bond formation ability of the functional groups with the solvents in the eluent.

The first eluent compositions in both systems can be chosen on the basis of sample characterization, as discussed above and shown in Table I.

The data in Table I are based on our practical experience and some examples of its use have been published[8–13]. However, it should be emphasized that the applicability of the eluent compositions indicated in Table I has some limitations, as follows:

(i) The retention data obtained from the first experiments can be considered only as a starting point for the optimization of eluent composition, as discussed in detail in Part I and here. The prediction of correct percentage of the organic component in an initial study seems impossible in most instances.

(ii) The elutropic strength of the mobile phase compositions in Table I is higher than can be expected on the basis of the chromatographic characterization of the sample to exclude the possibility that late-eluting bands may not show up in initial isocratic separations.

(iii) Reversed-phase retention data vary considerably with the molecular weight of the sample. In our practice the data in Table I may be applicable to the separation of compounds in the molecular weight range 100–700.

(iv) For the separation of highly polar samples necessitating the use of a reversed-phase mobile phase with a very low organic solvent content (less than 10%), the data in Table I cannot be applied.

When using the recommended eluent compositions for normal-phase chromatography in Table I to establish the experimental conditions for initial isocratic runs, the application of two-component eluent systems containing an apolar (Class N) and a polar (Class AB) constituent is proposed. The "solvent strength" optimization[1,14] was started with two binary eluent compositions (hexane–isopropanol and chloroform–isopropanol).

Plots of log k' (capacity factor) *vs.* volume fraction of isopropanol in hexane (Fig. 1) and in chloroform (Fig. 2) indicate a non-linear correlation between the data points, as shown together with the corresponding window diagrams. Using the linearizing equation of Soczewinski[15] a significant deviation was also found. However, using the iterative lattice method[16] for the optimization of ternary mobile phases the window diagrams are corrected with the retention data from the experimental runs

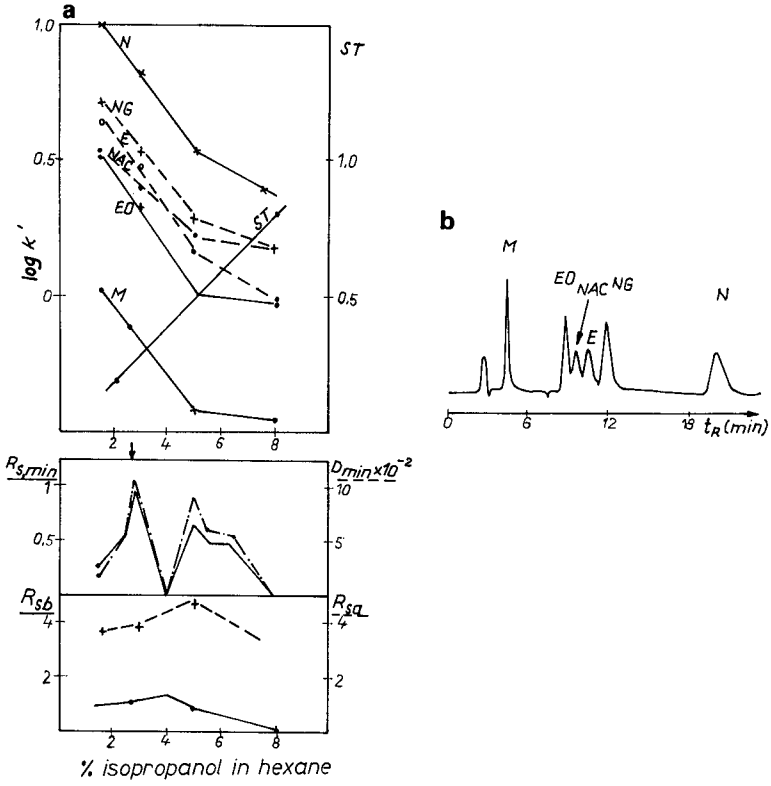

Fig. 1. Plots of log k' *vs.* volume fraction of isopropanol in hexane to illustrate the resolution of the steroid samples. (a) Window diagram; (b) chromatogram of model mixture [hexane–isopropanol (97.25:2.75); eluent strength calculated from the data in Table II according to eqn. 1, ST = 0.275]. Column: LiChrosorb Si 60 (5 μm) (250 × 4.6 mm I.D.); flow-rate, 1 ml/min; detection at 254 nm. Compounds and abbreviations: norethindrone (N), ethinylestradiol (E), norgestrel (NG), estrone (EO), norethindrone acetate (NAC) and mestranol (M). Solid lines, $R_{s,min}/R_{sb}$; broken lines, D_{min}/R_{sa}. t_R = Retention time.

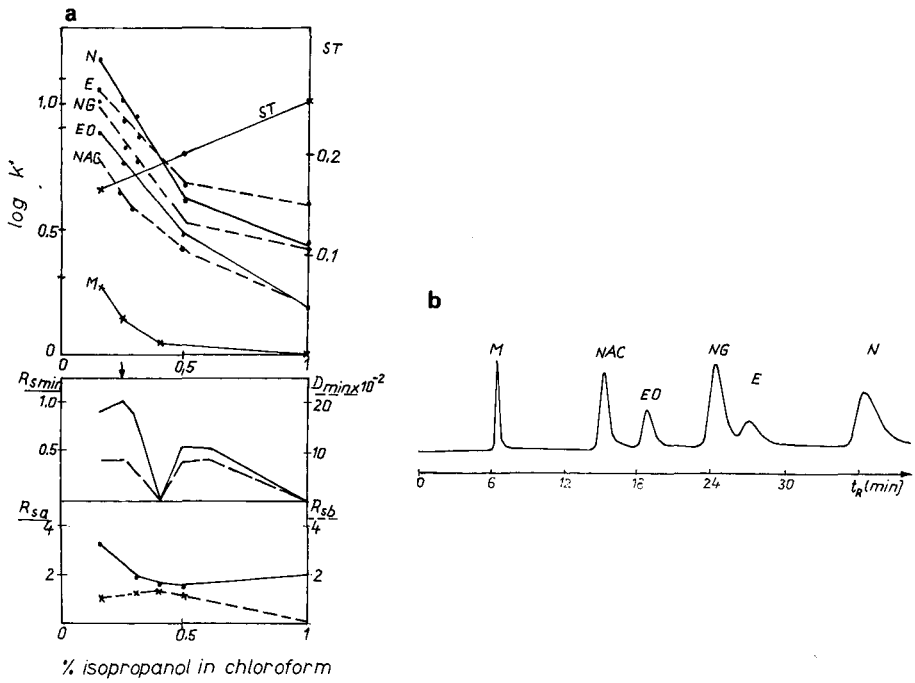

Fig. 2. Plots of log k' *vs.* volume fraction of isopropanol in chloroform. (a) Window diagram; (b) chromatogram of model mixture [chloroform–isopropanol (99.75:0.25); ST = 0.18]. Details as in Fig. 1.

step by step, assuming a linear correlation between the measured data points of the log k' *vs.* volume fraction of isopropanol plots.

Regarding the hexane–isopropanol eluent, three optima can be found (isopropanol concentrations 2.75, 4.9 and 6.4%). Similarly to the procedure described in Part I[1], norgestrel (NG) was chosen as main component when the values of R_{sb} and R_{sa} have been calculated. The optimum found at 2.75% isopropanol was selected for further experiments, giving the best values for $R_{s,min}$ and D_{min} and acceptable values for R_{sb} and R_{sa} (system A). A chromatogram obtained with this eluent is shown in Fig. 1.

Similar results were obtained with chloroform–isopropanol eluents. From the three optima (isopropanol concentration 0.25, 0.5 and 0.6%) the first was selected (system B) as it gave the highest $R_{s,min}$ value (the values for D_{min}, R_{sb} and R_{sa} were similar). A chromatogram obtained with this eluent is shown in Fig. 2.

Comparing the two selected systems, it can be concluded that both systems provide acceptable $R_{s,min}$ values (about 1.0), and system A gave better R_{sa} and worse R_{sb} values. NG is well separated from N and poorly separated from E; with system B the reverse applies, NG being separated well from EO (better R_{sb}) and poorly from E (R_{sb}).

The study was continued using the iterative lattice method[16]. The initial eluent composition for the first experimental run with a ternary eluent was selected from the window diagram shown in Fig. 3 [A–B (40:60)]. The resulting chromatogram is also shown in Fig. 3.

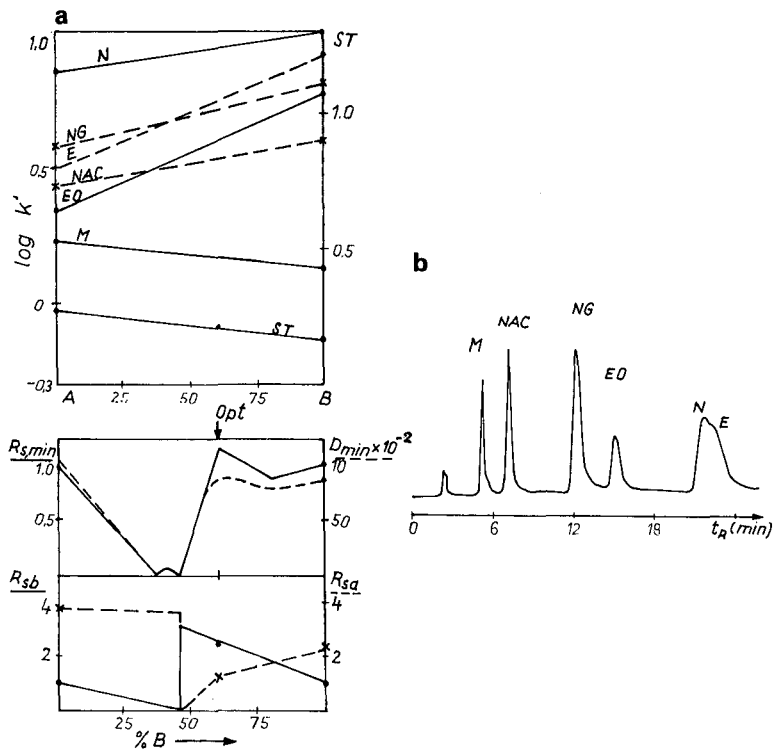

Fig. 3. Window diagram for the selection of initial three-component eluent mixture. System A, hexane–isopropanol (97.25:2.75); system B, chloroform–isopropanol (99.75:0.25). (a) Window diagram; (b) chromatogram obtained with the initial ternary eluent mixture [hexane–chloroform–isopropanol (38.90:59.85:1.25); ST = 0.215]. Details as in Fig. 1.

Contrary to expectation, a poor separation for N and E was obtained ($R_{s,min}$ = 0.54). The window diagram was corrected using the retention data from this run, resulting in a new optimum [A–B (80:20)], as shown in Fig. 4 together with the chromatogram obtained with this eluent system.

As shown in Fig. 4, the separation with this newly selected eluent does not also meet expectation, and no improvement in the separation efficiency was achieved. Re-correcting the window diagram again with the retention data, the next optimum was A–B (58:42), as shown in Fig. 5 together with the chromatogram obtained.

Fig. 5 shows that the separation was improved (N and E can be separated) and the system seems to be applicable for purity testing ($R_{s,min}$ = 0.82, R_{sb} = 4.2 and R_{sa} = 2.3).

The experiment was continued using an eluent composition indicated by the corrected window diagram shown in Fig. 6 [A–B (65:35)]. A better separation was achieved ($R_{s,min}$ = 0.88, R_{sb} = 3.66 and R_{sa} = 2.33) and this composition of mobile phase, corresponding to hexane–chloroform–isopropanol (63.2:34.9:1.9), is considered to be optimal because on re-correction of the window diagram the same optimum was obtained (Fig. 7).

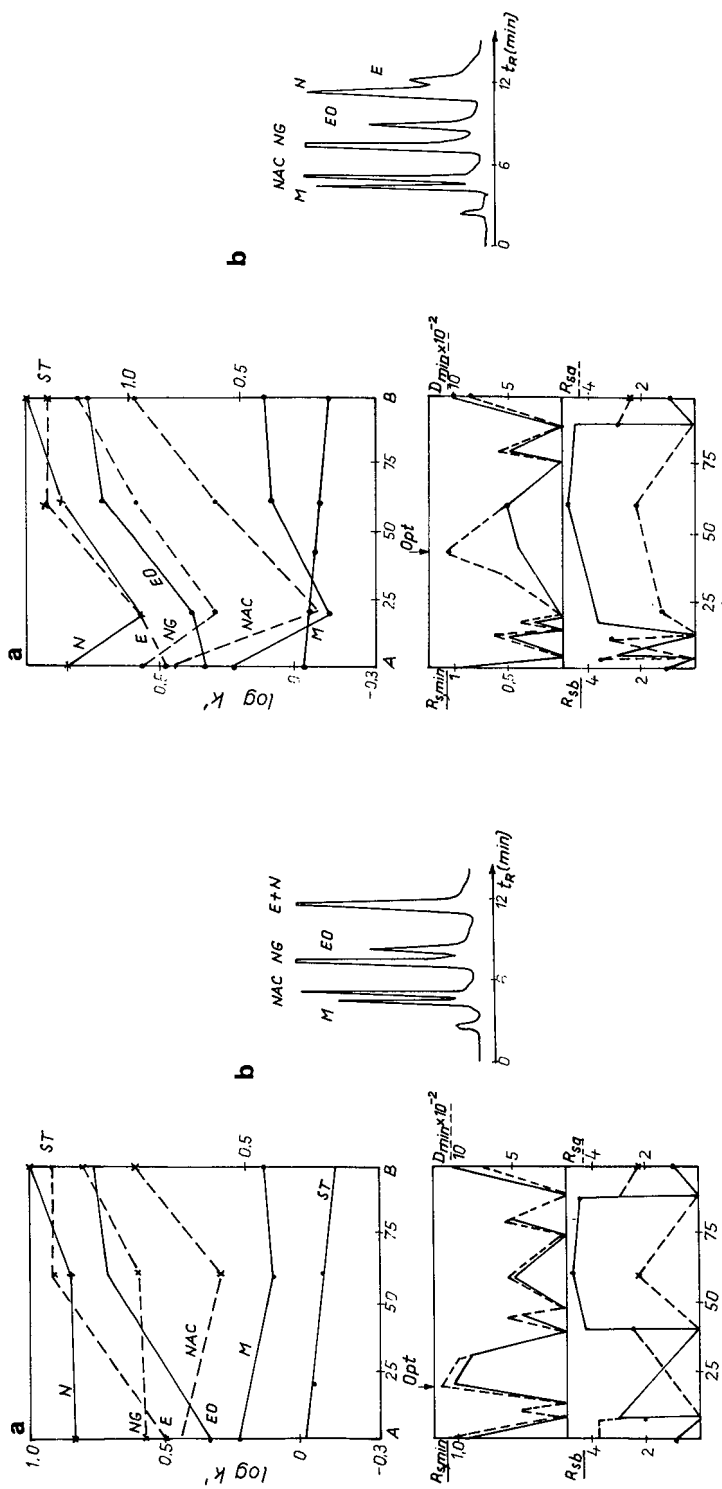

Fig. 4. First correction of window diagram (a) based on the retention data of the resulting chromatogram (Fig. 3b). (a) Window diagram; (b) chromatogram obtained at the selected optimum. Mobile phase composition in (b): hexane–chloroform–isopropanol (77.8:19.95:2.25); ST = 0.255. Details as in Fig. 1.

Fig. 5. Second correction of window diagram (a) based on the retention data of the resulting chromatogram (Fig. 4b). (a) Window diagram; (b) chromatogram obtained at the selected optimum. Mobile phase composition in (b): hexane–chloroform–isopropanol (56.4:41.9:1.7); ST = 0.233. Details as in Fig. 1.

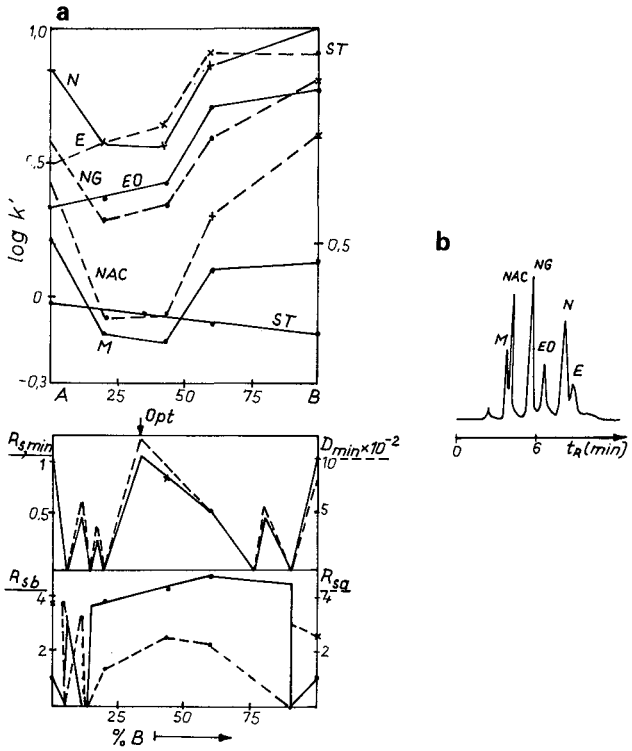

Fig. 6. Third correction window diagram (a) based on the retention data of the resulting chromatogram (Fig. 5b). (a) Window diagram; (b) chromatogram obtained at the selected optimum. Mobile phase composition in (b): hexane–chloroform–isopropanol (63.2:34.9:1.9); ST = 0.242. Details as in Fig. 1.

To improve further the selectivity of the separation, replacement of chloroform with other solvents belonging to the same group of solvents (Class P) in the ternary mobile phase was studied. As a practical approach, the elutropic strength of ternary mobile phases was calculated using an equation similar to that used in reversed-phase chromatography[17]:

$$ST = \sum s_i v_i \tag{1}$$

where ST is the elutropic strength of the eluent, s_i is the strength of individual solvents and v_i is the percentage volume fraction of the solvent in the eluent.

When the elutropic strengths of the eluents were calculated according to literature data[18] some deviations were observed. Based on our recent experimental data[9,11,12] obtained for different groups of compounds separated using different mobile phase compositions, an empirical order for the solvent strengths was established. The solvent strengths of two solvents were fixed (hexane = 0, isopropanol = 10) and the other solvents were placed in order by calculating the eluent strength according to eqn. 1, considering the concentrations of other solvents providing similar retentions for the same components.

Some large deviations in the solvent strengths were found (Table II) when our

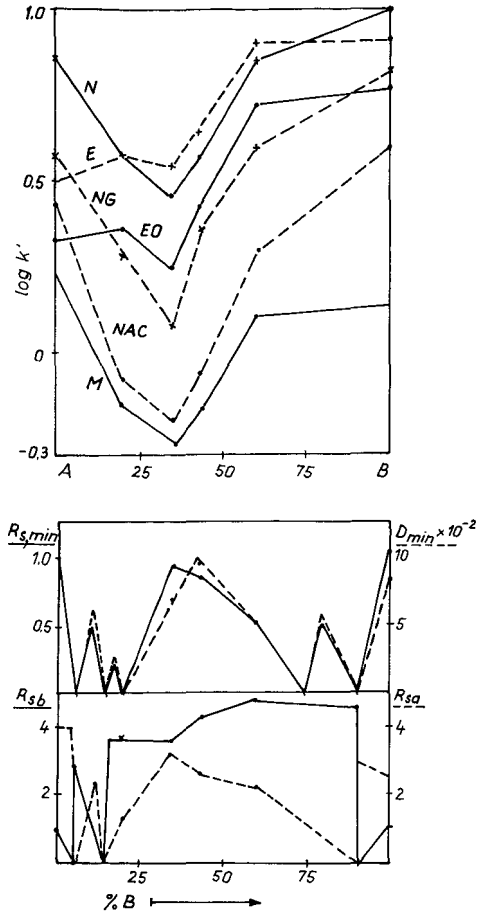

Fig. 7. Re-corrected window diagram.

TABLE II

SOLVENT STRENGTHS OF DIFFERENT SOLVENTS

Solvent	*Solvent strength*	
	Experimental	*Literature*[18]
Hexane	0	0.01
Dichloromethane	0.11	0.42
Chloroform	0.15	0.40
Dioxane	2.50	0.56
Acetonitrile	4.00	0.65
Tetrahydrofuran	4.50	0.45
Methanol	6.70	0.95
Isopropanol	10.0	0.82

data were compared with the data published in the literature[18]. According to our findings the solvent strength of chlorinated hydrocarbons (chloroform and dichloromethane) seems to be weaker than expected. Similarly, the order of solvent strengths for solvents belonging to Class P is different. According to our previous assumption, the significant deviations may be due to the change in separation mechanism with binary and ternary mobile phase compositions from liquid–solid adsorption to liquid–liquid partition chromatography as a result of the dynamically coated thin liquid layer formed on the silica surface.

A more likely explanation was given by Snyder[19] based on two effects. The first is derived from the fact that very low concentrations of strong solvents (Class AB) are used and under these conditions the strong (localizing) solvent has a much higher strength than normal, as was shown by Snyder and co-workers[3,4,6]. Second, all polar solvent systems have large secondary solvent effects (interactions between solute and solvent molecules in the adsorbed phase), resulting in deviations from the predicted solvent strength.

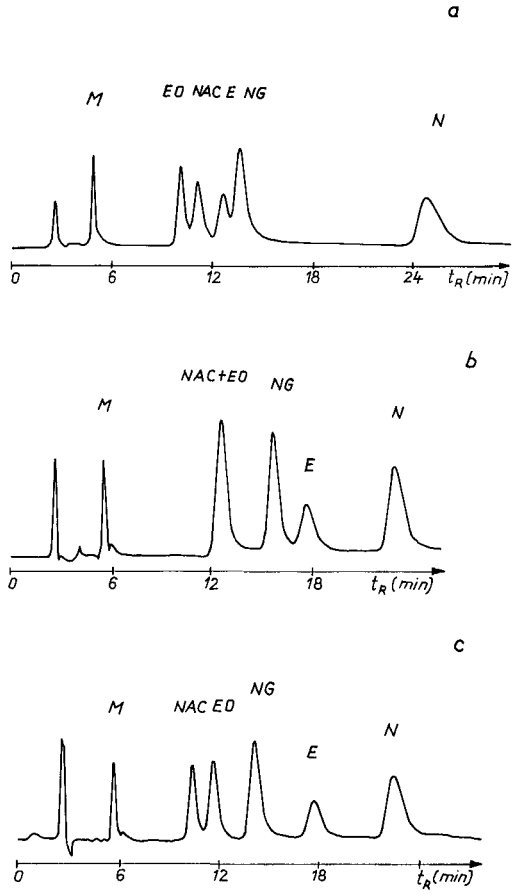

Fig. 8. Replacement of chloroform with other solvents belonging to Class P. (a) Hexane–tetrahydrofuran–isopropanol (97:1:2); ST = 0.245; (b) hexane–acetonitrile–isopropanol (97:1:2); ST = 0.240; (c) hexane–dioxane–isopropanol (96:2:2); ST = 0.250. Details as in Fig. 1.

Based on this explanation, the solvent strength values in Table II can be considered to represent a good practical approach, particularly for low concentrations of the polar modifier.

As a continuation of our experiments, the possible replacement of chloroform with tetrahydrofuran, acetonitrile and dioxane in the eluent (the calculated eluent strength according to eqn. 1 is 0.24) was studied. The chromatograms are shown in Fig. 8.

Comparing the chromatograms shown in Fig. 8, two important conclusions can be drawn. First, similar retentions were obtained for NG, M and N (first, last and main components). This seems to support our expectation regarding the calculation possibilities of elutropic strength. Second, replacement of chloroform with dioxane

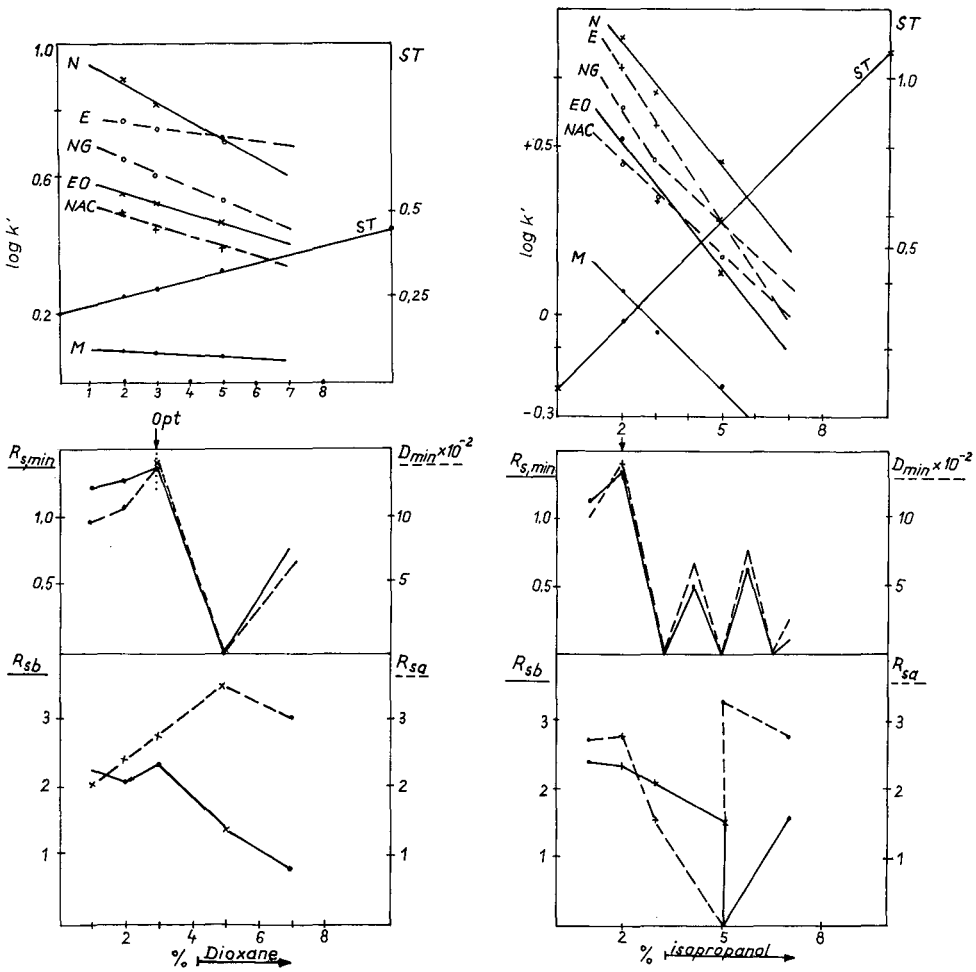

Fig. 9. Plots of log k' *vs.* volume fraction of dioxane in the mobile phase. Mobile phase: hexane–dioxane containing 2% of isopropanol. Details as in Fig. 1.

Fig. 10. Plots of log k' *vs.* volume fraction of isopropanol in the mobile phase. Mobile phase: hexane–isopropanol containing 3% of dioxane. Details as in Fig. 1.

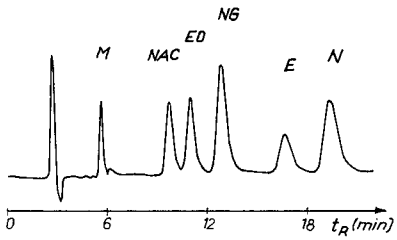

Fig. 11. Chromatogram obtained with the optimal eluent composition. Mobile phase: hexane–dioxane–isopropanol (95:3:2); ST = 0.275. Details as in Fig. 1.

can significantly improve the selectivity of the separation, and therefore this system was subjected to further investigations.

Plots of log k' *vs.* concentration of dioxane using a constant concentration of isopropanol (2%) and of log k' *vs.* concentration of isopropanol using a constant concentration of dioxane (3%) are shown in Figs. 9 and 10, respectively. The data show that the mobile phase hexane–dioxane–isopropanol (95:3:2) can be considered optimal. The chromatogram obtained with this eluent is shown in Fig. 11.

CONCLUSIONS

Six different mobile phase compositions (two binary and four ternary systems) were compared with respect to their selectivity. The elution orders obtained with these systems are shown in Fig. 12.

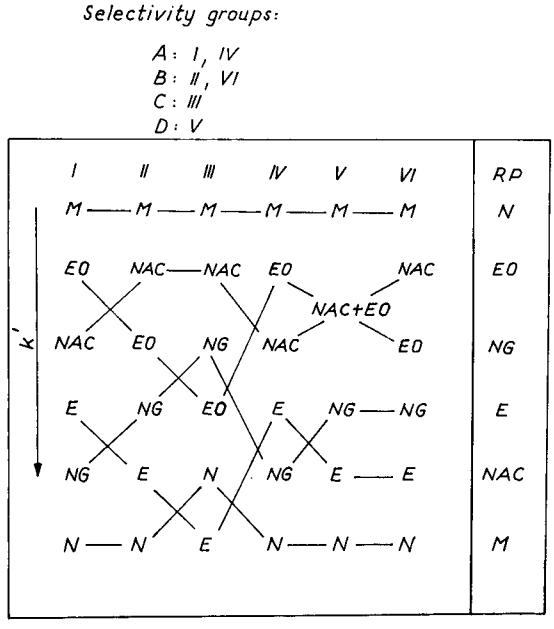

Fig. 12. Dependence of elution order on eluent composition. RP = Reversed phase. Solvent systems: I = Hexane–isopropanol; II = chloroform–isopropanol; III = hexane–chloroform–isopropanol; IV = hexane–tetrahydrofuran–isopropanol; V = hexane–acetonitrile–isopropanol; VI = hexane–dioxane–isopropanol.

All the ternary systems differ from each other, which supports our recent experience that the difference in selectivity of solvents available for normal-phase chromatography is greater than that of solvents applied in reversed-phase chromatography, and this can advantageously be used to improve the selectivity of separations.

This was the main reason why normal-phase chromatography was selected as a second alternative approach for optimizing HPLC separations in pharmaceutical analysis. The elution order with the optimal reversed-phase system is also indicated in Fig. 12.

ACKNOWLEDGEMENT

The authors are grateful to Dr. L. R. Snyder (LCResources, Orinda, U.S.A.) for his kind help and contributions to this work.

REFERENCES

1 M. Gazdag, G. Szepesi and E. Szeleczki, *J. Chromatogr.*, 454 (1988) 83.
2 L. R. Snyder, M. D. Palamareva, B. J. Kurtev, L. Z. Viteva and J. N. Stefanovsky, *J. Chromatogr.*, 354 (1986) 107.
3 L. R. Snyder and J. L. Glajch, *J. Chromatogr.*, 214 (1981) 1.
4 J. L. Glajch and L. R. Snyder, *J. Chromatogr.*, 214 (1981) 21.
5 L. R. Snyder, J. L. Glajch and J. J. Kirkland, *J. Chromatogr.*, 218 (1981) 299.
6 L. R. Snyder, in Cs. Horváth (Editor), *High-Performance Liquid Chromatography*, Vol. 3, Academic Press, New York, 1983, p. 157.
7 L. R. Snyder and J. L. Glajch, *J. Chromatogr.*, 248 (1982) 165.
8 L. Szepesy, I. Fehér, G. Szepesi and M. Gazdag, *J. Chromatogr.*, 149 (1978) 271.
9 G. Szepesi, M. Gazdag and L. Terdy, *J. Chromatogr.*, 191 (1980) 101.
10 G. Szepesi and M. Gazdag, *J. Chromatogr.*, 204 (1981) 341.
11 G. Szepesi and M. Gazdag, *J. Chromatogr.*, 205 (1981) 57.
12 M. Gazdag, G. Szepesi and K. Csomor, *J. Chromatogr.*, 243 (1982) 315.
13 G. Szepesi and M. Gazdag, in H. Kalász and L. Ettre (Editors), *Chromatography, the State of the Art*, Vol. 1, Akadémiai Kiadó, Budapest, 1985, p. 467.
14 M. A. Quarry, R. L. Grob, L. R. Snyder, J. W. Dolan and M. P. Rigney, *J. Chromatogr.*, 384 (1987) 163.
15 E. Soczewinski, *Anal. Chem.*, 41 (1969) 179.
16 P. J. Schoenmakers, A. C. J. H. Drouen, H. A. H. Billiet and L. de Galan, *Chromatographia*, 5 (1982) 688.
17 L. R. Snyder, *J. Chromatogr. Sci.*, 16 (1983) 223.
18 L. R. Snyder, J. W. Dolan and J. R. Gant, *J. Chromatogr.*, 165 (1979) 3.
19 L. R. Snyder, personal communication, 1987.

Journal of Chromatography, 454 (1988) 109–120
Elsevier Science Publishers B.V., Amsterdam — Printed in The Netherlands

CHROM. 20 760

AUTOMATED ANALYSIS OF VARIOUS COMPOUNDS WITH A WIDE RANGE OF BOILING POINTS BY CAPILLARY GAS CHROMATOGRAPHY BASED ON RETENTION INDICES

HAJIME TOKUDA*, EIJI SAITOH, YUKIO KIMURA and SATOSHI TAKANO
Tochigi Research Laboratories, Kao Corporation, 2606, Akabane, Ichikaimachi, Tochigi 321-34 (Japan)
(First received February 17th, 1988; revised manuscript received June 20th, 1988)

SUMMARY

A simple and reliable automated method has been developed for the analysis of various compounds with a wide range of boiling points by temperature-programmed capillary gas chromatography (GC). It consists of the identification based on corrected retention indices and the quantitation by a multi-internal standard technique. The full automation of the analysis was achieved by the connection of a GC system to a personal computer. Some factors affecting the reproducibility of retention indices and the quantitation are discussed. As an example of the application of the method, the analysis of a commercial cosmetic product was demonstrated.

INTRODUCTION

Gas chromatography (GC) is one of the best methods for the analysis of mixed unknown volatiles. There are many chromatographic techniques for the identification of unknown compounds, involving parameters such as absolute retention time, relative retention time, equivalent chain length (ECL) and retention index (*I*). Among them, the *I* system proposed by Kováts[1] in 1958 is considered to be the most suitable technique for routine GC analysis, in terms of reliability and ease of measurement.

Recent progress in fused-silica capillary column technology and the improvement of GC instruments in the 1980s have made it more useful, and many studies on its applications have been reported[2–11]. Anderson and Stafford[6] reported the screening of drugs based on the *I* system. D'Agostino and Provost[3] also applied it to the analysis of chemical warfare agents in environmental samples. The reproducibility of *I* in temperature-programmed capillary GC analysis has been investigated in detail by Schepers *et al.*[5] and Knöppel *et al.*[2]. However, these reports describe only the behaviour of compounds with low or medium boiling points, and there has been no study of compounds with high boiling points.

On the other hand, the quantitative analysis of the compounds is also required. This has been scarcely discussed for compounds with a wide range of boiling points analysed by temperature-programmed capillary GC. Unknown samples frequently

0021-9673/88/$03.50

contain a variety of compounds with low to high boiling points. Therefore, the development of a versatile method for the analysis of such samples is required.

In the present paper we will discuss the factors affecting the reproducibility of retention indices and quantitation in the simultaneous analysis of compounds with a wide range of boiling points by temperature-programmed capillary GC, and report a reliable automated method.

EXPERIMENTAL

Gas chromatography

All experiments were carried out using an Hewlett-Packard Model 5890A gas chromatograph equipped with a flame ionization detector and a split/splitless injection system. A 12.5 m × 0.20 mm I.D. fused-silica capillary column, Ultra 1, with a film thickness of 0.11 μm of a cross-linked dimethylpolysiloxane was used. The oven temperature was programmed from 120 to 325°C at a rate of 5°C/min with a 5-min hold at 325°C. The injection and detector temperatures were set at 340°C. Helium was used as a carrier gas at a linear velocity of 45 cm/s at 120°C. A split injection technique was used with a splitting rato of 80:1 in all analyses. All samples were automatically injected into the gas chromatograph by an Hewlett-Packard Model 7671A automatic sampler. Peak areas and retention times were obtained by an Hewlett-Packard Model 3392A integrator. These data were transferred to a personal computer, PC-98XA (NEC, Japan) with a 20-Mbyte hard disk, connected to the integrator by RS-232C interfaces, and were then processed by the personal computer.

Reagents and chemicals

Authentic hydrocarbons with even carbon numbers in the range of *n*-C_{12}–*n*-C_{44} were used as references for the calculation of retention indices. The *n*-C_{42} alkane, which is not commercially available, was synthesized from behenic acid by the Kolbe reaction[12]. Other hydrocarbons and all the standard compounds used in the present study were obtained from various suppliers and were used without further purification. All the reagents were of reagent grade.

Preparation of samples

A solution of reference hydrocarbons and all solutions of standard compounds were prepared by mixing 25 mg of each hydrocarbon or standard compound with 100 ml of chloroform. An unknown sample solution was prepared as follows; a sample containing 0.5–10 mg of each compound of interest was placed in a 30-ml beaker, and was dried in an electrical drying oven at 105°C for 2 h. To the sample, 10 ml of chloroform with (for the quantitation) or without (for the identification) a known amount of internal standards were added.

Automated capillary GC analysis

Fig. 1 illustrates an outline of the automated GC analysis. All sample solutions (2 μl) were injected into a gas chromatograph by using an automatic sampler. After the analysis of each sample, the data on retention times and peak areas were transferred to a personal computer. For the reference hydrocarbons, standard retention times were determined and the new retention times used to calculate retention indices in the

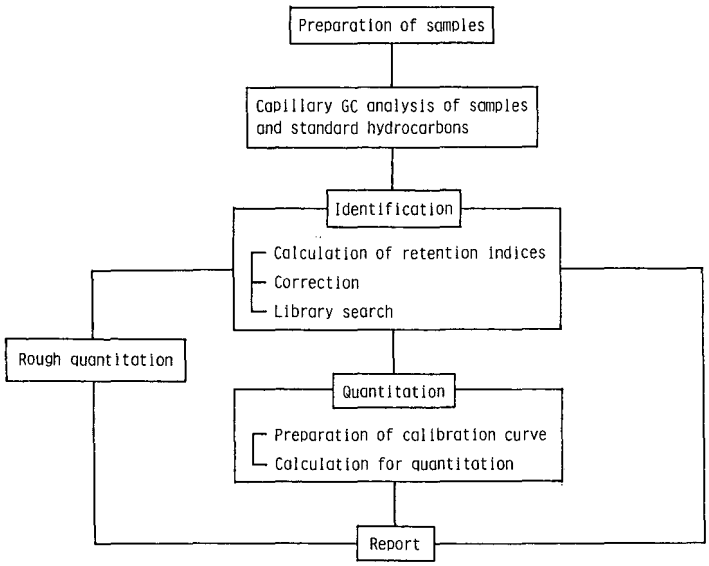

Fig. 1. An outline of the automated analysis system.

subsequent analysis. For an unknown sample, the retention indices, $I_{org.}$, of each peak were calculated using the expression proposed by Van den Dool and Kratz[13]

$$I_{org.} = 100n + 2 \cdot 100 \cdot \frac{T_X - T_{Cn}}{T_{Cn+2} - T_{Cn}} \quad (1)$$

where X is a compound of interest, C is a standard hydrocarbon, T is the retention time and n is the carbon number of a standard hydrocarbon immediately prior to the compound X. Then, the corrected retention indices, $I_{corr.}$, were calculated according to

$$I_{corr.} = I_{org.}\,(aX^3 + bX^2 + cX + d + 1) \quad (2)$$

where X is the peak area of the compound of interest, and a,b, c and d are constants (see Fig. 6). The corrected retention indices were then searched with an in-house retention index data base to identify the compounds. The results were printed out in a suitable format. A series of such processes was carried out automatically. When n-C_{28} alkane was added to the sample as an internal standard, semiquantitative analysis was carried out and the results printed out together with those for the identification. The subsequent quantitative analysis of the compounds identified, including the preparation of calibration graphs, quantitation and printing out of the results, was also carried out automatically.

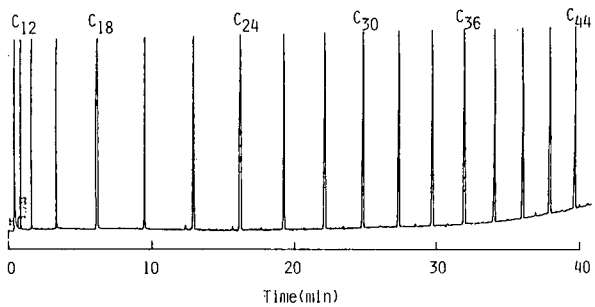

Fig. 2. Gas chromatogram of a mixture of standard hydrocarbons.

RESULTS AND DISCUSSION

Optimization of the GC conditions

The GC conditions were investigated with respect to the analysis time, resolving power and thermal stability of the columns. Polar columns with polyethylene glycol as a liquid phase gave unsatisfactory results because of the insufficient long-term stability and the strong retention of compounds with high boiling points. On the other hand, an Ultra 1 column with a thin film (0.11 μm) of cross-linked methyl silicone gave symmetrical peaks and good resolving power for compounds not only with low and medium boiling points but also with high boiling points. A column with a thick film of the same liquid phase afforded unsuitably long retention times for compounds with high boiling points. Therefore, the Ultra 1 column was used in the subsequent studies.

Based on the results described above and the investigation of other factors such as the column temperature, length and inner diameter of the column, the linear velocity of the carrier gas, etc., the optimum GC conditions were established as shown in the Experimental section. Under these conditions, a variety of compounds with I values in the range of 1200–4400 were analyzed within 40 min, as shown in Fig. 2. This method

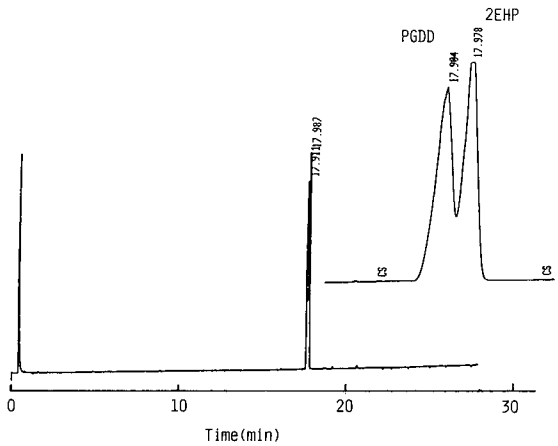

Fig. 3. Resolving power of the proposed method. Peaks: PGDD = propylene glycol didecanoate (I = 2482.3); 2EHP = 2-ethylhexyl palmitate (I = 2488.3).

gave relatively good resolving power in spite of the use of a short column (15 m), as shown in Fig. 3 which indicates a 20% valley separation of two compounds differing by 6.0 index units in retention indices, PGDD (I = 2482.3) and 2EHP (I = 2488.3).

Reproducibility of retention indices

The practical usefulness of the method proposed depends strongly on the reproducibility of the retention indices. Therefore, several factors affecting the reproducibility were investigated. Table I shows the effect of the injection methods on the reproducibility of retention indices in the replicate analyses (n = 10). A standard sample solution containing five compounds was separately injected, or co-injected together with the reference hydrocarbons. Both injection methods gave satisfactory reproducibilities within 0.5 index units standard deviation for all the compounds. However, slightly poorer reproducibility was obtained for compounds with high boiling points when a separate injection method was applied. In the present study, a separate injection method was chosen because of the convenience of the analysis of practical samples.

In GC analysis of compounds with high boiling points over a long period, the remaining compounds in a column and the use of high temperatures frequently result in thermal decomposition of the liquid phase, which greatly affects the reproducibility of retention indices. Therefore, the long-term reproducibility of retention indices under nominally unchanged chromatographic conditions was investigated using the various types of compounds listed in Table II. As shown in Fig. 4, the variations in the retention indices over a period of 6 months were within 3 index units for almost all the compounds, and no variation in the resolving power and the peak shape was observed during this period. These results indicate that the method proposed permits the relatively reliable identification of compounds with a wide range of boiling points over a long period.

Table III shows the retention indices of several compounds, determined with three columns having different lot numbers. Excellent inter-column reproducibility was obtained for all the compounds. Other factors affecting the reproducibility of retention indices, such as the solvents and the linear velocity of the carrier gas had no

TABLE I

EFFECT OF THE INJECTION METHODS ON THE REPRODUCIBILITY OF RETENTION INDICES IN REPLICATE ANALYSES

Sample	*Retention index*	*Standard deviation*	
		Separate injection	*Co-injection*
Lauryl alcohol	1442.8	0.44	0.05
Methyl stearate	2109.4	0.30	0.09
Propylene glycol didecanoate	2482.5	0.25	0.10
Myristyl myristate	2947.2	0.18	0.20
Octyldodecyl erucate	4129.2	0.42	0.35

TABLE II
COMPOUNDS USED AND THEIR RETENTION INDICES

Sample	*Retention index*
Methyl caprate	1281.5
Laurylamine	1426.2
Lauryl alcohol	1441.7
o-Hydroxybiphenyl	1455.6
2,6-Di-*tert.*-butylhydroxytoluene	1471.2
Cetyl alcohol	1856.4
Methyl palmitate	1904.7
Stearyl alcohol	2060.9
Methyl stearate	2108.2
Ethylene glycol monopalmitate	2200.2
Ethylene glycol monostearate	2403.1
Propylene glycol didecanoate	2481.6
Glycerol tri-2-ethylhexanoate	2602.5
Squalene	2663.1
Myristyl myristate	2946.3
Cholesterol	3003.5
dl-α-Tocopherol acetate	3132.2
Pentaerythritol tetra-2-ethylhexanoate	3267.4
2-Tetradecyloctadecanol	3381.2
Diisostearyl malate	3465.3
Ethylene glycol dipalmitate	3656.0
Distearylmethylamine	3699.9
2-Hexadecyleicosanol	3782.1
Ethylene glycol distearate	4056.8
Octyldodecyl erucate	4126.3

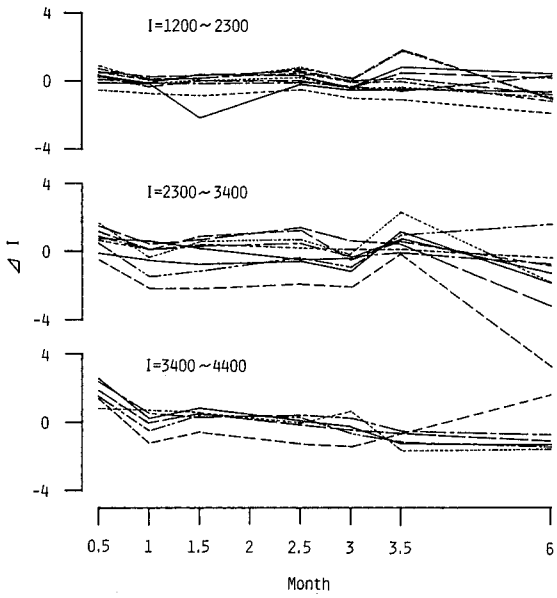

Fig. 4. Long-term reproducibility of retention indices of various compounds.

TABLE III
COMPARISON OF RETENTION INDICES DETERMINED WITH THREE COLUMNS HAVING DIFFERENT LOT NUMBERS

Sample	*Retention index*		
	Column 1	*Column 2*	*Column 3*
Methyl caprate	1281.5	1282.9	1283.8
Laurylamine	1426.2	1427.2	1427.2
Di-*tert.*-butylhydroxytoluene	1471.2	1472.7	1472.8
Stearyl alcohol	2060.9	2062.3	2061.4
Propylene glycol didecanoate	2481.6	2482.5	2482.1
Glycerol tri-2-ethylhexanoate	2602.5	2603.5	2602.5
dl-α-Tocopherol acetate	3132.2	3132.1	3131.4
Ethylene glycol dipalmitate	3656.0	3658.9	3656.8
Distearylmethylamine	3699.9	3700.2	3700.5

influence on the reproducibility. On the basis of these results, the error window of retention indices in the identification of unknown compounds was determined to be 4 index units.

Influence of the concentration of a compound on the retention index

As described above, the method proposed gave excellent reproducibility of the retention indices for various compounds with the same concentration. However, it was found that the retention indices were dependent upon the concentration of the compound of interest, as shown by the dotted line in Fig. 5. The retention indices gradually increased with increasing concentration of the compounds, and a ten-fold increase in the concentration resulted in an increase of 4–8 retention index units. Similar results were obtained for all the compounds listed in Table II. The

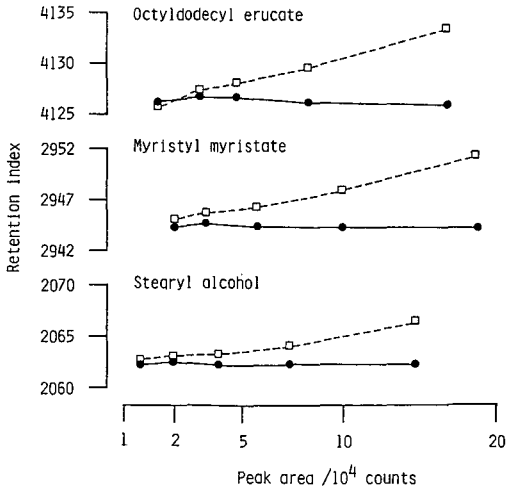

Fig. 5. Relationship between peak areas and retention indices: □---□, before correction; ●—●, after correction.

concentration dependence of retention indices is a significant problem in the practical use of the method proposed. The dependence decreased on a capillary column with a thick film of liquid phase, however the column was not suitable for the present study as described above. This behaviour suggests that the degree of the variation was related to the amounts of compounds injected. Therefore, the relationship between the degree of the variation in retention indices and the peak areas which are proportional to the amounts was examined. As shown in Fig. 6, a definite correlation was found to exist between these two, which could be expressed approximately as the third degree of a function of the peak areas. Therefore, we attempted to correct retention indices on the basis of peak areas. The full line in Fig. 5 shows the relationship between the peak areas and retention indices after this correction. No variation in the corrected retention indices was observed over the whole range of peak areas. Thus, the concentration dependence of the retention indices can be cancelled by the correction based on peak areas.

Quantitation

The on-column injection technique gives superior quantitation and high sensitivity, having been used in quantitative capillary GC analysis. However, this technique is not suitable for routine analysis because of the tendency to column decomposition and the need for special equipment for automatic analysis. This led us to investigate the quantitation by a split injection technique which is most widely used in capillary GC analysis.

Fig. 7 shows the reproducibility of the response factors for eight compounds relative to *n*-C_{28} alkane (an internal standard). The single internal standard technique gave good reproducibility within 3% relative for compounds which were eluted in the proximity of the internal standard, however poor reproducibility was observed for other compounds. The reason for this behaviour is considered to be that non-uniformity of splitting of the components vaporized in an injection port takes place

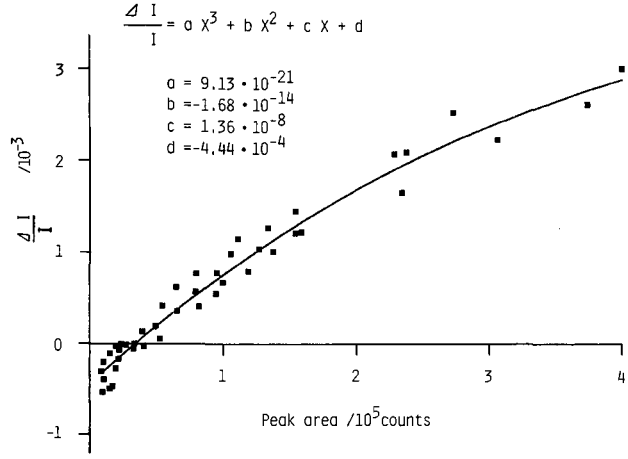

Fig. 6. Relationship between peak areas and the degree of the variation in retention indices, $\Delta I/I = (I_X - I)/I$, where I_X is the retention index of a target compound the peak area of which is X, I is the retention index of the target compound in concentration of 0.025%.

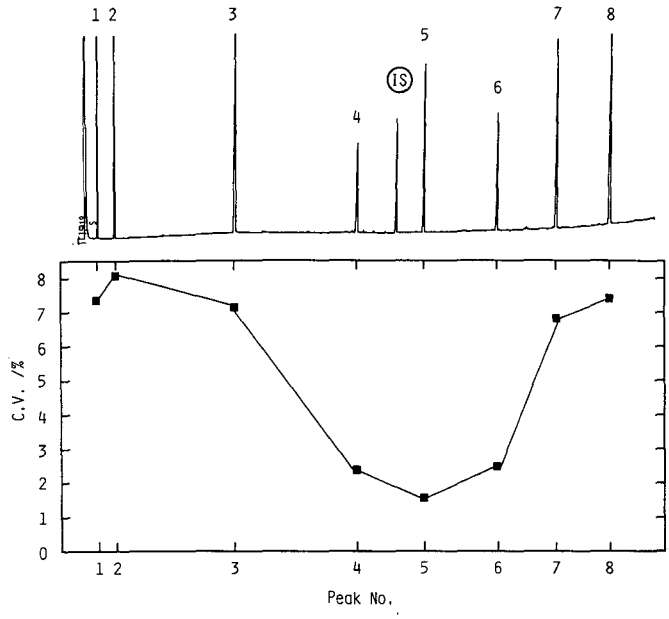

Fig. 7. Reproducibility of relative response factors in replicate analyses by a single internal standard (IS) technique.

depending on the differences in volatility of the components. Therefore, when a compound with a boiling point similar to that of a compound to be quantified is used as an internal standard, relatively good reproducibility can be obtained since these compounds are thought to undergo a similar degree of preferential loss. This suggests that the use of several internal standards with different boiling points would make it possible to quantify simultaneously compounds with a wide range of boiling points. Therefore, the use of a multi-internal standard technique was examined. The chromatogram was divided into three regions (A, B and C in Fig. 8) and an internal standard eluting in the same region as the unknown compounds was used to calculate their relative response factors. As shown in Fig. 8, this technique gave good reproducibility for all the compounds.

The accuracy of the method was tested by adding known amounts of six compounds with a wide range of boiling points to a commercial rinse and lotion. The recoveries were 97–101% as shown in Table IV. Fig. 9 shows the long-term reproducibility of the relative response factors. Satisfactory reproducibility was obtained over a period of 28 days.

The use of more than three internal standards was also investigated, however, similar reproducibilities were observed. Therefore, the number of internal standards employed was three.

These results indicate that the multi-internal standard technique permits the simultaneous quantitation of compounds with a wide range of boiling points in capillary GC analysis by a split injection technique.

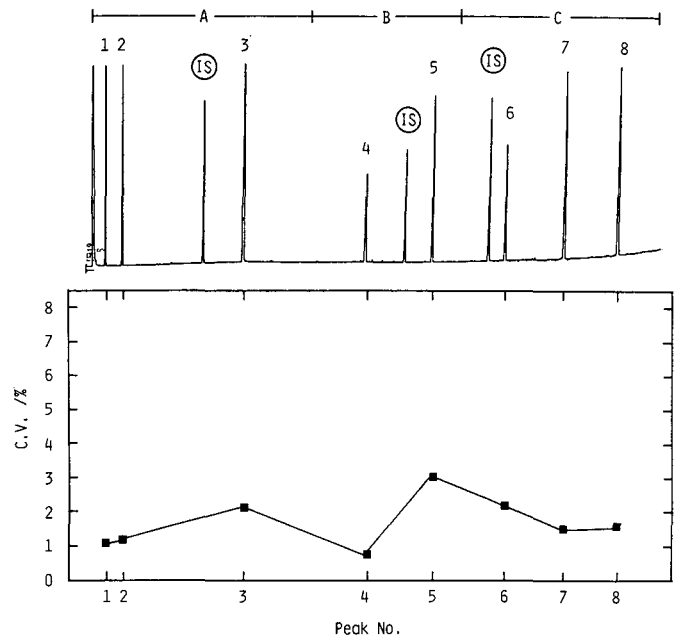

Fig. 8. Reproducibility of relative response factors in replicate analyses by a multi-internal standard technique.

Automation

The method proposed involves several time-consuming and cumbersome processes; the calculation and correction of retention indices, a library search based on corrected retention indices, etc. Therefore, a series of the processes were fully automated by connection of the GC system to a personal computer as shown in the Experimental section. All the analyst has to do is to place the samples in an automatic sampler and then push a button on the integrator attached to the gas chromatograph in

TABLE IV

RECOVERY IN THE ANALYSIS OF A COMMERCIAL RINSE AND LOTION BY THE METHOD PROPOSED

Compound added	*Added (%)*	*Found (%)*		*Recovery (%)*	
		Rinse	*Lotion*	*Rinse*	*Lotion*
Methyl caprate	0.300	0.296	0.291	98.7	97.1
2-Heptylundecanol	0.300	0.302	0.300	100.6	100.0
Eicosanol	0.300	0.295	0.290	98.2	96.6
2-Ethylhexyl palmitate	0.300	0.304	0.297	101.2	99.0
Cholesterol caprylate	0.300	0.295	0.295	98.4	98.4
Pentaerythritol tetra-2-ethylhexanoate	0.300	0.298	0.304	99.4	101.3

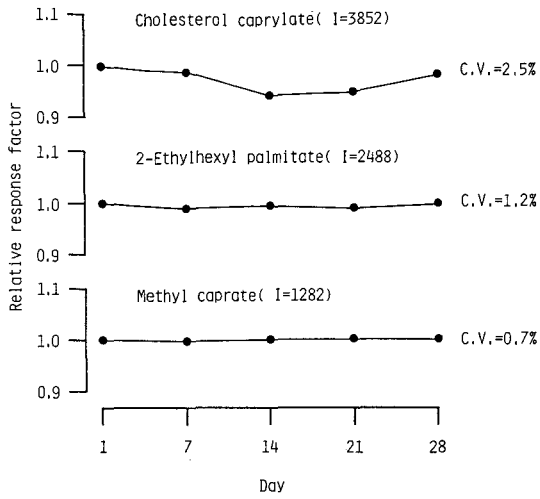

Fig. 9. Long-term reproducibility of relative response factors over a period of 28 days.

order to start the analysis. The automation of these processes would make the method more useful.

Application

The method proposed was applied to the analysis of a commercial cosmetic product. Fig. 10 shows the chromatogram of the analysis of a commercial lotion. All the compounds of interest could be identified by the library search based on their corrected retention indices and quantified, as shown in Table V. These results are in good agreement with those obtained by GC–mass spectrometry. This method was successfully applied also to the analysis of other cosmetic products and several kinds of industrial materials.

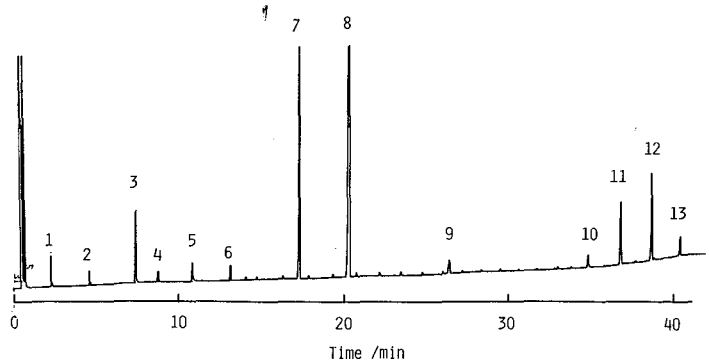

Fig. 10. Analysis of a commercial lotion. See Table V for peak identification.

TABLE V
RESULTS OF THE ANALYSIS OF THE COMMERCIAL LOTION BY THE METHOD PROPOSED

Peak No.	*Retention time (min)*	*Retention index*	*Difference**	*Compound identification*	*Content (%)*
1	2.475	1467.0	2.2	Ethyl *p*-hydroxybenzoate	0.06
2	4.743	1671.1	3.3	*n*-Butyl *p*-hydroxybenzoate	0.08
3	7.565	1856.3	2.3	Cetyl alcohol	0.24
4	8.952	1938.4	2.4	Oxybenzone**	0.07
5	11.041	2060.9	0.7	Stearyl alcohol	0.14
6	13.397	2198.5	3.6	Escalol 507***	0.09
7	17.648	2460.3	0.6	Cetyl isooctanoate	1.68
8	20.628	2660.1	−1.6	Stearyl isooctanoate	0.44
9	26.938	3130.7	1.8	Tocopherol acetate	1.01
10	35.523	3895.4	−0.8	Jojoba oil	0.81
11	37.535	4097.2	2.0	Jojoba oil	0.81
12	39.456	4300.9	2.7	Jojoba oil	0.89
13	41.259	4470.0	0.9	Jojoba oil	0.99

* The difference between the *I* of a target compound and that of the corresponding compound in our data base.

** 2-Hydroxy-4-methoxybenzophenone.

*** 2-Ethylhexyl *p*-dimethylaminobenzoate.

CONCLUSION

A simple and reliable automated method has been developed for the simultaneous analysis of compounds with a wide range of boiling points by using temperature-programmed capillary GC. It is based on the use of a corrected retention index system and a multi-internal standard technique, which permits the reliable identification and precise quantitation of such compounds. The method provides a very useful means for the simultaneous analysis of mixed unknown volatiles.

REFERENCES

1 E. sz. Kováts, *Helv. Chim. Acta*, 41 (1958) 1915.
2 H. Knöppel, M De Bortoli, A. Peil and H. Vissers, *J. Chromatogr.*, 279 (1983) 483.
3 P. A. D'Agostino and L. R. Provost, *J. Chromatogr.*, 331 (1985) 47.
4 K. Tanaka and D. G. Hine, *J. Chromatogr.*, 239 (1982) 301.
5 P. Schepers, J. Wijsbeek, J. P. Franke and R. A. de Zeeuw, *J. Forensic Sci.*, 27 (1982) 49.
6 W. H. Anderson and D. T. Stafford, *J. High Resolut. Chromatogr. Chromatogr. Commun.*, 6 (1983) 247.
7 W. G. Jennings and T. Shibamoto, *Quantitative Analysis of Flavor and Fragrance Chemicals by Glass Capillary Gas Chromatography*, Academic Press, New York, 1980.
8 M. Y. Tsai, C. Oliphant and M. W. Josephson, *J. Chromatogr.*, 341 (1985) 1.
9 D. L. Vassilaros, R. C. Kong, D. W. Later and M. L. Lee, *J. Chromatogr.*, 252 (1982) 1.
10 A. Yasuhara, M. Morita and K. Fuwa, *J. Chromatogr.*, 328 (1985) 35.
11 G. L. Hall, W. E. Whitehead, C. R. Mourer and T. Shibamoto, *J. High Resolut. Chromatogr. Chromatogr. Commun.*, 9 (1986) 266.
12 L. Eberson, in S. Patai (Editor), *The Chemistry of Carboxylic Acids and Esters*, Wiley-Interscience, New York, 1969, pp. 53–101.
13 H. van den Dool and P. D. Kratz, *J. Chromatogr.*, 11 (1963) 463.

Journal of Chromatography, 454 (1988) 121–128
Elsevier Science Publishers B.V., Amsterdam — Printed in The Netherlands

CHROM. 20 810

SOLID SORBENT SAMPLING AND CHROMATOGRAPHIC DETERMINATION OF GLYCIDYL ETHERS IN AIR

JAN-OLOF LEVIN*, KURT ANDERSSON and ROSE-MARIE KARLSSON
National Institute of Occupational Health, Research Department in Umeå, Analytical Chemistry Division, P.O. Box 6104, S-900 06 Umeå (Sweden)
(First received May 2nd, 1988; revised manuscript received July 8th, 1988)

SUMMARY

Activated charcoal, Amberlite XAD-2 and XAD-7 were evaluated as solid sorbents for air sampling of isopropyl glycidyl ether (IGE), allyl glycidyl ether (AGE), *n*-butyl glycidyl ether (BGE), phenyl glycidyl ether (PGE) and *o*-cresyl glycidyl ether (CGE). IGE, AGE and BGE were determined by capillary gas chromatography and flame ionization detection, PGE and CGE by high-performance liquid chromatography and ultraviolet detection. Amberlite XAD-7 was the best sorbent for all glycidyl ethers except IGE, which showed insufficient retention on this sorbent. Activated charcoal gave good recoveries only for IGE, AGE and BGE. The storage stability was acceptable on all three sorbents, and relative humidity had little effect on retention and recovery.

INTRODUCTION

Glycidyl ethers may be considered ethers of 2,3-epoxypropanol ("glycidol"):

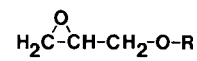

According to IUPAC nomenclature, the glycidyl ethers are derivatives of the three-membered oxirane ring. Since this ring is highly strained, epoxide-containing compounds will react with almost all nucleophilic (electron-donating) substances. Glycidyl ethers have become important because of this reactivity. The major industrial use of these compounds is as reactive diluents in epoxy resin systems, where the epoxide groups react to form cross-linkages within the resin. The glycidyl ethers most commonly used today include allyl glycidyl ether (AGE), *n*-butyl glycidyl ether (BGE), isopropyl glycidyl ether (IGE), phenyl glycidyl ether (PGE) and *o*-cresyl glycidyl ether (CGE). The oligomer with the lowest molecular weight of the glycidyl ether of bisphenol A, diphenylol propane diglycidyl ether, is probably the most common component of uncured epoxy resin[1]. In view of its toxicity, diglycidyl ether (DGE) is rarely found in industry today[1].

0021-9673/88/$03.50

TABLE I

OCCUPATIONAL LIMITS FOR GLYCIDYL ETHERS IN SWEDEN AND THE UNITED STATES, AS TIME-WEIGHTED AVERAGES FOR 8 h

Compound	*Occupational limit value (mg m^{-3})*	
	Sweden	*U.S.A.*
Isopropyl glycidyl ether	–	240
Allyl glycidyl ether	–	22
n-Butyl glycidyl ether	50	135
Phenyl glycidyl ether	60	6
o-Cresyl glycidyl ether	70	–

The primary effects of glycidyl ethers on workers are irritation and skin sensitization[2]. In 1978 NIOSH (U.S. National Institute for Occupational Safety and Health) estimated that 118 000 workers in the U.S.A. were exposed to glycidyl ethers and that an additional 1 000 000 workers were exposed to epoxy resins[1].

Table I shows the occupational limits for certain glycidyl ethers in Sweden[3] and the U.S.A.[4].

The use of solid sorbents for air sampling is preferable for the determination of workers exposure. NIOSH recommends activated charcoal for the sampling of IGE, BGE and PGE[5]. The charcoal tubes are desorbed with carbon disulphide and the glycidyl ethers are determined by gas chromatography (GC). Sampling on Tenax GC and diethyl ether desorption is recommended for AGE[6]. No recovery studies have been reported. In 1981 a method for determining μg/l amounts of BGE, using high-performance liquid chromatography (HPLC) and ultraviolet detection at 245 nm, was published[7]. Attempts to reproduce this method failed since BGE shows practically no absorption in the ultraviolet region.

For several years we have been evaluating the Amberlite XAD porous polymers for sampling organics in workroom air[8–18]. In the present work we have evaluated XAD-2 and XAD-7, together with activated charcoal, for the sampling of industrially important glycidyl ethers in combination with chromatographic determination.

EXPERIMENTAL

Reagents

The solvents used were dichloromethane (B & J), acetonitrile (Rathburn, HPLC Grade) and water (Milli RQ-purified). The glycidyl ethers used were BGE (Fluka, purum), IGE (Merck, zur synthese), AGE (Fluka, purum), PGE (Merck, puriss) and CGE (Polysciences, purum). All were of 99% or higher purity, as determined by GC or HPLC .

The solid sorbents used were activated charcoal (SKC 226-01. Lot 120), Amberlite XAD-2 (SKC 226-30, Lot 285) and XAD-7 (SKC 226-30-11-07, Lot 260). The sorbents (20–40 mesh) were packed in sealed glass tubes (60 mm × 4 mm I.D.) with a 15-mm trapping section (100 mg) and an 8-mm back-up section (50 mg).

Recovery experiments

Recovery experiments were performed using air with known relative humidity. The humidified air was produced by saturation with water in gas dispersion bottles and dilution with dry air in an apparatus described previously[15]. To provide constant flow-rates for seven parallel adsorbent tubes, the humidified air was split between eight glass capillary tubes. Glass capillaries with a diameter of 0.30 mm and a length of 20 mm, giving a flow-rate of 200 ml min^{-1}, were used. One of the capillaries was connected to a relative humidity meter (Humicap 14; Vaisala OY, Helsinki, Finland). A glass tube, 80 mm × 4 mm I.D., provided with an injection port, was connected to each of the other capillaries. The glycidyl ether to be investigated was dissolved in dichloromethane (IGE, BGE) or acetonitrile (AGE, PGE, CGE), and 10 μl of this solution were injected through the injection port into the glass tube. The adsorbent tubes were directly connected to the injection tubes. When 5 or 25 l of air had been sampled, the glycidyl ether was desorbed by shaking the adsorbent beads for 30 min with 3.0 ml of dichloromethane or acetonitrile. IGE, AGE and BGE were generated at room temperature, PGE at 80°C and CGE at 125°C.

GC

The recoveries of IGE, AGE and BGE were determined by capillary GC. An Hewlett-Packard 5890 gas chromatograph and a cross-linked 5% phenylmethylsilicone fused-silica capillary column, 25 m × 0.32 mm I.D., and film thickness 1.05 μm, were used. The splitting ratio was 1/30. The flame ionization detector temperature was 250°C for all three compounds. The column temperature was 60°C for IGE, 90°C for AGE and 130°C for BGE. Detection limits for IGE, AGE and BGE were all below 5% of the occupational limit, calculated for a 5-l air sample, a 3.0-ml desorption volume and a 2-μl injection volume.

HPLC

The recoveries of PGE and CGE were determined by HPLC. A Waters HPLC system, consisting of an M-6000 A pump, an M-710 B autosampler, an M-730 integrator and an M-440 absorbance detector, was used. The column was a Waters Radial-Pak Resolve (100 mm × 5 mm I.D., octadecylsilane, 10-μm particles). The mobile phase was 50% water in acetonitrile, and the flow-rate was 1.0 ml min^{-1}. The glycidyl ethers were detected at 280 nm with a detection limit of approximately 5 ng, corresponding to 0.3 mg m^{-3} in a 5-l air sample with an injection volume of 10 μl.

RESULTS

Recovery from activated charcoal

Since activated charcoal is the most frequently used sorbent for air sampling, it was evaluated for all five glycidyl ethers. Carbon disulphide and dichloromethane were evaluated for desorption of IGE and BGE. Both solvents gave satisfactory recoveries, but dichloromethane was chosen since it contaminated the GC detector to a smaller extent than did carbon disulphide. AGE, PGE and CGE were desorbed with acetonitrile.

Table II reports the recoveries from activated charcoal. The recoveries were determined with glycidyl ether amounts corresponding to 0.1, 1 and 10 times the

TABLE II

RECOVERY OF GLYCIDYL ETHERS FROM ACTIVATED CHARCOAL

Air volume: 5 l. Added amounts of 1200 μg, 110 μg, 250 g, 300 μg and 350 μg correspond to 240, 22, 50, 60 and 70 mg m^{-3}, respectively, in a 5-l air sample. R.S.D. = Relative standard deviation.

Compound	*Amount added (μg)*	*Relative humidity (%)*	*Recovery (%)*	*R.S.D.$_{n=6}$ (%)*
IGE	6000	20	98	3
		85	88	2
	1200	20	101	3
		85	100	5
		85	100	4
		85	98*	4
	120	20	100	4
		85	103	6
IGE**	1200	20	91	4
		85	94	3
AGE	550	20	98	2
		85	96	3
	110	20	98	2
		85	95	5
		85	85*	3
	11	20	96	4
		85	95	1
AGE**	110	20	87	4
		85	88	4
BGE	1250	20	96	2
		85	95	2
	250	20	95	4
		85	94	3
		85	98*	3
	25	20	93	3
		85	92	4
BGE**	25	20	93	2
		85	91	3
PGE	300	20	27	6
		85	26	5
CGE	350	20	8	8
		85	8	8

* A 25-l air sample.

** Stored for 2 weeks at room temperature in the dark.

occupational limits in a 5-l air sample. All recovery experiments were performed at 20 and 85% relative humidity. Exact breakthrough volumes were not determined, but a 25-l air sample was always taken at 85% relative humidity. A breakthrough volume > 25 l means that an 8-h sample with a flow-rate 50 ml min^{-1} can be taken without risk of breakthrough.

As Table II shows, recoveries from activated charcoal are in the range 88–103% for IGE, AGE and BGE. Recoveries at 85% relative humidity are generally somewhat lower. However, the difference is not significant in most cases.

Recoveries of PGE and CGE are considerably lower. The use of more polar or non-polar solvents for desorption did not increase the recovery.

In view of the reactivity of the glycidyl ethers, it was important to determine the storage stability of exposed sorbent tubes. The tubes were stored for 2 weeks at room temperature in the dark before desorption and analysis. Table II also shows the recoveries of IGE, AGE and BGE from charcoal after storage. There is a decrease (statistically significant) in the recovery of IGE and AGE. For BGE, the slight decrease is not statistically significant.

Recovery from Amberlite XAD-2

Table III shows the recoveries of all five glycidyl ethers from XAD-2. IGE and AGE are insufficiently retained on XAD-2. For IGE, there is a substantial

TABLE III

RECOVERY OF GLYCIDYL ETHERS FROM AMBERLITE XAD-2

Compound	*Amount added (μg)*	*Relative humidity (%)*	*Recovery (%)*	*R.S.D.$_{n=6}$ (%)*
IGE	6000	85	49 (20% in back-up)	8
AGE	550	85	72* (16% in back-up)	5
BGE	1250	20	96	2
		85	96	2
	250	20	99	4
		85	97	1
		85	99*	2
	25	20	93	3
		85	99	1
BGE**	25	20	90	1
		85	89	1
PGE	1500	20	89	5
		85	91	3
	300	20	93	4
		85	94	1
		85	94*	5
	30	20	99	2
		85	97	1
PGE**	300	20	95	1
		85	94	3
CGE	1750	20	91	3
		85	77	8
	350	20	92	2
		85	79	5
		85	94*	4
CGE	35	20	90	4
		85	91	4
CGE**	350	20	83	4
		85	79	5

* A 25-l air sample.

** Stored for 2 weeks at room temperature in the dark.

breakthrough, even when only 5 l of air are sampled, For AGE, 16% is found in the back-up section when 25 l of air are sampled. For BGE, the recoveries range between 93 and 99%. PGE is recovered to 89–99%, with no significant differences between 20 and 85% relative humidity. As Table III shows, CGE is recovered to more than 90% at most levels and relative humidities. At 85% relative humidity, however, there is

TABLE IV

RECOVERY OF GLYCIDYL ETHERS FROM AMBERLITE XAD-7

Compound	*Amount added (μg)*	*Relative humidity (%)*	*Recovery (%)*	*R.S.D.$_{n=6}$ (%)*
IGE	6000	85	77 (18% in back-up)	4
AGE	550	20	98	2
		85	96	3
		85	87* (5% in back-up)	3
	110	20	98	2
		85	95	5
		85	96*	1
	11	20	96	4
		85	95	1
AGE**	110	20	93	2
		85	93	3
BGE	1250	20	97	3
		85	96	2
	250	20	96	3
		85	97	2
		85	98*	1
	25	20	92	7
		85	97	4
BGE**	25	20	89	4
		85	88	2
PGE	1500	20	90	2
		85	90	5
	300	20	93	3
		85	91	4
		85	94*	4
	30	20	95	3
		85	98	3
PGE**	300	20	95	2
		85	91	3
CGE	1750	20	87	4
		85	77	7
	350	20	89	3
		85	95	2
		85	94*	3
	35	20	82	1
		85	92	1
CGE**	350	20	77	10
		85	77	2

* A 25-l air sample.

** Stored for 2 weeks at room temperature in the dark.

a decrease in recovery at 1750 and 350 μg. This decrease is not due to a breakthrough.

Table III also shows the storage stability data for the glycidyl ethers BGE, PGE and CGE on XAD-2. The exposed tubes were stored for 2 weeks at room temperature in the dark. In the case of BGE there is a 10% decrease ib recovery. PGE is unaffected by storage, but for CGE the decrease is approximately 10%.

Recovery from XAD-7

The recoveries of IGE, AGE, BGE, PGE and CGE are given in Table IV. IGE is not sufficiently retained on XAD-7; a 18% breakthrough to be back-up section is observed. The retention of AGE is excellent, but a small breakthrough is noted at 85% relative humidity at the 550-μg level when 25 l of air are drawn through the sorbent tube. BGE is well retained under all conditions studied, with a mean recovery of 96%. The recoveries of PGE are in the range 90–98%, with a mean of 93%. For CGE, there is a decrease in recovery at 85% relative humidity at the highest level. The mean recovery at all levels and relative humidities for CGE is 88%.

Table IV also shows the results of storage of AGE, BGE, PGE and CDE on XAD-7. For AGE and PGE, there is no significant decrease in recovery following storage in the dark for 2 weeks at room temperature. A 5–10% decrease is observed for BGE, and the decrease in recovery of CGE is 10–20%.

DISCUSSION

The use of solid sorbents is the most important method for monitoring harmful organic substances in workplace atmospheres. The most frequently used method is sampling on an activated charcoal sorbent, followed by carbon disulphide desorption and GC determination. Reactive organic compounds like the glycidyl ethers often decompose or absorb irreversibly on activated charcoal. For such compounds, sorbents of the porous polymer type, *e.g.*, Amberlite XAD, Tenax, Porapak and the Chromosorb 100 series, are useful alternatives.

We have previously shown that phenols[8,18], polychlorinated aromatics[9], glycol ethers[11], polycyclic aromatics[12], organic nitro compounds[13], nitrates[14], amines[16] and ketones[17] are examples of compounds that may adsorb irreversibly or decompose on activated charcoal but may be successfully sampled on XAD polymers. The XAD polymers which have proved most useful are XAD-2, a styrene–divinylbenzene polymer with an active surface of 330 $m^2 g^{-1}$, XAD-4, the same polymer with an active surface of 750 $m^2 g^{-1}$, and XAD-7, a more polar polyacrylic ester with a surface area of 450 $m^2 g^{-1}$.

From Table II it is evident that PGE and CGE show low recoveries from activated charcoal. The poor recoveries are not caused by low retention; no breakthroughs are observed. It is likely that PGE and CGE are adsorbed strongly on, or react with, active sites on the charcoal sampling bed. The aliphatic glycidyl ethers, IGE, AGE and BGE all show recoveries in the range 90–100% if the sorbent tubes are desorbed and analyzed immediately. All three compounds show a decrease in recovery on storage, probably owing to their reactivity. They may, however, be stored for 2 weeks at room temperature in the dark with a loss that is not greater than approximately 10%.

Amberlite XAD-2 retains only 49 and 72% of IGE and AGE, respectively. The

breakthrough volumes of these compounds are less than 5 l on XAD-2, owing to the low polarity and small active surface of this adsorbent. The less volatile BGE, PGE and CGE are quantitatively retained. PGE shows good storage stability, but BGE and CGE show a small decrease in recovery on storage.

Amberlite XAD-7 has a larger surface area and is more polar than XAD-2. Accordingly, the glycidyl ethers should be better retained on this adsorbent. This can indeed be seen from Table IV. Only IGE, the most volatile of the glycidyl ethers, shows a significant breakthrough at the highest level. A 5% breakthrough was noted for AGE at 85% relative humidity at the highest level. Like the other sorbents, on XAD-7 there is some decrease in recovery on storage, especially in the case of CGE. The occasional lower recoveries noted for CGE may, however, be a result of difficulties in the generation of this high-boiling compound.

In summary, the best overall adsorbent appears to be Amberlite XAD-7. Except for the most volatile, IGE, all glycidyl ethers are effectively retained on XAD-7, and can be recovered in high yields. The relative humidity has little influence on recovery. As a rule, no more than 5–10% is lost if the samples are stored no longer than 2 weeks in the dark at room temperature. In addition, activated charcoal enables good recoveries and acceptable storage stability for the aliphatic glycidyl ethers (IGE, AGE, BGE).

ACKNOWLEDGEMENT

A grant from the Swedish National Board of Occupational Safety and Health is gratefully acknowledged.

REFERENCES

1 *Criteria for a Recommended Standard: Occupational Exposure to Glycidyl Ethers*, U.S. Department of Health, Education and Welfare, National Institute for Occupational Safety and Health, Cincinnati, OH, 1978.
2 N. I. Sax, *Dangerous Properties of Industrial Materials*, Van Nostrand-Reinhold, New York, 4th ed., 1975.
3 *Occupational Limits for Chemical Substances in Work-room Environment*, National Swedish Board of Occupational Safety and Health, AFS 1987:12, Stockholm, 1987.
4 *Threshold Limit Values and Biological Exposure Indices for 1987–88*, American Conference of Governmental Industrial Hygienists, ACGIH, Cincinnati, OH, 1987.
5 *Manual of Analytical Methods*, Vol. 2, DHEW, National Institute for Occupational Safety and Health, Cincinnati, OH, 2nd ed. 1977, methods S77, S81 and S74.
6 *Manual of Analytical Methods*, Vol. 4, DHEW, National Institute for Occupational Safety and Health, Cincinnati, OH, 1978, Method S346.
7 V. M. S. Ramanujam, T. H. Connor and M. S. Legator, *Microchem. J.*, 26 (1981) 217–220.
8 J.-O. Levin, C.-A. Nilsson and K. Andersson, *Chemosphere*, 6 (1977) 595–598.
9 K. Andersson, J.-O. Levin and C.-A. Nilsson, *Chemosphere*, 10 (1981) 137–142.
10 K. Andersson, J.-O. Levin, R. Lindahl and C.-A. Nilsson, *Chemosphere*, 10 (1981) 143–146.
11 K. Andersson, J.-O. Levin, R. Lindahl and C.-A. Nilsson, *Chemosphere*, 11 (1982) 1115–1119.
12 K. Andersson, J.-O. Levin and C.-A. Nilsson, *Chemosphere*, 12 (1983) 197–207.
13 K. Andersson, J.-O. Levin and C.-A. Nilsson, *Chemosphere*, 12 (1983) 377–384.
14 K. Andersson, J.-O. Levin and C.-A. Nilsson, *Chemosphere*, 12 (1983) 821–826.
15 K. Andersson, J.-O. Levin, R. Lindahl and C.-A. Nilsson, *Chemosphere*, 13 (1984) 437–444.
16 K. Andersson and B. Andersson, *Anal. Chem.*, 58 (1986) 1528–1529.
17 J.-O. Levin and L. Carleborg, *Ann. Occup. Hyg.*, 31 (1987) 31–38.
18 J.-O. Levin, *Chemosphere*, 17 (1988) 671–679.

Journal of Chromatography, 454 (1988) 129–143
Elsevier Science Publishers B.V., Amsterdam — Printed in The Netherlands

CHROM. 20 805

GAS CHROMATOGRAPHIC SEPARATION OF HALOGENATED COMPOUNDS ON NON-POLAR AND POLAR WIDE BORE CAPILLARY COLUMNS

G. CASTELLO*, A. TIMOSSI and T. C. GERBINO
Istituto di Chimica Industriale, Università, Corso Europa 30, I-16132 Genova (Italy)
(First received February 24th, 1988; revised manuscript received June 7th, 1988)

SUMMARY

Thirty five halogenated compounds (chloro-, bromo- and iodomethanes, ethanes and ethenes, with one or more different halogen atoms in the molecule) which can be found as contaminants in surface or waste water were analysed on non-polar (SPB-1) and polar (Supelcowax-10) wide bore capillary columns (60 m × 0.75 mm I.D.). Adjusted retention times and retention index values with respect to homologous series of *n*-alkanes and 1-iodoalkanes were measured for identification purposes. The use of capillary columns permits a more efficient separation than by using packed columns, mainly when non-polar stationary phases are used. Only 9 compounds were not resolved on SPB-1 (compared with 14 on packed OV-1), while compounds (different from those not separated on SPB-1) remained poorly resolved on Supelcowax-10 and on packed SP-1000, owing to coincidence of the partition coefficients. The simultaneous use of polar and non-polar capillary columns permits analysis of all of the components of the mixture.

INTRODUCTION

Gas chromatographic (GC) analysis of chlorinated contaminants in drinking water was previously carried out by using headspace and liquid–liquid extraction[1–3]. Packed columns of different polarities were used[4–8] that did not permit the complete separation of very complex mixtures of compounds. The connection of two columns of different polarities or the use of mixed polar–non-polar liquid phases[9,10] allowed a more efficient resolution of trihalogenomethanes and other halogenated compounds.

When these methods are applied to environmental samples, such as waste waters, surface water, contaminated soil and underground water supplies, many peaks, not identified as commonly used solvents, but probably formed by cracking or biological degradation of halogenated polymers, paints, pesticides, etc., are detected by specific electron-capture detection (ECD) and packed columns do not ensure their complete separation. Packed columns, having a maximum of about 4000 theoretical plates when a practically suitable length is used (the mixed polar–non-polar columns previously described[10] had about 2600 theoretical plates for trichloroethylene), do not

0021-9673/88/$03.50

permit the complete separation of all of the possible compounds. By changing the column polarity by use of different amounts of polar and non-polar liquid phases and by using the window diagram method[11,12] to select the best temperature for a given separation[13], a suitable resolution can be achieved between many compounds, but some groups of peaks are still partially overlapped. The retention indices of many halogenated aliphatic and alicyclic compounds were measured by using a fused-silica narrow bore (0.2 mm I.D.) capillary column coated with a non-polar liquid phase (methylsilicone)[14], and a linear relationship was found between the retention index values and the boiling points. Narrow bore capillary columns (0.20–0.25 mm I.D.) show a great resolving power (up to 150 000 plates) but are easily saturated (maximum load capacity 50–100 ng per component). Organic halogenated pollutants are often found in a very wide range of concentrations. The injection of sample volumes large enough to permit the detection of the less concentrated compounds can overload the column with too large amounts of the most common contaminants, yielding non-symmetrical and tailing peaks. Furthermore, the use of the splitting systems necessary in order to inject into the capillary column very small amounts of sample may result in a non-constant splitting ratio as a function of the molecular weight and vapour pressure of the halocarbons, which contributes to the differences in partition ratio during the liquid–liquid or headspace extraction, and to the lack of linearity of some specific detectors. For this reason, many EPA methods[3] still suggest the use of packed columns. Wide-bore glass capillary columns[15–19] permit direct sample injection without better inlet splitting and have higher efficiency compared with packed columns and a good inertness. They were used for the analysis of volatile priority pollutants in water by purge-and-trap extraction and gas chromatography–mass spectrometry (GC–MS)[20] and the factors influencing the behaviour of wide bore columns and their interfacing with the purge-and-trap device were investigated[21].

The search for analysis conditions that permit the best resolution of very complex mixtures, and the possibility of obtaining a positive identification of many compounds on the basis of different polarities, require an exhaustive investigation of many analytical parameters, as the carrier gas flow-rate and the column temperature. This paper describes the results of experiments carried out with polar and non-polar wide-bore capillary columns, for the separation of complex mixtures of halogenated methanes, ethanes and ethenes.

EXPERIMENTAL

The analyses were carried out by using a Varian 3700 gas chromatograph (Varian Associates, Palo Alto, CA, U.S.A.) equipped with nickel-63 electron-capture detection (ECD), linear temperature programming and a Varian Vista 402 integration and data acquisition computer. Flame ionization detection (FID) was also used in order to analyze non-electron-absorbing compounds (alkanes, alcohols) whose GC behaviour was compared with those of halogenated compounds.

Two wide-bore capillary columns (0.75 mm I.D.) were used: non-polar SPB-1 (dimethylpolysiloxane polymer, maximum allowable temperature 320°C) and polar Supelcowax-10 (polyethylene glycol, maximum allowable temperature 280°C with FID, 200°C with ECD) (Supelco, Bellefonte, PA, U.S.A.) both 60 m long. In both columns the stationary phase was chemically bonded to the column wall. The analyses

TABLE I

RETENTION TIMES, t_R, AND NUMBER OF THEORETICAL PLATES, n, ON NON-POLAR (SPB-1) AND POLAR (SUPELCOWAX-10) COLUMNS

Nitrogen flow-rate 4 ml/min.

Compound	*SPB-1*		*Supelcowax-10*	
	t_R *(min)*	$n \cdot 10^{-3}$	t_R *(min)*	$n \cdot 10^{-3}$
Tribromomethane	15.7	76		
Pentachloroethane	25.7	59		
Hexachloroethane	47.3	51		
Bromodichloromethane			22.3	50
Chloroiodomethane			27.9	53
1,1,1,2-Tetrachloroethane			37.5	41
Dibromochloromethane			46.3	45

were carried out on the two columns installed in the GC oven by using the Supelco conversion kit for direct injection and a make-up gas detector adapter in order to supply the proper amount of carrier gas for ECD without influencing the flow-rate into the capillary column. Nitrogen was used as the carrier gas, at a flow-rate of 4 ml/min, selected after a series of experiments carried out to determine the resolving power of the columns as a function of the carrier gas velocity. Flow-rates below 3 ml/min should give an higher number of theoretical plates, n, but the detector response becomes irregular, probably due to imperfect mixing between the gas coming from the column and the make-up gas (30 ml/min). The flow-rate selected represents a good compromise between speed and efficiency. Table I shows the values of t_R and n for some compounds on polar and non-polar columns.

The true temperature of the column was monitored by inserting between its coils a thermocouple connected to a digital thermometer with 0.1°C precision. The gas pressure at the column inlet was monitored by connecting a mercury micromanometer to a capillary T-piece at the injection port. The increase in dead volume was negligible (no appreciable effect on the values of n was found) and the pressure was measured within $\pm$ 1 Torr (133 Pa). The injector and detector temperatures were set at 210 and 260°C, respectively.

Standard solutions of the compounds listed in Table II were prepared at concentrations ranging between 10^{-3} and 1 g/l, taking into account the different sensitivity of ECD to various compounds, in order to have peaks with similar areas. The sample volume injected was 0.5 μl; therefore, the most concentrated samples contained about 0.5 μg of halocarbons, too low to saturate the columns, having a capacity of about 15 μg per peak.

RESULTS AND DISCUSSION

Table II shows the analysed compounds, their boiling points, molecular weights, t'_R and retention relative to 1,1,2-trichloroethylene, r, on SPB-1 and Supelcowax-10 columns at 75°C. Figs. 1 and 3 show the chromatograms of the mixture on the

TABLE II

ADJUSTED RETENTION TIMES, t'_R, AND RETENTION RELATIVE TO 1,1,2-TRICHLOROETHYLENE, r, OF HALOGENATED HYDROCARBONS ANALYZED ON NON-POLAR AND POLAR WIDE BORE CAPILLARY COLUMNS AT 75°C

Boiling points and molecular weights are also reported.

No.	*Compound*	*B.p. (°C)*	*Mol.wt.*	*SPB-1*		*Supelcowax-10*	
				t'_R	r	t'_R	r
1	1,1,1,2-Tetrabromoethane	112	345.67	2.72	0.96	6.24	1.17
2	1,1,1,2-Tetrachloroethane	130.5	167.85	8.14	2.88	29.55	5.53
3	1,1,2,2-Tetrabromoethane	243.5	345.67	19.19	6.80	–	–
4	1,1,2,2-Tetrachloroethane	146.2	167.85	11.66	4.13	145.78	27.27
5	1,1,2-Trichloroethane	113.8	133.41	4.32	1.53	30.30	5.67
6	1,1,2-Trichloroethylene	87	131.39	2.82	1.00	5.35	1.00
7	1,1-Dichloroethane	57.28	98.96	1.06	0.38	2.57	0.48
8	1,1-Dichloroethylene	37	96.94	0.74	0.26	0.96	0.18
9	1,2-Dibromoethane	131.36	187.87	5.73	2.03	29.55	5.53
10	1,2-Dichloroethane	83.74	98.96	1.76	0.63	8.65	1.62
11	1,2-Diiodoethane	200	281.86	24.72	8.77	–	–
12	1-Bromo-2-chloroethane	107	143.20	3.19	1.13	15.84	2.96
13	Bromochloromethane	68.11	129.39	1.24	0.44	7.62	1.43
14	Bromoethane	38.4	108.97	0.74	0.26	1.23	0.23
15	Tribromomethane	149.5	252.75	9.99	3.54	91.05	17.03
16	Tetrabromomethane	189	331.65	33.93	12.03	91.42	17.09
17	Tetrachloromethane	76.54	153.82	2.26	0.80	2.57	0.48
18	*cis*-1,2-Dichloroethylene	60.3	96.94	1.23	0.44	5.20	0.97
19	Trichloromethane	61.7	119.38	1.23	0.44	6.24	1.17
20	Chloroiodomethane	109	176.38	3.10	1.10	20.62	3.86
21	Dibromochloromethane	119	208.29	5.31	1.89	37.62	7.04
22	Dibromomethane	97	173.85	2.72	0.96	16.62	3.11
23	Dichlorobromomethane	90	163.83	2.82	1.00	15.37	2.88
24	Dichloromethane	40	84.93	0.74	0.26	3.44	0.64
25	Diiodomethane	182	267.84	11.98	4.25	116.93	21.88
26	Hexachloroethane	186	236.74	41.80	14.82	80.53	15.07
27	Iodoethane	72.3	155.97	1.28	0.46	2.57	0.48
28	Triiodomethane	218	393.73	20.08	7.12	–	–
29	Iodomethane	42.4	141.94	0.74	0.26	1.67	0.31
30	1,1,1-Trichloroethane	74	133.41	1.91	0.68	2.57	0.48
31	Pentachloroethane	162	202.30	20.08	7.12	84.47	15.80
32	Tetrachloroethylene	121	165.83	6.61	2.34	6.63	1.24
33	*trans*-1,2-Dichloroethylene	47.5	96.94	1.00	0.36	2.18	0.41
34	Trichlorobromomethane	104.7	198.28	4.54	1.61	8.45	1.58
35	1-Iodopropane	102.4	169.99	–	–	4.76	0.89
36	1-Iodobutane	130.5	184.02	–	–	8.45	1.58
37	1-Iodopentane	157	198.05	–	–	15.84	2.96
38	1-Iodohexane	181.3	212.08	–	–	29.55	5.53
39	1-Iodoheptane	204	226.10	–	–	56.33	10.54

non-polar and polar columns respectively. Numbers refer to the compounds listed in Table II. Some compounds were not included in the complete sample, due to the presence of impurities that could interfere with other peaks. Fig. 2 shows an example of a chromatogram of these compounds on the non-polar column.

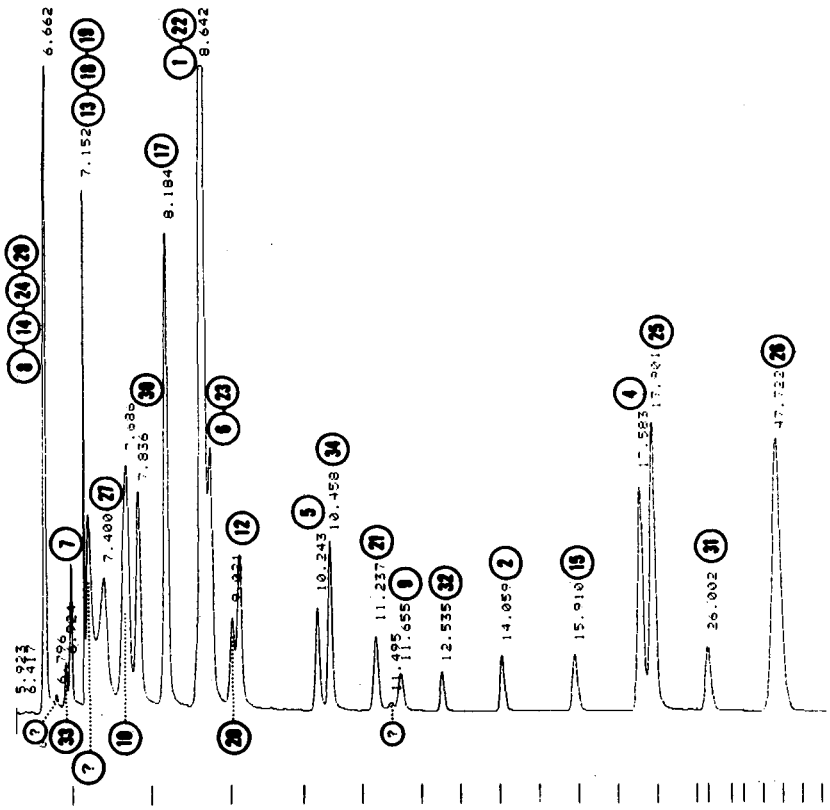

Fig. 1. Chromatogram of halogenated compounds on an SPB-1 wide bore capillary column, 60 m × 0.75 mm I.D., 1.0-μm film. Carrier gas (nitrogen) flow-rate: 4 cm^3/min. Temperature: 75°C. Peak numbers as in Table II.

Some experiments were carried out in order to investigate the effect of temperature on the resolution. On a non-polar column, five groups of peaks are not well resolved (see Fig. 1) at 75°C. (a) 1,1-dichloroethylene; bromoethane; dichloromethane; iodomethane (peaks 8, 14, 24, 29); (b) bromochloromethane; *cis*-1,2-dichloroethylene; chloroform (peaks 13, 18, 19); (c) 1,1,1,2-tetrabromoethane; dibromomethane (peaks 1, 22); (d) 1,1,2-trichloroethylene; dichlorobromomethane (peaks 6, 23); (e) iodoform; pentachloroethane (peaks 28, 31) (see Fig. 2).

Group (a) consists of low boiling compounds, and therefore is suitable to investigate the influence of decreasing temperature. Fig. 4 shows the separation at 33 and 22°C and with temperature programming from 8 to 15°C at about 0.5°C/min obtained by a subambient temperature accessory. Groups (b)–(d) are resolved [except for peaks 1 and 22 (1,1,1,2-tetrabromoethane and dibromomethane)] at 45°C in about 15 min (see Fig. 5). The resolution of group (c) at low temperature on the non-polar column is also possible, but the retention times are too long for practical purposes.

It is known that sometimes the resolution of closely eluting compounds increases with increasing temperature, and that at different temperatures the elution order can

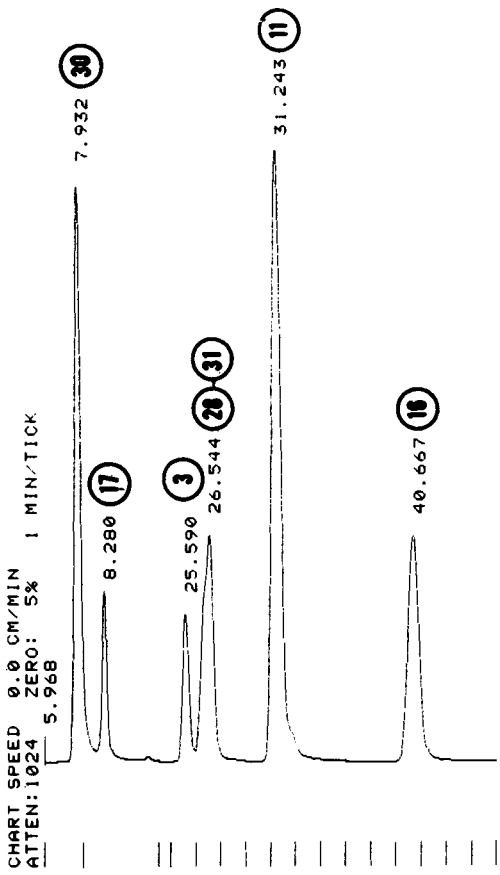

Fig. 2. Chromatogram of halogenated compounds (not included in the mixture of Fig. 1) on an SPB-1 wide bore capillary column. Other details as in Fig.

change. Also in the analysis of these compounds this phenomenon has to be taken into account. As an example, Fig. 6 shows the effect of temperature on the separation of 1,1,1,2-tetrabromoethane, 1,1,2-trichloroethylene, chloroform, tetrachloroethylene (peaks 1,6,19,32), which exhibits an inversion of the elution times between peaks 1 and 19 and a perfect coincidence at 75.5°C. Fig. 7 shows the relative retention, r, of compounds 1, 19 and 32 as a function of the reciprocal of the absolute temperature (Arrhenius plot).

In general, temperature programming offers the best way for separation of complex mixtures, due to both the reduction in analysis time and to the enhanced resolution when intersection of the Arrhenius plots takes place, because peaks separated at low temperature are not combined again when the temperature increases. Therefore, some different programming rates were tested for the separation of the complete mixture. A good compromise between resolution and analysis time was obtained by an initial isotherm at 75°C followed by a linear increment of 20°C/min for

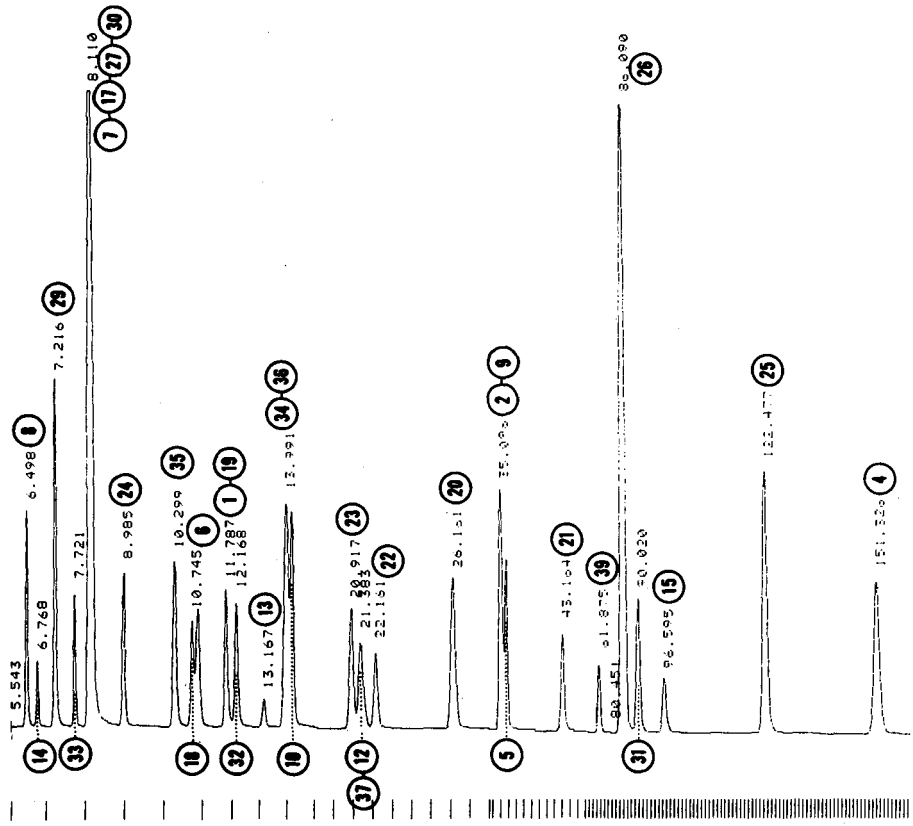

Fig. 3. Chromatograms of halogenated compounds and 1-iodoalkanes on Supelcowax-10 wide bore capillary column, 60 m × 0.75 mm I.D., 1.0-μm film. Carrier gas (nitrogen) flow-rate: 4 cm^3/min. Temperature: 75°C. Peak numbers as in Table II.

the non-polar and of 10°C/min for the polar column up to 120 and 110°C, respectively. Figs. 8 and 9 show the resulting chromatograms. A better resolution can be obtained by using a lower initial temperature, but the time needed for complete analysis strongly increases, as a programming rate greater than 25°C/min may damage the columns.

Polar and non-polar columns can be connected in parallel, by using two detectors and two injectors or a 50/50 capillary splitter on the same injector. Existing data processing systems, such as the dedicated Varian Vista 402 with the two-channel option or the all-purpose software Nelson Series 3000 Laboratory Data System (Nelson Analytical, Cupertino, CA, U.S.A.) with one standard two-channel Model 760 intelligent interface, can automatically integrate and correlate both chromatograms, which ensures a satisfactory resolution of the majority of the peaks of the mixture tested, because the results are complementary. As an example, simultaneous elution of the compounds belonging to group (a), discussed above, which on the non-polar column gives an unique peak at 6.66 min (see Fig. 1) and can be resolved only by decreasing the column temperature with sub-ambient temperature programming, were

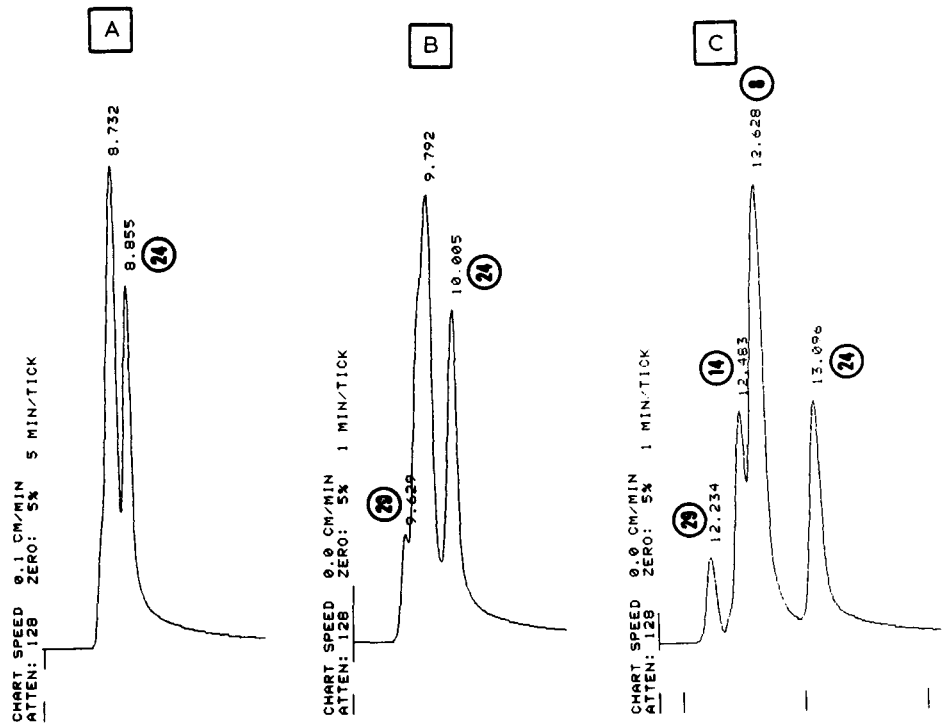

Fig. 4. Chromatogram of incompletely resolved halogenated compounds on an SPB-1 wide bore capillary column at various temperatures: (A) column temperature = 33°C; (B) column temperature = 22°C; (C) temperature programmed from 8 to 15°C at about 0.5°C/min.

completely resolved on the polar column (see Fig. 2). On the contrary, the compounds that coeluted in a peak at 8.11 min on the polar column (1,1-dichloroethane; carbon tetrachloride; iodoethane and methylchloroform, peaks 7, 17, 27 and 30) were easily separated on the non-polar phase.

Nine compounds only were not resolved on non-polar capillary SPB-1, compared with 14 compounds not resolved by using the non-polar packed column OV-1[3–5]. The performance of polar Supelcowax-10 and packed SP-1000 was about the same: 8 compounds (different from those not resolved on SPB-1) were coeluted on both the capillary and packed column; this is due to identical or very similar partition coefficients on the polyethylene glycol liquid phase of the two polar columns, because the efficiency was much greater for the capillary column (40 000–70 000 theoretical plates compared with 3000–4000 for packed columns).

The identification of the compounds on the basis of GC analysis requires a knowledge of the elution order and of the relative positions of the peaks more accurate than that permitted by the use of retention relative to 1,1,2-trichloroethylene, *r* mainly for substances with longer retention times. The use of the retention index, *I*, is more suitable, because this parameter refers to the elution of an homologous series. In the analysis of halogenated compounds, the use of linear alkanes as in the standard

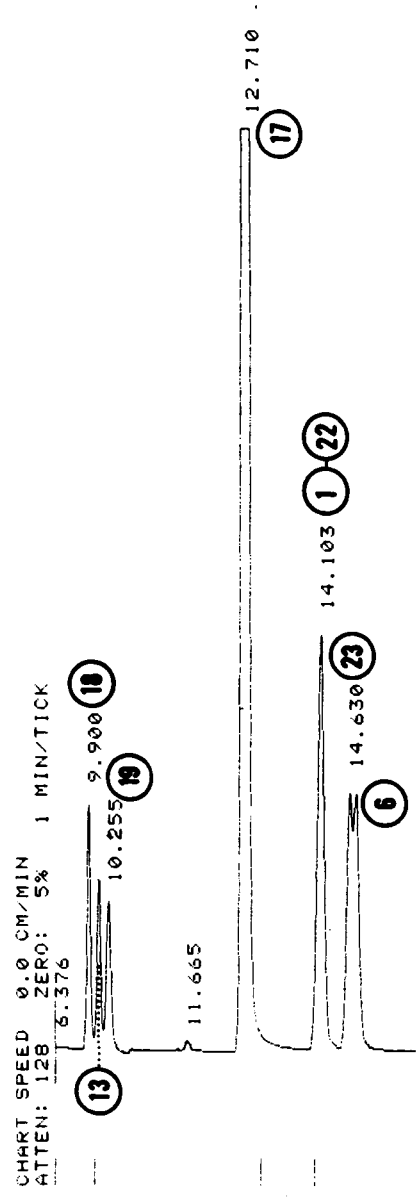

Fig. 5. Chromatogram of incompletely resolved halogenated compounds on an SPB-1 wide bore capillary column at 45°C. Other details as in Fig. 1.

Kováts method[22] is impractical when ECD is used, which is not sensitive to saturated compounds. The homologous series of 1-iodoalkanes was therefore used[23,24] and a correlation between the Kováts I and the I_{ni} with respect to normal iodides can be calculated by using FID and injecting similar amounts of *n*-alkanes and 1-iodoalkanes. Fig. 10 and Table III respectively show the linear behaviour of these homologous series

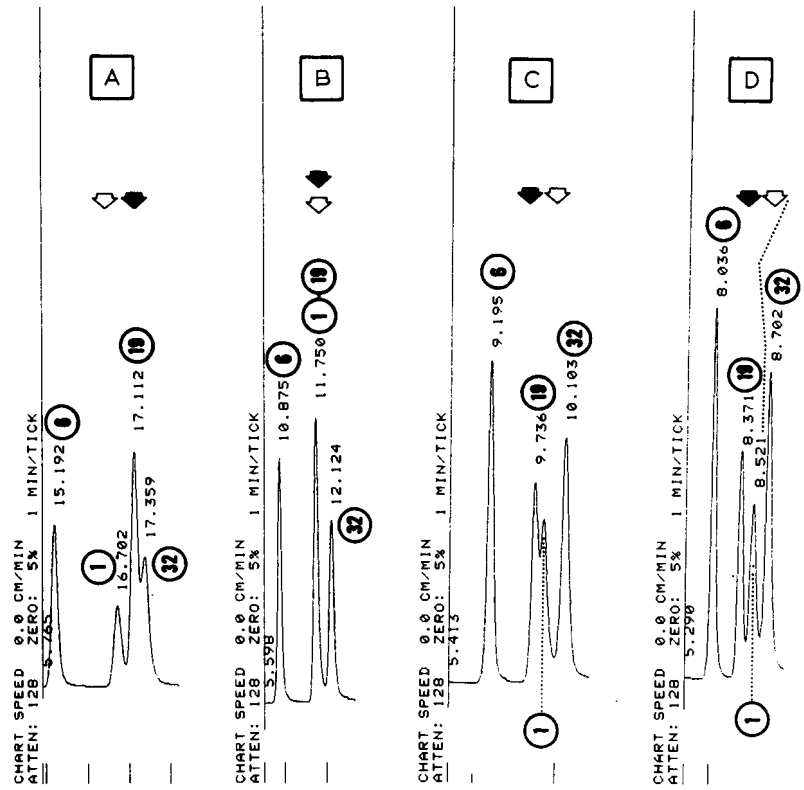

Fig. 6. Effect of temperature on the separation of incompletely resolved halogenated compounds on a Supelcowax-10 wide bore capillary column, showing inversion of the elution order. Column temperatures: (A) 59.8; (B) 75.5; (C) 85.6; (D) 96.3°C.

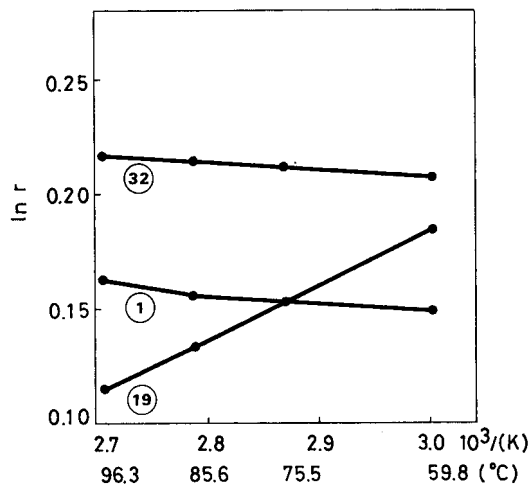

Fig. 7. Logarithm of the retention relative to trichloroethylene as a function of the reciprocal of the absolute temperature for some of the halogenated compounds listed in Table II.

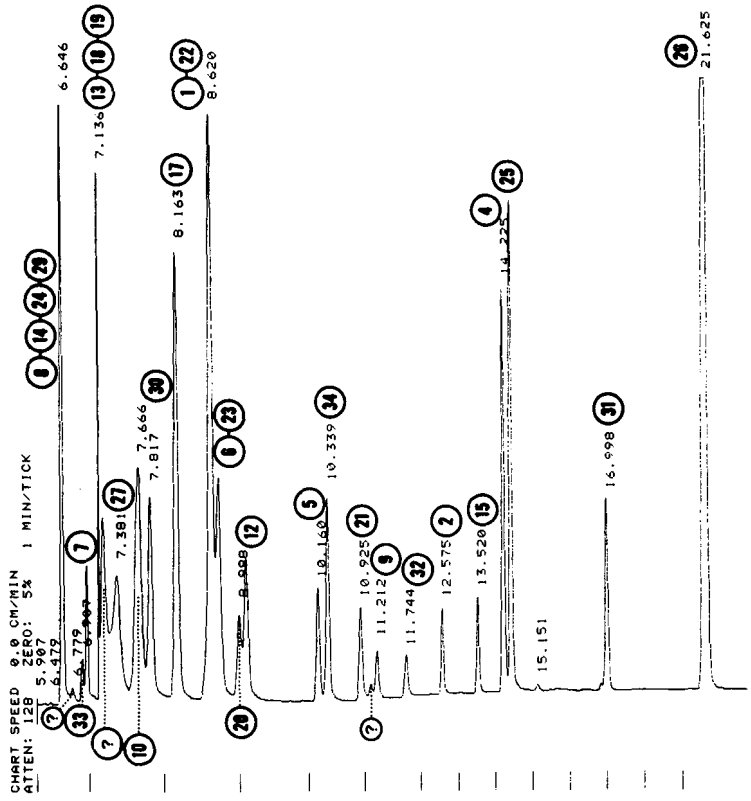

Fig. 8. Chromatograms of halogenated compounds on SPB-1. Temperature programming: isothermal at 75°C for 10 min, then increased at 20°C/min up to 120°C. Peak numbers as in Table II. Other details as in Fig. 1.

on non-polar and polar column, and the slope, m, and intercept, q, of the equations:

$$y_i = q_i + (m_i I_{ni}/100) \quad \text{for 1-iodoalkanes}$$

$$y_p = q_p + (m_p I/100) \quad \text{for } n\text{-alkanes}$$

The Kováts retention index with respect to n-alkanes, I, can therefore be calculated

$$I = \frac{(q_i - q_p) \cdot 100}{m_p} + \frac{m_i - I_{ni}}{m_p} = A_0 + A_1 I_{ni}$$

and the constants A_0 and A_1 permit a quick conversion of I_{ni} into I values. For the columns used, the values of these constants are: SPB-1, $A_0 = 418.35$, $A_1 = 0.973$; Supelcowax-10, $A_0 = 715.3$, $A_1 = 0.927$. The parallel behaviour of the lines in Fig. 10 also permits a graphical determination of the I values, with horizontal lines drawn from the position of the substance on the 1-iodoalkane line to cross the n-alkane line.

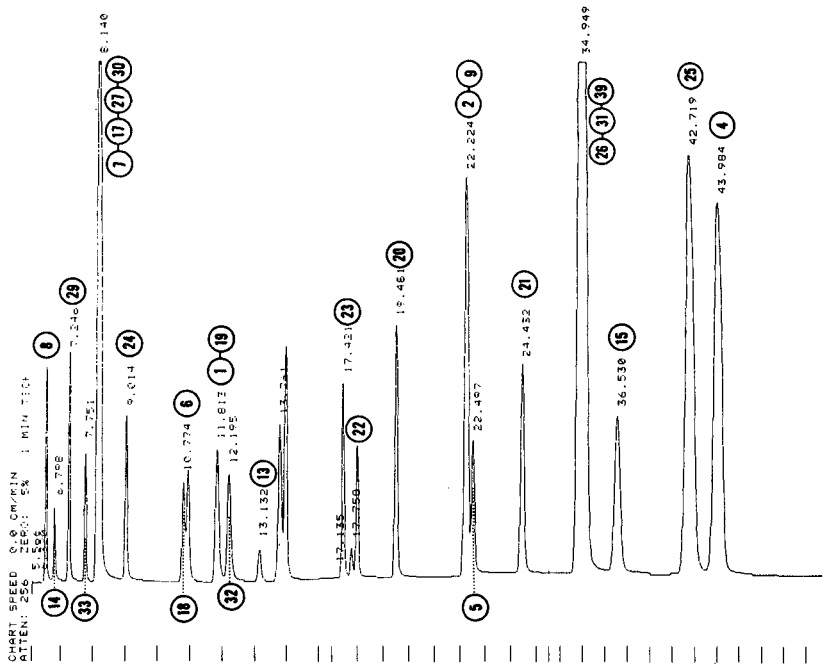

Fig. 9. Chromatograms of halogenated compounds on Supelcowax-10. Temperature programming: isothermal at 75°C for 10 min, then increased at 10°C/min up to 110°C. Peak numbers as in Table II. Other details as in Fig. 3.

Fig. 10 and Table III also show the linear behaviour of other homologous series (1-bromoalkanes and 1-alcohols), which were analyzed in order to test the validity of a quick method for the determination of the column polarity. The Rohrschneider's and McReynolds' constants[25,26] calculated from the I values are the most often used

TABLE III

SLOPE, m, INTERCEPT, p, CORRELATION COEFFICIENT, r, OF STRAIGHT LINES ln t'_R AS A FUNCTION OF THE NUMBER OF CARBON ATOMS IN VARIOUS HOMOLOGOUS SERIES, AND HORIZONTAL DISTANCE BETWEEN PARALLEL LINES IN FIG. 10, ΔC, USED AS A MEASUREMENT OF THE COLUMN POLARITY

	m	p	r	ΔC
Non-polar				
n-Alkanes	0.774	−4.182	1.000	–
1-Iodoalkanes	0.753	−0.944	1.000	4.11
1-Bromoalkanes	0.757	−1.521	1.000	3.36
1-Alcohols	0.781	−2.231	0.998	2.55
Polar				
n-Alkanes	0.673	−4.977	1.000	–
1-Iodoalkanes	0.623	−0.163	0.999	7.01
1-Bromoalkanes	0.655	−1.027	1.000	5.79
1-Alcohols	0.618	0.303	0.991	7.75

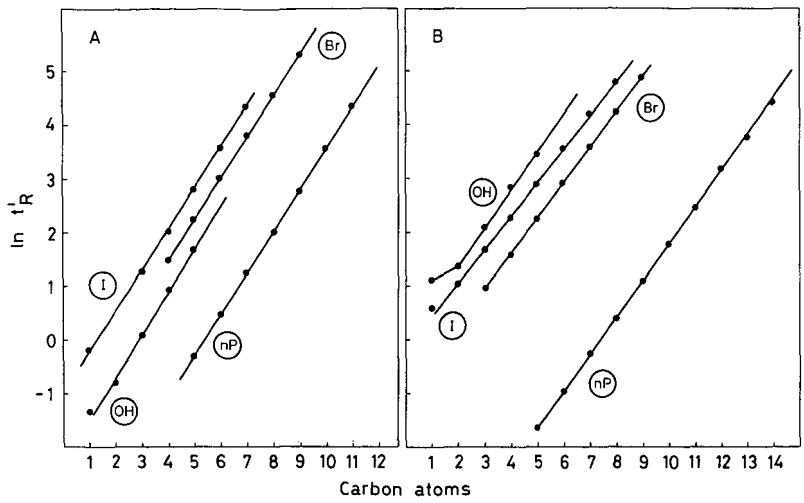

Fig. 10. ln t'_R for different homologous series as a function of number of carbon atoms in the linear chain: (A) non-polar column; (B) polar column; nP = linear alkanes; OH = alcohols; Br = 1-bromoalkanes; I = 1-iodoalkanes.

method for polarity classification. Table IV shows the values of t'_R, I and of the ΔI (difference between the I values on polar and non-polar liquid phases) on SPB-1 and Supelcowax capillary columns for the Rohrschneider's and some of the McReynolds' probes. The latter values cannot correctly be identified with the McReynolds

TABLE IV

VALUES OF t'_R AND I OF ROHRSCHNEIDER'S AND McREYNOLDS' PROBES ON A NON-POLAR AND POLAR CAPILLARY COLUMN, AND DIFFERENCES CORRELATED TO POLARITY (SEE TEXT)

t_M = Column dead time (min).

Compound	*SPB-1* $t_M = 6.701$		*Supelcowax-10* $t_M = 6.516$		$I^{(P)} - I^{(NP)}$
	t'_R	I	t'_R	I	
1 Benzene	2.59	661.6	4.69	967.7	306.1
2 Ethanol	0.38	414.4	3.89	940.7	526.3
3 1-Butanol	2.53	658.7	16.44	1145.9	487.2
4 Methyl ethyl ketone	1.40	582.7	3.44	923.3	340.6
5 Methyl propyl ketone	2.66	664.8	5.78	997.6	332.8
6 Nitromethane	1.03	543.6	18.11	1160.9	617.3
7 Nitropropane	3.77	709.8	26.16	1219.3	509.5
8 Pyridine	4.45	731.5	21.86	1190.1	458.6
9 1-Iodobutane	7.88	806.2	9.61	1067.0	260.8
Sum ΔI Rohrschneider (1+2+4+6+8)					2248.6
Sum ΔI McReynolds (1+3+5+7+8)					2094.2

constants, because the polarity of the SPB-1 liquid phase (dimethylpolysiloxane polymer) is probably higher than that of the standard squalane liquid phase, taken as the non-polar reference term in both polarity classification methods. The relative distances of the parallel lines in Fig. 10, expressed by the values of the corresponding intercepts or by the horizontal distance ΔC along the x axis (Table III), are correlated to the column polarity. The distance, ΔC, between n-alkanes and 1-alcohols is probably the best and most rapid way to identify the difference in polarities of two liquid phases. It can be obtained by injecting only four compounds (two n-alkanes and two alcohols) with carbon atom numbers different enough to permit a precise calculation of the parameters of the straight lines in Fig. 10. This procedure is much easier than the determination of the Rohrschneider's and McReynolds' constants, requiring the analysis of the polarity probes on squalane and on the column under evaluation, and can be useful mainly when different columns are connected in series.

CONCLUSIONS

The use of wide bore capillary columns for the analysis of volatile chlorinated compounds in water supplies offers some advantages from the point of view of resolution of complex mixtures when compared with classical packed columns. At the same time, the introduction of the whole sample without inlet splitting, owing to the relatively high capacity of these columns compared to narrow bore capillaries, permits the use of different extraction and concentration procedures without introducing further uncertainty due to the splitting system. Simultaneous analysis on polar and non-polar stationary phases permits resolution of the 39 compounds tested. Suitable identification procedures on the basis of tabulated retention index values can be carried out. The analysis of homologous series of polar and non-polar compounds also permits the relative polarity of the columns to be measured more easily than by using Rohrschneider's or McReynolds' methods.

REFERENCES

1 *The Analysis of Trihalomethanes in Finished Waters by the Purge and Trap Method*, U.S. Environmental Protection Agency, Environmental Monitoring and Support Laboratory, Cincinnati, OH, 1979, Method 501.1.
2 *The Analysis of Trihalomethanes in Drinking Water by Liquid/liquid Extraction*, U.S. Environmental Protection Agency, Environmental Monitoring and Support Laboratory, Cincinnati, OH, 1979, Method 501.2.
3 G. Castello, T. C. Gerbino and S. Kanitz, *J. Chromatogr.*, 351 (1986) 165.
4 L. D. Hinshaw, *J. Gas Chromatogr.*, 8 (1966) 300.
5 D. A. Solomons and J. S. Ratcliffe, *J. Chromatogr.*, 76 (1973) 101.
6 L. Žilka and M. Matucha, *J. Chromatogr.*, 148 (1978) 229.
7 E. A. Dietz, Jr. and K. F. Singley, *Anal. Chem.*, 51 (1979) 1809.
8 G. Agazzotti and G. Predieri, *Water Res.*, 8 (1986) 959.
9 G. Castello, T. C. Gerbino and S. Kanitz, *J. Chromatogr.*, 247 (1982) 263.
10 G. Castello and T. C. Gerbino, *J. Chromatogr.*, 366 (1986) 59.
11 R. J. Laub and J. H. Purnell, *J. Chromatogr.*, 112 (1975) 71.
12 J. H. Purnell, in F. Bruner (Editor), *The Science of Chromatography* (*Journal of Chromatography Library*, Vol. 32), Elsevier, Amsterdam, 1985, p. 362.
13 G. Castello and T. C. Gerbino, *J. Chromatogr.*, 437 (1988) 33.
14 A. Yasuhara, M. Morita and K. Fuwa, *J. Chromatogr.*, 328 (1985) 35.
15 L. S. Ettre, *Chromatographia*, 17 (1983) 553.

16 L. S. Ettre, *Chromatographia*, 18 (1984) 477.
17 M. L. Duffy, *Int. Lab.*, April (1986) 78.
18 R. T. Wiedermer, S. L. McKinley and T. W. Rendl, *Int. Lab*, May (1986) 68.
19 L. Blomberg, J. Buijten, K. Markides and T. Wännman, *J. Chromatogr.*, 279 (1983) 9.
20 V. Lopez-Avila, R. Wood, M. Flanagan and R. Scott, *J. Chromatogr. Sci.*, 25 (1987) 286.
21 N. H. Mosesman, L. M. Sidinsky and S. D. Corman, *J. Chromatogr. Sci.*, 25 (1987) 351.
22 E. Kovats, *Helv. Chim. Acta*, 41 (1958) 1915.
23 G. Castello and G. D'Amato, *J. Chromatogr.*, 76 (1973) 293.
24 G. Castello and G. D'Amato, *J. Chromatogr.*, 79 (1973) 33.
25 L. Rohrschneider, *J. Chromatogr.*, 22 (1966) 6.
26 W. A. McReynolds, *J. Chromatogr. Sci.*, 8 (1970) 685.

Journal of Chromatography, 454 (1988) 145–155
Elsevier Science Publishers B.V., Amsterdam — Printed in The Netherlands

CHROM. 20 798

FORMATION OF POLYCHLORINATED DIBENZO-*p*-DIOXIN FROM 2,4,4'-TRICHLORO-2'-HYDROXYDIPHENYL ETHER (IRGASAN® DP300) AND ITS CHLORINATED DERIVATIVES BY EXPOSURE TO SUNLIGHT

AKIO KANETOSHI*, HIROSHI OGAWA, EIJI KATSURA and HIROYASU KANESHIMA
Hokkaido Institute of Public Health, North 19, West 12, Kita-ku, Sapporo 060 (Japan)
and
TOSHIAKI MIURA
College of Medical Technology of Hokkaido University, North 12, West 5, Kita-ku, Sapporo 060 (Japan)
(First received February 23rd, 1988; revised manuscript received June 1st, 1988)

SUMMARY

Exposure to sunlight in the solid state of 2,4,4'-trichloro-2'-hydroxydiphenyl ether (Irgasan® DP300) (I) produced dichlorodibenzo-*p*-dioxin(s) (di-CDD) and a trace amount of trichlorodibenzo-*p*-dioxin (tri-CDD) together with three chlorinated derivatives of Irgasan DP300, 2',3,4,4'-tetrachloro-2-hydroxydiphenyl ether (II), 2',4,4',5-tetrachloro-2-hydroxydiphenyl ether (III) and 2',3,4,4',5-pentachloro-2-hydroxydiphenyl ether (IV). These chlorinated derivatives gave various polychlorinated dibenzo-*p*-dioxins (PCDDs) upon exposure to sunlight; *i.e.*, II gave 1,2,8-tri-CDD and a tetrachlorodibenzo-*p*-dioxin (tetra-CDD); III gave di-CDD(s), 2,3,7-tri-CDD and a tetra-CDD and IV gave three pentachlorodibenzo-*p*-dioxins (penta-CDDs) with two tri-CDDs and four tetra-CDDs. Upon exposure to sunlight of commercial textile products containing Irgasan DP300, 0.02–0.03% of the agent was converted into di-CDD(s). These results suggest that Irgasan DP300 is one of the precursors of various PCDDs in the environment.

INTRODUCTION

The environmental pollution by polychlorinated dibenzo-*p*-dioxins (PCDDs) has recently become a serious problem[1–4]. The PCDDs are considered to originate from not only the contamination in chemicals[5] and accidents in chemical plants[6,7] but also the thermal and photochemical reactions of their precursors such as chlorinated phenols[8–10]. For example, PCDDs are formed upon the incineration of municipal refuse[11–15]. Therefore, it is of environmental and toxicological importance to study their formation mechanism and precursors[16–18].

2,4,4'-Trichloro-2'-hydroxydiphenyl ether (Irgasan® DP300) (I) is a chlorinated phenol that is widely used as an antimicrobial agent for textile products and as a bacteriostat for shampoo, toilet soap and cosmetics[19–25]. We reported previously[26] that Irgasan DP300 was chlorinated with sodium hypochlorite, a domestic bleaching

0021-9673/88/$03.50

agent, to afford 2',3,4,4'-tetrachloro-2-hydroxydiphenyl ether (II), 2',4,4',5-tetrachloro-2-hydroxydiphenyl ether (III) and 2',3,4,4',5-pentachloro-2-hydroxydiphenyl ether (IV). Furthermore, Irgasan DP300 and the three chlorinated derivatives (II, III and IV) were shown to be converted to various PCDDs by heating or UV irradiation[26]. The combustion of fabrics containing them also gave PCDDs[27].

Recently, Miyazaki *et al.*[28] detected methylated Irgasan DP300 in fish and shellfish from the Tama River and the Tokyo Bay in Japan. Moreover, Onodera *et al.*[29] reported that the three chlorinated derivatives were formed upon disinfection and deodorization with sodium hypochlorite of water containing Irgasan DP300. In order to prevent pollution by PCDDs, it is important to study whether or not these compounds give PCDDs under environmental conditions.

In this paper, we examined, by means of capillary gas chromatography–mass spectrometry (capillary GC–MS), the possibility that exposure of Irgasan DP300 and its chlorinated derivatives to sunlight gives PCDDs.

EXPERIMENTAL

Reagents

2,4,4'-Trichloro-2'-hydroxydiphenyl ether (Irgasan DP300) (I) was obtained from Ciba-Geigy (Basle, Switzerland), 1,2,4-trichlorodibenzo-*p*-dioxin (1,2,4-tri-CDD) and 2,3,7,8-tetrachlorodibenzo-*p*-dioxin (2,3,7,8-tetra-CDD) from Gasukuro Kogyo (Tokyo, Japan). The three chlorinated derivatives (II, III and IV) of Irgasan DP300 and dichlorodibenzo-*p*-dioxin (di-CDD, a mixture of 2,7- and 2,8-di-CDD) were synthesized as reported previously[26]. All organic solvents were of residual pesticide analysis quality (Wako Pure Chemical, Tokyo, Japan). Other reagents were of analytical reagent grade.

Fabrics

Of the commercial textile products treated with antimicrobial agents, fabrics in which Irgasan DP300 was detected[22] were used as samples.

Conditions for capillary GC–MS

A Shimadzu DF2000 GC–MS system equipped with a GC-MSPAC 1100 data-processing system was used with an Shimadzu CBP5-50-05 capillary column (50 m × 0.35 mm I.D.). The column temperature was programmed from 140 to 260°C at 4°C/min. The injection temperature and the separator temperature were set at 260 and 280°C, respectively. Helium was used as the carrier gas at 1.3 kg/cm^2.

Exposure of Irgasan DP300 and its chlorinated derivatives to sunlight

A 5-mg amount of Irgasan DP300 or each chlorinated derivative was dissolved in 1 ml of acetone and placed in a glass plate (diameter 120 mm). The solvent was evaporated at room temperature and the resulting thin layer was exposed to sunlight, (8–10) · 10^4 lux), for 18 h. The photolysate was dissolved in an adequate volume of acetone and the aliquot was analysed by high-performance liquid chromatography (HPLC) was previously reported[26] to quantify the residual amount of Irgasan DP300. After elution of Irgasan DP300 from the column, the eluate containing the chlorinated derivatives was pooled and evaporated to dryness. The residue was methylated with

ethereal diazomethane and analyzed by capillary GC–MS for identification and quantitation of compounds II–IV.

For the determination of PCDD(s) formed, the residual acetone solution of the photolysate was concentrated to *ca.* 0.1 ml. The concentrate was diluted in 10 ml of *n*-hexane and placed on a silica gel column (160 mm × 12 mm I.D.) packed with 10 g of Kieselgel 60 (Merck). The PCDD(s) was eluted from the column with 200 ml of *n*-hexane. The dioxin fraction was concentrated to 0.1 ml and analysed by capillary GC–MS. To quantify the amount of PCDD(s) originally present in the parent compound, a 5-mg amount of each compound was dissolved in 1 ml of *n*-hexane, chromatographed on a silica gel column and analysed by capillary GC–MS in the manner described above. Without photolysis, no PCDD ($<0.0004\%$) was detected in each compound.

Exposure of commercial textile products containing Irgasan DP300 to sunlight

Samples used as textile products were two commercial men's socks with differing loadings of Irgasan DP300. Each sample was cut into two equal pieces, one of which was weighed and exposed to sunlight, $(8–10) \cdot 10^4$ lux, for 18 h. The fabric was refluxed with 250 ml of methanol–acetic acid (9:1) for 30 min and filtered through a glass filter (3G2). Then, the fabric was refluxed again with 250 ml of ethyl acetate for 30 min and filtered. The filtrates were pooled and the solvent was evaporated. The residue was dissolved in a small volume of ethyl acetate and chromatographed on silica gel as described above. The dioxin fraction eluted from the column with *n*-hexane was evaporated and the residue was dissolved in an adequate volume of *n*-hexane for repeated clean up by silica gel column chromatography using *n*-hexane as an eluent. The eluate was concentrated and placed on an alumina column[30] (55 mm × 15 mm I.D.) packed with 10 g of basic aluminium oxide (Alumina Woelm B, Akt. 1; Woelm Pharma). The interfering substances were removed by eluting successively with 50 ml of *n*-hexane and 100 ml of 2% dichloromethane in *n*-hexane. PCDD(s) was then eluted from the column with 200 ml of 20% dichloromethane in *n*-hexane. The dioxin fraction was concentrated to 0.1 ml and analyzed by capillary GC–MS. For correction of the background amount(s) of PCDD(s), another piece of the sock was treated in the same manner except that exposure to sunlight was omitted. Prior to photolysis no PCDD (<0.002 μg/g) was detected in the fabrics.

Quantitation of PCDDs

Di-CDD was quantified by the intensity of the molecular ion (M^+) peak at *m/z* 252 (base peak) in the mass spectrum using a mixture of 2,7- and 2,8-di-CDD as a standard. Similarly, the amounts of tri-CDD and tetra-CDD were determined from the intensities of the M^+ peaks at *m/z* 286 and 320 in the mass spectra using 1,2,4-tri-CDD and 2,3,7,8-tetra-CDD as standards, respectively. Pentachlorodibenzo-*p*-dioxin (penta-CDD) was quantified by the intensity of the M^+ peak at *m/z* 354 which was assumed to be the same as that at *m/z* 320 of tetra-CDD because of the lack of an authentic standard.

RESULTS AND DISCUSSION

Exposure of Irgasan DP300 and its chlorinated derivatives (II–IV) to sunlight

Irgasan DP300 and its chlorinated derivatives were exposed to sunlight and the amounts of chlorinated 2-hydroxydiphenyl ethers or PCDDs in the photolysates were determined as follows.

Intermolecular migration of a chlorine atom(s). Exposure of Irgasan DP300, II, III and IV to sunlight gave chlorinated and dechlorinated products by intermolecular chlorine atom migration. Table I shows the amounts of II, III and IV formed from Irgasan DP300. The commercially available Irgasan DP300 originally contained 0.003% of III as a contaminant. Upon exposure of Irgasan DP300 to sunlight, the amount of compound III was markedly increased with the appearance of an equal amount of II and a trace amount of IV. These results indicate that Irgasan DP300 can yield the three chlorinated derivatives not only by treatment with sodium hypochlorite[26,29] but also by exposure to sunlight.

Table II shows the intermolecular chlorine atom migration of compounds II–IV upon exposure to sunlight. Both II and III were chlorinated to IV and dechlorinated to Irgasan DP300, whereas IV gave Irgasan DP300, II and III by loss of chlorine atoms.

Formation of PCDDs. Fig. 1 shows the total ion monitoring (TIM) and mass chromatograms of the dioxin fraction separated from the photolysate of Irgasan DP300 (capillary GC–MS). Di-CDD(s) (M^+ peak at *m/z* 252) and a trace amount of tri-CDD (M^+ peak at *m/z* 286) were detected at 20.6 and 24.7 min, respectively. Other peaks were almost entirely due to phthalic acid esters as contaminants.

Though the di-CDD(s) showed the same retention time as that of 2,8-di-CDD, which is formed by intramolecular dehydrochlorination between the 2-chlorine atom and 2′-hydroxyl group of Irgasan DP300, its structure remains uncertain because 2,8-di-CDD was not separated from 2,7-di-CDD under the conditions employed in this study. On the other hand, the tri-CDD was neither 1,2,8- nor 2,3,7-tri-CDD. Therefore, it was not produced by the intramolecular dehydrochlorination of compound II and III once formed.

TABLE I

INTERMOLECULAR CHLORINE ATOM MIGRATION UPON EXPOSURE OF 2,4,4′-TRICHLORO-2′-HYDROXYDIPHENYL ETHER (IRGASAN DP300) (I) TO SUNLIGHT

Each compound was quantified by HPLC.

Sample	*Amounts of Irgasan DP300 and its chlorinated derivatives detected (%)*			
	I	*II*	*III*	*IV*
Untreated*	99.4 ± 0.04	N.D.	0.003 ± 0.0001	N.D.
Photolysate**	53	0.14	0.13	0.02
	(45–61)	(0.07–0.21)	(0.09–0.16)	(Trace–0.04)

* Values are the averages ±S.D. of four experiments and calculated on the basis of the initial amount. N.D. is below 0.0003%.

** Values are the averages of two experiments with the ranges of the data in parentheses and calculated on the basis of the initial amount.

TABLE II

INTERMOLECULAR CHLORINE ATOM MIGRATION UPON EXPOSURE OF THE CHLORINATED DERIVATIVES (II–IV) OF IRGASAN DP300 (I) TO SUNLIGHT

Each compound was quantified by HPLC. Values are calculated on the basis of the initial amount (5 mg) and are the averages of two experiments with the ranges of the data in parentheses.

Starting material of photolysate	*Amounts of Irgasan DP300 and its chlorinated derivatives (%)*			
	I	*II*	*III*	*IV*
II	0.85 (0.58–1.12)	69 (63–75)	0.29* (0.24–0.34)	0.3* (0.14–0.31)
III	0.87 (0.54–1.19)	0.12* (Trace–0.24)	51 (39–62)	0.62* (0.34–0.89)
IV	0.11 (0.10–0.12)	Trace* (Trace–0.02)	2.74* (1.84–3.63)	35 (33–36)

* Values are corrected by the background amount and the recovery of each compound. Trace is between 0.01 and 0.02%.

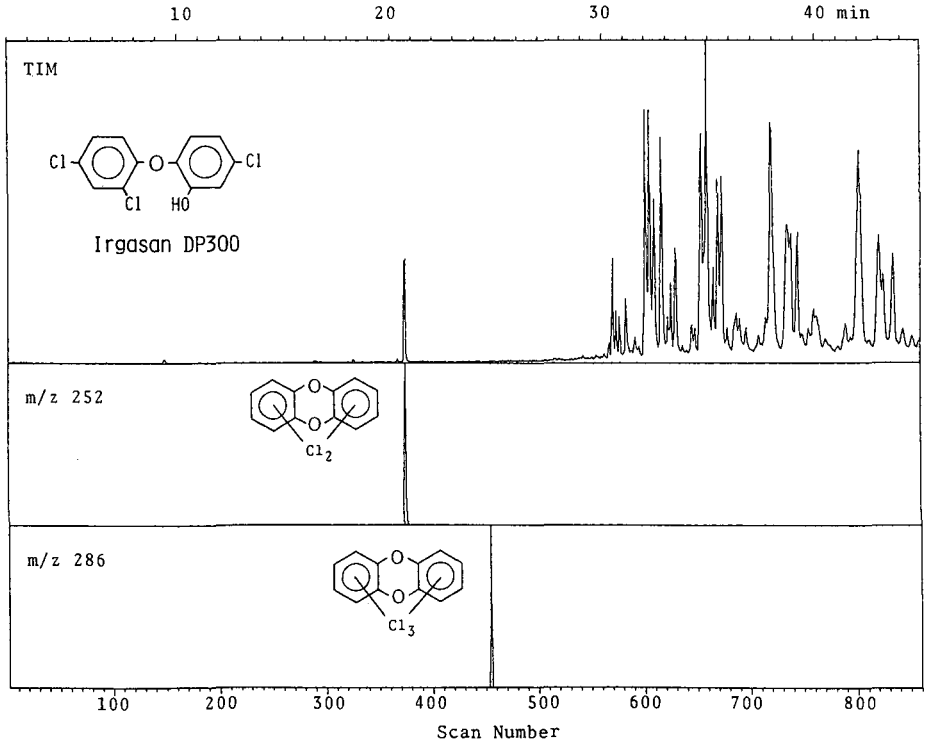

Fig. 1. TIM and mass chromatograms of the dioxin fraction from the photolysate of Irgasan DP300 with sunlight.

Fig. 2 shows the TIM and mass chromatograms of the dioxin fraction from the photolysate of compound II. A major peak at 26.0 min was assigned due to 1,2,8-tri-CDD according to its retention time[27], which was presumably formed by the intramolecular dehydrochlorination of II. In addition, small amounts of tetra-CDD (M^+ peak at *m/z* 320) and tetrachlorodiphenyl ether (M^+ peak at *m/z* 306) were detected at 29.6 and 24.8 min, respectively.

The TIM and mass chromatograms of the dioxin fraction from the photolysate of compound III are shown in Fig. 3. 2,3,7-Tri-CDD[27] was detected at 25.6 min with di-CDD(s) at 20.6 min and tetra-CDD at 29.3 min. The 2,3,7-tri-CDD was a major product formed by the intramolecular dehydrochlorination of III. Tetrachlorodiphenyl ether and two isomers of pentachlorodiphenyl ether (M^+ peak at *m/z* 340) were also found at 24.8, 27.6 and 28.5 min, respectively. Since the tetra-CDDs formed from compounds II and III were not 1,2,3,8-tetra-CDD as judged by their retention times, they were not produced by the intramolecular dehydrochlorination of IV once formed from II or III.

As shown previously[26], the di-CDD, 1,2,8-tri-CDD and 2,3,7-tri-CDD were formed upon UV irradiation of Irgasan DP300, II and III, respectively, though their amounts were small as those obtained in this study. However, no evidence was obtained for the formation of PCDD(s) from compound IV by UV irradiation. On the

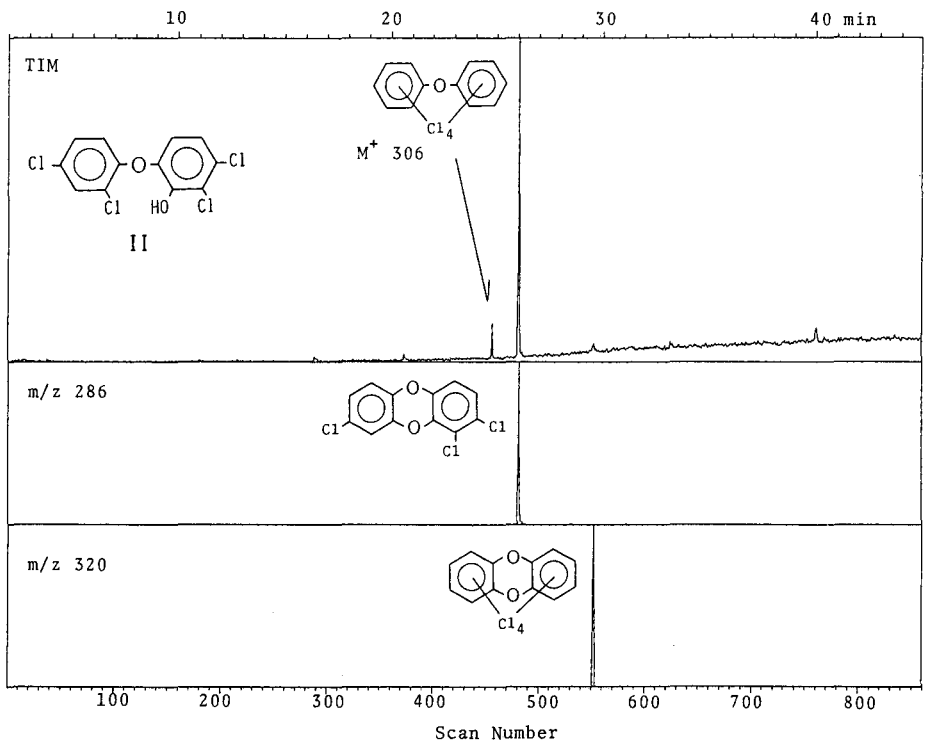

Fig. 2. TIM and mass chromatograms of the dioxin fraction from the photolysate of compound II with sunlight.

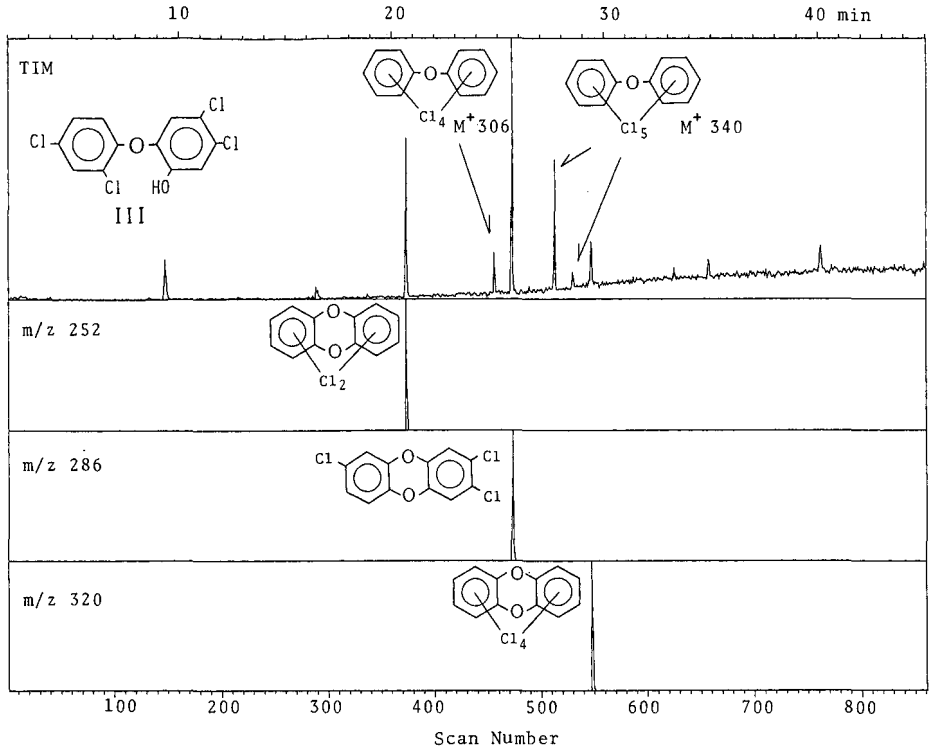

Fig. 3. TIM and mass chromatograms of the dioxin fraction from the photolysate of compound III with sunlight.

contrary, exposure of IV to sunlignht gave various PCDDs as shown in Fig. 4, though their amounts were very small; two tri-CDDs were detected at 24.7 and 25.6 min. The latter was identified as 2,3,7-tri-CDD[27]. Four tetra-CDDs were detected at 28.2, 29.3, 29.6 and 30.2 min. The last one is identified by its retention time as 1,2,3,8-tetra-CDD[27] formed by the intramolecular dehydrochlorination of IV. The amounts of the tetra-CDDs at 28.2 and 29.6 min were very small. The former was detected in only one of two experiments. Furthermore, three penta-CDDs were detected at 34.2, 34.6 and 35.8 min, though the amount of the second was very small and detected in one of two experiments.

These results are summarized in Table III. Irgasan DP 300, II and III gave two, two and three PCDDs, respectively, whereas IV gave nine PCDDs. The extent of conversion of each compound into PCDDs reached 0.09–0.18%.

Though the tri-CDDs, major products from compounds II and III, were presumably formed by intramolecular dehydrochlorination of II and III, the occurrence of some of the other PCDDs cannot be explained by the mechanism that Irgasan DP300 and its chlorinated derivatives were further chlorinated by intermolecular chlorine atom migration followed by intramoleclar dehydrochlorination. Buser[31] reported that octachlorodibenzo-*p*-dioxin, a major contaminant at levels up to hundreds of ppm in commercial chlorinated phenols[32], was dechlorinated by UV

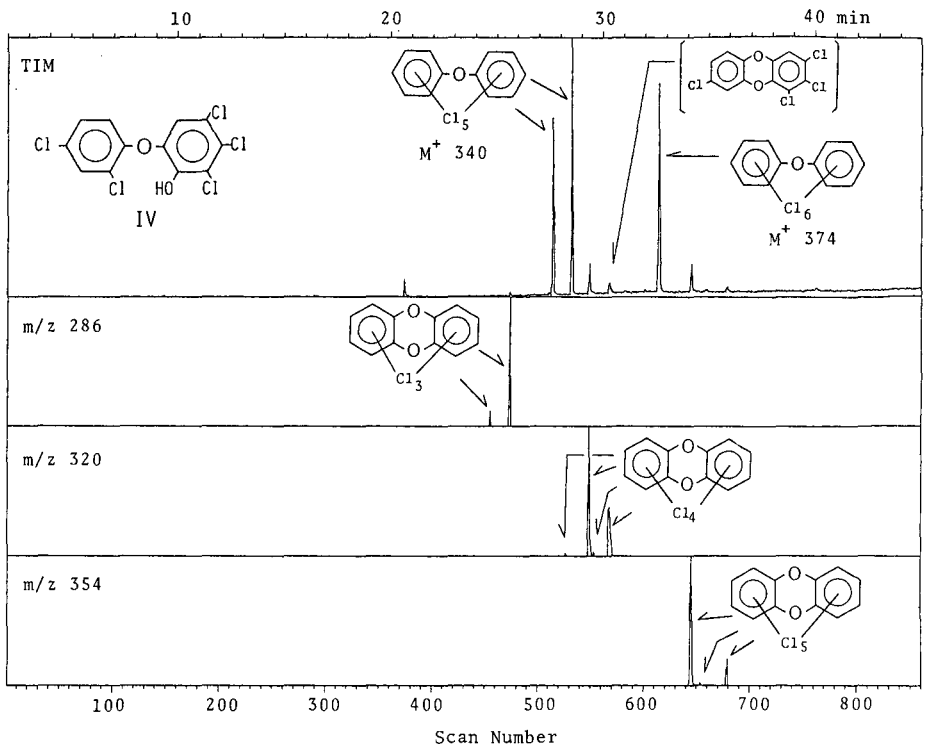

Fig. 4. TIM and mass chromatograms of the dioxin fraction from the photolysate of compound IV with sunlight.

irradiation to give trace amounts of tetra-CDDs, penta-CDDs, hexachlorodibenzo-*p*-dioxins and heptachlorodibenzo-*p*-dioxins. The present study shows that sunlight exposure of Irgasan DP300 and chlorinated derivatives gave further chlorinated PCDDs as well as dechlorinated PCDDs. These results indicate that intermolecular chlorine atom migration occurs not only in Irgasan DP300 and its chlorinated derivatives but also in PCDDs once formed. Therefore, more complicated mechanisms may operate for the formation of various PCDDs upon photolysis with sunlight, *i.e.*, ring closure of compounds II–IV without elimination of a chlorine atom and intermolecular chlorine atom migration of PCDDs to give the higher chlorinated PCDDs, as observed in the pyrolysis of II–IV[26].

These results suggest that Irgasan DP300 is converted into various PCDDs *via* its chlorinated derivatives in the environment.

Formation of PCDDs from Irgasan DP300 contained in commercial textile products by exposure to sunlight

Fig. 5 shows the TIM and mass chromatograms of the dioxin fraction of the extract from the men's sock containing Irgasan DP300 exposed to sunlight. A small amount of di-CDD(s) was detected at 20.6 min in the chromatograms, determined to be 0.04 and 0.27 μg/g from the fabrics containing 158 and 789 μg/g Irgasan DP300

TABLE III

AMOUNTS OF PCDDs FORMED UPON EXPOSURE OF IRGASAN DP300 (I) AND ITS CHLORINATED DERIVATIVES (II–IV) TO SUNLIGHT

Values are the averages of two experiments with the ranges of the data in parentheses. The retention time of each PCDD is as follows; di-CDD, 20.6; tri-CDD; (a) 24.7, (b) 26.0, (c) 25.6; tetra-CDD; (d) 29.6, (e) 29.3, (f) 28.2, (g) 30.2; penta-CDD; (h) 34.2, (i) 34.6, (j) 35.8 min.

Compound	*Amounts of PCDDs formed (%)**				
	Di-CDD	*Tri-CDD*	*Tetra-CDD*	*Penta-CDD*	*Total*
I	0.095 (0.080–0.110)	0.002[a] (0.002 × 2)	N.D.	N.D.	0.097
II	N.D.	0.18[b] (0.14–0.22)	0.004[d] (0.004 × 2)	N.D.	0.184
III	0.014 (0.012–0.015)	0.093[c] (0.061–0.124)	0.016[e] (0.014–0.017)	N.D.	0.123
IV	N.D.	0.001[a] (0.001 × 2) 0.009[c] (0.006–0.012)	0.001[d] (Trace–0.001) 0.038[e] (0.033–0.042) Trace[f] (N.D.–Trace) 0.016[g] (0.016 × 2)	0.023[h] (0.019–0.026) Trace[i] (N.D.-Trace) 0.004[j] (0.003–0.004)	0.092

* Values are calculated on the basis of the initial amount (5 mg). N.D. is below 0.0004%. Trace is about 0.0004%.

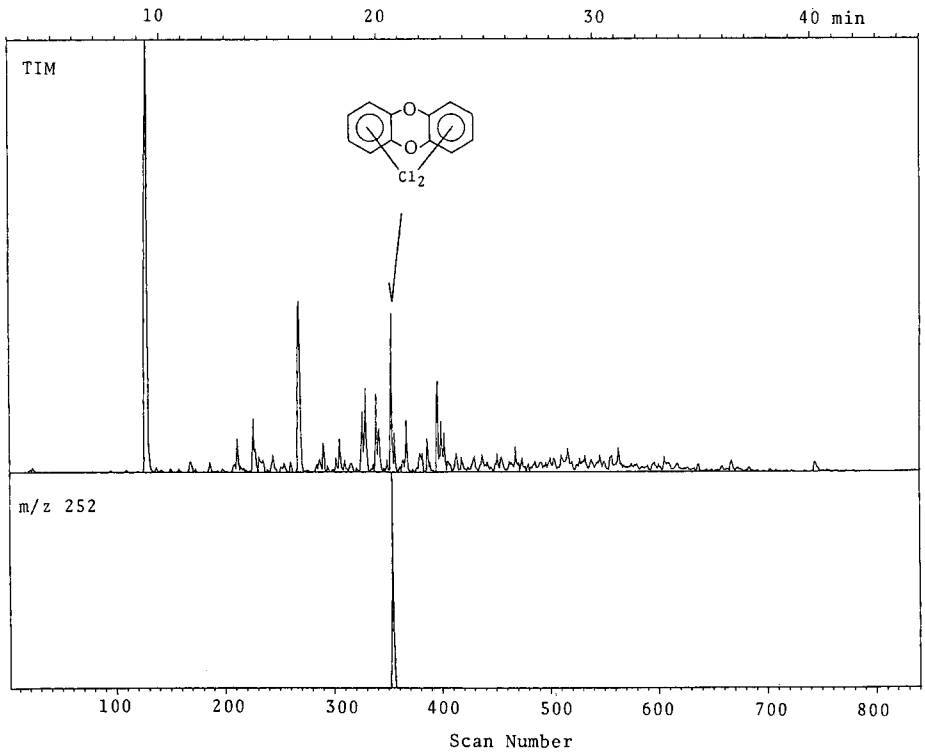

Fig. 5. TIM and mass chromatograms of the dioxin fraction from commercial men's socks containing Irgasan DP300 after exposure to sunlight.

respectively. Thus, the photolytic conversions of Irgasan DP300 into di-CDD(s) in the two fabrics were estimated to be 0.02 and 0.03%, respectively. Although 2,7- and 2,8-di-CDD derived from Irgasan DP300 are less toxic than other higher chlorinated PCDDs[33,34], the formation of di-CDD(s) in fabrics is undesirable for users.

In this study, we have demonstrated that the three chlorinated derivatives II–IV, the precursors[8,26,27] of more toxic PCDD[33,34], were formed from Irgasan DP300 upon exposure to sunlight, though their amounts were less than those formed by bleaching with sodium hypochlorite[26]. As with UV irradiation, the extents of conversion of Irgasan DP300 and its chlorinated derivatives into PCDDs upon exposure to sunlight were less than those obtained by the thermal conversion[26,27]. However, such photolytic conversion into PCDDs with sunlight may easily occur under the conditions of our daily life and environment. Thus, the use of Irgasan DP300 and its abandonment in the environment may be causative of the pollution by various PCDDs.

REFERENCES

1 T. Yamagishi, T. Miyazaki, K. Akiyama, M. Morita, J. Nakagawa, S. Horii and S. Kaneko, *Chemosphere*, 10 (1981) 1137.
2 A. J. Schecter, J. J. Ryan and J. D. Constable, *Chemosphere*, 15 (1986) 1613.
3 J. J. Ryan, A. Schecter, W. F. Sun and R. Lizotte, in C. Rappe (Editor), *Chlorinated Dioxins and Dibenzofurans in Perspective*, Lewis Publishers, Chelsea, MI, 1986, p. 3.
4 A. Schecter, J. J. Ryan and G. Gitlitz, in C. Rappe (Editor), *Chlorinated Dioxins and Dibenzofurans in Perspective*, Lewis Publishers, Chelsea, MI, 1986, p. 51.
5 H.-R. Buser, *J. Chromatogr.*, 107 (1975) 295.
6 C. Rappe, *Environ. Sci. Technol.*, 18 (1984) 78A.
7 Y. Takizawa, *Toxicology Forum*, 10 (1987) 583.
8 C.-A. Nilsson, K. Andersson, C. Rappe and S.-O. Westermark, *J. Chromatogr.*, 96 (1974) 137.
9 H.-R. Buser, *J. Chromatogr.*, 114 (1975) 95.
10 T. Humppi and K. Heinola, *J. Chromatogr.*, 331 (1985) 410.
11 K. Olie, P. L. Vermeulen and O. Hutzinger, *Chemosphere*, 6 (1977) 455.
12 G. A. Eiceman, R. E. Clement and F. W. Karasek, *Anal. Chem.*, 51 (1979) 2343.
13 G. A. Eiceman, R. E. Clement and F. W. Karasek, *Anal. Chem.*, 53 (1981) 955.
14 F. W. Karasek and A. C. Viau, *J. Chromatogr.*, 265 (1983) 79.
15 M. Suter-Hofmann and O. Schlatter, *Chemosphere*, 15 (1986) 1733.
16 W. M. Shaub and W. Tsang, *Environ. Sci. Technol.*, 17 (1983) 721.
17 A. Liberti, D. Brocco, A. Cecinato and A. Natalucci, *Pergamon Ser. Environ. Sci.*, 7 (1982) 281.
18 L. C. Dickson and F. W. Karasek, *J. Chromatogr.*, 389 (1987) 127.
19 M. Kazama, K. Mizuishi, Y. Nakamura, H. Harada and T. Totani, *Eisei Kagaku*, 20 (1974) 248.
20 A. Y. K. Chow, G. H. Hirsch and H. S. Buttar, *Toxicol. Appl. Pharmacol.*, 42 (1977) 1.
21 M. Kazama, Y. Nakamura and H. Harada, *Annu. Rep. Tokyo Metrop. Res. Lab. Public Health*, 31 (1980) 91.
22 O. Yuge, *J. Antibact. Antifung. Agents*, 11 (1983) 76.
23 T. Amemiya, M. Sakai, K. Mori, S. Suzuki and M. Kazama, *Annu. Rep. Tokyo Metrop. Res. Lab. Public Health*, 35 (1984) 133.
24 T. Amemiya, M. Sakai, K. Ikeda, K. Mori, S. Suzuki and Y. Watanabe, *Annu. Rep. Tokyo Metrop. Res. Lab. Public Health*, 36 (1985) 123.
25 A. Kanetoshi, H. Ogawa, M. Anetai, E. Katsura and H. Kaneshima, Eisei Kagaku, 31 (1985) 245.
26 A. Kanetoshi, H. Ogawa, E. Katsura and H. Kaneshima, *J. Chromatogr.*, 389 (1987) 139.
27 A. Kanetoshi, H. Ogawa, E. Katsura, H. Kaneshima and T. Miura, *J. Chromatogr.*, 442 (1988) 289.
28 T. Miyazaki, T. Yamagishi and M. Matsumoto, *Bull. Environ. Contam. Toxicol.*, 32 (1984) 227.
29 S. Onodera, M. Ogawa and S. Suzuki, *J. Chromatogr.*, 392 (1987) 267.
30 P. W. Albro and C. E. Parker, *J. Chromatogr.*, 197 (1980) 155.

31 H.-R. Buser, *J. Chromatogr.*, 129 (1976) 303.
32 H.-R. Buser, *Anal. Chem.*, 48 (1976) 1553.
33 E. E. McConnell, J. A. Moore, J. K. Haseman and M. W. Harris, *Toxicol. Appl. Pharmacol.*, 44 (1978) 335.
34 A. Poland and E. Glover, *Mol. Pharmacol.*, 9 (1973) 736.

Journal of Chromatography, 454 (1988) 157–167
Elsevier Science Publishers B.V., Amsterdam — Printed in The Netherlands

CHROM. 20 779

ON-LINE HIGH-PERFORMANCE LIQUID CHROMATOGRAPHY–POST-COLUMN REACTION–CAPILLARY GAS CHROMATOGRAPHY ANALYSIS OF LIPIDS IN BIOLOGICAL SAMPLES

THOMAS V. RAGLIONE
E. R. Squibb and Sons, New Brunswick, NJ 08903 (U.S.A.)
and
RICHARD A. HARTWICK*
Department of Chemistry, Rutgers University, Piscataway, NJ 08854 (U.S.A.)
(First received March 23rd, 1988; revised manuscript received June 13th, 1988)

SUMMARY

The versatility of on-line liquid chromatography and gas chromatography is further expanded by the addition of on-line derivatization. The on-line fractionation, derivatization and separation system is applied to the characterization of lipids in biological samples. Separation of the triglycerides from the phospholipids was accomplished on a narrowbore (2.0 mm I.D.) 5 μm silica column. The entire triglyceride fraction was transferred to a heated fixed bed reactor for esterification of the fatty acid constituents. Transfer of the derivatized zones to the gas chromatograph was accomplished by the use of a retention gap. Application of the system to the separation and characterization of *Staphylococcus aureus* is presented.

INTRODUCTION

The combination of liquid and gas chromatographic (LC and GC) separations as two modes in a multidimensional separation is hindered by the need for chemical derivatization of many polar compounds prior to their introduction into a gas chromatograph. Therefore the next logical progression in the development of on-line LC–GC interfacing[1,2] is the addition of post-column derivatization prior to GC analysis. Such a system would be ideally suited for biological separations where often the sample complexity requires both prefractionation to reduce interferences as well as derivatization to increase volatility and/or thermal stability.

One such area of application would be the analysis of biomass and community structure of bacteria. In studying the biomass community the determination of lipid constituents and their relative abundance is important. Researchers in this field have relied on a variety of techniques including agar films[3], colorimetric methods[4], and chitin assays[5] however each of these methods has its own shortcomings, which can lead to erroneous results. White *et al.*[6] developed a method, based on chromatography, requiring multiple separation steps, for determining community structure of

0021-9673/88/$03.50

TABLE I

COMPARISON OF THE OFF-LINE AND ON-LINE METHODS OF SEPARATION, ESTERIFICATION AND IDENTIFICATION OF TRIGLYCERIDES

Step	*Manual method*	*Time*	*On-line method*	*Time*
1	Develop preparative TLC plate	1 h*	Separate by LC	2 min
2	Scrape plate and extract lipids from plate media	20 min	Trap on fixed bed reactor	30 s
3	Esterification with methanolic hydrochloric acid	1 h	React on fixed-bed reactor	2 h
4	Extract into hexane add internal standard and blow down	20 min	Flush into GC injector	30 s
5	Reconstitute in hexane and vortex	15 min	Evaporate solvent in retention gap	25 min
6	GC analysis	30 min	GC analysis	30 min
	Total:	3 h 25 min		2 h 58 min
Automate:	No		Yes	

* 1–4 Samples/plate.

estuarine sediments. By purifying and measuring individual components, it is possible to begin to define some of the key components necessary to resolve the fungal population structure as a part of the total microbial assembly. The method was very labor intensive and time consuming, requiring many transfer steps which compromised sample intergity (Table I).

The method, described by White *et al.*[6], is carried out in a number of steps. First, the phospholipids and lipids are separated on a preparative thin-layer chromatography (TLC) plate. The plate is then scraped and the lipids extracted from the plate media. The triglycerides are then converted to the methyl esters with a methanolic hydrochloric acid solution and extracted into hexane. Internal standards are added and the solvent evaporated. After reconstitution the samples are injected on to a GC system for separation and identification. The major problem with such an approach is that the sample is subjected to several transfer steps leaving the sample liable to contamination and loss. Also the method requires a substantial amount of operator involvement thus limiting the sample throughput due to the inability to automate.

The use of on-line LC–GC with post-column derivatization would eliminate the manual transfer steps and thus the risk of loss or contamination, while increasing sample throughput through automation. In developing an on-line derivatization scheme for LC–GC several factors must be considered: (1) solvent miscibility (if solvents are immiscible reaction kinetics are severely impeded), (2) high-performance liquid chromatography (HPLC) and post-column reaction (PCR) solvent compatibility with GC column, (3) reaction time, and (4) side products. Preliminary work based on the method of White *et al.*[6], utilizing acidic esterification solvents proved unsatisfactory due to the susceptibility of GC stationary phases to acid hydrolysis. Thus, alternative reaction schemes were investigated.

The use of a fixed bed resin was found to be both compatible with the GC stationary phase and a good catalyst for esterification. Key to the success of the system described was the use of a strong cation-exchange resin, of high capacity

(mequiv./g) for the catalysis of the esterification. The on-line system incorporated the use of a retention gap for the transfer of the large derivatized zones. The triglycerides tripalmitin and tristearitin, which are commonly found in biological systems, were used for evaluating the on-line system. Application of the system to the analysis of *Staphylococcus aureus* is presented.

EXPERIMENTAL

Liquid chromatography equipment

All LC separations were performed with a Waters M6000 pump (Waters-Millipore, Milford, MA, U.S.A.) and a Rheodyne injector (Rheodyne, Cotati, CA, U.S.A.) equipped with a 50-μl loop. The column used was 250 × 2.0 mm I.D. packed with LiChrosorb 60 A, 5 μm (EM Labs., Elmsford, NY, U.S.A.). The flow-rate was 0.3 ml/min and the mobile phase was heptane–isopropanol (7:3). The isopropanol was added to aid the misciblity of the LC mobile phase and the PCR solvent. Verification of triglyceride retention times was accomplished by connecting a refractive index detector (Waters Chromatography) or a UV detector (Kratos, Applied Biosystems, Foster City, CA, U.S.A.) set at 220 nm to the end of the column. The detector was then removed to prevent flow cell damage due to the back pressure of the PCR system. All solvents were HPLC grade and purchased from J. T. Baker (Phillipsburg, NJ, U.S.A.).

TLC

All TLC experiments were preformed on pre-coated silica gel 60 A plates (EM Labs.). The development solvent was heptane–isopropanol (7:3). Triglyceride standards, tripalmitin and tristearitin, and phospholipid standards, dimyristoyl, dipalmitoyl and distearoyl, were purchased from Sigma (St. Louis, MO, U.S.A.) and solutions prepared in heptane at 1.0 mg/ml. Plates were spotted with 50 μl of solution. Upon development and drying, the plates were sprayed with 20% sulfuric acid in methanol and charred to determine migration distances.

Post-column reaction

All post-column reactions were performed using a Varian (Sunnyvale, CA, U.S.A.) 8500 syringe pump. The initial acidic esterification PCR system, consisted of a mixing/reaction loop of PTFE tubing, 0.010 in. I.D. and 1.0 ml total volume (Kratos), which had been tightly woven to minimize laminar dilution. Reaction solvents were methanol–isopropanol–acid (100:100:1) at 0.3 ml/min. The acids investigated were hydrochloric and trifluoroacetic acid.

The fixed-bed reactor system consisted of a column, 150 × 4.6 mm packed with a strong cation exchanger HC-15 (Hamilton, Reno, NV, U.S.A.). The fixed-bed reactor was packed by slurrying and packing in 5% glycerine under constant flow conditions. The PCR solvent was methanol–isopropanol (4:6). The isopropanol was added to the PCR solvent to aid in the miscibility of the mobile phase. The fixed-bed reactor was placed in an oven (Carle Instruments, Anaheim, CA, U.S.A.) and kept at 85–90°C. Elution times of the methyl esters were confirmed by placing a refractive index detector at the column outlet, the detector was then removed to prevent damage to the flow cell due to the system back pressure.

GC equipment

All GC experiments were preformed on a Varian 3400 equipped with a flame ionization detector. A "retention gap", consisting of an uncoated 50 m × 0.32 mm fused-silica capillary (Polymicro Technologies, Phoenix, AZ, U.S.A.), was connected to the head of the column with a zero dead volume union. The column used was a 25 × 0.32 mm I.D. 5% phenylmethyl silicone (Hewlett-Packard, Palo Alto, CA, U.S.A.). Deactivation of the retention gap was achieved[7] by filling with a solution of hexamethyldisilazane–pentane (1:1) (Petrarch Systems, Bristol, PA, U.S.A.) capping the ends, and placing in an oven set at 100°C for 17 h. After heating the retention gap was then connected to an LC pump and washed with toluene and methanol prior to use. The retention gap was connected to a Rheodyne 7040 switching valve mounted directly above the injection port. A short length of 0.020 in. I.D. stainless-steel tubing was epoxied to the end of the fused-silica retention gap to both eliminate dead volume and make a gas tight seal to the switching valve. Injections were on-column with a sample volume of 50 μl. The carrier gas was helium at a linear velocity of 52 cm/min. The GC oven was maintained at 100°C for 25 min during the injection/evaporation procedure and then ramped at the rate of 7°C/min to 250°C.

Sample preparation

Dried *Staphylococcus aureus* cells were purchased from Sigma. The lipids were extracted from the *Staphylococcus aureus* using the Bligh-Dyer[8] technique. Approximately 100 mg of dried cells were weighed and transferred to a 250-ml separatory funnel containing water (15 ml), methanol (37.5 ml) and chloroform (18.8 ml). After allowing the sample to react overnight, 18.8 ml each of water and chloroform were added to the solution breaking the system into two phases. The lipid containing layer (chloroform) was collected and the chloroform evaporated by placing under a stream of air. The sample was then redissolved in heptane and analyzed with the LC–PCR–GC system. A portion of the heptane solution was blown down and reacted without any preseparation. A solution of methanol–chloroform–hydrochloric acid (10:1:1) was added to the residue and allowed to reacted for 1 h at 100°C. The methyl esters were then extracted into heptane and analyzed directly by GC.

RESULTS AND DISCUSSION

Phospholipid detection

In developing the LC separation it was necessary to find an alternative method of detection for the phospholipids, due to insensitivity of the refractive index detector. At the concentrations used in this study the phospholipids could not be distinguished from the baseline with the refractive index detector. The phospholipids were believed to be retained on the head of the silica column due to the highly polar phosphate groups. Since the phospholipids lack a good chromophore, UV and fluorescence detection could not be used, and an alternative method was needed for determining the retention time of the phospholipids. Thus, silica gel plates were obtained which were manufactured from the same gel as the HPLC column, and the triglyceride and phospholipid standards were chromatographed under the same mobile phase conditions as the HPLC column. Development of the plates confirmed that the phospholipids were contained at the head of the LC column, thus preventing their

fatty acid constituents from interfering with the GC analysis. The LC column was periodically backflushed to remove the phospholipids from the head of the column.

Typical off-line separation and derivatization schemes

Analysis of the triglycerides is usually carried out off-line by the formation of the fatty acid methyl ester in the presence of a strong acid, with subsequent extraction of the methyl ester into an organic solvent and separation by GC[9–11]. Table I lists the steps involved in an off-line separation and derivatization scheme. Initially an acidic PCR solvent was used with the on-line LC–PCR–GC system. To increase the reaction rate of the lipid (organic layer) and the reaction solvent (aqueous layer) isopropanol was added forming a single-phase system. To verify that the addition of the isopropanol did not cause the formation of the isopropyl esters of the fatty acids, the isopropyl esters by palmitic and stearic acid were synthesized and chromatographed by GC. No response was ever detected for the isopropyl esters of either fatty acid.

Acidic PCR solvent

The preliminary results obtained with an acidic post column reactor solvent and a mixer/reaction loop proved to be quite unsatisfactory. The first acidic solution

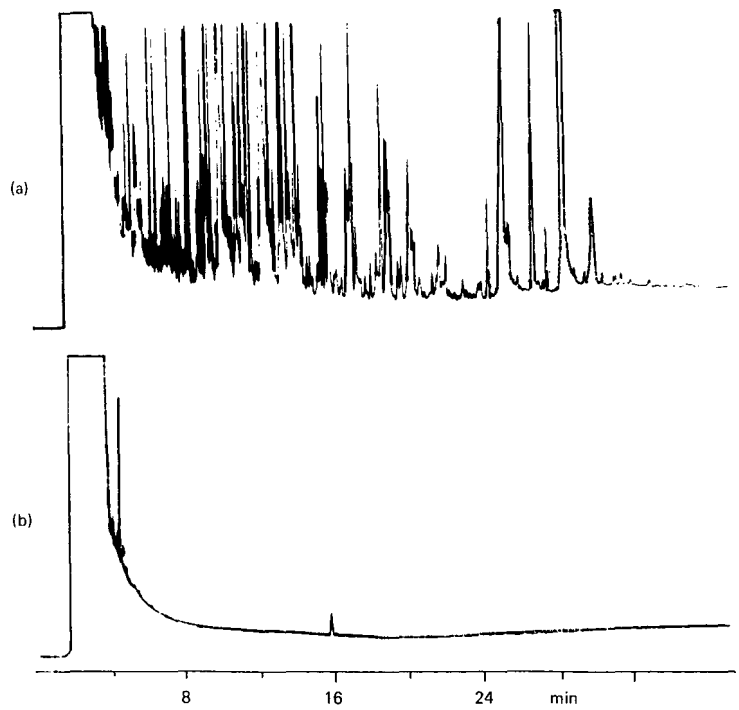

Fig. 1. GC traces of (a) the on-line separation and derivatization of a standard solution of tripalmitin using an acidic post-column derivatization solution of methanol–isopropanol–trifluoroacetic acid (100:100:1) (Notice the excessive column bleed due to the injection of an acidic solution); (b) off-line derivatization prior to GC with methanol–chloroform–hydrochloric acid (10:1:1), with extraction into hexane. (Notice lack of sensitivity, 10 μl injection.)

employed, methanol–isopropanol–hydrochloric acid (100:100:1), produced several major peaks in the GC separation, which interfered with the resulting methyl ester separation. Dilution of the acid was examined as a means of eliminating the spurious peaks. Though the intensity of these peaks were greatly reduced they were not eliminated. Furthermore, the reaction rate of the methanolysis was severely decreased. An organic acid, trifluoroacetic acid, was examined as a catalyst. However, once again the separation showed several interfering peaks (Fig. 1). Reduction of the acid content did not eliminate this problem and therefore other reaction schemes were investigated. The spurious peaks in the acid catalyzed reactions were throught to be due to column phase hydrolysis caused by the injection of the acidic solutions.

Alternative derivatization schemes

Many off-line derivatization schemes for the formation of methyl esters of fatty acids are commercially available[10,11] however, the chemicals employed were not readily compatible with the post-column reactor pump. Thus, it was felt that the acid catalyzed reaction scheme used previously had to be modified in one of two ways: (1) addition of an anion-exchange column after the reaction loop to remove the acid prior to GC injection, or (2) removal of the acid from flow stream completely with the substitution of a strong cation-exchange column for the reaction loop.

The first of these choices was not investigated for several reasons including: (1) removal of the acid would deplete the anions thus requiring either continuous replacement of the anion-exchange column or additional pumping capability for regenerating the ion-exchange capability of the column, and (2) the column would add to the variance of the transfer zone thus increasing the volume of the zone.

Fixed-bed reactor

The second alternative, the addition of a strong cation-exchange column, was chosen since complete removal of the acid would eliminate the acidic hydrolysis of the GC stationary phase. Since the acid groups on the cation-exchange column are used as a catalyst, they will not be consumed by the reaction, thus eliminating the need for column regeneration. Also, by carrying out the reaction in a packed bed of very small particles (10 μm) the zone should maintain its narrow width, whereas the original mixer/reaction loop, though modified to minimize the differences in the laminar flow, adds a significant amount of variance to the zone. The width of the zone transferred is an important criteria for successful LC–GC interfacing[12,13] due to the minute injection volumes tolerated by GC.

Zone transfer

Because of the large transfer volumes (column diameters of 2.0 mm generate transfer volumes of approximately 0.2 ml) and the low concentration of triglycerides (note Fig. 1b, 10 μl injection of methylpalmitate standard) the retention gap[14–18] technique was employed. The retention gap technique is ideally suited for trace work since it allows the transfer of several hundred microliters of sample to the GC system, and as shown by Grob[19]. The application of Grob's method to the LC–GC interface is an obvious and effective extension of the technique. Injections of up to 2 ml have been reported in the literature[14] when using concurrent solvent evaporation. Initially short retention gaps were examined (10 and 21 m) in this work. However, as noted by

Grob[19] polar molecules such as methanol and isopropanol require longer retention gaps due to their higher heats of vaporization. Grob also noted that heptane floods a longer section of capillary than hexane or pentane, therefore requiring a longer retention gap. The 10- and 21-m retention gaps were not sufficiently long enough to allow complete solvent evaporation, because the sample loop was injected by flushing with carrier gas (fast injection). The alternative injection technique, concurrent solvent evaporation, was not used because the high PCR temperatures did not allow accurate flow-rates, a requirement for this technique. Therefore, a long, 50 m, retention gap was used to accommodate the longer evaporation times required by the polar LC and PCR solvents.

On-line LC–PCR–GC

Fig. 2 shows a block diagram of the apparatus used for this study. The system was simplified by the removal of the LC detector prior to the post column reactor, since the triglycerides were completely excluded from the separation column. The LC detector at the exit of the fixed-bed reactor column was also removed, since the (non-polar) methyl esters did not exhibit any retention on the (polar) reactor column.

The first switching valve (Fig. 2) allows the trapping of the triglyceride zone on the reactor column (to prevent evaporation of the solvent, the inlet and outlet ports in the trapped position of the valve were plugged). A multicapillary eluent splitter[20] was initially used to skim the derivatized zone, as it eluted from the fixed-bed reactor column, and transfer it to the second valve. However, the splitter was removed due to the excessive back pressure (> 2000 p.s.i.g.) caused by the high viscosity of the eluent (33% isopropanol). This was necessary because the reactor column was a medium pressure resin (< 1500 p.s.i.g.). The second switching valve is used for trapping the derivatized lipid zones for on column injection.

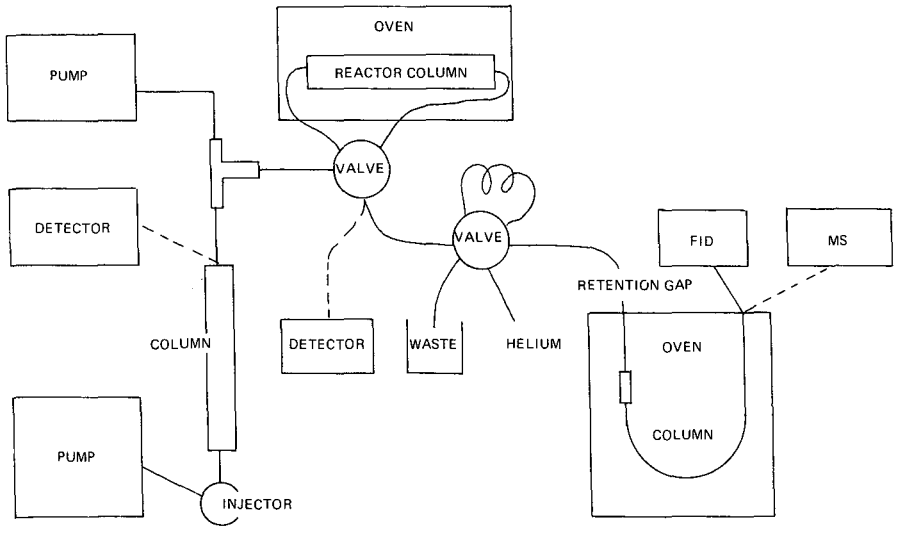

Fig. 2. Block diagram of the on-line LC–PCR–GC system. The detectors were removed after determining the elution times of the triglycerides and methyl esters respectively. The use of a retention gap allowed the transfer of the large derivatized zone. FID = Flame ionization detector; MS = mass spectrometer.

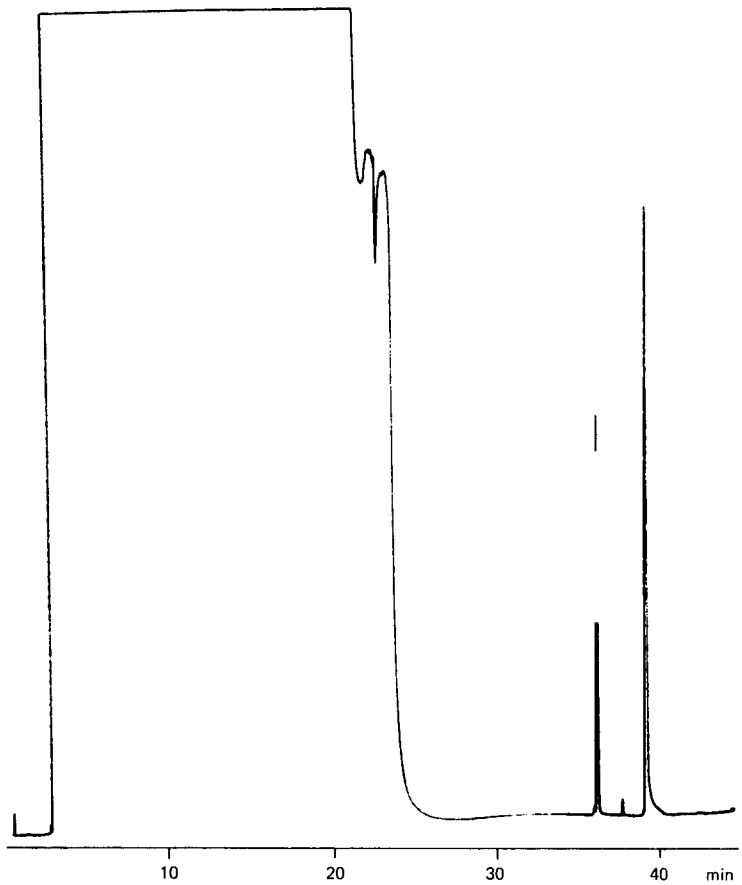

Fig. 3. Separation and derivatization of standards, tripalmitin and tristearitin, on the on-line LC–PCR–GC system using the fixed bed reactor catalysis column. LC conditions: mobile phase, heptane–isopropanol (7:3); flow-rate, 0.3 ml/min; column, LiChrosorb Si 60 A 250 mm × 2.0 mm. PCR conditions: solvent, isopropanol–methanol (4:6); flow-rate, 0.3 ml/min. GC conditions: on-column injection, 50 μl; retention gap, 50 m × 0.32 mm deactivated; separation column, 25 m × 0.32 mm 5% phenylmethylsilicone; hold 100°C for 25 min; ramp at 7°C/min to 280°C.

Reproducibility and kinetics of the esterification

Fig. 3 shows the derivatization and separation of the standards tripalmitin and tristearitin on the LC–PCR–GC system. The reaction rate of the esterification was determined by injecting a solution of tripalmitin (1.2 mg/ml) on the LC–PCR–GC system and varying the reaction time while recording the GC response. Fig. 4 is a plot of the data from this experiment. From the graph it appears that a reaction time of 2 h was sufficient to convert all of the triglyceride present to the methyl ester. Reproducibility of the system was determined by injecting a solution, containing tripalmitin and an internal standard, tristearitin, on the system using a reaction time of 2 h. The average relative standard deviation using the internal standard averaged 9%. Tristearitin was chosen as the internal standard to account for any changes in reac-

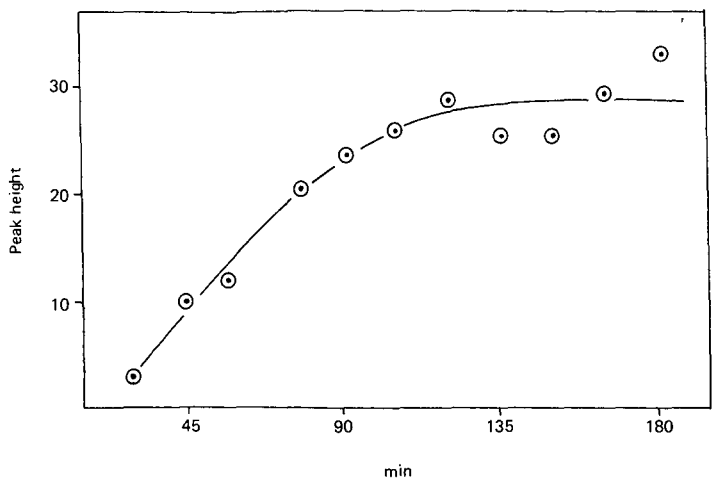

Fig. 4. Plot of the GC response *versus* reaction time for the fixed-bed reactor system. GC injection volume was 50 μl.

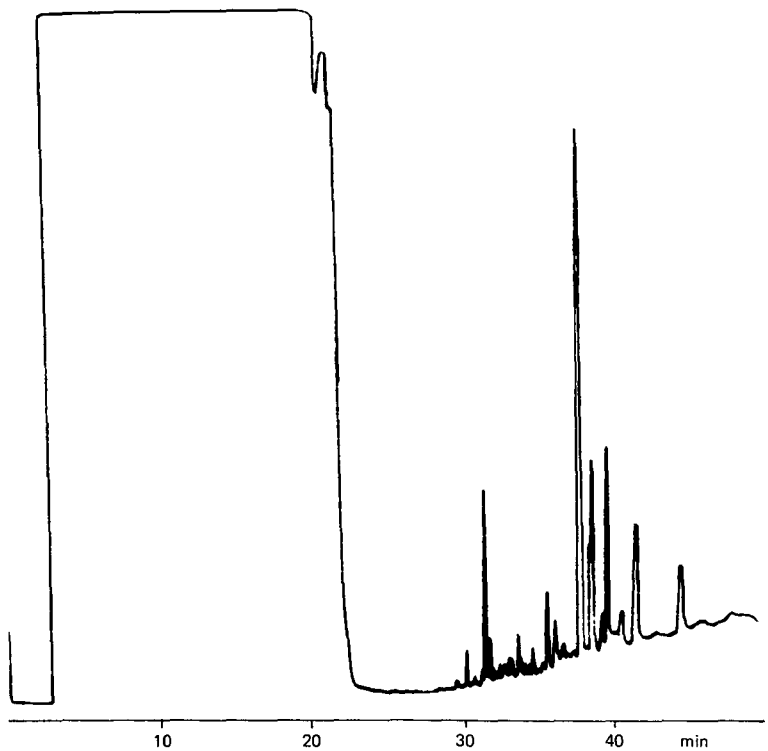

Fig. 5. Derivatization of the entire lipid fraction of *Staphylococcus aureus* separated by the Bligh-Dyer technique. GC conditions as in Fig. 3.

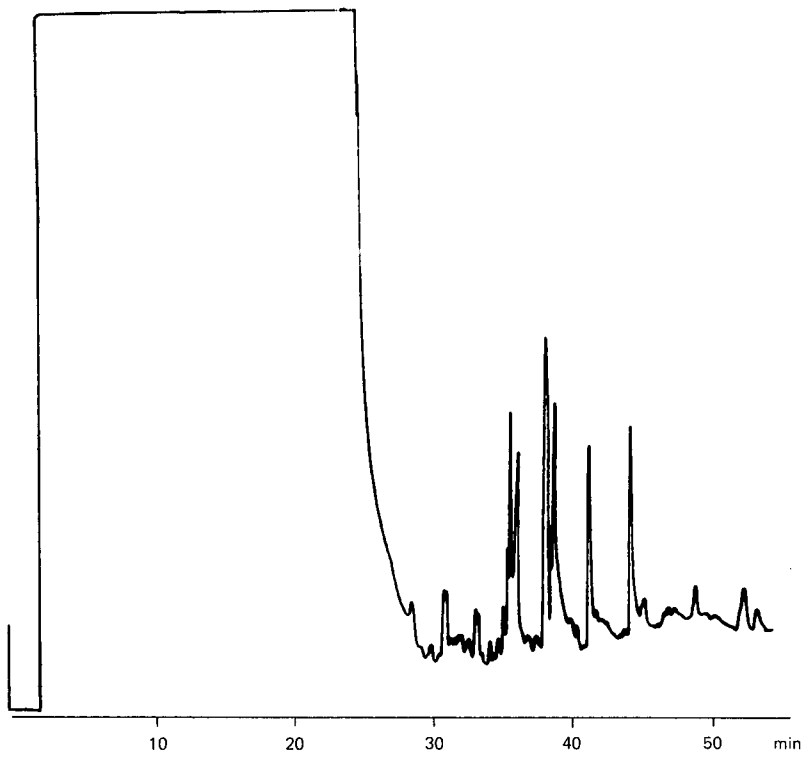

Fig. 6. Separation and derivatizaton of the *Staphylococcus aureus* lipid fraction on the on-line LC–PCR–GC system. LC and GC conditions as in Fig. 3. Note the elimination of the fatty acid constituents from the phospholipids, see Fig. 5.

tion rate caused by fluctuations in temperature and solvent composition. Linearity of the system was determined by injecting solutions of the lipids in the concentration range 0.09–0.5 mg/ml. The correlation coefficients for tripalmitin was 0.992. Examination of a plot of the residuals indicated good linearity over this range.

Application to samples of biological interest

The system was applied to the separation and identification of the triglycerides which are contained in *Staphylococcus aureus*. Fig. 5 is a GC trace of all of the lipid constituents that were extracted by the Bligh-Dyer technique from the *Staphylococcus aureus* cells (*i.e.* no LC fractionation prior to GC). The sample was then run on the LC–PCR–GC system (Fig. 6) with a noticeable difference in composition due to the exclusion of the phospholipids from the derivatization and GC separation steps. Confirmation of the lipid constituent was performed by GC–mass spectrometry off-line. Information gained by determining the fatty acids which compose the biomass community is important for determining whether communities have suffered genetic damage due to environmental pollution.

CONCLUSIONS

The addition of a post column reactor to the on-line LC–GC increases the range of analyses for the multidimensional LG–GC experiment dramatically. Although the system presented did not decrease analysis time significantly for the lipid separations as compared to existing TLC methods (Table I), it did show the feasibility of the technique. Unfortunately, the particular reaction chosen was limited by slow kinetics, while the use of faster reagents, such as boron trifluoride, would be prohibitively expensive unless pulsed into a reactor coil only while the peak of interest elutes. Nevertheless, the value of having a completely automated system is significant as compared to the manual procedures currently in use. Future work will focus on improving the kinetics of the derivatization reaction, and applying PCR to other biological samples.

ACKNOWLEDGEMENTS

The authors thank Dan Lee of Hamilton Company for supplying the cation exchanger. Steven Fazio and Roger Hsu are gratefully acknowledged for many helpful discussions during the course of this work. The authors gratefully acknowledge the Center for Advancement of Food Technology, the Petroleum Research Fund (AC3-16161), the Bush Memorial Fund and the PQ Corporation for support of this research.

REFERENCES

1 T. V. Raglione, J. A. Troskosky and R. A. Hartwick, *J. Chromatogr.*, 409 (1987) 205.
2 F. Munari and K. Grob, *J. High Resolut. Chromatogr. Chromatogr. Commun.*, 11 (1988) 172.
3 J. C. Frankland, *Soil Biol. Biochem.*, 7 (1975) 339.
4 C. M. Hepper, *Soil. Biol. Biochem.*, 9 (1977) 15.
5 M. J. Swift, *Soil. Biol. Biochem.*, 5 (1973) 321.
6 D. C. White, W. M. Davis, J. S. Nickels, J. D. King and R. J. Bobbie, *Oecologia*, 40 (1979) 51.
7 K. Grob, G. Grob, W. Blum and W. Walther, *J. Chromatogr.*, 244 (1982) 197.
8 E. G. Bligh and W. J. Dyer, *Can. J. Biochem. Physiol.*, 37 (1959) 911.
9 D. C. White, R. J. Bobbie, J. S. Nickels, S. D. Fazio and W. M. Davis, *Botanica Marina*, 23 (1980) 239.
10 *Pierce Chemical Catalog (NSTFA method)*, Pierce, Rockford, IL, 1987, p. 187.
11 *Pierce Chemical Catalog (BF_3)*, Pierce, Rockford, IL, 1987, p. 202.
12 J. C. Giddings, *J. High Resolut. Chromatogr. Chromatogr. Commun.*, 10 (1987) 312.
13 T. V. Raglione, N. Sagliano, Jr. and R. A. Hartwick, *Chromatography*, (1987) 42.
14 K. Grob, Jr., *J. Chromatogr.*, 237 (1982) 15.
15 K. Grob, Jr. and R. Müller, *J. Chromatogr.*, 244 (1982) 185.
16 K. Grob, Jr. and K. Grob, *J. Chromatogr.*, 270 (1983) 17.
17 K. Grob, Jr., *J. Chromatogr.*, 279 (1983) 225.
18 F. Munari, A. Trisciani, G. Mapelli, S. Trestianu, K. Grob, Jr. and J. M. Colin, *J. High Resolut. Chromatogr. Chromatogr. Commun.*, 8 (1985) 601.
19 K. Grob, Jr., *J. Chromatogr.*, 213 (1981) 3.
20 T. V. Raglione, J. A. Troskosky and R. A. Hartwick, *J. Chromatogr.*, 409 (1987) 205.

Journal of Chromatography, 454 (1988) 169–183
Elsevier Science Publishers B.V., Amsterdam — Printed in The Netherlands

CHROM. 20 820

POLYMERIC BENZOTRIAZOLE REAGENT FOR THE OFF-LINE HIGH-PERFORMANCE LIQUID CHROMATOGRAPHIC DERIVATIZATION OF POLYAMINES AND RELATED NUCLEOPHILES IN BIOLOGICAL FLUIDS*

T.-Y. CHOU, C.-X. GAO, S. T. COLGAN and I. S. KRULL*
Department of Chemistry, The Barnett Institute, 341 Mugar Building, Northeastern University, 360 Huntington Avenue, Boston, MA 02115 (U.S.A.)
and
C. DORSCHEL and B. BIDLINGMEYER
Applications Department, Waters Chromatography Division, Millipore Corporation, 34 Maple Street, Milford, MA 01757 (U.S.A.)
(First received March 22nd, 1988; revised manuscript received July 11th, 1988)

SUMMARY

A polymeric benzotriazole reagent containing a 9-fluorenylmethyleneoxycarbonyl (FMOC) group has been synthesized, characterized, and its derivatizations, off-line, for three polyamines, have been optimized with regard to solvent, time, and temperature. An authentic FMOC derivative of cadaverine has been prepared, characterized, and used as the external standard for quantitation of off-line derivatizations and identification of final derivatives. Actual percent derivatizations have been determined, rather than just percent disappearance of starting material. The polyamines in urine or other biological fluids can be derivatized without organic solvent or solid phase extraction, but rather *in situ* by the simple addition of the polymeric reagent to the fluid, incubation for a few minutes at room or elevated temperature, filtration and direct injection. Derivatizations could also be performed by transferring a small volume of the hydrolyzed and filtered biological fluid to a disposable pipette containing the polymeric reagent. Derivatization was then followed by elution, filtration, and direct injection onto the high-performance liquid chromatographic (HPLC) system. Automation of the overall polymeric derivatization, filtration, HPLC injection, separation, detection, quantitation, and data acquisition-interpretation is suggested.

The polymeric reagent has been utilized for the qualitative and quantitative determination of cadaverine and putrescine, normally occurring polyamines, in human urine. These levels were compared with the corresponding literature values for healthy human subjects, and the values were found to be in excellent agreement. This novel derivatization approach, though off-line, provides for a much simpler, more rapid, and more efficient conversion of these and related polyamines or nucleophiles

* Contribution No. 363 from the Barnett Institute at Northeastern University.

0021-9673/88/$03.50

to derivatives having vastly improved chromatographic detection properties in HPLC. The final derivatives contain the FMOC group, making them extremely chromophoric and fluorophoric, and providing trace detection at ppb (μg/l) and sub-ppb levels. The overall approach is recommended for these and other biologically occurring polyamines, in fluids and tissues, as well as related bioorganic and biologically active nucleophiles, including drugs and their metabolites.

INTRODUCTION

In recent years, we and others have described certain novel polymeric or solid phase reagents that have proven advantageous in both off-line and on-line derivatizations related to final high-performance liquid chromatographic (HPLC) determinations[1–15]. We have most recently described the synthesis, characterization, optimization of derivatizations, percent derivatizations, and analytical figures of merit for a particular polymeric benzotriazole reagent containing the 9-fluorenylmethylene oxycarbonyl (FMOC) tag[15]. The derivatization of standard nucleophiles using this polymeric benzotriazole reagent provided additional selectivity, and also decreased detection limits for primary and secondary amines or polyamines by both ultraviolet (UV) and fluorescence detection in HPLC. However, no real world applications for this polymeric reagent were described. The label or tag was designed to be detector versatile, so that the derivative(s) would be amenable to several different detection modes, in this case UV–fluorescence[15]. Gao *et al.*[15] have done a complete study using a related polymeric benzotriazole *o*-acetylsalicyl reagent for derivatizations of simple amines. These particular derivatives were totally analogous to others described by us for a related polymeric anhydride reagent containing the same tag[13].

When one performs an analysis involving a derivatization, solution or solid phase, the derivative must often be separated from excess derivatizing reagent and any other species present in the sample matrix. Of course, in the case of solid phase reagents, excess derivatizing reagent is not present in the final derivative solution, though sample components still are[1,2]. The separation of analyte derivative from potential interferents may be achieved through chromatography, but if several detection modes are available, separation of the derivative may be more easily accomplished through selective detection. This was singularly exemplified in the recent reports by Colgan *et al.*[11,12,14].

Polyamines, such as putrescine and cadaverine, were chosen as analytes due to their physiological and biochemical significance. The concentrations of polyamines in the urine of cancer patients and in the plasma of uremic patients are elevated[16–18]. Accurate and precise quantitation for polyamines in physiological fluids have been of considerable importance and interest. HPLC coupled with fluorescence detection offers high sensitivity and good specificity as a general approach for polyamine assays at trace levels, following appropriate derivatization. Various solution derivatizing reagents, such as: *o*-phthalaldehyde (OPA), fluorescamine (Fluram), and 5-dimethylaminonaphthalene-1-sulphonyl (Dansyl) chloride have been used for polyamine derivatizations in the past[19–26].

All of these solution reagents and reactions lead to polyamine derivatives with strong fluorescent properties and excellent detection limits. However, none of the

existing derivatizations have involved solid phase reagents, such as the polymeric benzotriazole FMOC[15]. This new polymeric reagent has been synthesized using standard procedures, based on a polystyrene–divinylbenzene support, commercially available. The FMOC tagging moiety was purposely incorporated into the final polymeric reagent, which resulted in fluorenylamino type derivatives, actually carbamates.

This reagent has been used in an off-line, pre-column mode, prior to HPLC injection, for a number of polyamines. Its use in the on-line, pre-column mode, has been attempted, but found unsuccessful in a repetitive manner[27]. A standard FMOC derivative of cadaverine was prepared, characterized by physical and spectral properties, as well as elemental analysis, and used as an external standard to determine percent derivatizations with the polymeric reagent[15]. The reagent itself was characterized by its method of synthesis and loading determinations. The feasibility and applicability of this reagent for the derivatization of polyamines, such as cadaverine and putrescine, in biological fluids has now been examined under optimized conditions. This approach can provide significant advantages over all related solution type derivatizations with the same and related nucleophiles. The approach may be applicable for routine clinical and biomedical–biochemical analyses in most, if not all, aqueous, organic, or aqueous–organic sample matrices.

The limits of detection (LODs) with fluorescence are 1–2 pmol for typical polyamines using the above approach, which is comparable to or better than all existing solution derivatization methods[19–26]. The linear calibration range is 3–4 orders of magnitude concentration of each polyamine.

EXPERIMENTAL

Chemicals, reagents and solvents

Macroporous polystyrene–divinylbenzene copolymer (particle size, d_p 60–90 μm, Porapak Q) was obtained from Waters Chromatography Division (Millipore, Milford, MA, U.S.A.). Chemicals used were obtained from a variety of commercial sources, including: Aldrich (Milwaukee, WI, U.S.A.), Burdick & Jackson Labs. (Muskegon, MI, U.S.A.), J. T. Baker (Phillipsburg, NJ, U.S.A.), Alfa Products (Danvers, MA, U.S.A.), Sigma (St. Louis, MO, U.S.A.). These chemicals were of the highest purity available and were used without further purification. HPLC solvents were obtained from EM Science (Cherry Hill, NJ, U.S.A.), as their Omnisolv HPLC grade. All HPLC solvents were used after filtration through a 0.45-μm solvent filter (GVWP, Millipore, Bedford, MA, U.S.A.) and degassed under vacuum with stirring.

Apparatus

The HPLC system consisted of a Waters Model 6000A solvent delivery system, a Waters Model U6K syringe loading injection valve, and a Brown Boveri Model SE 120 dual-pen recorder (Brown Boveri, Metrawatt/Goerz Division, Vienna, Austria). Chromatographic columns consisted of a Waters μBondapak™ C_{18} reversed-phase, 30 cm × 7.8 mm I.D. (semipreparative), a Waters μBondapak C_{18} reversed-phase, 30 cm × 3.9 mm I.D., or an 8 mm I.D. Radial-Pak Resolve™ C_{18} column used in a Model RCM-100 radial compression module. The detectors consisted of a Waters Model 480 variable-wavelength UV detector and a Hitachi Model F1000 fluorescence

spectrophotometer. At times, a Hewlett-Packard Model 3380A reporting integrator (Hewlett Packard, Palo Alto, CA, U.S.A.) was used.

The instrumentation used to characterize the isolated standards or monitor creatinine levels consisted of a Varian Model XL-300 NMR Spectrometer (Varian, Palo Alto, CA, U.S.A.), a Perkin-Elmer Model 599B infrared spectrophotometer (Perkin-Elmer, Analytical Instruments, Norwalk, CT, U.S.A.), a Thomas Hoover capillary melting point apparatus (Arthur H. Thomas, Philadelphia, PA, U.S.A.), a Perkin-Elmer Model Lambda 3B UV–VIS spectrophotometer equipped with the Perkin-Elmer data station, a Milton Roy Model Spectronic 1201 scanning UV–VIS spectrophotometer [Milton Roy, Analytical Products Division (formerly division of Bausch & Lomb), Rochester, NY, U.S.A.], and a Nuclide magnetic sector mass spectrometer (Nuclide, State College, PA, U.S.A.). At times a Hewlett-Packard Model HP 1040A linear diode array UV–VIS detector was used to confirm the purity of standards.

Preparation and reaction conditions of the polymeric benzotriazole FMOC reagent

The entire synthetic procedure for preparation of the final polymeric benzotriazole FMOC reagent (I) was indicated in our previous paper[15]. Because the method of synthesis and its reactions with standard amines or polyamines have been presented elsewhere in the literature, these are not repeated here. The reader is referred to the literature for additional, specific information[15,27,28].

Characterization of the polymeric reagent

The amount of labelling moiety in one gram of the polymeric support was determined by a base-initiated hydrolysis of the polymeric reagent. This procedure was used to demonstrate if the synthesis was successful. It also indicated how much derivatizing reagent or tag had been incorporated into the final polymeric support. Though we have previously described the method of characterization for the analogous polymeric benzotraizole *o*-acetylsalicyl reagent, the hydrolysis information for the FMOC incorporated reagent I was not described[15].

Hydrolysis reaction of polymeric benzotriazole FMOC reagent. Hydrolysis and quantitation of the released tag or its analogue is an accepted method for the determination of loading of a polymeric tagging/derivatizing reagent. The polymeric benzotriazole FMOC reagent (137 mg) (I) was added to 10 ml dioxane and 20 ml potassium hydroxide solution (0.2 *M*) and refluxed for 4 h. After hydrolysis, the solution was acidified to pH 3, and the reaction product was extracted twice by 50 ml chloroform. The organic phase was collected and the solvent was evaporated under vacuum. The reaction product was redissolved in 20 ml acetonitrile, and 25 μl of this solution was injected into the HPLC system. The same procedure was repeated for a reaction blank, except that there was no potassium hydroxide added. The LC–UV chromatogram of the hydrolysis product showed an unknown peak at a retention time of 3.2 min under the following chromatographic conditions: 8 mm I.D. Radial-Pak Resolve C_{18} column used in a RCM-100 module; mobile phase: acetonitrile–water (90:10); flow-rate: 2.0 ml/min; UV at 254 nm.

Preparation, isolation and characterization of dibenzofulvene. Hydrolysis of the polymeric benzotriazole FMOC reagent gave essentially an unknown product which was suspected to be dibenzofulvene (II)[29]. The possible mechanism of this

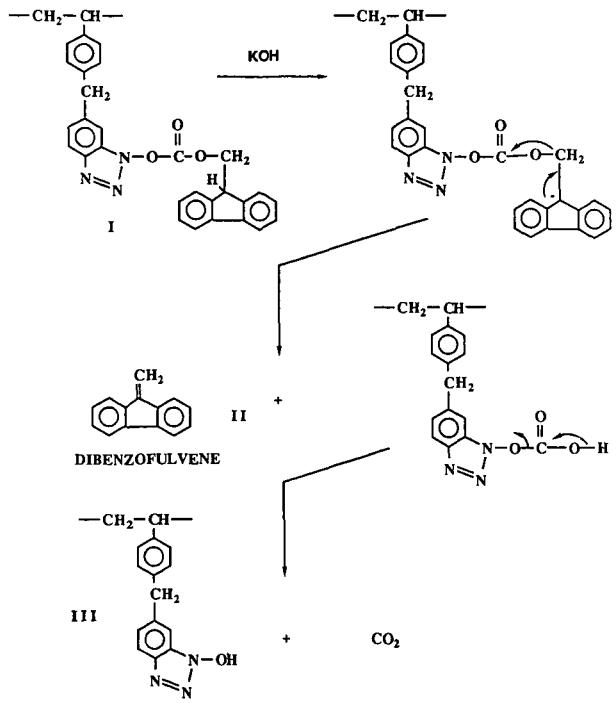

Fig. 1. Possible mechanism of the hydrolysis reaction of polymeric benzotriazole fluorenylmethyl (FMOC) reagent, I, leading to formation of dibenzofulvene, II.

hydrolysis reaction is shown in Fig. 1. To characterize the polymeric benzotriazole FMOC reagent, it was necessary to quantitate this product and thereby determine the loading. Base-catalyzed hydrolysis of 9-fluorenylmethanol could have provided the desired dibenzofulvene, and that could have been used as an external standard. Base hydrolysis of 9-fluorenylmethanol by potassium hydroxide did give one major product. 9-Fluorenylmethanol (1.27 mmol) was dissolved in 15 ml acetonitrile, and this was mixed with 15 ml potassium hydroxide solution (1.27 mmol). The mixture was refluxed for 2 h, and the reaction mixture was extracted with 80 ml chloroform. A white precipitate in the organic layer, which might have been an insoluble polymer of dibenzofulvene, was discarded. The organic solvent was evaporated under vacuum, and the residue was partially dissolved in acetonitrile. The solution was filtered again, and the filtrate was injected into the HPLC system, with conditions as above. Again, a single peak at 3.2 min was observed, strongly suggesting the hydrolysis formation of the same product from the polymeric FMOC reagent (I).

To isolate the desired product, the solution from the above hydrolysis reaction was subjected to semipreparative LC using isopropanol–hexane (3:97) as the mobile phase. Dibenzofulvene (15 mg) was isolated. Since dibenzofulvene was only partially soluble in various solvents, such as acetonitrile, dioxane, chloroform and hexane, and no sharp melting point was observed up to 250°C, we believed most of the dibenzofulvene was polymerized during the collection procedure[29]. The electron impact (EI) mass spectrum of dibenzofulvene showed a base peak at *m/e* 179, which may

have been the molecular ion. Due to the solubility problem in chloroform, the NMR spectrum was not reliable. However, it did show an olefinic methylene group at 6.1 ppm (singlet) and aromatic hydrogens between 7.2–7.8 ppm (multiplet), as demanded by the structure. Because the dibenzofulvene hydrolysis product was not stable to the hydrolysis conditions, the amount determind, as above, could not be a reliable indicator of the original loading of the FMOC tag on the polymeric reagent I. Elemental analysis was attempted as an alternative approach. The data for the C, H, N analyses of the FMOC reagent was consistent with the theoretical value calculated[15].

Preparation, isolation and characterization of external standard of cadaverine

The authentic, external standard of fluorenylmethyl cadaverine was prepared in-house and characterized. This was prepared by reacting 9-fluorenylmethyl chloroformate (18:4 mmol) with cadaverine (9.2 mmol) in 15 ml chloroform at room temperature for 30 min. The organic solvent was then evaporated under vacuum. The derivative of cadaverine was isolated by preparative HPLC conditions as follows. Column: Waters μBondapak C_{18} reversed-phase, 30 cm × 7.8 mm I.D. (semipreparative); mobile phase: acetonitrile–water (70:30); flow-rate: 2.5 ml/min; retention time: 14.4 min.

The physical and spectral properties for this compound have been reported previously, and the reader is referred to the literature for further details. Since all of the analytical and structural data were consistent with the expected structure, the characterized compound was then used as an external standard to determine percent reactions with the polymeric reagent for cadaverine, putrescine, and 1,7-diaminoheptane, under different reaction conditions. These data were reported previously[15]. Since a standard addition technique was used here to quantitate for cadaverine and putrescine in urine, starting with the base polyamines, no external standards were needed, other than to qualitatively identify the presence of such polyamines in urine after derivatization.

Procedure for derivatization of polyamines

The step-by-step procedure for derivatization of both polyamines, cadaverine and putrescine, has been reported elsewhere[15]. Approaches leading to these optimization conditions were similarly described. The derivatization reaction for a typical polyamine with this reagent is shown in Fig. 2. The HPLC–UV/fluorescence conditions used for the determination of the polyamine derivatives from urine were: acetonitrile–water (70:30), flow-rate 1.5 ml/min, 100 mm × 8 mm I.D. Radial-Pak Resolve C_{18} column, 5 μm, used in an RCM-100 module, fluorescence at 275/315 nm, UV at 254 nm.

Optimization of excitation and emission wavelengths

The excitation and emission wavelengths of the FMOC derivatives of amino acids have been reported to be 264 and 340 nm[30]. These wavelengths were optimized using flow injection analysis (FIA) by changing the emission wavelength, while holding the excitation wavelength constant. Knowing the optimum emission wavelength, the excitation wavelength was further optimized. The optimal excitation and emission wavelengths were 275 and 315 nm for the polyamine derivatives of the polymeric benzotriazole fluorenylmethyl reagent, I.

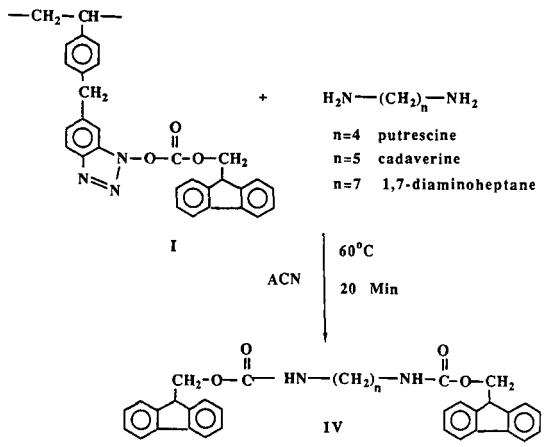

Fig. 2. The derivatization reaction of typical polyamines with the polymeric benzotriazole fluorenylmethyl (FMOC) reagent. ACN = Acetonitrile.

Urine sample preparation and derivatization of polyamines

Sample preparation and collection. It was necessary to have a bottle of about 2 l capacity. The bottle was clean, and toluene (as preservative) was added before collection was started. At a convenient time in the morning, the bladder was emptied and the specimen was discarded. This voiding represented urine produced by the kidneys before the period of collection. Thereafter all urine voided up to and including the time corresponding to that of the discarded specimen of the previous morning was placed in the bottle, which was kept in a refrigerator. Analyses were carried out as soon as possible after collection of the specimen.

Measurement of volume. Since the amount of a polyamine in the whole specimen was found by calculation from the amount determined in an aliquot, it was necessary to know the exact volume of the 24-h specimen. Hence the volume was carefully measured before any other determination was made.

Procedure for hydrolysis and derivatization of urine samples. A urine sample was collected during a 24-h period. The total volume was 1.8 l. To develop a suitable procedure for derivatization of 24-h urine, several factors had to be taken into consideration. The overall scheme for hydrolysis and derivatization of a typical urine sample was as follows: urine (or spiked urine) → hydrolysis → centrifuge → neutralization → derivatization → dilution → injection into HPLC system.

Since the polyamines were present in human urine predominantly as conjugates, it was necessary to hydrolyze the sample prior to analysis in order to liberate any polyamines from their conjugates. Most reports indicate total polyamines present, as free and conjugates in urine. A modified procedure from the literature is described as follows[31]. A 5 ml 24-h urine sample was added with 1.2 ml conc. hydrochloric acid in a reaction vial. After hydrolysis for 16 h at 110°C in an oil bath, the hydrolysate was neutralized with 6 *M* sodium hydroxide and the pH was adjusted to 9. The solution was centrifuged at 4000 rpm for 10 min and any precipitate was discarded. The clear solution was condensed to a volume of 1.5 ml. This aqueous solution (50 μl) was derivatized with the polymeric benzotriazole FMOC reagent in a

disposable Pasteur pipette at 60°C for 30 min. After reaction, the product was washed from the reaction cartridge with acetonitrile to a volume of 1 ml and 20 μl was injected into the HPLC system.

Method for determining creatinine levels in human urine. Most methods for determining creatinine are based on the Jaffe reaction described in 1886. Creatinine, in this reaction, reacts with alkaline picrate to form an amber-yellow solution that is measured photometrically. The nature of the substance formed is thought to be a salt of creatinine, picric acid, and sodium hydroxide[32].

Reagents used. The reagents used are sodium hydroxide, 0.75 *M* and picric acid. Since picric acid is explosive when it is dry, a certain amount of water was added. To determine the concentration of picric acid, a standard solution of sodium hydroxide (0.75 *M*) was used to titrate against a solution of picric acid. The concentration of picric acid was calculated to be 0.056 *M*. Creatinine was used as the working standard. Various concentrations (5, 10 and 20 ppm) of creatinine solutions were prepared by dissolving creatinine standard (free base, purchased from Sigma) in 0.1 *M* hydrochloric acid.

Procedure. Dilute 5 ml of 24-h urine to 500 ml in a volumetric flask and mix well. Pipet 6 ml of the diluted urine into a test tube and add 2 ml of 0.056 *M* picric acid and 2 ml of 0.75 *M* sodium hydroxide, mix well. Treat 6 ml of distilled water (this was used as a blank) and 6 ml of working standard creatinine in the same way. Allow to stand for 15 min and read spectrophotometrically within next 30 min.

RESULTS AND DISCUSSION

Percent derivatizations of cadaverine as a function of solvent

We had previously shown that of all the solvents tested, acetonitrile offered the highest percent derivatizations under optimal time and temperature conditions. More specific conditions for both derivatizations and HPLC for the polyamine standards have been reported elsewhere[15]. There was a significant decrease in percent derivatization as the solvent was changed from acetonitrile to hexane to water (72.1 ± 5.8%, 39.1 ± 2.5% and 7.1 ± 0.5%, respectively, average ± S.D., n = 9–11). The fact that an aqueous solution provided the lowest percent reactions of all was significant, since the polymeric reagent was to be used for polyamines in aqueous–biological fluids. The overall reproducibility of the derivatizations in water was excellent, with a relative standard deviation (R.S.D.) of about 7%, less than the R.S.D. in some other solvents. Thus, even for a low percent derivatization, reproducibility can be acceptable. However, using water as the solvent had two major advantages: (i) convenience; and (ii) no extraction was needed. As will be seen, even with this reduced reactivity, the extreme sensitivity of the final derivatives by fluorescence overcame a potential reactivity deficiency. Though most analysts would prefer percent derivatizations that approach 100% at all times, this becomes a moot point if the final derivatives formed can be detected at the trace levels needed, even with a 1% derivatization. That was exactly the case with polyamines in urine using the polymeric fluorescent derivatizing reagent, I.

Using aqueous samples, it is likely that water reacts as a nucleophile and causes hydrolysis of the polymeric reagent and thus bleeding. However, based on our studies, we have not seen excess bleeding using water as a solvent as compared to that

using acetonitrile. More strenuous conditions are required to hydrolyze this polymeric reagent.

Analysis of cadaverine and putrescine in 24-h urine samples

Usually, 24-h samples of urine are used in any quantitative analysis of polyamines in urine. Quantitative determinations of the polyamines of random voiding are of no value or significance in the interpretation of metabolic processes. it is only when all the urine produced by the kidneys over a known period of time is analyzed, that conclusions can be drawn as to what the body is doing with various foodstuffs. A 24-h sample is usually preferable. This was done here, and a literature modified procedure was perfected for collection of urine, storage of urine, hydrolysis, and pH neutralization (see Experimental).

The final urine solution after hydrolysis was derivatized in one of two ways: (1) by adding a small aliquot of a known volume of the urine to a fixed amount of the polymeric reagent in a disposable pipette (see Experimental and ref. 15); or (2) by adding a fixed amount of the polymeric reagent to an aliquot solution of the hydrolyzed and neutralized urine, *en toto*. That is, derivatizations could be successfully performed just by adding some of the polymeric reagent to the hydrolyzed urine, followed by mild heating (60 °C) for a short period of time (10–20 min). This probably represented the simplest derivatization method for any bioorganic found in urine, since it did not require any liquid–liquid extractions nor solid phase removal of the analyte prior to derivatization.

A chromatogram of an unspiked, hydrolyzed urine sample after derivatization is shown in Fig. 3. The HPLC conditions involved: acetonitrile–water (70:30) isocratic; 1.5 ml/min; Waters μBondapak C_{18} reversed-phase, 30 cm × 3.9 mm I.D.; Hitachi Model F1000 fluorescence spectrophotometer; sensitivity setting: 1.0/10 mV; excitation (ex)/emission (em) wavelengths: 275 nm/315 nm. Other HPLC mobile phase conditions involved acetonitrile–water (80:20), isocratic, also at 1.5 ml/min flow-rate. Quite different retention times were obtained just by altering the acetonitrile–water ratio. An authentic standard of the FMOC cadaverine derivative was used to identify the cadaverine peak in the urine sample chromatograms, under two HPLC conditions. The peak areas of cadaverine and putrescine derivatives under each HPLC condition appeared approximately the same. Additional confirmation for the two analytes in question came from the standard addition spiking studies, which resulted in increases in peak heights and areas for only two of the peaks present in Fig. 3. The recoveries of cadaverine and putrescine after the above hydrolysis conditions have been reported to be nearly 100%[33]. We did not perform separate polyamine recovery studies here, but have assumed our recoveries equal to those of the literature.

It did not seem likely that the peaks assigned to cadaverine and putrescine could have been due to interferences or artifacts of the analytical method. Such potential interferences would have had identical retention times to the FMOC-polyamine derivatives, under two different reversed-phase conditions, and to have identical fluorescence responses at these particular wavelengths (ex/em) to those of the FMOC-polyamines. In addition, the potential interferents would have had to have been present, underivatized or after derivatization, at levels exactly equal to those of the incurred polyamines, so that they would yield standard addition plots with excellent coefficients of linearity. It seems highly unlikely that there would have been two

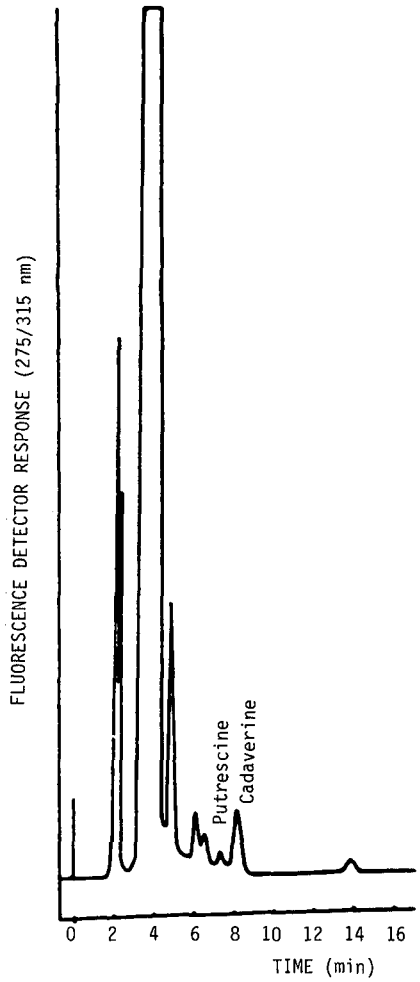

Fig. 3. Chromatogram of an unspiked, hydrolyzed urine sample after derivatization, showing the presence of cadaverine and putrescine. HPLC conditions involved: acetonitrile–water (70:30) isocratic; 1.5 ml/min; Waters μBondapak C_{18} reversed-phase, 30 cm × 3.9 mm I.D.; Hitachi Model F1000 fluorescence spectrophotometer; sensitivity setting: 1.0/10 mV; excitation/emission wavelengths: 275 nm/315 nm.

interferents that would meet all of these criteria and thereby provide false positives in both cases that agree so well with known, incurred levels of these two polyamines, as below.

Determination of the creatinine excretion

Since polyamine excretion is more nearly constant from day-to-day when expressed in mg/g creatinine, and to make it possible to make a comparison with reported values, it was essential to determine the creatinine extracted in urine. This followed a standard assay for creatinine described elsewhere[33].

Normal value of creatinine coefficient. It has been known for more than 50 years

that the 24-h excretion of creatinine per kilogram of body weight is approximately constant[33]. When the kidney function is normal, creatinine synthesis and excretion of creatinine in the urine is directly proportional to the muscle mass, and is independent of the physical effort from hour-to-hour. For a given individual it is approximately constant from day-to-day. It is possible therefore to control the reliability of the urine collection by determination of the creatinine. The following normal values[33] of creatinine coefficient can be applied for the creatinine excretion: males: 20–26 mg of creatinine per kg body weight per 24 h; women: 14–22 mg of creatinine per kg body weight per 24 h.

Calculation of creatinine in 24-h urine. UV spectra for a urine sample and creatinine standards of various concentrations (5, 10 and 20 ppm) were obtained in order to quantitate creatinine in urine. A calibration curve was obtained by plotting absorbance at 490 nm *vs.* concentration of creatinine. Based on the calibration curve of creatinine standard, the amount of creatinine excreted in the urine sample was 1.65 g/24 h, which was within the range of normal values: from the normal value of creatinine coefficient for males and the body weight of the subject (142 lbs.; 64.545 kg), the normal value of creatinine excreted could be calculated as 1.29–1.68 g/24 h.

Determination of cadaverine and putrescine levels in 24-h urine

Standard addition method. In order to determine the levels of cadaverine and putrescine present in the 24-h urine sample, we used the standard addition method, lacking an authentic standard of the FMOC putrescine derivative. We also did not know the exact percent derivatizations for each polyamine in a urine matrix. Thus, the simplest approach appeared to be that of standard addition. A urine sample was spiked with both polyamines of different levels (24 and 46 ppm for putrescine, and 8 and 46 ppm for cadaverine). These levels were chosen based on the literature values for these polyamines in normal, healthy human subjects. The same hydrolysis and derivatization procedures as described before were followed. A urine sample spiked with 24 ppm putrescine, 8 ppm cadaverine, and 1,7-diaminoheptane (internal standard), followed by derivatization, is shown in Fig. 4, with conditions indicated. Though there was no 1,7-diaminoheptane present in the normal urine sample, it was also spiked into the urine just to show the possible elution order and baseline separation for three very similar polyamines. Standard addition plots were obtained by plotting peak height *vs.* concentration spiked. The regression line equations and correlation coefficients are shown in Table I.

Cadaverine and putrescine levels in a urine sample were calculated based on the line equations for the standard addition plots.

For putrescine: $y = 2.85x + 3.164$
when $y = 0$, $x = 1.1$ ppm
1.1 ppm · 1800 ml/1.65 g creatinine = 1.20 mg/g creatinine.

For cadaverine: $y = 1.394x + 2.574$
when $y = 0$, $x = 1.8$ ppm
1.8 ppm · 1800 ml/1.65 g creatinine = 1.96 mg/g creatinine.

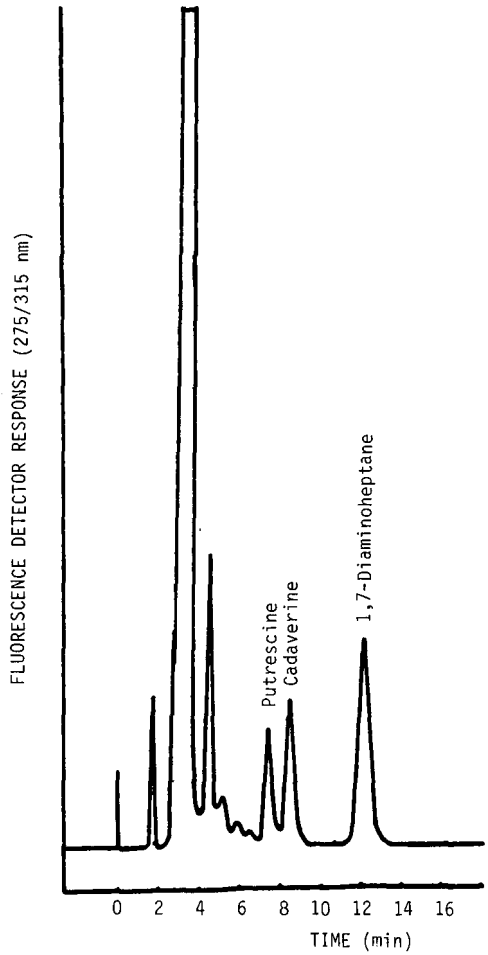

Fig. 4. Chromatogram for a typical hydrolyzed and spiked urine sample after derivatization, showing the presence of the cadaverine and putrescine peaks at higher levels. HPLC conditions as in Fig. 3.

TABLE I

STANDARD ADDITION LINE EQUATIONS AND CORRELATIONS FOR POLYAMINES IN URINE

m = Slope of the line, b = the y-intercept, r = the correlation coefficient: $y = mx + b$ for a straight line equation, as here.

Compound	*m*	*b*	*r*
Putrescine	2.850	3.164	0.999
Cadaverine	1.394	2.574	0.998

Comparison of determined polyamine values to reported ones. It has been reported that cadaverine and putrescine levels in cancer patients were significantly higher than those in normal subjects[34]. Polyamine values are generally expressed in mg/g creatinine, because polyamine excretion is more nearly constant from day-to-day when expressed in mg per day. Different expressions have been used such as μg/ml, mg/24 h, and mmol/mg creatinine. The cadaverine and putrescine levels in normal urines are 0.26–2.06 and 1.06–2.92 mg/g creatinine, respectively. However, for cancer patients the levels of putrescine and cadaverine are 50–85% and 21–31% exceeding the normal upper limits. Our determined values of cadaverine and putrescine (1.96 ± 0.07 and 1.20 ± 0.05 mg/g creatinine ± S.D., $n = 9$), using a standard addition method, were in the ranges of reported values for healthy, normal subjects. The detection limits for the determination of the polyamines, cadaverine and putrescine, in urine were 21 pmol and 24 pmol, respectively.

Suggestions on possible automation of the overall polymeric derivatization. Automated pre-column derivatizations have the same basic requirements and limitations as non-automated techniques. However, automation generally increases throughput and decreases operator attendance and analysis cost. In principle, automation should have been widely employed and described for derivatization in LC, but quite the opposite has been the case. Perhaps the necessity of extra instrumentation, method codification and sophistication, or method development has dissuaded many from employing this approach. As the hardware and software become less expensive and easier to use, automated techniques should become prevalent.

Various commerical firms have developed solid phase extraction tubes which are filled with silica-based, monomerically bonded packings, and have been used for sample cleanup[35]. The polymeric benzotriazole reagent could be easily packed into such tubes in the same manner as the bonded phases used today for cleanup. The Visiprep™ solid phase extraction vacuum manifold developed, *e.g.*, by Supelco, contains a built-in vacuum bleed valve and gauge, a heavy duty glass basin, chemical resistant cover and seals, stainless-steel solvent guide needles, adjustable screw-type valves built into the cover, a collection rack, and a plate for autosampler vials. This device allows one to accurately adjust the vacuum, and thus control the time of a solid phase derivatization reaction and final filtration of derivatized sample. The polypropylene collection vessel rack accommodates autosampler and vials, and thus injection could be automated[35]. Similar solid phase extraction devices (*e.g.* Baker-10 SPE System by J. T. Baker) could be used in the same manner for the purpose of automation of derivatizations.

CONCLUSIONS

Polystyrene-bound benzotriazole reagents are feasible and practical for the off-line derivatization of nucleophiles, such as simple amines and polyamines, in connection with HPLC for trace analysis. In addition to the advantages usually possible for related supported reagents in heterogeneous reactions, these particular polymeric reagents have exhibited higher derivatization yields and lower detection limits. This has been a direct result of the tag/label selected. The choice of a label that can impart multiple detection capabilities, such as UV–fluorescence for the fluorenyl reagent or UV–electrochemical detection for the *o*-acetylsalicyl reagent, has further expanded

the overall utility and applicability of such newer reagents for improved detection in HPLC.

Detection limits for the derivatives were excellent, usually 2–3 orders of magnitude lower than for the starting polyamines. Derivatization yields were high, and reactions required mild conditions (low temperature, short time, mild solvents). Derivatizations with the polymeric fluorenyl reagent for polyamines have occurred at room temperature within 10 min, in mild solvents (acetonitrile, dioxane, etc.). The derivatives were formed in yields of about 50% using the above conditions. Reactions were also successful, though with lower percent conversions, in aqueous or aqueous–organic solutions. Derivatizations have been possible simply by adding the polymeric reagent to the aqueous sample solution, derivatizing, filtering off the unused reagent, and injecting the derivatized solution into the HPLC. Sample work-up and extraction of the bioorganics of interest, such as polyamines, have been greatly reduced over all current approaches. Polyamine levels in urine samples of normal subjects or cancer patients can now be quantitated using this approach, with automation entirely feasible. Further applications to serum, plasma, and tissue samples should prove just as successful.

ACKNOWLEDGEMENTS

We gratefully acknowledge the many contributions and encouragements provided by our various colleagues at Northeastern University (NU) and Waters Chromatography Division, Millipore Corporation (WCD/MC). Special thanks are due C. Selavka, M. Y. Chang, B. D. Karcher, D. Bushee, and W. LaCourse at NU for their technical assistance and cooperation. Financial assistance, instrumentation donations, and technical support/collaboration for this joint research and development program were provided to NU by WCD/MC. We are grateful for all support provided this joint R&D program at NU/Waters.

The HP Model 1040A linear diode array UV–VIS detector for HPLC was donated to NU by Hewlett-Packard, with the assistance of S. A. George, for which we are appreciative. The Model Spectronic 1201 scanning UV–VIS spectrophotometer was donated by Milton Roy/Analytical Products Division (formerly Division of Bausch & Lomb), through the direct assistance of R. Jarrett and R. Flores, for which we are most grateful. A Hitachi Model D2000 ChromatoIntegrator was donated to NU by EM Science, through the gracious assistance of M. Gurkin and G. Desotelle.

REFERENCES

1 I. S. Krull (Editor), *Reaction Detection in Liquid Chromatography, (Chromatographic Science Series*, Vol. 34), Marcel Dekker, New York, 1986.
2 I. S. Krull, S. T. Colgan and C. M. Selavka, in P. R. Brown and R. A. Hartwick (Editors), *High Performance Liquid Chromatography*, Wiley-Interscience, New York, 1988, in press.
3 S. T. Colgan and I. S. Krull, in I. S. Krull (Editor), *Reaction Detection in Liquid Chromatography*, Marcel Dekker, New York, 1986, p. 227.
4 J. M. Rosenfeld and R. A. McLeod, in D. J. Harvey (Editor), *Marihuana '84, Proceedings of the Oxford Symposium on Cannabis*, IRL Press, Oxford, England, 1984, p. 151.
5 L. Nondek, R. W. Frei and U. A. Th. Brinkman, *J. Chromatogr.*, 282 (1983) 141.
6 H. Jansen, U. A. Th. Brinkman and R. W. Frei, *Chromatographia*, 20 (1985) 453.
7 I. S. Krull and E. P. Lankmayer, *Am. Lab. (Fairfield, Conn.)*, May (1982) 18.

8 I. S. Krull, K.-H. Xie, S. Colgan, T. Izod, U. Neue, R. King and B. Bidlingmeyer, *J. Liq. Chromatogr.*, 6 (1984) 605.
9 K.-H. Xie, S. Colgan and I. S. Krull, *J. Liq. Chromatogr.*, 6 (S-2) (1983) 125.
10 I. S. Krull, S. Colgan, K.-H. Xie, U. Neue, R. King and B. Bidlingmeyer, *J. Liq. Chromatogr.*, 6 (1983) 1015.
11 S. T. Colgan, I. S. Krull, U. Neue, A. Newhart, C. Dorschel, C. Stacey and B. Bidlingmeyer, *J. Chromatogr.*, 333 (1985) 349.
12 S. T. Colgan, I. S. Krull, C. Dorschel and B. Bidlingmeyer, *Anal. Chem.*, 58 (1986) 2366.
13 T.-Y. Chou, S. T. Colgan, D. M. Kao, I. S. Krull, C. Dorschel and B. Bidlingmeyer, *J. Chromatogr.*, 367 (1986) 335.
14 S. T. Colgan, I. S. Krull, C. Dorschel and B. Bidlingmeyer, *J. Chromatogr. Sci.*, (1988) in press.
15 C.-X. Gao, T.-Y. Chou, S. T. Colgan, I. S. Krull, C. Dorschel and B. Bidlingmeyer, *J. Chromatogr. Sci.*, 26 (1988) 449.
16 M. M. Abdel-Monem and J. L. Merdink, *J. Chromatogr.*, 222 (1981) 363.
17 C. E. Prussak and D. H. Russell, *J. Chromatogr.*, 229 (1982) 47.
18 T. Takagi, T. G. Chung and A. Saito, *J. Chromatogr.*, 272 (1983) 279.
19 M. Mach, H. Kersten and W. Kersten, *J. Chromatogr.*, 223 (1981) 51.
20 T. Skaaden and T. Greibrokk, *J. Chromatogr.*, 247 (1982) 111.
21 H. Veening, W. W. Pitt, Jr. and G. Jones, Jr., *J. Chromatogr.*, 90 (1974) 129.
22 M. Kai, T. Ogata, K. Haraguchi and Y. Ohkura, *J. Chromatogr.*, 163 (1979) 151.
23 N. E. Newton, K. Ohno and M. M. Abdel-Monem, *J. Chromatogr.*, 124 (1976) 277.
24 F. L. Vandemark, G. J. Schmidt and W. Slavin, *J. Chromatogr. Sci.*, 16 (1978) 465.
25 N. D. Brown, R. B. Sweet, J. A. Kintzios, H. D. Cox and B. P. Doctor, *J. Chromatogr.*, 164 (1979) 35.
26 B. Brossat, J. Straczek, F. Belleville, P. Nabet and R. Metz, *J. Chromatogr.*, 277 (1983) 87.
27 C.-X. Gao, *M.S. Thesis*, Northeastern University, Boston, MA, 1986.
28 R. Kalir, A. Warshawsky, M. Fridkin and A. Patchornik, *J. Biochem.*, 59 (1975) 55.
29 L. A. Carpino and G. Y. Han, *J. Org. Chem.*, 37 (1972) 3404.
30 R. Cunico, A. G. Mayer, C. T. Wehr and T. L. Sheehan, *BioChromatography*, 1 (1986) 6.
31 F. L. Vandemark, G. J. Schmidt and W. Slavin, *J. Chromatogr. Sci.*, 16 (1978) 465.
32 I. Greenwald, *J. Biol. Chem.*, 80 (1928) 103.
33 R. Richterich, *Clinical Chemistry: Theory and Practice*, Academic Press, New York, London, 1969, p. 73.
34 K. Fujita, T. Nagatsu, K. Shinpo, K. Maruta, R. Teradaira and M. Nakamura, *Clin. Chem.*, 26/11 (1980) 1577.
35 *Supelco Chromatography Supplies*, Supelco, Bellefonte, PA, Catalog No. 26, 1988, p. 216.

Journal of Chromatography, 454 (1988) 185–193
Elsevier Science Publishers B.V., Amsterdam — Printed in The Netherlands

CHROM. 20 800

PRELIMINARY APPLICATIONS OF CROSS-AXIS SYNCHRONOUS FLOW-THROUGH COIL PLANET CENTRIFUGE FOR LARGE-SCALE PREPARATIVE COUNTER-CURRENT CHROMATOGRAPHY

TIAN-YOU ZHANG*
Laboratory of Technical Development, National Heart, Lung, and Blood Institute, National Institutes of Health, Bethesda, MD 20892 (U.S.A.)
Y.-W. LEE and Q. C. FANG
Research Triangle Institute, Research Triangle Park, NC 27709 (U.S.A.)
RONG XIAO
Institute of Pharmaceutical Sciences, West China Medical University, Chengdu, Sichuan (China)
and
YOICHIRO ITO*
Laboratory of Technical Development, National Heart, Lung and Blood Institute, National Institutes of Health, Bethesda, MD 20892 (U.S.A.)
(Received May 27th, 1988)

SUMMARY

The cross-axis synchronous flow-through coil planet centrifuge with a 20-cm revolutional radius and a total capacity of 1600 ml was successfully applied to preparative counter-current chromatography of various biological samples, which include sea buckthorn extract, steroid reaction mixture, indole plant hormones, and dinitrophenylamino acids. The present system offers advantages of stable balance of the centrifuge, a large column capacity, and high resolution.

INTRODUCTION

The advantages of counter-current chromatography (CCC) have been described and demonstrated using a variety of support-free chromatographic systems[1–3]. Recently, a cross-axis synchronous flow-through coil planet centrifuge (X-axis CPC) has been developed for performing large-scale CCC[4,5]. The axes of revolution and the planetary motion form a cross to each other. The centrifugal-force field generated by this planetary motion provides efficient three-dimensional mixing of two solvent phases in a coiled column, thus doubling the partition efficiency of this unique CCC system. The preparative capability of this method has been demonstrated on gram-quantity separation of test samples with a pair of multilayer coiled columns connected in series[5].

* Visiting scientist from the Beijing Institute of New Technology Application, Beijing, China.

0021-9673/88/$03.50

The present paper describes the preliminary applications of the X-axis CPC to the separations of various samples, which include crude sea buckthorn extract, steroid reaction products, indole auxins, and dinitrophenyl (DNP)-amino acid mixtures with suitable two-phase solvent systems.

EXPERIMENTAL

Apparatus

A second prototype of the X-axis CPC with a 20-cm revolutional radius was employed in the present experiments. Fig. 1 shows a photograph of the apparatus, which is equipped with a pair of identical multilayer coiled columns symmetrically mounted on each side of the centrifuge frame to provide perfect balance of the centrifuge system. The apparatus can be rotated up to 500 rpm which produces about 56 *g* on the axis of the column holder. Each separation column was prepared from 2.6-mm I.D. polytetrafluoroethylene (PTFE) tubing (Zeus Industrial Products, Raritan, NJ, U.S.A.) by winding it onto the holder hub of 15-cm O.D. making multiple coiled layers. The β values (ratio of the radius of rotation to the radius of revolution) of the multilayer coil ranged from 0.375 at the internal terminal to 0.625 at the external terminal. Two multilayer coils were connected in series with a 0.85-mm I.D. PTFE tubing (Zeus Industrial Products) to provide a capacity of about 1600 ml. Each column consisted of 14 coiled layers between the flanges spaced 5 cm apart. These columns were laterally positioned at a distance of 10 cm left from the center of the holder shafts to improve the retention of the stationary phase[4].

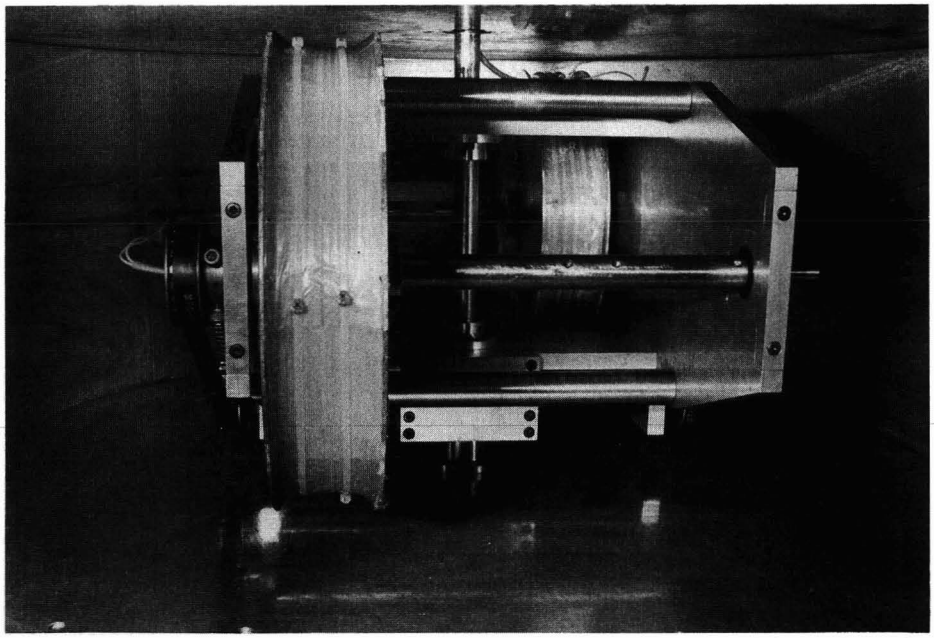

Fig. 1. Photograph of the second prototype of the cross-axis synchronous flow-through coil planet centrifuge with a 20-cm revolutional radius. A pair of large multilayer coils is symmetrically mounted, one on each side of the centrifuge frame, in the lateral position.

Sample and two-phase solvent system

Separations were performed on four sets of samples, *i.e.*, crude ethanol-extracted dried powder from sea buckthorn (*Hippophae rhamnoides* obtained from China), crude steroid reaction products, indole auxins (Sigma, St. Louis, MO, U.S.A.) and DNP-amino acids (Sigma). A suitable two-phase solvent system was selected for each set of these samples on the basis of solubility and partition coefficient values of the sample components. The solvent mixture was thoroughly equilibrated in a separatory funnel at room temperature and two phases separated shortly before application to the separation column.

Crude sea buckthorn extract. This sample is a dried powder from a crude ethanol extract of a medicinal herb called sea buckthorn (*H. rhamnoides*) and known to contain five major flavonoid compounds[6]. A two-phase solvent system composed of chloroform–methanol–water at a volume ratio of 4:3:2 was used for the separation. The sample solution was prepared by dissolving 100 mg of the crude powder in 50 ml of the above solvent mixture consisting of equal volumes of the upper and lower phases.

Steroid mixture. This crude synthetic steroid product was a complex mixture which contained more than ten different components detected by thin-layer chromatographic (TLC) analysis[7]. The separation was performed with a two-phase solvent system composed of *n*-hexane–ethyl acetate–methanol–water at a volume ratio of 6:5:4:2. The sample solution was prepared by dissolving 2.3 g of the steroid mixture in 20 ml of the above solvent system consisting of equal volumes of the upper and the lower phases.

Indole auxins. A synthetic mixture of indole-3-acetamide, indole-3-acetic acid, and indole-3-butyric acid was separated with a two-phase solvent system composed of *n*-hexane–ethyl acetate–methanol–water at a volume ratio of 3:7:5:5. The sample solution was prepared by dissolving 1 g of each compound, the total weight of 3 g, in 140 ml of the above solvent mixture consisting of equal volumes of the upper and the lower phases.

DNP-Amino acids. Two sets of sample mixtures were prepared, one used for the lower phase elution and the other for the upper phase elution, both with the same solvent system of chloroform–acetic acid–0.1 *N* hydrochloric acid at a volume ratio of 2:2:1. The first sample set for the lower phase elution consisted of 400 mg DNP-L-leucine (DNP-leu), 800 mg DNP-L-proline (DNP-pro), 800 mg DNP-β-alanine (DNP-β-ala), 400 mg diDNP-L-cystine [diDNP-$(cys)_2$], and 1600 mg DNP-DL-glutamic acid (DNP-glu). A total of 4 g of the above sample mixture was dissolved in 100 ml of the above solvent mixture consisting of equal volumes of the two phases. The second sample set for the upper phase elution consisted of 400 mg δ-N-DNP-L-ornithine (DNP-orn), 800 mg DNP-L-aspartic acid (DNP-asp), 800 mg DNP-DL-glutamic acid (DNP-glu), 400 mg diDNP-L-cystine [diDNP-$(cys)_2$], and 1600 mg DNP-L-alanine (DNP-ala). A total of 4 g of the above sample mixture was similarly dissolved in 100 ml of the solvent mixture.

Experimental procedure

Each separation was performed as follows: a pair of multilayer coils was first entirely filled with the stationary phase. This was followed by injection of the sample solution through the sample port. Then the centrifuge was rotated at the optimum

TABLE I

SUMMARY OF EXPERIMENTAL CONDITIONS

Expt. No.	*Sample*	*Solvent system*	*Volume ratio*	*Mobile phase*	*Flow-rate*	*Planetary* motion*	*Elution mode*	*Revolution speed*
1	Sea buckthorn extract (100 mg)	Chloroform Methanol Water	4 3 2	Lower phase	120 ml/h	P_I	Head-Tail	450 rpm
2	Steroid reaction mixture (2.4 g)	*n*-Hexane Ethyl acetate Methanol Water	6 5 4 2	Lower phase	240 ml/h	P_I	Head-Tail	450 rpm
3	Indole auxins Indole-3-acetamide (1 g) Indole-3-acetic acid (1 g) Indole-3-butyric acid (1 g)	*n*-Hexane Ethyl acetate Methanol Water	3 7 5 5	Lower phase	240 ml/h	P_I	Head-Tail	450 rpm
4	DNP-amino acid mixture DNP-L-leucine (400 mg) DNP-L-proline (800 mg) DNP-β-alanine (800 mg) diDNP-L-cystine (400 mg) DNP-DL-glutamic acid (1600 mg)	Chloroform Acetic acid 0.1 *N* Hydrochloric acid	2 2 1	Lower phase	120 ml/h	P_{II}	Tail-Head	500 rpm
5	DNP-amino acid mixture DNP-L-ornithine (400 mg) DNP-L-aspartic acid (800 mg) DNP-DL-glutamic acid (800 mg) diDNP-L-cystine (400 mg) DNP-L-alanine (1600 mg)	Chloroform Acetic acid 0.1 *N* Hydrochloric acid	2 2 1	Upper phase	120 ml/h	P_{II}	Head-Tail	500 rpm

* Planetary motion P_I: 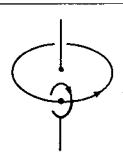 ; P_{II}: 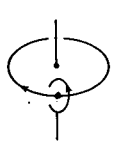

Large circles indicate revolution around the central axis of the centrifuge and small circles, rotation around the holder axis.

revolutional speed while the mobile phase was pumped into the column at a selected flow-rate in the proper elution mode predetermined by the preliminary experiments (see Table I). Effluent from the outlet of the coiled column was continuously monitored with a UV monitor (LKB Uvicord S) at 278 nm and collected in test tubes with a fraction collector (LKB Ultrorac). Aliquot of each fraction was diluted with a known volume of methanol and the absorbance was determined at a suitable wavelength with a spectrophotometer (Zeiss Model PM 6).

Determination of proper elution mode

The CCC method utilizing a CPC requires a knowledge of hydrodynamic motion and distribution of two solvent phases in the rotating coil. In the high-speed CCC system, two solvent phases are usually distributed unilaterally in the coil in such a way that one phase (head phase) occupies the head and the other phase (tail phase) the tail of the coil. (Here, head–tail relationship refers to the Archimedean screw force which tends to drive all objects of different density toward the head of the coil.) Consequently, satisfactory retention of the stationary phase is attained by eluting either the head phase from the tail toward the head or the tail phase from the head toward the tail.

In the present X-axis CPC method, the above hydrodynamic distribution is further modified by the mode of planetary motions P_I and P_{II} illustrated in Table I (bottom) when the coil is mounted in the lateral position on the holder[4]. Although various mechanisms involved in the above hydrodynamic phenomena are extremely complex and difficult to explain on the basis of our present knowledge, the proper elution mode can be easily determined by a series of simple preliminary runs using a

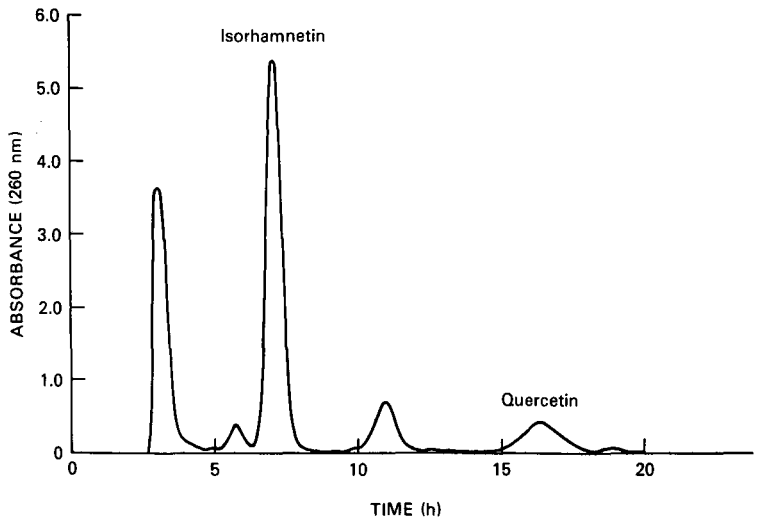

Fig. 2. Chromatogram of crude sea buckthorn extract (100 mg) with chloroform–methanol–water (4:3:2). Experimental conditions: column: multilayer coil, 2.6 mm I.D., 1600 ml capacity; mobile phase: lower non-aqueous phase; elution mode: head to tail; flow-rate: 120 ml/h; revolution: 450 rpm (P_I); retention: 85.5%.

short coil. In addition, a set of phase distribution diagrams previously reported[4] will predict the hydrodynamic behavior of the two phases in a variety of commonly used two-phase solvent systems. The experimental conditions employed in the present studies are summarized in Table I.

RESULTS

Separation of crude sea buckthorn extract

Fig. 2 shows a chromatogram of the sea buckthorn extract obtained from a set of experimental conditions indicated in the diagram. A 100-mg quantity of the crude sample was completely separated into five major flavonoid components. Partition efficiency can be calculated from the chromatogram according to the conventional gas chromatographic formula, $N = (4\ t_R/W)^2$, where N is a partition efficiency expressed in terms of theoretical plates, t_R, retention time of the peak maximum, and W,

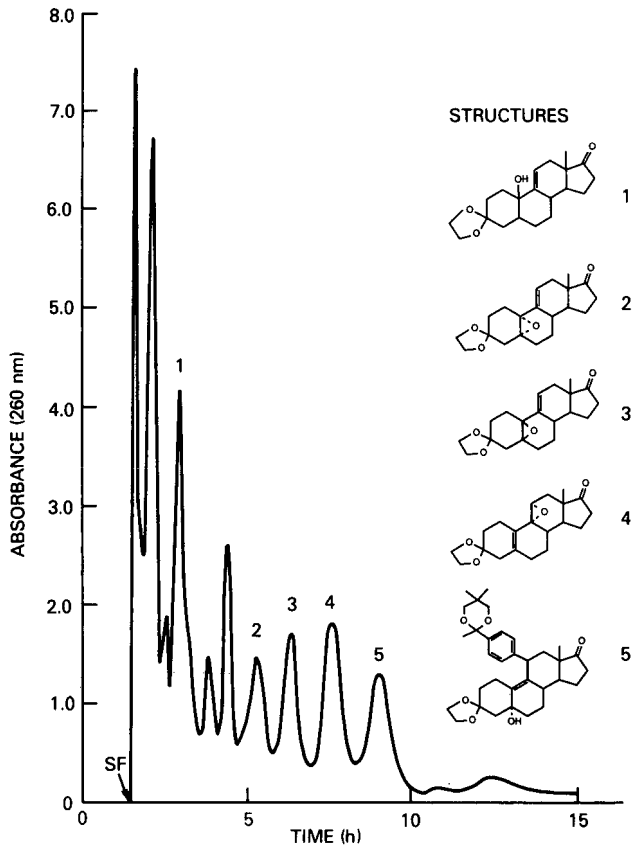

Fig. 3. Chromatogram of steroid reaction mixture (2.4 g) with *n*-hexane–ethyl acetate–methanol–water (6:5:4:2). Experimental conditions: column: multilayer coil, 2.6 mm I.D., 1600 ml capacity; mobile phase: lower aqueous phase; elution mode: head to tail; flow-rate: 240 ml/h; revolution: 450 rpm (P_1); retention: 71.3%.

the peak width expressed in the same unit as t_R. Partition efficiencies of peaks 3, 4, and 5 in Fig. 2 were calculated by the above formula as 720, 900, and 720, respectively. In this experiment, the head to tail elution mode was applied and planetary motion P_I was used at a revolutional speed of 450 rpm. The retention of the stationary phase was 85.5% of the total column capacity.

Separation of steroid mixture

The chromatogram of a crude reaction mixture of synthetic steroids showed fairly well resolved multiple peaks (Fig. 3). A total of 2.4 g of the crude steroid mixture was efficiently separated in 15 h. In this separation, planetary motion P_I was applied at a revolutional speed of 450 rpm. Retention of the stationary phase was 72%. Five steroids corresponding to peaks 1–5 were determined by NMR analysis as indicated on the right side of the chromatogram (Fig. 3). The desired product was found at peak 5 and yielded 310 mg of the crystalline material at high purity.

Separation of indole auxins

Fig. 4 shows a chromatogram of the synthetic mixture of indole plant hormones. A 3-g quantity of the sample was well separated. Planetary motion P_I was applied at the revolutional speed of 450 rpm. Retention of the stationary phase was 33.5%. Partition efficiencies of indole-3-acetamide, indole-3-acetic acid, and indole-3-butyric acid were calculated as 580, 580, and 590, respectively.

Separation of DNP-amino acids

In the first experiment, the lower non-aqueous phase was used as the mobile phase and the separation was performed under planetary motion P_{II} at a revolutional

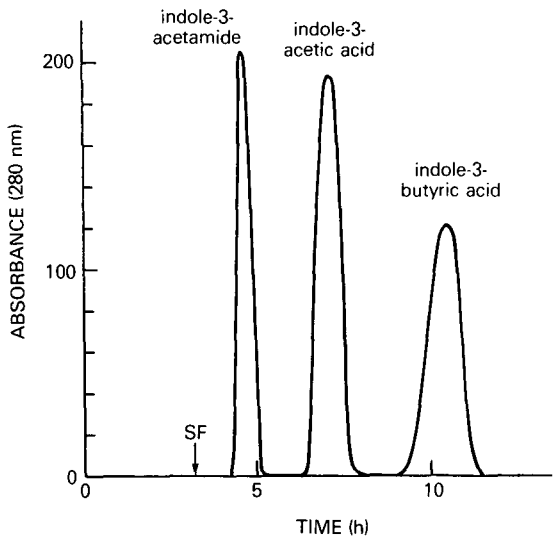

Fig. 4. Chromatogram of indole auxins (3 g) with *n*-hexane–ethyl acetate–methanol–water (3:7:5:5). Experimental conditions: column: multilayer coil, 2.6 mm I.D., 1600 ml capacity; mobile phase: lower aqueous phase; elution mode: head to tail; flow-rate: 240 ml/h; revolution: 450 rpm (P_I); retention: 34%.

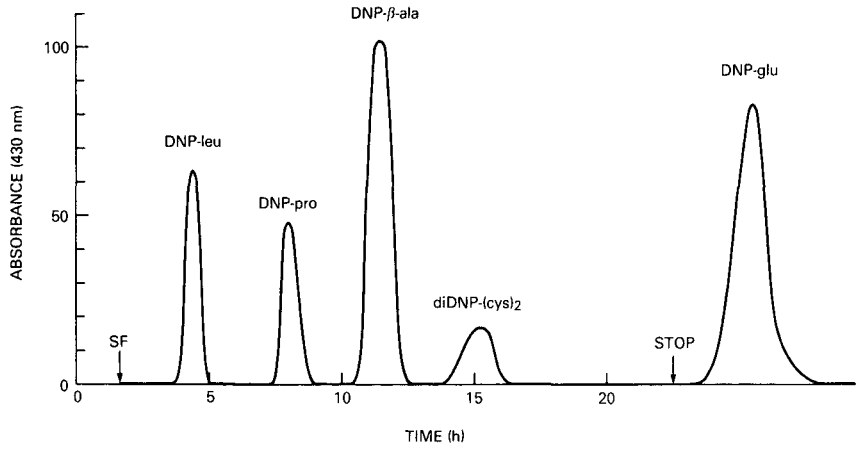

Fig. 5. Chromatogram of DNP-amino acid mixture (4 g) with chloroform–acetic acid–0.1 *N* hydrochloric acid (2:2:1). Experimental conditions: column: multilayer coil, 2.6 mm I.D., 1600 ml capacity; mobile phase: lower non-aqueous phase; elution mode: tail to head; flow-rate: 120 ml/h; revolution: 500 rpm (P_{II}); retention: 83%.

speed of 500 rpm. Fig. 5 shows the chromatogram in which 4 g of the sample mixture were efficiently separated in 23 h. Retention of the stationary phase was 83%.

In the second experiment, the upper aqueous phase was used as the mobile phase in the head to tail elution mode while planetary motion P_{II} was applied at 500 rpm. Fig. 6 shows the chromatogram obtained from a 4-g quantity of the sample mixture. All components are well separated in 22 h. Retention of the stationary phase was 45%.

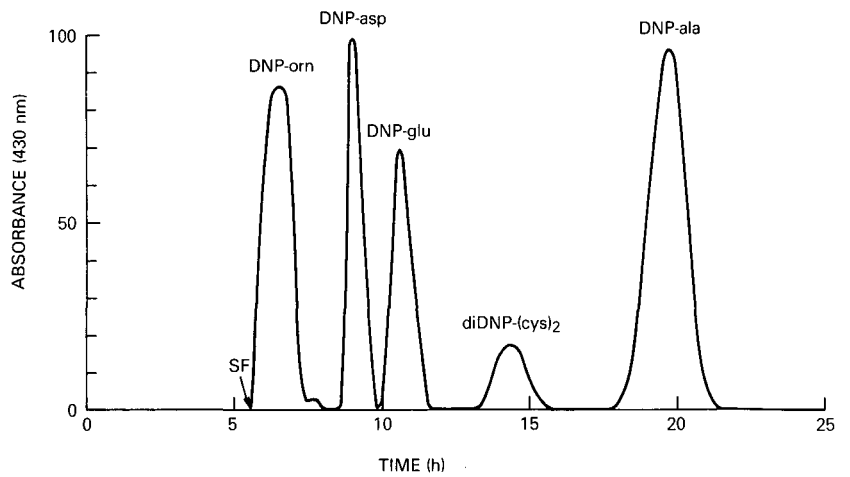

Fig. 6. Chromatogram of DNP-amino acid mixture (4 g) with chloroform–acetic acid–0.1 *N* hydrochloric acid (2:2:1). Experimental conditions: column: multilayer coil, 2.6 mm I.D., 1600 ml capacity; mobile phase: upper aqueous phase; elution mode: head to tail; flow-rate: 120 ml/h; revolution: 500 rpm (P_{II}); retention: 45%.

DISCUSSION

In the present experiments, preparative capacity of the X-axis CPC was demonstrated in gram-quantity separations of various samples. Partition efficiencies of these separations are mostly over several hundred theoretical plates. These results clearly demonstrate that the present method is capable of separating several grams of samples at a high partition efficiency.

In the separation of the cruder sea buckthorn extract with the chloroform–methanol–water (4:3:2) system, an increase of the sample size to 1 g or more resulted in extensive carryover of the stationary phase from the column. This detrimental effect may be attributed to emulsification in the rotating column as suggested by a long settling time of the sample solution[8]. This clearly suggests that one must search for better conditions to improve the retention of the stationary phase mainly by trial and error experiments using the settling time as a parameter. In the present applications, both retention of the stationary phase and effective partition process were produced by the unique three-dimensional force field generated by the X-axis CPC. The method is suitable for gram-quantity separations of natural and synthetic products with various two-phase solvent systems with a broad spectrum in physical properties.

The operational conditions of the X-axis CPC can be properly adjusted in not only the revolutional speed, flow-rate of the mobile phase, and elution mode of the head to tail or tail to head, but also the mode of planetary motion P_I or P_{II}. Selection of multiple parameters and conditions will facilitate the choice of various kinds of solvent systems suitable for particular applications.

A pair of identical multilayer coils was connected in series and symmetrically mounted one on each side of the centrifuge frame. This doubles the capacity of the separation column to improve both partition efficiency and sample loading capacity. It further provides an important advantage of the care-free stable balance of the centrifuge system without the use of a counterweight which would require accurate weight adjustment according to the density of the applied solvent system. In order to perform large-scale preparative separations, the present centrifuge was designed to hold a pair of large columns at a 20-cm revolutional radius, and to operate at a revolutional speed not exceeding 500 rpm. The present X-axis CPC system will be extremely useful for large-scale separation and extraction in research laboratories and industrial plants.

REFERENCES

1 Y. Ito and R. Bhatnager, *J. Liq. Chromatogr.*, 7 (1984) 257.
2 J. L. Sandlin and Y. Ito, *J. Liq. Chromatogr.*, 7 (1984) 323.
3 J. L. Sandlin and Y. Ito, *J. Liq. Chromatogr.*, 8 (1985) 2153.
4 Y. Ito and T. Y. Zhang, *J. Chromatogr.*, 449 (1988) 135.
5 Y. Ito and T. Y. Zhang, *J. Chromatogr.*, 449 (1988) 153.
6 T. Y. Zhang, R. Xiao, X. Hua and S. Kong, *J. Liq. Chromatogr.*, 11 (1988) 233.
7 Y.-W. Lee and Q. C. Fang, unpublished results.

Journal of Chromatography, 454 (1988) 195–203
Elsevier Science Publishers B.V., Amsterdam — Printed in The Netherlands

CHROM. 20 797

ANALYSIS OF DOUBLE-STRANDED POLY(A) · POLY(U) MOLECULES BY REVERSED-PHASE HIGH-PERFORMANCE LIQUID CHROMATOGRAPHY

J. LIAUTARD, S. COLOTE, C. FERRAZ and J. SRI-WIDADA
U-249 INSERM, CRBM du CNRS et Université Montpellier I, B.P. 5051, 34033 Montpellier Cedex (France)
A. PICHOT
Laboratoire EXPANSIA, B.P. 6, 30390 Aramon (France)
and
J. P. LIAUTARD*
U-249 INSERM, CRBM du CNRS et Université Montpellier I, B.P. 5051, 34033 Montpellier Cedex (France)
(First received March 11th, 1988; revised manuscript received May 18th, 1988)

SUMMARY

The behaviour of different batches of synthetic Poly(A) · Poly(U) in reversed-phase high-performance liquid chromatography (HPLC) was studied. They consist of large molecules mainly in the form of a double strand. Differences in the elution patterns were correlated with properties detected by conventional methods such as electrophoresis, centrifugation, fusion analysis or enzymatic digestions. Under the present conditions, contamination by products and precursors used during synthesis was detectable, but was absent in most of the preparations. The differences in elution patterns between batches appear to be correlated with the size of the molecules synthesized. The chromatograms suggested that Poly(A) · Poly(U) molecules contain single-strand portions at least transiently. The presence of such portions was confirmed by enzymatic digestion with S1 nuclease. The rapidity, reproducibility and ease of reversed-phase HPLC qualify this technique as a tool for routine analysis.

INTRODUCTION

The homoribopolymers Poly(A) and Poly(U) associate to form a helix, whose structure resembles that of a native DNA[1]. In some cases, however, more complex structures have been described in mixtures of Poly(A) and Poy(U). For example, associations of two Poly(U) molecules with one Poly(A) molecule[1–3] or two Poly(A) molecules with one molecule of Poly(U) have been reported. Moreover, because they are synthesized *in vitro* using polymerizing enzymes such as polynucleotide phosphorylase (PNPase), the length of the resulting polymers is heterogeneous. Partly single-stranded polymers could therefore be present in the mixture.

Poly(A) · Poly(U) molecules are known to exert biological effects on the immune system[5]. For instance, spontaneous mammary tumours have been reduced by treatment with Poly(A) · Poly(U) molecules[6].

0021-9673/88/$03.50

Analysis of the biological properties of these molecules calls for an exact determination of the degree of purity and especially the exact structure of the different batches. Many methods can be used to analyze such molecules, *e.g.*, gel electrophoresis, centrifugation, melting analysis and enzymatic studies. However, a single method giving a general view of most of the properties, would be of great value. We have used reversed-phase high-performance liquid chromatography (HPLC) because the separation of large nucleic acids on a reversed phase is relatively complex, depending on the base composition[7], secondary structure[8] and constraints present in the molecule[9].

In the present study, we analyzed Poly(A) · Poly(U) polymers by reversed-phase HPLC and compared the results with those obtained by conventional methods. We show that most of the properties found by conventional analysis can be correlated with the particularities of the reversed-phase HPLC elution profile.

MATERIALS AND METHODS

Materials used

Poly(A), Poly(U) and Poly(A) · Poly(U) were obtained from Boehringer (F.R.G.) and from Expansia (France). Agarose type II was obtained from Sigma, acetonitrile (HPLC grade) from Touzart & Matignon and phosphate and polynucleotide kinase from Boehringer.

Methods employed

Reversed-phase HPLC. Reversed-phase HPLC was performed on a Gilson apparatus equipped with a LiChrosorb RP-18 column (25 cm × 0.4 cm; particle size, 10 μm; pore size, 75 Å; Merck) and an UV detector at 254 nm, essentially as described previously[7]. Poly(A) · Poly(U) was analyzed using a linear gradient elution, from 100% (v/v) buffer I (0.2 *M* ammonium acetate, pH 6.5) to 40% (v/v) buffer II (50% acetonitrile in water) in 40 min. A flow-rate of 1 ml/min was used throughout Poly(A) · Poly(U) was dissolved in 150 m*M* sodium chloride and kept overnight at 4°C before injection. The nucleosides were analyzed using the same buffers, but the gradient was performed in 20 min.

Other methods. Electrophoresis was performed on 1.5% agarose gel in TBE buffer (90 m*M* Tris–borate pH 8, 5 m*M* EDTA[9] with ethidium bromide at 3 V/cm for 4 h.

To analyze the base composition, the polymers were hydrolysed overnight in 0.3 *M* potassium hydroxide at 37°C. After neutralization, the phosphate groups were removed with alkaline phosphatase.

Centrifugation in a 5–20% sucrose gradient in 150 m*M* sodium chloride and 10 m*M* Tris–HCl, pH 7.4, was performed in a Kontron centrifuge using a TST 41-14 rotor at 30 000 rpm for 20.5 h. Gradients were fractionated and the optical density was determined. A mean sedimentation coefficient was deduced at the maximum absorption, according to McEwen[10].

The buoyant density in caesium chloride at 42°C was determined by centrifugation in 50% caesium chloride at 30 000 rpm for 72 h using a TST 41-14 rotor. The resulting gradient was fractionated and the refractive index and optical density at 260 nm were determined in each fraction.

Melting point and hyperchromicity [(OD_{260} max − OD_{260} min)/OD_{260} min] were determined in 10 m*M* Tris–HCl, pH 7.4 and 150 m*M* sodium chloride by increasing the temperature from 20°C to 70°C in 25 min.

RESULTS

Conventional analysis of Poly(A) · Poly(U) batches

Numerous preparations were studied. We present only three batches, A, B and C, which summarize the results obtained.

The mean molecule size was determined by two methods, *i.e.*, sucrose centrifugation and agarose electrophoresis, which gave similar results. Fig. 1 shows the gel electrophoretic pattern of the nucleic acid. The molecular weight was estimated by comparison with standards obtained by digestion of lambda-phage DNA with restriction enzymes. Preparation C consisted of heterogeneous polymers with a maximum of around 300 base pairs, preparation B had larger molecules and preparation A contained essentially large molecules. These results were confirmed by sucrose gradient centrifugation (Table I).

The base composition was determined by HPLC after alkaline hydrolysis and removal of the phosphates with alkaline phosphatase. The only bases present were uridine and adenosine, and their molar ratio was close to 1 (see Table I).

The secondary structure was analyzed by the melting point method. The results summarized in Table I confirm that Poly(A) · Poly(U) molecules are indeed double-stranded, with a melting point corresponding to published data[11]. The shape of the melting curve shows the presence of small molecules in preparation C, and to a lesser extent in preparation B. The melting curve of batch A confirms that the molecules are large, with few small molecules if any. The double-stranded nature of the

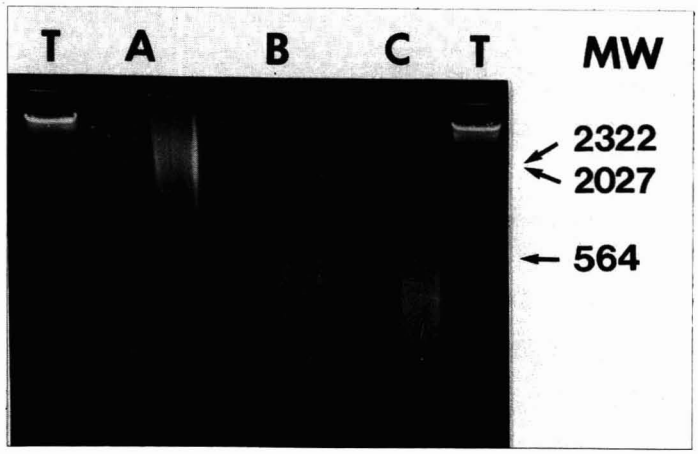

Fig. 1. Size determination of the three representative batches of Poly(A) · Poly(U) by agarose gel electrophoresis. The three batches (A, B, C), dissolved in 150 mM sodium chloride and 30% sucrose, were applied to a 1.5% agarose gel in TBE buffer containing 0.5 μg/ml ethidium bromide (see Materials and Methods). Electrophoresis was performed at 3 V/cm for 4 h. Lambda-phage DNA digested by Hind III was added for size markers (T). MW = Molecular weight.

TABLE I

ANALYSIS OF THE Poly(A) · Poly(U) PREPARATIONS BY CONVENTIONAL METHODS

The three batches were analyzed by sucrose gradient centrifugation, caesium chloride buoyant density, melting point, T_m, and nucleoside ratio determination, as described in Materials and Methods.

	Batch C	*Batch B*	*Batch A*
Mean sedimentation constant	6S	7S	7–9S
Density in CsCl	1.84	1.84	1.85
Melting point, T_m (°C)	56	57	60
Hyperchromicity (%)	49	56	57
Uridine/adenosine molar ratio	1.1	1.03	1.06

Poly(A) · Poly(U) solution was confirmed by buoyant density centrifugation analysis in caesium chloride (Table I).

Reversed-phase HPLC analysis of Poly(A) · Poly(U)

The three batches of Poly(A) · Poly(U) were analyzed by reversed-phase HPLC. Although they were prepared using the same protocol, the analysis showed significant differences, as seen in Fig. 2. The behaviour of each batch was very different. For example, batch A exhibited only one peak with an elution time of 27 min, whereas batch B and especially batch C were eluted as three different components, each appearing heterogeneous.

These differences between the three batches cannot be attributed to the quantity of Poly(A) · Poly(U) loaded on the column, first because the same amount of material was used in each case that is 60 μg of polynucleotide in 200 μl of buffer (Fig. 2). Furthermore we have studied the influence of the quantity applied to the column on the elution profile. There was a very small change in the appearance of the profile, less

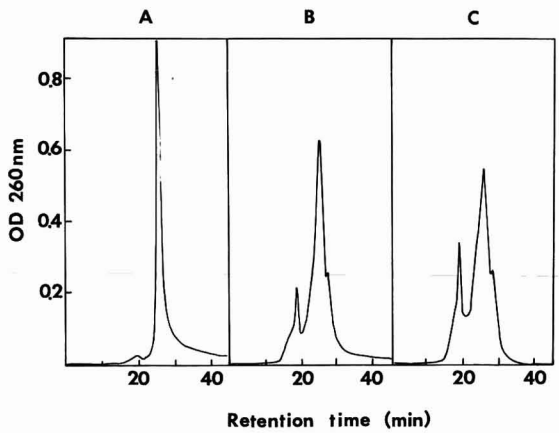

Fig. 2. Elution profiles of representative preparations of Poly(A) · Poly(U). Three representative preparations were analyzed by reversed-phase chromatography on a C_{18} column as described in Materials and Methods. In each case 60 μg of lyophilized Poly(A) · Poly(U) were dissolved in 200 μl of 0.15 *M* sodium chloride. In order to obtain a good dissolution, the preparation was kept for at least 16 h at 4°C before loading. OD = Absorbance. Retention times: (A) 27 min; (B) 19, 27 and 29 min; (C) 19, 27 and 29 min.

than 5% when doubling the quantity. This result is in accord with an equilibrium between the single stranded and double stranded portions proposed below.

Several other hypotheses can be proposed to account for these results. The first is a possible contamination by products other than Poly(A) · Poly(U), particularly the precursors in their synthesis (ADP and UDP, or degradation products of the polymers, AMP, UMP, nucleotides, nucleosides and oligonucleotides). Consequently we analyzed, under the same conditions, ADP, UDP and the products obtained from degradation by alkaline hydrolysis (*i.e.*, adenosine 3′-phosphate and uridine 3′-phosphate) or the nucleosides obtained by further phosphatase digestion. Nuclease-degraded Poly(A) · Poly(U) was also analyzed. The retention times of these products are shown in Table II. They are very different from those of Poly(A) · Poly(U). Only adenosine exhibited a retention time close to that of Poly(U), *i.e.*, 18 min compared to 19 min, but they differed slightly when analyzed together.

We also analyzed the behaviour of Poly(A) and Poly(U) separately (Table II), and were very surprised to find that their retention times were exactly the same as those of peaks 1 and 2 of Poly(A) · Poly(U). It is thus possible that under the chromatographic conditions the two strands are dissociated and eluted separately. However, this hypothesis does not take two facts into account: (i) the melting point of these molecules is around 57°C and (ii) the different batches gave different results (see Fig. 1). Therefore we further analyzed the products obtained after separation by HPLC.

Furthermore when two different batches were mixed and analyzed by HPLC the resulting chromatogram was the sum of the chromatograms obtained for each batch analyzed separately.

Analysis of fractions separated by HPLC

The three fractions separated by HPLC were precipitated with 2 volumes of ethanol and purified twice by HPLC. The materials corresponding to peaks 1 and 2 were easily separated but molecules corresponding to peak 3 were not totally pure. This unsuccessful purification may have been due to the very small amounts and

TABLE II

RETENTION TIMES OF SOME OF THE MOLECULES THAT MAY CONTAMINATE THE PREPARATION

To examine whether molecules used during the synthesis of the Poly(A) · Poly(U) or degradation products could produce the complex Poly(A) · Poly(U) elution profile, we determined their retention times under the conditions of analysis used in Fig. 2 and described in Materials and Methods.

Molecule analyzed	*Retention time (min)*
ADP	8.75
UDP	3.5
Uridine	9
Adenosine	18.25
Digest	3–15
Poly(A)	27
Poly(U)	19

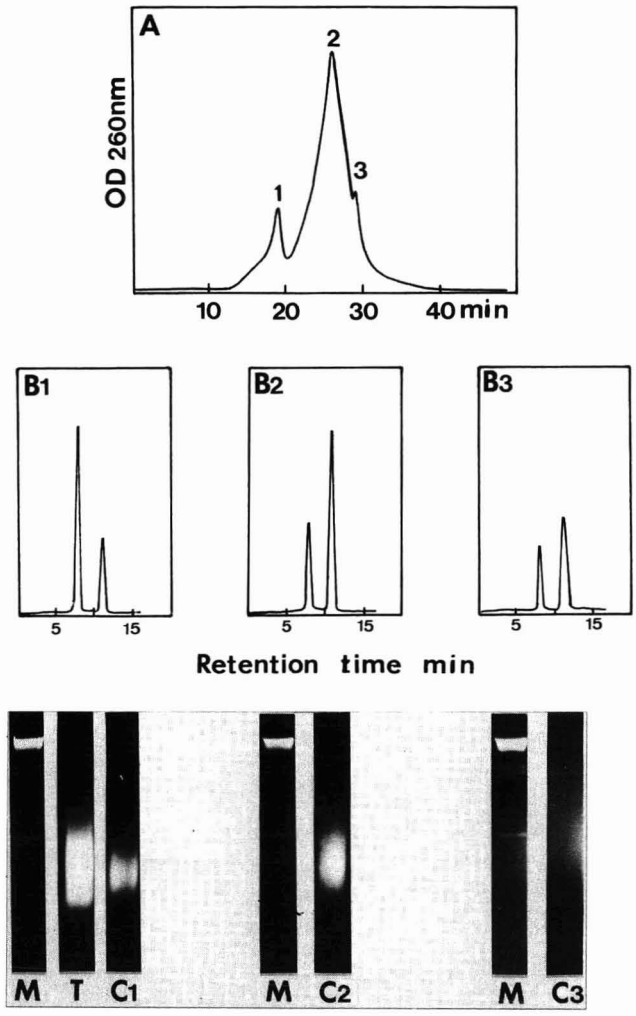

Fig. 3. Analysis of the materials separated by HPLC. Poly(A) · Poly(U) (batch B, 0.5 mg) was chromatographed as described in Fig. 2 (Fig. 3A). Fractions corresponding to the three peaks were pooled and precipitated with 75% ethanol. A second round of purification was performed on each fraction. They were then analyzed for base composition (Fig. 3B) or for size determination by gel electrophoresis (Fig. 3C) as described in Materials and Methods. (B) The HPLC profile obtained after hydrolysis and thus depicts the the base composition of the different peaks: 1 = peak 1; 2 = peak 2 and 3 = peak 3. (C) The size analysis determination by agarose gel electrophoresis. In each case M represents for the size markers; there were obtained by digestion of lambda phage with restriction enzyme Hind III. T is the Poly(A) · Poly(U) before separation by HPLC and is thus given as a reference. The three components separated by HPLC in (A) were analysed: 1, peak 1, 2, peak 2 and 3, peak 3.

minimum differences in the retention times of the contaminating products, or to the apparent conversion of this peak into peak 2 during purification. In any case, we analyzed the size agarose gel electrophoresis and the base composition (alkaline hydrolysis, HPLC) of the material separated in peaks 1, 2 and 3 (Fig. 3). Peak 1 contained material of small size, with a mean of around 250–300 base pairs. Base

composition analysis revealed that uridine was the major component, but adenosine was also present, in a molar ratio A/U of 0.6. Peak 2 contained molecules of a mean size close to that of the starting material and a molar ratio (A/U = 1.2) showing a slight increase in the A base. Peak 3 contained molecules of large size and a molar ratio A/U of around 1.

Interpretation of the results

These results can be explained by the theory of multiple interactions and the behaviour of nucleic acids in reversed-phase HPLC as described previously[7–9,12]. Assuming that Poly(A) · Poly(U) molecules have gaps in their secondary structures, *i.e.*, single-stranded regions, these portions would interact strongly with the stationary phase as previously shown[8]. Thus, there are three possibilities, *i.e.*, the molecule contains: (i) stretches of single-stranded Poly(U), (ii) single-stranded Poly(A) or (iii) both. In the case where the single-strand stretchers are only on Poly(U), the double-stranded part would detach from the stationary phase and the molecule would be attached by the single-stranded Poly(U) (see ref. 8); the whole molecule would consequently be eluted with Poly(U) and exhibit the same retention time. In other words, in this case, the retention time of the molecule would be determined by the single-stranded region and the whole molecule would exhibit the elution profile of Poly(U). In contrast, if a molecule contains both single-stranded Poly(U) and single-stranded Poly(A) [where higher hydrophobicity of Poly(A) would dominate], the retention time of the whole molecule would be that of Poly(A). None of these molecules contains two perfectly matching strands, or they would be eluted earlier[8]. It can be assumed that when the molecules of Poly(A) and Poly(U) are small, the fraction of molecules containing only single-stranded Poly(U) increases, as does the fraction containing only single-stranded Poly(A), but the latter is eluted with molecules also containing single-strand Poly(U). Thus the smaller the molecules are, the greater is the ratio of peak 1 to peak 2, and thus reversed-phase HPLC measures the mean size of the polymers. If this interpretation is correct, single strands should be detectable in the molecule. To test for the presence of such single strands we have digested the molecules with single-strand-specific S1 nuclease. Fig. 4 shows that Poly(A) · Poly(U) was digested by this nuclease, implying the presence of single-stranded regions. Analysis by HPLC was also performed under the conditions used for native Poly(A) · Poly(U). Degradation products corresponding to oligonucleotides and finally to nucleotides have been observed (results not shown). However a peak corresponding to genuine Poly(A) · Poly(U) was still observed but disappeared when digestion was performed for 3 h. Thus Poly(A) · Poly(U) contains single-stranded parts that are sensitive to S1 nuclease.

The nature of peak 3 is more difficult to explain. It may represent an unidentified complex structure, or could be the result of a contaminant protein, but such a protein was not detected. We have not detected protein contamination by colorimetric protein content analysis, gel electrophoresis, nor using a radioimmunologic assay directed against PNPase the enzyme used for synthesis of Poly(A) · Poly(U).

CONCLUSIONS

We have shown the advantages of reversed-phase HPLC in analyzing synthetic

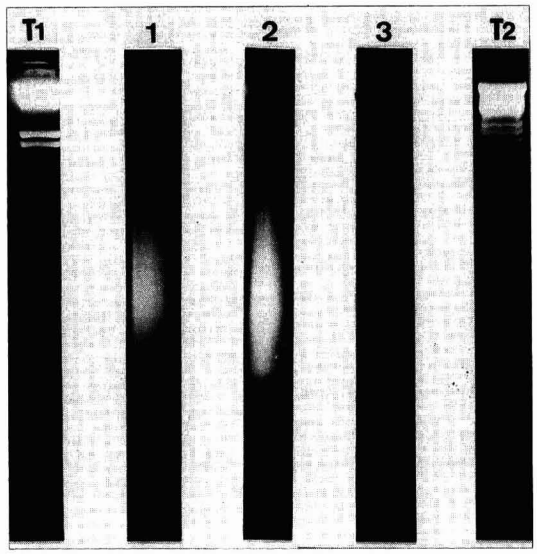

Fig. 4. Degradation of Poly(A) · Poly(U) by S1 nuclease. Batch B of Poly(A) · Poly(U) (0.1 mg) was incubated with 30 units of S1 nuclease for 1 h at 37°C in the buffer recommended by the supplier. The reaction was stopped at 0°C, the mixture diluted 10 times in sucrose buffer and immediately deposited on the gel and electrophorized as described in Fig. 1. Lanes: 1, Poly(A) · Poly(U) control; 2, Poly(A) · Poly(U) incubated at 37°C without nuclease; 3, Poly(A) · Poly(U) digested by S1 nuclease; T, lambda DNA digested by restriction enzyme Hind III (T1) or Pst I (T2) as the size marker. Lane 3 reveals that Poly(A) · Poly(U) has been digested by the single-strand-specific enzyme: first because the mean molecular weight has decreased and secondly because the quantity revealed by ethidium bromide coloration, which binds only long double-stranded molecules, has considerably decreased.

Poly(A) · Poly(U) preparations. A single chromatographic analysis revealed most of the biochemical properties of the preparations. The method is rapid, reproducible and easy to perform. It is particularly suitable for analyzing preparations for industrial or pharmacological use, as well as those used in biological experiments.

Based on the results, we hypothesized that these molecules contain stretches of single strands, and this was confirmed by enzymatic digestion with the S1 nuclease known to degrade only single strands. The result may be of interest in explaining the biological properties of the molecule.

These results complement the analysis of nucleic acids previously reported[7–9,12]. They show that large nucleic acids can be separated by their secondary and tertiary structures. This property has potential applications in the field of molecular biology and genetic engineering.

ACKNOWLEDGEMENTS

This work was mainly supported by a contract between Expansia and the Université de Montpellier I which financed a fellowship for one of us (J.L.). This work was also supported by INSERM and CNRS.

REFERENCES

1 G. Felsenfeld, D. Davies and A. Rich, *J. Am. Chem. Soc.*, 78 (1956) 2023–2028.
2 R. Blake, J. Massoulie and J. R. Fresco, *J. Mol. Biol.*, 30 (1967) 291–308.
3 A. Michelson, J. Massoulie and W. Guschlbauer, *Prog. Nucleic Acid Res. Mol. Biol.*, 6 (1967) 83–141.
4 S. Broitman, D. Im and J. R. Fresco, *Proc. Natl. Acad. Sci. U.S.A.*, 84 (1987) 5120–5124.
5 W. Braun and M. Nakano, *Science (Washington, D.C.)*, 157 (1967) 819–821.
6 F. Laceau, G. Delage and C. Chianale, *Science (Washington, D.C.)*, 187 (1975) 256–259.
7 S. Garcia and J. P. Liautard, *J. Chromatogr. Sci.*, 21 (1983) 398–404.
8 J. P. Liautard, *J. Chromatogr.*, 285 (1984) 221–225.
9 S. Colote, C. Ferraz and J. P. Liautard, *Anal. Biochem.*, 154 (1986) 15–20.
10 D. R. Mc Ewen, *Anal. Biochem.*, 20 (1967) 114–149.
11 H. Sober (Editor), *Handbook of Biochemistry*, CRC Press, Boca Raton, FL, 2nd ed., 1970, p. H19.
12 S. Garcia and J. P. Liautard, *J. Chromatogr.*, 296 (1984) 355–362.

Journal of Chromatography, 454 (1988) 205–215
Elsevier Science Publishers B.V., Amsterdam — Printed in The Netherlands

CHROM. 20 788

STRUCTURAL CHARACTERIZATION OF RECOMBINANT CONSENSUS INTERFERON-α

MICHAEL L. KLEIN, TIMOTHY D. BARTLEY, POR-HSIUNG LAI and HSIENG S. LU*
Amgen Inc., 1900 Oak Terrace Lane, Thousand Oaks, CA 91320 (U.S.A.)
(First received November 26th, 1987; revised manuscript received March 4th, 1988)

SUMMARY

Recombinant consensus interferon-α is derived from genetically modified *Escherichia coli* containing a synthetic gene constructed from a consensus of interferon sequences. The purified and biologically active protein has been subjected to detailed structural characterization including sequence determination and peptide isolation and identification. The homogeneous consensus interferon-α preparation contains two chromatographically indistinguishable homologous polypeptides with one containing an extra methionyl residue at the amino terminus. The delineated amino acid sequence of the protein is identical to that expected from the coding sequence of the gene. Correct oxidation of the molecule has been confirmed with two intramolecular disulfide linkages observed at Cys(1)–Cys(99) and Cys(29)–Cys(139).

INTRODUCTION

Interferons (IFNs) are a group of closely related soluble cellular proteins acting as potent biological response modifiers *in vivo* (for reviews, see refs. 1 and 2). It has been demonstrated that homogeneous interferon preparations elicit various biological activities such as antiviral effect, cell growth inhibition and immunomodulation[3]. Interferons-α are differentiated as "leucocyte type" interferons and are antigenically, physicochemically and biologically distinguishable from interferons-β (fibroblast type) and -γ (immune type)[1].

Approximately fourteen distinct human IFN-α genes coding for proteins which contain 164–166 amino acid residues have been cloned[4–6]. All the interferon-α genes yield products that are about 80% homologous at the amino acid level. At Amgen (Thousand Oaks, CA, U.S.A.), a consensus interferon-α (IFN-Con_1) gene, a hybrid of the fourteen IFN-α subtypes, was developed. The polypeptide derived from this hybrid gene corresponds to the amino acid sequence representing the most frequently observed amino acid at each position when the sequences for the fourteen IFN-α subtypes are aligned[7]. This synthetic hybrid gene was cloned into *Escherichia coli* and the expressed recombinant product was purified to homogeneity. The final product was confirmed to have a specific antiviral activity of more than $5 \cdot 10^8$. In this communication, the entire amino acid sequence of IFN-Con_1 was elucidated by direct N-

0021-9673/88/$03.50

and C-terminal sequence analyses of the intact protein and by characterization of various overlapping peptide fragments. In addition, the covalent disulfide structures in IFN-Con_1 were confirmed to be correctly oxidized and identical to the structures in authentic IFN-α[9,10].

EXPERIMENTAL

Materials

Trypsin [L-1-tosylamide-2-phenylethyl chloromethyl ketone (TPCK)-treated] and iodoacetate were obtained from Sigma. Iodoacetic acid was recrystallized from light petroleum prior to use. [2-^{3}H]Iodoacetate was a product of New England Nuclear. *Staphylococcus aureus* V8 (SV8) protease was purchased from Miles, and carboxypeptidase P from the Peptide Institute (Osaka, Japan). Trifluoroacetic acid (TFA), acetonitrile and water were obtained from Burdick & Jackson. Crystalline cyanogen bromide was from EASTMAN-Kodak. All of the sequencing reagents and solvents were purchased from Applied Biosystems.

Purification of IFN-Con_1

A hybrid gene coding for IFN-Con_1 was synthesized and cloned into *E. coli*. Recombinant IFN-Con_1 produced by this organism was purified to homogeneity as follows. Intact cells of *E. coli*, harvested from fermenatation broth by centrifugation, were lysed in a Manton–Gaulin press. The insoluble pellet, containing IFN-Con_1, was collected by centrifugation at 3500 *g* and solubilized in 6 *M* guanidine–HCl, 2 m*M* dithiotreitol (DTT), 25 m*M* Tris–HCl (pH 8.5). Guanidine–HCl and DTT were removed by buffer exchange against 25 m*M* Tris–HCl (pH 8.5) to initiate refolding and oxidation. The IFN-Con_1 was purified by sequential chromatography using DEAE-Sepharose Fast Flow and Sephacryl S-200 (Pharmacia).

S-Carboxymethylation of IFN-Con_1

IFN-Con_1 [in 25 m*M* phosphate (pH 7), 0.1 *M* sodium chloride (phosphate buffered saline, PBS)] was desalted by passing over a Pharmcia PD-10 (Sephadex G-25) column equilibrated with HPLC-grade water. A 1-mg amount of desalted material was dried down, reconstituted with 6 *M* guanidine–HCl in 0.2 *M* ammonium bicarbonate (pH 8.2) and gently stirred at 37°C. DTT was added at a 50-fold molar excess while flushing with nitrogen gas, and stirred at 37°C for 2 h. After wrapping the reaction vessel with alumninum foil, iodoacetic acid was added at a 10-fold molar excess to DTT. Diluted sodium hydroxide (10 m*M*) was added to bring the reaction mixture back to pH 8.2. The mixtured was stirred at 37°C for 30 min, after which the reaction was quenched by the addition of 60 μl β-mercaptoethanol (5%, v/v). The mixture was immediately transferred to a dialysis bag (Spectra-Por 8000 mol.wt. cut-off), and was extensively dialyzed against 0.1 *M* ammonium bicarbonate (pH 7.8) at 4°C in the dark. The dialyzed derivative was then subjected to further analysis.

Amino acid sequence analysis

Polypeptides were sequenced from their amino termini by automated Edman degradation on an Applied Biosystems 470A gas phase sequencer. The phenylthiohydantoin (PTH) amino acids were analyzed by high-performance liquid chromato-

graphy (HPLC) according to the method of Hewick *et al.*[11]. When the entire IFN-Con_1 molecule was to be sequenced, it was spotted on a TFA-activated glass fiber (Whatman GF/C) disc; when cleavage products (peptides) were to be sequenced, they were spotted on TFA-activated GF/C discs which were treated with Polybrene containing 6.7 mg/ml sodium chloride and preconditioned with at least three sequencer cycles.

Amino acid analysis

Samples containing IFN-Con_1 were transferred to WISP vials (Waters Assoc.), dried and hydrolyzed using the vapor hydrolysis method[12]. Vials containing dried samples were placed in sealed, evacuated screw-top vacuum vials (Waters Assoc.) containing 1.5 ml of 6 *M* hydrochloric acid, 0.1% β-mercaptoethanol and 0.05% phenol. The tubes were placed in an oven at 110°C for 24 h, after which the vials were removed and dried by vacuum. The dried hydrolysates were reconstituted with 0.2 *M* sodium citrate and analyzed by high-performance cation-exchange chromatography followed by ninhydrin detection on a Beckman 6300 amino acid analyzer.

The amino acid composition of the peptide fragments was determined by a pre-column derivatization method using phenylisothiocyanate (PITC)[13,14]. The phenylthiocarbamyl (PTC) amino acids were analyzed by reversed-phase HPLC on a 3-μm Rainin C_{18} column (10 × 0.46 cm I.D.) using a Spectra-Physics 8700 HPLC system, a Waters WISP 710B autosampler, and a Waters 440 detector (254 nm detection wavelength).

Peptide mapping derived from enzymatic and chemical cleavages

Tryptic digestion. Cys(Cm)-IFN-Con_1 [Cys(Cm) is S-carboxymethylcysteine] derivative was diluted to 0.23 mg/ml with 0.1 *M* ammonium bicarbonate (pH 7.8). This solution and a solution of native IFN-Con_1 (0.23 mg/ml PBS) were treated with trypsin (trypsin:IFN-Con_1, 1:50, w/w) and incubated at 37°C for 4 h. The reactions were stopped by placing the vessels on ice. The digests were injected directly by a Waters WISP 710B onto a reversed-phase C_4 column (Vydac; 25 × 0.46 cm I.D.), and eluted with a gradient of acetonitrile in 0.1% TFA generated by a Spectra-Physics 8700 pumping system. Tryptic maps were generated by monitoring the absorbance of the effluent with a Spectraflow 757 detector (Kratos) at 220 nm. Peaks were collected in glass test tubes using a Gilson Model 202 fraction collector.

SV8 protease digestion. A solution of native IFN-Con_1 (0.23 mg/ml PBS) was teated with SV8 protease (enzyme-to-substrate ratio = 1.25) and incubated at 37°C for 18 h. The reaction was stopped by placing the vessel on ice. Mapping was performed as described above for tryptic mapping. SV8 cleavage is expected to occur at Glu-X and, to a lesser extent, Asp-X bonds.

Cyanogen bromide cleavage. A 500-μg amount of Cys(Cm)-IFN-Con_1 in 0.1 *M* ammonium bicarbonate (pH 7.8) was dried and reconstituted with 190 μl of a 10% (w/v) cyanogen bromide solution in 70% formic acid (pre-purged with nitrogen gas). The reaction was run for 16 h in the dark at room temperature. The mixture was then dried to near-completion in a hood with a stream of nitrogen, followed by the addition of 200 μl of 0.1% TFA, which gave a turbid solution. To alleviate much of the turbidity, one crystal of guanidine–HCl was added. Using this solution, cyanogen bromide mapping was performed as described above for tryptic mapping.

C-terminal analysis

Desalted IFN-Con$_1$ (in water) was brought to 0.05% (w/v) Brij-35 at pH 4.0 (final IFN-Con$_1$ concentration of 0.36 mg/ml). Carboxypeptidase P was added at a 1:400 (w/w) ratio with IFN-Con$_1$ and left to digest at room temperature. Time point aliquots were removed and quenched by adding TFA to a 10% concentration. The samples were immediately dried and subjected to amino acid analysis using pre-column PITC derivatization and narrow bore HPLC[15].

Peptide nomenclature

Peptide numbers were designated according to the elution order of each HPLC peptide map. Those peaks not numbered were recovered in low concentration and yielded no sequencing results.

RESULTS AND DISCUSSION

Amino acid analysis

Table I shows the amino acid composition of IFN-Con$_1$ derived from acid

TABLE I

AMINO ACID COMPOSITION ANALYSIS OF RECOMBINANT IFN-Con$_1$

Recombinant IFN-Con$_1$ was hydrolyzed and the hydrolysate analyzed as described in the Experimental section.

Amino acid	*Number of residues*	
	Theoretical	*Calculated*
Cys(Cm)*	–	3.85
Asx	14	14.14
Thr	8	8.29
Ser**	13	11.55
Glx	28	28.26
Pro	5	6.17
Gly	4	6.01
Ala	10	10.04
Cys	4	N/A***
Val	8	7.23
Met	4	3.65
Ile	8	7.50
Leu	20	20.59
Tyr	5	4.73
Phe	10	9.97
Lys	9	9.12
His	3	2.93
Arg	11	10.94
Trp§	2	1.82
Total	166	

* Cysteine was determined as carboxymethylated cysteine by analysis of Cys(Cm)-IFN-Con$_1$.
** Content of Ser is not corrected.
*** Not analyzed.
§ Tryptophan was recovered by 4 *M* methanesulfonic acid hydrolysis of IFN-Con$_1$.

hydrolysis. The calculated numbers of residues correspond very well with the expected values except for the low values for serine and valine, and the high values for proline and glycine. Cysteine was determined as its S-carboxymethyl derivative, and tryptophan was separately determined by hydrolysis using 4 *M* methanesulfonic acid[16]. The low value for serine is due to partial destruction during acid hydrolysis and was estimated without correction. The compositional analysis of IFN-Con_1 indicates that it is a product derived from the IFN-Con_1 gene.

N-terminal sequence of IFN-Con_1

When purified Cys(Cm)-IFN-Con_1 was subjected to N-terminal sequencing, two distinct sequences were revealed. Once sequence corresponded to a species starting with the initiator methionine. The other sequence began with cysteine as the N-terminus, indicating the removal of the initiator methionine by the host expression system. The ratio of N-terminal methionine to cysteine is approximately 1.1:1, suggesting that the *E. coli* methionyl aminopeptidase[17] is able to process approximately half of the protein initiator under the conditions used to express IFN-Con_1. The N-terminal sequence analysis of the protein results in the elucidation of the first 33 amino acid residues from the amino terminus as shown in Fig. 1. Cys-1 and Cys-29 were positively identified by sequencing the Cys(Cm)-IFN-Con_1 derivative. However, due to the interference of the two N-terminal sequences of IFN-Con_1, the extended sequencing run yielded inconclusive results, as carryover and lag made further assignment unclear after cycle 33.

C-terminal sequence analysis

The intactness of the C-terminal sequence of IFN-Con_1 was confirmed by two separate analyses. The C-terminal sequence was identified by isolation of an SV8 protease-cleaved peptide, peptide S-1 (Figs. 1 and 2). The peptide contains six amino acids and has a sequence of Arg-Leu-Arg-Arg-Lys-Glu-COOH as revealed by compositional and sequence analyses. This C-terminal sequence is supported by carboxypeptidase P digestion of the intact protein (Table II). Kinetic analysis of the data is consistent with the fact that the C-terminal sequence of the protein is · · · (R)-L-R-R-K-E, indicating that the recombinant IFN-Con_1 indeed contains the intact C-terminal amino acid sequence as predicted from gene sequence. The release of arginine at higher value is expected as two arginine groups are located at the third and fourth positions near the C-terminal of the molecule. No degradation or further C-terminal processing generated by *E. coli* proteases was observed.

Isolation and characterization of peptides

To elucidate the complete amino acid sequence of IFN-Con_1, the native protein or S-carboxymethylated derivative was subjected to a series of enzymatic and chemical cleavages and the resulting peptide mixtures subjected to separation by reversed-phase HPLC. Fig. 2–5 represent HPLC peptide maps obtained from various cleavages of IFN-Con_1. All peaks were collected and analyzed by PTC-amino acid analysis (data not shown). All of the numbered peptides were characterized and actually found in the IFN-Con_1 sequence (Fig. 1). Those fractions which showed low recovery in amino acid analysis were not further analyzed.

Fig. 3 shows the HPLC peptide map obtained after chromatography of a tryp-

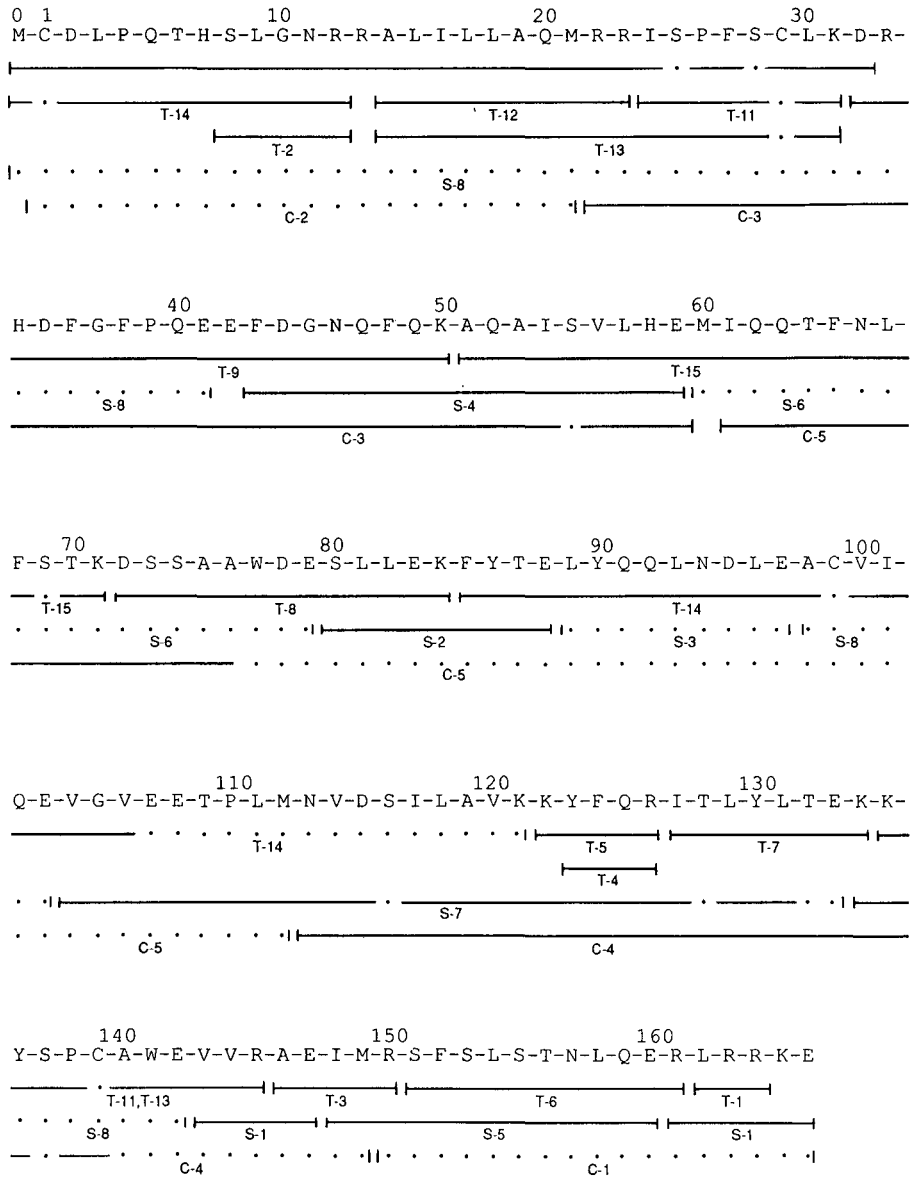

Fig. 1. Amino acid sequence of recombinant IFN-Con_1. Sequences analyzed with intact Cys(Cm)-IFN-Con_1, and peptides derived from native and S-carboxymethylated IFN-Con_1 are indicated by solid lines under the residues comprising the protein or the peptide. The letter codes below these solid lines correspond to the peptides generated by enzymatic or chemical cleavage of native and S-carboxymethylated IFN-Con_1 which were separated and isolated by HPLC (refer to Figs. 2–5): T = tryptic peptides; S = SV8 peptides; C = cyanogen bromide peptides. The solid line without a letter code corresponds to the sequence of intact Cys(Cm)-IFN-Con_1. Solid lines indicate the results of automated Edman degradation. Dots indicate residues deduced from amino acid analysis but not identified by automated Edman degradation.

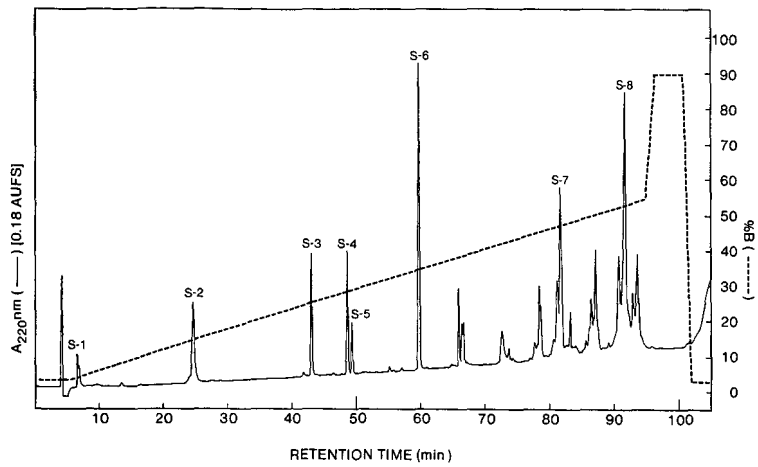

Fig. 2. HPLC peptide map of SV8 protease derived peptide from native IFN-Con_1. Native IFN-Con_1 was incubated with *S. aureus* V8 protease, and 46 μg of the resulting peptide mixture was separated by reversed-phase HPLC (see Experimental section). Peaks which were analyzed after collection are numbered according to order of elution. Solvent A, 0.1% TFA in water; solvent B, 0.1% TFA in acetonitrile–water (90:10).

sin digest of the native protein. At least 15 peptides were sequenced and the results are summarized in Fig. 1. Both peptides T-11 and T-14 were found to contain two distinct sequences, corresponding to the two disulfide-containing peptides [Cys(29)–Cys (139), and Cys(1)–Cys(99), respectively]. Further characterization of disulfide assignment is described below. A broader peak which eluted at 95 min. in the tryptic map corresponds to uncleaved or incompletely cleaved IFN-Con_1, indicating that the present cleavage conditions result in incomplete digestion of the protein substrate.

The alignment of tryptic peptides was obtained by isolation and characterization of overlapping peptides derived from SV8 protease digestion (Fig. 2) and cyanogen bromide cleavage (Fig. 4) of IFN-Con_1. Eight SV8 protease-derived peptides and five cyanogen bromide-cleaved fragments are actually analyzed to construct the entire sequence as shown in Fig. 1. In summary, proteolytic and chemical cleavages of both native and S-carboxymethylated IFN-Con_1, along with sequencing of the

TABLE II

RELEASED AMINO ACIDS FROM CARBOXYPEPTIDASE P DIGESTION OF RECOMBINANT IFN-Con_1

Data were obtained and calculated as number of residues released per mol of protein (see Experimental).

Amino acid	*Time (min)*				
	0	*5*	*10*	*20*	*40*
Glu	0	0.18	0.48	0.75	0.86
Arg	0	0.17	0.57	1.14	1.80
Leu	0	0.10	0.12	0.19	0.22
Lys	0	0.14	0.38	0.53	0.78

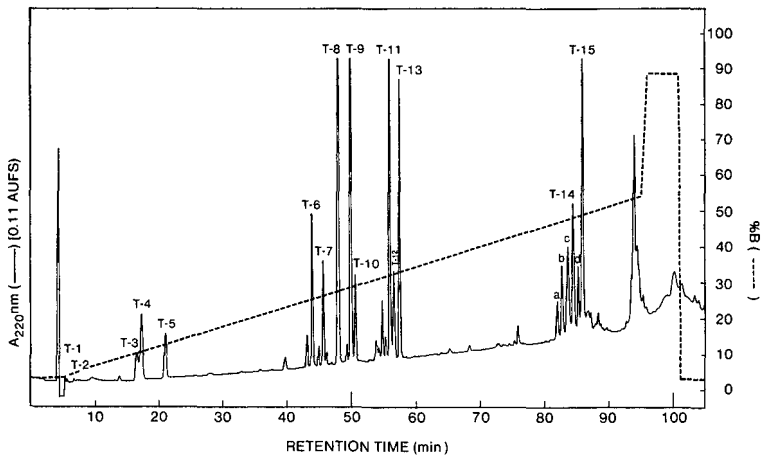

Fig. 3. HPLC peptide map of tryptic peptides derived from native IFN-Con$_1$. Native IFN-Con$_1$ was incubated with trypsin, and 46 μg of the resulting peptide mixture was separated by reversed-phase HPLC (see Experimental section). For details see Fig. 2.

N- and C-termini of the intact protein, provide for a complete overlapping sequence of this molecule. This analysis confirms that the sequence of recombinant IFN-Con$_1$ protein corresponds exactly to the coding sequence of the synthetic gene.

Assignment of disulfide bonds

Recombinant IFN-Con$_1$ when produced by genetically modified *E. coli* cells is recovered using processes including the denaturation–renaturation step. This step also allows formation of two disulfide bonds. The fully active, recombinant protein was analyzed to identify and characterize the disulfide structures.

When the protein was reacted with a 20-fold molar excess of [^{3}H]iodoacetate in

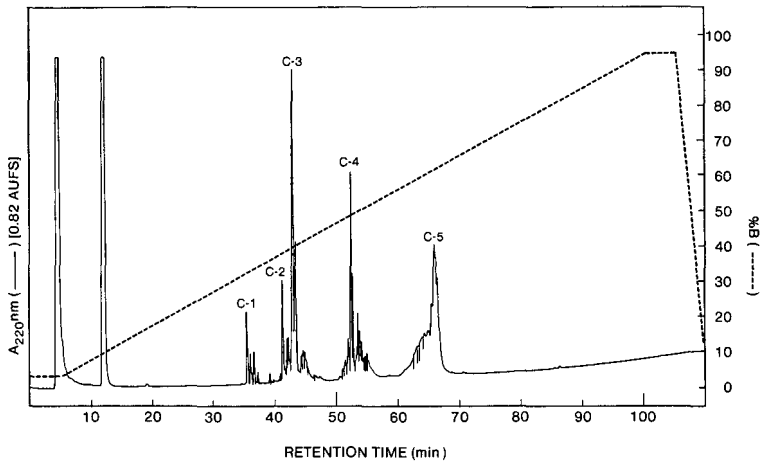

Fig. 4. HPLC peptide map of cyanogen bromide cleaved peptides from Cys(Cm)-IFN-Con$_1$. Cys(Cm)-IFN-Con$_1$ was incubated with cyanogen bromide, and 83 μg of the resulting peptide mixture was separated by reversed-phase HPLC. For details, see Fig. 2.

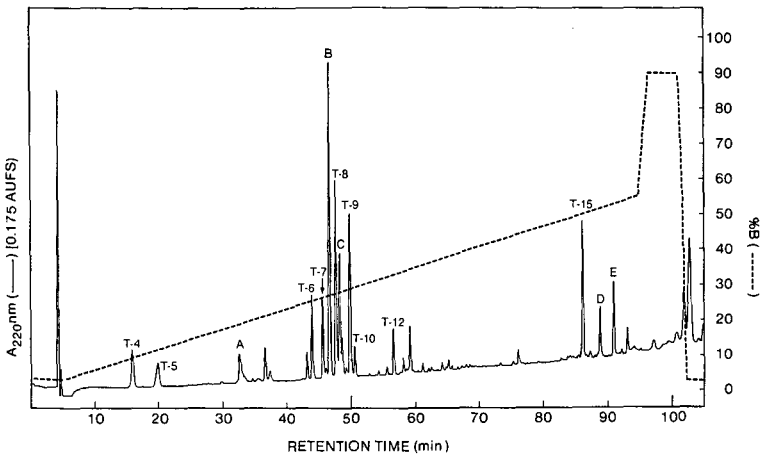

Fig. 5. HPLC peptide map of tryptic peptides from Cys(CM)-IFN-Con_1. Cys(Cm)-IFN-Con_1 was incubated with trypsin, and 46 μg of the resulting peptide mixture was separated by reversed-phase HPLC (see Experimental section). Peaks labeled A, B, C, D and E correspond to peptides containing SA-carboxymethylcysteine (see Table III).

0.2 *M* ammonium bicarbonate (pH 8.2) containing 6 *M* guanidine–HCl, 0.01 mol of radioactive label was incorporated per mol of protein. This result confirmed that all the cysteinyl residues in the molecule are involved in disulfide bond formation, and no residual unpaired cysteine was observed. This observation was further corroborated by Ellman's reaction[18], since no free sulfhydryl could be detected. When the protein was first reduced with DTT in 0.2 *M* ammonium bicarbonate (pH 8.2) containing 6 *M* guanidine–HCl and followed by alkylation with [2-^{3}H]iodoacetate (see Experimental section), 3.9 mol of radioactive label was incorporated per mol of protein. This result further indicated that the four cysteinyl residues in recombinant IFN-Con_1 form two pairs of disulfide bonds.

Determination of the location of the correct disulfide bonds was performed by

TABLE III

IDENTIFICATION OF PEPTIDES CONTAINING DISULFIDE OR S-CARBOXYMETHYLCYSTEINE

Conditions used for isolation of these peptides are described in Figs. 3 and 5. These peptides were identified by sequence and/or amino acid analysis as described in the Experimental section.

Peptides containing disulfide	*Sequence positions*	*Peptides containing S-carboxymethylcysteine*	*Sequence positions*
11	24–31/135–145	A	0–12
13	14–31/135–145	B	135–145
14	0–12/85–121	C	24–31
a	0–13/85–122	D	85–122
b	0–12/85–122	E	85–122
c	0–12/85–121		
d	1–13/85–122		

isolation, characterization and sequencing of the cysteine-containing peptides. As shown in Fig. 3, two tryptic peptides, peptides T-11 and T-14, were confirmed to be disulfide-containing peptides by amino acid analysis and direct sequence determination. Peptide T-11 contains residues 24–31 and 135–145; and peptide T-14 contains residues 0–12 and 85–121 (Table III). Both are held together by disulfide bonds at Cys(29)–Cys(139) and Cys(1)–Cys(99), respectively. Peptide T-13, which was confirmed to contain residues 14–31 and 135–145, also contains the Cys(29)–Cys(139) disulfide. It is interesting to note that other fractions, designated as a, b, c and d shown in Fig. 3, are also Cys(1)–Cys(99) disulfide-containing peptides (Table III). This heterogeneity is explained by the fact that the C-termini of the peptides on each side of the disulfide bond contain two possible cleavage sites [Arg(11)–Arg(12) and Lys(121)–Lys(122)], and that the amino terminus of the final product contains both methionine and cysteine, giving several disulfide-containing peptides.

To further assign the disulfide bonds, a tryptic map of Cys(Cm)-IFN-Con$_1$ was developed in comparison to the map of native protein (Fig. 5). Peptides T-11, T-13 and T-14 together with a, b, c and d shown in Fig. 3 disappear in the map of the reduced and alkylated protein, further supporting that these fractions correspond to the disulfide-paired peptides. Peaks corresponding to the S-carboxymethylcysteine-containing peptides appear in place of the disulfide-paired peptides, and are labeled A–E shown in Fig. 5. Amino acid composition and sequence analyses allowed the assignment of these half-cysteine peptides (Table III and Fig. 1). These results unambiguously corroborate previous evidence determining that the two disulfide bonds of IFN-Con$_1$ are Cys(1)–Cys(99) and Cys(29)–Cys(139), and are identical to the structures of IFN-α isolated from natural sources[9,10]. HPLC of SV8 protease-digested protein also allowed recovery of a disulfide-containing peptide, peptide S-8 (see Fig. 2). Peptide S-8 is composed of three distinct peptide sequences, residues 0–41, 98–103, 134–142, and these sequences are held together by two disulfide bonds (Fig. 1). Characterization of peptide S-8 was not pursued.

In summary, detailed structural characterization indicates that the primary structure of recombinant IFN-Con$_1$ expressed in *E. coli* completely matches that deduced from the IFN-Con$_1$ gene. The incomplete N-terminal processing of the protein by the host enzyme, methionyl aminopeptidase, results in the generation of two homologous species, *i.e.*, methionyl and desmethionyl IFN-Con$_1$. These two forms behave similarly so that they tend to co-elute in various chromatographic procedures. IFN-Con$_1$ purified through denaturation–renaturation–reoxidation steps was found to properly oxidize to form a biologically active molecule that is similar to natural IFN-α[8].

REFERENCES

1 W. E. Stewart, in E. Mihich (Editor), *Biological Response in Cancer —Progress towad Potential Applications*, Vol. 2, Plenum Press, New York, London, 1984, pp. 19–44.
2 N. Stebbing, *Trends Pharmacol. Sci.*, 4 (1983) 390–393.
3 W. E. Stewart II, in L. Gresser (Editor), *Interferon —1979*, Academic Press, London, 1979, pp. 20–52.
4 S. Nagata, H. Tiara, A. Hall, L. Johnsrud, M. Streuli, J. Escordi, W. Bol, K. Cantell and C. Weissman, *Nature*, 284 (1980) 316–320.
5 D. V. Goeddel, D. W. Leung, T. J. Dull, M. Cross, R. M. Lawn, R. McCandliss, P. H. Seeburg, A. Ulrich, E. Yelverton and P. W. Gray, *Nature (London)*, 390 (1981) 20–26.

6 A. E. Franke, H. M. Shepard, C. M. Houck, P. W. Leung, D. V. Goeddel and R. M. Lawn, *DNA*, 1 (1982) 225–230.
7 N. Stebbing, *Adv. Exp. Med. Biol.*, 166 (1983) 23–25.
8 K. Alton, Y. Stabinsky, R. Richards, B. Ferguson, L. Goldstein, B. Altrock, L. Miller and N. Stebbing, in E. de Maeyer and H. Schellekens (Editors), *The Biology of the Interferon System*, Elsevier, Amsterdam, 1983, pp. 119–128.
9 R. Wetzel, H. L. Levine, D. A. Estell, S. Shire, J. Fimer-Moore, R. M. Stroud and T. A. Bewley, in T. Merigan, R. Friedman and C. F. Fox (Editors), *Chemistry and Biology of Interferons, UCLA Symp. Mol. Cell Biol.*, Vol. 25, Academic Press, New York, 1982, pp. 365–376.
10 R. Wetzel, P. D. Johnston and D. W. Czarniecki, in E. de Maeyer and H. Schellekens (Editors), *The Biology of the Interferon System*, Elsevier, Amsterdam, 1983, p. 101.
11 R. W. Hewick, M. W. Hunkapiller, L. E. Hood and W. J. Dreyer, *J. Biol. Chem.*, 256 (1981) 7990.
12 B. A. Bidlingmeyer, S. A. Cohen and T. L. Tarvin, *J. Chromatogr.*, 336 (1984) 93–104.
13 H. S. Lu, M. L. Klein, R. E. Everett and P. H. Lai, in J. L'Italien (Editor), *Modern Methods in Protein Chemistry*, Plenum, New York, 1987, pp. 493–501.
14 H. S. Lu and P. H. Lai, *J. Chromatogr.*, 368 (1986) 215–231.
15 H. S. Lu, M. L. Klein and P. H. Lai, *J. Chromatogr.*, 447 (1988) 351–354.
16 R. J. Simpson, M. R. Neuberger and T. Y. Liu, *J. Biol. Chem.*, 251 (1976) 1936–1940.
17 F. Sherman, J. W. Stewart and S. Tsunasawa, *Bioassays*, 3 (1985) 27–31.
18 G. L. Ellman, *Arch. Biochem. Biophys.*, 82 (1959) 70–77.

Journal of Chromatography, 454 (1988) 217–232
Elsevier Science Publishers B.V., Amsterdam — Printed in The Netherlands

CHROM. 20 771

FREON FC-113, AN ALTERNATIVE TO METHYLENE CHLORIDE FOR LIQUID–LIQUID EXTRACTION OF TRACE ORGANICS FROM CHLORINATED DRINKING WATER*

E. A. IBRAHIM and I. H. SUFFET*
Department of Chemistry and Environmental Studies Institute, Drexel University, Philadelphia, PA 19104 (U.S.A.)
(First received December 30th, 1987; revised manuscript received June 24th, 1988)

SUMMARY

Methylene chloride is the U.S. Environmental Protection Agency solvent of choice for the liquid–liquid extraction of base-neutral organic compounds from water. The presence of cyclohexene as a preservative in the methylene chloride becomes a serious constraint when a 10^5 concentration factor is needed to isolate ng/l amounts of the trace constituents for biological testing (*e.g.* Ames bioassay) and/or gas chromatographic (GC) and GC–mass spectrometric (MS) analysis of chlorinated water samples. Cyclohexene reacts with the residual free chlorine in the samples to produce many chlorinated and oxidized cyclohexene products. These artifacts mask large portions of the early chromatogram (Kovats index <700–1300) of a capillary GC analysis on a non-polar stationary phase. Also, dechlorination by a reducing agent can affect any electrophiles present in the sample which are analyzed in the Ames procedures. This study evaluates the replacement of methylene chloride with freon FC-113 for the isolation of trace organics from chlorinated water samples that will be used for biological testing and/or GC and GC–MS analysis. Freon was found to minimize the interferences from solvent artifacts.

A continuous liquid–liquid extractor is used to compare the extraction efficiency of methylene chloride and freon. The results showed that the extraction efficiency of both solvents are comparable when 100–300 ng/l of non-polar organics are extracted and concentrated 1000-fold. Solvent blanks showed freon to have no contaminants at 200-fold concentration and, when used to extract chlorinated water, no byproducts were observed. Field sampling and quality assurance considerations show that freon is an acceptable alternative to methylene chloride for the isolation of trace organic compounds when large volumes of chlorinated waters are concentrated 10^5-fold for toxicity testing or GC and GC–MS analysis.

* Paper presented at the *American Water Works Association, Water Quality Technology Conference, Baltimore, MD, U.S.A., November, 1987.*

0021-9673/88/$03.50

INTRODUCTION

The potentially hazardous ng–μg amounts of trace organic contaminants present in environmental water samples must be isolated and concentrated before they can be analyzed by gas chromatography–mass spectrometry (GC–MS) or tested for toxicity (*e.g.* Ames bioassay). A 10^5-fold concentration factor (100 l to 1 ml) for drinking water is needed for chemical identification by GC–MS and bioassay procedures. This translates into 1 ng/l in water being concentrated from 100 l to 0.1 μg/ml solvent or 0.5 ng/5 μl injected into a GC–MS system.

A major objective of the isolation and concentration methods are to assure minimum chemical alteration of the sample, and minimize blank artifacts of the method. This can be a difficult problem, especially when chlorinated drinking water is sampled, since free chlorine in water is very reactive. However, dechlorination by a reducing agent would react with electrophiles that may be in the sample. These electrophiles, in fact, are the compounds that would affect the Ames bioassay procedure. This study will consider 1,1,2-trichloro-1,2,2-trifluoroethane (freon FC-113) as an alternative to methylene chloride for the extraction of base–neutral organic compounds from water.

Methylene chloride is the solvent of choice for the liquid–liquid extraction of base–neutral organic compounds from water by EPA method 625[1] and the Master Analytical Scheme (MAS)[2]. The presence of cyclohexene as a preservative in the methylene chloride becomes a serious constraint for the extraction of chlorinated water samples[3]. Cyclohexene reacts with the residual free chlorine in the samples to produce many chlorinated and oxidized cyclohexene products[3]. The reaction products can mask a large portion of the beginning of a capillary GC chromatogram (Kovats index <700–1300) therefore limit the quantification of compounds eluting in this region of the chromatogram. At the present time, attempts to separate cyclohexene from methylene chloride have failed and the use of a more appropriate preservative for methylene chloride has not yet been developed by manufacturers for commercial use.

Toxicological concern exists for methylene chloride. A national EPA toxicology program studying lifetime inhalation of methylene chloride showed carcinogenic effect on mice[4]. Accordingly, the highest time-weighed average (TWA) allowable air exposure limit was decreased from 500 ppm to 100 ppm[5].

Some of the general criteria for choice of solvent are: (1) stability and chemical reactivity, (2) solvent character (*e.g.* polarity), (3) solubility in water, (4) solvent handling (*e.g.* volatility, viscosity, etc.), (5) toxicity, (6) flammability and (7) cost. In the last few years, freon FC-113 was introduced as a solvent for today's needs[6]. For example, the TWA allowable exposure limit of FC-113 is 1000 ppm. Table I summarizes the physical properties of FC-113 and methylene chloride. FC-113 is stable, non-flammable and chemically inert which makes it attractive as a solvent. It does not react with strong acids (*e.g.* sulphuric acid), inorganic bases (*e.g.* sodium hydroxide) and oxidizing agents (*e.g.* perchlorates, N_2O_4, O_3, liquid O_2 and H_2O_2). Its low heat of vaporization allows evaporation with comparatively small amounts of energy. However, the lower solubility parameter (7.3 *vs.* 9.6 for methylene chloride) makes freon less efficient than methylene chloride for extracting polar organic compounds. Environmental concern related to the earth's ozone layer can associate with uncontrolled evaporation of either methylene chloride or freon[7]. However, recovery of the solvent from the distillation process can be achieved.

TABLE I

PHYSICAL PROPERTIES OF FREON FC-113 AND METHYLENE CHLORIDE[20,21]

	FC-113	*Dichloromethane*
Formula	CCl_2FCClF_2	CH_2Cl_2
Molecular weight	187.37	84.93
Boiling point (°C) at 1 atm	47.57	39.75
Latent heat of vaporization (cal/g)	35.07	78.6
Vapor pressure (Torr) at 25°C	330	436
Freezing point (°C)	− 36.4	− 95.14
Viscosity at 20°C (cP)	0.711	0.44
Liquid density at 25°C (g/ml)	1.564	1.317
Refractive index at 25°C	1.356	1.424
UV cutoff (nm)	231	250
Surface tension (dyn/cm) at 20°C	17.3	28.12
Solubility of water at 20°C (%)	0.009	0.24
Solubility in water at 20°C and saturation pressure (%)	0.017	1.60
Dielectric constant (ε) at 25°C	2.4	8.93
Hildebrand solubility parameter, δ	7.3	9.6

Trichlorotrifluoroethane (no exact structure given) has been used to extract organic solutes from water[8]. Comparative recovery data for extracting toluene by hexane, freon, carbon tetrachloride and chloroform was reported. Of the four solvents, freon gave the best extraction efficiency for toluene. Surprisingly, freon was more efficient than benzene, hexane and chloroform for the extraction of 2-pentanol, which is more polar than toluene. No comparative recovery data involving methylene chloride was reported.

This paper investigates the partitioning characteristics of both solvents and studies the possibility of using freon FC-113 as an alternative to methylene chloride for liquid–liquid extraction of non-polar trace organics from chlorinated drinking water samples.

Apparatus

The continuous liquid–liquid extractor (CLLE) developed and modified by Suffet and co-workers[9–15] to isolate and concentrate detectable amounts of trace organic compounds from water samples was further modified in this study. The CLLE glassware was redesigned by introducing the evaporative concentration system (EVACS)[16] as the evaporation chamber. A schematic diagram of the entire process is shown in Fig. 1. The new design of the CLLE glassware with the EVACS is shown in Fig. 2 and a photograph of the apparatus is shown in Fig. 3. The most significant changes of the present CLLE from the previous one used by Baker *et al.*[14,15] are as follows.

(1) The distillation chamber with the previous heating element is replaced by the EVACS with a Mica band heater (Watlow B1A1JN3) which allows smoother operation especially when used with a variable voltage supply (Variac) to have full control over the heater. The new heater eliminated the problem of cracking the glass tube surrounding the old heater (Fig. 4)[14]. The solvent loss during recycle in the system is reduced from 300 to 150 ml with the new design. The final volume of the extract after

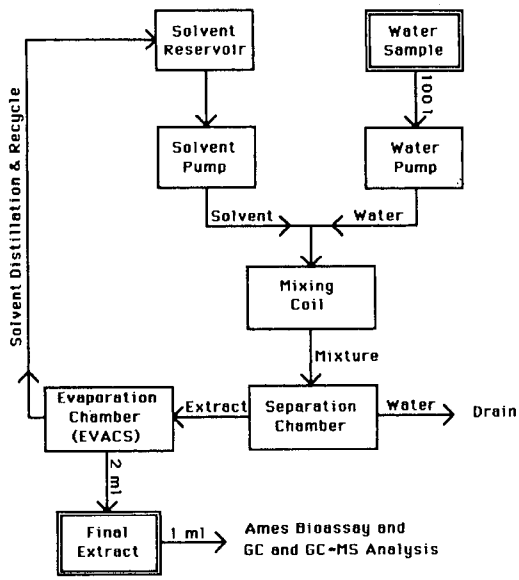

Fig. 1. Schematic diagram of the CLLE process.

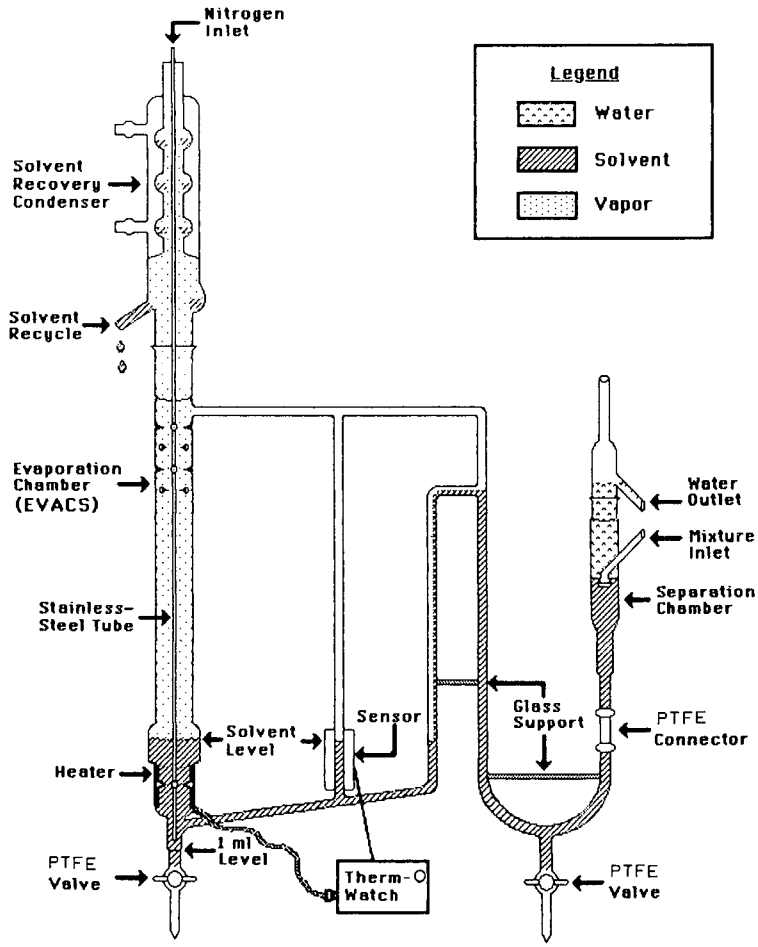

Fig. 2. Modified CLLE glassware.

introducing EVACS is 1 ml which can be injected directly in a GC or GC–MS system without any subsequent evaporation.

(2) The solvent level is sensed with a solid state sensor which uses conductance instead of the level sensor which was used with a glass-float containing copper wire wrapped in aluminum foil. The new sensor eliminated the operational problems of the

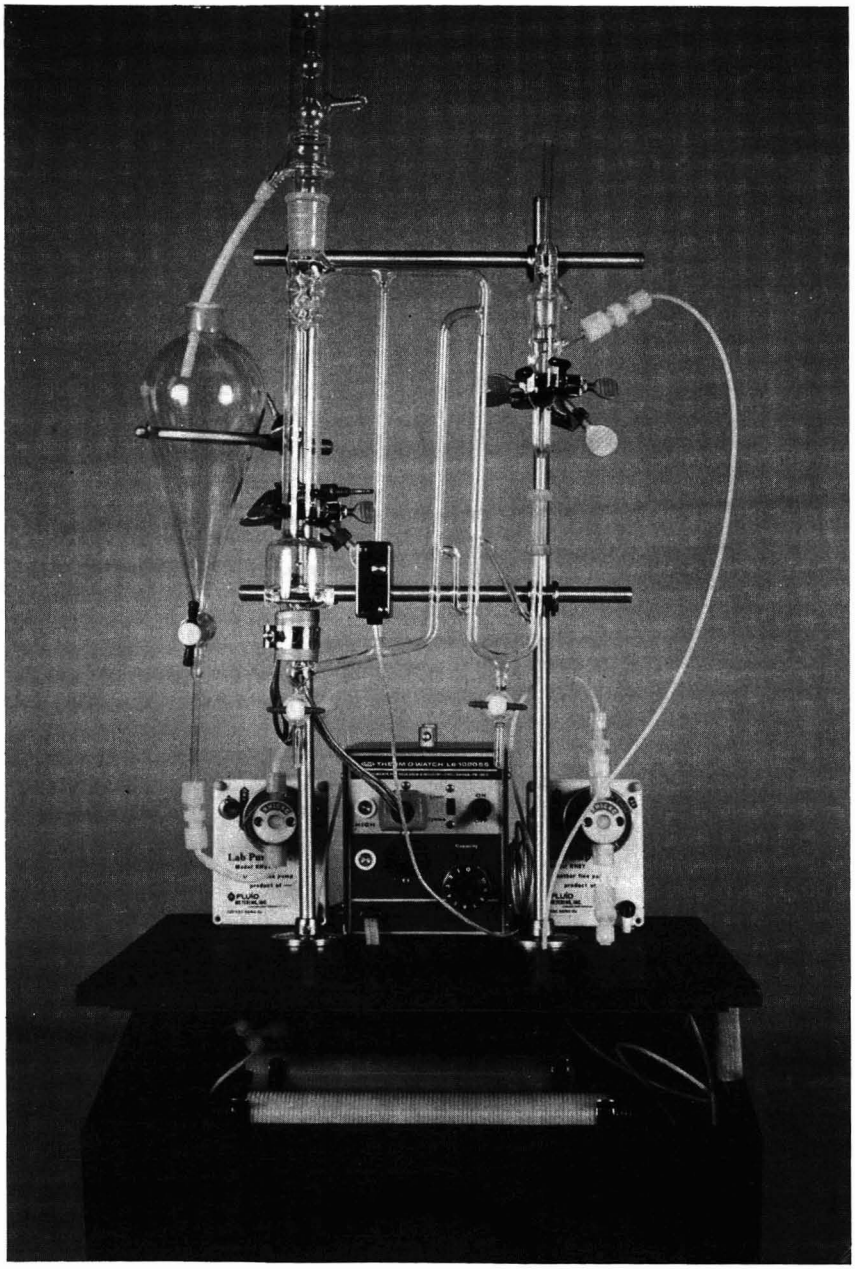

Fig. 3. Photograph of the CLLE apparatus made by E. M. Becker Co. (Philadelphia, PA, U.S.A.).

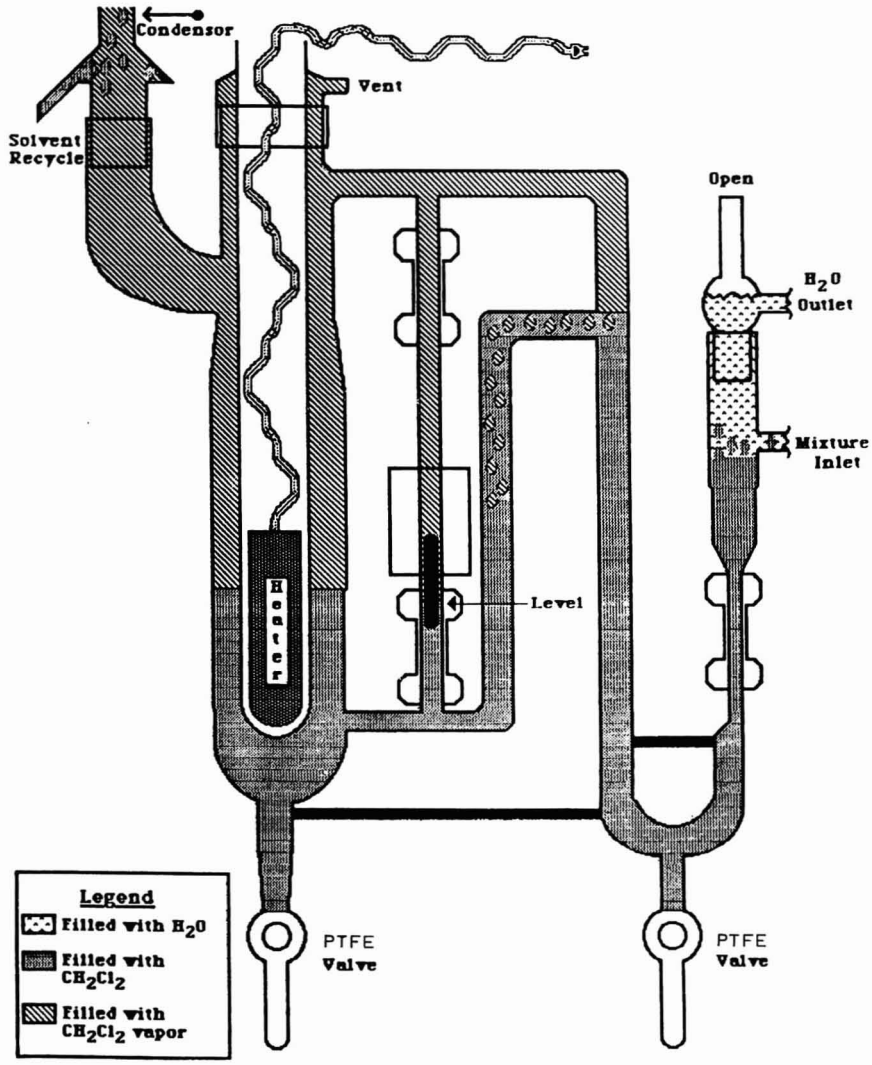

Fig. 4. Previous version of CLLE apparatus (Baker *et al.*[14]).

float with its adherence to the walls of the level tube. The manufacture states that the new solid state sensor is sensitive to liquids with dielectric constant (ε) greater than 4. However, it works for FC-113 with a dielectric constant of only 2.5.

(3) The positive displacement pumps Models RH1CKC and PG 20 (Fluid Metering, Oyster Bay, NY, U.S.A.) for water and solvent, respectively, were replaced by two identical positive displacement pumps Model RHSY1CKC (Fluid Metering). The new pumps are smaller in size, lighter in weight (4 instead of 9 lbs. for the old pumps) and safer in operation as they can operate dry.

The CLLE apparatus was designed to be run by one operator with minimum

downtime and adjustments. The latest unit made by E. M. Becker Co. (Philadelphia, PA, U.S.A.) was assembled on a rigid box with the two coils inside and the other parts (pumps, glassware, and Therm-O-Watch) outside (Fig. 3).

EXPERIMENTAL

The solvents used in the study were HPLC–GC-grade freon FC-113 from Burdick & Jackson (Muskegon, MI, U.S.A.) and distilled in glass LC–GC methylene chloride from EM Science (Cherry Hill, NJ, U.S.A.). The following laboratory experiments were conducted to study the extraction efficiency of FC-113.

(1) A 200-ml volume of FC-113 was evaporated to 1 ml in the EVACS[14] and analyzed by capillary GC for quality assurance.

(2) A set of organic compounds representing different functional groups and different polarities were used to evaluate the partitioning characteristics of FC-113 at pH 7. Table II lists those selected compounds, their functionality, boiling points and Kovats indices.

(3) A mixture of lower boiling compounds (Table III) was also used in a comparative study of FC-113 *versus* methylene chloride for extracting Milli-Q water samples. A 1-l volume of Milli-Q water was spiked with 5 μl of 1% solution (in acetone) of each of these compounds. Continuous liquid–liquid extraction of these spiked chemicals into FC-113 was completed using the modified CLLE (Fig. 3). At the end of each run the solvent was recycled in the system for 10 min to rinse the coils and separation chamber. Further concentration of the sample to 1 ml was continued in the evaporation chamber (EVACS). The sample was stored in a 1-ml vial with a PTFE-lined cap after adding 10 μl of 2000 ppm of six internal standards (C_8, C_9, C_{10},

TABLE II

ORGANICS SELECTED FOR EVALUATION OF FC-113

GC conditions: Carlo Erba 2150 gas chromatograph with flame ionization detector using a 60 m × 0.32 mm fused-silica column with a SE-30 bonded phase. Nitrogen carrier gas at a flow-rate of 0.4 ml/min and detector gases; air at 400 ml/min and hydrogen at 40 ml/min. Temperature program: isothermal at 50°C for 8 min; 5°C/min to a final temperature of 275 then isothermal at 275°C for 10 min; injector and detector temperatures were 250°C and 300°C, respectively. Sample size was 2.5 μl and split ratio was 20:1. Peak integration was done with a Spectra-Physics SP 4100 computing integrator using 1 cm/min chart speed and attenuation 4.

Compound	*Functional group*	*Boiling point (°C)*	*Kovats index*
Acetophenone	Ketone	202.6	1029.3
Isophorone	Ketone	214.0	1083.8
2,4-Dichlorophenol	Phenol	210.0	1143.1
Quinoline	Benzopyridine	238.0	1202.7
1-Chlorodecane	Chlorinated hydrocarbon	223.4	1255.7
2-Methylnaphthalene	Polyaromatic hydrocarbon	241.0	1264.3
Biphenyl	Hydrocarbon	255.9	1344.6
1-Chlorododecane	Chlorinated hydrocarbon	260.0	1431.9
Diacetone-L-sorbose	Sugar derivative	–	1570.7
Anthracene	Polyaromatic hydrocarbon	340.0	1742.6
Dioctylphthalate	Phthalate	384.0	2501.8

TABLE III

LOWER BOILING ORGANICS SELECTED FOR EVALUATION OF FC-113

GC conditions: the same as Table II except the temperature program was isothermal at 50°C for 8 min then 3°C/min to 150°C and 35°C/min to 275°C, then 10 min at 275°C.

Compound	*Functional group*	*Boiling point (°C)*	*Kovats index*
Toluene	Aromatic hydrocarbon	110.6	765.6
Ethyl butyrate	Ester	121.0	787.6
Ethyl benzene	Aromatic hydrocarbon	136.2	844.0
Cyclohexanone	Ketone	155.6	857.1
Anisole	Ether	155.0	893.3
1,4-Dichlorobenzene	Aromatic chloro-hydrocarbon	174.0	987.3
2-Ethylhexanol	Alcohol	185.0	1014.4
Acetophenone	Ketone	202.6	1031.6
Tolunitrile	Aromatic nitrile	205.0	1050.4
Isophorone	Ketone	214.0	1087.8
2,4-Dichlorophenol	Phenol	210.0	1144.0
Naphthalene	Polyaromatic hydrocarbon	218.0	1160.2
Benzothiazole	Heterocyclic thiazole	231.0	1190.2
Quinoline	Benzopyridine	238.0	1205.1
1-Chlorodecane	Chlorinated hydrocarbon	223.4	1255.3
2-Methylnaphthalene	Polyaromatic hydrocarbon	241.0	1271.4
Biphenyl	Hydrocarbon	255.9	1368.2
Ethyl cinnamate	Aromatic ester	271.0	1459.0
Diacetone-L-sorbose	Sugar	–	1534.1
Tributyl phosphate	Phosphate ester	289.0	1552.0

C_{11}, C_{13} and C_{15} hydrocarbons). The sample was stored at 0°C until analysis. Triplicate samples of both FC-113 and methylene chloride were completed and analyzed by capillary GC chromatography. Quantitation was done using standard curves *vs.* internal standards.

(4) A 10-l sample of distilled water was extracted by both methylene chloride and freon FC-113 using two modified CLLEs to test the efficiency of a distillation apparatus. The flow was adjusted to a rate of 2 l/h. The extracts were concentrated in the EVACS chamber to approximately 10 ml. Further concentration to 0.5 ml was completed in the EVACS chamber using nitrogen stripping at 1 ml/min flow-rate. Each concentration stack was rinsed with 1 ml of solvent and added to each sample. It was observed that less time was needed for the final concentration and stripping steps of the freon extracts. Sample vials were kept at 0°C until the GC and GC–MS analysis.

(5) A finished chlorinated drinking water sample was extracted using both methylene chloride and FC-113 in the same way. The sampling run was terminated after 45 l of water were extracted by both methylene chloride and FC-113. The samples were concentrated down to 0.5 ml by a stand alone EVACS[16] and analyzed by capillary GC and GC–MS. The concentration factor of the detected organic compounds in the original water sample is 10^5.

RESULTS AND DISCUSSION

Solvent blanks showed FC-113, to have no contaminants at 200-fold concentration, and when used to extract chlorinated Milli-Q water no byproducts were observed. FC-113 would not be expected to have better extraction efficiency than methylene chloride because of its lower polarity shown by its solubility parameter (7.3 *vs.* 9.6 for methylene chloride). The azeotropic mixture of FC-113 and methylene chloride has a solubility parameter of 8.4. Spinning band distillation (30 plates) failed to separate the cyclohexene preservative from the azeotrope[3]. The formation of cyclohexene artifacts when extracting chlorinated water with the azeotrope remained unsolved. Therefore, the azeotropic mixture of FC-113 and methylene chloride cannot be used for the extraction. Methanol, acetone, acetonitrile and ethyl alcohol form azeotropes with FC-113 but they are miscible with water and this can affect the partitioning of organics between the water sample and the solvent. Another approach to improve the extraction efficiency is to saturate the water sample with salt (salting out). This is easily done for the analysis of small sample volumes. It is more difficult for large volumes of water samples (50–100 l) which are needed to extract detectable amounts of the trace organics for instrumental analysis or for any biological testing.

Table IV represents the partitioning characteristics (*E*- and *p*-values) of methylene chloride and FC-113. The extraction method described by Suffet and Faust[17] was used in this study. Some of the compounds tested showed lower *E*- and *p*-values for FC-113 than those of methylene chloride. The only compound that is dramatically lower with FC-113 was diacetone-L-sorbose which is a very polar sugar derivative.

The comparative recoveries of methylene chloride and FC-113 for the organic compounds listed in Table III are shown in Table V. Table VI represents the statistical

TABLE IV

PARTITIONING CHARACTERISTICS OF CH_2Cl_2 AND FC-113

E-Value = fraction extracted at an equilibrated water-to-solvent ratio of 10:1. *p*-Value = fraction extracted at an equilibrated water-to-solvent ratio of 1:1. Method of calculation: Suffet and Faust[17]. Number of determinations = 4. GC conditions are the same as Table II.

Compound	*E-Value*		*p-Value*	
	CH_2Cl_2	*FC-113*	*CH_2Cl_2*	*FC-113*
Acetophenone*	0.92 ± 0.01	0.82 ± 0.04	0.99	0.98
Isophorone*	0.93 ± 0.01	0.75 ± 0.03	0.99	0.97
2,4-Dichlorophenol*	0.79 ± 0.02	0.56 ± 0.03	0.97	0.93
Quinoline	0.88 ± 0.01	0.70 ± 0.02	0.99	0.96
1-Chlorodecane	0.94 ± 0.01	0.73 ± 0.09	0.99	0.96
2-Methylnaphthalene	0.95 ± 0.01	1.11 ± 0.08	0.99	1.01
Biphenyl	0.93 ± 0.02	0.94 ± 0.04	0.99	0.99
Ethyl cinnamate	0.92 ± 0.00	1.01 ± 0.04	0.99	0.98
Diacetone-L-sorbose	0.57 ± 0.01	0.03 ± 0.00	0.93	0.28
Dioctylphthalate*	0.84 ± 0.01	0.89 ± 0.13	0.98	0.99

* U.S. EPA Priority Pollutant[19].

TABLE V

COMPARATIVE RECOVERIES OF CH_2Cl_2 AND FC-113

From 1 l water to 1 ml solvent. GC conditions are the same as Table III.

Compound	*Concentration in water (μg/l)*	*Recovery ± standard deviation (%)*	
		CH_2Cl_2	*FC-113*
Toluene	19	53 ± 7	37 ± 3
Ethyl butyrate	17	80 ± 3	80 ± 11
Ethyl benzene	20	54 ± 9	39 ± 7
Cyclohexanone	17	70 ± 1	23 ± 3
Anisole	17	74 ± 5	69 ± 4
1,4-Dichlorobenzene	16	66 ± 8	61 ± 6
2-Ethylhexanol	8	46 ± 5	53 ± 3
Acetophenone	9	61 ± 2	56 ± 4
Tolunitrile	8	61 ± 1	77 ± 5
Isophorone	17	79 ± 0	61 ± 3
Naphthalene	16	64 ± 4	77 ± 2
Benzothiazole	1	N.D.	58 ± 6
1-Chlorodecane	20	14 ± 1	14 ± 1
2-Methylnaphthalene	16	60 ± 3	78 ± 1
Biphenyl	10	65 ± 2	89 ± 2
Ethyl cinnamate	14	N.D.	100 ± 6
Diacetone-L-sorbose	7	51 ± 2	N.D.
Tributyl phosphate	26	100 ± 4	97 ± 10

TABLE VI

ANALYSIS OF VARIANCE (ANOVA) OF EXTRACTION RECOVERY DATA OF CH_2Cl_2 AND FC-113

From 1 l water to 1 ml solvent. Extraction efficiencies of freon, FC-113 and methylene chloride are equivalent. The theoretical Student $t_{0.975}$ value is 2.4469.

Compound	$t_{0.975}$	*ANOVA*
Toluene	4.202	Reject — freon lower
Ethyl butyrate	0.00	Accept — equivalent
Ethyl benzene	2.731	Reject — freon lower
Cyclohexanone	29.725	Reject — freon lower
Anisole	1.562	Accept — equivalent
1,4-Dichlorobenzene	1.00	Accept — equivalent
2-Ethylhexanol	2.401	Accept — equivalent
Acetophenone	2.236	Accept — equivalent
Toluonitrile	6.276	Reject — freon higher
Isophorone	12.00	Reject — freon lower
Naphthalene	5.814	Reject — freon higher
1-Chlorodecane	0.00	Accept — equivalent
2-Methylnaphthalene	11.358	Reject — freon higher
Biphenyl	16.971	Reject — freon higher
Tributyl phosphate	0.557	Accept — equivalent

significance of the ANOVA (analysis of variance) comparison using the Student-*t* test. Tables V and VI indicate that the CLLE efficiency of 1 l of Milli-Q water by FC-113 is comparable to methylene chloride when 1–30 ng/l of organics are extracted and concentrated 1000 fold. Seven compounds: ethyl butyrate, anisole, 1,4-dichlorobenzene, 2-ethylhexanol, acetophenone, 1-chlorodecane and tributyl phosphate gave statistically similar recoveries for both solvents. Of the rest, eleven compounds of the mixture FC-113 showed higher extraction efficiency when using FC-113 for seven compounds while four compounds were better extracted by methylene chloride. For unexplained reasons benzothiazole and ethyl cinnamate were not detected in the methylene chloride extracts but gave recoveries of 58 ± 6 and 100 ± 6%, respectively, with FC-113. However, previous analysis with methylene chloride could detect ethyl cinnamate[14]. Only diacetone-L-sorbose was not detected in the FC-113 extracts and gave 51 ± 2% recovery with methylene chloride.

Table VII shows the compounds identified by GC–MS in the four distilled and drinking water sample extracts. These samples are: (1) $2 \cdot 10^4$-fold concentration of 10 l of distilled water extracted by FC-113 (Fig. 5a); (2) $2 \cdot 10^4$-fold concentration of 10 l of distilled water extracted by methylene chloride (Fig. 5b); (3) 10^5-fold concentration of 45 l of finished water sample extracted by FC-113 (Fig. 6a); (4) 10^5-fold concentration of 45 l of finished water sample extracted by methylene chloride (Fig. 6b).

Fig. 7 shows computer reconstructed chromatograms of the four extracts to demonstrate the difference between FC-113 and methylene chloride. Peak-by-peak comparison of both distilled and finished water extracts (excluding the cyclohexene peaks) indicate that FC-113 is as efficient as methylene chloride for extracting organic compounds from aqueous samples. Methylene chloride was expected to be more efficient than FC-113 because of its higher solubility parameter, δ (9.6 *vs.* 7.3 for FC-113). At present, there is no explanation of why the FC-113's efficiency is equivalent to that of the methylene chloride.

Of particular interest is the area on the chromatograms between Kovats indices 600 and 1300 (Fig. 7) which contains very large peaks only in the methylene chloride samples. These large peaks are air oxidation or oxidation and chlorination byproducts of cyclohexene, the preservative in methylene chloride, which result from the reaction with residual chlorine in the finished drinking water[3]. In the methylene chloride distilled water extract the large peaks affected the resolution of other chromatographic peaks present in the sample between retention time (t_R) 30.02 and 35.22 min (Fig. 5) which corresponds to a Kovats index of 1000–1200 (Fig. 7). In the chlorinated water extract the larger number of peaks are both oxidation and chlorination cyclohexene byproducts. These peaks are located at t_R 11.31–38.39 (Fig. 6) which corresponds to a Kovats index of 600–1300 (Fig. 7). Peaks observed in the FC-113 extracts in that region (Kovats index 600–1300) could not be observed by GC or GC–MS in the methylene chloride samples because they are masked by the cyclohexene artifacts.

Table VII lists the compounds identified in the four samples. There are mainly three groups of impurities:

(a) Cyclohexene artifacts which originate from the oxidation and chlorination reactions occurring between methylene chloride and cyclohexene, the preservative in the solvent. In presence of the free chlorine residual used as a disinfectant in the finished water, the number and concentration of the cyclohexene derivatives was dramatically greater than those in the distilled water extracts[3];

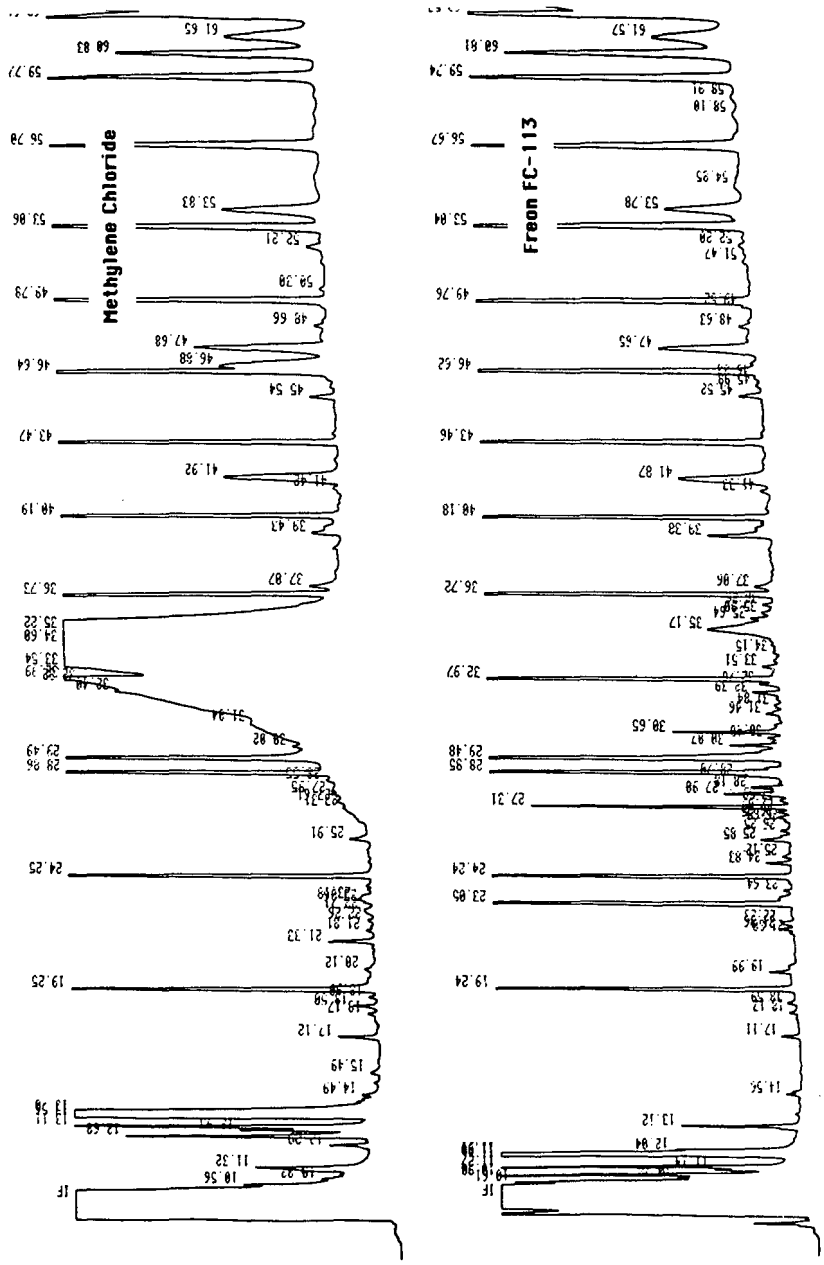

Fig. 5. Chromatograms of distilled water extracts.

TABLE VII

GC–MS COMPOUND IDENTIFICATION

GC and GC–MS conditions: Hewlett-Packard 5890 gas chromatograph with a flame ionization detector and a capillary DB-1, 30 m × 0.25 mm I.D. column. Sample sizes of 1.0 μl were injected on column at 50°C. The temperature programme was isothermal at 50°C for 8 min, 5°C/min to 275°C final temperature, then isothermal at 275°C for 10 min. The GC–MS apparatus was a Hewlett-Packard 5970 MSD. The mass range for the MS was 40–400 a.m.u. using a scan rate of 500 a.m.u./s. EM multiplier voltage was 1800 V and the transfer line temperature was 280°C.

Compound	*Distilled water*		*Finished water*	
	FC-113	*CH_2Cl_2*	*FC-113*	*CH_2Cl_2*
Cyclohexene related compounds				
Cyclohexene		X		X
Chlorocyclohexene				2
Cyclohexen-1-one				X
Dichlorocyclohexane		X		3
Chlorocyclohexanol		X		2
Chlorocyclohexanone				X
Bromocyclohexanol				X
Haloform related compounds				
Bromoform*			X	X
Dibromochloromethane*				X
1,1,1-Trichloroacetone			X	X
Other compounds				
Benzaldehyde	X		X	
Benzothiazole	X	X		
Tetrachloroethylene*				X
C_3-benzene isomer			2	X
C_4-benzene isomer				X
Trichloromethylbenzene			X	
Methyl phenyl hexanone			X	
Tolunitrile or phenylacetonitrile			X	X
Naphthalene*			X	X
Methyl naphthalene			2	X
Biphenyl			X	
Dichlorobiphenyl*	X			
Ethyl cinnamate			X	
Dihydroactinidiolide			X	X
Tributyl phosphate			X	
C_{12} Fatty acid		X		
C_{14} Fatty acid	X	X		
C_{16} Fatty acid	X	X		X
C_{18} Fatty acid				X
Diethyl phthalate*	X	X	X	
Dibutyl phthalate*	X	X	X	X
Dioctyl phthalate*	X	X		

* Represent EPA priority pollutant[19]. GC–MS analysis was not confirmed by standards. Numbers represent isomers.

(b) Phthalates, which are used in all types of plastic products and may originate from laboratory contamination;

(c) Long chain fatty acids.

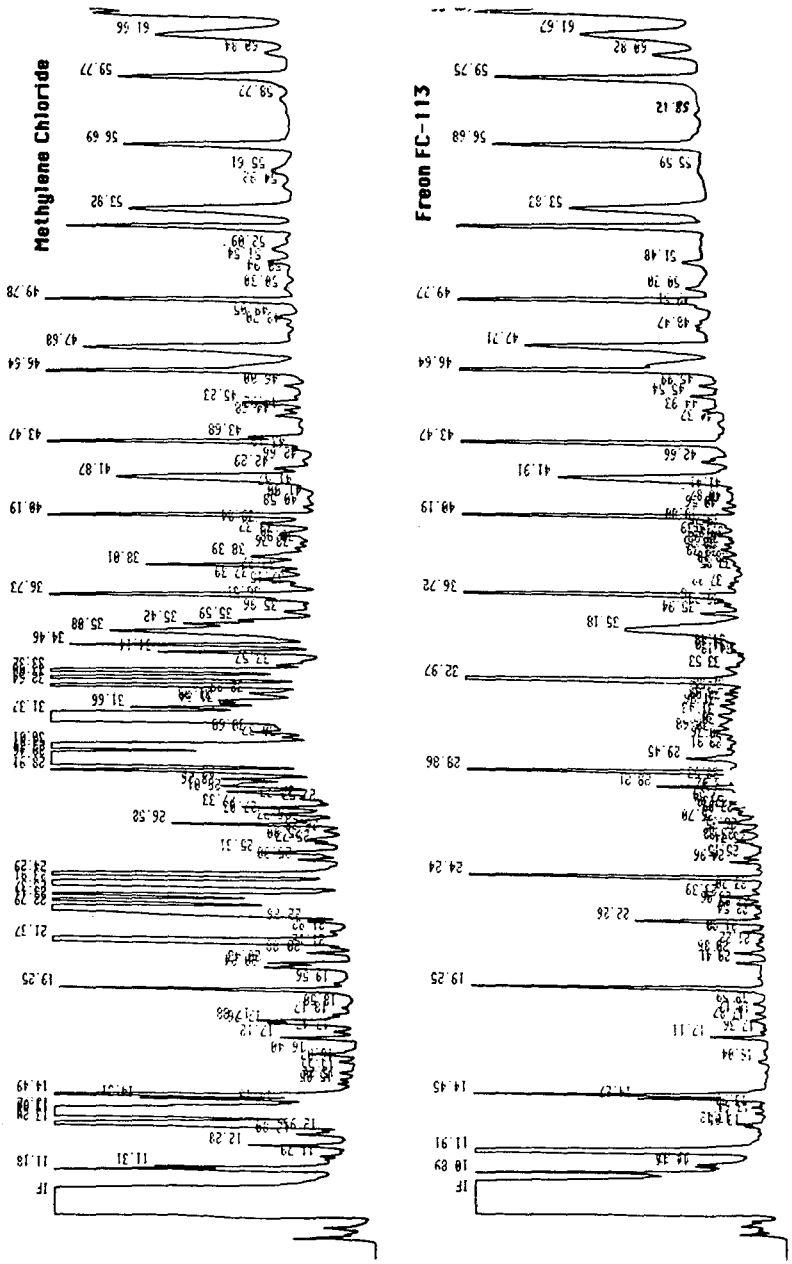

Fig. 6. Chromatograms of finished water extracts.

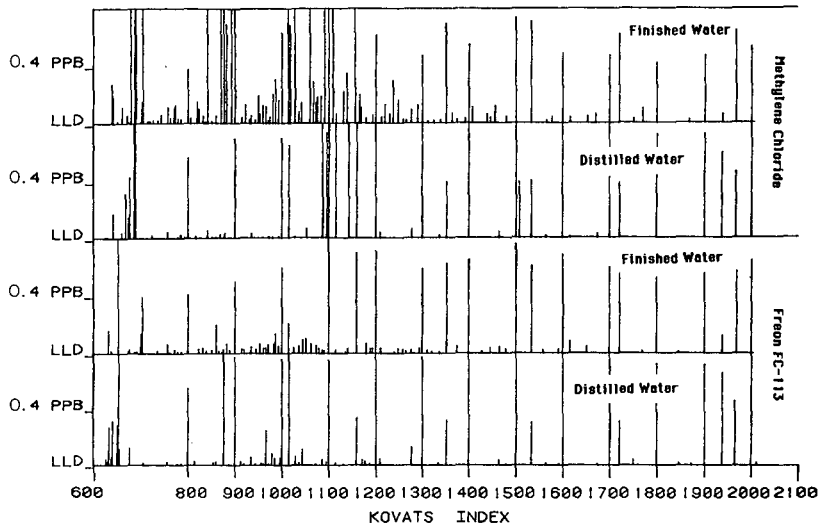

Fig. 7. Computer reconstructed chromatograms of the four extracts. ppb = parts per billion = μg/l (the American billion is 10^9). LLD = Lower limit of detection.

In addition to these impurities, other compound classes of organics were found to be present which originate from the water samples. These included:

(a) Haloforms originating from the reaction between chlorine and natural humic or industrial organic compounds. Trichloroacetone is an important intermediate in the haloform reaction[18] and has been observed in many extracts of chlorinated drinking water samples. Bromoform and chlorodibromomethane are specified as priority pollutants[19];

(b) Aromatic compounds (alkyl benzenes, naphthalene, methyl naphthalene and biphenyl). These compounds are commonly found in crude oil distillates such as gasoline and general organic solvents. Naphthalene is specified as a priority pollutant[19];

(c) Tetrachloroethylene is a degreasing agent and is considered a priority pollutant[19];

(d) Ethyl cinnamate is an ester used as fixative for perfumes and in glass prisms and lenses. Tributyl phosphate is used as plasticizer for cellulose esters, lacquers, plastics and vinyl resins;

(e) The remaining compounds represent a variety of aldehydes, esters, ketones, etc. The hazard of these chemicals at trace levels is unknown.

CONCLUSION

The comparative study of freon FC-113 and methylene chloride proved that FC-113 can be used to extract non-polar organic compounds (*e.g.*,. EPA method 625 compounds) from chlorinated drinking water samples. The use of FC-113 is safer, takes less time for evaporation and eliminates the cyclohexene problem associated with the methylene chloride extracts. Identification of more compounds in the FC-113 extracts which were masked by the cyclohexene derivatives in the methylene chloride extracts shows that FC-113 can be an alternative to methylene chloride.

ACKNOWLEDGEMENTS

This research was partially supported by the Microanalytical Center of Cairo University, Cairo, Egypt, Dr. A. B. Sakla Director and the New Jersey Department of Environmental Protection, Office of Research, Project Officer, Dr. Judy Lewis. The authors thank A. Abas and L. Brenner for their technical assistance during sample preparation and interpretation of GC–MS data.

REFERENCES

1 J. E. Longbottom and J. J. Lichtenberg (Editors), *Methods for Organic Chemical Analysis of Municipal and Industrial Wastewater*, U.S. Environmental Protection Agency, Cincinnati, OH, 1982.
2 E. D. Pellizzari, L. S. Sheldon, J. T. Bursey, L. C. Michael and R. A. Zweidinger, *Master Analytical Scheme for Organic Compounds in Water, Part I: Protocols*, U.S. Environmental Protection Agency, Athens, GA, 1984.
3 E. A. Ibrahim, R. L. Lippincott, L. Brenner, I. H. Suffet and R. E. Hannah, *J. Chromatogr.*, 393 (1987) 237–253.
4 *Chem. Eng. News*, 63 (19) (1985) 14.
5 *Chem. Eng. News*, 64 (48) (1986) 18.
6 P. L. Barlett, *Chemtech.*, June (1980) 354–355.
7 *EPA-400/1-87/00B Assessing the Risks of Trace Gases That Can Modify the Stratosphere*, Vol. 11, United States Environmental Protection Agency, Washington, DC, 1987, Ch. 1–5.
8 M. C. Goldberg, L. DeLong and M. Sinclair, *Anal. Chem.*, 45 (1973) 89–93.
9 C. Wu and I. H. Suffet, in *Water Pollution Assessment: Automatic Sampling and Measurement (ASTM STP 582)*, American Society for Testing and Materials, Philadelphia, PA, 1975, pp. 90–108.
10 C. Wu and I. H. Suffet, *Anal. Chem.*, 49 (1977) 231–237.
11 T. L. Yohe, I. H. Suffet and R. J. Grochowski, in C. E. Van Hall (Editor), *Measurement of Organic Pollutants in Water and Wastewater (ASTM STP 686)*, American Society for Testing and Materials, Philadelphia, PA, 1979, pp. 47–67.
12 T. L. Yohe, I. H. Suffet and J. T. Coyle, in M. J. McGuire and I. H. Suffet (Editors), *Activated Carbon Adsorption of Organics from the Aqueous Solution*, Vol. 2, Ann Arbor Science, Ann Arbor, MI, 1980, pp. 27–69.
13 T. L. Yohe, I. H. Suffet and P. R. Cairo, *J. Am. Water Works Assoc.*, 73 (1981) 402–410.
14 R. J. Baker, J. Gibs, A. K. Meng and I. H. Suffet, *Water Res.*, 21 (1987) 179–190.
15 R. J. Baker and I. H. Suffet, in I. H. Suffet and M. Malaiyandi (Editors), *Organic Pollutants in Water: Sampling, Analysis and Toxicity Testing*, American Chemical Society, Washington, DC, 1987, Ch. 27, pp. 572–591.
16 E. A. Ibrahim, I. H. Suffet and A. B. Sakla, *Anal. Chem.*, 59 (1987) 2091–2098.
17 I. H. Suffet and S. D. Faust, *J. Agric. Food Chem.*, 20 (1972) 52–56.
18 I. H. Suffet, L. Brenner and B. Silver, *Environ. Sci. Technol.*, 10 (1976) 1273–1275.
19 *EPA-440/4-79/029a Water-Related Environmental Fate of 129 Priority Pollutants*, Vol. 1, United States Environmental Protection Agency, Washington, DC, 1979.
20 C. D. Hodgman, R. C. Weast and S. M. Selby (Editors), *Handbook of Chemistry and Physics*, CRC Press, Cleveland, OH, 41st ed., 1960.
21 R. C. Weast, M. J. Astle and W. H. Beyer (Editors), *Handbook of Chemistry and Physics*, CRC Press, Boca Raton, FL, 64th ed., 1984.

Journal of Chromatography, 454 (1988) 233–242
Elsevier Science Publishers B.V., Amsterdam — Printed in The Netherlands

CHROM. 20 768

HIGH-PERFORMANCE LIQUID CHROMATOGRAPHIC METHOD FOR DETERMINING TRIAZINE HERBICIDE RESIDUES IN SOIL

MASSIMO BATTISTA, ANTONIO DI CORCIA* and MARCELLO MARCHETTI
Dipartimento di Chimica, Università "La Sapienza" di Roma, Piazzale Aldo Moro 5, 00185 Rome (Italy)
(Received July 2nd, 1988)

SUMMARY

The extraction of eight triazines from soil and their isolation from the soil extract were simultaneously performed using two mini-columns connected in series, one containing the soil sample and the other filled with a strong acid exchanger. By allowing 3 ml of acetone to flow along the two cartridges in tandem, triazines were removed from the soil particles and then selectively readsorbed via salt formation on the exchanger surface. After disconnecting the two cartridges, the triazines were eluted from the exchanger trap by potassium chloride-saturated methanol. This procedure was also adopted to desorb from the soil surface residual amounts of chemically adsorbed triazines, which acetone is unable to remove. After removal of methanol from the two combined eluates, the triazines were fractionated and quantified by reversed-phase high-performance liquid chromatography with UV detection at 220 nm. Using this procedure, the recoveries of triazines were greater than 90% and independent of the triazine concentration, the type of soil samples and their ageing on storage. The mean limit of detection was about 1 ng/g in soil. The results obtained were compared with those obtained by two techniques of known efficiency (reflux extraction and Soxhlet extraction). Some effects on the adsorption of triazines of the type of soil and its ageing on storage are discussed.

INTRODUCTION

Since their introduction around 1960, triazine derivatives have become widely used in agriculture as selective herbicides and, consequently, they can give rise to residues in soil. Methods for the determination of triazine herbicides in soil are important from both agricultural[1,2] and environmental[3,4] points of view. A wide variety of solvents have been used for the extraction of triazines from soil[5–8], including agitation of the soil and a solvent for various periods of time at various temperatures, sonication and Soxhlet extraction. Clean-up procedures are generally needed for most soil types in order to attain a satisfactory limit of detection, such as 20 ng/g. However, these procedures are invariably tedious, time consuming, not highly selective and require excessive manipulation of the sample.

Triazine derivatives are very weakly basic compounds with pK_b values ranging

0021-9673/88/$03.50

between 10 and 12, depending on the nature of the substituent. It has been shown[9] that, under strictly anydrous conditions, very weakly basic compounds can be adsorbed on a strong acid exchanger via salt formation.

This paper describes an original, simple and rapid procedure for accurately determining trace amounts of eight triazines in soil samples.

The extraction and isolation of triazines were simultaneously performed by connecting two mini-columns in tandem, the upper column being packed with soil and the lower column with a sulphonic acid-type silica-based cation exchanger (SCX). Solvent percolation through a soil column is a technique already performed with success by Mangani *et al.*[10] for the extraction of chlorinated pesticides from soil. Subfractionation and quantitation of triazines were performed by high-performance liquid chromatography (HPLC) with UV detection at 220 nm.

EXPERIMENTAL

Reagents

Authentic triazine derivatives were obtained from Supelco (Bellefonte, PA, U.S.A.) as follows: 2-chloro-4,6-bis-ethylamino-*s*-triazine (simazine), 2,4-bis-ethylamino-6-methylthio-*s*-triazine (simetryn), 2-chloro-4-ethylamino-6-isopropylamino-*s*-triazine (atrazine), 2,4-bis-isopropylamino-6-methoxy-*s*-triazine (prometon), 2-isopropylamino-4-ethylamino-6-methylthio-*s*-triazine (ametryn), 2-chloro-4,6-bis-isopropylamino-*s*-triazine (propazine), 2,4-bis-isopropylamino-6-methylthio-*s*-triazine (prometryn) and 2-ethylamino-4-*tert*.-butylamino-6-methylthio-*s*-triazine (terbutryn). The pK_a values of chlorotriazines are *ca.* 2 and those of the other triazines considered are *ca.* 4[11]. A standard solution was prepared by dissolving 100 mg/l of each herbicide in acetone. This solution was further diluted to obtain a working standard solution of 10 mg/l.

For HPLC, distilled water was further purified by passing it through a Norganic cartridge (Millipore, Bedford, MA, U.S.A.). Acetonitrile was of HPLC grade from Carlo Erba (Milan, Italy). All other solvents were of analytical-reagent grade (Carlo Erba) and were used as supplied.

Sample preparation

Soil samples were taken from three different sites located in Italy. The soils were chosen on the basis of differences in physical characteristics (Table I). Moisture was eliminated by heating at 80°C. Soil was ground and sieved to obtain a particle size range between 120 and 270 mesh. Herbicide-fortified soil samples were prepared in a manner similar to that reported elsewhere[10,12]. To a known amount of soil in a flat dish, an appropriate volume of the working, standard solution containing herbicides was added. Additional acetone was added until the solvent completely covered the soil particles. The bulk of the solvent was slowly evaporated at room temperature so that the soil particles became a slush-like mass, which was then stirred thoroughly with a spatula until the material appeared dry. Soil was resieved to maintain the required mesh range and stored in glass containers at room temperature until analysed.

TABLE I

PHYSICAL AND CHEMICAL CHARACTERISTICS OF THE SOILS USED IN THE RECOVERY EXPERIMENTS

Soil No.	*Clay (%)*	*Silt (%)*	*Sand (%)*	*pH*	*Organic matter (%)*
1	26	60	14	8.1	2.1
2	39	38	24	5.9	1.9
3	12	2.1	86	7.5	4.2

Apparatus

Percolation of solvents through the cartridges was carried out using a vacuum manifold with a water pump. Both soil and the cation exchanger were packed in cylindrical polypropylene tubes (6 cm × 0.9 cm I.D.) (Supelco). They were one quarter filled with 1 g of soil, taking care to vibrate the tube in order to avoid loose packing of soil particles. Polyethylene frits (Supelco) were located above and below the soil column to hold minute particles in place and keep the column intact.

The SCX cartridge was prepared in the same way with 1 g of the exchanger material having a particle size range between 200 and 400 mesh (Supelco). Before use, this material was washed with 4 ml of 0.12 mol/l hydrochloric acid in methanol at a flow-rate of about 1 ml/min, followed by 3 ml of methanol and 3 ml of acetone. Washing of the cartridge was stopped when the level of acetone was about 2 cm higher than the SCX bed.

The two cartridges, one containing soil and the other the exchanger material, were then connected in series through an adapter (Supelco) and inserted in the vacuum system. Acetone (3 ml) was allowed to percolate through the soil bed at a flow-rate of 0.8 ml/min to desorb the triazine herbicides, which were readsorbed on the SCX column as the soil extract passed along the second tube. After this, the two cartridges were disconnected and the residual amount of triazine herbicides was extracted from the soil column by passing through it 3 ml of potassium chloride-saturated methanol, which were collected separately. After washing the SCX cartridge with 2 ml of acetone, the herbicides were eluted with 2.5 ml of potassium chloride-saturated methanol at a flow-rate of 0.8 ml/min into the same glass tube containing the methanolic soil extract. Before removal of the solvent, 200 μl of a methanolic solution of ammonia (0.1 mol/l) were added to this solution to neutralize the acidity, which causes some decomposition of chlorotriazines. Methanol was removed at 32°C under a stream of nitrogen and the residue was reconstituted with 100 μl of the mobile phase for HPLC. A 50-μl volume of this solution was injected into the HPLC apparatus.

HPLC apparatus

A Model 5000 liquid chromatograph (Varian, Walnut Creek, CA, U.S.A.) equipped with a Rheodyne Model 7125 injector having a 50-μl loop and with a Model 2050 UV detector (Varian) was used. A 25 cm × 4.6 mm I.D. column filled with 5-μm (average particle size) LC-18-DB reversed-phase packing and a guard column containing Pelliguard (both from Supelco) were used. The mobile phase was acetonitrile–phosphate buffer (10 mmol/l; pH 6.7) (38:62, v/v) and the flow-rate was 1.5 ml/min. Triazines were monitored with the detector set at 220 nm.

The concentrations of the herbicides in soil samples were calculated by comparing the heights of the peaks obtained with the sample and with a standard solution. The latter was prepared by adding an appropriate volume of the herbicide working standard solution to 5 ml of potassium-chloride-saturated methanol, by eliminating the solvent and dissolving the residue in 100 μl of the HPLC mobile phase.

RESULTS AND DISCUSSION

Recovery studies

The abilities of various organic solvents to extract triazine herbicides quantitatively from a soil column were evaluated. These experiments were performed by adding herbicides directly to the top of the soil column and allowing the solvent to be removed by vacuum. In Table II, recovery data for some selected solvents are reported.

Several mechanisms or combination of mechanisms can be postulated for the adsorption of organic basic compounds by aluminosilicates of the soil particulates. These include physical adsorption, hydrogen bonding, coordination complexes and chemical adsorption. The soil can be considered as a natural "direct phase" whose surface is contaminated to varying extents by chemical groups which may give rise to strong, anomalous adsorption depending on the nature of the adsorbate and the chemical characteristics of the soil. Therefore, it is not surprising that chloroform is unable to desorb relatively polar compounds, such as triazine derivatives, quantitatively from the soil bed. From the results obtained, acetone and methanol appeared to be of comparable value in extracting herbicides from a freshly contaminated soil surface. However, when a soil cartridge was connected in series with that containing the ion exchanger and the extracting solvent flowed down from the first cartridge directly into the second, about a 40 % loss of chlorotriazines occurred when methanol

TABLE II

RECOVERIES OF TRIAZINES USING DIFFERENT EXTRACTION SOLVENTS

Herbicide concentrations: 200 ng/g each.

Triazine	*Recovery (%)**								
	Chloroform			*Acetone*			*Methanol*		
	*I***	*II***	*III***	*I***	*II***	*III***	*I***	*II***	*III***
Simazine	30	23	3	63	27	3	66	26	2
Simetryn	28	25	2	63	28	2	64	27	2
Atrazine	30	25	2	64	26	3	63	27	2
Prometon	27	27	1	65	34	–	67	31	–
Ametryn	26	25	3	63	30	2	64	29	1
Propazine	28	24	2	63	29	1	63	30	2
Prometryn	25	23	2	63	33	1	64	31	1
Terbutryn	25	23	2	64	32	–	63	31	1

* Mean values obtained from duplicate determinations.

** Fractions I–III consisted of 1-ml aliquots of the solvent considered (chloroform, acetone or methanol).

TABLE III

RECOVERIES OF TRIAZINES FROM DIFFERENT SOIL TYPES

Herbicide concentrations: 50 ng/g each.

Triazine	*Recovery (%)**			
	Soil 1: acetone (3 ml)	*Soil 2: acetone (3 ml)*	*Soil 3***	
			Acetone (6 ml)	*Methanol (3 ml)*
Simazine	93	92	75	17 (92)***
Simetryn	93	94	73	16 (89)
Atrazine	92	93	72	19 (91)
Prometon	99	98	84	13 (97)
Ametryn	92	93	83	9 (92)
Propazine	94	93	82	11 (93)
Prometryn	97	96	86	9 (95)
Terbutryn	97	96	85	9 (94)

* Mean values obtained from triplicate measurements.
** Methanol was passed through the soil bed after passage of acetone.
*** Overall recoveries.

was used instead of acetone. Competition of methanol with very weakly basic compounds for binding on exchange sites may be responsible for this loss, as this solvent is able to form a stable hydrogen bond with strong acids.

It has been found that the recovery of atrazine can vary with the soil type[13,14]. With the view of assessing the extent to which the matrix effect could affect the extraction of the eight triazines studied, recovery studies were performed for soil samples with various physical and chemical characteristics (see Table I). Herbicide-fortified soils were prepared as described under Experimental. The results are reported in Table III. A 3-ml volume of acetone failed to elute quantitatively triazines adsorbed on sample soil 3. No further increase in the recovery of herbicides was achieved even by doubling the volume of acetone passing through the soil bed. The residual amount of triazines still remaining adsorbed on soil sample 3 could be removed by methanol.

Various hypotheses have been put forward to explain the recovery of triazines from different soil types. Hayes[15] noted that the clay content of soils could have a considerable influence on the adsorption of triazines in instances where the organic carbon contents of the soils were less than 5%. A high permanent negative charge was considered to be responsible for lower recoveries of hydroxytriazines[16]. With our samples the opposite was true, as anomalies in the adsorption of triazines were found just in the soil type having the lowest clay content and the largest amount of organic matter. Probably, the particular chemical nature of the clay mineral, more than its relative content, influences the mechanism of adsorption of triazine herbicides, as found by Knight and Tomlinson[17] for the adsorption of paraquat on soil. That methanol is able to remove the fraction of triazines remaining adsorbed after extraction with acetone can be then explained assuming that, compared with the other two soil types considered, soil sample 3 has particular and/or easily accessible adsorption sites which are able to establish strong, specific interactions, *e.g.*, hydrogen bonding, with triazines.

The extractable atrazine content of soil has been found to decrease with ageing of samples stored at room temperature[18,19]. This loss was traced to either slow degradation of atrazine or a tighter association of the atrazine with the soil components during storage, so that the extraction system failed to remove it completely from the soil.

Analogous experiments were performed on soil sample 3, which was fortified with the eight herbicides studied and stored in a screw-capped glass jar at 20°C for 3 months. Recovery data are given in Table IV. As can be seen, the extraction method with acetone followed by methanol, which effectively removed triazines from soil samples after about 1–3 days following their deposition, showed some difficulty in desorbing triazines, particularly simetryn, from a 3-months aged soil sample. The reason for this effect is not clear to us. It seems that the mode of adsorption of triazines turns slowly from physical to chemical adsorption. It may be that basic compounds adsorbed on the silicate surface, even in the absence of an effective means of movement, such as water, migrate slowly from certain adsorption sites to ion-exchange sites where they are chemisorbed via salt formation. This supposition may account for the fact that the extractable triazine content of a soil sample aged on storage increases when an effective organic cation displacer, such as potassium ion, is added to the methanol. If this mechanism of adsorption of triazines takes place even on actually contaminated soils, it follows that the extraction method developed by us is certainly more effective than other, conventional procedures proposed for measuring triazine herbicide content in agricultural samples.

Whatever the mechanism of adsorption, potassium chloride-saturated methanol was able to elute triazines from the soil column. However, using this solvent system alone obviously precluded any possibility of purifying the extract using an ion exchanger. The best compromise was to pass acetone through the soil bed first, in order to remove neutral and acidic compounds together with triazines, followed by potassium chloride-saturated methanol to elute residues of herbicides chemically bound to the soil surface. The former extract also passed through the SCX column,

TABLE IV

RECOVERIES OF TRIAZINES AFTER 3 MONTHS OF SOIL AGEING

Herbicide concentration: 50 ng/g each.

Triazine	*Recovery (%)**	
	Methanol following acetone	*KCl-saturated methanol following acetone*
Simazine	81	93
Simetryn	74	92
Atrazine	83	93
Prometon	87	97
Ametryn	84	92
Propazine	85	94
Prometryn	88	95
Terbutryn	88	95

* Mean values obtained from triplicate measurements.

which was bypassed by the latter. The potassium chloride-saturated methanol fractions from both the soil and SCX columns were then combined and submitted to the solvent removal step.

The effectiveness of the extraction procedure was compared with those obtained by following two other proposed extraction methods. The first procedure involves extraction with water–acetonitrile (10:90, v/v) by refluxing for 1 h[20] and the second procedure was Soxhlet extraction with methanol for 24 h[21]. For these experiments, soil sample 3 was selected and spiked with triazines at individual concentrations of 200 ng/g. At this high contamination level, it was unnecessary to apply clean-up steps. Recovery data are reported in Table V. It can be seen that the water–acetonitrile reflux procedure gave poorer recoveries than those obtained by our method. Moreover, the recovery of atrazine obtained by us using acetonitrile extraction was in good agreement with that obtained by Vermeulen *et al.*[13].

In comparison with data reported by Xu *et al.*[21], unexpectedly low recoveries of chlorotriazines (simazine, atrazine and propazine) were obtained by us using the 24-h Soxhlet extraction from soil sample 3. Reducing the extraction time to 3 h increased the recovery of the chlorotriazines considerably. Moreover, no significant loss of chlorotriazines occurred by Soxhlet extracting them from the other two soil types considered for 24 h. These results suggest that, on 24-h repeated treatment with hot methanol, some strongly adsorbed, unknown components present in particular soil types can be co-extracted and slowly react with chlorotriazines in hot methanol.

Precision

The analytical recovery and the precision of the method at high and low triazine contents of soil samples were assessed by extracting a spiked composite soil sample (Table VI). The recovery of triazines was unaffected by their concentrations in soil, confirming that no procedural loss occurred.

TABLE V

RECOVERIES OF TRIAZINES FROM SOIL BY THE PROPOSED METHOD COMPARED WITH TWO OTHER EXTRACTION METHODS

Herbicide concentrations: 200 ng/g each.

Triazine	*Recovery (%)**		
	19	*20*	*This method*
Simazine	77	46	92
Simetryn	74	76	92
Atrazine	75	43	91
Peometon	84	90	98
Ametryn	76	83	93
Propazine	78	47	93
Prometryn	79	77	96
Terbutryn	80	75	95

* Mean values obtained from triplicate measurements.

TABLE VI

ACCURACY AND PRECISION OF THE METHOD WITH HIGH AND LOW TRIAZINE CONTENTS IN SOIL SAMPLES

Triazine	*Recovery ± S.D.* (%)*	
	400 ng/g	*10 ng/g*
Simazine	92.3 ± 1.6	91.8 ± 3.1
Simetryn	93.2 ± 1.9	91.9 ± 5.0
Atrazine	91.5 ± 1.8	92.6 ± 3.2
Prometon	97.4 ± 1.5	98.1 ± 2.4
Ametryn	94.1 ± 1.8	94.0 ± 2.8
Propazine	92.6 ± 2.0	91.8 ± 3.4
Prometryn	95.3 ± 1.7	94.1 ± 3.9
Terbutryn	96.8 ± 1.9	94.0 ± 3.7

* Standard deviation calculated from six determinations.

Limits of detection

Under the chromatographic conditions selected, the limits of detection (signal-to noise ratio = 3) varied from 0.8 to 3 ng/g in soil, respectively, for simazine and terbutryn, which are the first and last compounds, respectively, to be eluted from the HPLC column. For the more retained herbicides, these limits could be further decreased by using gradient elution for HPLC fractionation. However, isocratic elution was used for simplicity and economy. With this method, the mobile phase could be recycled at least three times without appreciable changes in the retention times of the analytes considered or the sensitivity.

Fig. 1 shows a typical chromatogram obtained by this procedure. It must be pointed out that, except for the compounds under consideration, most of the peaks were for unknown substances released by the plastic tubes used to pack both the soil and the ion exchanger. However, none of these extraneous compounds interfered with the analysis.

Activation and re-usability of the SCX cartridge

When the acetone extract of soil was passed through the untreated exchanger bed, 20% of each chlorotriazine was unaccounted for in the acetone effluent. This effect was traced to the presence of residual water still present in soil samples after drying. Water being removed by acetone was able to compete with chlorotriazines for binding on the exchange sites chemically bonded to the silica surface. This loss of chlorotriazines was eliminated by an acidic washing of the SCX cartridge prior to its use. Probably this washing increased the retention of chlorotriazines by replacing with H^+ ions inorganic cations that are unable to establish sufficiently strong interactions with very weakly basic compounds.

The reusability of the SCX cartridge was investigated by making repeated extractions of herbicides from 1-g aliquots of soil. After each extraction, the exchanger bed was restored by passing 10 ml of 0.12 mol/l hydrochloric acid in methanol, followed by 3 ml of methanol and 3 ml of acetone, at flow-rates of about 1.5 ml/min. Only after ten such extractions was a slight loss of chlorotriazines observed.

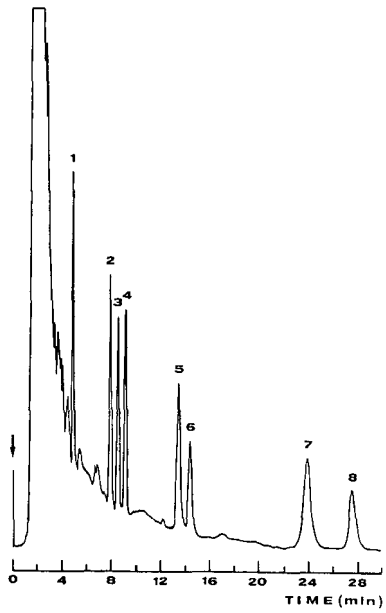

Fig. 1. Chromatogram obtained for 1 g of soil spiked with 10 ng of each herbicide: 1 = simazine; 2 = simetryn; 3 = atrazine; 4 = prometon; 5 = ametryn; 6 = propazine; 7 = prometryn; 8 = terbutryn.

Analytical variables

The influence that the flow-rate at which solvents passing through both the soil and the SCX columns could have on the recovery of triazines was evaluated. Some loss of triazines was observed only when acetone was passed through the two cartridges at flow-rates higher than 1 ml/min. The same effect was observed when the flow-rate of potassium chloride-saturated methanol passing through the soil bed was varied. Less critical was the flow-rate at which the potassium chloride-saturated methanol was passed through the SCX bed to displace triazines. No loss of triazines was observed even at a flow-rate of 1.5 ml/min.

As described under Experimental, the SCX tube was partially filled with acetone before connecting the two cartridges in series. When this precaution was not followed, the initial non-steady-state condition caused the very first drops of acetone flowing from the soil column to be passed too rapidly along the SCX column, which resulted in a loss of chlorotriazines.

REFERENCES

1 R. Frank, *Weeds*, 14 (1966) 82.
2 G. J. Sirons, R. Frank and T. J. Sawyer, *J. Agric. Food Chem.*, 21 (1973) 1016.
3 R. Frank, G. J. Sirons and B. D. Ripley, *Pestic. Monit. J.*, 13 (1979) 120.
4 M. D. Erickson, C. W. Frank, D. P. Morgan, *J. Agric. Food Chem.*, 27 (1979) 140.
5 E. Knusli, H. P. Burchfield and E. E. Storrs, in G. Zweig (Editor), *Analytical Methods for Pesticides, Plant Growth Regulators, and Food Additives*, Vol. IV, Academic Press, New York, 1964, p. 44.
6 C. A. Benfield and E. D. Chillwell, *Analyst (London)*, 89 (1964) 475.
7 T. J. Sheets and P. C. Kearny, *Weed Soc. Am. Abstr.*, (1964) 10.

8 A. Ambros, J. Lantos, E. Visi, I. Csatlos and L. Sarvari, *J. Assoc. Off. Anal. Chem.*, 164 (1981) 733.
9 J. E. Gordon, *J. Chromatogr.*, 18 (1965) 542.
10 F. Mangani, G. Crescentini and F. Bruner, *Anal. Chem.*, 53 (1981) 1627.
11 J. B. Weber, *Spectrochim. Acta, Part A*, 23 (1967) 458.
12 H. B. Lee and A. S. Y. Chom, *J. Assoc. Off. Anal. Chem.*, 66 (1983) 1322.
13 N. M. J. Vermeulen, Z. Apostolides, D. J. J. Potgieter, P. C. Nel and N. S. H. Smit, *J. Chromatogr.*, 240 (1982) 247.
14 D. C. G. Muir and B. E. Baker, *J. Agric. Food Chem.*, 26 (1978) 420.
15 M. H. B. Hayes, *Residue Rev.*, 32 (1970) 132.
16 K. P. Goswaml and R. E. Gree, *Soil Sci. Soc. Am. Proc.*, 37 (1973) 702.
17 R. M. Knight and W. F. Tomlinson, *J. Soil Sci.*, 18 (1967) 233.
18 D. J. Swain, *J. Agric. Food Chem.*, 27 (1979) 915.
19 L. A. Birk and F. E. B. Roadhouse, *Can. J. Plant Sci.*, 44 (1964) 21.
20 A. M. Mattson, R. A. Kabrs and R. T. Murphy, *Residue Rev.*, 32 (1970) 371.
21 Y. Xu, W. Lorenz, G. Pfister, M. Bahadir and F. Korte, *Fresenius' Z. Anal. Chem.*, 325 (1986) 377.

Journal of Chromatography, 454 (1988) 243–251
Elsevier Science Publishers B.V., Amsterdam — Printed in The Netherlands

CHROM. 20 762

PHASE-SYSTEM SWITCHING AS AN ON-LINE SAMPLE PRETREATMENT IN THE BIOANALYSIS OF MITOMYCIN C USING SUPERCRITICAL FLUID CHROMATOGRAPHY

W. M. A. NIESSEN*, P. J. M. BERGERS, U. R. TJADEN and J. VAN DER GREEF
Division of Analytical Chemistry, Center for Bio-Pharmaceutical Sciences, Gorlaeus Laboratories, Leiden University, P.O. Box 9502, 2300 RA Leiden (The Netherlands)
(First received May 5th, 1988; revised manuscript received June 24th, 1988)

SUMMARY

One of the problems of the application of supercritical fluid chromatography (SFC) in bioanalysis is the fact that many sample pretreatment procedures deliver the solutes of interest in a polar solvent, which upon injection will dramatically disturb the phase system characteristics of the SFC system. The phase-system switching approach, recently introduced for liquid chromatography—mass spectrometry, can be used to avoid this problem. Plasma samples containing the thermolabile and pH-sensitive cytostatic drug Mitomycin C (MMC) were injected onto a short precolumn. After washing and drying of the precolumn the compound of interest was desorbed using a supercritical fluid and analyzed by SFC. Up to 1 ml of plasma containing 20 ng of MMC has been analyzed in this way.

INTRODUCTION

Supercritical fluid chromatography (SFC) is a powerful tool for solving analytical problems in various areas. The perspectives of SFC have been discussed in several excellent reviews[1–5]. Our interest in SFC lies in its potential to solve some of the challenging problems in bioanalysis, for SFC has several attractive features. Being complementary to gas chromatography (GC) and liquid chromatography (LC), SFC broadens the field of chromatography. Several applications indicating the bioanalytical potential of SFC have been described, *e.g.*, refs. 6–9. The possibilities of open-capillary columns in SFC, *i.e.*, very high efficiencies, which are useful in difficult separations for instance of enantiomeric compounds[10], the use of sensitive and selective GC detectors such as the nitrogen–phosphorus detector[11] and the ease of coupling with a mass spectrometer[4], have all been demonstrated with compounds of biological and pharmaceutical origins. Interesting features of packed columns in SFC are the possibility to perform rapid separations with moderate efficiencies[2], and the use of powerful LC detectors, such as UV absorbance and fluorescence. An important advantage of packed columns over open-capillary columns is the higher sample loadability of the former.

0021-9673/88/$03.50

Before SFC can be successfully applied in bioanalysis some additional analytical technology has to be developed. An important aspect of bioanalysis is the selection of an appropriate sample pretreatment. Many procedures are based either on liquid–liquid extractions or on liquid–solid isolations. Especially in bioanalysis, the solutes will be reconstituted in relatively polar solvents after these pretreatment procedures. In SFC the direct injection of such a solution may disturb the chromatographic system dramatically, considering the strong influence of small percentages of organic modifier on the retention characteristics in SFC[6]. Therefore, a new approach has been developed in our laboratory. In order to avoid the injection of polar solvents in the SFC system the phase-system switching (PSS) approach, which was originally developed for liquid chromatography–mass spectrometry[12,13], has been adopted and applied in SFC. The aqueous sample, *e.g.*, plasma is pumped through a small precolumn containing an hydrophobic adsorbent. Then the precolumn is washed with water in order to remove hydrophilic compounds and subsequently dried with a stream of nitrogen in order to remove the polar solvent. Desorption of the analytes and transfer to the separation column is performed using a supercritical fluid, which is also used for the chromatographic separation. In this way the introduction of polar solvents into the SFC system can be avoided. An additional perspective of this approach lies in the possibility to combine the phase-system switching step with an on-line sample pretreatment based on liquid–solid extraction. The potential of this approach is demonstrated by the bioanalysis of the anti-cancer drug Mitomycin C (MMC)[14,15] in human plasma. For the analysis of MMC in biological fluids and tissue homogenates a fully automated system based on the use of a dialysis membrane, a short concentration column and an HPLC separation has been described[15]. In the present investigations MMC is merely used as a test compound, particularly because it is thermally labile and is degraded in solutions of both low and high pH[14].

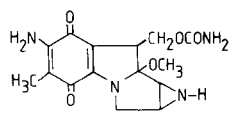

The sample pretreatment system described here shows some similarities with supercritical fluid extraction (SFE). Various examples have been reported of the use of supercritical fluid extraction of solids in combination with chromatographic techniques, either high-performance liquid chromatography (HPLC)[16], GC[17] or SFC[18,19]. However, in these cases the solid samples to be analyzed are extracted directly with the supercritical fluid, and the compounds of interest are transferred to the appropriate chromatographic technique, while in the PSS system described here the compounds of interest are chromatographically retained on a solid phase material and desorbed with a supercritical fluid.

This paper describes the analysis of Mitomycin C in plasma samples and the development of the phase-system switching technique; a comparison has been made between off-line and on-line sample pretreatment.

EXPERIMENTAL

Equipment

The supercritical fluid chromatograph used was constructed from various, in most cases commercially available, components, some of which were slightly modified. A schematic diagram of the system is given in Fig. 1. The system consisted of a MWG Lauda K2R Cooling Unit (Beun de Ronde, Amsterdam, The Netherlands), a Model 2150 reciprocating HPLC pump (LKB, Bromma, Sweden), a syringe pump (BrownLee, Santa Clara, CA, U.S.A.), a MUST valve-switching unit (Spark Holland, Emmen, The Netherlands), a Constametric III reciprocating pump (Milton Roy, Riviera Beach, FL, U.S.A.), a Model 7125 injection valve (Rheodyne, Berkeley, CA, U.S.A.), a Fractovap 2101 system, which was used as a column oven (Carlo Erba, Milan, Italy), a Spectroflow 757 UV detector (ABI Kratos, Ramsey, NJ, U.S.A.) equipped with an ABI Kratos high-pressure flow cell (Brownlee Scientific) and a Type BD40 recorder (Kipp & Zn., Delft, The Netherlands).

The Model 2150 reciprocating pump was used for the delivery of the supercritical mobile phase. It was modified by replacing the PTFE inlet capillaries of the

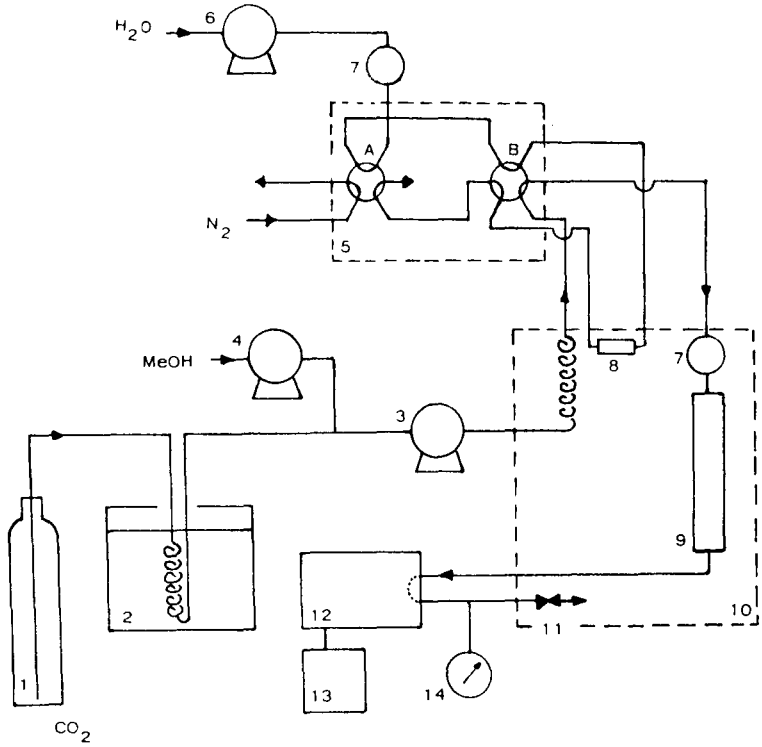

Fig. 1. Schematic diagram of the equipment used in the PSS-SFC experiments. For details see text. 1 = Carbon dioxide cylinder; 2 = cooling unit; 3 = modified reciprocating pump; 4 = syringe pump; 5 = valve switching unit; 6 = reciprocating pump; 7 = rheodyne injection valve; 8 = precolumn; 9 = analytical column; 10 = GC oven; 11 = back-pressure regulator; 12 = UV detector; 13 = recorder; 14 = manometer. MeOH = Methanol.

pump with stainless-steel capillaries, and by adding a brass water-jacket around the pump heads, through which was pumped 20% ethyleneglycol in water at −5°C. The syringe pump was used for the addition of methanol to the carbon dioxide. The third pump was used for sampling and washing the precolumn in the PSS system.

A flow-rate of 2 ml/min was used in all experiments. UV detection was done at the wavelength of maximum absorbance of MMC (in methanol) at 360 nm. Other components of the system were a carbon dioxide cylinder with a siphon tube (Hoekloos, Amsterdam, The Netherlands), a line filter (0.5 μm; Nupro, Willoughby, OH, U.S.A.) at the outlet of the carbon dioxide cylinder, a Rosil C_{18} analytical column (150 mm × 4.6 mm I.D.) (Alltech, Deerfield, IL, U.S.A.), a Nupro Model SS-SS1-A fine-metering valve used as a back-pressure regulator and a Bourdon-type pressure gauge. The precolumn (10 mm × 3.2 mm I.D.) was laboratory-made and hand-packed with the stationary phase material, which was enclosed between two frits.

Materials

The column used in the SFC experiments was 150 mm × 4.6 mm I.D. packed with 5-μm Rosil C_{18} material (Alltech). Similar columns packed with other materials (silica, NH_2, C_8) were also tested.

Carbon dioxide was of technical grade (grade 2.5). Analytical grade methanol from J. T. Baker Chemicals (Deventer, The Netherlands) was filtered over a 0.45-μm membrane filter (Sartorius, Göttingen, F.R.G.) before use. The water was purified using a Milli Q Water Purification System (Millipore, Bedford, MA, U.S.A.). XAD-2 (150–200 μm) was obtained from Serva (Heidelberg, F.R.G.) and Polygosil C_{18} (40–63 μm) from Macherey-Nagel (Düren, F.R.G.). Mitomycin C was from Kyowa Hakko Kogyo (Tokyo, Japan). Pooled human plasma was used, centrifuged at 1000 *g* for 10 min before injection.

RESULTS AND DISCUSSION

SFC of Mitomycin C

The behaviour of MMC in SFC has not been studied previously. In order to evaluate the chromatography of MMC under SFC conditions, various experimental parameters were varied.

Several column materials have been tested. The best results were obtained with a C_{18} stationary phase. The other materials tested were silica, aminopropyl- and octyl-silica. With the C_8 material poor peak shapes of MMC were observed, while with silica and aminopropyl material no peaks of MMC were detected, indicating a capacity factor above 25.

No elution of MMC was observed from a packed C_{18} column when pure carbon dioxide was used as the mobile phase. At least 5% methanol must be added to the carbon dioxide as a modifier in order to obtain capacity factors below 10 (at 30-MPa and 60°C). The influence of the percentage of methanol in the mobile phase on the capacity factor has been investigated at a constant back-pressure of 30 MPa. The results are given in Fig. 2. The influence of the modifier content of the mobile phase is dramatic. The capacity factor decreases fromn a value of 27 at 2.5% methanol to a value of 1 at 10% methanol. At a constant percentage of methanol added to the mobile phase the back-pressure also has some influence on the capacity factor of

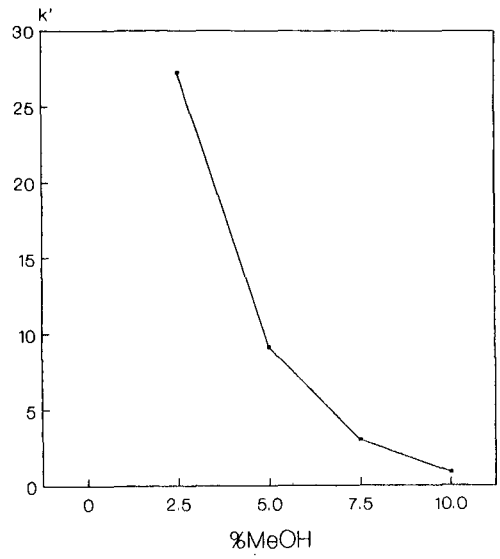

Fig. 2. Capacity factor (k') of MMC as a function of the percentage of methanol in the mobile phase. Conditions: C_{18} column (150 mm × 4.6 mm I.D., 5 μm); back-pressure 30 MPa; flow-rate 2.0 ml/min; oven temperature 50°C; UV detection at 360 nm.

MMC. However, this influence is less dramatic than the influence of the modifier content. This is in agreement with published data for other compounds, *e.g.*, see ref. 6. With 10% methanol in the mobile phase and a temperature of 50°C the capacity factor decreases from 1.6 at 18 MPa to 0.8 at 33 MPa. Variation of the temperature does not result in significant changes as far as the retention characteristics are concerned. However, due to thermal degradation of the MMC, the peak heights and peak areas decrease rapidly at temperatures above 60°C.

As seen from the typical MMC chromatogram in Fig. 3a, the peak of MMC suffers from tailing. At first sight, this may be due to the interaction of MMC with the free silanol groups at the surface of the stationary phase. Similar effects have been reported by others[20] with highly polar compounds. However, with 12% methanol present in the mobile phase such an interaction is not expected.

In most of the experiments described in this paper, 12% methanol was used at a column temperature of 50–60°C at a back-pressure of 28–30 MPa. Under these optimized conditions a calibration plot for MMC in SFC analysis was obtained, which was linear over at least two decades from 10 to 500 ng per injection. The detection limit based on a signal-to-noise ratio of 3 was calculated to be 0.4 ng, which compares well with the detection limit of 0.25 ng found in HPLC[15].

Off-line sample pretreatment

Two off-line sample pretreatment procedures have been tested. The first procedure consists of the denaturation of proteins by methanol and centrifugation of the samples (10 min at 1000 *g*). The 5-μl injections of the supernatant in the SFC system resulted in pressure fluctuations in the system and an unstable UV signal. Therefore, a more elaborate procedure based on liquid–solid isolation was tested[21]. The procedure

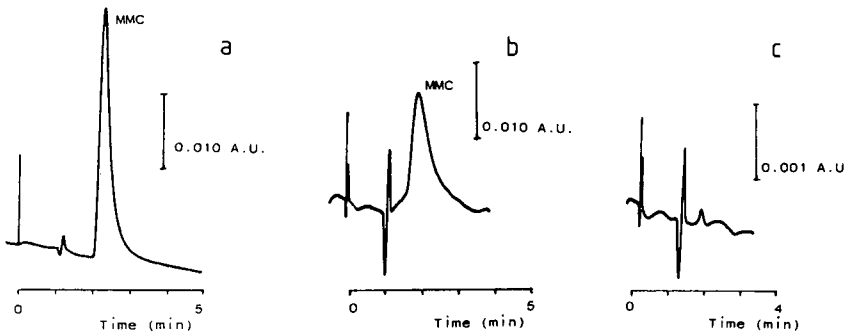

Fig. 3. Chromatograms of MMC dissolved in methanol: with injection of (a) 5 μl of 40 μg/ml MMC in methanol, (b) 5 μl of extract after the off-line simple pretreatment of 1 ml plasma containing 100 μg MMC and (c) 5 μl of extract after the off-line sample pretreatment of 1 ml blank plasma. Conditions: as in Fig. 2, except that the percentage of methanol is 12%.

consists of the following steps. A Pasteur pipette is filled with 100 mg XAD-2 (particle size 150–200 μm). The solid phase material is first activated with 6 ml of methanol and washed with 6 ml of water. Then the plasma sample (1 ml) is extracted. After washing the material with 6 ml of water, the analytes are eluted with 6 ml of methanol. The eluate is evaporated to dryness by blowing nitrogen gas over it at ambient temperature. The residue is dissolved in 100 μl of methanol. A 5-μl volume of this solution is injected directly onto the analytical column. This procedure is straightforward; recoveries are 93%. A typical chromatogram is given in Fig. 3b. The determination limit is estimated to be 30 ng/ml.

Phase-system switching and on-line sample pretreatment

A liquid–solid isolation procedure as described above can easily be implemented on-line in an HPLC system by the use of valve-switching techniques. This approach is used for instance in the automatic HPLC determination method for MMC[15]. However, in combination with SFC a phase-system switching step must be performed in order to step from aqueous solutions to supercritical mixtures of carbon dioxide and methanol. A system has been designed which performs such a phase-system switching in combination with SFC. The procedure consists of five distinct steps. In the first step the plasma sample, after centrifugation, is injected into a stream of water, which transports the sample to a short precolumn. Adsorption onto the surface of the precolumn material takes place. In the second step the precolumn is washed with 1 ml water. In the third step the precolumn is dried, removing residual water, with a stream of nitrogen flowing in the backflush direction. In the fourth step the compounds are desorbed from the precolumn by a stream of supercritical carbon dioxide with 12% methanol and transferred to the separation column. In the last step the compounds are separated on the analytical column and selectively detected at 360 nm with an UV detector. After each experiment the precolumn is washed with 10 ml of water. The various steps in this procedure have been studied in more detail.

Using an adsorption step from aqueous solutions and a desorption step with 12.5% acetonitrile in water, the retention characteristics of the precolumn in the

analysis of MMC in plasma were investigated. It was found that nearly complete recoveries (between 90 and 104%) can be obtained in such a system.

Injection of 5 μl water into the SFC system does not result in serious problems the first few times, but cannot be done frequently as it results in pressure fluctuations and disturbance of the UV signals. This is expected, as only 0.1–0.2% water can be dissolved in supercritical carbon dioxide under the present conditions. By using solutions of MMC in mixtures of water and methanol the influence on the chromatography of MMC has been investigated. It was found that the peak shapes rapidly deteriorate with increasing water content of the sample. From these experiments it can be concluded that it is necessary to dry the precolumn. Drying of a precolumn has also been described by Noorozian *et al.*[22] in LC–GC experiments. In the present experiments a stream of nitrogen at a flow-rate 300–400 ml/min was used to dry the precolumn. It has been found that drying times up to 25 min at ambient temperature do not result in complete removal of the water on the precolumn. Therefore, it was decided to place the precolumn in the SFC column oven at 50–60°C. Drying at 60°C for 10 min resulted in significant decrease of the chromatographic signals, probably due to thermal degradation of the MMC. Lowering the temperature to 50°C gave better results.

Two types of adsorbents have been investigated. The silica-based Polygosil C_{18} material gave irreproducible results. Better results were obtained with the XAD-2 resin material with particle size 150–200 μm.

When during the procedure the supercritical fluid is switched to the dried precolumn a significant pressure drop of about 6 MPa takes place in the system. However, it takes about 30 s to restore the original condition.

The liquid–solid isolation step is surprisingly selective. UV detection at 215 nm after sampling blank plasma samples onto the precolumn and analyzing with the same procedure results in a broad peak, with similar capacity factors as for MMC. However, considering the complexity of plasma, far more extensive signals are expected. In the analysis of MMC in plasma samples the compounds coeluted from the

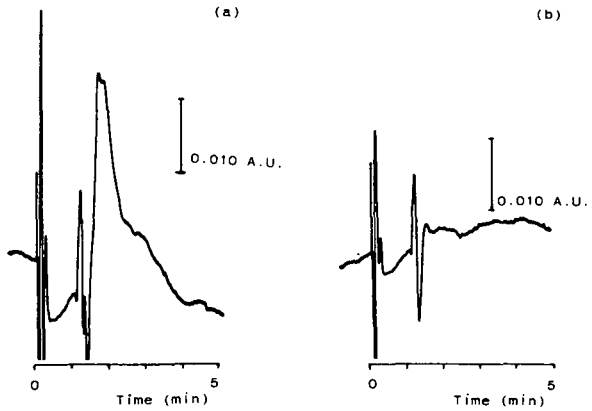

Fig. 4. Chromatograms after injection of 20 μl of blank plasma onto the precolumn with UV detection at (a) 215 nm and (b) 360 nm. Conditions: precolumn (10 mm × 3.2 mm I.D.) packed with XAD-2; sampling with 1.0 ml/min for 1 min; other conditions as in Fig. 3.

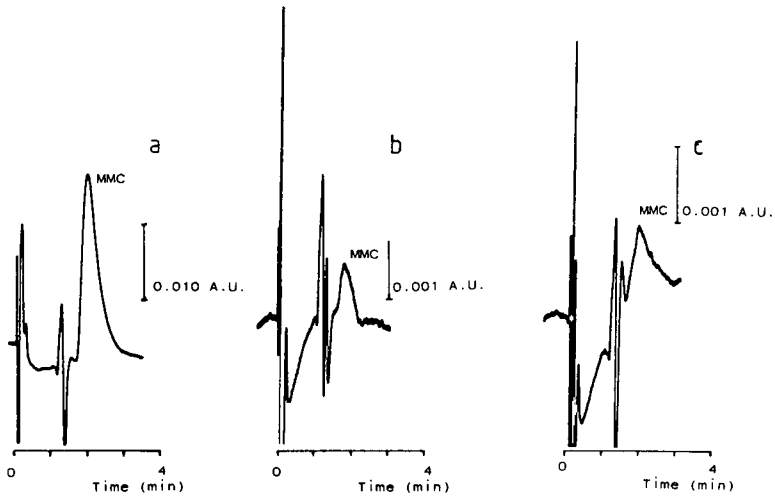

Fig. 5. Chromatograms after on-line liquid–solid extraction of MMC from plasma samples with sampling of (a) 20 μl plasma containing 200 ng MMC, (b) 20 μl plasma containing 20 ng MMC and (c) 1 ml plasma containing 20 ng MMC. For conditions see Fig. 4.

precolumn do not interfere. At the wavelength of maximum absorbance of MMC, *i.e.*, 360 nm, the blank plasma samples give clean UV signals (see Fig. 4). These results indicate that the phase-system switching approach in this case is quite a selective sample pretreatment procedure.

One of the drawbacks of the off-line sample pretreatment procedure lies in the fact that it is hardly possible to dissolve the residue reproducibly in volumes smaller than 100 μl. As only 5 μl of the methanolic solution can be injected on the SFC column, it is not possible to analyze directly the equivalent of 1 ml plasma in such a system. In the on-line sample pretreatment system the volume of the plasma samples injected has been varied between 20 and 1000 μl, keeping the absolute amount of MMC in the samples constant (either 20 or 200 ng). Typical chromatograms are given in Fig. 5, showing that it is possible to analyze with the system described 1 ml of plasma directly. Typical recoveries in the determination are 70% (with an oven temperature of 50°C). Thus, some (thermal) degradation of MMC appears to take place during the procedure, as there is no evidence for significant break-through of MMC on the precolumn. However, lower temperatures cannot be used, as SFC will not be stable under those conditions. The calculated detection limit of the complete procedure is 1.48 ng MMC. The determination limit is about 5 ng/ml.

With the precolumn used in these experiments it is possible to inject, at least 15 times, 1 ml of plasma before the precolumn has to be replaced.

CONCLUSIONS

The analysis of Mitomycin C in plasma samples with SFC is described. MMC is used merely as a test compound. It has been shown that MMC can be analyzed successfully by using an off-line liquid–solid isolation procedure. However, the off-

line procedure is time-consuming and laborious. An on-line liquid–solid isolation can also be performed by using valve-switching techniques. In this system 1 ml of plasma can be sampled directly. On the precolumn a phase-system switching is performed, in which the polar liquid phase which disturbs the SFC analysis is removed, and the compound of interest is desorbed from the precolumn with a supercritical mixture of carbon dioxide and methanol, also used as the mobile phase in SFC. The determination limit of this procedure is 5 ng/ml. The present system can easily be coupled to a continuous-flow system equipped with a dialysis membrane in order to obtain a fully automated system for Mitomycin C analysis. Other applications of the phase-system switching approach in SFC are now under investigation and will be reported separately.

ACKNOWLEDGEMENT

ABI Kratos Brownlee Scientific is greatly acknowledged for the loan of the syringe pump and the high-pressure flow-cell.

REFERENCES

1 P. J. Schoenmakers and L. G. M. Uunk, *Eur. Chromatogr. News*, 1 (1987) 14.
2 P. J. Schoenmakers, *J. High Resolut. Chromatogr. Chromatogr. Commun.*, 11 (1988) 278.
3 M. Novotný and S. R. Springston, *J. Chromatogr.*, 279 (1983) 417.
4 R. D. Smith, H. T. Kalinoski and H. R. Udseth, *Mass Spectrom. Rev.*, 6 (1987) 445.
5 T. L. Chester, *J. Chromatogr. Sci.*, 24 (1986) 226.
6 J. B. Crowther and J. F. Henion, *Anal. Chem.*, 57 (1985) 2711.
7 A. J. Berry, D. E. Games and J. R. Perkins, *J. Chromatogr.*, 363 (1986) 147.
8 D. W. Later, B. E. Richter, D. E. Knowles and M. R. Anderson, *J. Chromatogr. Sci.*, 24 (1986) 249.
9 C. M. White, D. R. Gere, D. Boyer, F. Packolec and L. K. Wong, *J. High Resolut. Chromatogr. Chromatogr. Commun.*, 11 (1988) 94.
10 W. Röder, F.-J. Ruffing, G. Schomburg and W. H. Pirkle, *J. High Resolut. Chromatogr. Chromatogr. Commun.*, 10 (1987) 665.
11 R. Wall, *Int. Analyst*, Nov. (1987) 28.
12 J. van der Greef, W. M. A. Niessen and U. R. Tjaden, *J. Pharm. Biomed. Anal.*, accepted for publication.
13 E. R. Verheij, H. J. E. M. Reeuwijk, G. F. La Vos, W. M. A. Niessen, U. R. Tjaden and J. van der Greef, *Biomed. Environ. Mass Spectrom.*, accepted for publication.
14 J. H. Beijnen, H. Lingeman, H. A. van Munster and W. J. M. Underberg, *J. Pharm. Biomed. Anal.*, 4 (1986) 275.
15 U. R. Tjaden, E. A. de Bruijn, R. A. M. van der Hoeven, C. Jol, J. van der Greef and H. Lingeman, *J. Chromatogr.*, 420 (1987) 53.
16 K. K. Unger and P. Roumeliotis, *J. Chromatogr.*, 282 (1983) 519.
17 S. B. Hawthorne and D. J. Miller, *J. Chromatogr. Sci.*, 24 (1986) 258.
18 H. Engelhardt and A. Gross, *J. High Resolut. Chromatogr. Chromatogr. Commun.*, 11 (1988) 38.
19 M. E. P. McNally and J. R. Wheeler, *J. Chromatogr.*, 435 (1988) 63.
20 P. J. Schoenmakers, F. C. C. J. G. Verhoeven and H. M. van den Bogaert, *J. Chromatogr.*, 371 (1986) 121.
21 U. R. Tjaden, J. P. Langenberg, K. Ensing, W. P. van Bennekom, E. A. de Bruijn and A. T. van Oosterom, *J. Chromatogr.*, 232 (1982) 355.
22 E. Noorozian, F. A. Maris, M. W. F. Nielen, R. W. Frei, G. J. de Jong and U. A. Th. Brinkman, *J. High Resolut. Chromatogr. Chromatogr. Commun.*, 10 (1987) 17.

Journal of Chromatography, 454 (1988) 253–259
Elsevier Science Publishers B.V., Amsterdam — Printed in The Netherlands

CHROM. 20 761

GRADIENT ELUTION WITH NORMAL PHASES ON SILICA

A COMPARISON BETWEEN HIGH-PERFORMANCE LIQUID AND SUPERCRITICAL FLUID CHROMATOGRAPHY

W. STEUER, M. SCHINDLER and F. ERNI*
Analytical Research and Development, Pharma Division, Sandoz Ltd., Basle (Switzerland)
(First received April 11th, 1988; revised manuscript received June 21st, 1988)

SUMMARY

Gradient elution on silica in supercritical fluid chromatography (SFC) and high-performance liquid chromatography (HPLC) was compared. The instrumental set-up for the measurement of the equilibration volumes in SFC and HPLC is described. It was demonstrated by k' measurements that 300–1000 column volumes in normal-phase HPLC are needed in order to achieve constant chromatographic conditions after a change of eluent. For this reason normal-phase gradient elution is an impracticable and irreproducible HPLC method for routine application. On the other hand, pressure gradient elution with supercritical carbon dioxide on silica showed very small equilibration volumes (*ca.* 2 column volumes). Thermodynamic equilibration in the column is achieved instantly. The modifier change in SFC needs only 10–30 column volumes. Here the equilibration volume depends strongly on the density and diffusivities in the supercritical fluid. Consequently, the use of pressure and modifier gradients in SFC has great advantages over the use of gradient elution in normal-phase HPLC.

INTRODUCTION

In recent years, interest in supercritical fluid chromatography (SFC) has increased continuously as it combines promising kinetic properties[1] with interesting solvent behaviour of the fluids. The solvent power and therefore the retention of substances in SFC depend strongly on the density of the solvent, and pressure programmed SFC[2] is comparable to gradient elution in high-performance liquid chromatography (HPLC).

Supercritical carbon dioxide at low densities possesses solubility parameters[3] similar to those of liquid pentane and at high densities of liquid toluene. Therefore, carbon dioxide is an advantageous eluent in normal-phase chromatography. A major disadvantage of normal phases in HPLC is the sensitive dependence of the selectivity on the amount of water; normal-phase HPLC often seems to be an irreproducible method and gradient elution on pure silica is nearly impossible. The equilibration

0021-9673/88/$03.50

volumes needed to obtain stable chromatographic conditions are between 300 and 1000 column volumes. Polar bonded phases are better than pure silica[4] and normal-phase HPLC was gradually replaced by reversed-phase HPLC (RP-HPLC), although many separation problems such as the separation of isomeric compounds are often better solved by normal-phase HPLC than by RP-HPLC. With supercritical carbon dioxide as the eluent one should be able to combine the advantages of both SFC and normal-phase HPLC. The aim of these investigations was to compare gradient elution on silica in SFC and HPLC with respect to the equilibration volumes necessary for constant and reproducible chromatographic conditions.

EXPERIMENTAL

Apparatus

The determination of the pressure gradient equilibration volumes in SFC was carried out on the instrumental set-up shown in Fig. 1. This made possible an immediate change of the pressure conditions in the column without any change in flow-rate. Two independent SFC systems at different pressure levels were coupled by a Rheodyne 7010 switching valve. LC 420 and LC 410 pumps for carbon dioxide were obtained from Kontron (Zürich, Switzerland). The pump heads for the carbon dioxide-delivering pumps were equipped with head exchangers that allowed the carbon dioxide to be cooled to below −10°C. Pressure was monitored by LCP 501 pressure transducers (Innovativ-Labor, Wallisellen, Switzerland). The injector was

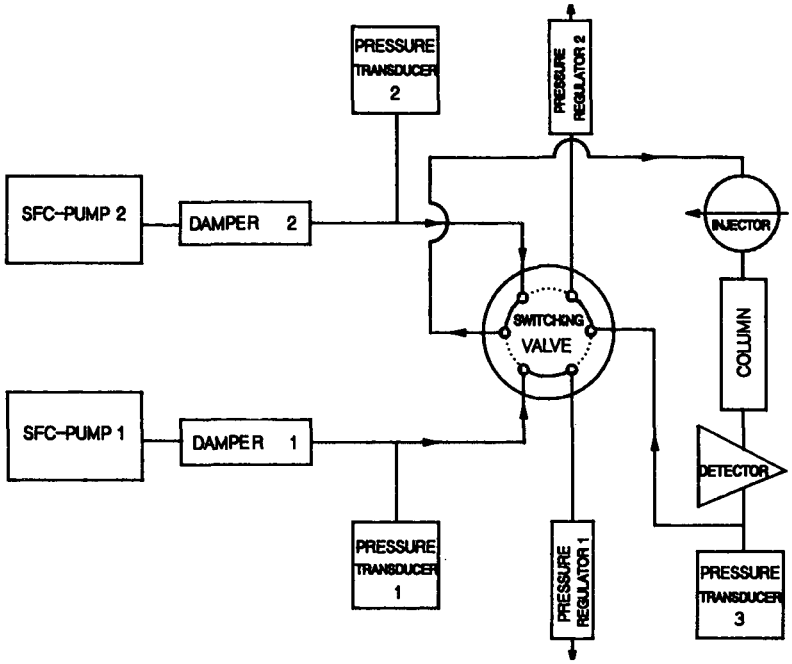

Fig. 1. Instrumental set-up for the measurement of relaxation time and pressure gradient equilibration time in SFC.

a Rheodyne 7010 valve. Uvikon 720 LC UV detector (Kontron) equipped with laboratory-made high-pressure-resistant cell was used. The system back-pressure was maintained and adjusted with 26-1761 pressure regulators (Tescom, Elk River, MA, U.S.A.).

For the measurement of the equilibration volumes in solvent-programmed HPLC the SFC set-up shown in Fig. 1 was used without pressure regulators and pressure transducers. One pulse damper was replaced with an alumina column (200 × 30 mm I.D.) in order to guarantee a constant small amount of water in the *n*-heptane.

Chemicals

Carbon dioxide (48 grade) was obtained from Carba Gas (Basle, Switzerland), and *n*-heptane (HPLC grade) from Merck (Darmstadt, F.R.G.). Wet *n*-heptane, directly from the bottle, contained 80 ppm of water. The dried *n*-heptane (50 ppm of water) was pumped through a column filled with neutral alumina (Woelm, Eschwege, F.R.G.), pretreated in an oven at 600°C for 4 h. Methanol was obtained from Rathburn (Walkerburn, U.K.). Anthracene, naphthalene, perylene, nitrobenzene and 1,2-diphenylethandione were purchased from Merck. In all experiments silica columns from Brownlee Labs. (Santa Clara, CA, U.S.A.) were used. The columns (100 × 4.6 mm I.D.) were packed with 5-μm particles.

RESULTS AND DISCUSSION

It is of practical importance to know the equilibration times in pressure programmed SFC to prevent irreproducible results being obtained owing to a lack of thermodynamic equilibrium in the column. The reproducibility of retention times could be influenced by the heat generated by the compression of the carbon dioxide during the pressure gradient. The dependence of the retention on the pressure drop was described by Schoenmakers and Verhoeven[5]. It might be that at high pressures an effect similar to capillary condensation causes the existence of a liquid carbon dioxide phase within the pores of the packing material[5]. Water dissolved in the carbon dioxide[6] could be adsorbed on to the silica surface. All these effects would influence the retention and, hence, the reproducibility of the separation. The faster the chromatographic equilibrium is obtained the better is the reproducibility. The disturbance of the equilibrium can be caused by a change of pressure in SFC or of solvent in silica HPLC. The solvent volume that is necessary to give constant capacity factors (k') after changing the chromatographic conditions serves as a criterion of reproducibility. This equilibration volume is expressed as the number of column volumes.

Modifier change in normal-phase HPLC

The influence of water on retention is demonstrated in Fig. 2. More than 1000 column volumes of dried *n*-heptane (40 ppm of water) are necessary to give stable conditions after changing the eluent from wet (80 ppm of water) to dry *n*-heptane. The water is strongly adsorbed on the polar silica surface[7] and also it has very low solubility in *n*-heptane. Both of these factors are responsible for the slow exchange of adsorbed water. A problem arises when solvents are used in gradient elution with different solubilities of water. It is very time consuming to establish the initial chromatographic

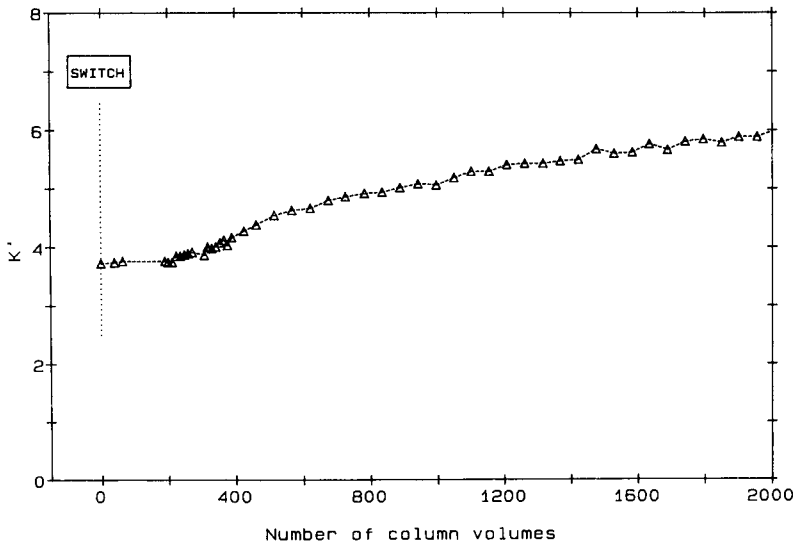

Fig. 2. Relaxation volumes in HPLC on silica. Switch from *n*-heptane (80 ppm of water) to *n*-heptane (50 ppm of water); flow-rate, 3.0 ml/min; sample, nitrobenzene.

conditions because of the insufficient solubility of water in the weaker eluent. Hence it is essential to control exactly the content of water in the solvents.

With methanol as a modifier in *n*-heptane the new equilibrium seems to be obtained after nearly 300 column volumes (Fig. 3). Methanol is more soluble in *n*-heptane. However, the retarded recovery of the equilibrium may indicate that the

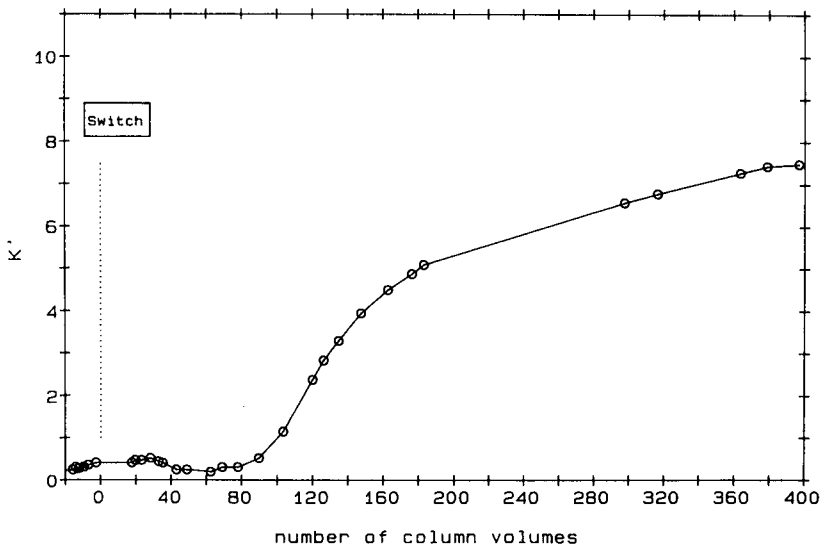

Fig. 3. Relaxation volumes in HPLC on silica. Switch from *n*-heptane–methanol (98.4:1.6) to *n*-heptane; flow-rate, 3.5 ml/min; sample, nitrobenzene.

equilibrium between methanol and *n*-heptane is superimposed by an equilibrium between adsorbed water from the methanol and the *n*-heptane.

Pressure change in normal-phase SFC

Fig. 4 shows that in contrast to solvent gradients in silica HPLC, pressure changes in silica SFC result in a very rapid establishment of the equilibrium. For all substances constant chromatographic conditions are obtained within two column volumes after switching the pressure from 150 to 180 bar. Apparently the heat of compression has no significant influence on retention. One gains considerable time in

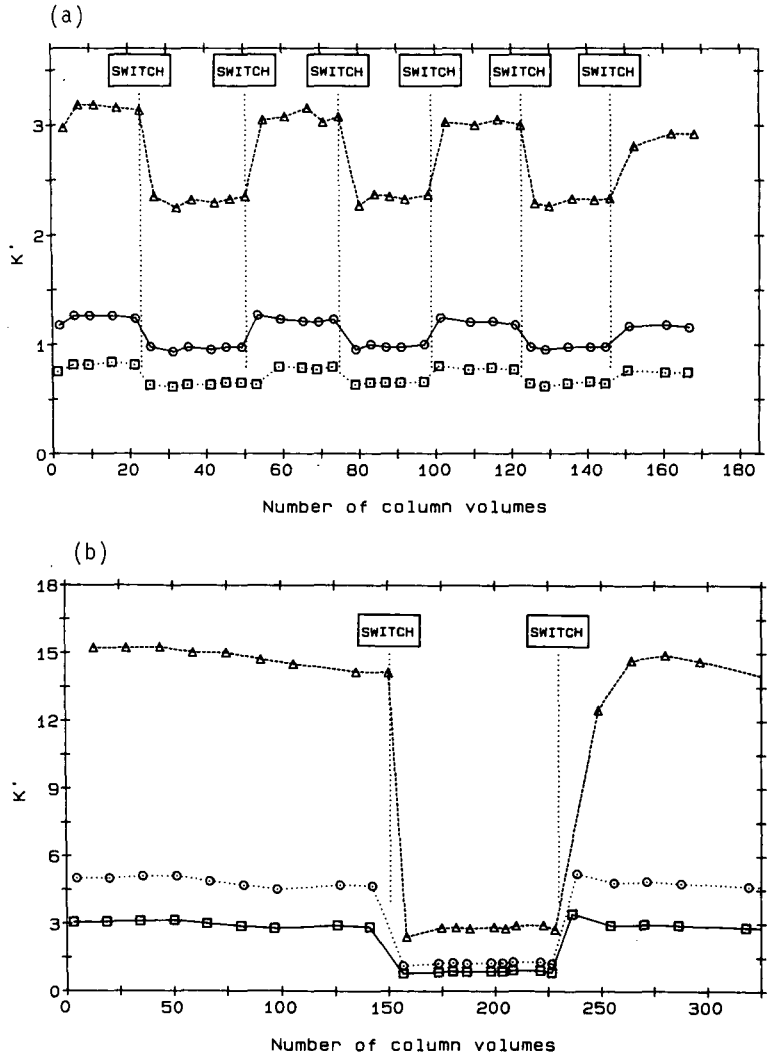

Fig. 4. Relaxation volumes in SFC on silica. (a) Switch from 150 to 180 bar; temperature, 40°C; flow-rate, 3.0 ml/min. (b) Switch from 100 to 200 bar. Conditions as in (a). △ = Perylene; ○ = pyrene; □ = anthracene.

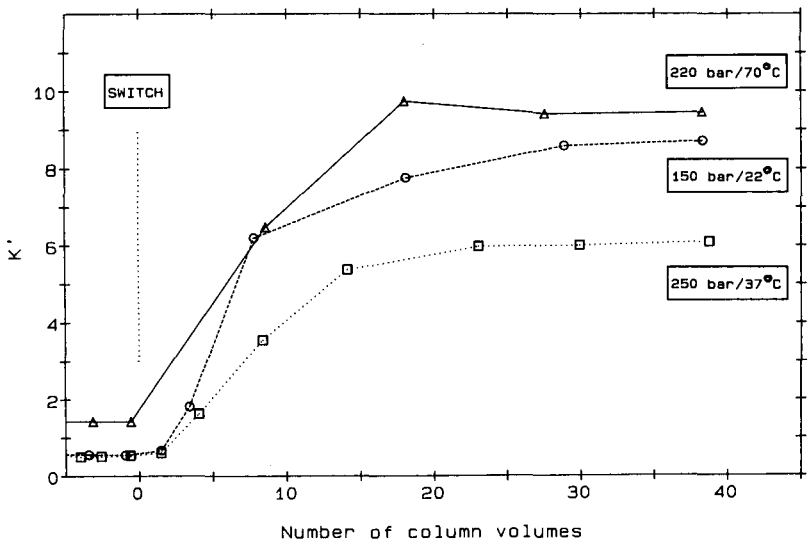

Fig. 5. Relaxation volumes in SFC on silica at different densities and diffusivities. Switch from carbon dioxide–methanol (98:2) to carbon dioxide; flow-rate, 4.0 ml/min; sample, 1,2-diphenylethandione.

SFC not only in gradient chromatography but also when optimizing an isocratic constant pressure method. Within a few seconds new constant chromatographic conditions are obtained.

Modifier change in SFC

Often it is essential to add polar modifiers to the carbon dioxide in order to improve the retention behaviour of the samples. It is important to know mainly during the optimization when the chromatographic equilibrium has been obtained. Fig. 5 and Table I demonstrate that after 10–30 column volumes completely constant chromatographic conditions are obtained. The number of equilibration volumes depends on the density of the fluid. There is a faster exchange of modifier at lower densities and consequently at higher diffusivities. The diffusion coefficients in carbon dioxide increase from 0.9 to 0.7 g/cm^3 and from lower temperature to higher temperature[8]. It

TABLE I

COMPARISON OF THE EQUILIBRATION VOLUMES (NUMBER OF COLUMN VOLUMES) FOR PRESSURE CHANGE AND MODIFIER CHANGE IN SFC AND MODIFIER CHANGE IN NORMAL-PHASE HPLC

Method	*No. of column volumes*
Pressure change in SFC	< 2
SFC 1 (70°C/220 bar), CO_2 + 2% methanol	10
SFC 2 (37°C/250 bar) → pure CO_2	18
Subcritical (22°C/150 bar)	28
HPLC 1 [*n*-heptane–methanol (98.4:1.6) to *n*-heptane]	300
HPLC 2 [*n*-heptane + 80 ppm water to *n*-heptane + 50 ppm water]	> 1000

seems possible that because of the 10-fold higher diffusivities of supercritical fluids compared with those of liquid heptane, the rate of desorption of the polar modifier molecules from the pores of the silica into the mobile phase is also much higher.

CONCLUSION

The retention in HPLC on silica is heavily dependent on the water content. Gradient silica HPLC is a time-consuming and often irreproducible chromatographic method because equilibrium is obtained only after about 300–1000 column volumes.

In contrast there are very short equilibrium times in pressure gradient SFC compared with gradients in silica HPLC. This leads to shorter times of analysis in pressure gradient SFC and higher reproducibility in normal-phase SFC. Moreover, modifier changes in SFC are much faster than in normal-phase HPLC. Therefore, the times necessary to develop optimized separations are much shorter in SFC than in HPLC. In addition, there are more possibilities in SFC of optimizing separations because both the density and the organic modifier affect selectivity.

Hence the most important objectives of a chromatographic method, namely reproducibility of retention times, time of analysis and time to develop a separation method, are much better fulfilled in SFC than in HPLC. A combination of SFC with the undisputed advantages of normal phases should be a powerful alternative to normal-phase HPLC.

REFERENCES

1 H. E. Schwartz, P. J. Barthel, S. E. Moring and B. H. Lauer, *LC · GC, Mag. Liq. Gas Chromatogr.*, 5 (1987) 490–497.
2 E. Klesper and F. P. Schmitz, *J. Chromatogr.*, 402 (1987) 1–39.
3 J. C. Giddings, M. N. Myers, L. McLaren and R. A. Keller, *Science (Washington, D.C.)*, 162 (1968) 67–73.
4 E. L. Weiser, A. W. Salotto, S. M. Flach and L. R. Snyder, *J. Chromatogr.*, 303 (1984) 1–12.
5 P. J. Schoenmakers and F. C. C. J. G. Verhoeven, *J. Chromatogr.*, 352 (1986) 315–328.
6 C. R. Coan and A. D. King, Jr., *J. Am. Chem. Soc.*, 93 (1971) 1857.
7 R. L. Snyder, *J. Chromatogr. Sci.*, 7 (1969) 595.
8 P. Mourier, P. Sassiat, M. Caude and R. Rosset, *Analysis*, 12 (1984) 229–248.

Journal of Chromatography, 454 (1988) 261–272
Elsevier Science Publishers B.V., Amsterdam — Printed in The Netherlands

CHROM. 20 749

DETERMINATION OF ORGANOPHOSPHORUS ACIDS BY THERMOSPRAY LIQUID CHROMATOGRAPHY–MASS SPECTROMETRY

E. R. J. WILS* and A. G. HULST
Prins Maurits Laboratory TNO, P.O. Box 45, 2280 AA Rijswijk (The Netherlands)
(First received March 16th, 1988; revised manuscript received June 13th, 1988)

SUMMARY

The determination of thirteen organophosphorus acids, hydrolysis products of nerve agents and pesticides, by a combination of ion-pair liquid chromatography on a reversed-phase C_{18} column and thermospray mass spectrometry was investigated. Ammonium acetate and three tetraalkylammonium salts with different alkyl groups (methyl, ethyl and *n*-butyl) were applied as ion-pair reagents. All the organophosphorus acids could be eluted using water or water–methanol mixtures. Capacity factors (k') were measured for some selected acids using water as eluent.

The recorded thermospray mass spectra using ammonium acetate as electrolyte gave the $[M + NH_4]^+$ ion as a predominant peak, whereas with the tetraalkylammonium salts cluster ions were found. This difference in ionization mechanism was also reflected in the sensitivity. An amount of 100 pg of dimethylthiophosphoric acid could be detected by selected ion monitoring using ammonium acetate, whereas with tetramethylammonium hydroxide the amount was 5 ng. To obtain lower detection levels preconcentration could be achieved with a Sep-Pak C_{18} cartridge pretreated with a tetra-*n*-butylammonium salt.

INTRODUCTION

Alkyl-substituted organophosphorus acids are the primary hydrolysis products of physiologically active organophosphorus compounds such as nerve agents and pesticides. With a few exceptions the first group of substances contain a methyl group directly linked to a phosphorus atom, leading to alkylmethylphosphonic acids after hydrolysis. organophosphorus pesticides are mainly (thio)phosphates which hydrolyse to dialkyl(thio)phosphoric acids. In recent years various analytical procedures for the determination of these hydrolysis products in environmental and biological samples have been developed. Generally, these procedures are based on the isolation of the organophosphorus acids from the aqueous phase followed by derivatization and determination by gas chromatography (GC) using phosphorus-specific or mass spectrometric (MS) detection.

Direct analysis of these acids in aqueous solution by reversed-phase liquid chromatography (LC) seems more straightforward. However, sensitive detection is a

problem because these acids do not contain ultraviolet (UV)-absorbing or fluorescing groups. This has been overcome by precolumn derivatization into compounds with UV[1] or fluorescence properties[2]. Combining LC with a phosphorus-specific GC detector is another approach[3,4]. This detection problem can also be solved by using a mass spectrometer as an LC detector. A compound such as nitric acid with similar detection limits to the organophosphorus acids has successfully been determined by thermospray (TSP)–LC–MS[5]. In the investigation described here a combination of tetra-*n*-butylammonium (TBA) hydroxide and ammonium acetate was used as ion-pair reagent in chromatography on a reversed-phase C_{18} column.

Organophosphorus acids are relatively strong acids and exist as anions at neutral pH. Until now conventional ion chromatography has offered limited possibilities for the determination of these organophosphorus acids[4,6]. Some experiments on the determination of phosphonic acids used in the detergent industry by ion-pair chromatography on a reversed-phase C_{18} column have been reported[3]. Hence, a study was started to investigate the determination of a number of hydrolysis products of nerve agents and organophosphorus pesticides (Table I) by ion-pair TSP–LC–MS on conventional C_{18} columns. Recently, in the course of this study, the determination of four hydrolysis products of nerve agents by ion-pair reversed-phase chromatography on a polystyrene–divinylbenzene (PSDVB) column has been published[6]. TBA hydroxide was used as the ion-pair reagent and detection was carried out by means of a conductivity detector after suppression of the TBA ions. These cations are mostly applied during ion-pair chromatography of anions on reversed-phase columns. However, tetraalkylammonium ions with smaller alkyl groups and even the ammonium ion itself have been used as counter ions, in particular for the determination of anions containing hydrophobic groups[7]. Therefore ammonium acetate, generally used in

TABLE I

ORGANOPHOSPHORUS ACIDS USED AS TEST COMPOUNDS

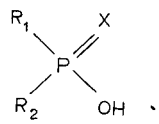

No.	*Acid*	R_1	R_2	*X*	*MW*
1	Methylphosphonic	OH	CH_3	O	96
2	Dimethylphosphoric	CH_3O	CH_3O	O	126
3	Ethylmethylphosphonic	C_2H_5O	CH_3	O	124
4	Dimethylthiophosporic	CH_3O	CH_3O	S	142
5	Ethylmethylthiophosphonic	C_2H_5O	CH_3	S	140
6	Isopropylmethylphosphonic	$(CH_3)_2CHO$	CH_3	O	138
7	Diethylphosphoric	C_2H_5O	C_2H_5O	O	154
8	Diethylthiophosphoric	C_2H_5O	C_2H_5O	S	170
9	Cyclopentylmethylphosphonic	C_5H_9O	CH_3	O	164
10	Diisopropylphosphoric	$(CH_3)_2CHO$	$(CH_3)_2CHO$	O	182
11	Cyclohexylmethylphosphonic	$C_6H_{11}O$	CH_3	O	178
12	Diisopropylthiophosphoric	$(CH_3)_2CHO$	$(CH_3)_2CHO$	S	198
13	Pinacolylmethylphosphonic	$(CH_3)_3CCH(CH_3)O$	CH_3	O	180

TSP–LC–MS as an electrolyte for the ionization of organic molecules, could also serve as an ion-pair reagent in chromatography.

This paper describes the effects of ammonium acetate and tetraalkylammonium salts with different alkyl groups (methyl, ethyl and *n*-butyl) on the chromatographic behaviour and on the TSP ionization of organophosphorus acids.

EXPERIMENTAL

Chemicals

Ammonium acetate (A.C.S. reagent grade) was obtained from Aldrich (Milwaukee, WI, U.S.A.). Tetramethylammonium hydroxide was purchased from Sigma (St. Louis, MO, U.S.A.), tetraethylammonium hydroxide (20% solution in water) from Aldrich (Steinheim, F.R.G.) and tetra-*n*-butylammonium hydroxide (40% solution in water) from BDH (Poole, U.K.). Glacial acetic acid (UCB, Leuven, Belgium), used to adjust the pH of the eluent as indicated, and methanol (Merck, Darmstadt, F.R.G.) were of analytical-reagent grade. Polyethylene glycols (PEG-200 and PEG-400) were purchased from Fluka (Buchs, Switzerland). For all purposes water was purified in a Milli-Q water purification system (Millipore, Bedford, MA, U.S.A.). Organophosphorus acids were prepared in the laboratory and gave satisfactory elemental analyses and spectral (IR, NMR and mass) data. Standard solutions of the acids were prepared in water, with the exception of pinacolylmethylphosphonic acid, which was dissolved in water–methanol (80:20, v/v). The solutions were diluted to the appropriate concentrations with water before use.

Liquid chromatography

The LC system included the following components: a Waters Model 590 solvent delivery system (Waters Assoc., Milford, MA, U.S.A.), a Valco injector (Bester, Amsterdam, The Netherlands) with a 10-μl sample loop and a stainless-steel column (250 mm × 5 mm I.D.) which was packed in the laboratory with LiChrosorb C_{18}, 5-μm particles (Merck). The connection between the column and the TSP interface consisted of a low-dead-volume tee, a Valco injector with a 5-μl sample loop for flow injections and a 2-μm screen filter (Waters Assoc.). A second high-pressure pump (Waters Model 501) combined with a pulse damper (Touzart et Matignon, Vitry sur Seine, France) was connected to the low-dead-volume tee for post-column addition of an ammonium acetate solution or for the introduction of the mass axis calibration mixture.

A flow-rate of 1.5 ml/min was used in all experiments, except during post-column addition. In this instance a flow-rate of 1.2 ml/min was maintained through the column, while 0.3 ml/min of a 0.3 *M* ammonium acetate solution was added at the end of the column.

Capacity factors (k') were calculated by using the hold-up time of ^2H_2O, which was injected into an eluent of pure water at a flow-rate of 1.5 ml/min. Detection of the ^2H_2O signal was carried out after post-column addition of ammonium acetate. Retention times of the acids were measured after equilibration of the LC system. Column loading, especially with the TBA salt, required at least 30 min to reach a steady state.

Mass spectrometry

A Nermag (Rueil Paris, France) R 10-10 C quadrupole instrument, equipped with a TSP ion source (Nermag), was coupled with the LC system via a Vestec TSP interface (Vestec, Houston, TX, U.S.A.). The mass spectrometer was operated in the positive ion mode, with the filament off. Mass axis (m/z) calibration from m/z 60 to 800 was performed with a mixture of PEG-200 and PEG-400. Maximal sensitivity was tuned in the mass range of the expected ions.

The scan range used was dependent on the application, whereas the scan time was dependent on the mass range and varied between 0.6 and 0.9 s. During single ion monitoring experiments the integration time was set at 0.2 s. The TSP vaporizer temperature was optimized for the particular kind of analysis and was normally in the range 190–240°C. The ion block temperature was maintained at 240°C during experiments with ammonium acetate. This temperature was raised to 280°C when tetraalkylammonium salts were applied.

Preconcentration of pinacolylmethylphosphonic acid

Sep-Pak C_{18} cartridges (Waters Assoc.) were prewashed with 10 ml of methanol and 5 ml of water. To equilibrate the C_{18} phase, 20 ml of a 10 mM solution of TBA hydroxide (adjusted to pH 6.0) were forced through the cartridge at a flow-rate of approximately 10 ml/min. A volume of 50 ml of a solution of pinacolylmethylphosphonic acid (2.5 ng/ml) in 10 mM TBA hydroxide (previously adjusted to pH 6.0) was forced through the pretreated cartridge. After drying both ends of the cartridge with a tissue, 2 ml of methanol were used to elute the ion pair. This solution was evaporated to 200 μl by gently blowing nitrogen over the liquid surface. The recovery was determined by comparing the signal obtained after LC–MS analysis of this concentrated solution with that of an appropriate standard solution.

RESULTS AND DISCUSSION

Ammonium acetate as ion-pair reagent

The effect of the ammonium acetate concentration on the capacity factor (k') of three organophosphorus acids was measured (Fig. 1). Without ammonium acetate a negative k' value was obtained, indicating that the acids did not penetrate the pores of the silica particles when using pure water as the eluent. This phenomenon had been observed before on C_{18} columns and was explained by an electrostatic exclusion mechanism[8]. Above the concentration level of 0.02 M no substantial enhancement of the k' values was noticed. Generally, a concentration of 0.1 M ammonium acetate is used during TSP–LC–MS analysis, providing optimal ionization of the analyte[9]. Therefore, further experiments were carried out at this concentration level.

The reconstructed ion chromatograms (RIC) obtained after analysing mixtures of organophosphorus acids are presented in Figs. 2 and 3. Although the more hydrophilic acids (1–4) eluted very fast, separation was still complete. In order to analyse acids with longer alkyl chains the addition of an organic solvent was necessary. Pinacolylmethylphosphonic acid (13), the hydrolysis product of the nerve agent soman, is the most hydrophobic of the compounds studied. By means of a mixture containing 30% methanol this acid eluted within 12 min at the chosen flow-rate. If all the acids need to be analysed in one LC run, gradient elution will be necessary; this will be the subject of a future investigation.

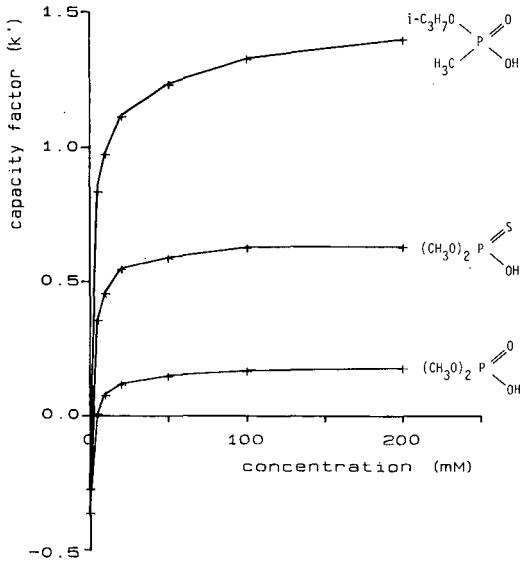

Fig. 1. Effect of ammonium acetate concentration on the capacity factors (k') of three acids. Eluent, water containing the indicated amount of counter ion (pH 5.8).

The influence of the pH of the mobile phase on the retention behaviour was investigated. Small but significant changes in the retention times were found between pH 4.5 and 7.0. The retention times of thiophosphoryl acids decreased at lower pH, whereas methylphosphonic acids showed the opposite behaviour. This different retention behaviour might be attributed to the differences in pK_a values. Thiophosphoryl acids ($pK_a < 1$) are stronger acids than methylphosphonic acids ($pK_a \approx 2$). By selecting an appropriate pH a separation could be achieved of ethylmethylthiophosphonic acid (5) and isopropylmethylphosphonic acid (6), the hydrolysis products of

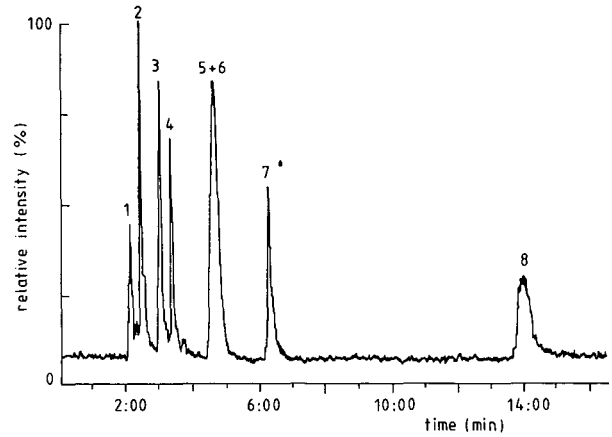

Fig. 2. Reconstructed ion current chromatogram. Eluent, 0.1 *M* ammonium acetate (pH 6.8). Analyte concentration, 2–3 ng/μl. See Table I for compound numbers.

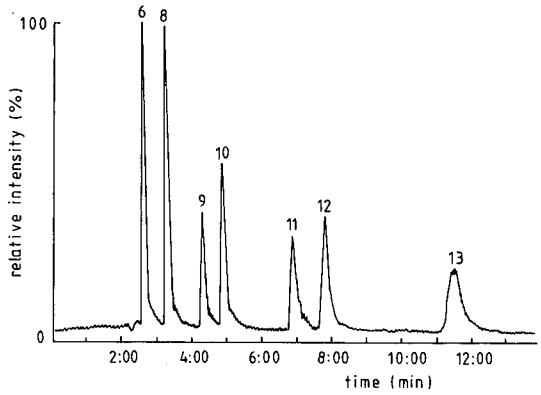

Fig. 3. Reconstructed ion current chromatogram. Eluent, water (0.1 *M* ammonium acetate)–methanol (70:30) (pH 6.8). Analyte concentration, 4–6 ng/μl. See Table I for compound numbers.

the nerve agents VX and sarin, respectively. At pH 6.8 both acids coeluted (Fig. 2), whereas at pH 5.0 baseline separation was achieved.

Tetraalkylammonium salts as ion-pair reagents

The major disadvantage of the use of ammonium acetate as an ion-pair reagent is the small k' values obtained for the more hydrophilic organophosphorus acids. By using tetraalkylammonium salts these values could be enhanced. With tetramethylammonium (TMA) ions a small enhancement of the k' values was achieved. However, the use of tetraethylammonium (TEA) ions led to a k' value above 1 for dimethylphosphoric acid (Fig. 4). For the three selected acids a rapid increase was

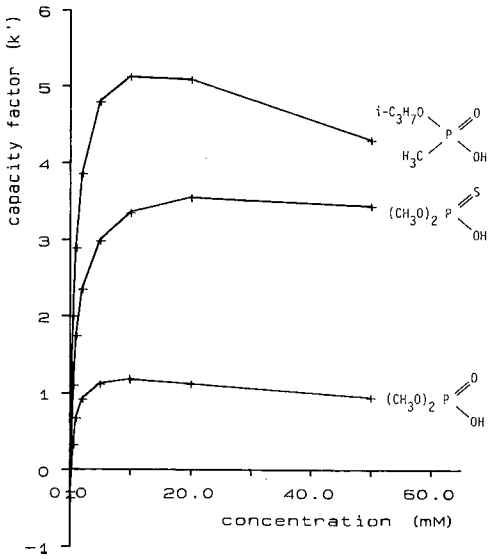

Fig. 4. Effect of TEA hydroxide concentration on the capacity factors (k') of three acids. Eluent, water containing the indicated amount of counter ion (pH 5.2).

observed, leading to a maximal k' value at a counter-ion concentration of around 10 mM, followed by a gradual decrease at higher concentrations. This concentration dependence of the k' value has been described theoretically[10].

A different behaviour was observed for the more hydrophobic TBA ions, which were strongly adsorbed on the C_{18} stationary phase. Consequently, the nature of the column after preconditioning was changed and resembled an ion-exchange resin[10]. The effect of the TBA ion concentration on the k' value of dimethylphosphoric acid is presented in Fig. 5. A relatively high concentration (> 10 mM) was necessary to elute this acid. The elution of acids with larger alkyl groups was only possible after the addition of methanol. In Table II the retention times of twelve monovalent organophosphorus acids obtained using a water–methanol mixture are presented. The effect of increasing the TBA ion concentration on the retention was the opposite of that with the use of water as the eluent. When using water–methanol, increased salt concentrations led to increased retention times. The acids with the smaller alkyl groups were well separated. However, the retention times became long for the more hydrophobic acids such as pinacolylmethylphosphonic acid.

Attempts were made to determine methylphosphonic acid using TBA ions. The determination of this bivalent acid on a PSDVB column has been described[6] using, in addition to TBA hydroxide, sodium carbonate as a modifier to shorten the retention time. However, it was impossible to obtain a reasonable peak shape for this acid on a C_{18} column. Very broad peaks were obtained in the pH range tested (3.0–6.0). Probably this acid can only be measured at a pH far above the second dissociation constant (pK_{a_2} in water *ca.* 6.5). Unfortunately, C_{18} columns cannot be used at high pH values.

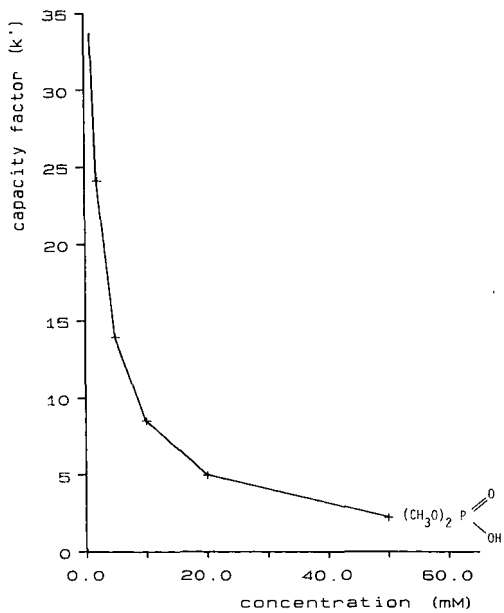

Fig. 5. Effect of TBA hydroxide concentration on the capacity factor (k') of dimethylphosphoric acid. Eluent, water containing the indicated amount of counter ion (pH 5.2).

TABLE II

EFFECT OF THE TBA ION CONCENTRATION ON THE RETENTION TIMES OF TWELVE ORGANOPHOSPHORUS ACIDS

Column, 250 × 5 mm I.D., 5-μm LiChrosorb C_{18}; eluent, water–methanol (60:40), pH 5.0; flow-rate, 1.5 ml/min.

No.	*Acid*	*Retention time (min)*	
		1 mM	*5 mM*
2	Dimethylphosphoric	3.15	4.05
3	Ethylmethylphosphonic	3.35	4.38
4	Dimethylthiophosphoric	3.37	4.48
5	Ethylmethylthiophosphonic	4.07	5.42
6	Isopropylmethylphosphonic	4.17	5.53
7	Diethylphosphoric	4.26	6.09
8	Diethylthiophosphoric	5.02	8.00
9	Cyclopentylmethylphosphonic	7.12	11.17
10	Diisopropylphosphoric	7.52	12.54
11	Cyclohexylmethylphosphonic	12.10	19.38
12	Diisopropylthiophosphoric	13.15	23.16
13	Pinacolylmethylphosphonic	20.52	33.00

The use of tetraalkylammonium salts (especially TBA salts) at high concentrations had some drawbacks. The C_{18} column degraded fairly rapidly, resulting in a reduction of the number of plates. Further, partial or complete blockage of the TSP interface occurred, probably owing to silica material originating from the degrading column. Although the use of TBA salts did not lead to an extremely contaminated ion source, the salt was difficult to eliminate. Changing to another mobile phase required extensive rinsing of the whole LC–MS system with methanol. Even then the TBA ion at *m/z* 242 could still be found in the TSP mass spectra after several weeks. Strong memory effects from alkylammonium salts have been reported before[11].

Positive ion TSP mass spectra

The ammonium adduct ion $[M + NH_4]^+$ was a predominant peak in the positive ion TSP mass spectra of the organophosphorus acids recorded during the LC–MS analysis using ammonium acetate as electrolyte. The spectra correspond to those obtained for organophosphorus pesticides which also showed strong $[M + NH_4]^+$ ions[9]. The ratio between the ammonium adduct ion and the protonated molecular ion $[M + H]^+$ varied for the acids studied. In acids with small alkyl groups the $[M + H]^+$ ion was relatively small (Fig. 6), but became more abundant in acids with larger alkyl groups (Fig. 7). No great difference in the $[M + NH_4]^+/[M + H]^+$ ratio was found between phosphoryl and thiophosphoryl compounds containing the same alkyl groups. The $[M + NH_4]^+/[M + H]^+$ ratio depended on the temperature of the vaporizer and to a minor extent on the ion source block. Normally, owing to contamination of the capillary tip after a number of analyses, the vaporizer temperature was increased to obtain the same stable signal. An increase in the vaporizer temperature reduced the $[M + NH_4]^+/[M + H]^+$ ratio. Variations of a factor 3 in these ratios were observed over the temperature range used. Therefore, the spectra presented

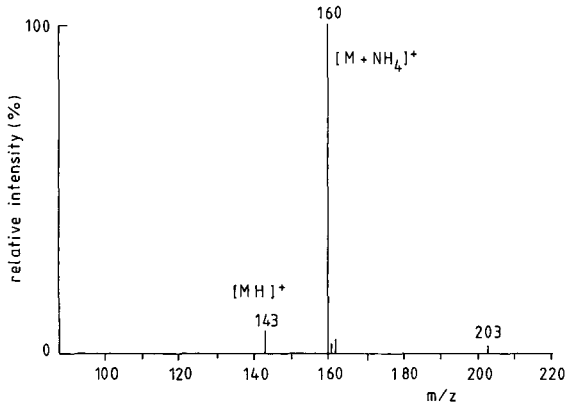

Fig. 6. TSP mass spectrum of dimethylthiophosphoric acid. Eluent, 0.1 *M* ammonium acetate.

should be regarded only as typical examples. A small ion corresponding to the addition of acetic acid to the $[M + H]^+$ ion was sometimes noticed, *e.g.*, *m/z* 203 in the TSP mass spectrum of dimethylthiophosphoric acid (Fig. 6). Fragments derived from methylphosphonic acid (*m/z* 97 and 114) were noticed in the TSP mass spectrum of pinacolylmethylphosphonic acid (Fig. 7). The intensities of these fragments increased with increasing ion source block temperature, indicating that decomposition of this compound can take place.

Two kinds of ions were formed during TSP–LC–MS analysis of the organophosphorus acids using tetraalkylammonium salts as electrolytes. In addition to an ion due to the addition of the cation to the acid ($[M + C]^+$), a cluster ion, $[A][C]_2^+$ (A = anion, C = cation), was found. Higher cluster ions were not observed. This $[A][C]_2^+$ ion was of moderate intensity in the TSP mass spectra recorded with TMA salts, but became predominant using TEA and TBA salts (Fig. 8). The cation adduct ion $[M + C]^+$ corresponds to the $[M + Na]^+$ ion frequently found in the TSP mass

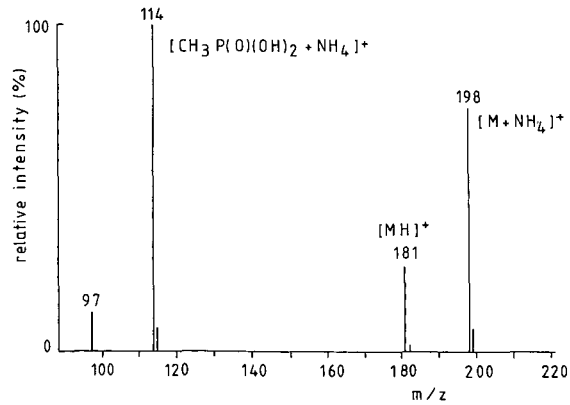

Fig. 7. TSP mass spectrum of pinacolylmethylphosphonic acid. Eluent, water (0.1 *M* ammonium acetate)–methanol (70:30).

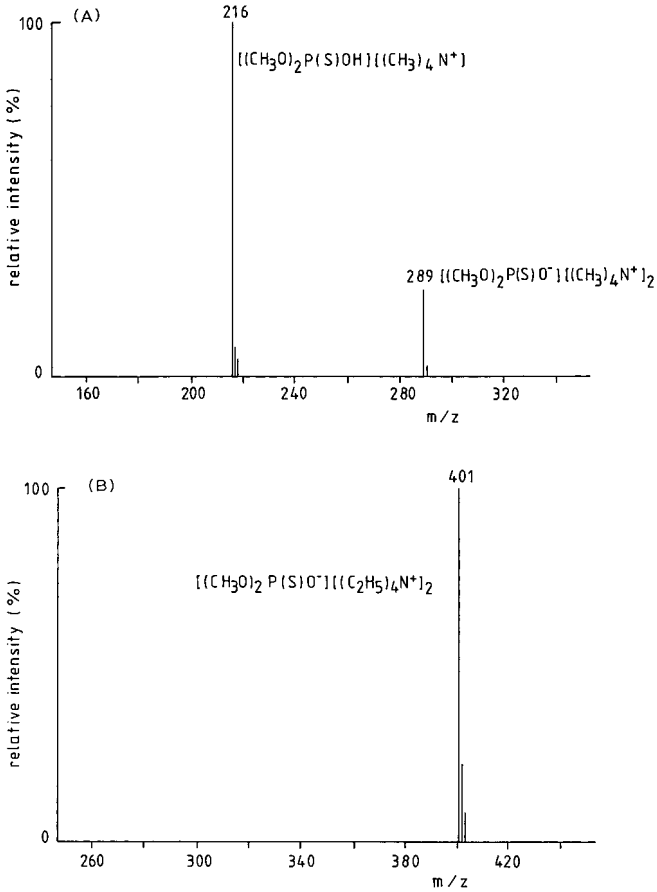

Fig. 8. TSP mass spectrum of dimethylthiophosphoric acid obtained using 5 m*M* TMA hydroxide (A) and TEA hydroxide (B) (pH 5.2).

spectra of polar organic compounds and whose formation has recently been discussed in nucleotides[12]. A similar $[A][C]_2^+$ cluster ion has been found in the TSP and fast atom bombardment (FAB) mass spectra of sodium butanesulphonate[13]. In both spectra the major peak was assigned to the cluster ion $[C_4H_9SO_3][Na]_2^+$. As observed previously[12,13], the similarity between TSP and FAB mass spectra is supported by the results obtained here with the organophosphorus acids. Recently, the same kinds of ions have been detected in the FAB mass spectra of several alkylammonium salts[14,15].

Sensitivity considerations

An advantage of the use of ammonium acetate as an ion-pair reagent is the high water content of the eluent, which is the most preferential situation in TSP ionization[16]. To demonstrate the sensitivity achieved in the positive ion detection mode, the signal-to-noise (S/N) ratio obtained after injecting an amount of 100 pg of di-

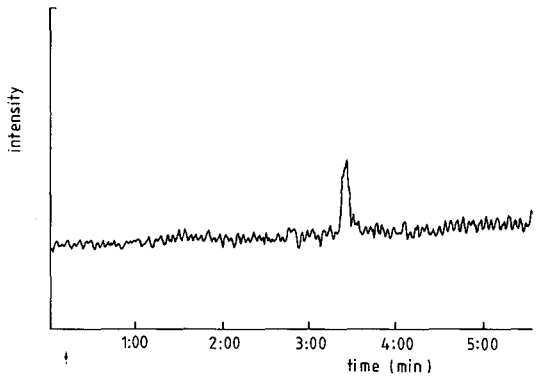

Fig. 9. Selected ion monitoring at *m/z* 160, the ammonium adduct ion of dimethylthiophosphoric acid (100 pg). Eluent, 0.1 *M* ammonium acetate (pH 6.8).

methylthiophosphoric acid is shown in Fig. 9. Selected ion monitoring (SIM) was applied to the ammonium adduct ion. Owing to peak broadening at longer retention times and the addition of methanol to the eluent (resulting in a decrease in the TSP ionization), the minimal amount detected was higher for acids containing longer alkyl chains. For instance, to achieve a detectable signal with SIM for pinacolylmethylphosphonic acid an amount of 1 ng had to be injected.

The sensitivity using tetraalkylammonium salts as electrolytes was much reduced in comparison with ammonium acetate. The S/N ratio obtained after injecting an amount of 5 ng of dimethylthiophosphoric acid using an eluent containing 5 m*M* of TMA hydroxide was similar to that shown in Fig. 9, indicating a reduction in sensitivity by a factor of 50. Although the absolute intensity of the TMA adduct ion was enhanced on increasing the salt concentration, the noise was also increased and consequently no improvement in the S/N ratio was achieved. This phenomenon was also observed on increasing the ammonium acetate concentration[9].

The TSP ionization of dimethylthiophosphoric acid by mixtures of 0.1 *M* ammonium acetate and various concentrations of tetraalkylammonium salts was investigated. After reducing the salt concentration to 0.1 m*M* the formation of the $[M + NH_4]^+$ ion was favoured instead of the above-mentioned cluster ions. At this low concentration TBA ions could still interact with the organophosphorus anions during elution through a C_{18} column. By post-column addition of ammonium acetate the acids could be detected as the $[M + NH_4]^+$ ions formed in the TSP ion source. In this way 1 ng of dimethylthiophosphoric acid could be determined with a similar S/N ratio to that shown in Fig. 9, using a mobile phase consisting of 0.1 m*M* TBA hydroxide–methanol (70:30).

This reduced sensitivity in comparison with the experiments using only ammonium acetate as the mobile phase (Fig. 9) must mainly be attributed to the reduced ionization efficiency of water–methanol mixtures[16].

Although the results obtained for the determination of organophosphorus acids are promising, further research will be necessary. Generally, the measured sensitivity is insufficient for analysing real samples of environmental or biological origin. An SIM detection limit of around 1 ng leads to a minimum detectable concentration of 20 ng/ml when using a relatively large injection volume of 50 μl. Future improve-

ments to the equipment (incorporation of negative ion detection and a repeller in the TSP source) may lead to lower detection limits. Experiments at the Nermag application laboratory pointed to an increase in sensitivity by a factor of 4 for pinacolylmethylphosphonic acid[17]. However, to detect organophosphorus acids in aqueous solution below a concentration level of 1 ng/ml, preconcentration will be necessary. Preconcentration of organophosphorus acids by means of an ion-exchange resin or a polymeric adsorbent such as XAD-4 has been reported[18,19]. On the basis of the results obtained here with ion-pair chromatography, Sep-Pak C_{18} cartridges can also be used for preconcentration. Pinacolylmethylphosphonic acid was trapped quantitatively from a volume of 50 ml of water with a Sep-Pak C_{18} cartridge using TBA salts. The ion pair formed was removed from the cartridge with methanol. After evaporation of the methanol a preconcentration factor of greater than 100 was easily achieved. The overall recovery of the procedure described was around 90%.

REFERENCES

1 P. C. Bossle, J. J. Martin, E. W. Sarver and H. Z. Sommer, *J. Chromatogr.*, 267 (1983) 209.
2 M. C. Roach, L. W. Ungar, R. N. Zare, L. M. Reimer, D. L. Pompliano and J. W. Frost, *Anal. Chem.*, 59 (1987) 1059.
3 T. L. Chester, *Anal. Chem.*, 52 (1980) 1621.
4 A. Verweij, C. E. Kientz and J. van den Berg, *Int. J. Environ. Anal. Chem.*, in press.
5 L. R. Hogge, R. K. Hynes, L. M. Nelson and M. L. Vestal, *Anal. Chem.*, 58 (1986) 2782.
6 P. C. Bossle, D. J. Reutter and E. W. Sarver, *J. Chromatogr.*, 407 (1987) 399.
7 J. Weiss, *J. Chromatogr.*, 353 (1986) 303.
8 B. A. Bidlingmeyer, S. N. Deming, W. P. Price, Jr., B. Sachok and M. Petrusek, *J. Chromatogr.*, 186 (1979) 419.
9 R. D. Voyksner and C. A. Haney, *Anal. Chem.*, 57 (1985) 991.
10 W. R. Melander and Cs. Horváth, *J. Chromatogr.*, 201 (1980) 211.
11 G. Schmelzeisen-Redeker, M. A. McDowall, U. Giessmann, K. Levsen and F. W. Röllgen, *J. Chromatogr.*, 323 (1985) 127.
12 R. D. Voyksner, *Org. Mass Spectrom.*, 22 (1987) 513.
13 C. Fenselau, D. J. Liberato, J. A. Yergey, R. J. Cotter and A. L. Yergey, *Anal. Chem.*, 56 (1984) 2759.
14 K. G. Furton and C. F. Poole, *Org. Mass Spectrom.*, 22 (1987) 210.
15 K. G. Furton and C. F. Poole, *Org. Mass Spectrom.*, 22 (1987) 377.
16 D. J. Liberato and A. L. Yergey, *Anal. Chem.*, 58 (1986) 6.
17 F. de Maack and M. Lesieur, Nermag, Rueil Paris, personal communication.
18 A. Verweij, C. E. A. M. Degenhardt and H. L. Boter, *Chemosphere*, 8 (1979) 115.
19 C. G. Daughton, D. G. Crosby, R. L. Garnas and D. P. H. Hsieh, *J. Agric. Food Chem.*, 24 (1976) 236.

Journal of Chromatography, 454 (1988) 273–284
Elsevier Science Publishers B.V., Amsterdam — Printed in The Netherlands

CHROM. 20 782

SEPARATION OF MOLECULAR SPECIES OF TRIACYLGLYCEROLS BY HIGH-PERFORMANCE LIQUID CHROMATOGRAPHY WITH A SILVER ION COLUMN

W. W. CHRISTIE
Hannah Research Institute, Ayr KA6 5HL (U.K.)
(First received April 21st, 1988; revised manuscript received June 20th, 1988)

SUMMARY

Molecular species representative of the wide range of triacylglycerols occurring in nature, ranging from relatively saturated fats such as that from sheep adipose tissue through polyunsaturated seed oils, including sunflower and linseed oils, to an oligounsaturated fish oil, have been resolved by high-performance liquid chromatography in the silver ion mode. The stationary phase consisted of an ion-exchange medium, which was a silica gel matrix with bonded sulphonic acid moieties, loaded with silver ions. The mobile phase for the more saturated fractions was a gradient of acetone into 1,2-dichloroethane–dichloromethane, then acetonitrile was introduced to elute polyunsaturated fractions. A mass detector was employed to monitor separations. Fractions were collected via a stream-splitter for identification and quantification by gas chromatography as methyl esters. Excellent resolution was obtained on the silver ion column with no contamination of fractions with silver ions, while the column was stable and retained its activity in prolonged use.

INTRODUCTION

Silver ion chromatography has long been valued by lipid analysts, because it permits separation of distinct molecular fractions, differing solely in the degree of unsaturation[1,2]. The technique has been used largely in conjunction with thin-layer chromatography (TLC), with silver nitrate being incorporated into the silica gel layer. While this has given excellent results, there are a number of disadvantages in practice. For example, relatively large amounts of expensive silver nitrate are required, the separated components are not always easily visualised, autoxidation can occur on the TLC plate and some silver ions are generally eluted together with the fractions. There have been many attempts to adapt the technique to high-performance liquid chromatography (HPLC), but until relatively recently these had met with limited success only[3]. On the other hand, a stable ion-exchange column loaded with silver ions has been developed that has proved of value in some applications[4]. The procedures are rapid, reproducible and give clean fractions, uncontaminated by silver ions. HPLC with this column has recently been used to simplify complex mixtures of fatty acids of

0021-9673/88/$03.50

natural origin for subsequent identification by gas chromatography (GC)–mass spectrometry[5].

One of the more important applications of silver ion chromatography has been for the separation of molecular species of intact lipids, especially the triacylglycerols of the commercially important fats and oils[6]. By utilising aprotic mobile phases, it has been demonstrated that it is possible similarly to fractionate relatively simple natural fats, such as palm oil, by HPLC with the silver-loaded ion-exchange medium[4]. It is shown here that the method can be extended to a much wider range of natural triacylglycerols, including some that are highly unsaturated.

EXPERIMENTAL

Samples and reagents

The vegetable oils, *i.e.* sunflower, maize (corn), safflower, linseed and evening primrose, were obtained from local shops. A sample of subcutaneous fat was obtained from a sheep of the institute flock and one of rat parametrical adipose tissue was from a female Wistar rat; lipids were extracted with chloroform–methanol (2:1, v/v). The fish oil was a commercial sample of South African origin, probably from anchovies and pilchards, and was donated by Dr. R. J. Henderson of the NERC Unit of Aquatic Biochemistry in the University of Stirling. With each of the samples, triacylglycerols were purified, prior to HPLC analysis, by elution from a short column of Florisil™, with hexane–diethyl ether (4:1) as the mobile phase. All solvents were Analar or HPLC grades and were supplied by FSA Scientific (Loughborough, U.K.).

High-performance liquid chromatography

The HPLC equipment and the silver ion column were as described previously[4]. In brief, a Spectra-Physics Model 8700 solvent delivery system was used (Spectra-Physics, St. Albans, U.K.), together with an ACS Model 750/14 mass detector [Applied Chromatography Systems, (ACS), Macclesfield, U.K.]. When required, a stream-splitter (approximately 10:1) was inserted between the column and the detector. A column (250 × 4.6 mm I.D.) of Nucleosil™ 5SA (kindly donated by ACS) was flushed with 1% aqueous ammonium nitrate solution at a flow-rate of 0.5 ml/min for 1 h, then with distilled water at 1 ml/min for 1 h. Silver nitrate (0.2 g) in water (1 ml) was injected onto the column via the Rheodyne valve in 50-μl aliquots at 1-min intervals; silver began to elute from the column after about 10 min. 20 min after the last injection, the column was washed with methanol for 1 h, then with 1,2-dichloroethane–dichloromethane (1:1, v/v) for a further hour.

The three solvent reservoirs contained the following: (A) 1,2-dichloroethane–dichloromethane (1:1, v/v); (B) acetone; (C) acetone–acetonitrile (9:1, v/v). For the separation of sheep subcutaneous fat, a linear gradient of A to B was generated over 40 min at a flow-rate of 0.75 ml/min. With rat adipose tissue and linoleic acid-rich seed oils, gradients of A to 50% A–50% B over 15 min, then to 50% B–50% C over a further 25 min, and held at this for 5 min, were employed. For linolenic acid rich seed oils, C was changed to acetone–acetonitrile (4:1, v/v) and the flow-rate was increased to 1 ml/min; gradients of A to 50% A–50% B over 10 min, then to 70% B–30% C over 20 more min, and finally to 100% C over a further 30 min, were utilised. The last elution scheme was also used with the fish oil except that the final solvent mixture was

maintained for an additional 10 min. Samples (0.25–0.8 mg) were applied to the column in dichloroethane solution (5–10 μl). Fractions were collected manually via the stream splitter and methyl nonadecanoate was added to each as an internal standard.

Gas chromatography

The methyl ester derivatives of the fatty acids from each fraction were prepared by sodium methoxide-catalyzed transesterification[7]. A Carlo Erba Model 4130 capillary gas chromatograph (Carlo Erba, Crawley, U.K.), fitted with split/splitless injection, was equipped with a capillary column (25 m × 0.22 mm I.D.) of fused silica coated with Carbowax 20M (Chrompak, London, U.K.). It was temperature-programmed from 165°C (held at this for 3 min) at 4 to 195°C, and held at this point for a further 20 min. Hydrogen was the carrier gas. Components were quantified by electronic integration.

RESULTS

The utility of a gradient of acetone into 1,2-dichloroethane–dichloromethane for the separation of simple natural triacylglycerols was demonstrated earlier[4]. With aprotic solvents of this kind, there is no danger of transesterification of solutes being catalysed by residual free sulphonic acid groups in the stationary phase, as has been observed by others in related circumstances[8]. However, this basic elution scheme is only of value with triacylglycerols containing relatively low amounts of linoleic acid. The separation of one such sample is illustrated in Fig. 1, *i.e.* of triacylglycerols from sheep subcutaneous adipose tissue. In this instance, one additional complication is the presence of fatty acids with *trans* double bonds or with conjugated diene systems (largely 9-*cis*-11-*trans*-octadecadienoic acid[9]). The more abundant fractions such as SSS, SSM and SMM (see Table I for abbreviations) are clearly apparent and are particularly well resolved. In addition, there are a number of other peaks and some of these were found to contain *trans*-monoenes and the conjugated diene following

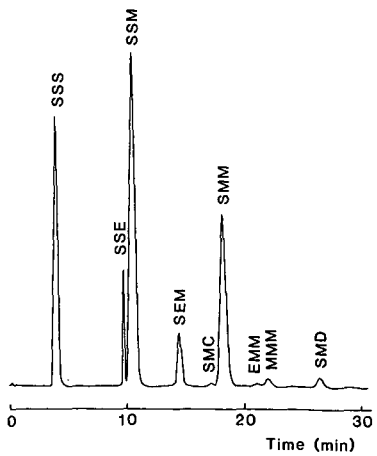

Fig. 1. Separation of triacylglycerols from sheep subcutaneous adipose tissue by HPLC with a silver ion column and mass detection. See the Experimental section for practical details, and Table I for abbreviations.

TABLE I

FATTY ACID COMPOSITION (MOL% OF THE TOTAL) OF THE TRIACYLGLYCEROLS OF SHEEP SUBCUTANEOUS ADIPOSE TISSUE AND OF FRACTIONS OF THIS OBTAINED BY SILVER ION HPLC

Abbreviations: S = saturated; M = monoenoic (*cis*-); E = elaidic (*trans*-monoenoic); C = conjugated dienoic; D = dienoic; T = trienoic fatty acids; br-i = isomethyl branched; ai = ante-isomethyl branched.

	Total	*SSS*	*SSE*	*SSM*	*SEM*	*SMC*	*SMM*	*SSD*	*EMM*	*MMM*	*SMD*	*Check*
14:0	3.3	6.5	5.4	3.7	1.0	1.1	1.2	2.2			1.0	2.9
15:0	0.9	1.3	0.6	0.8	0.4	0.5	0.4	1.1			0.6	0.6
16:0	26.1	44.3	31.7	29.9	15.9	17.5	17.0	35.1			19.3	25.3
16-br-i	0.6	0.9	0.5	0.7	0.3	0.2	0.4	0.7			0.7	0.6
16-br-ai	0.9	1.5	1.1	1.1	0.5	0.4	0.6	0.9			0.8	0.9
16:1	2.3		0.5	1.4	2.2	1.5	3.0		13.4	3.5	1.5	2.0
17:0	1.7	3.1	2.1	2.1	1.2	1.1	1.1	2.5			1.1	1.7
17:1	0.5			0.5	0.5	0.6	1.2		1.0	1.1	0.4	0.6
18:0	21.2	42.4	32.8	26.8	14.0	13.4	10.3	32.8			10.9	21.7
18:1($n-9$)	34.9		22.6	32.6	34.2	32.7	63.2		68.0	90.3	31.9	38.2
18:1($n-7$)	4.4		2.8	0.4	28.2	1.7	1.6		17.6	5.2	1.3	3.9
18:2	1.4					8.9		24.8			30.5	1.0
18:3	0.6											
18:2conj.	1.2				1.6	20.3						0.7
% of the total		14.3	5.1	35.6	9.6	2.6	25.2	1.5	2.1	2.6	1.5	

transesterification and analysis by capillary GC and silver ion HPLC[10] as indicated. Thus, fractions containing one mole of *trans*-monoene with two of saturated fatty acids and one saturated, one *cis*- and one *trans*-monoenoic fatty acid are present. A similar result was obtained with bovine milk fat (not illustrated). No comparable separation appear to have been recorded by silver ion TLC.

Each of the fractions was collected via the stream-splitter and transesterified in the presence of an internal standard for identification and quantification by GC. The mass (or "light-scattering") detector itself can only be used for quantification purposes after extensive calibration, although it permits a wide range of solvents and gradients to be used and is exceedingly useful when developing methodology[3]. The results are shown in Table I. Each of the fractions contain broadly the spectrum and proportions of fatty acids expected, the deviations being greatest in minor fractions or those which are incompletely resolved. As many trace fatty acids were resolved by capillary GC and were omitted from the calculations as unidentifiable, the results are perhaps better than is immediately apparent. As a check on the recoveries, the fatty acid composition of the whole was computed from the relative proportions in each of the fractions; the agreement is acceptable for most of the components.

In order to elute triacylglycerols containing higher proportions of linoleic acid, it was necessary to introduce some acetonitrile into the mobile phase. As an example, the separation of the triacylglycerols of rat parametrical adipose tissue is illustrated in Fig. 2. Many more distinct fractions are seen than in the previous sample. Some of these have shoulders or appear to be double, and this may be because of partial resolution of positional isomers in the triacylglycerols or because of chainlength differences or variations in the positions of the double bonds in fatty acids. Thus the two components of the trimonoenoic fraction are 18:1–18:1–18:1 and 18:1–18:1–16:1 respectively. All of the early fractions are well resolved, but fractions containing linolenic acid tend to overlap with those containing two dienoic acids. The relative proportions of each can, however, be determined from the fatty acid compositions, which were obtained as before and are listed in Table II. Again each fraction contains the relative proportions

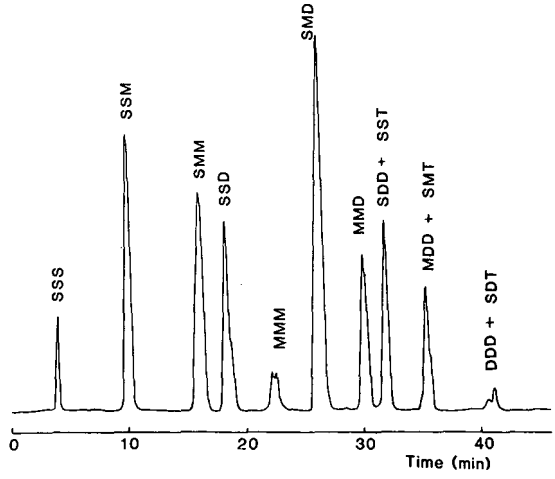

Fig. 2. Separation of triacylglycerols from rat parametrial adipose tissue by HPLC with a silver ion column and mass detection. See the Experimental section for practical details, and Table I for abbreviations.

TABLE II

FATTY ACID COMPOSITIONS (MOL% OF THE TOTAL) OF THE TRIACYLGLYCEROLS OF RAT PARAMETRIAL ADIPOSE TISSUE AND OF FRACTIONS OF THIS OBTAINED BY SILVER ION HPLC

Abbreviations: see Table I.

	Total	*SSS*	*SSM*	*SMM*	*SSD*	*MMM*	*SMD*	*MMD*	*SDD + SST*	*MDD + SMT*	*DDD + SDT*	*Check*
14:0	2.3	2.3	1.4	0.9	1.8		1.0		1.2	0.3	0.9	1.0
15:0	0.5	0.9	0.6	0.4	0.7		0.3		0.5	0.2	0.4	0.4
16:0	32.6	84.8	55.9	28.6	54.7		27.4		28.9	6.7	18.2	32.3
16:1	7.6		5.7	12.3		17.2	5.9	12.0		5.9		6.1
17:0	0.3	0.6	0.5	0.2	0.4		0.3		0.3			0.3
18:0	3.3	11.4	6.8	3.2	6.3		2.9		3.0	1.0	2.0	3.7
18:1($n-9$)	22.7		26.8	48.9		72.0	23.6	44.3		21.0		24.4
18:1($n-7$)	3.2		2.3	5.6		10.7	3.7	8.1		4.2		3.4
18:2	26.1				36.1		34.9	35.6	64.1	54.8	65.7	27.3
18:3	1.4								2.0	6.2	12.8	1.0
% of the total		3.8	14.3	15.5	12.5	3.2	22.1	8.9	9.5	7.5	2.7	

of the various types of fatty acid expected, and the check on the recovery by computation of the overall composition from those of the fractions is excellent.

A more challenging separation perhaps is that of the linoleic acid-rich seed oils used for human consumption, and the separation of sunflower seed oil, in which the same gradient elution scheme as for the last sample was used, is illustrated in Fig. 3. Again, well-shaped peaks are obtained and excellent resolution of all the main fractions is achieved with species containing linoleic acid being predominant. The quantitative data on the fatty acid compositions and the proportions of the various molecular species is listed in Table III. As before, the check on the overall composition indicates that the recovery is essentially complete. Very similar results were obtained with maize (corn) and safflower oils (not illustrated) except that the relative heights of the main peaks varied somewhat. In some commercial samples of these vegetable oils, there appeared to be some isomerised linoleic acid, and additional small peaks containing these components eluted in front of the corresponding main peaks on silver ion chromatography.

By increasing the proportion of acetonitrile in the final stages of elution to a higher level, it proved possible to obtain good separations of molecular species of seed oils containing trienoic acids. Fig. 4 illustrates the separation of linseed oil, which contains a high proportion of 18:3 ($n-3$), and the compositional data are listed in Table IV. In this instance also, a large number of fractions, up to and including trilinolenin, are resolved. Many of these comprise single molecular fractions, and only those species containing a single linolenoyl residue tend to overlap with those having two linoleoyl residues. In spite of the high degree of unsaturation, the compositions of each fraction contain close to the expected proportions of the fatty acids, while the check involving summation of the composition of the various fractions confirms that quantitative recoveries are obtained. With evening primrose oil, which contains 8% of γ-linolenic acid [18:3($n-6$)], fractions up to DDT were eluted but some small changes in the order of elution were observed in comparison to linseed oil that were presumably

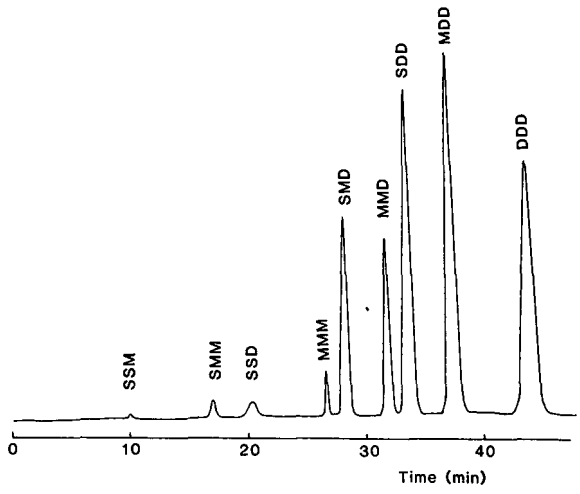

Fig. 3. Separation of triacylglycerols from sunflower seed oil by HPLC with a silver ion column and mass detection. See the Experimental section for practical details, and Table I for abbreviations.

TABLE III

FATTY ACID COMPOSITIONS (MOL% OF THE TOTAL) OF THE TRIACYLGLYCEROLS OF SUNFLOWER SEED OIL AND OF FRACTIONS OF THIS OBTAINED BY SILVER ION HPLC

Abbreviations: see Table I.

	Total	*SSM*	*SMM*	*SSD*	*MMM*	*SMD*	*MMD*	*SDD*	*MDD*	*DDD*	*Check*
16:0	7.3	37.2	17.5	36.9		19.6		17.4			6.7
18:0	4.9	27.7	12.8	27.5		11.7		14.4			5.0
18:1	21.9	35.1	69.6		100.0	34.2	61.9		31.9		23.4
18:2	65.9			35.5		34.5	38.1	68.2	68.1	100.0	64.9
% of the total		0.6	2.3	2.8	3.9	10.2	9.3	17.7	26.8	26.6	

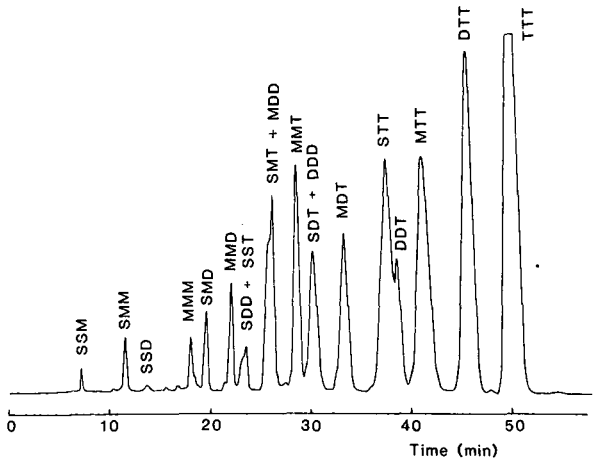

Fig. 4. Separation of triacylglycerols from linseed oil by HPLC with a silver ion column and mass detection. See the Experimental section for practical details, and Table I for abbreviations.

due to the different position of the double bonds in the trienoic component (separation not illustrated). Thus, SST and MMD elute together, SDT elutes just ahead of DDD, while MDT elutes just after DDD, *i.e.* fractions containing 18:3($n-6$) tend to elute before those containing 18:3($n-3$).

The ultimate test of the methodology is whether it will give acceptable separations of molecular fractions from a fish oil that contains substantial amounts of polyunsaturated fatty acids including 20:5($n-3$) and 22:6($n-3$). In the sample of triacylglycerols from a commercial fish oil of South African origin used here, these comprised 18.3 and 7.4% respectively of the total fatty acids. With an elution scheme

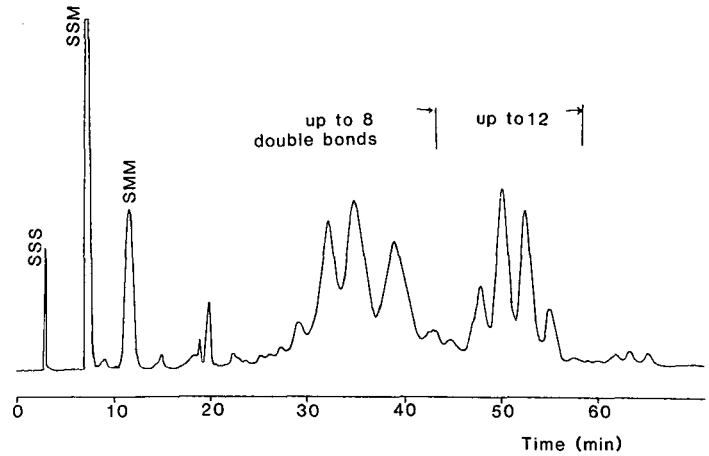

Fig. 5. Separation of triacylglycerols from a commercial fish oil of South African origin by HPLC with a silver ion column and mass detection. See the Experimental section for practical details, and Table I for abbreviations.

TABLE IV

FATTY ACID COMPOSITIONS (MOL% OF THE TOTAL) OF THE TRIACYLGLYCEROLS OF LINSEED OIL AND OF FRACTIONS OF THIS OBTAINED BY SILVER ION HPLC

Abbreviations: see Table I.

	Total	*SSM*	*SMM*	*SSD*	*MMM*	*SMD*	*MMD*	*SST + SDD*
16:0	6.3	32.4	14.0	28.5		15.9		28.5
18:0	3.2	32.7	20.6	32.8		12.0		16.5
18:1	17.0	34.8	65.5		100.0	36.7	64.8	
18:2	15.8			38.7		35.4	35.2	40.4
18:3	57.7							14.6
% of the total		0.3	0.8	0.6	1.3	1.4	2.1	1.9

similar to that for linseed oil but extended somewhat, the separation shown in Fig. 5 was obtained. The resolution is far from perfect, but some considerable simplification is obviously possible. Because of the complexity, a few representative fractions only were analysed to determine the nature of the separations, but it is evident that species with twelve and more double bonds in total are eluted. Unfortunately, it appeared that in spite of a careful purification some autoxidised or polymerised material remained that contributed to peak broadening. As many positional isomers of unsaturated fatty acids, differing in chain length, are also present, some peak broadening is probably inevitable. The potential of the procedure for this type of separation is evident, nonetheless, and the work will be repeated when a better defined and fresher sample of fish triacylglycerols is available.

DISCUSSION

The results described above illustrate that HPLC in the silver ion mode can replace analogous TLC procedures for the separation of the full range of triacylglycerols likely to be encountered in natural samples. Excellent resolution is obtained in general, and indeed the time for each fractionation can be reduced appreciably by increasing the flow-rate of the mobile phase or the rate of change of the gradient. The mass detector could certainly be used for quantification purposes if need be following careful calibration, but better results would probably be obtained with a detector operating on the transport-flame ionisation principle. However, the lengthy procedure of transesterification in the presence of an internal standard for GC determination, that is employed here, has the merit of giving detailed information on the composition of each fraction. In contrast to fractions obtained by silver ion TLC, the solvent eluting from the silver ion HPLC column contains no silver as an impurity so no clean-up step is required prior to transesterification. Most of the natural samples analysed here have been analysed previously by silver ion TLC (as reviewed by Litchfield[6]), but never with the convenience and clarity obtained here.

A column of this type has been in continuous use in the author's laboratory for miscellaneous separations with no detectable loss of resolution for more than one year. Periodically, there is a build up in the operating pressure, that appears to be due to the

SMT + MDD	*MMT*	*SDT + DDD*	*MDT*	*STT + DDT*	*MTT*	*DTT*	*TTT*	*Check*
13.9		14.9		11.0				4.5
9.6		9.1		8.6				3.3
32.6	65.1		33.1		31.8			15.9
17.7		48.3	33.2	21.3		31.3		15.7
26.2	34.9	27.8	33.7	59.1	68.2	68.7	100.0	60.7
6.6	6.2	5.0	6.3	15.1	12.1	14.4	25.9	

presence of material tightly bound to the stationary phase, but this can be cleared with relative ease by elution with methanol–acetonitrile (1:1, v/v) into which a solution of a few milligrams of silver nitrate in acetonitrile is injected.

The order of elution of triacylglycerol species is comparable but not identical to that obtained by TLC, but this may be due in part to variation in the mobile phases used by analysts. However, the only important difference is that those fractions containing one linoleoyl residue are sometimes separated from those containing two dienoic fatty acids in the TLC procedures[11,12]. With the HPLC elution schemes described here, the order of migration is SSS > SSM > SMM > SSD > MMM > SMD > MMD > SDD = SST > SMT = MDD > MMT > SDT = DDD > MDT > STT $\geqslant$ DDT > MTT > DTT > TTT, where T is 18:3($n-3$). When the positional isomer of linolenic acid, *i.e.* 18:3($n-6$), is present, the species containing this component are retained less strongly. Internal double bonds in polyunsaturated fatty acids almost certainly interact less strongly with silver ions than do outer ones, otherwise fractions with twelve or more double bonds from fish oils would not have eluted in a reasonable time. It should, therefore, be possible to analyse triacylglycerols from any natural source by this means.

In recent years many excellent separations of triacylglycerol species have been obtained by HPLC in the reversed-phase mode[3]. Separations are then attained both according to the combined chainlengths of the fatty acyl residues, and the total number of double bonds, each one reducing the retention time of the species by the equivalent of about two methylene groups. It is then rarely easy to identify components of complex mixtures. Fewer fractions are obtained when HPLC in the silver ion mode is employed, but as the separation is on the basis of a single molecular property, it is a rather simpler problem to identify components. In the analysis of confectionary fats especially, it can be important to determine the proportions of the trisaturated and disaturated–monounsaturated species by a rapid method as these govern the physical properties. The technique described here should permit analyses of this kind in a manner suited to routine quality control. On the other hand, it may be of particular value to consider silver ion chromatography as a complementary technique to reversed-phase procedures rather than as a rival. Many more molecular species can be isolated by subjecting fractions isolated by silver ion HPLC to reversed-phase

chromatography than would be possible using either technique on its own.

Although the elution schemes described here are for triacylglycerols only, they could almost certainly be adapted with little difficulty to the fractionation of other simple lipids, such as cholesterol esters or wax esters, and to the analysis of diacylglycerol derivatives prepared by the phospholipase C-catalysed hydrolysis of phospholipids. A priori, there would appear to be no reason why intact glycosphingolipids or phospholipids should not be resolved in a similar manner after further modifications to the mobile phase.

REFERENCES

1 L. J. Morris, *J. Lipid Res.*, 7 (1966) 717.
2 F. Mikěs, V. Schuring and E. Gil-Av, *J. Chromatogr.*, 83 (1973) 91.
3 W. W. Christie, *High-Performance Liquid Chromatography and Lipids*, Pergamon, Oxford, 1987.
4 W. W. Christie, *J. High Resolut. Chromatogr. Chromatogr. Commun.*, 10 (1987) 148.
5 W. W. Christie, E. Y. Brechany and K. Stefanov, *Chem. Phys. Lipids*, 46 (1988) 127.
6 C. Litchfield, *Analysis of Triglycerides*, Academic Press, New York, 1972.
7 W. W. Christie, *J. Lipid Res.*, 23 (1982) 1072.
8 R. O. Adlof and E. A. Emken, *J. Am. Oil Chem. Soc.*, 57 (1980) 276.
9 W. W. Christie, *Progress Lipid Res.*, 17 (1978) 111.
10 W. W. Christie and G. H. M. Breckenridge, unpublished results.
11 F. D. Gunstone and F. B. Padley, *J. Am. Oil Chem. Soc.*, 42 (1965) 957.
12 J. N. Roehm and O. S. Privett, *Lipids*, 5 (1970) 353.

Journal of Chromatography, 454 (1988) 285–291
Elsevier Science Publishers B.V., Amsterdam — Printed in The Netherlands

CHROM. 20 801

GAS CHROMATOGRAPHIC DETERMINATION OF INDOLEACETONITRILES IN RAPESEED AND *BRASSICA* VEGETABLES

B. A. SLOMINSKI and L. D. CAMPBELL*
Department of Animal Science, University of Manitoba, Winnipeg, Manitoba R3T 2N2 (Canada)
(First received March 2nd, 1988; revised manuscript received May 19th, 1988)

SUMMARY

Indole glucosinolates are susceptible to thermal decomposition with the production of indoleacetonitriles. The indoleacetonitriles are only one of several enzymatic degradation products of indole glucosinolates which have been reported to have both beneficial and harmful effects in animal and human studies. A gas chromatography (GC) method was developed for the quantification of 3-indoleacetonitrile and 4-hydroxy-3-indoleacetonitrile, which correspond to the indole glucosinolates glucobrassicin (3-indolylmethyl) and 4-hydroxyglucobrassicin (4-hydroxy-3-indolylmethyl), respectively. Following extraction with methylene chloride, trimethylsilyl derivatives of indoleacetonitriles from commercial low-glucosinolate rapeseed meal and cooked *Brassica* vegetables were effectively separated by GC with a total run time of 20 min and detected by using a flame ionization detector. Extraction of samples with methylene chloride was maximal at 15 min extraction time and sample to water ratios (w/v) of 1:2 for rapeseed meal and 1:10 for freeze-dried vegetables were shown to be effective. Derivatization of the indoleacetonitriles was effected at room temperature.

INTRODUCTION

The indole glucosinolates, glucobrassicin (3-indolylmethyl) and 4-hydroxyglucobrassicin (4-hydroxy-3-indolylmethyl), represent the major portion (40–60%) of the total glucosinolate content of low-glucosinolate rapeseed and *Brassica* vegetables[1,2]. It was shown for both of the indole glucosinolates that they are markedly susceptible to thermal degradation with thiocyanate ion (SCN) as a major thermal degradation product[1,3]. Recent studies have indicated the presence of two new thermal degradation products of indole glucosinolates in rapeseed meal[4] and *Brassica* vegetables[5]. These compounds were identified as 3-indoleacetonitrile (IAN) and 4-hydroxy-3-indoleacetonitrile (OH-IAN), which correspond to the intact indole glucosinolates glucobrassicin and 4-hydroxyglucobrassicin, respctively. A scheme showing the thermal decomposition of indole glucosinolates to SCN and indoleacetonitriles is given in Fig. 1.

Since thermally treated cruciferous crops are widely used as human foods and animal feedstuffs, there is a growing interest in the potential antinutritive properties of

0021-9673/88/$03.50

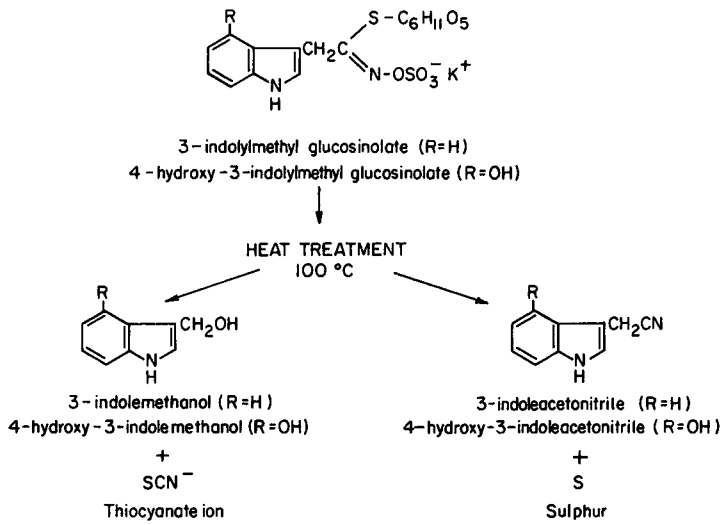

Fig. 1. Proposed pathway of the thermal degradation of indole glucosinolates.

the thermal degradation products of indole glucosinolates. In contrast to the potential antinutritive effects of *Brassica* vegetables, studies have indicated a possible beneficial effect in humans due to the fact that some indole compounds originating from the intact glucosinolates in the vegetables were shown to be inhibitors of chemically induced carcinogenesis and to stimulate the activity of key enzymes involved in cellular detoxification systems[6]. Further research in these areas is warranted and the procedure reported herein for determining indoleacetonitriles should facilitate such research.

EXPERIMENTAL

Materials

Commercial low-glucosinolate rapeseed meal samples were obtained from crushing plants located in Western Canada and the *Brassica* vegetable samples were purchased at a local supermarket. Indole-3-acetic acid, 3-indoleacetonitrile and *n*-octadecane were obtained from Sigma (St. Louis, MO, U.S.A.). Pyridine and bis(trimethylsilyl)-trifluoroacetamide (BSTFA) were purchased from Pierce (Rockford, IL, U.S.A.). Methylene chloride was from Burdick and Jackson (Muskegon, MI, U.S.A.).

Gas chromatographic analysis of indoleacetonitriles

Rapeseed meal or *Brassica* vegetable samples (0.5 g) were weighed into 125-ml erlenmeyer flasks. Distilled water was then added and the mixture was allowed to stand for 5 min to form a paste. The standard procedure involved the use of 1 and 5 ml of water for rapeseed meal and freeze-dried vegetable samples, respectively. Portions of 20 and 30 ml of methylene chloride were then added, respectively to rapeseed meal and vegetable samples, followed by 1 ml of a methylene chloride solution of internal standard (0.25 μmol ml^{-1} *n*-octadecane). The flasks were sealed and shaken in an orbit shaker for 15 min at 200 rpm. Following extraction, the methylene chloride extracts

were filtered (Whatman No. 3 filter paper) into 50-ml evaporating flasks, concentrated under vacuum to approximately 1 ml and transferred by Pasteur pipette into 4-ml silylation vials. Following drying under a stream of nitrogen the samples were derivatized at room temperature by adding 50 μl pyridine and 50 μl BSTFA to each vial which was then capped and mixed well prior to gas chromatographic (GC) analysis. The trimethylsilyl (TMS) derivatized indoleacetonitriles were separated by using a Varian Vista 6000 gas chromatograph equipped with a flame ionization detector and a Vista 402 computer. A glass column (1.8 m × 2 mm I.D.) packed with 3% OV-1 on Chromosorb W (HP) (100–120 mesh) was used with helium gas at a flow-rate of 40 ml min^{-1}. The oven temperature was programmed from 120 to 220°C at 5°C min^{-1}. Injection port and detector temperatures were 200 and 250°C, respectively.

During development of the method, sample to water ratio and extraction time were studied to effect complete extraction of indoleacetonitriles from the samples. In addition, time and temperature conditions of derivatization with BSTFA were also studied.

Determination of relative response factors

Relative response factors (RRF) were determined by using pure IAN (Sigma) and a sample of isolated OH-IAN. A known amount (1 μmol) of each compound was used with *n*-octadecane as internal standard in the determination of the response factors.

Isolation of OH-IAN was done since this compound is not commercially available. Column chromatography (CC, Sepahdex LH-20) and thin-layer chromatography (TLC, silica gel 60) as described by Slominski and Campbell[4] were used in the isolation and purification. In the quantification of OH-IAN, GC of a 80% methanol TLC eluate was conducted while using indole-3-acetic acid as a reference compound. Following derivatization with pyridine and BSTFA (1:1, v/v) for 15 min at 50°C[7] indole-3-acetic acid and OH-IAN were separated on a 3% OV-1 column with the response set at 1.00. This was based on the assumption that both compounds would respond identically in the flame ionization detector due to similar chemical structures, *i.e.*, two TMS groups attached to the molecule and the same number of carbon atoms.

Indoleacetonitrile analysis and recovery studies

Seven samples of low-glucosinolate rapeseed meal and four samples of cooked *Brassica* vegetables were analyzed for content of indoleacetonitriles by using the proposed procedure. The samples of *Brassica* vegetables included white and red cabbage, broccoli and Brussels sprouts. Prior to analysis the vegetable samples were boiled (100°C) for 40 min, freeze-dried and ground. Three recovery experiments were conducted using rapeseed meal and white cabbage with a known amount (1 μmol g^{-1}) of IAN added to each sample.

RESULTS AND DISCUSSION

Examples of gas chromatograms of trimethylsilyl derivatives of indoleacetonitriles from commercial low-glucosinolate rapeseed meal and cooked white cabbage leaves are shown in Fig. 2. Although both indoleacetonitriles were well separated in a total run time of 17 min, the analysis was continued for an additional 3 min to allow the removal of impurities from the column.

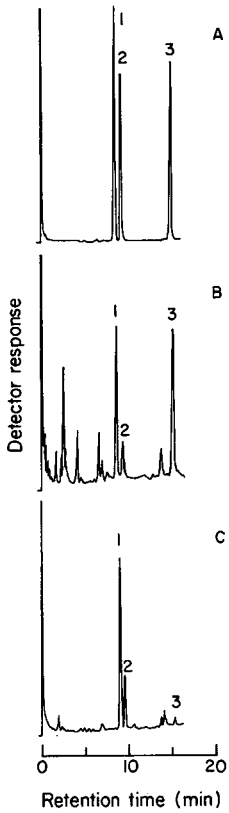

Fig. 2. Gas chromatogram of TMS derivatives of indoleacetonitriles from (A) a mixture of pure compounds, (B) low-glucosinolate rapeseed meal and (C) cooked white cabbage leaves. Peaks: 1 = *n*-octadecane (internal standard); 2 = IAN; 3 = OH-IAN.

The influence of the amount of water added to rapeseed meal samples on the extraction of indoleacetonitriles by methylene chloride is shown in Fig. 3. The data indicated that a ratio of 1:1 (w/v) was sufficient to result in maximal extraction of both IAN and OH-IAN from rapeseed meal samples. As a standard procedure, however, it is recommended that for air-dry rapeseed meal samples a ratio of sample to water of 1:2 be used. In the case of freeze-dried vegetable samples the ratio of sample to water to effectively extract the indoleacetonitriles was found to be 1:10. No additional water was required, however, for the analysis of non-freeze-dried (*i.e.* fresh) cooked or steamed samples of vegetables.

The effect of time of extraction on the recovery of indoleacetonitriles is shown in Fig. 4. Extraction was maximal within 10–15 min and consequently an extraction time of 15 min was adopted for the standard procedure. Derivatization of a methylene chloride extract of rapeseed meal under different conditions showed no significant differences with respect to the times (1–20 min) or temperatures (20 and 60°C) applied (Fig. 5). In previous work derivatization of indoleacetonitriles was carried out at 60°C for 15 min[4]. Under those conditions it was demonstrated that the nitrogen atom of the indole ring of both IAN and OH-IAN and the hydroxyl group of OH-IAN were

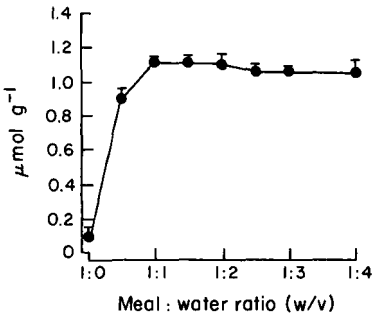

Fig. 3. Effect of different meal to water ratios on the extraction of indoleacetonitriles with methylene chloride.

effectively trimethylsilylated. The results from the current study indicated that derivatization is effective at 20°C and consequently it is recommended that derivatization be conducted at room temperature in the proposed procedure.

The RRF values determined for IAN and OH-IAN are given in Table I. The RRF values for both compounds are approximately 15% higher than values calculated based on TMS-nitrile and *n*-octadecane carbon number. This apparent discrepancy may be explained by a differential response between aromatic and aliphatic compounds in the flame ionization detector. A similar response difference between aromatic and aliphatic glucosinolates has been reported[1,8]. It should be noted that the RRF values reported herin cannot be applied arbitrarily and should be determined for specific column and chromatographic conditions.

The recoveries of IAN added to samples of rapeseed meal and white cabbage leaves are shown in Table II. Since IAN is readily soluble in methylene chloride and due to the fact that no clean-up procedure is used in the proposed method, the data demonstrating complete recovery (98–101%) are more a confirmation of the accuracy of the RRF value for IAN than recovery *per se*. Another estimate of recovery, however, can be obtained from the data presented in Fig. 3 and 4. The constant amounts of indoleacetonitriles determined in samples of rapeseed meal and cabbage leaves subjected to varying but optimum extraction conditions is an indication of adequate recovery of the nitriles from these samples.

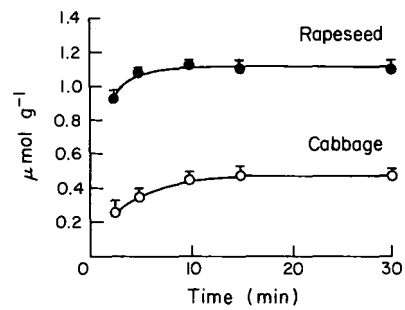

Fig. 4. Effect of varying times of extraction on the recovery of indoleacetonitriles from rapeseed meal and cooked white cabbage leaves.

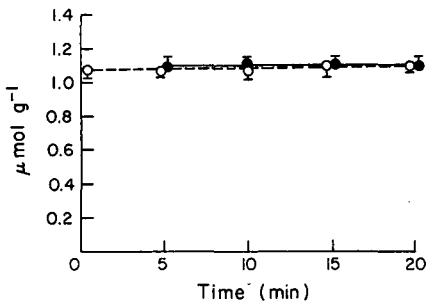

Fig. 5. Effect of different derivatization conditions on the recovery of indoleacetonitriles. (●) 60°C; (○) 20°C.

A number of samples of low-glucosinolate rapeseed meal and of cooked *Brassica* vegetables were analyzed for IAN and OH-IAN by the proposed method (Table III). Total indoleacetonitriles content averaged at 0.8 μmol g^{-1} for the seven rapeseed meal samples. The predominant indoleacetonitrile was OH-IAN which would be expected since 4-hydroxyglucobrassicin is the major intact indole glucosinolate in low-glucosinolate rapeseed meal[1]. Results have shown that in rapeseed meal approximately 5–6 μmol g^{-1} of intact indole glucosinolates are decomposed during heat treatment and that of the decomposed indoles 2.0 μmol g^{-1}, on average, appear as free SCN[1]. The results from the current study indicate that indoleacetonitriles may account for an additional 0.8 μmol g^{-1} which leaves approximately 2–3 μmol g^{-1} of decomposed indoles unaccounted for. This confirms that degradation products other than SCN or indoleacetonitriles are formed during the heat treatment of indole glucosinolates as suggested by Campbell and Slominski[3].

TABLE I

RELATIVE RESPONSE FACTORS (RRF) FOR IAN AND OH-IAN WITH *n*-OCTADECANE AS INTERNAL STANDARD (RRF = 1)

Compound	*Relative response factor*	
	Calculated	*Determined*
IAN	1.38	1.58
OH-IAN	1.12	1.36

TABLE II

PERCENT RECOVERY OF IAN ADDED TO SAMPLES OF RAPESEED MEAL AND WHITE CABBAGE LEAVES

Sample	*Recovery (%)**
Rapeseed meal	101.0 ± 1.0
White cabbage	98.2 ± 2.3

* Mean ± S.D.

TABLE III

CONTENTS OF IAN AND OH-IAN IN COMMERCIAL LOW-GLUCOSINOLATE RAPESEED MEAL AND COOKED *BRASSICA* VEGETABLES

Sample	*IAN*	*OH-IAN*	*Total*
Rapeseed meal (μmol g^{-1} air-dry weight)			
Meal 1	0.15	0.60	0.75 ± 0.02*
Meal 2	0.11	0.66	0.77 ± 0.02
Meal 3	0.24	0.68	0.92 ± 0.01
Meal 4	0.10	0.56	0.66 ± 0.03
Meal 5	0.31	0.82	1.13 ± 0.03
Meal 6	0.14	0.61	0.74 ± 0.02
Meal 7	0.09	0.64	0.73 ± 0.01
Vegetable (μmol g^{-1} dry weight)			
White cabbage	0.41	0.07	0.48 ± 0.01
Red cabbage	0.19	0.07	0.26 ± 0.03
Broccoli	0.20	0.03	0.23 ± 0.02
Brussels sprouts	2.43	0.11	2.54 ± 0.06

* Mean of duplicate determinations, ±S.D.

The amount of indoleacetonitriles in *Brassica* vegetables (Table III) was more variable than that noted for the rapeseed meal samples, which could be explained by the high variability in intact indole glucosinolate content among and within species of cruciferous vegetables[2]. In contrast to the rapeseed meal samples, IAN rather than OH-IAN was the predominant indoleacetonitrile which corresponds to the high amount of glucobrassicin in these vegetables[2]. In addition, the highest level of IAN was present in Brussels sprouts which are known to contain a relatively high amount of glucobrassicin[9]. The data presented in Table III, however, does not represent a total amount of IAN and OH-IAN produced upon the thermal decomposition of indole glucosinolates in *Brassica* vegetables since substantial leaching may occur during the cooking process[5].

ACKNOWLEDGEMENTS

Partial funding provided by the Canola Utilization Assistance Program of the Canola Council of Canada and by the Natural Sciences and Engineering Research Council of the Government of Canada is gratefully acknowledged.

REFERENCES

1 B. A. Slominski and L. D. Campbell, *J. Sci. Food Agric.*, 40 (1987) 131.
2 G. R. Fenwick, R. K. Heaney and W. J. Mullin, *J. CRC Crit. Rev. Food Sci. Nutr.*, 18 (1983) 123.
3 L. D. Campbell and B. A. Slominski, *J. Sci. Food Agric.*, in press.
4 B. A. Slominski and L. D. Campbell, *J. Sci. Food Agric.*, in press.
5 B. A. Slominski and L. D. Campbell, *J. Agric. Food Chem.*, submitted for publication.
6 National Research Council, *Diet, Nutrition and Cancer*, National Academy Press, Washington, DC, 1982, Ch. 15, p. 151.
7 R. S. Bandurski and A. Schulze, in J. R. Hillman (Editor), *Isolation of Plant Growth Substances*, Cambridge University Press, London, New York, Melbourne, 1978, p. 12.
8 J. K. Daun and D. I. McGregor, *Glucosinolate Analysis of Rapeseed (Canola)*, Agriculture Canada, Winnipeg, 1983.
9 R. K. Haeney and G. R. Fenwick, *J. Sci. Food Agric.*, 31 (1980) 785.

Journal of Chromatography, 454 (1988) 293–301
Elsevier Science Publishers B.V., Amsterdam — Printed in The Netherlands

CHROM. 20 819

DETERMINATION OF COTININE IN URINE USING GLASS CAPILLARY GAS CHROMATOGRAPHY AND SELECTIVE DETECTION, WITH SPECIAL REFERENCE TO THE BIOLOGICAL MONITORING OF PASSIVE SMOKING

GUNNAR SKARPING*
Department of Occupational Medicine, University Hospital, S-221 85 Lund (Sweden)
STEFAN WILLERS
Department of Occupational Medicine, Malmö General Hospital, S-214 01 Malmö (Sweden)
and
MARIANNE DALENE
Department of Occupational Medicine, University Hospital, S-221 85 Lund (Sweden)
(First received March 7th, 1988; revised manuscript received July 20th, 1988)

SUMMARY

A capillary gas chromatographic (GC) method using selected-ion monitoring (SIM) was developed for the analysis of cotinine (C.A.S. No. 486-56-6) in human urine. The method is based on basic extraction of cotinine from 2 ml of urine into dichloromethane. After evaporation of the dichloromethane solution to dryness, 100 μl of toluene were added, prior to GC–mass spectrometric (MS) analysis. Trideuterated cotinine (C.A.S. No. 97664-65-8) was used as the internal standard. More than 1000 automatic chromatographic analyses were made without column degradation. Molecular ions (M) of cotinine and trideuterated cotinine, (m/e = 176 and 179), were monitored in the electron impact (EI) mode and m/e = 177 (M + 1) and m/e = 180 (M + 1) in the chemical ionization (CI) mode with isobutane. The correlation coefficient with SIM and EI was 0.998 (5–20 ng/ml) and with CI was (0.2–2 ng/ml). For thermionic specific detection the correlation coefficient was 0.998 (10–510 ng/ml). Only capillary columns with an apolar bonded stationary phase film thickness of 1 μm showed sufficient inertness for cotinine analysis at the sub ng/ml level. The relative standard deviations for 5 and 20 ng/ml were 5.2 and 3.5% respectively (n = 12) using EI. Spiked urine samples from six non-smokers (5 ng/ml) showed a relative standard deviation of 5%. The overall recovery (25 ng/ml) was 100 $\pm$ 4%. The minimum detectable concentration, using SIM, was *ca.* 2 ng/ml in the EI mode and *ca.* 0.2 ng/ml in the CI mode. The half-time for cotinine was *ca.* 18 h for both active smokers and non-smokers.

INTRODUCTION

Passive smoking, *i.e.*, the exposure of non-smokers to tobacco smoke, has been shown to be an health hazard. Monitoring the exposure to environmental tobacco

0021-9673/88/$03.50

smoke[1–3] is important because passive smoking has created health problems in homes and work places[4–10]. Due to its relatively long half-life, cotinine, a major nicotine metabolite, has been shown to be the intake marker of choice[11–14]. The purpose of a marker of passive smoking is to evaluate exposure, quantitate the intake, validate non-smokers status[15–17] and provide feedback to encourage smokers to stop smoking.

Several analytical techniques have been used for the determination of cotinine in biological fluids. The methods described in the literature have been compared by Daenens[18]. The most frequently used methods of the low nanograms per ml level are radioimmunoassay (RIA), liquid chromatography (LC)[19] and gas chromatography (GC) with flame ionization, electron-capture, and nitrogen selective detection[20–23] or selected-ion monitoring (SIM)[18,24–26]. Interlaboratory studies have recently been performed for the determination of cotinine in urine[23,27].

Glass capillary GC and nitrogen selective detection has successfully been used[21,23] with detection limits, for cotinine in plasma, of 0.4 ng/ml; N-ethyl-norcotinine was used as the internal standard. SIM of cotinine in plasma or urine, with methylprylone or trideuterated cotinine as the internal standard, has been demonstrated. The detection limit was found to be below 1 ng/ml with electron impact ionization.

In this work we present a method for determination of cotinine at the low ng/ml level in human urine samples using fused-silica capillary columns and SIM. The detection is performed both in the electron impact (EI) mode and in the chemical ionization mode with isobutane as the reagent gas. The main purpose is to evaluate the involuntary exposure to tobacco smoke.

EXPERIMENTAL

Apparatus

A Varian 3500 gas chromatograph equipped with Varian thermionic specific detection (TSD) and a Varian 8035 automatic on-column injector was employed. The injector was cooled with liquid nitrogen. The temperature of the injector was initially 105°C for 5 s and thereafter programmed at 150°C/min to 280°C. After 2 min isothermal, the column oven was programmed at 20°C/min to 290°C and then held for 5 min. Typical settings for the detector were: bead heating current 3.10 A; bias voltage −3.9 V; detector temperature 270°C, gas flow-rates 3 ml/min of hydrogen, 175 ml/min of air and 20 ml/min of nitrogen as the make-up gas. Chromatograms were recorded on Servogor Model 310 linear recorders and Shimadzu CR3A integrators were used for peak evaluation.

A Shimadzu GC–MS QP1000 EI/CI quadrupole mass spectrometer was connected to a Shimadzu GC 9A gas chromatograph equipped with a split/splitless injection system spl-69 and a Shimadzu autosampler AOC-9. The starting temperature of the column oven was set near to the solvent boiling point, and in the case of toluene it was 95°C isothermal for 3 min. The split exit valve was kept closed for 1 min after injection. After elution of the solvent, the column was programmed at 5°C/min to 110°C, then at 30°C/min to a final temperature of 280°C which was maintained for 5 min. The capillary column outlet was mounted directly in the ion source. The gas chromatograph–mass spectrometer interface and the ion source were held at 250°C. The pressure in the ion source was *ca.* $1.5 \cdot 10^{-5}$ Torr. Instrument characteristics for

the QP 1000 were set as follows: *m/e* 176 and 179, molecular ions (M) of cotinine and trideuterated cotinine, were monitored in the EI mode and *m/e* = 177 (M + 1) and *m/e* = 180 (M + 1) in the chemical ionization (CI) mode. The filament in the ion source was turned on after 6 min and off after 14 min. Five measurements were made per second (rate 3). The tuning of the instrument (autotuning) was performed using a standard sample inlet system and the standard sample used was perfluorotributylamine (PFTBA), according to standard procedures (70 eV). The resolution was set to maximum. Three reagents gases, isobutane, ammonia and methane, were tested for CI of cotinine. The pressure in the ion source was kept at *ca.* $3 \cdot 10^{-5}$ Torr. The gas chromatography–mass spectrometry (GC–MS) conditions were set as follows: Samples were introduced into the chromatographic system with an autosampler using a splitless injection technique at 250°C with an inlet pressure of helium of 0.2 kg/cm^2. The amount injected was typically 1–2 μl using an Hamilton 701RN syringe with a point style 5 needle with a conical point and a sidehole to minimize septum coring. A Sigma 3E-1 centrifuge (Sigma Harz, F.R.G.) was employed for phase separation.

Columns

Four different types of fused-silica capillary columns with chemically bonded stationary phases were used: NORDION® (Helsinki, Finland) flexibond capillary columns NB-54 (25 m × 0.32 mm I.D.) with film thickness of 0.1, 0.25, 0.5 and 1.0 μm.

Chemicals

Chemicals used were toluene and dichloromethane from Janssen (Beerse, Belgium), cotinine (C.A.S. no. 486-56-6) and trideuterated cotinine (C.A.S. no. 97664-65-8) picrate from the Swedish Tobacco Company (Stockholm, Sweden) and PFTBA from E. Merck (Darmstadt, F.R.G.).

Preparation of standard solutions

Standard solutions of cotinine were prepared by dissolving accurately weighed amounts of cotinine (*ca.* 50 mg) in 100 ml aqueous solution of 0.1 *M* hydrochloric acid, and further dilution of this solution in hydrochloric acid to the desired concentrations. Typically, solutions containing 5 or 20 ng/ml were used in the work-up procedure where the addition of 1 ml of water was exchanged for the described standard solution. Standard solutions of trideuterated cotinine were prepared by dissolving *ca.* 10 mg of the compound in the manner described above.

Storage of standards

Standard solutions were stored in acidic aqueous solutions at room temperature and diluted solutions of concentrations less than 100 ng/ml were kept in a refrigerator. Diluted standard solutions could be used only for *ca.* 2 weeks.

Sampling and storage of samples

In the application the total urine volume from the test persons was sampled and each batch was analysed for creatinine, pH, density and cotinine concentration according to the method presented. All urine samples were kept frozen until analyzed, and no losses of cotinine were observed during this storage. Urine samples were stored in 10 ml test-tubes kept in a deep-freezer at −20°C.

Procedure

A 2-ml urine sample was added to a mixture of 1 ml water, 0.5 ml of a standard solution containing 202.5 ng/ml of trideuterated cotinine as the internal standard, 2 ml 5 *M* sodium hydroxide and 3 ml dichloromethane. The mixture was shaken for 10 min and centrifuged at 4000 rpm for 20 min. The main part of the aqueous layer was removed. The sample tube was then taken to a cooling solution consisting of solid carbon dioxide and acetone until the remaining water was frozen. The dichloromethane solution was then transferred to the test-tube. The solvent was evaporated to dryness at 30°C in a vacuum desiccator connected to an aspirating pump where several test-tubes containing sample solutions could simultaneously be evaporated. The vacuum desiccator was equipped with an electrically heated oven for the simultaneous treatment of 25 sample tubes. The residue was dissolved in 100 μl toluene and transferred to an autosampler vial, with an 100-μl conical insert, ready for the GC–MS analysis. For each sample, two determinations with duplicate injections were performed and the average values of the peak area or peak height ratios were used.

Standard solutions of cotinine in water were added to blank urine and injected in series with real samples. Every third sample was a standard (5 and 20 ng/ml).

For GC-TSD, the dry residue was dissolved in 100 μl of toluene containing the isobutyl chloroformate derivative of di-*n*-butylamine (200 ng/ml).

RESULTS AND DISCUSSION

Standards

Cotinine and trideuterated cotinine were identified by GC–MS and the purity was checked by GC-TSD and GC-FID. The purity was found to be better than 99%.

Chromatography

The NB-54 apolar columns with a film thickness of 1 μm gave symmetrical peaks and virtually no adsorption in the investigated range of 10–1000 ng/ml of cotinine in toluene. The elution temperature for cotinine (*ca.* 280°C) resulted in no column bleeding, after conditioning the column for 48 h, that interfered with SIM.

Several capillary columns were tested. Due to the adsorption, only capillary columns with an apolar bonded stationary phase film thickness of 1 μm showed sufficient inertness for cotinine analysis in the sub ng/ml range. The bonded Carbowax columns showed considerable column bleeding at the elution temperature of cotinine, giving unstable conditions and higher detection limits for cotinine compared with those obtained on apolar stationary phases. The removal of water (freezing out), described in the Procedure, increased the column lifetime considerably, making possible 1000 chromatographic experiments without any noticeable column degradation and absorption losses. Frequent testing is recommended to evaluate the adsorption behaviour of cotinine and N-ethylnorcotinine in the chromatographic system.

Detection

Nitrogen selective detection. TSD is as sensitive as SIM in the CI mode and ten times more sensitive than in the EI mode. The use of high resolution capillary columns has made it possible to use TSD for detection of cotinine. However, when analysing

cotinine in urine several nitrogen-containing compounds appear in the chromatogram and the matrix[28] is not constant. Considerable care must be taken to avoid contaminants in the concentration range of passive smoking (a few nanograms per ml). The detection limit is mainly set by the matrix. Inter-individual variations in urine composition can influence the analysis.

In order to obtain detection limits with TSD in the same order of magnitude as with SIM, further work-up is necessary.

Mass selective detection. Trace determination of cotinine with the procedure described in the Experimental demands introduction of 1 μl or more of the resulting toluene solution into the chromatographic system. However, the ion source and the high vacuum system can be severely damaged and contaminated when large volumes of solvents are introduced. Usually the solvent is eliminated using a solvent cut and a jet separator. This may result in sample losses and poor reproducibility. The low carrier gas flow in the capillary column enables a direct inlet of the capillary column into the ion source without disturbing the high vacuum system. Attempts were made to perform the analysis with the column connected directly to the ion source. This however resulted in poor reproducibility with a decreasing sensitivity and short lifetime of the filament. The ion source became severely contaminated after some injections and frequent rinsing was therefore necessary. When the filament was switched off during the entrance of the solvent and later turned on during the chromatographic analysis these problems were eliminated. Using this procedure, we performed several hundreds of analyses without a decrease in sensitivity and with excellent reproducibility during several weeks. It was sufficient to tune the instrument once a month which makes this procedure very well suited for routine analysis.

As mentioned earlier the chromatographic behaviour of cotinine is excellent in our system. The mass spectrometer was employed in the EI mode at 70 eV. Fig. 1 shows the peaks of the molecular ion of cotinine and trideuterated cotinine from an urine sample at a concentration of 20 ng/ml. No interfering peaks were observed in the urine samples studied. The mass spectrometer was also employed in the CI mode with isobutane as the reaction gas. Fig. 2 shows the peaks of cotinine and trideuterated cotinine in urine, using CI.

Quantitative analysis

Calibration graphs. The calibration graphs for cotinine in toluene solution using capillary GC-TSD with an automated cold on-column injector gave virtually linear calibration plots of the peak area ratio or peak height ratio *vs.* concentration. The calibration graph of the peak area ratio passed through the origin with a correlation coefficient of 0.999 ($n = 34$, $p = 0.0001$) in the concentration range investigated (10–510 ng/ml and peak area ratio 0.06–2.5) of cotinine in toluene. The slope was 0.004 and the intercept was 0.03 for peak area measurements.

The calibration graphs for cotinine in urine using capillary GC and SIM in the EI mode and the CI mode were constructed as follows. Different amounts of cotinine were added to aqueous solutions or to urine and the entire work-up was performed as described above. For each concentration, duplicate determinations with duplicate injections were made and the average values of the peak area or peak height were plotted. In the case of EI the average value of the ratio of the signal of the $m/e = 176$ molecular ion to that of the molecular ion of the internal standard, $m/e = 179$, was

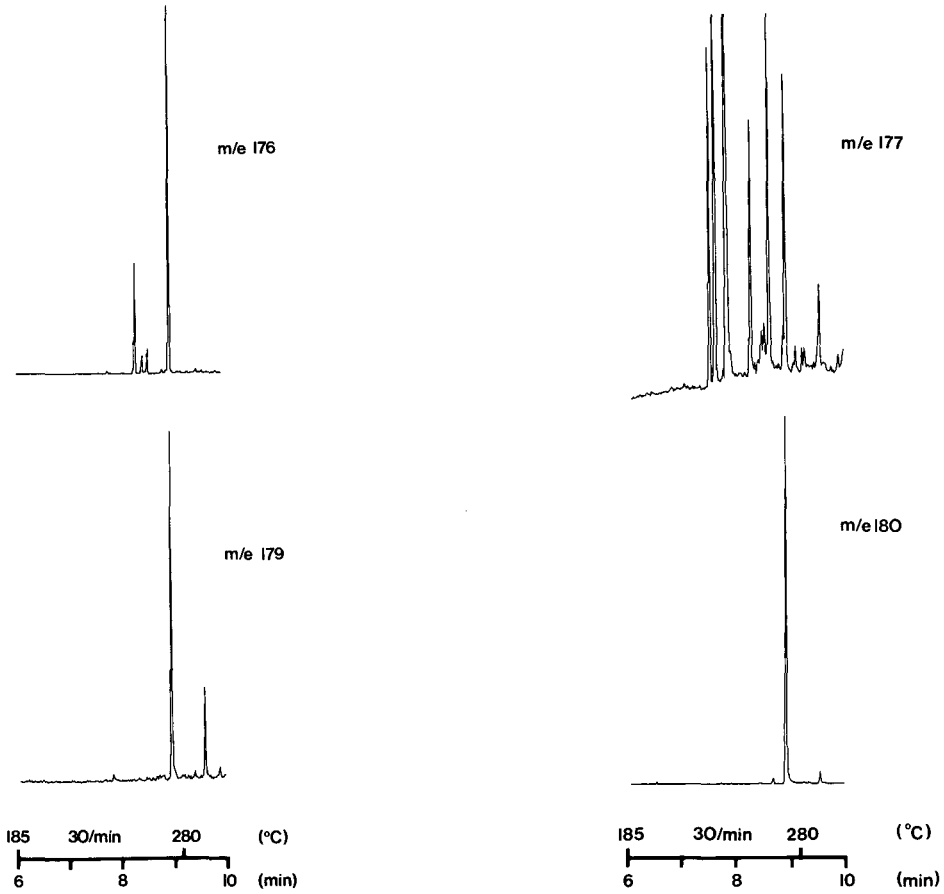

Fig. 1. Selected ion monitoring of urine samples using the EI ionization mode. The upper chromatogram shows the molecular ion of cotinine (176) from an urine sample from a 5-year-old asthmatic boy, whose parents both smoked *ca.* 20 cigarettes each evening. The peak corresponds to a concentration of *ca.* 40 ng per ml of urine, the lower chromatogram shows the molecular ion of trideuterated cotinine (179) used as an internal standard. Column: fused silica coated with SE-54 bonded stationary phase (25 m × 0.32 mm I.D.), film thickness 1.0 μm. Inlet pressure of the carrier gas (helium); 0.2 kg/cm^2. Splitless injection (1 min) of 1 μl toluene. Temperature programming: isothermal at 95°C (3 min), raised at 5°C/min to 110°C, then at 30°C/min to a final temperature of 280°C which was maintained for 5 min.

Fig. 2. Selected ion monitoring of cotinine in a spiked urine sample corresponding to a concentration of 0.5 ng/ml of cotinine, using CI with isobutane as the ionization gas and the M + 1 ion for detection. Upper: molecular ion (M + 1) of cotinine (177). Lower: molecular ion (M + 1) of trideuterated cotinine (180). Chromatographic conditions as in Fig. 1.

plotted. The calibration graph for the concentration range investigated (0–20 ng/ml and peak height ratio 0.007–1.72) of cotinine in urine and peak height ratio measurements gave a correlation coefficient of 0.998 ($n = 5$, $p = 0.0001$). The slope was 0.085 and the intercept was −0.004. No noticeable difference was found between aqueous solutions and urine and no significant difference between peak area or peak height ratio measurements. The use of CI with isobutane gave a linear calibration plot

in the concentration range investigated (0.2–2 ng/ml and peak height ratio 0.01–0.055) of cotinine in urine. The correlation coefficient was 0.996 ($n = 6, p = 0.0001$) for the average peak area ratio six concentrations with duplicate injections. The slope and the intercept were 0.02 and 0.01 respectively. The response curve was linear for the GC–MS mode in the ranges 1–100 ng/ml (EI) and 0.2–10 ng/ml (CI) and in the case of GC-TSD in the range 5–50 000 ng/ml for an injected volume of 1 μl.

The detection limit determined from the intercept according to Miller and Miller[29] was 2.2 ng/ml of urine with GC–MS using the EI mode and 0.20 ng/ml in the CI mode using isobutane as the reagent gas. For the calibration plots above we used urine from one of our non-smoking colleagues having a very low estimated exposure to tobacco smoke. In no urine tested so far was the concentration of cotinine found to be zero. For water solutions no cotinine was found, resulting in a practically zero intercept. The detection limit in aqueous solutions is therefore at least one decade lower than in human urine.

Recovery. The overall recovery was studied by working-up ten urine samples spiked with cotinine to a concentration of 25 ng/ml. Ten urine samples of the same concentration were then worked up by the same procedure but with no internal standard present. In the final step of the work-up procedure before the evaporation of the dichloromethane solution, 1 ml of dichloromethane containing the same amount of internal standard was added. The separately prepared solutions yielded a ratio between cotinine and internal standard of 100 $\pm$ 5% and 98 $\pm$ 5.2% for the peak height ratio comparison and 100 $\pm$ 5 and 102 $\pm$ 4.6% for the peak area ratio comparison. The values are given with a 95% confidence range.

The procedure of extraction of cotinine from urine samples to the dichloromethane solution was investigated and the recovery was *ca.* 100%. The recovery in the evaporation step was also studied. After working-up ten urine samples, 10 μl of a toluene solution containing 2500 ng/ml of cotinine were added to the dichloromethane solution in the final step before evaporation of the solvent. The following samples were then compared with a solution containing 250 ng/ml. For a confidence range of 95%, the recovery in the evaporation step was 98.8 $\pm$ 3% based on peak areas $n = 10$. Standard solutions of cotinine and internal standard were injected, and the peak height and peak area ratio were established. The temperature-controlled vacuum desiccator, designed at our laboratory, made it possible to evaporate 25 samples containing 1 ml dichloromethane within 1 h and to study the possible evaporation losses in detail. No artefact and no carry over was found during this procedure.

Accuracy and precision. The usefulness of a deuterium-labelled internal standard is shown by the very good precision in the analysis even at the low ng/ml level. When analysing twelve different standard samples in urine at concentrations of 5 and 20 ng/ml respectively with the entire work-up procedure followed by GC with multiple ion detection (MID) during 2 weeks, the relative standard deviations of the ratio between the area of the cotinine and the trideuterated cotinine molecular ion peak were 5.2 (100 $\pm$ 3%) and 3.5% (100 $\pm$ 2%) respectively. When analysing urine from six non-smoking colleagues spiked to a concentration of 5 ng/ml (the blank was subtracted), the relative standard deviation of the peak height ratio between cotinine and trideuterated cotinine was 5% (100 $\pm$ 5%). The values in brackets are given with a 95% confidence range.

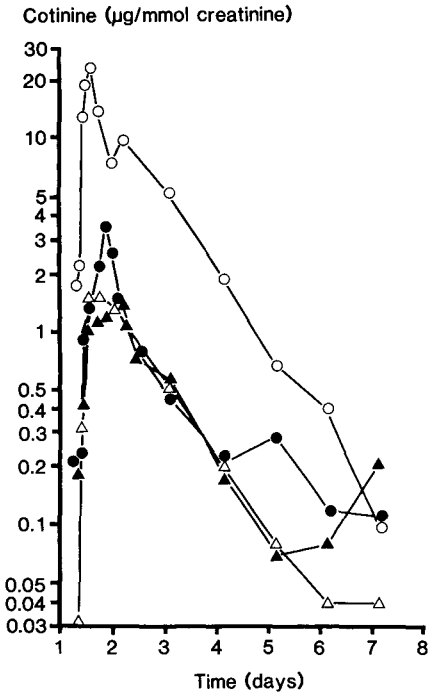

Fig. 3. Elimination curves of cotinine in urine from four male persons, one active smoker (○) and three passive smokers (△, ▲, ●). The active smoker consumed 20 cigarettes during 1.5 h in the presence of the three non-smokers while driving a car with closed windows and normal ventilation.

Applications

Four male persons were placed in a car, which was driven for 1.5 h. One person was an active smoker who consumed 20 cigarettes during this hour and the other three persons were non-smokers. The three non-smokers were told not be exposed for tobacco smoke for 1 week before and 1 week after this test was applied. The cotinine concentrations in urine, using GC-SIM and EI, *versus* creatinine concentrations were monitored for all four persons and the results are plotted in Fig. 3. This figure shows *ca.* 20 times higher cotinine levels for the active smokers *versus* the three non-smokers. Actually, person 1 visited a public restaurant on day 5 for less than 2 h and person 3 was in an apartment on day 6 where another person smoked a few cigarettes. From the elimination curve it is possible to estimate the half-time of cotinine in urine. It was found to be *ca.* 18 h for both active smokers and non-smokers, in agreement with findings by other workers[12,14]

CONCLUSIONS

The method described for the determination of cotinine in human urine based upon high resolution gas chromatography–mass fragmentography makes it possible to determine cotinine in a more complex matrix than is the case with GC-TSD. No special clean-up procedure is necessary and several samples can be worked up simultaneously. Very selective and sensitive determinations of cotinine at the

sub ng/ml level are possible. The use of trideuterated cotinine as the internal standard gave accurate and precise determinations. The combination of high resolution chromatography and selective detection is an appropriate choice for the analysis of cotinine in biological matrixes at the low ng/ml level. Mass fragmentography is well suited to this task.

ACKNOWLEDGEMENTS

We are indebted to Professor Staffan Skerfving, head of the department of Occupational Medicine, for his interest in this work. We also gratefully acknowledge the skilful technical assistance of Miss Anita Hultberg, and the Swedish Work Environment Fund for financial support. We thank Dr. Antti Manninen, NORDION instruments Oy Ltd. (Finland) for supplying dedicated capillary columns and Dr. Margareta Curvall for deuterium-labelled standards. We also gratefully acknowledge Dr. Sven Jackobsson (Apotekarnas Compositae, Stockholm, Sweden) for valuable discussion, especially concerning automatization of the filament on/of procedure for the ion source.

REFERENCES

1 Y. Saint-Jalm and P. Moree-Testa, *J. Chromatogr.*, 198 (1980) 188–192.
2 I. Schmeltz and D. Hoffmann, *Chem. Rev.*, 77 (1977) 295.
3 R. F. Severson, K. L. McDuffie, R. F. Arrendale, G. R. Gwynn, J. F. Chaplin and A. W. Johnson, *J. Chromatogr.*, 211 (1981) 111.
4 R. A. Greenberg, *New England J. Med.*, 310 (1984) 1075.
5 E. N. Pattishall, G. L. Strope, R. A. Etzel, R. W. Helms, N. J. Haley and F. W. Denny, *Am. J. Dis. Child.*, 139 (1985) 1101.
6 S. Matsukura, T. Taminato, N. Kitano, Y. Seino, H. Hamada, M. Uchihashi, H. Nakajima and Y. Hirata, *New England J. Med.*, 311 (1984) 828.
7 M. J. Jarvis, A. D. McNeill, M. A. H. Russell, R. J. West, A. Bryant and C. Feyerabend, *Lancet*, i (1987) 1324–1325.
8 M. J. Jarvis, M. A. H. Russell, C. Feyerabend, J. R. Eiser, M. Morgan, P. Gammage and E. M. Gray, *Br. Med. J.*, 291 (1985) 927.
9 M. J. Jarvis, M. A. H. Russell and C. Feyerabend, *Thorax*, 38 (1983) 829.
10 A. Weber and T. Fischer, *Int. Arch. Occup. Environ. Health*, 47 (1980) 209.
11 D. T. Darby, J. E. McNamee and J. M. van Rossum, *Clin. Pharmacokin.*, 9 (1984) 435.
12 L. C. Johnson, H. Letzel and J. Kleinschmidt, *Int. Arch. Environ. Health*, 56 (1985) 99.
13 N. J. Wald, J. Boreham, A. Bailey, C. Ritchie, J. E. Haddow and G. Knight, *Lancet*, i (1984) 230–231.
14 R. Hopkins, L. E. Wood, M. I. Biol and N. M. Sinclair, *Clin. Pharmacol. Ther.*, 36 (1984) 788.
15 K. Husgafvel-Pursiainen, *Doctoral thesis*, ISBN 951-801-585-6, Helsinki, 1987.
16 P. N. Lee, *Toxicol. Lett.*, 35 (1987) 157.
17 K. Überla, *Int. Arch. Occup. Environ. Health*, 58 (1987) 421.
18 P. Daenens, L. Laruelle, K. Callewaert, P. de Schepper, R. Galeazzi and J. van Rossum, *J. Chromatogr.*, 342 (1985) 79.
19 D. A. Machacek and N. Jiang, *Clin. Chem.*, 32 (1986) 979.
20 C. Feyerabend and M. A. H. Russell, *Analyst (London)*, 105 (1980) 998.
21 M. Curvall, E. Kazemi-Vala and C. R. Enzell, *J. Chromatogr.*, 232 (1982) 283–293.
22 G. Stehlik, J. Kainzbauer, H. Tausch and O. Richer, *J. Chromatogr.*, 232 (1982) 295.
23 R. A. Davies, *J. Chromatogr. Sci.*, 24 (1986) 134.
24 J. Dow and K. Hall, *J. Chromatogr.*, 153 (1978) 521.
25 J. A. Thompson, Ming-Shan Ho and D. R. Petersen, *J. Chromatogr.*, 231 (1982) 53.
26 G. C. Norbury, *J. Chromatogr.*, 414 (1987) 449.
27 A. Biber, G. Scherer, I. Hoepfner, F. Adlkofer, W-D. Heller, J. E. Haddow and G. J. Knight, *Toxicol. Lett.*, 35 (1987) 45.
28 A. Zlatkis, W. Bertsch, H. A. Lichtenstein, A. Tishbee, F. Shunbo, H. M. Liebich, A. M. Coscia and N. Fleischer, *Anal. Chem.*, 45 (1973) 1973.
29 J. C. Miller and J. N. Miller, *Statistics for Analytical Chemistry*, Wiley, Chichester, 1984.

Journal of Chromatography, 454 (1988) 303–310
Elsevier Science Publishers B.V., Amsterdam — Printed in The Netherlands

CHROM. 20 796

DETERMINATION OF CYCLIC GLUCANS BY ANION-EXCHANGE CHROMATOGRAPHY WITH PULSED AMPEROMETRIC DETECTION

KYOKO KOIZUMI*, YOKO KUBOTA, TOSHIKO TANIMOTO and YASUYO OKADA
Faculty of Pharmaceutical Sciences, Mukogawa Women's University, 11-68 Koshien Kyuban-cho, Nishinomiya 663 (Japan)
(Received June 8th, 1988)

SUMMARY

Anion-exchange chromatography with pulsed amperometric detection was applied to the determination of cyclodextrins (CDs), branched CDs and cyclosophoraoses. These cyclic glucans with degree of polymerization 6–25 were well resolved in each series by using simple isocratic elution with 150 m*M* sodium hydroxide solution containing 140–200 m*M* sodium acetate. The separation mode was not only simple anion exchange, but also involved some hydrophobic interactions and, moreover, inclusion interactions also seemed to take part in the retention. The detector response per glucose unit of these cyclic glucans was almost the same, regardless of the molecular weight and linkage form. The limit of determinaton of the cyclic glucans was 5–10 pmol and the detection limit was 2.5–5 pmol with a signal-to-noise ratio of 3.

INTRODUCTION

In recent years, research on cyclodextrins (CDs) has made remarkable progress, and particularly research on the pharmaceutical application of CDs is very active at present. The use of CD-containing drugs such as alprostadil-α-CD, limaprost-α-CD (both from Ono Pharmaceutical, Japan) and benexate hydrochloride-β-CD (Shionogi, Japan) in therapy has been authorized by the Japanese Government. In Europe piroxicam-β-CD, developed by Chiesi (Italy), is now registered by the Italian Drug Authorities[1]. Moreover, studies on the preparation and application of branched CDs are continuing energetically[2–11]. The microanalysis of CDs and branched CDs is necessary in this connection.

Recently, a sensitive high-performance liquid chromatographic (HPLC) procedure for carbohydrates using an anion-exchange method and triple-pulse amperometric detection (PAD) at a gold electrode has been developed[12–15]. PAD can detect not only reducing aldoses and ketoses but also non-reducing sugars such as xylitol and sucrose.

In this work we examined anion-exchange chromatography for the determination of CDs and branched CDs, using PAD, and also investigated the chromatographic behaviour and detector response of another series of cyclic glucans, cyclosophoraoses [CyS A–I, cyclic (1→2)-β-D-glucans] for comparison.

0021-9673/88/$03.50

EXPERIMENTAL

Materials

The CDs were gifts from Sanraku (Fujisawa, Japan) and purified by recrystallization from hot water. Maltosyl (G_2)-, maltotriosyl (G_3)-, maltotetraosyl (G_4)- and maltopentaosyl (G_5)-CDs were synthesized from CDs and maltooligosaccharides [degree of polymerization (DP) 2–5] by the reverse action of *Pseudomonas* isoamylase[6] or *Klebsiella aerogenes* pullulanase[16]. Glucosyl (G_1)-CDs were prepared from G_2- or G_3-CDs by hydrolysis with purified *Rhizopus delemar* glucoamylase GIII[17]. These branched CDs were purified by high-performance liquid chromatography (HPLC) on YMC-Pack ODS columns[18] to a high state of purity. The CySs were isolated from culture filtrates of *Agrobacterium* and *Rhizobium*[19] and purified by reversed-phase HPLC[20].

Sodium hydroxide and sodium acetate used for preparation of eluents were of analytical-reagent grade. The eluents were 150 m*M* sodium hydroxide solution containing 140–300 m*M* sodium acetate as a modifier to elute oligo- and polysaccharides; 300 m*M* sodium hydroxide solution was prepared by dilution of carbonate-free 50% sodium hydroxide solution with deionized water (18 MΩ cm) purified using a NANO-pure II (Barnstead, Newton, MA, U.S.A.) and diluted with the same volume of sodium acetate solution, prepared with 18 MΩ cm deionized water and filtered through a 0.2-μm membrane filter.

Apparatus and column

HPLC was performed on a Dionex BioLC Model 4000i system equipped with a Model PAD II pulsed amperometric detector consisting of an amperometric flow-through cell with a gold working electrode and a silver – silver chloride reference electrode and a potentiostat. The sample loop size was 50 μl. The column used was a Dionex HPIC-AS6 (10 μm) (250 × 4 mm I.D.) equipped with an AG6 guard column (50 × 4 mm I.D.) (all from Dionex, Sunnyvale, CA, U.S.A.). A Chromatopac C-RIA digital integrator (Shimadzu, Kyoto, Japan) was used to calculate peak areas.

Chromatographic conditions and measurements

PAD utilizes a repeating sequence of three applied potentials: E_1 set to a small positive value for sample oxidation, E_2 set near the positive potential limit of the working electrode in the eluent to clean the electrode surface electrochemically and E_3 set near the negative potential limit to reduce gold oxide to gold. The three potentials are applied for specific durations, t_1, t_2 and t_3, respectively. To produce an increase in sensitivity, a decrease in the background current and an overall increase in detectability, the following pulse potentials and durations were optimal for analyses of cyclic glucans at Range 2 (sampling period, 200 ms): $E_1 = 0.10$ V ($t_1 = 300$ ms), $E_2 = 0.60$ V ($t_2 = 120$ ms) and $E_3 = -0.80$ V ($t_3 = 300$ ms). The response time of the PAD II detector was set to 1.0 s. The eluents, prepared daily, were degassed before use and kept under a stream of nitrogen. The sample solutions were prepared using 18 MΩ cm deionized water and filtered through a 0.2-μm membrane filter. All separations were carried out at ambient temperature with a flow-rate of 1 ml/min.

RESULTS AND DISCUSSION

Analysis of CDs and branched CDs

Fig. 1a shows the chromatogram of a mixture of α-, β- and γ-CD. The column used was a strongly basic anion-exchange column in the hydroxide form and carbohydrates can be separated by anion exchange with highly alkaline eluents, as carbohydrates have pK values ranging from 12 to 14[21]. In general, retention of a homologous series of carbohydrates on this column increases as the degree of polymerization (DP) increases. However, the elution order of CDs was α-CD (DP 6), γ-CD (DP 8) and β-CD (DP 7). This result indicates that there are some hydrophobic interactions on this column, but the interaction may be weaker than that on the ODS column; the retention order of CDs on the ODS column is γ-CD < α-CD ≪ β-CD[22]. The ion-exchange resin used for the column consists of a 10-μm substrate coated with a monolayer of anion-exchange latex. It is said[23] that the ion-exchange capacity is less than 1% of that of ordinary anion-exchange resin.

Fig. 1 shows the elution profiles of (b) branched α-CDs, (c) branched β-CDs and

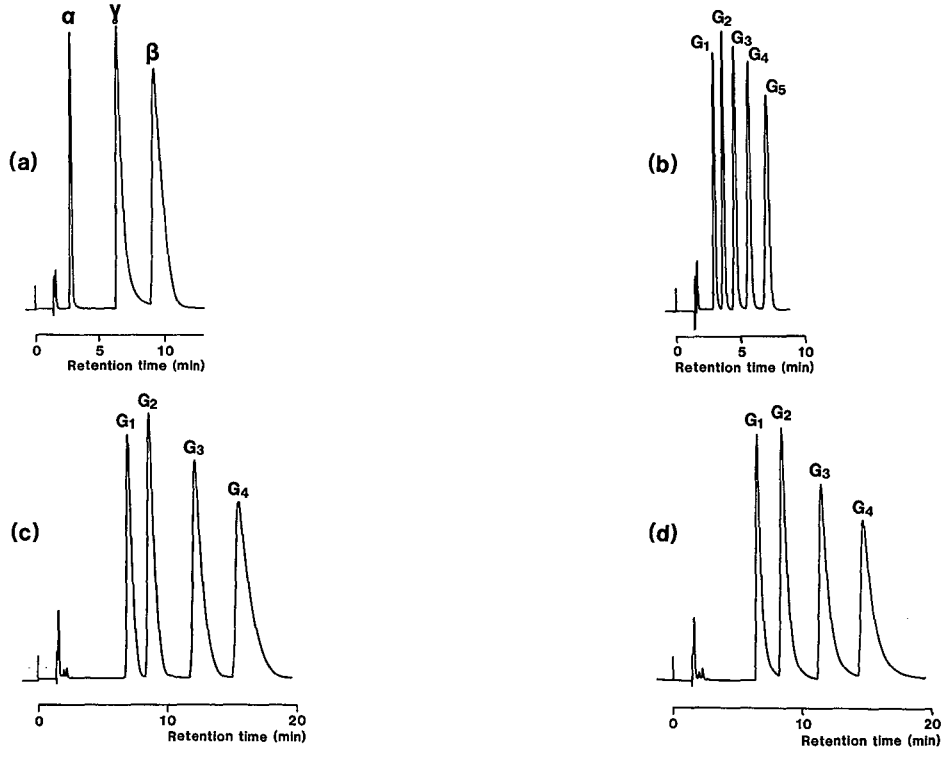

Fig. 1. Elution profiles of (a) α-, β- and γ-CD, (b) branched α-CDs, (c) branched β-CDs and (d) branched γ-CDs on a HPIC-AS6 column (250 × 4 mm I.D.). α = α-CD; β = β-CD; γ = γ-CD; G_1 = glucosyl; G_2 = maltosyl; G_3 = maltotriosyl; G_4 = maltotetraosyl; G_5 = maltopentaosyl. Chromatographic conditions: eluent, 150 mM sodium hydroxide–200 mM sodium acetate; flow-rate, 1 ml/min; detector, PAD II; meter scale, $10 \cdot 10^3$ nA; temperature, ambient (25 ± 1°C). Sample size: α-CD, 6.25; β-CD, 18.75; γ-CD, 12.5; branched α-CD, 3; branched β-CD, 10; branched γ-CD, 7.5 nmol.

(d) branched γ-CDs. For a series of branched CDs the retention increases as the length of the branch increases. G_1-CD to G_4-CD in each series showed similar elution profiles to that on C_{18}-bonded silica whereas the elution order of G_5-α-CD was different from that on C_{18}-bonded silica, which was abnormal, G_5-α-CD eluting before G_3-α-CD[18].

Although the peak shapes of α-CD and branched α-CDs were all good, those of the β-CD and especially the γ-CD series were poor. These peaks showed tailing, the extent of which increased with decrease in the sample concentration, particularly with the γ-CD series. As the peak shapes of CySs, having much longer retention times (t_R), are excellent, as shown in Fig. 3, the peak shape is independent of t_R. This phenomenon may arise from inclusion of benzyltrialkylammonium in the stationary phase with the cyclic glucan. For this interaction the cavity of γ-CD may be of the most suitable size (cavity diameter = 9.5 Å)[24] and the cavity size of β-CD (7.8 Å)[24] may also be suitable, whereas that of α-CD (5.7 Å)[24] is too small and those of CySs must be too large.

For control of retention sodium acetate was added to the eluent. The effect of sodium acetate concentration on the capacity factors for CDs and branched CDs is shown in Fig. 2. Changes in the sodium acetate concentration did not affect the mutual elution order of branched CDs, whereas the elution order of β-CD and γ-CD in each series changed with the sodium acetate concentration in the eluent.

PAD at a gold electrode is applicable to the sensitive detection of the HCOH group in carbohydrates. Although the exact oxidation reaction mechanism is not clear, a high pH is required in order to obtain adequate sensitivity. pH 13 is the optimum for detection. On the basis of this information, quantitative analyses of CDs and branched CDs by anion-exchange chromatography with PAD were carried out using 150 m*M* sodium hydroxide–200 m*M* sodium acetate as the eluent. First the relative detector response was evaluated from chromatograms of standard mixtures of α-, β- and γ-CD,

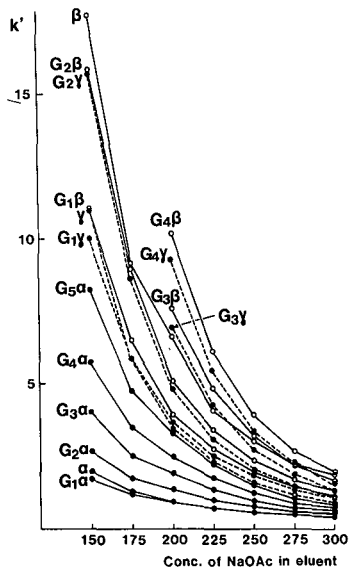

Fig. 2. Relationship between sodium acetate (NaOAc) concentration in the eluent and the capacity factor of each CD and branched CD. Sample size, 5 nmol each. Chromatographic conditions other than eluent as in Fig. 1.

TABLE I

RELATIVE DETECTOR RESPONSE OF CDs AND BRANCHED CDs

Chromatographic conditions as in Fig. 1. The amounts of CDs and branched CDs used were 5 nmol each.

CD	*R.D.R.**	*CD*	*R.D.R.*	*CD*	*R.D.R.*	*CD*	*R.D.R.*
α-	1.0	α-	1.0	β-	1.0	γ-	1.0
β-	1.7	G_1-α-	1.4	G_1-β-	1.1	G_1-γ-	1.2
γ-	2.0	G_2-α-	1.6	G_2-β-	1.5	G_2-γ-	1.5
		G_3-α-	2.0	G_3-β-	1.8	G_3-γ-	1.6
		G_4-α-	2.3	G_4-β-	2.0	G_4-γ-	1.8
		G_5-α-	2.6				

* R.D.R. = Relative detector response.

and each series of branched α-, β- and γ-CDs (5 nmol each) (Table I). The results indicated that the sensitivity of detection does not decrease with increasing molecular weight. The detector response per HCOH group in CDs and branched CDs varied only in limited ranges.

The linearity of the detector response was investigated by injection of progressive dilutions of a mixture of α-, β- and γ-CD and a mixture of branched α-CDs under the same chromatographic conditions as in Fig. 1. The calibration graph of peak height *vs.* concentration of α-CD was linear in the range 10 pmol–1 nmol ($r = 0.999$), whereas those of β-CD and γ-CD were linear in the range 25 pmol–500 pmol ($r = 0.996$ and 0.995, respectively). The detection limits for α-, β- and γ-CD were 5, 10 and 10 pmol, respectively, with a signal-to-noise ratio of 3. The reason for the poorer sensitivities for β- and γ-CD appears to be retardation of the retention time (t_R) accompanying peak broadening with decreasing CD concentration (Table II). This phenomenon could be explained by a relative increase in the surface area accessible to the aforesaid interaction with β- and γ-CD. A reduction in t_R by using 150 m*M* sodium hydroxide–300 m*M* sodium acetate as the eluent avoided these effects and increased the sensitivities for β- and γ-CD to the same level as for α-CD or even higher; the detection limit for γ-CD was 2.5 pmol.

Table III gives quantitative results for branced α-CDs. The limits of determination and detection of G_1-, G_2- and G_3-α-CD, which have shorter t_R and give very sharp peaks, were lower. The reproducibility of the peak heights at 1 nmol, 200 pmol and 50 pmol was good.

TABLE II

VARIATION OF RETENTION TIME WITH CONCENTRATION OF CD

Chromatographic conditions as in Fig. 1.

Concentration (pmol)	*Retention time (min)*		
	α-CD	*β-CD*	*γ-CD*
500	2.92	10.47	7.07
50	2.92	11.13	8.23
25	2.92	11.32	8.92

TABLE III
CALIBRATION GRAPHS AND DETECTION LIMITS FOR BRANCHED α-CDs
Chromatographic conditions as in Fig. 1.

CD	t_R *(min)*	*Calibration graph*					*Detection limit (pmol) for S/N = 3***
		Linear region (pmol)		*C.V.** (n = 5) at*			
				1 nmol	*200 pmol*	*50 pmol*	
G_1-α-	3.0	10–1000	0.999	0.92	1.13	1.36	5
G_2-α-	3.6–3.7	10–1000	0.999	0.87	1.18	2.07	5
G_3-α-	4.4–4.5	10–1000	0.999	1.04	1.17	2.05	5
G_4-α-	5.4–5.6	20–1000	0.999	0.87	0.98	2.05	10
G_5-α-	6.7–6.9	20–1000	0.999	1.18	2.31	2.81	10

* r = Correlation coefficient.
** C.V. = Coefficient of variation.
*** S/N = Signal-to-noise ratio.

Analysis of CySs

For comparison, analyses of CyS A–I, having a different linkage form [β-(1→2)] from CDs [α-(1→4)] and much higher DPs (17–25), were performed. Fig. 3 shows the elution profile of CyS A–I. The elution pattern was different from those obtained on amino-bonded silica with acetonitrile–water as eluent and also on C_{18}-bonded silica with methanol–water as eluent[20]: in the former instance there was an increased retention with increasing molecular size of CyS, and in the latter probably an increased retention with decreasing solubility in water, the elution order of CyS-C and -D, and CyS-E and -F being reversed. On this anion-exchange column with 150 m*M* sodium hydroxide solution containing sodium acetate as the eluent, the elution order of CyS-D and -E was reversed. Moreover, in spite of their much larger molecular sizes, CySs moved faster on this column (Fig. 4).

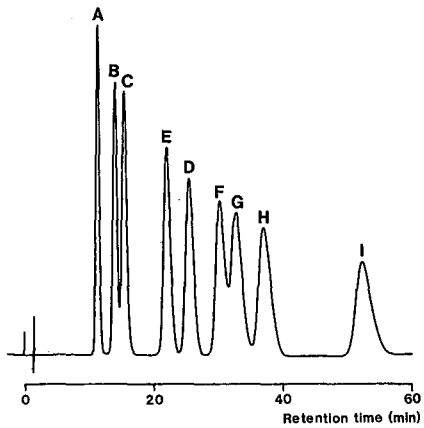

Fig. 3. Separation of CyS A–I. DP: A = 17; B = 18; C = 19; D = 20; E = 21; F = 22; G = 23; H = 24; I = 25. Chromatographic conditions: eluent, 150 m*M* sodium hydroxide–140 m*M* sodium acetate; other conditions as in Fig. 1. Sample size, 5 nmol each.

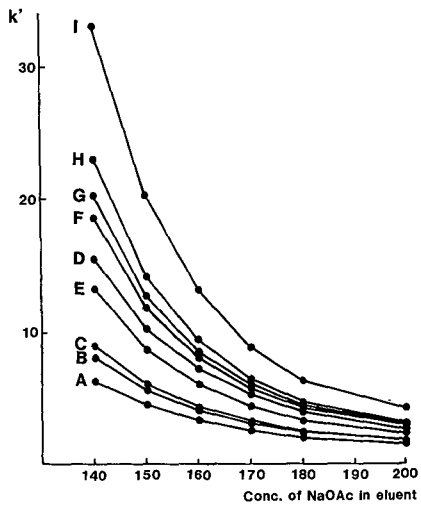

Fig. 4. Relationship between sodium acetate (NaOAc) concentration in the eluent and the capacity factor of each CyS. Sample size, 5 nmol each. Chromatographic conditions other than eluent as in Fig. 1.

The retention times and relative detector responses of CyS A–I under the same chromatographic conditions as in Table I are summarized in Table IV and compared with the data for CDs. The detector responses per glucose unit of β- and γ-CD and CySs are almost the same.

Under the same chromatographic conditions as in Table IV, the CySs gave calibration graphs having good linearity (all with $r = 0.999$) in the ranges 5–500 pmol for CyS A–H and 10–500 pmol for CyS I. The detection limits were 2.5 pmol for CyS A–H and 5 pmol for CyS I.

TABLE IV

COMPARISON OF RETENTION TIMES (t_R) AND RELATIVE DETECTOR RESPONSES OF CySs WITH THOSE OF CDs

Chromatographic conditions as in Fig. 1. The amounts of CDs and CySs used were 5 nmol each.

Glucan	t_R *(min)*	*R.D.R.**	*DP***	*R.D.R. per Glc unit*
α-CD	2.92	0.61	6	0.7
β-CD	10.47	1.00	7	1.0
γ-CD	7.07	1.10	8	1.0
CyS-A	3.83	2.54	17	1.1
CyS-B	4.19	2.59	18	1.0
CyS-C	4.33	2.88	19	1.1
CyS-D	5.70	3.09	20	1.1
CyS-E	5.13	3.04	21	1.0
CyS-F	6.04	3.34	22	1.1
CyS-G	6.23	3.66	23	1.1
CyS-H	6.26	3.68	24	1.1
CyS-I	8.08	3.38	25	1.0

* R.D.R. = Relative detector response.
** DP = Number of glucose (Glc) units.

CONCLUSION

The combination of anion-exchange separation with a highly alkaline eluent and PAD provides a powerful new technique for the analysis of cyclic glucans. As cyclic glucans have no reducing end, they are stable to the highly alkaline eluent. For the separation of cyclic glucans, 150 m*M* sodium hydroxide solution having the optimum pH for detection by PAD can be used as the eluent and therefore no post-column addition of a strong base is needed. The sensitivity of detection of β-CD by PAD is 20 times that using a refractive index detector of high sensitivity, used together with a pump-minimized pulsating flow[25].

ACKNOWLEDGEMENTS

The authors are indebted to Professor S. Hizukuri (Kagoshima University) for the preparation of branched CDs, and also thank Dr. A. Amemura (Osaka University) and Dr. M. Hisamatsu (Mie University) for the preparation of CySs.

REFERENCES

1 J. Szejtli and J. Pagington, *Cyclodextrin News*, 2, No. 8 (1988) 6–7.
2 S. Kobayashi, N. Shibuya, B. M. Young and D. French, *Carbohydr. Res.*, 126 (1984) 215–224.
3 Y. Sakano, M. Sano and T. Kobayashi, *Agric. Biol. Chem.*, 49 (1985) 3391–3398.
4 J. Abe, Y. Takeda, S. Hizukuri, K. Yamashita and N. Ide, *Carbohydr. Res.*, 131 (1984) 175–179.
5 K. Koizumi, T. Utamura, M. Sato and Y. Yagi, *Carbohydr. Res.*, 153 (1986) 55–67.
6 J. Abe, N. Mizowaki, S. Hizukuri, K. Koizumi and T. Utamura, *Carbohydr. Res.*, 154 (1986) 81–92.
7 S. Kitahata, Y. Yoshimura and S. Okada, *Carbohydr. Res.*, 159 (1987) 303–313.
8 Y. Yoshimura, S. Kitahata and S. Okada, *Carbohydr. Res.*, 168 (1987) 285–294.
9 K. Koizumi, Y. Okada,Y. Kubota and T. Utamura, *Chem. Pharm. Bull.*, 35 (1987) 3413–3418.
10 P. Fügedi, P. Nánási and J. Szejtli, *Carbohydr. Res.*, 175 (1988) 173–181.
11 Y. Okada, Y. Kubota, K. Koizumi, S. Hizukuri,T. Ohfuji and K. Ogata, *Chem. Pharm. Bull.*, 36 (1988) 2176–2185.
12 R. D. Rocklin and C. A. Pohl, *J. Liq. Chromatogr.*, 6 (1983) 1577–1590.
13 G. G. Neuberger and D. C. Johnson, *Anal. Chem.*, 59 (1987) 203–204.
14 K. Ohsawa, Y. Yoshimura, S. Watanabe, H. Tanaka, A. Yokota, K. Tamura and K. Imaeda, *Anal. Sci.*, 2 (1986) 165–168.
15 M. R. Hardy, R. R. Townsend and Y. C. Lee, *Anal. Biochem.*, 170 (1988) 54–62.
16 S. Hizukuri, S. Kawano, J. Abe, K. Koizumi and T. Tanimoto, *Biotech. Appl. Biochem.*, in press.
17 J. Abe, H. Nagano and S. Hizukuri, *J. Appl. Biochem.*, 7 (1985) 235–247.
18 K. Koizumi, Y. Kubota, Y. Okada, T. Utamura, S. Hizukuri and J.-I. Abe, *J. Chromatogr.*, 437 (1988) 47–57.
19 M. Hisamatsu, A. Amemura, K. Koizumi, T. Utamura and Y. Okada, *Carbohydr. Res.*, 121 (1983) 31–40.
20 K. Koizumi, Y. Okada, T. Utamura, M. Hisamatsu and A. Amemura, *J. Chromatogr.*, 299 (1984) 215–224.
21 J. A. Rendleman, *Carbohydrates in Solution*, Advances in Chemistry Series, No. 117, American Chemical Society, Washington, DC, 1973, p. 51.
22 K. Koizumi, T. Utamura, T. Kuroyanagi, S. Hizukuri and J.-I. Abe, *J. Chromatogr.*, 360 (1986) 397–406.
23 J. Weiss, in E. L. Johnson (Editor), *Handbook of Ion Chromatography*, Dionex Co., Sunnyvale, CA, 1986, p. 26.
24 J. Szejtli, *Cyclodextrins and Their Inclusion Complexes*, Akadémiai Kiadó, Budapest, 1982, p. 25.
25 K. Koizumi, Y. Kubota, Y. Okada and T. Utamura, *J. Chromatogr.*, 341 (1985) 31–41.

Journal of Chromatography, 454 (1988) 311–316
Elsevier Science Publishers B.V., Amsterdam — Printed in The Netherlands

CHROM. 20 781

REVERSED-PHASE HIGH-PERFORMANCE LIQUID CHROMATOGRAPHY TECHNIQUE FOR TAURINE QUANTITATION*

DALE W. PORTER

Division of Animal and Veterinary Sciences, College of Agriculture and Forestry, West Virginia University, P.O. Box 6108, Morgantown, WV 26506 (U.S.A.)

MELANIE A. BANKS and VINCENT CASTRANOVA

Division of Respiratory Disease Studies, National Institute of Occupational Safety and Health, 944 Chestnut Ridge Road, Morgantown, WV 26505 (U.S.A.)

and

WILLIAM G. MARTIN*

Division of Animal and Veterinary Sciences, College of Agriculture and Forestry, West Virginia University, P.O. Box 6108, Morgantown, WV 26506 (U.S.A.)

(First received April 25th, 1988; revised manuscript received June 13th, 1988)

SUMMARY

Taurine (2-aminoethanesulfonic acid) was quantitated by reversed-phase chromatography on a C_{18} Resolve column using a linear gradient of 9–11% methanol in water. Glutamine was used as the internal standard. Pre-column derivatization of the amino acid with *o*-phthalaldehyde allowed the detection of as little as 0.1 pmol taurine. Dual ion-exchange column chromatography was employed to remove other amino acids and metabolic precursors of taurine from the samples. Cysteic acid and cysteine sulfinic acid did not interfere with taurine analysis by the high-performance liquid chromatographic method.

For sample deproteinization, boiling and picric acid precipitation were used. Recovery of taurine averaged 93.5 ± 5.0% ($\bar{x}$ ± standard error of the mean) from standard solutions and was not affected by the method of deproteinization.

Using this procedure, plasma taurine concentrations for the rat and chick were determined to be 100.7 ± 13.1 μM and 108.0 ± 0.3 μM, respectively. Recovery of taurine from plasma samples averaged 97.2 ± 4.7%.

INTRODUCTION

The presence and quantity of taurine (2-aminoethanesulfonic acid) has been reported in a wide variety of animal species and tissues[1]. The function of this non-protein amino acid in animal cells and fluids, other than bile acid conjugation in

* Published with approval of the Director of West Virginia University Agricultural Experiment Station as publication No. 2096 of the Journal Series.

0021-9673/88/$03.50

liver, is not known, although it has been suggested that taurine functions as a neuromodulator[2], membrane stabilizer[3], and antioxidant[4].

Early techniques used to quantitate taurine in biological samples included thin-layer chromatography[5], paper chromatography[6], and colorimetric determinations[7,8]. Applications of these techniques are limited because they require large sample size and lack sensitivity.

The application of high-performance liquid chromatography (HPLC) to the quantitation of taurine has overcome the limitations of the earlier techniques. Existing HPLC methods for taurine determinations lack resolution[9] or require complicated buffer systems for the analyses[10].

We have developed a new, simple HPLC method for the analysis of taurine in biological samples which has high sensitivity and resolution. The technique is based on adsorption chromatography of the *o*-phthaldehyde (OPA)-taurine derivative, using a linear gradient of 9–11% methanol in water. Separation of taurine from the internal standard glutamine is rapidly achieved.

MATERIALS AND METHODS

Equipment

The HPLC system consisted of a Perkin-Elmer Series 4 liquid chromatograph equipped with a microprocessor controlled solvent delivery system, a Rheodyne Model 7125 injector with a 20-μl injection loop, a Perkin-Elmer PC-75 absorbance detector and a Varian Model 4270 integrator. A Waters (Milford, MA, U.S.A.) C_{18} Resolve (5 μm) reversed-phase column was used. Scintillation counting was performed on a Beckman LS-1800 liquid scintillation counter (Fullerton, CA, U.S.A.).

Reagents

Taurine (external standard), L-glutamine (internal standard), *o*-phthalaldehyde (OPA) and β-mercaptoethanol were obtained from Sigma (St. Louis, MO, U.S.A.). Potassium borate buffer (fluoraldehyde reagent dilutent, pH 10.4) was obtained from Pierce (Rockford, IL, U.S.A.). Picric acid (2,4,6-trinitrophenol), HPLC-grade methanol and water were obtained from Fisher Scientific (Pittsburgh, PA, U.S.A.). HPLC-grade methanol was filtered with a Millipore (Bedford, MA, U.S.A.), HAWP, 0.45-μm filter. HPLC-grade water was filtered with a Millipore HVHP filter. Analytical ion-exchange resins AG 1-X8 (100–200 mesh, Cl^-) and AG 50W-X8 (100–400 mesh, H^+) were obtained from Bio-Rad (Richmond, CA, U.S.A.). Cysteic acid and cysteine sulfinic acid were obtained from ICN Nutritional Biochemicals (Cleveland, OH, U.S.A.). [1,2-^{14}C]taurine was obtained from New England Nuclear (Willmington, DE, U.S.A.). Scinti-Verse II scintillation fluid was obtained from Fisher Scientific.

Animals

Male Sprague-Dawley rats (200–250 g) were obtained from Charles River (Boston, MA, U.S.A.). Peterson male × Hubbard female chickens (five-weeks of age) were obtained from Rocco Hatchery (Harrisonburg, VA, U.S.A.).

Preparation of standards and derivatizing reagent

A 1.0 m*M* stock solution of taurine was diluted with HPLC-grade water to prepare the 5–30 μM standards. To 97 μl of the taurine standard, 3 μl of 0.4 m*M* glutamine was added.

The derivatizing reagent was formulated by adding 0.4 ml of β-mercaptoethanol and 50 mg OPA to 10 ml of HPLC-grade methanol. After gently shaking to dissolve the OPA, the volume of the solution was then brought to 100 ml with 0.4 *M* potassium borate buffer. This reagent was prepared fresh daily and stored at room temperature in a dark bottle during use.

Plasma collection

Rats were anesthetized with pentabarbital sodium (110 mg/kg body weight). Blood samples (6 ml) were drawn from the inferior vena cava using heparinized syringes. Chickens were anesthetized with chloroform. Blood samples (10 ml) were collected by cardiac punture using heparinized syringes.

Plasma from rats and chickens was obtained by centrifugation (1400 *g*, 10 min) of the whole blood. Samples from four rats and three chickens were analyzed in triplicate to determine plasma taurine levels.

Sample preparation

Plasma samples (1 ml) were deproteinized either by boiling for 15 min or addition of saturated picric acid (1 ml of 2 g/100 ml water). After centrifugation at 15 000 *g* for 10 min, the supernatants (200–500 μl) were removed and placed on dual-bed ion-exchange columns (0.5 cm I.D.) which were prepared by layering 2.5 cm AG 1-X8 over 2.5 cm of AG 50W-X8[9]. After loading the sample onto the column with 0.6 ml distilled water, the taurine fraction was collected using 2.0 ml distilled water. The eluants were placed in a drying oven at 70°C, and the dried samples were stored at room temperature until reconsitution with HPLC-grade water prior to analysis.

Standard taurine solutions used for estimation of recovery were treated identically to the tissue samples. To determine whether metabolic precursors of taurine interfere with the estimation of taurine, a solution of 1 mg/ml cysteic acid and 1 mg/ml cysteine sulfinic acid was subjected to analysis by the same method. To determine the volume of water needed to elute the samples from the ion-exchange columns, 0.002 μCi of [1,2-^{14}C]taurine was chromatographed and 0.5-ml fractions were collected and counted.

HPLC analysis

Standards or samples to which internal standard had been added just prior to the HPLC analysis were reacted for 1 min with an equal volume of the OPA reagent, then injected onto the HPLC[10]. A linear gradient of 9–11% methanol in water was run at a flow-rate of 1.0 ml/min for 10 min to achieve separation of taurine from glutamine. The absorbance of the OPA adducts of these amino acids were monitored at 340 nm, at a sensitivity of 0.01 absorbance units full-scale (a.u.f.s.). The taurine concentration of the sample was calculated by the peak area: weight ratio method from known concentrations of internal and external standards in the standard curve.

RESULTS

Elution of isotope from the preparative ion-exchange column with 2.0 ml of water resulted in recovery of 96.9% of the sample applied (Fig. 1).

A representative chromatogram, showing retention times for taurine (5.65 min) and the internal standard glutamine (2.69 min), is shown in Fig. 2. The standard curve is shown in Fig. 3. Taurine concentrations in 20 μl of the sample (injection volume) were calculated from the equation:

$$[\text{Tau}] = \frac{RT}{S} \cdot [\text{Gln}]$$

where RT = (peak area for taurine)/(peak area for glutamine), and S = slope of standard curve.

Recovery of taurine from standard solutions (10–30 μM) treated by either boiling or addition of picric acid, followed by ion-exchange chromatography and HPLC, was 93.5 ± 8.7% and 93.5 ± 5.0% [$\bar{x}$ ± standard error of the mean (S.E.M.) for four added concentrations, each determined in triplicate], respectively. Recovery from plasma samples to which taurine (10–40 μM) was added did not significantly

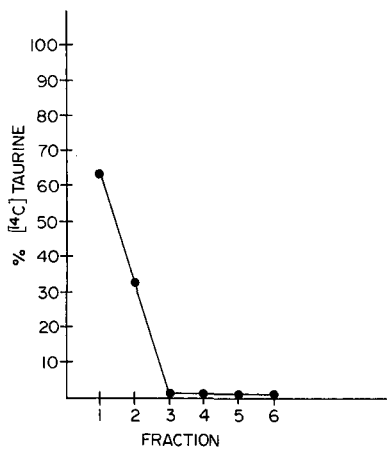

Fig. 1. Percentage of [1,2-^{14}C]taurine eluted by water from dual ion-exchange column in successive 0.5-ml fractions.

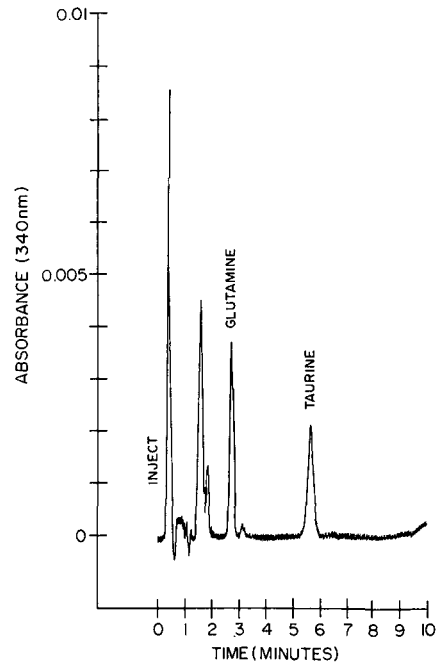

Fig. 2. Representative chromatogram showing elution of taurine and glutamine peaks. The absorbance detector was set at a wavelength of 340 nm, and a sensitivity of 0.01 a.u.f.s.

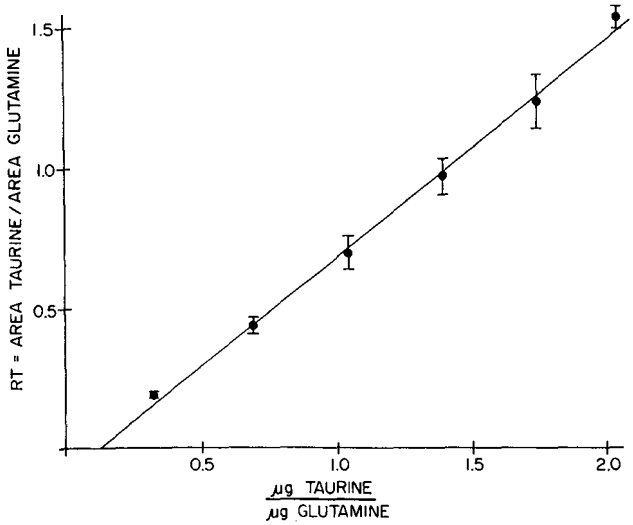

Fib. 3. Taurine standard curve. Values represent the mean ± S.E.M. of five analysis at each concentration. Slope = 0.780, intercept = −0.100.

differ by the method of sample deproteinization, and averaged 97.2 ± 4.7% ($\bar{x}$ ± S.E.M. for two added concentrations, each determined in triplicate).

Cysteice acid and cysteine sulfinic acid eluted in the solvent front, before the internal standard. However, when standards were subjected to preparative ion-exchange chromatography, peaks attributable to either of these metabolic precursors of taurine were not detected in the chromatogram.

Plasma taurine concentrations for the rat and the chick were determined to be 100.7 ± 13.1 μM and 108.0 ± 0.3 μM, respectively.

DISCUSSION

The HPLC procedure presented allows accurate quantitation of as little as 0.1 pmol of taurine. Lower quantities of taurine are detectable using our method, but baseline noise prevents accurate quantitation at these levels. A previous method which used isocratic elution of the taurine-OPA adduct reported a 5-pmol lower limit of detection[10].

Although recovery of taurine from biological samples which are deproteinized by boiling or picric acid did not significantly differ, the former method does offer some advantages. Picric acid explodes when rapidly heated or upon percussion[11], thus care must be exercised when using this compound. Also, for samples with high protein content (for example, rat plasma), multiple picric acid precipitation steps are required for complete deproteinization. This is necessary because use of inadequately deproteinized samples will accumulate on and decrease the life of the HPLC column.

As demonstrated previously[10], the sample preparation method which we used removes contaminating metabolic precursors of taurine such as cysteic acid and cysteine sulfinic acid. Use of the methanol–water gradient and the reversed-phase column provided excellent separation of the taurine and glutamine peaks.

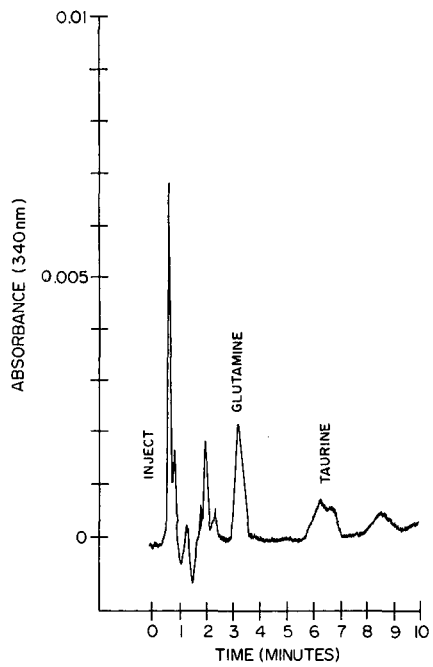

Fig. 4. Representative chromatogram showing shouldering of taurine peak caused by use of old OPA reagent.

To avoid shouldering of the taurine peak (Fig. 4), the OPA derivatizing reagent should be made fresh. Also, vigorous stirring of the OPA reagent should be avoided, since this caused shouldering of the taurine peak even if fresh derivatizing reagent was used.

REFERENCES

1 J. G. Jacobsen and L. H. Smith, Jr., *Physiol. Rev.*, 48 (1968) 424.
2 K. Kuriyama, *FEBS Lett.*, 39 (1980) 2680.
3 H. Pasantes-Marales, C. E. Wright and G.E. Gaull, *J. Nutr.*, 114 (1984) 2256.
4 J. G. Alvarez and B. T. Storey, *Biol. Reprod.*, 29 (1984) 548.
5 A. Guidotti, G. Badiani and G. Pepeu, *J. Neurochem.*, 19 (1972) 431.
6 C. Wu, *J. Biol. Chem.*, 207 (1954) 775.
7 E. I. Pentz, C. H. Davenport, W. Glover and D. D. Smith, *J. Biol. Chem.*, 288 (1957) 433.
8 B. Sarlro, *Clin. Chim. Acta*, 6 (1961) 87.
9 Z. K. Shihabi and J. P. White, *Clin. Chem.*, 25 (1979) 1368.
10 B. R. Larsen, D. S. Grosso and S. Y. Chang, *J. Chromatogr. Sci.*, 18 (1980) 233.
11 *The Merck Index*, Merck, Rahway, NJ, 10th ed., 1983, p. 1304.

Journal of Chromatography, 454 (1988) 317–326
Elsevier Science Publishers B.V., Amsterdam — Printed in The Netherlands

CHROM. 20 774

HIGH-PERFORMANCE SIZE-EXCLUSION CHROMATOGRAPHY OF OILS AND FATS*

SAJID HUSAIN*, G. S. R. SASTRY, N. PRASADA RAJU and R. NARASIMHA
Analytical Chemistry Division, Regional Research Laboratory, Hyderabad-500 007 (India)
(First received April 5th, 1988; revised manuscript received June 24th, 1988)

SUMMARY

A simple high-performance size-exclusion chromatographic (HPSEC) method for the determination of the molecular weights of various oils and fats and their binary mixtures is described. The weight-average molecular weights, ($\overline{M}_w$), of refined oil samples thus obtained are in close agreement with those predicted from conventional saponification data. The results obtained for pure butter fats and binary mixtures of coconut oil and castor oil by HPSEC are discussed. The method may be suitable for the determination of adulteration in oils and fats.

INTRODUCTION

Oils and fats are essentially triglyceride mixtures of long chain fatty acids of carbon number ranging from C_4 to C_{24}. Generally, they differ in their fatty acid composition depending on their origin and nature. In addition to the above components, a number of foreign substances such as diglycerides, monoglycerides, free fatty acids and unsaponifiable matter are also present in oils and fats.

Several analytical methods[1,2] and specifications[3,4] based on physical, chemical and physicochemical aspects are available to characterize oils and fats. Among these, the saponification value (SV) occupies the most important position as it correlates the average molecular weight (SE) of fatty acids of glycerides. The relationship between SV and SE is :

$$SE = 56\,100/SV \tag{1}$$

The average molecular weight of oils and fats can be predicted by[5,6]

$$\text{Average molecular weight} = \frac{3 \cdot 56\,100}{SV} + 38 \tag{2}$$

but is not truly representative of all the components present in the sample as it does not

* RRL(H) Communication No. 2170.

0021-9673/88/$03.50

include the contributions of low molecular weight and unsaponifiable fractions. Therefore, the accuracy of this prediction is considered to be very low, particularly for crude samples. Further it does not convey any information about the molecular weight distribution (MWD). The MWD is a key property which is needed to understand the compositional nature of oils and fats. It may also be helpful in studying adulteration in oils and fats.

Many techniques such as cryoscopy, ebullioscopy, osmometry, viscometry, light scattering, sedimentation and ultracentrifugation based on colligative and bulk properties are used for determining molecular weights[7]. However, all these techniques yield approximate data.

High-performance size-exclusion chromatography (HPSEC) is a valuable technique in providing information about sample complexity, accurate molecular weights and their distribution pattern. In a SEC column, the analytes are eluted in accordance with their molecular sizes, *i.e.*, hydrodynamic volume in a mobile phase solvent.

Though the technique was originally developed for characterizing macromolecules, it has also been successfully used for studying low-molecular-weight mixtures by introducing more efficient column packings and making innovations in instrumentation[8–10]. A thorough literature survey has revealed that only limited studies have been carried out with on the SEC retention behaviour of oils and fats. White and Wang[11] employed HPSEC for evaluating heated soya bean oil.

The present investigation was undertaken with a view to collecting information about the HPSEC retention behaviour of various oils and fats and to extend the utility of this technique to the prediction of saponification values of unknown samples and also the relative contributions of impurities and their detection. This technique may also find application in the detection of adulteration in oils and fats.

EXPERIMENTAL

Apparatus

HPSEC was performed on an LC-6A high-performance liquid chromatograph (Shimadzu Corporation, Kyoto, Japan) with a loop injector (capacity 12 μl) having an high-pressure six-way valve. A refractive index detector Model RID-6A was connected after the column for eluate monitoring. The work was carried out on a high speed gel permeation chromatographic column (HSG-15H, Shimadzu) 300 mm $\times$ 7.9 mm I.D. As per the specifications from the supplier, the number of theoretical plates of the column ranges between 20 000 to 30 000 per meter. The column was packed with spherical beads (size 10 μm) of styrene–divinylbenzene copolymer. The chromatograms and the integrated data were recorded by a Chromatopac C-R3A processor (Shimadzu).

Reagents and samples

HPLC-grade tetrahydrofuran (THF) was obtained from Spectrochem Pvt. (India) and other chemicals such as potassium hydroxide, hydrochloric acid, etc., were of reagent grade. Ethanol was freshly distilled before use. Polyethylene glycols of different molecular weights (800, 580, 400 and 200) were obtained from S.D. Fine Chemicals (India).

Samples of vegetable oils and fats were obtained from local industries. Butter fats were extracted from different samples of processed buffalo milk collected from two different regions. Animal body fats such as mutton tallow, broiler chicken and beef fats were obtained by solvent extraction of the respective crude animal tissues.

Chromatographic conditions

The mobile phase used was the HPLC grade THF with a flow-rate of 0.3 ml/min. The samples were dissolved in the mobile phase used. A 12-μl loop with an high-pressure six-way valve was used for injecting the sample. Chromatograms were recorded on $16 \cdot 10^{-6}$ refractive index unit scale (RIUS) ranges and the sample concentration was about 15 mg/ml. Analyses were performed at ambient temperature. The samples were filtered using 0.45-μm pore size filters supplied by Waters Assoc. (Milford, MA, U.S.A.) before injection.

Reference materials

Polyethylene glycol standards of various molecular weights (800, 580, 400 and 200) were employed for calibrating the retention data of oils and fats. Stearic acid and the unsaponifiable fraction extracted from palm oil were used as reference materials to study the retention behaviour of free fatty acids and the unsaponifiable matter of oils and fats. To estimate the theoretical efficiency of the method, the $\overline{M}_w$ obtained (in case of refined samples) was compared with that predicted from the experimental saponification value. By use of the AOCS method[1], the SV data for refined samples were determined.

Calibration of the retention data

HPSEC retention times of standard polyethylene glycols on a single HSG-15H (Shimadzu) column were determined by injecting individual samples with THF as the eluent at a flow-rate of 0.3 ml/min. The retention data and a linear calibration graph of retention *vs.* log $\overline{M}_w$ are shown in Table I and Fig. 1 respectively. The data for the calibration graph were stored on a floppy disk FDD-1A (Shimadzu) coupled with the

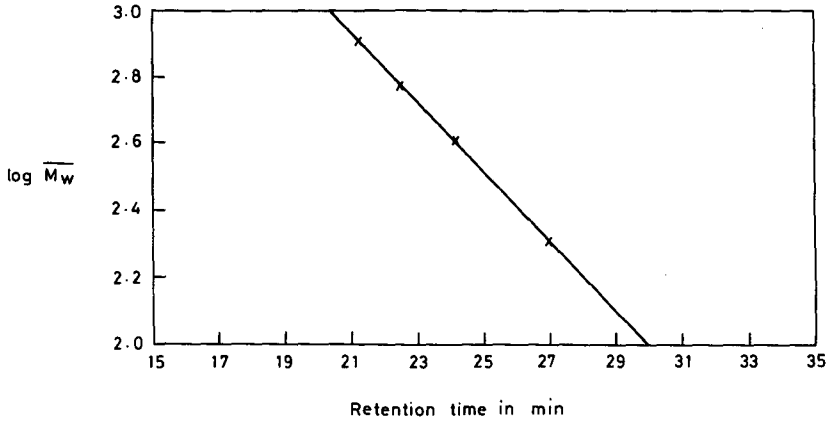

Fig. 1. Calibration graph using polyethylene glycols as standards.

TABLE I

HPSEC RETENTION DATA FOR STANDARD POLYETHYLENE GLYCOLS (PEG)

Sample No.	*Average molecular weight of PEG, $\bar{M}_w$*	*Retention time (min)*
1	800	21.3
2	580	22.5
3	400	24.2
4	200	27.0

Chromatopac C-R3A processor for molecular weight determination of the analytes. The reproducibility of this method was tested by injecting triplicate samples of standards and analytes. The coefficient of variation for molecular weights ranged from 1 to 2% and the $\bar{M}_w$ obtained for refined samples is in close agreement with that predicted from the average experimental saponification value.

RESULTS AND DISCUSSION

Determination of molecular weights

$\bar{M}_w$, the number-average molecular weight, $\bar{M}_n$, the viscosity average molecular weight, $\bar{M}_v$, and the Z-average molecular weight, $\bar{M}_z$, of some oils and fats are given in Table II and HPSEC chromatograms of refined and crude oil samples are shown in Fig. 2A and B respectively. The $\bar{M}_w$ and $\bar{M}_v$ values for all samples are found to be almost identical. The difference between $\bar{M}_w$ and $\bar{M}_n$ is much less for refined samples. In case of the crude samples it is about 100 units. This large difference between M_w and $\bar{M}_n$ values in crude samples is indicative of a significant contribution of low-molecular-weight fractions like free fatty acids and unsaponifiable matter. A standard

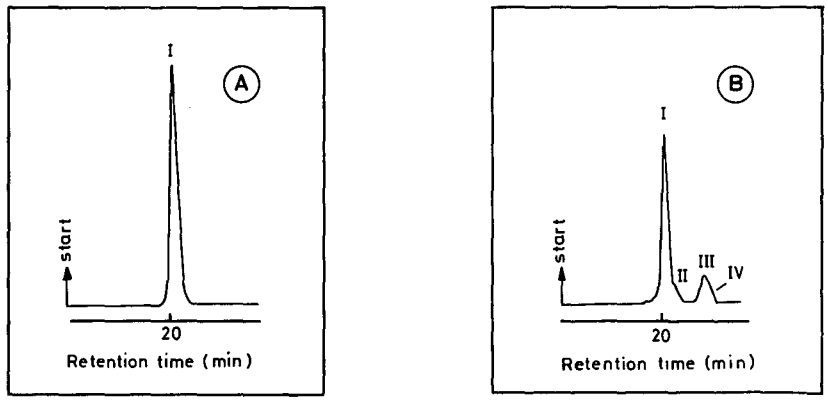

Fig. 2. (A) HPSEC chromatogram of refined safflower oil showing the molecular weight distribution of glycerides (I). (B) HPSEC chromatogram of crude neem oil showing the molecular weight distribution of triglycerides (I), mono- and diglycerides (II), free fatty acids (III) and the unsaponifiable fraction (IV).

TABLE II

MOLECULAR WEIGHTS OF VARIOUS OILS AND FATS DETERMINED BY HPSEC

Calculated from the total constituents present in the analyte.

Sample No.	*Name*	$\overline{M}_w$	$\overline{M}_n$	$\overline{M}_z$	$\overline{M}_v$	$\overline{M}_w/\overline{M}_n$
1	Coconut oil	712	701	723	720	1.0157
2	Butter fats					
	a $(BF)_W$	814	799	829	812	1.0188
	b $(BF)_H$	831	808	850	828	1.0285
3	Palm oil	886	876	896	884	1.0114
4	Cotton seed oil	889	869	915	886	1.0230
5	Soya bean oil	845	837	854	844	1.0096
6	Linseed oil	916	902	927	914	1.0155
7	Safflower oil	898	878	915	885	1.0228
8	Sesame oil	875	866	884	874	1.0104
9	Groundnut oil	903	894	911	901	1.0101
10	Ricebran oil					
	a Neutral oil	910	900	919	909	1.0201
	b Oil with 14.8% acid value	856	798	890	849	1.1152
11	Castor oil	965	953	979	964	1.0126
12	Mustard oil	1019	1014	1023	1018	1.0049
13	Corn oil	874	847	890	871	1.0319
14	Neem oil	811	703	876	799	1.1536
15	Vanaspathi					
	a S	896	887	906	894	1.0101
	b D	898	885	911	896	1.0147
	c T	906	892	919	904	1.0157
	d A	928	912	944	926	1.0175
16	Mahua oil	903	870	922	900	1.0379
17	Ram fat	941	917	951	939	1.0262
18	Broiler chicken fat	928	925	932	928	1.0032
19	Beef fat	918	877	932	915	1.0468

sample of stearic acid and an unsaponifiable fraction extracted from palm oil were injected for comparison of retention times. Stearic acid was eluted after 24.1 min which corresponds to the molecular weight, $\overline{M}_w$, of 380 according to the standard calibration graph (Fig. I). However, the true molecular weight of stearic acid is lower than the value obtained by HPSEC. This may be due to strong hydrogen bonding interactions between fatty acids and the mobile phase solvent.

From Table III and Fig. 3, in the case of refined samples the $\overline{M}_w$ obtained by HPSEC and that predicted from their SV data are seen to be in good agreement. The slope and intercept of the correlation graph are in accord with eqn. 2.

Molecular weight distributions of oils and fats

Fig. 2A shows that the moleclar weight distribution for mixtures of glycerides present in all vegetable oils and fats and animal body fats is represented by a symmetric gaussian peak at their respective retention times. However, two partially resolved peaks are observed in the case of butter fats. The first peak which corresponds to $\overline{M}_w$ of *ca.* 900 is due to the presence of high-molecular-weight glycerides containing $C_{18.1}$

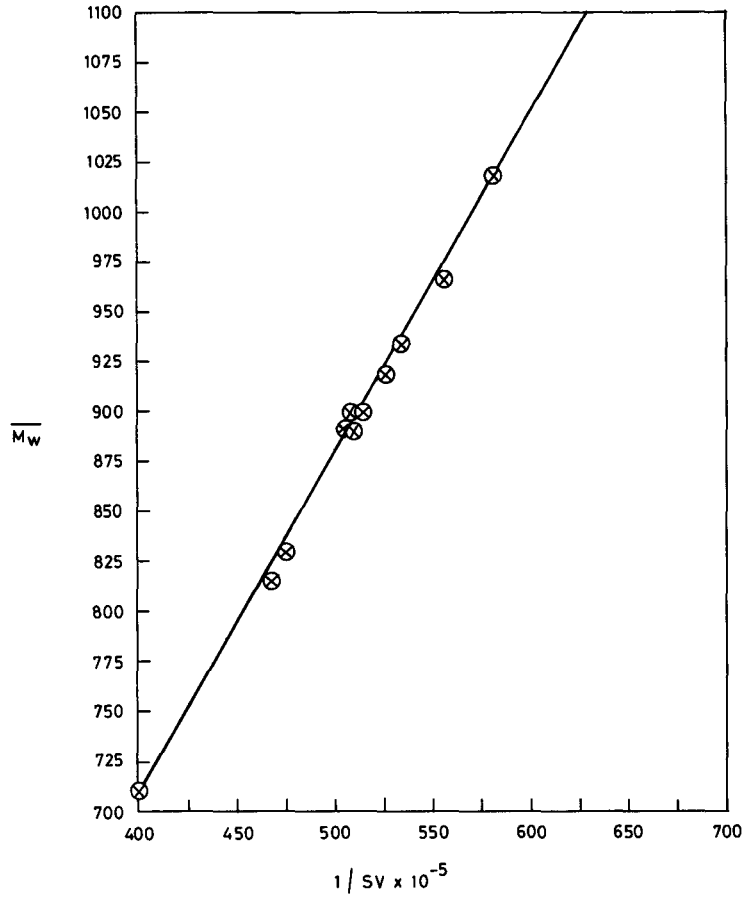

Fig. 3. Correlation of weight-average molecular weight, $\overline{M}_w$, and reciprocal of average experimental saponification value, 1/SV.

unsaturated fatty acid, whereas the second peak corresponds to $\overline{M}_w$ of *ca.* 700 due to low-molecular-weight glycerides containing saturated fatty acids of carbon numbers less than sixteen.

Two butter fats from different regions were studied in respect of their MWD and fatty acid composition using HPSEC and conventional gas–liquid chromatographic[12] techniques respectively. Fig. 4A and B show the MWD of two butter fats labelled as $(BF)_H$ and $(BF)_W$ respectively. It is seen that the high-molecular-weight glycerides are relatively more abundant in sample $(BF)_H$ than in $(BF)_W$. The fatty acid compositions of these samples are given in Table IV, and are in close agreement with the MWD.

MWD of binary mixtures of oils and fats

The MWD of glycerides for a pure oil is symmetric, whereas binary mixtures of oils having molecular weight differences of more than 100 units have unsymmetric molecular weight distributions. A number of binary systems, *viz.*, coconut oil (CCO)–castor oil (CO), butter fat (BF)–Vanaspathi (V), BF–CCO and CCO–mineral oil

TABLE III

COMPARISON BETWEEN $\overline{M}_w$ OBTAINED BY HPSEC AND THE MOLECULAR WEIGHT PREDICTED FROM SV DATA USING EQN. 2 FOR REFINED SAMPLES

Sample No.	*Name*	M_w	*Mol.wt. predicted*	*SV*	*% Error*
1	Coconut oil	712	708	251	0.5
2	Palm oil	886	892	197	0.7
3	Cotton seed oil	889	892	197	0.4
4	Safflower oil	898	903	194.5	0.5
5	Groundnut oil	903	915	192	1.3
6	Mahua oil	903	910	193	0.8
7	Linseed oil	916	920	191	0.5
8	Castor oil	965	973	180	0.9
9	Mustard oil	1019	1013	172.5	0.6
10	Butter fats				
	a $(BF)_W$	814	817	216	0.4
	b $(BF)_H$	831	836	211	0.6
11	Vanaspathi	928	933	188	0.6
12	Broiler chicken fat	928	905	194	2.5

(liquid paraffin) were studied to understand the MWD of binary mixtures of oils and fats.

Typical HPSEC chromatograms of these mixtures are presented in Fig. 5A, B, C and D respectively. Two partially resolved peaks for their respective triglyceride groups are seen in a CCO–CO mixture containing more than 5% CO. The resolution of the two peaks increases with increasing percentage of CO. A similar pattern was obtained for mixtures of CCO with other oils and fats, except BF.

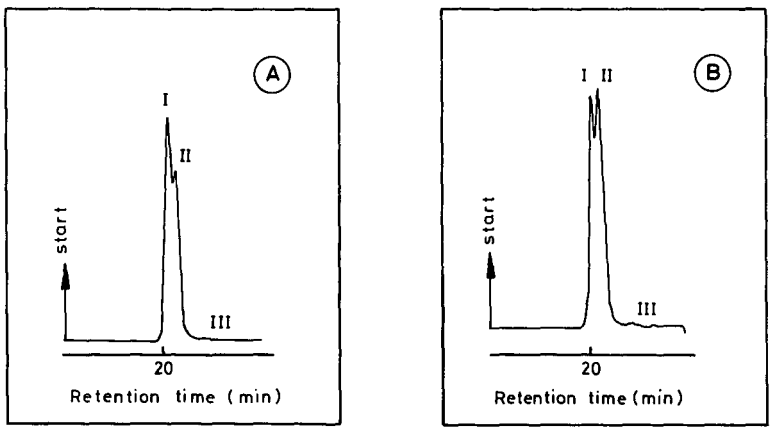

Fig. 4. HPSEC chromatograms of butter fat $(BF)_H$ (A) and butter fat $(BF)_w$ (B) showing the molecular weight distribution of relatively high-molecular-weight glycerides (I), relatively low-molecular-weight glycerides (II) and free fatty acids and the unsaponifiable fraction (III).

TABLE IV

FATTY ACID COMPOSITION (%) OF BUTTER FATS

	Fatty acid	*Sample code*	
		$(BF)_H$	$(BF)_W$
(A) Saturates			
1	Butyric acid ($C_{4:0}$)	1.8	1.6
2	Caproic acid ($C_{6:0}$)	0.4	0.8
3	Caprylic acid ($C_{8:0}$)	0.3	0.7
4	Capric acid ($C_{10:0}$)	0.6	1.0
5	Lauric acid ($C_{12:0}$)	1.0	1.7
6	Myristic acid ($C_{14:0}$)	5.8	7.7
7	Palmitic acid ($C_{16:0}$)	23.2	27.6
8	Stearic acid ($C_{18:0}$)	16.4	14.8
9	$C_{20:0}$, $C_{22:0}$, etc.	6.6	6.7
(B) Unsaturated			
1	Myristoleic acid ($C_{14:1}$)	1.6	2.1
2	Palmitoleic acid ($C_{16:1}$)	4.6	4.7
3	Palmitolinoleic acid ($C_{16:2}$)	3.1	2.9
4	Oleic acid ($C_{18:1}$)	23.8	18.0
5	Linoleic acid ($C_{18:2}$)	5.0	4.7
(C) Unusual fatty acids		5.8	5.0

It has already been mentioned that BF gives two peaks for its glycerides. The addition of any other oil or fat to it changes the intensities of these two peaks. It is seen from Fig. 5C that when CCO is added to BF the intensity of the low-molecular-weight peak is increased whereas Fig. 5B reveals that when vanaspathi is added to BF the intensity of the high-molecular-weight peak is increased. This observation may find application in detecting the adulteration of some oils and fats.

It is also observed that the ratio $\bar{M}_w/\bar{M}_n$ is almost unity for pure samples. Any change in the value of $\bar{M}_w/\bar{M}_n$ is indicative of adulteration. A typical example for admixtures of CCO–CO is shown in Fig. 5A(a) to (e) and Table V. It is also possible to detect the adulteration of mineral oil in edible oil by applying this method, as seen from Fig. 5D.

TABLE V

MOLECULAR WEIGHTS OF CCO–CO BINARY MIXTURES

Calculated from MWD of glycerides only.

Sample No.	*CCO (%)*	*CO (%)*	$\bar{M}_w$	$\bar{M}_n$	$\bar{M}_w/\bar{M}_n$
1	100.0	0.0	718	716	1.0028
2	97.5	2.5	734	721	1.0180
3	95.0	5.0	748	732	1.0218
4	90.0	10.0	768	747	1.0281
5	85.0	15.0	788	765	1.0301
6	80.0	20.0	801	775	1.0335

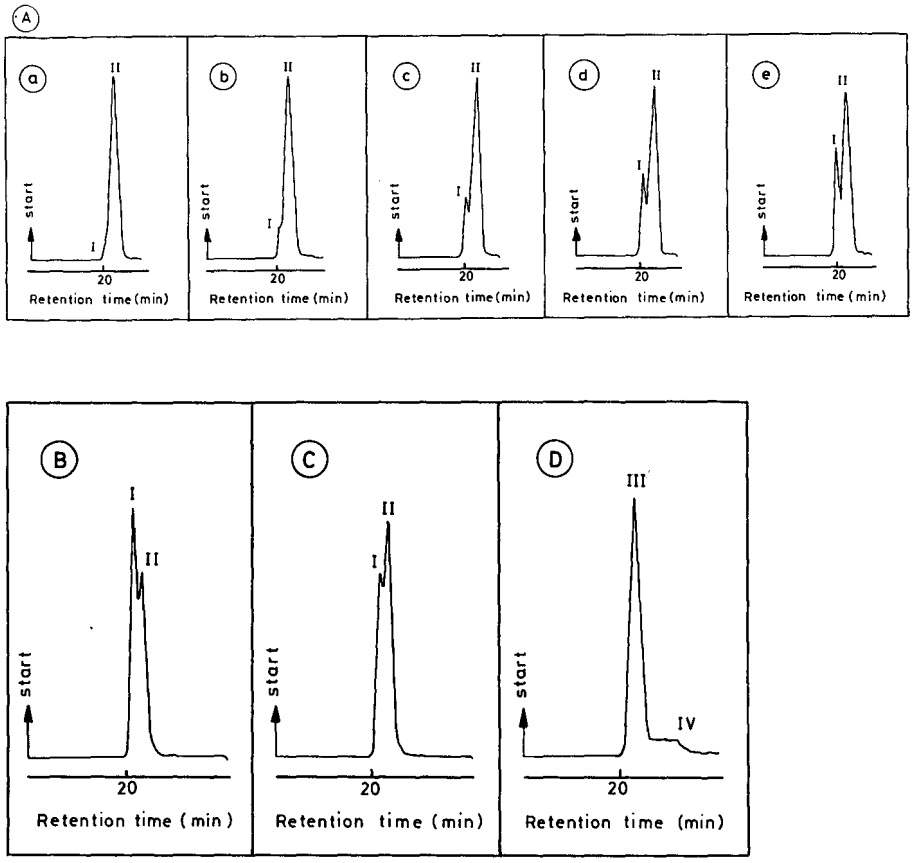

Fig. 5. (A) HPSEC chromatograms of coconut oil (CCO)–castor oil (CO) binary mixtures: (a) 97.5:2.5, (b) 95.0:5.0, (c) 90.0:10.0, (d) 85.0:15.0 and (e) 80.0:20.0. Molecular weight distributions: I, CO glycerides; II, CCO glycerides. (B) HPSEC chromatogram of $(BF)_W$ containing vanaspati, (C) containing CCO and (D) CCO containing mineral oil. Molecular weight distributions; III, CCO glycerides; IV, mineral oil fraction.

CONCLUSION

The determination of molecular weights and their distribution in oils and fats by HPSEC is reported for the first time. The data can be used for the characterization of various oils and fats. This method can be extended to the determination of adulteration in oils and fats.

REFERENCES

1 *Official and Tentative Methods of the American Oil Chemists' Society AOCS*, Vols. I and II, American Oil Chemists' Society, IL, 3rd ed., 1973.
2 *Methods of Sampling and Tests for Oils and Fats, IS:548*, Part I, Indian Standards Institution, New Delhi, 1964.
3 *British Standard Year Book and Catalogue of Publications*, British Standards Institution, London, 1983.

4 *Handbook of Indian Standards Institution*, Indian Standards Institution, New Delhi, 1987.
5 R. J. Hamilton and J. B. Rossell, *Analysis of Oils and Fats*, Elsevier, Barking, New York, 1986, p. 37.
6 E. Woollatt, *The Manufacture of Soaps, other Detergents and Glycerine*, Ellis Horwood, Chichester, 1st ed., 1985, p. 143.
7 A. Tager, *Physical Chemistry of Polymers (English translation)*, MIR, Moscow, 2nd ed., 1978, pp. 489–527.
8 V. F. Gaylor and H. L. James, *Anal. Chem.*, 48 (1976) 44R.
9 V. F. Gaylor and H. L. James, *Anal. Chem.*, 50 (1978) 29R.
10 J. Sjöström and B. Holmbom, *J. Chromatogr.*, 411 (1987) 363.
11 P. J. White and Y.-C. Wang, *J. Am. Oil Chem. Soc.*, 63 (1986) 914.
12 *Analysis of Oils and Fats by Gas Liquid Chromatography, IS:548*, Part III, Indian Standards Institution, New Delhi, 1976.

Journal of Chromatography, 454 (1988) 327–334
Elsevier Science Publishers B.V., Amsterdam — Printed in The Netherlands

CHROM. 20 815

Note

Theoretical aspects of the application of head-space analysis to the investigation of reaction kinetics in solutions

A. N. MARINICHEV and B. V. IOFFE*
Leningrad State University, Department of Chemistry, 199034 Leningrad (U.S.S.R.)
(First received February 18th, 1988; revised manuscript received June 14th, 1988)

The monographs on head-space analysis[1,2] contain no information concerning its application to kinetic investigations, although it has been suggested that head-space analysis may be used for the determination of rate constants and reaction order[1]. However, in a recent review of modern trends in the development of head-space analysis[3], particular attention has been paid to the study of reaction systems.

A number of papers deal with the problem of the kinetics of emission of harmful volatile impurities from polymer materials. However, either simply the time dependence of the amount of volatile components evolved is recorded or only particular cases are considered in which the progress of evolution of volatile substances may be approximated by a simple exponential function.

If the term "head-space analysis" is interpreted in a broad sense[4], its should encompass also the procedure of gas chromatography with flow stop and reversal, which has been applied to the study of reactions on the surface of solid catalysts (see, *e.g.*, ref. 5). However, the investigation of the possible applications of head-space analysis to the study of the kinetics of volatile product formation in solutions is only just beginning. The first paper in this field[6] was based on the periodical sampling of vapour from the reaction mixture and empirical detector calibration according to the volatile products in the vapours above solutions of known concentrations. Nevertheless, only one example of the determination of rate constants by this method is known[7] (oxidation of mercaptans with aqueous dimethyl sulphoxide).

Preliminary communications[8,9] have been concerned with the relationships concerning discrete and continuous gas extraction of volatile products of slow liquid-phase first-order reactions in heterogeneous systems with high mass exchange rates. In this paper the consideration of the possibility of using head-space analysis for obtaining kinetic information is continued, including cases in which the attainment of the phase equilibrium is hindered and methods of calculating the rate constants.

Symbols

$C_L(t)$ and $C_G(t)$ are the concentrations (mass-volume concentrations) of the volatile product in a liquid, L, and in a gas, G, at the time t.

τ is the time interval (min) between the replacements of the gas phase contacting the reaction mixture.

0021-9673/88/$03.50

$K = C_L/C_G$ is the partition coefficient.

$K^{(q)} = C_{Lq}/C_{Gq}$ is the concentration ratio of the reaction product in the liquid and the gas phase in the qth stage of extraction.

$B_{\tau q} = C_{G(q+1)}/C_{Gq}$ is the "dynamic buffer coefficient"[10].

V_L and V_G are the volumes of the liquid and the gas phases, respectively; $r = V_G/V_L$.

$B^{(q)} = K^{(q)}/(r + K^{(q)})$ is the buffer coefficient[10].

K_1 is the rate constant for the process of transformation of the reagent into the volatile product; $E = \exp(-K_1\tau)$.

ω is the carrier gas flow-rate (ml/min).

$V_0 = \omega t$ is the gas volume passing during time t.

C_0 is the concentration (g/ml) of the non-volatile reagent in the liquid phase before the reaction start; $a = \omega/(KV_L)$; $b = C_0^0 K_1/K$; $\rho = a/K_1$.

Repeated gas extraction of reaction mixtures

Let us consider consecutive extraction stages of the volatile product of first-order reactions in the liquid phase by identical volumes of a pure inert gas. For the first extraction ($q = 1$) the material balance equations in the above system of designations are given by

$$(K^{(1)} + r)C_{G1} = C_0^0(1 - E) \tag{1}$$

and for the following extractions ($q = 2, \ldots, n$) by:

$$(K^{(q)} + r)C_{Gq} = C_0^0 E^{q-1}(1 - E) + K^{(q-1)}C_{G(q-1)} \tag{2}$$

Here the establishment of the phase equilibrium in the system is not assumed, and if the value characterizing the contribution of the volatile component in the gas phase is introduced

$$1 - B^{(q)} = r/(r + K^{(q)}) \tag{3}$$

we obtain the expressions for the concentrations of this component after the first and the subsequent extraction stages:

$$C_{G1} = \frac{C_0^0}{r}(1 - E)(1 - B^{(1)}) \tag{4}$$

$$C_{Gq} = \frac{C_0^0}{r}(1 - E)(1 - B^{(q)})\{E^{q-1} + B^{(q-1)}[E^{q-2} + B^{(q-2)}(\ldots)]\} \tag{5}$$

$(q = 2, \ldots, n)$

As already mentioned[11], it is not desirable to carry out a great number of gas extractions because of the possibility of a "memory" effect of the instrumentation and the great expenditure of time. Restricting ourselves to the minimum number of extractions required for calculations, we will assume the simplest proportional

dependence between the contributions of the volatile component in the gas phase in consecutive extractions

$$1 - B^{(q)} = \alpha(1 - B^{(q+1)}) \tag{6}$$

where α is a constant characterizing the deviation of component partition between the phases from the equilibrium partition ($0 \leqslant \alpha \leqslant 1$). Then the values of the dynamic buffer coefficients determined directly are:

$$B_{\tau 1} = C_{G2}/C_{G1} = (E + B^{(1)})/\alpha \tag{7}$$

$$B_{\tau 2} = C_{G3}/C_{G2} = \left(\frac{E^2}{E + B^{(1)}} + B^{(2)}\right)\Big/\alpha \tag{8}$$

$$B_{\tau 3} = C_{G4}/C_{G3} = \left(\frac{E^3}{E^2 + B^{(2)}(E + B^{(1)})} + B^{(3)}\right)\Big/\alpha \tag{9}$$

In order to determine the kinetic parameters by the iterative method, it is convenient to rewrite eqns. 7–9 in the forms

$$\alpha = (E + B^{(1)})/B_{\tau 1} \tag{10}$$

$$B^{(1)} = 1 - \alpha + \alpha^2 B_{\tau 2} - E^2/B_{\tau 1} \tag{11}$$

$$E = \sqrt[3]{B_{\tau 1} B_{\tau 2} [1 - B^{(1)} - \alpha^2(1 - \alpha B_{\tau 3})]} \tag{12}$$

and to assume as zero (initial) approximation that these values are equal to 0.5.

An indispensable condition of a relatively precise measurement of rate constants K_1 for a limited number of consecutive extractions is the optimum choice of duration of each extraction stage, τ. Since $E = \exp(-K_1\tau)$, the errors in K_1 and E are related to each other by:

$$\frac{|\Delta K_1|}{K_1} = \frac{1}{|\ln E|} \cdot \frac{|\Delta E|}{E} \tag{13}$$

Hence, the precision of determination of the rate constants K_1 attainable with the experimental error, ΔE, depends on the value of E and consequently on the ratio of K_1 to τ. Thus, if $\Delta E/E \approx 0.02$ and the required precision of the determination of K_1 is $\pm 10\%$, the value of E should be equal to $\exp(-0.02/0.1) = 0.82$. This value implies that at $K_1 \approx 0.1$ the duration of each extraction stage should be approximately 2 min, at $K_1 \approx 0.01$ it should be 20 min, etc. Arbitrary choice of the time τ can lead to excessive error or can even make the calculation of the parameters impossible[8–10]. Since it is difficult to reduce manually the duration of the gas phase replacement to a few seconds, the measurements of constants for rates higher than 0.1 min^{-1} would require special automatic instrumentation. Moreover, the measurement of constants

for slow reactions ($K_1 < 10^{-3}$ min^{-1}) can be carried out only during several hours and even longer.

If the reaction rate in the liquid phase is relatively slow (in order that the phase equilibrium may be considered to be virtually established at any moment of time) then $\alpha \approx 0$ and in this case, which has been considered previously[8], equations of the type 4 and 5 can be written in the form:

$$B_{\tau n} = B + E\left[\sum_{q=0}^{n-1} (B/E)\right]^{-1} \tag{14}$$

Since at $n \to \infty$ the sum contained in this equation acquires the value of ∞ at $(B/E) \geqslant 1$ and at $(B/B) < 1$ becomes equal to $[1 - (B/E)]^{-1}$, it is evident that with increasing extraction number the value of the dynamic buffer coefficient, $B_{\tau n}$) decreases, tending in the limit to the larger of the numbers B or E.

In order to determine parameters E and B, only the data on the first three extractions, *i.e.*, the values of $B_{\tau 1}$ and $B_{\tau 2}$ may be used. Indeed, eqns. 7 and 8 become

$$B_{\tau 1} = B + E \tag{15}$$

$$B_{\tau 2} = B + E^2/(B + E) \tag{16}$$

and

$$\left.\begin{matrix} E/B_{\tau 1} \\ \text{and} \\ B/B_{\tau 1} \end{matrix}\right\} = 0.5 \pm \sqrt{(B_{\tau 2}/B_{\tau 1}) - 0.75} \tag{17}$$

The values of E, *i.e.*, the desired reaction rate K_1 proper, and B, *i.e.*, the partition coefficient K, may be found if $1 > B_{\tau 2}/B_{\tau 1} \geqslant 0.75$. However, it is impossible to determine which of the roots in eqn. 17 refers to E and which refers to B without supplementary information. This information may be provided by repeated experiments at a different extraction time, τ, other conditions being equal (when the value of E will vary) or at a different ratio of the phase volumes, r (when the value of B will vary).

Continuous gas extraction of the reaction mixtures

The change in the concentration of the volatile product of chemical liquid-phase reaction which is entrained by an inert gas passing above the liquid (or through it) is described by a linear non-homogeneous differential equation[8]:

$$\frac{dC_G}{dt} = -aC_G + be^{-K_1 t} \tag{18}$$

As a result of the differentiation of eqn. 18 over t and exclusion of b we have:

$$\frac{d^2C_G}{dt^2} + (a + K_1)\frac{dC_G}{dt} + (aK_1)C_G = 0 \tag{19}$$

It is known that to solve eqn. 19 it is necessary to find the roots of the supplementary quadratic equation:

$$\lambda^2 + (a + K_1)\lambda + (aK_1) = 0 \tag{20}$$

The roots of eqn. 20 are evidently $-a$ and $-K_1$. If a and K_1 are real values and $a \neq K_1$

$$C_G(t) = C_1 e^{-at} + C_2 e^{-K_1 t} \tag{21}$$

where C_1 and C_2 are integration constants. In the case when $a = K_1$, we have:

$$C_G(t) = (C_1 t + C_2) e^{-at} \tag{22}$$

In combination with the initial condition $C_G(0) = 0$, eqns. 21 and 22 become, respectively:

$$C_G(t) = \frac{b}{K_1 - a}(e^{-at} - e^{-K_1 t}) \tag{23}$$

$$C_G(t) = bte^{-at} \tag{24}$$

The form of the corresponding functions is shown in Fig.1. Both curves exhibit a maximum at t_m and an inflexion at $t_b = 2t_m$. The values of t_m and t_b may prove to be useful for increasing the precision of the time-scale and for the establishment of the initial moment of time, $t = 0$ (moment of the start of chemical interaction). For example, it is important in the case when the moment of introduction of the reagent into the chromatographic system does not coincide with that of the beginning of its interaction with the other reactants or with the catalyst. Moreover, since at $a \neq K_1$ we have $t_m = \ln\rho/K_1(\rho - 1)$ and at $a = K_1$ we have $t_m = 1/a$, it is evident that if one of the constants, a or K_1, is known, it is possible to calculate the other constant by using the value of t_m.

It follows from ref. 12 that eqns. 23 and 24 are the solutions of the homogeneous difference second-order equation

$$C_G(t + 2) + pC_G(t + 1) + qC_G(t) = 0 \tag{25}$$

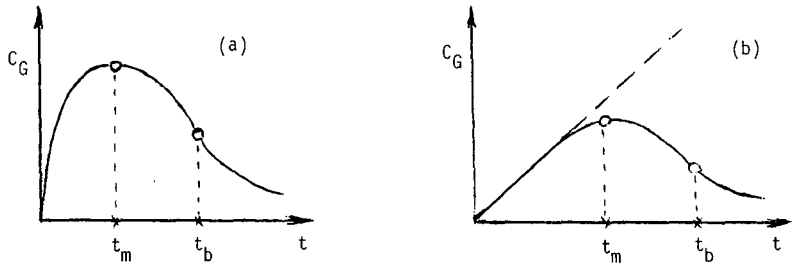

Fig. 1. Dependence of $C_G(t)$ according to eqns. 23 (a) and 24 (b).

with the initial condition $C_G(0) = 0$. Moreover:

$$\left.\begin{aligned} -p &= \exp(-K_1) + \exp(-a) \\ q &= 1/\exp(K_1 + a) \end{aligned}\right\} \tag{26}$$

The coefficients p and q can be calculated from the experimental data for $C_G(t)$ by the least-square method (as linear regression coefficients). As the sum and the products of the values $\exp(-K_1)$ and $\exp(-a)$ are known, the constants K_1 and a can easily be determined. For the experimental data $C_G(0) = 0$, $C_G(\Delta t)$, $C_G(2\Delta t)$, ... with equal intervals between the measurements of $\Delta t \neq 1$, eqn. 25 becomes:

$$C_G(t + 2\Delta t) + pC_G(t + \Delta t) + qC_G(t) = 0 \tag{27}$$

Now the values of p and q are expressed by equations similar to eqn. 26:

$$\left.\begin{aligned} -p &= \exp(-K_1\Delta t) + \exp(-a\Delta t) \\ q &= 1/\exp[(K_1 + a)\Delta t] \end{aligned}\right\} \tag{28}$$

In practice the value of C_G is usually replaced by that of $H(t)$ proportional to it: this is the height or the surface area of the chromatographic peak representing the product content in the gas phase at the time t.

The first two points should be borne in mind. First, if it is not known which of the parameters, K_1 or a, is larger, eqns. 25 and 28 cannot be uniquely identified with the roots of K_1 and a. In these cases it is necessary to use additional information from experiments carried out under different conditions (temperature, gas flow-rate, etc.). Secondly, the "restoration" of the parameters K_1 and a in eqns. 23 and 24 is possible only if the experimental data for $H(t)$ are sufficiently precise[12].

In order to establish the effect of random errors in chromatographic measurements (peak heights or areas), a computer simulation of experiments was carried out. It consisted of two stages: (1) On the basis of the initial values of b, K_1 and a, the value of $H(t)$ was calculated according to eqn. 23 and using the random number generator a random error was introduced into this value. This error corresponded to the standard deviation of 2% consistent with the possibilities provided by the gas chromatograph. (2) The values of $H(t)$ obtained in this manner were used to "restore" the desired parameters K_1 and a by the above procedure. Among cases with $\rho > 1$, such cases were considered in which t_m ranged from 5 to 10 min. It is in this range of t_m that the results of this restoration are most uncertain *a priori*.

Table I gives the results of the application of this method of determining the parameters K_1 and a from the data on $H(t)$ with a relative error of 2%. Each ine of the table contains the results of the treatment of 6–12 computer simulations. In each simulation, up to 22 points were taken into account. It is seen that at $\rho = 2$ the restoration of the values of both parameters was observed for all Δt intervals, whereas at $\rho \geqslant 10$ it was usually possible to obtain a reliable value only for the smaller parameter. In order to explain this fact, let us analyze the equation of errors for the value of $H_m = H(t = t_m)$ determined by the relation

$$H_m = CK_1\rho^{1/(1-\rho)}$$

TABLE I

VALUES OF THE PARAMETERS K_1 AND a FROM THE RESULTS OF 6–12 COMPUTER SIMULATIONS

Initial data					*Results of calculations*	
$K_1 \cdot 10^{-3}$ (min^{-1})	a (min^{-1})	ρ	t_m (min)	t (min)	$K_1 \cdot 10^{-3}$ (min^{-1})	a (min^{-1})
5	0.5	100	9	10	4.93	–
				5	4.82	–
				2	3.7	0.61
10	1.0	100	5	10	9.97	–
				5	9.92	–
				2	9.2	–
10	0.5	50	8	10	9.9	–
				5	9.8	–
				2	8.3	0.56
50	0.5	10	5	10	49.9	–
				5	49.5	–
				2	49.4	0.57
50	0.2	4	9	10	49.9	0.20
				5	49.3	0.22
				2	52	0.21
100	0.2	2	7	10	98	0.21
				5	99	0.22
				2	97	0.24

where C is a constant

$$\frac{\Delta H_m}{H_m} = \frac{\Delta K_1}{K_1} + \varphi(\rho)\frac{\Delta \rho}{\rho} \tag{29}$$

where $\varphi(\rho) = (1 - \rho)^{-2}(1 - \rho + \rho\ln\rho) \in [0 + 1]$

In the cases considered here $\Delta H_m/H_m = 0.02$ and evidently:

$$\frac{\Delta \rho}{\rho} = \frac{\Delta K_1}{K_1} = \frac{\Delta a}{a} \leqslant \frac{1}{\varphi(\rho)}\left(\frac{\Delta H_m}{H_m} + \frac{\Delta \rho}{\rho}\right) \tag{30}$$

The relative error in the larger constant a is determined from eqn. 30: since $1/\varphi(\rho)$ greatly increases with ρ, the value of $(\Delta a/a)$ also increases with ρ. As a result of this increase, the smaller of the roots $\exp(-K_1)$ and $\exp(-a)$ becomes (as a rule at $\rho \geqslant 10$) negative and it is impossible to restore the values of both parameters from the data for $H(t)$ by the non-iterative method.

REFERENCES

1 H. Hachenberg and A. P. Schmidt, *Gas Chromatographic Headspace Analysis*, Heyden & Son, London, 1977.

2 B. V. Ioffe and A. G. Vitenberg, *Head-Space Analysis and related Methods in Gas Chromatography*, Wiley, New York, 1984.
3 B. V. Ioffe, *Zh. Anal. Khim.*, 42 (1987) 197.
4 B. V. Ioffe, *J. Chromatogr.*, 290 (1984) 363.
5 N. A. Katsanos and G. Karaiskakis, *Adv. Chromatogr. (N.Y.)*, 24 (1984) 125.
6 I. Ya. Levitin, *Kinet. Katal.*, 12 (1971) 227.
7 B. Zygmunt and A. Przyjazny, *J. Chromatogr.*, 294 (1984) 117.
8 B. V. Ioffe, L. A. Kokovina and B. V. Stoljarov, *Dokl. Akad. Nauk SSSR*, 286 (1986) 117.
9 A. N. Marinichev and B. V. Ioffe, *Dokl. Akad. Nauk SSSR*, 292 (1987) 1181.
10 B. V. Ioffe and T. L. Reznik, *Zh. Anal. Khim.*, 36 (1981) 2191.
11 B. V. Ioffe, A. G. Vitenberg and T. L. Reznik, *Zh. Anal. Khim.*, 37 (1982) 902.
12 C. Lanczos, *Applied Analysis*, Prentice-Hall, New York, 1957.

Journal of Chromatography, 454 (1988) 335–339
Elsevier Science Publishers B.V., Amsterdam — Printed in The Netherlands

CHROM. 20 766

Note

Sedimentation focusing field-flow fractionation in channels of triangular cross-section

STANISLAV WIČAR
Hvězdárenská 3, 61600 Brno (Czechoslovakia)
(Received June 30th, 1988)

Sedimentation focusing field-flow fractionation in channels with modulated cross-sectional permeability has been proposed by Janča and Jáhnová[1]. Later Janča and Chemelík[2] published some preliminary results obtained in a gravitational field.

A limiting case of focusing based on Archimedes' forces is focusing in a pseudo-discontinuous density field. Let us consider a channel of triangular cross-section containing three layers of liquids differing only slightly in their densities. The lower part of the channel is occupied by the most dense, the middle part by a less dense and the upper part by the least dense liquid. The density gradients necessary for focusing are concentrated in the diffusional zones around the interfaces separating homogenous liquids. If a binary mixture of particles differing merely in density is introduced at the channel inlet, then after relaxation both particle species are focused at the interfaces, provided that the particle densities match those of liquid layers.

The initial particle distribution could be expressed in terms of spatial resolution, R_y:

$$R_y = \frac{y_1 - y_0}{\overline{W}} \tag{1}$$

where y_1 and y_0 are the coordinates of the two interfaces and $\overline{W}$ is the effective thickness of the interface zone. As the thickness of each diffuse zone does not depend on the medium layer height, $y_1 - y_0$, the initial spatial resolution could be generated over wide limits.

During the subsequent field-flow fractionation process the spatial resolution, R_y, is transformed into a time-based resolution, R_t. The efficiency of this process, R_t/R_y, is controlled by convective diffusion within both interface zones. To evaluate the efficiency, we have first to describe the hydrodynamics in a channel of triangular cross-section.

Janča and Jáhnová[1] modified Takahashi and Gill's[3] approximate solution of the Poisson equation for fully developed laminar flow in rectangular channels:

$$u(x,y) = \frac{\Delta P b^2}{2\eta L}(1-y^2/b^2)\left[1 - \frac{\cosh(\sqrt{3}\,x/b)}{\cosh(\sqrt{3}\,w/b)}\right] \tag{2}$$

0021-9673/88/$03.50

by multiplying the right-hand side of eqn. 2 by the function

$$\left[1 + x/w\left(\frac{y_2 - y_1}{y_2 + y_1}\right)\right]^2 \tag{3}$$

to satisfy the new boundary problem for a trapezoidal cross-section. In eqn. 2 $\Delta P/L$ is the pressure drop applied to the channel, η is fluid viscosity and b and w are the channel dimensions. In expression 3 y_2 and y_1 are the channel widths at both sides of the channel.

Unfortunately, the resulting $u(x,y)$ function does not satisfy the basic Poisson equation

$$\frac{\partial^2 u}{\partial x^2} + \frac{\partial^2 u}{\partial y^2} = -\frac{\Delta P}{\eta L} \tag{4}$$

To find the solution of eqn. 4 for a channel of triangular cross-section, we may start with the construction of a function $f(x,y)$ that vanishes at the channel walls (Fig. 1):

$$f(x,y) = (y - ax)(y + ax) \tag{5}$$

where

$$a = \tan \alpha = \operatorname{cotan} \beta/2 = \frac{\sin \beta}{1 - \cos \beta}$$

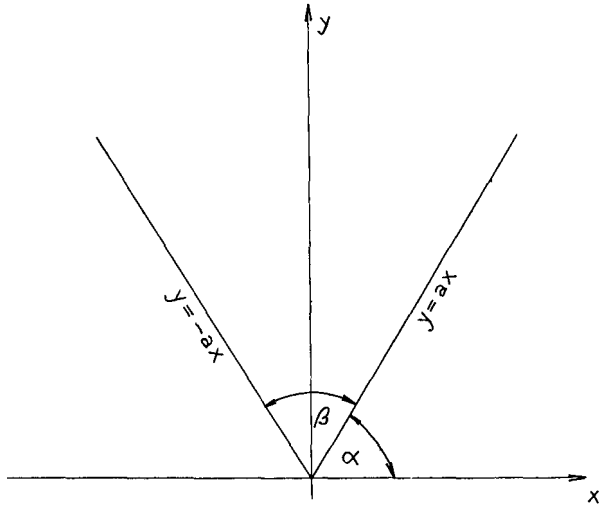

Fig. 1. Orientation of the channel in the rectangular coordinate system.

As the Laplacean of f(x,y) equals a constant:

$$\frac{\partial^2 f}{\partial x^2} + \frac{\partial^2 f}{\partial y^2} = -2(a^2 - 1)$$

we may use function 5 to form the solution of eqn. 4:

$$u(x,y) = \frac{\Delta P}{2\eta L(a^2 - 1)} (y^2 - a^2x^2) \tag{6}$$

Eqn. 6 expresses the velocity profiles in an open channel of triangular cross-section, provided that $\beta < \pi/2$. For a closed channel, the profiles are modified merely at the upper wall. The important central part of the profiles in eqn. 6 for $x = 0$ is parabolic and does not display any local minimum as the equation of Janča and Jáhnová[1] does.

The convective diffusion could be characterized by an HETP equation:

$$H = \frac{2D}{\bar{u}} + \frac{w^2\bar{u}}{\kappa D} \tag{7}$$

where w is the channel width, κ, according to Aris[4], is a dimensionless number, D is the diffusion coefficient of separated particles and $\bar{u}$ is the linear mean velocity.

For the mean velocity of each interface layer we obtain from eqn. 6, provided that $\eta_0 \doteq \eta_1 \doteq \eta_2 = \eta$,

$$\bar{u}(y) = \frac{K}{a^2 - 1} \cdot y^2 \tag{8}$$

where $K = \Delta P/3\eta L$ is the normalized pressure drop across the channel. By inserting from eqn. 8 into eqn. 7, taking into account that $w = 2y/a$,

$$H = \frac{2D(a^2 - 1)}{Ky^2} + \frac{4Ky^4}{a^2(a^2 - 1)\,\kappa D} \tag{9}$$

We may minimize H with respect to the normalized pressure drop K to obtain

$$K_m = \frac{\tau a(a^2 - 1)\,D}{y^3}$$

where $\tau = \sqrt{\kappa/2}$. Relating the minimum H to the first interface at y_0, we have

$$H_{m0} = \frac{4y_0}{a\tau}$$

and

$$\sigma_{t0} = \frac{\sqrt{H_{m0} L}}{\bar{u}_0} = \frac{1}{aD}\sqrt{\frac{4y_0^3 L}{a\tau^3}} \tag{10}$$

For H_1 and the time variance of the particle distribution at the second interface, y_1, we obtain

$$H_1 = \frac{2y_1}{a\tau}\left(\frac{y_0^3}{y_1^3} + \frac{y_1^3}{y_0^3}\right)$$

and

$$\sigma_{t1} = \frac{1}{aD}\sqrt{\frac{2L}{a\tau^3} \cdot \frac{y_0^6}{y_1^3}\left(\frac{y_0^3}{y_1^3} + \frac{y_1^3}{y_0^3}\right)} \tag{11}$$

The time-based resolution at the end of the channel is by definition

$$R_t = \frac{2L(1/\bar{u}_0 - 1/\bar{u}_1)}{4(\sigma_{t0} + \sigma_{t1})}$$

and after inserting from eqns. 8, 10 and 11 we obtain

$$R_t = \mathrm{f}(y_0,y_1)\sqrt{aL\sqrt{\kappa/2}}(y_1 - y_0) \tag{12}$$

where

$$\mathrm{f}(y_0,y_1) = \frac{1}{y_1^2} \cdot \frac{y_0(y_1 + y_0)}{2\sqrt{y_0^3} + \sqrt{2\frac{y_0^6}{y_1^3}\left(\frac{y_0^3}{y_1^3} + \frac{y_1^3}{y_0^3}\right)}}$$

Janča and Jáhnová[1] used a channel with $\beta = 2^0$ and a = 57.3; the length of the channel was 30 cm. For $y_0 = 1$ cm, $y_1 = 2$ cm, f(1,2) = 3/16. Taking κ according to Golay[5] as 105, we have $R_t = 20.9$.

Estimating the effective thickness of the interface zones as 0.5 mm, the efficiency of the transformation process is approximately 1. Unfortunately, if the effective diffusion coefficient of separated particles is of the order of 10^{-7} cm^2/s, the time for this separation is unrealistic:

$$\frac{L}{u_0} = \frac{Ly_0}{\tau aD} = 7.2 \cdot 10^5 \text{ s} = 200 \text{ h}$$

By increasing the optimum normalized pressure drop by a factor of 100, we obtain for the time-based resolution

$$R_{t100} = f_1(y_0,y_1)\frac{\sqrt{aL\sqrt{\kappa/2}}}{40}(y_1 - y_0) \tag{13}$$

where

$$f_1(y_0,y_1) = \frac{y_1 + y_0}{y_1^2\sqrt{2y_0}}$$

and for the same channel we have $R_{t100} = 1.4$ and the efficiency of the transformation is merely 0.1; the process requires about 2 h.

It is evidently questionable whether field-flow fractionation is the best solution for the conversion of the spatial resolution to the time-based resolution in sedimentation separations using gravitation. Apparently better results could be obtained if the sedimentation focusing process were accomplished in a burette-like vertical tube. Connecting the lower end of this tube directly to the detector, the direction of flow coincides with that of the gravitational force and, once obtained, the spatial resolution is converted to its time-based form directly with greater efficiency in a substantially shorter time. Such an arrangement, of course, could hardly be called field-flow fractionation.

REFERENCES

1 J. Janča and V. Jáhnová, *J. Liq. Chromatogr.*, 6 (1983) 1559.
2 J. Janča and J. Chmelík, *J. Liq. Chromatogr.*, 9 (1986) 55.
3 T. Takahashi and W. N. Gill, *Chem. Eng. Commun.*, 5 (1980) 367.
4 R. Aris, *Proc. R. Soc. London, Ser. A*, 252 (1959) 538.
5 M. J. E. Golay, in D. H. Desty (Editor), *Gas Chromatography 1959*, Academic Press, New York, 1959, p. 36.

Journal of Chromatography, 454 (1988) 340–344
Elsevier Science Publishers B.V., Amsterdam — Printed in The Netherlands

CHROM. 20 767

Note

Macrocyclic polyfunctional Lewis bases

XII. Influence of complex formation on chromatographic migration

J. KOSTROWICKI*, E. LUBOCH, B. MAKUCH, A. CYGAN, A. HORBACZEWSKI and J. F. BIERNAT
Institute of Inorganic Chemistry and Technology, Technical University of Gdańsk, 80-952 Gdańsk (Poland)
(First received February 25th, 1988; revised manuscript received July 1st, 1988)

Macrocyclic polyethers, their aza analogues, cryptands, some podands and numerous groups of biologically important compounds (such as the antibiotics valinomycin and nigericin) form complexes with metal ions, especially of alkali and alkaline earth metals, and ammonium cations[1]. The determination of the stability of these complexes permits a better understanding of the properties of ligand or the qualification of their biological action.

In crown ether chemistry[2–5] some qualitative tests have been introduced to establish whether the given ligand forms complexes with the cation under consideration. A simple thin-layer chromatographic (TLC) test described previously[6] is based on changes on the chromatographic R_F values of ligands caused by impregnation of the support with salts. The influence of complex formation on R_F values has been reported for many cations[7].

In this paper we present the results of experiments on and a simplified mathematical treatment of the chromatographic behaviour of ligands 1–13 (Fig. 1) in the presence of salts. Experiments were performed using TLC and high-performance liquid chromatography (HPLC) using impregnated silica gel as the stationary phase.

EXPERIMENTAL

Silufol plates (3 × 8 cm) were impregnated on one half with 2% solutions of alkali metal, strontium or barium chlorides by developing them perpendicularly along the longer edge. The plates were then dried and heated at 105°C for 2 h. The ligands were applied on the impregnated and unimpregnated parts of the plate and developed along the longer edge. The spots on the chromatograms were detected with iodine. The solvent systems used were selected to obtain R_F^0 values of 0.6–0.8. The results are summarized in Table I.

HPLC experiments were performed using a KB-5101 (Kabid-Warszawa) apparatus equipped with a UV detector (254 nm). The columns (100 × 3.3 mm I.D.) were dry packed with silica gel (particle diameter, d_P = 33 μm) obtained by multiple sedimentation of an H-60 (Machery, Nagel & Co.) gel. The solid phase was impregnated in the following way: a 1-g portion of silica gel was mixed with a solution of

0021-9673/88/$03.50

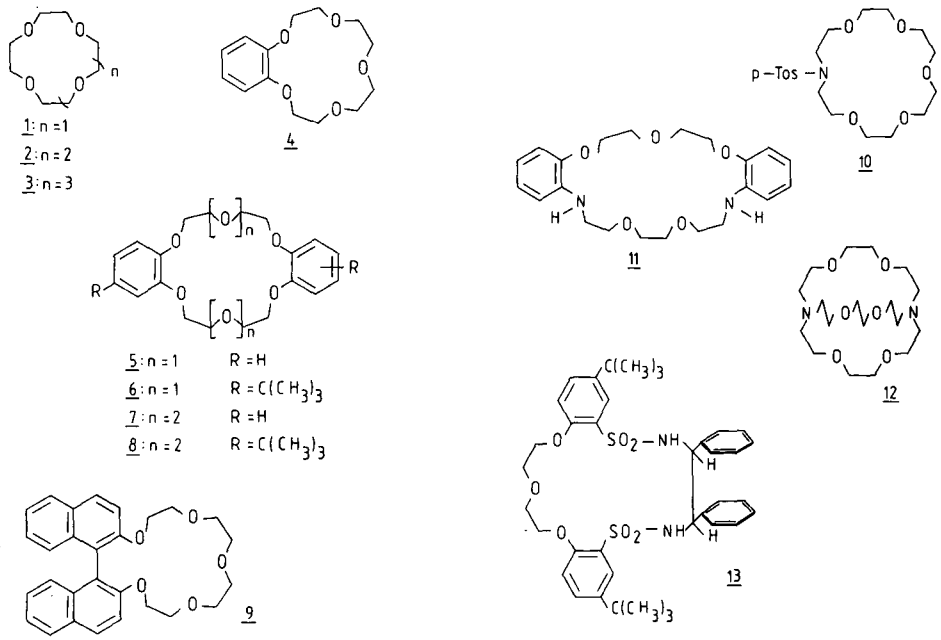

Fig. 1. Structures of compounds 1–13.

0.1 g of the respective salt in water (1 cm^3) and the mixture was dried for 2 h at 105°C. The results of the HPLC experiments are summarized in Table II.

RESULTS AND DISCUSSION

The changes in R_F values[8] may be expressed by the equation

$$\Delta R_M = \log (1/R_F^1 - 1) - \log (1/R_F^0 - 1) \quad (1)$$

where R_F^0 denotes the R_F valve on the unimpregnated support and R_F^1 that on the salt-impregnated support.

In the HPLC technique we should consider analogously the equation

$$\Delta V_M = \log (V_R^1/V^D - 1) - \log (V_R^0/V^D - 1) \quad (2)$$

where $V_R{}^0$ is the retention volume on the unimpregnated support. $V_R{}^1$ the retention volume on the salt-impregnated support and V^D the dead volume.

Migration in the presence of a salt differs because of complex formation. Most ligands exhibit retardation on the impregnated compared with the unimpregnated support. The greatest retardation was observed for ligands that form the strongest complexes. Ligand 12 is an interesting exception where acceleration is observed.

In order to explain this behaviour, let us assume that the chromatographic process is described by a partition mechanism and the species ligand L, metal ion M, complex ML and anion A exist in the stationary phase (water) and ligand L, ion pair

TABLE I

RESULTS OF TLC MEASUREMENTS

*Mobile phase**	*Ligand*	R_F^0	R_F^1 *and* ΔR_M	*Salt*							
				LiCl	*NaCl*	*KCl*	NH_4Cl	*RbCl*	*CsCl*	$SrCl_2$	$BaCl_2$
I	1	0.75	R_F^1	0.68	0.73	0.80	0.65	0.73	0.83	–	–
			ΔR_M	0.15	0.05	−0.12	0.21	0.05	−0.21		
I	2	0.80	R_F^1	0.65	0.63	0.65	0.60	0.70	0.75	–	–
			ΔR_M	0.33	0.37	0.33	0.42	0.23	0.12		
I	3	0.80	R_F^1	0.88	0.65	0.55	0.68	0.60	0.60	–	–
			ΔR_M	−0.27	0.33	0.51	0.27	0.42	0.42		
II	4	0.60	R_F^1	0.10	0.13	0.15	0.23	0.08	0.33	0.13	0.18
			ΔR_M	1.13	1.01	0.93	0.7	1.24	0.49	1.01	0.84
II	5	0.63	R_F^1	0.60	0.10	0.08	0.13	0.45	0.43	–	–
			ΔR_M	0.05	1.18	1.29	1.06	0.32	0.35		
II	6	0.62	R_F^1	0.80	0.20	0.15	0.22	0.20	0.37	–	–
			ΔR_M	−0.39	0.81	0.96	0.76	0.81	0.44		
II	7	0.62	R_F^1	0.50	0.27	0.20	0.25	0.15	0.17	0.52	0.20
			ΔR_M	0.21	0.64	0.81	0.69	0.96	0.9	0.18	0.81
II	8	0.70	R_F^1	0.62	0.27	0.22	0.30	0.17	0.15	–	–
			ΔR_M	0.16	0.8	0.92	0.74	1.06	1.12		
II	9	0.65	R_F^1	0.70	0.53	0.68	0.75	0.68	0.70	–	–
			ΔR_M	−0.1	0.22	−0.06	−0.21	−0.06	−0.1		
I	10	0.80	R_F^1	0.88	0.70	0.68	0.75	0.78	0.83	–	–
			ΔR_M	−0.27	0.23	0.27	0.12	0.05	−0.09		
III	11	0.74	R_F^1	0.74	0.70	0.47	–	0.25	0.29	0.56	0.74
			ΔR_M	0	0.08	0.5		0.93	0.84	0.35	0
IV	12	0.16	R_F^1	0.16	0.56	0.75	–	0.64	0.55	–	–
			ΔR_M	0	−0.82	−1.2		−0.97	−0.81		
III	13	0.81	R_F^1	–	–	0.78	–	–	–		–
			ΔR_M			0.08					

* Composition of mobile phases: I = chloroform–methanol (4:2); II = acetone–chloroform (3:2); III = acetone–chloroform (1:4); IV = acetone–methanol (1:1).

TABLE II

RESULTS OF HPLC MEASUREMENTS

Mobile phase for all ligands = dioxane–heptane (4:1).

Ligand	V_R^0	V_R^1 *and* ΔV_M	*Salt*		
			NaCl	*KCl*	*CsCl*
1	0.74	V_R^1	1.87	1.41	1.10
		ΔV_M	0.59	0.43	0.28
6	1.14	V_R^1	3.43	4.32	1.53
		ΔV_M	0.59	0.7	0.18
7	0.52	V_R^1	0.93	1.30	2.36
		ΔV_M	0.53	0.74	1.07
8	0.45	V_R^1	0.70	1.00	1.99
		ΔV_M	0.54	0.81	1.21
9	0.39	V_R^1	0.39	0.41	0.40
		ΔV_M	0	0.17	0.09

MA and ion pair MLA in the organic mobile phase. Let us define equilibrium constants:

$$k_L = (L)/[L];\ k_{MLA} = (ML)(A)/[MLA] \tag{3}$$

where (X) is the concentration of substance X in the stationary phase and [X] is the concentration of X in the mobile phase. The average partition coefficient of the ligand L in the presence of salt MA is expressed by

$$k^{av} = [(L) + (ML)]/([L] + [MLA]) \tag{4}$$

Applying the known equations

$$\begin{aligned} V_R^1 &= V^D (1 + k^{av}) \\ V_R^0 &= V^D (1 + k_L) \end{aligned} \tag{5}$$

we obtain

$$\Delta V_M = \log k^{av} - \log k_L \tag{6}$$

The relative difference between k^{av} and k_L:

$$(k^{av} - k_L)/k_L = \frac{(k_{MLA} - k_L(A))\,(ML)}{k_{MLA}\,(L) + k_L\,(A)\,(ML)} \tag{7}$$

$$k^{av} < k_L \Leftrightarrow k_{MLA} < k_L\,(A) \tag{8}$$

$$k^{av} > k_L \Leftrightarrow k_{MLA} > k_L\,(A) \tag{9}$$

According to eqns. 5, chromatographic acceleration, as a consequence of impregnation, takes place for those salts MA and ligands L for which relation 8 holds. Consequently, retardation occurs when relation 9 is valid. Relation 8 means that the complex prefers the mobile phase to the stationary one more than the free ligand does, and relation 9 means the opposite.

The model described is of course a simplified one. To prove its adequacy we chose compound 13 of macrocyclic structure, *i.e.*, similar to other compounds considered in this work. It has been reported[9] that it does not form complexes with potassium ion at any pH value. Results of TLC measurements on this substance (Table I) confirmed that for non-complexing agents the R_F values are the same for both sides of the plate. We have therefore assumed that complexation is the decisive, essential factor influencing the R_F changes, *i.e.*, modification of the physical properties of the phases due to impregnation may be neglected.

For ligands 1–11 we usually observe a retardation of migration, implying that relation 9 is valid. However, impregnation with lithium salts in some instances causes a reversed behaviour of the ligand. For compound 9, which forms weak complexes, the ΔR_M values are usually negative, implying a grain effect, which can be neglected for strong complexes.

Cryptand [2.2.2] is a special case. It illustrates the other possibility expressed by relation 8, *i.e.*, that the complex is less polar than the free ligand. It is possible to explain this fact by structural conversion from the out–out structure of the ligand to the in–in conformation of its complexes[10].

CONCLUSIONS

The chromatographic method described permits the following:

(a) the estimation of the complex-forming ability;

(b) the identification of the ionophoric properties of compounds present in a reaction mixture (coronands, cryptands, some podands) or in a mixture of natural products (antibiotics);

(c) the separation of compounds of identical R_F values if at least one of them forms complexes with salts; this may be important for the purification of ionophores by column chromatography or preparative HPLC;

(d) information to be obtained about the interactions of the complex and the free ligand with the solvent.

The determinations may be carried out quickly and with the use of trace amounts of pure compounds in addition to mixtures of compounds.

ACKNOWLEDGEMENT

This work was supported by the CPBP 01.15 project.

REFERENCES

1 Yu. A. Ovchinnikov, I. T. Ivanov and A. M. Shkrob, *Membranoaktivnije Kompleksoni*, Nauka, Moscow, 1974.
2 M. M. Htay and O. Meth-Cohn, *Tetrahedron Lett.*, (1976) 469.
3 A. R. Butler, *J. Chem. Soc., Perkin Trans. 1*, (1975) 1557.
4 V. Takaki, T. E. Hogen Esch and J. Smid, *J. Am. Chem. Soc.*, 93 (1971) 6760.
5 N. S. Poonia, *J. Am. Chem. Soc.*, 96 (1974) 1012.
6 J. F. Biernat and T. Wilczewski, *Pol. J. Chem.*, 53 (1979) 513.
7 B. Vonach and G. Schomburg, *J. Chromatogr.*, 149 (1978) 417.
8 K. Macek and Z. J. Vejdelek, *Nature (London)*, 176 (1955) 1173.
9 J. S. Bradshaw, H. Koyama, N. K. Dalley, R. M. Izatt, J. F. Biernat and M. Bocheńska, *J. Heterocycl. Chem.*, 24 (1987) 1077.
10 J. Cheney, J. P. Kintzinger and J. M. Lehn, *Nouv. J. Chim.*, 2 (1978) 411.

Journal of Chromatography, 454 (1988) 345–351
Elsevier Science Publishers B.V., Amsterdam — Printed in The Netherlands

CHROM. 20 822

Note

Nitroalkanes as a multidetector retention index scale for drug identification in gas chromatography

ROLF ADERJAN* and MACIEJ BOGUSZ
Institute of Forensic Medicine, Ruprecht Karl University, Vosstrasse 2, D-6900 Heidelberg (F.R.G.)
(First received February 12th, 1988; revised manuscript received May 24th, 1988)

The need for the standardization of retention data has been obvious from the first application of gas chromatograpy (GC). The retention index (RI) system based on homologues of *n*-alkanes proposed by Kováts[1] has been widely accepted in various fields of chromatographic analysis[2–4] and also in analytical toxicology, where the identification of unknown substances is particularly important. Compilations and libraries of RI values of toxicologically relevant compounds examined on packed columns have enabled the interlaboratory exchange and use of data[5–8]. More recently, RI values of various drugs determined on capillary columns have been shown to be comparable with those on packed columns[9–15] with only slight deviations.

Under normal working conditions, selective GC detectors do not respond to *n*-alkanes. Alternative standardization systems for GC data have therefore been developed, with the use of alkanoic acid methyl esters[16,17], steranes[18], 2-alkanones[19], straight chain alcohols[20], *n*-alkyltrichloroacetates[21,22], polycyclic aromatic hydrocarbons[23], dialkylsulphides[24], diisopropylaminoalkanes[8], *n*-alkylbis(trifluoromethyl)-thiophosphinates[25], *n*-bromoalkanes[26,27], *n*-trialkylamines[28,29], fused quinones[30] and *n*-alkylbis(trifluoromethyl)phosphine sulphides[31]. All these systems are not regarded as satisfactory by us, as they were usually designated for a particular detection. Only two series of closely related compounds proposed as an alternative RI scale meet the demands of multiple detectability[25,31], *i.e*, by electron-capture or thermionic detection (ECD or TID). However, the synthesis of these probably very toxic materials does not seem to be simple and is not described in the literature.

In a previous study the applicability and advantages of the lower 1-nitroalkanes (C_1–C_6) as a retention index system for high-performance liquid chromatography (HPLC) was shown in comparison with another scale[32,33]. In the present paper the use and preparation of higher 1-nitroalkanes as an alternative retention index scale in GC, applicable to all common detector systems, is described. To our knowledge, 1-nitroalkanes are the first series of homologues applicable as a retention index scale both for liquid chromatography (reversed-phase HPLC) and for GC with ECD, TID and flame ionization detection.

0021-9673/88/$03.50

MATERIALS AND METHODS

Nitroalkanes

Nitromethane, nitroethane, 1-nitropropane, 1-nitrobutane, 1-nitropentane and 1-nitrohexane were obtained from Fluka (Buchs, Switzerland). Higher homologues were synthesized according to Kornblum *et al.*[34,35] using the following procedure: 7.5 mmol (1.16 g) of silver nitrite were suspended in 3 ml anhydrous diethyl ether in a head-space vial 25 ml in volume covered with aluminium foil and equipped with a small size magnetic stirrer. The mixture was cooled to 4°C. In a second head-space vial a cold solution of 5 mmol of the corresponding *n*-bromo- (or iodo-) alkane in 3 ml of anhydrous diethyl ether was prepared. From this, every 30 min a portion of 0.5 ml was drawn up into a polypropylene syringe and injected into the stirred silver nitrite suspension. Contact with moisture was avoided as far as possible, and during the reaction the products were protected from light. The reaction mixture was kept at 4°C for 36–48 h and then at room temperature for 24–36 h until the reaction was complete. After filtration from the resulting silver halide, the solvent was evaporated with a stream of nitrogen. The 1-nitroalkanes were obtained in a nearly quantitative yield and with greater than 95% purity. No further purification was needed when the starting materials were of analytical grade. However, solid 1-nitroalkanes may be recrystallized from methanol, 4% water in methanol, or from acetone (homologues above C_{20}).

Other reagents and standard substances

n-Alkanes were supplied by Merck (Darmstadt, F.R.G.). Drugs were of analytical grade from various manufacturers. 1-Bromoalkanes (C_7–C_{18}), as well as *n*-alkanols with even carbon numbers (C_{20}–C_{30}), were from Fluka. 1-Iodoalkanes, used for the synthesis of 1-nitroalkanes with more than 18 carbon atoms, were prepared from the commercially available *n*-alcohols, red phosporus and iodine[36,37], according to the following procedure: 1 mmol *n*-alkanol, 1 mmol iodine and 0.33 mmol red phosphorus were kept at 160°C for 3 h. The individual iodides were extracted with toluene and the toluene extract was washed with water followed by 0.2 *M* sodium hydroxide solution. After washing with water again, the toluene was partially evaporated. On cooling the remaining toluene extract, the iodoalkanes crystallized in *ca.* 90% of the theoretical yield. After recrystallization from methanol or acetone no further purification was needed for the synthesis of 1-nitroalkanes.

Gas chromatography

Two Shimadzu (Model 9 A and Model 9 AM) gas chromatographs, equipped with ECD, TID (rubidium chloride bead, electrically heated) and FID were used. Fused-silica capillary columns (10 m × 0.53 mm I.D.), coated with CP-Sil 5 CB (methyl polysiloxane, film thickness 5 μm) and with CP-Sil 19 CB (50% phenyl methyl polysiloxane, film 2 μm) were supplied by Chrompack (Middelburg, The Netherlands). The columns were installed directly in the injector using a deactivated glass liner. Helium was used as the carrier gas at flow-rate of 7 ml/min, as in the previous screening toxicological procedures[38]. The gas flows to the detectors were: for FID, air 500 ml/min, hydrogen 50 ml/min; for TID, air 150 ml/min, hydrogen 3.5 ml/min; for ECD, argon–methane (95:5) 330 ml/min. No make-up gas was used.

The samples were analyzed isothermally at 160 and 220°C or using a temperature programme: 2 min at 100°C, then raised at 15°C/min to 200°C, at 10°C/min to 300°C, finally maintained for 8 min at 300°C. The two-step program gives a better approximation to a linear relationship between the k' values of n-alkanes and their carbon numbers than the simple one, and is commonly used in toxicological screening[38].

Calculations of retention indices

The retention indices of the drugs examined were calculated either from an isothermal experiment using

$$RI = 100n + 100(N - n) \cdot \frac{\log t_R(x) - \log t_R(n)}{\log t_R(N) - \log t_R(n)} \quad (1)$$

or from a temperature-programmed experiment according to

$$RI = 100n + 100(N - n) \cdot \frac{t_R(x) - t_R(n)}{t_R(N) - t_R(n)} \quad (2)$$

where n and N are the carbon numbers of consequentively eluted reference compounds (n-alkanes or 1-nitroalkanes), x is the substance examined and t_R is the net retention time. A linear elution of the reference substances during the temperature-programmed experiment was assumed[4,39]. The column dead time was determined with methane and FID.

RESULTS AND DISCUSSION

The stable, non-explosive 1-nitroalkanes having seven or more carbon atoms were easily prepared from the corresponding 1-bromoalkanes or 1-iodoalkanes by a heterogeneous SN1 reaction. All nitroalkanes gave symmetrical GC peaks. The relationship between the logarithm of k' and the carbon number was linear for 1-nitroalkanes analyzed isothermally on both columns (Fig. 1).

The 1-nitroalkanes are easily detectable with FID, ECD or TID. In the chromatograms of the unpurified 1-nitroalkanes, negligible impurities were found by FID or TID. With ECD, however, a few additional peaks were observed, but these can be distinguished from 1-nitroalkanes. Comparison of the magnitudes of the best detector signal for individual 1-nitroalkanes revealed a ratio of approximately 1:3:6 for FID, TID and ECD, respectively.

The RI values of thirteen selected drugs were determined using the n-alkane and the 1-nitroalkane scale on CP-Sil 5 and CP-Sil 19 columns. The relationship between the adjusted retention times and the carbon numbers of n-alkanes or 1-nitroalkanes under these conditions was approximately linear (Fig. 2). The RI values of the substances examined calculated with both reference systems are listed in Table I. The relationship between the RI values calculated on the two scales was linear for both polysiloxane columns. The data were fitted by regression lines expressed by

$$y = 1.02x + 430 \qquad r = 0.9999 \text{ (CP-Sil 5)} \quad (3)$$

$$y = 1.07x + 530 \qquad r = 0.9997 \text{ (CP-Sil 19)} \quad (4)$$

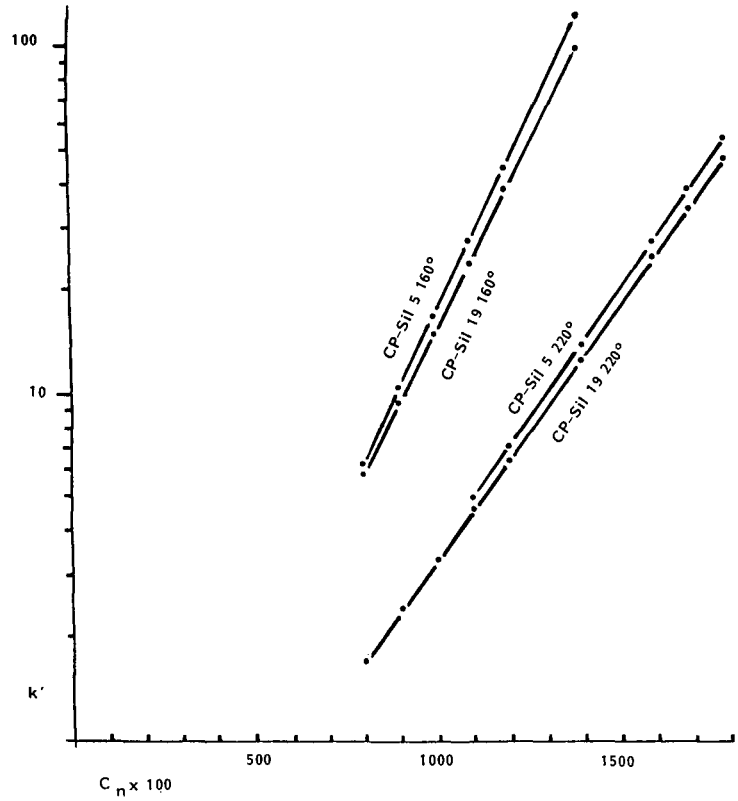

Fig. 1. Relationships between the k' values and the carbon numbers of 1-nitroalkanes at various temperatures on CP-Sil 5 and CP-Sil 19 columns. Semilogarithmic scale.

TABLE I

RETENTION INDEX VALUES OF SUBSTANCES EXAMINED ON CP-SIL 5 AND CP-SIL 19 COLUMNS, RELATIVE TO THE *n*-ALKANES (RI_{Kovats}) AND THE 1-NITROALKANES (RI_{NO_2})

Drug	*CP-SIL 5*		*CP-SIL 19*	
	RI_{Kovats}	RI_{NO_2}	RI_{Kovats}	RI_{NO_2}
Clomethiazole	1245	800	1398	810
Bromdecane	1370	919	1644	1052
Barbital	1495	1047	1828	1208
Aprobarbital	1619	1170	1875	1246
Amobarbital	1711	1253	1943	1313
Caffeine	1809	1341	2143	1527
Diphenhydramine	1869	1420	2025	1405
Parathion	1962	1516	2269	1634
Methaqualone	2152	1685	2466	1815
Amitriptyline	2208	1742	2440	1790
Nordiazepam	2494	2035	3054	2348
Nitrazepam	2744	2271	–	–
Strychnine	3146	2660	–	–

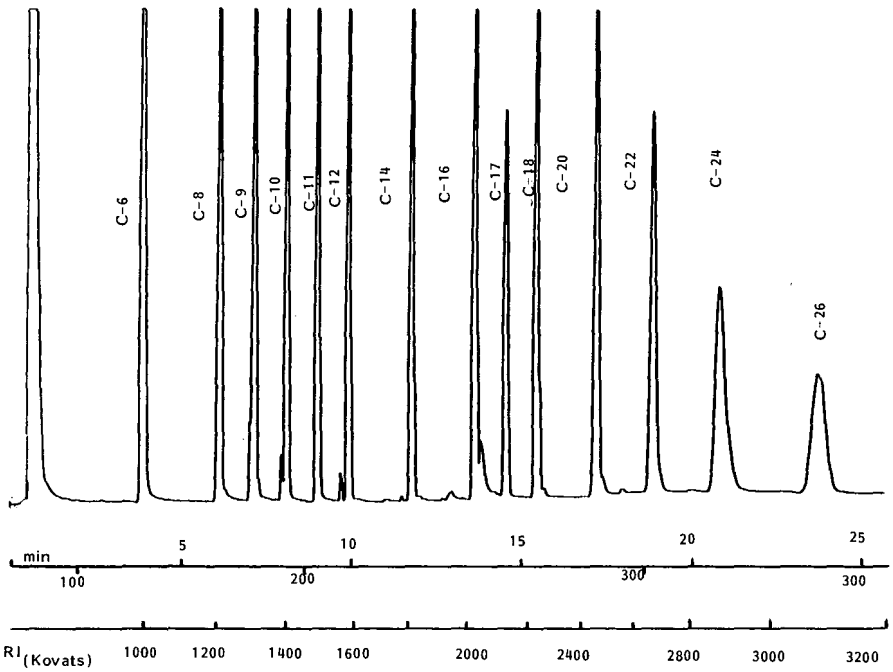

Fig. 2. Chromatogram of a mixture of 1-nitroalkanes (C_6–C_{26}) analyzed on a CP-Sil 5 column with thermionic detection. Temperature programme (°C) as in text. The lower scale shows the location of the *n*-alkanes.

TABLE II

KOVÁTS RETENTION INDICES OF DRUGS, MEASURED RELATIVE TO *n*-ALKANES AND CALCULATED FROM THE 1-NITROALKANE SCALE

CP-Sil 5 column. The reference values, on a packed OV-1 or SE-30 column[8], are given in parentheses.

Drug (RI ref.)	RI_{NO_2}	RI_{Kovats}	
		Calculated	*Measured*
Nicotine (1348)	887	1336	1332
Warfarin (1432)	949	1399	1395
Carbromal (1513)	1068	1520	1509
Demeton-S-methyl (1628)	1221	1676	1667
Lidocane (1870)	1412	1871	1881
Cyclobarbital(1963)	1498	1959	1967
Endosulfan α (2085)	1660	2124	2135
Endosulfan β (2175)	1760	2226	2236
Codeine (2376)	1935	2403	2391
Diazepam (2425)	1978	2448	2436
Diamorphine (2614)	2171	2644	2635
Fenetylline (2830)	2348	2825	2824

where y is the drug RI relative to n-alkane, x is the drug RI relative to 1-nitroalkane and r is the correlation coefficient. Thus it is possible to calculate the RI values from one scale by use of the other. This was checked by the determination of Kováts RI values of selected substances directly, using n-alkanes, and by the indirect method using RI of 1-nitroalkanes and the regression equation 3. The results, given in Table II, show good agreement between both sets of data. The homologues synthesize cover the whole range of toxicologically relevant substances, analyzed on an OV-1-like column (RI on n-alkane scale between 1000 and 3100).

CONCLUSIONS

1-Nitroalkanes are readily detectable with all GC detection systems used in modern toxicological analysis. Their chromatographic properties and close relation to n-alkanes allows the reliable calculation of retention index value from the Kováts n-alkane scale using our 1-nitroalkane scale and *vice versa*. This makes possible the convenient use of existing retention index libraries based on n-alkanes, for 1-nitroalkane work. No detector change is required. Apart from this immediate application, the 1-nitroalkanes may be a real alternative to the n-alkane scale in GC and HPLC.

REFERENCES

1 E. Kováts, *Helv. Chim. Acta*, 41 (1958) 1915.
2 J. Haken, *Adv. Chromatogr. (N.Y.)*, 14 (1976) 367.
3 M. V. Budahegyi,E. R. Lombosi, T. S. Lombosi, S. Y. Mészáros, Sz. Nyiredy, G. Tarján, I. Timár and J. M. Takács, *J. Chromatogr.*, 271 (1983) 213.
4 L. G. Blomberg, *Adv. Chromatogr. (N.Y.)*, 26 (1986) 229.
5 R. E. Ardrey and A. C. Moffat, *J. Chromatogr.*, 220 (1981) 195.
6 B. J. Perrigo and H. W. Peel, *J. Chromatogr. Sci.*, 19 (1981) 219.
7 T. Daldrup, M. Susanto and P. Michalke, *Fresenius' Z. Anal. Chem.*, 308 (1981) 413.
8 R. E. Ardrey, R. A. de Zeeuw, B. S. Finkle, A. C. Moffat, M. R. Möller and R. K. Müller, *Gas Chromatographic Retention Indices of Toxicologically Relevant Substances on SE-30 or OV-1*, VCH, Weinheim, 1985.
9 G. W. Hime and L. R. Bednarczyk, *J. Anal. Toxicol.*, 7 (1982) 247.
10 W. H. Anderson and D. T. Stafford, *J. High Resolut. Chromatogr. Chromatogr. Commun.*, 6 (1983) 247.
11 A. Eklund, J. Johnsson and . Schubert, *J. Anal. Toxicol.*, 7 (1983) 24.
12 P. Schepers, J. Wijsbeek, J. P. Franke and R. A. de Zeeuw, *J. Forensic Sci.*, 27 (1982) 49.
13 B. Newton and R. F. Foery, *J. Anal. Toxicol.*, 8 (1984) 129.
14 B. J. Perrigo, H. W. Peel and D. J. Ballantyne, *J. Chromatogr.*, 341 (1985) 81.
15 A. Stowell and L. Wilson, *J. Forensic Sci.*, 32 (1987) 1214.
16 R. G. Ackman, *J. Chromatogr. Sci.*, 10 (1972) 536.
17 F. P. Woodford and C. H. van Gent, *J. Lipid Res.*, 1 (1960) 188.
18 W. Van den Heuvel and E. C. Horning, *Biochim. Biophys. Acta*, 64 (1962) 41.
19 H. F. Dymond and K. D. Kilburn, in A. P. Littlewood (Editor), *Gas Chromatography 1966*, Institute of Petroleum, London, 1967, p. 353.
20 S. J. Hawkes, *J. Chromatogr. Sci.*, 10 (1972) 535.
21 H. J. Neu, M. Zell and K. Ballschmiter, *Fresenius' Z. Anal. Chem.*, 293 (1978) 193.
22 K. Ballschmiter and M. Zell, *Fresenius' Z. Anal. Chem*, 302 (1980) 20.
23 M. C. Lee,D. L. Vassilaros, C. M. White and M. Novotny, *Anal. Chem.*, 51 (1979) 768.
24 L N. Zotov, G. V. Golovkin and R. V. Golovnya, *J. High Resolut. Chromatogr. Chromatogr. Commun.*, 4 (1981) 6.
25 J. Enqvist, P. Sunila and U. M. Lakkisto, *J. Chromatogr.*, 279 (1983) 667.
26 F. Pacholec and C. P. Poole, *Anal. Chem.*, 54 (1982) 1019.
27 F. Pacholec and C. F. Poole, *J. Chromatogr.*, 302 (1984) 289.

28 G. L. Hall, W. E. Whitehead, C. R. Mourer and T. Shibamoto, *J. High Resolut. Chromatogr. Chromatogr. Commun.*, 9 (1986) 266.
29 V. W. Watts and T. F. Simonick, *J. Anal. Toxicol.*, 11 (1987) 210.
30 A. Boenke and K. Ballschmiter, *Fresenius Z. Anal. Chem.*, 327 (1987) 42.
31 A. Manninen, M.-L. Kuitunen and L. Julin, *J. Chromatogr.*, 394 (1987) 465.
32 M. Bogusz and R. Aderjan, *J. Chromatogr.*, 435 (1988) 43.
33 M. Bogusz, G. Neidl-Fischer and R. Aderjan, *J. Anal. Toxicol.*, (1988) in press.
34 N. Kornblum, B. Taub and H. E. Ungnade, *J. Am. Chem. Soc.*, 76 (1954) 3209.
35 N. Kornblum and H. E. Ungnade, *Org. Synth.*, Coll. Vol. IV (1963) 724.
36 G. Ställberg, S. Ställberg-Stenhagen and E. Stenhagn, *Acta Chem. Scand.*, 6 (1952) 313.
37 P. A. Levene, C. J. West and J. v.d. Scheer, *J. Biol. Chem.*, 20 (1915) 521.
38 M. Bogusz, J. Bialka, J. Gierz and M. Klys, *J. Anal. Toxicol.*, 10 (1986) 135.
39 H. van den Dool and P. D. Krantz, *J. Chromatogr.*, 11 (1963) 463.

Journal of Chromatography, 454 (1988) 352–356
Elsevier Science Publishers B.V., Amsterdam — Printed in The Netherlands

CHROM. 20 817

Note

Dual retention mechanism on commercial acetylcellulose as a stationary phase in planar chromatography*

JIŘÍ GASPARIČ
Faculty of Pharmacy, Charles University, Heyrovsky 1203, 501 65 Hradec Králové (Czechoslovakia)
(Received July 11th, 1988)

Acetylated paper was originally introduced by Koštíř and Slavík[1] as a carrier of less polar stationary phases in reversed-phase paper chromatography. Later, reversed-phase separations were achieved using acetylated paper alone as a stationary phase. Similarly, layers of acetylated cellulose powders were found suitable for reversed-phase thin-layer chromatography (TLC). Both the papers and powders are prepared by converting cellulose into its acetate esters. Up to three hydroxyl groups per cellulose structural unit can be esterified. The acetyl content may vary from 6% up to a maximum of *ca.* 45%, the latter value corresponding to the triacetate. A gradual change from the "aqueous" to the "organic non-polar" stationary phase can thus be effected through variation of the extent of acetylation[2]. Thus, acetylated cellulose is in principle suitable for the separation of lipophilic substances and good separations have been achieved in the case of aromatic hydrocarbons[2,3], disperse dyes[2], antioxidants[2], etc.

Commercially available papers and powders are manufactured with an acetyl content up to 37%. Because of the incomplete acetylation it is supposed that the free hydroxy groups can also exhibit some interactions with the chromatographed compounds. A similar "dual retention mechanism" was observed in the case of less polar and polar organic compounds chromatographed on cellulose paper or on silica gel layers impregnated with less polar organic stationary phases: polar organic compounds behaved as if no stationary liquid were present, whereas non-polar substances were chromatographed according to the rules common for reversed-phase chromatography[4,5]. Therefore, we tried to show that the commercially available acetylcellulose materials represent a dual stationary phase, *i.e.*, acetylcellulose as the stationary phase for reversed-phase chromatography of lipophilic compounds and cellulose for normal-phase chromatography of hydrophilic compounds.

MATERIALS AND METHODS

All dyes chromatographed were standard substances from our collection. Solvents used as mobile phases were of current reagent grade purity. Paper chromatogra-

* Presented at the *6th Danube Symposium on Chromatography, Varna, October 12–17, 1987*. The majority of papers presented at this symposium have been published in *J. Chromatogr.*, Vol. 446 (1988).

0021-9673/88/$03.50

phy was carried out using FN 7 paper (Papierfabrik Niederschlag, G.D.R.) and acetylated paper MN Cell 300Ac 10% (Macherey, Nagel & Co., Düren, F.R.G.). TLC was performed using commercial layers of microcrystalline cellulose Lucefol quick® (Sklárny Kavalier, Votice, Czechoslovakia) and of acetylated cellulose MN Polygram cel 300Ac-10 (Macherey, Nagel & Co). All chromatograms were developed by ascending development using C_1–C_4 alcohols in mixtures with water or ammonia, as the mobile phases.

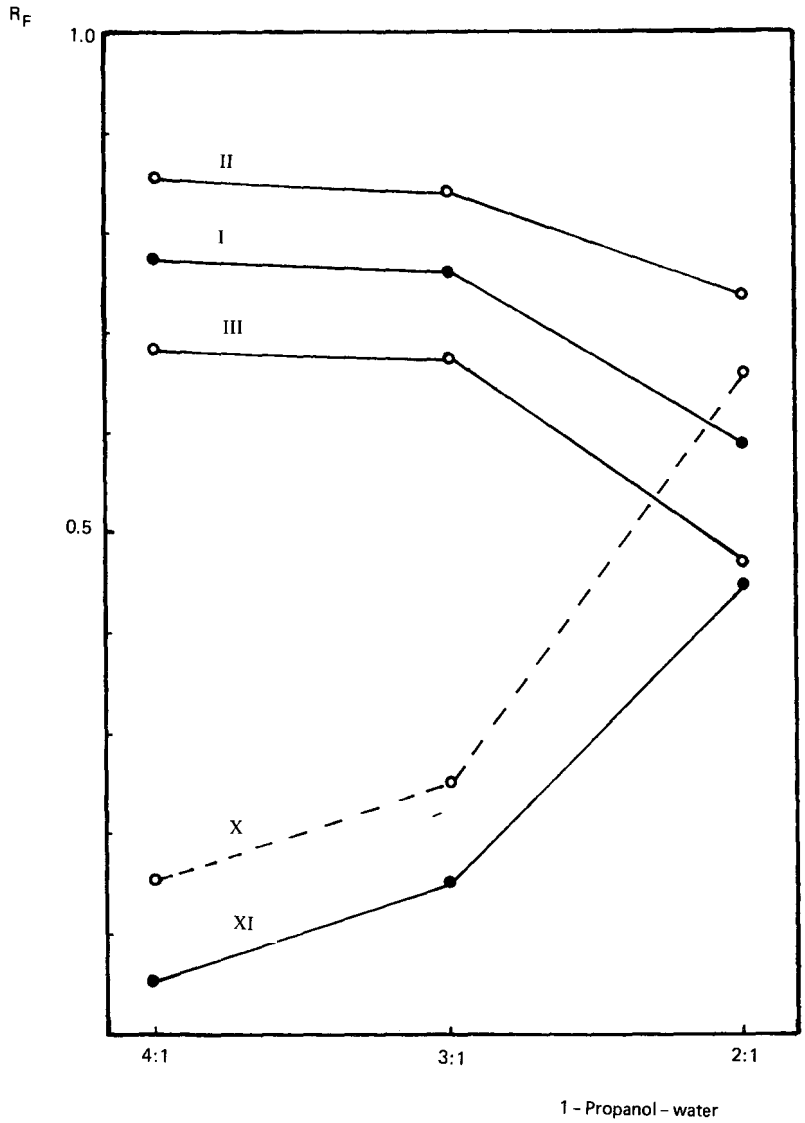

Fig. 1. Influence of the 1-propanol–water ratio on the retention of lipophilic dyes I–III and hydrophilic dyes X and XI.

TABLE I

R_F VALUES OF MODEL DYES ON CELLULOSE AND ACETYLATED CELLULOSE MATERIALS

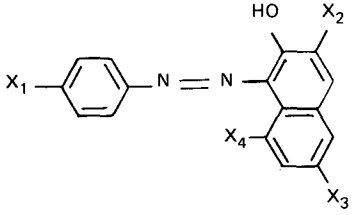

PC = Paper chromatography; ROH = aliphatic alcohol; C = cellulose; Ac = acetylated cellulose.

	Substituent				*TLC/80% ROH*								*TLC/1-propanol–water*						*PC/ROH–NH_3 (2:1)*			
	X_1	X_2	X_3	X_4	*Methanol*		*Ethanol*		*1-Propanol*		*1-Butanol*		*4:1*		*3:1*		*2:1*		*Ethanol*		*1-Butanol*	
					C	*Ac*	*C*	*Ac*	*C*	*Ac*	*C*	*Ac*	*C*	*Ac*	*C*	*Ac*	*C*	*Ac*	*C*	*Ac*	*C*	*Ac*
I	H	H	H	H	0.80	0.31	0.98	0.57	1.00	0.71	1.00	0.76	0.99	0.77	1.00	0.76	1.00	0.69	0.99	0.70	0.98	0.74
II	C_5H_{11}	H	H	H	0.58	0.16	0.90	0.51	1.00	0.84	1.00	0.84	1.00	0.85	1.00	0.84	1.00	0.74	0.99	0.84	0.98	0.86
III	C_6H_5	H	H	H	0.45	0.12	0.89	0.37	1.00	0.67	1.00	0.70	1.00	0.68	1.00	0.67	1.00	0.47	0.99	0.48	0.98	0.50
IV	H	H	SO_3H	H	0.80	0.87	0.92	0.96	0.92	0.89	0.80	0.74	0.92	0.92	0.89	0.95	0.96	0.93	0.86	0.81	0.83	0.72
V	C_5H_{11}	H	SO_3H	H	0.83	0.84	1.00	0.99	0.99	0.97	0.98	0.90	0.98	0.98	0.99	0.98	1.00	0.99	0.95	0.90	0.92	0.86
VI	C_6H_5	H	SO_3H	H	0.83	0.78	0.91	0.90	0.98	0.89	0.99	0.85	0.97	0.93	0.98	0.95	0.98	0.93	0.86	0.66	0.83	0.58
VII	H	SO_3H	SO_3H	H	0.80	0.84	0.69	0.80	0.35	0.50	0.05	0.12	0.32	0.43	0.39	0.50	0.65	0.84	0.72	0.89	0.62	0.82
VIII	C_5H_{11}	SO_3H	SO_3H	H	0.83	0.85	0.93	0.97	0.63	0.82	0.20	0.50	0.60	0.85	0.64	0.87	0.84	0.97	0.51	0.73	0.46	0.60
IX	C_6H_5	SO_3H	SO_3H	H	0.77	0.77	0.62	0.77	0.28	0.45	0.05	0.10	0.24	0.32	0.34	0.82	0.83	0.93	0.47	0.48	0.42	0.48
X	H	SO_3H	SO_3H	SO_3H	0.78	0.82	0.55	0.68	0.12	0.18	0.01	0.01	0.07	0.15	0.16	0.25	0.45	0.66	0.20	0.40	0.23	0.49
XI	SO_3H	SO_3H	SO_3H	SO_3H	0.70	0.77	0.38	0.60	0.05	0.07	0	0	0.04	0.05	0.10	0.15	0.36	0.45	0.15	0.30	0.09	0.44

RESULTS AND DISCUSSION

A series of eleven azo dyes of the basic structure I was used as model compounds. Dyes I–III represent compounds of lipophilic character, the lipophilicity of the basic compound I being increased by the presence of 1-pentyl or phenyl groups, in compounds II and III. Compounds IV–XI are hydrophilic. Their hydrophilicity increases with the number of sulpho groups, *i.e.*, in the sequence IV < VII < X < XI, whilst it is slightly decreased by the presence of the 1-pentyl or phenyl groups in compounds V, VI, VIII and IX. This series of compounds was simultaneously chromatographed on cellulose and acetylcellulose materials using the same mobile phases, *i.e.*, C_1–C_4 alcohols in mixtures with water or ammonia. The R_F values thus obtained are summarized in Table I.

The hydrophilic sulphonated compounds migrate on both materials in the same sequence, *i.e.*, their R_F values are decreased in the series IV > VII > X > XI. The sequence of the unsubstituted compound and that with the 1-pentyl and phenyl groups is also the same on both stationary phases. The increasing chain length of the alcohol in the mobile phase brings about a significant decrease in the R_F values with a reproducible exception in the case of methanol. The increasing water content of the mobile phase containing 1-propanol as the organic modifier is manifested by an increase in R_F values. All these phenomena are common to both the cellulose and acetylcellulose materials and are in accordance with the rules of normal (straight) phase chromatography. The absolute R_F values cannot reliably be compared since the corresponding cellulose and acetylcellulose materials are not from the same supplier. However, R_F values of higher sulphonated compounds are observably higher on acetylcellulose than on cellulose.

The lipophilic dyes I–III behave on cellulose and acetylcellulose as expected, in a quite different way. They migrate on cellulose with the solvent front in the case of all aqueous alcohols as mobile phases, with the exception of methanol. In 80% methanol as the mobile phase, however, their behaviour is similar to that in a reversed-phase system! Their retention on acetylated cellulose with 80% methanol or ethanol is as expected in reversed-phase chromatography, *i.e.*, it is decreased in the series I > II > III. On the other hand, the R_F values of these dyes decrease in the series II > I > III when 1-propanol or 1-butanol is used in the mobile phase. This sequence is not

TABLE II

R_F VALUES OF ALKYLPYRIDINIUM CHLORIDES USING 1-BUTANOL SATURATED WITH AMMONIA AS THE MOBILE PHASE

According to Kabil and Prey[6]. C = S + S 2043b paper; Ac = S + S 2043b acetylated paper.

Compound	R_F	
	C	*Ac*
Ethylpyridinium chloride	0.12	0.16
1-Butylpyridinium chloride	0.31	0.28
1-Octylpyridinium chloride	0.62	0.08
1-Dodecylpyridinium chloride	0.73	0.08
1-Cetylpyridinium chloride	0.89	0.06

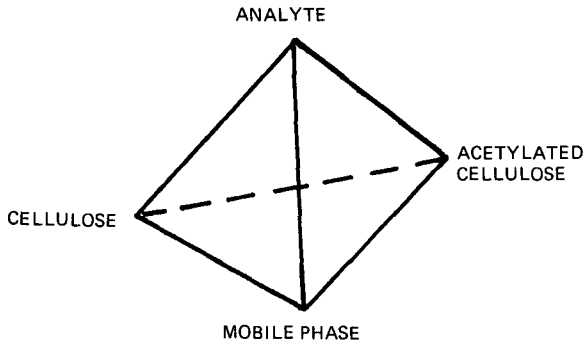

Fig. 2. Schematic representation of the chromatographic system using acetylated cellulose materials.

characteristic for a reversed-phase system. The increasing water content in the mobile phase containing 1-propanol brings about a decrease in the R_F values of the lipophilic compounds. The comparison of the response of lipophilic and hydrophilic compounds to the increasing water content in the mobile phase is illustrated also in Fig. 1.

A very interesting example which is in good accordance with our results can be found in the literature though the authors did not comment it: in 1958 Kabil and Prey[6] chromatographed a homologous series of alkylpyridinium salts on cellulose and acetylcellulose papers. The R_F values of those compounds increased with increasing length of the alkyl group on cellulose paper, whereas on acetylated cellulose paper the R_F values increased only up to the $\sim C_6$ alkyl compound and began then to decrease with increasing length of the alkyl chain (see Table II).

It can be concluded from our results that, due to incomplete acetylation, two stationary phases must be considered in commercial acetylated materials: cellulose and acetylated cellulose. Using one mobile phase, the analytes prefer one of these materials according to their hydrophilicity or lipophilicity. Thus, the hydrophilic analytes are separated according to the rules of normal (straight) phase chromatography and the lipophilic ones according to the rules of reversed-phase chromatography. There is also some influence of the organic modifier in the mobile phase. Some anomalies were observed using 80% methanol on cellulose and 1-propanol and 1-butanol on acetylated cellulose. Therefore the system considered is a complex one as illustrated in Fig. 2. This phenomenon is quite analogous to the action of free silanol groups in silica-bonded hydrocarbonaceous stationary phases in reversed-phase high-performance liquid chromatography[7–9].

REFERENCES

1 J. V. Koštíř and K. Slavík, *Collect. Czech. Chem. Commun.*, 15 (1950) 17.
2 P. Wollenweber, in E. Stahl (Editor), *Thin-layer Chromatography. A Laboratory Handbook*, Springer, Berlin, Heidelberg, New York, 2nd ed., 1961, p. 37.
3 J. Gasparič and J. Churáček, *Laboratory Handbook of Paper and Thin-layer Chromatography*, Ellis Horwood, Chichester, 1978, p. 89.
4 J. Gasparič, *J. Chromatogr.*, 47 (1970) 51.
5 J. Gasparič, *J. Chromatogr.*, 196 (1980) 391.
6 A. Kabil and V. Prey, *Monatsh. Chem.*, 87 (1956) 625.
7 A. Nahum and Cs. Horváth, *J. Chromatogr.*, 203 (1981) 53.
8 K. E. Bij, Cs. Horváth, W. R. Melander and A. Nahum, *J. Chromatogr.*, 203 (1981) 65.
9 T. Welsh and H. Frank, *Chromatographia*, 19 (1984) 457.

Journal of Chromatography, 454 (1988) 357–361
Elsevier Science Publishers B.V., Amsterdam — Printed in The Netherlands

CHROM. 20 775

Note

Effect of temperature difference between pump and column in molecular weight determination by gel permeation chromatography

KAZUYO MIYAZAKI, YUICHIROU TANAKA and MUNEO SAITO*
JASCO, Japan Spectroscopic Co., Ltd., 2967-5 Ishikawa-cho, Hachioji City, Tokyo 192 (Japan)
(First received January 25th, 1988; revised manuscript received June 20th, 1988)

Some years ago, the effect of temperature on retention times in liquid chromatography was studied by several workers[1–6], and the importance of column thermostating in order to obtain accurate and reproducible retention times (t_R) was emphasized. In gel permeation chromatography (GPC), however, the effect of temperature on retention time is less significant than that in any other mode of chromatography, because it is based on steric exclusion and there is little contribution to retention of adsorption or partition, which is very temperature dependent. Therefore, it was considered to be more important to measure the flow-rate accurately in order to reduce errors in molecular weight calculations[7,8].

The effect of column temperature on molecular weight determinations has been reported[9], including the influence of solvent expansion and contraction. However, there has been no systematic study of the errors caused by the temperature difference between the solvent discharged from a pump and the solvent in a thermostated column.

This paper demonstrates that the independent changes in temperature of the solvent in the pump head and in the column results in significant errors in molecular weight determinations, and these errors can be compensated for simply by taking thermal expansion into account.

EXPERIMENTAL

The retention volume, V_R, is expressed by using the mass flow-rate, F_m:

$$V_R = t_R F_m[V_0(1 + \alpha T + \beta T^2 + \gamma T^3)]$$

where V_0 = volume of 1 g of the solvent at 0°C, α, β and γ are coefficients of cubic expansion of the solvent and T (°C) = temperature of the solvent. The coefficients of cubic expansion of an organic solvent are generally $\alpha \approx 10^{-3}$, $\beta \approx 10^{-6}$ and $\gamma \approx 10^{-8}$. In most instances, it can simply be taken that the volume of an organic solvent linearly expands by 0.1%/°C because the second- and third-order terms are negligibly small.

By using a volumetric displacement-type pump [any high-performance liquid chromatographic (HPLC) pump is of this type] a given volume of the solvent is simply displaced irrespective of its density or temperature. This means that the volumetric

0021-9673/88/$03.50

flow-rate metered in the pump may be constant, but the mass flow-rate from the pump varies with the temperature of the solvent. When the solvent enters a column oven at an elevated temperature from a pump at room temperature, a reduction in solvent density or a volume expansion consequently takes place. Therefore, no matter how accurately the volumetric flow-rate of the pump and the temperature of the column are controlled, the actual volumetric flow-rate or the linear velocity in the column cannot be maintained constant unless the solvent temperature in the pump head is kept constant.

Solvent, sample and column

Tetrahydrofuran (THF) was used as the mobile phase in GPC measurements with a column system consisting of two Shodex A-80M columns (50 cm × 8 mm I.D.) connected in series and packed with a mixture of polystyrene gels of nominal pore size 10^3, 10^4, 10^5 and 10^6 Å (Showa Denko, Tokyo, Japan).

Monodisperse polystyrene (PS) standards having nominal molecular weights of $2880 \cdot 10^3$, $233 \cdot 10^3$, $17.5 \cdot 10^3$ and $2.8 \cdot 10^3$ were used to measure the effect on retention times of temperature differences between the solvent and pump head and the solvent and column. These standards were obtained from Toyo Soda (Tokyo, Japan) (mol.wt. $2880 \cdot 10^3$ and $2.8 \cdot 10^3$) and Pressure Chemical (Pittsburgh, PA, U.S.A.) (mol.wt. $233 \cdot 10^3$ and $17.5 \cdot 10^3$). Ten milligrams of each PS standard and benzene were dissolved in 20 ml of THF and 100 μl of the solution were injected into the GPC system.

Apparatus

The GPC system was assembled from JASCO (Tokyo, Japan) 800 series HPLC modules. The mobile phase solvent (THF) was supplied to the delivery pump through a Model 880-50 in-line degasser (JASCO) in order to remove dissolved air, which often causes instability of the flow-rate. To control the solvent temperature in the pump head, a thermostat jacket was attached to the pump head. A water circulating bath with a built-in LC-101 refrigerator (Scinics, Tokyo, Japan) circulated water to the jacket, which contained a thermal equilibration coil (2 m × 0.8 mm I.D. × 1.6 mm O.D.) for incoming solvent. THF in a glass bottle was placed in the bath. Using this arrangement, the temperature of THF discharged from the pump was controlled to an accuracy of ± 0.1°C at specified temperatures.

The columns were thermostated to ± 0.1°C at specified temperatures in an 860-CO air circulating oven (JASCO). An 855-AS autosampler (JASCO) was used to perform automated sample injection. A heat-exchanger coil (1 m × 0.25 mm I.D.) was connected between th sampler and the column and placed in the oven for temperature equilibrium of the mobile phase solvent and sample solution before entry into the column.

An 875-UV variable-wavelength UV detector and an 805-GI data processor (JASCO) were used for monitoring and processing the GPC results. To obtain molecular weight distributions, a refractive index detector is generally used because it offers a proportional response to the mass of a sample solute. However, it is very sensitive to temperature changes of the mobile phase and room temperature, and for this reason a UV detector, which is thermally stable, was employed here for GPC measurements.

GPC measurement procedure

In order to evaluate the effect of temperature differences between the solvent and pump head and the solvent and column on errors in molecular weight determinations by GPC measurement, a calibration graph was established by injecting the polystyrene standard mixture with a solvent/pump head temperature of 20°C and a column temperature of 40°C. Retention data for each PS standard were obtained at various solvent/pump head temperatures (17, 25 and 30°C) while the temperature of the column was maintained constant at 40°C.

The molecular weight of each PS standard was calculated using the obtained

TABLE I

EFFECTS OF SOLVENT/PUMP HEAD TEMPERATURE AND RETENTION TIME COMPENSATION USING THE COEFFICIENT OF CUBIC EXPANSION ON ERRORS IN MOLECULAR WEIGHT DETERMINATION FROM THE CALIBRATION GRAPH OBTAINED AT 20°C

GPC conditions: two columns, Shodex A-80M; column temperature, 40°C; mobile phase, THF at a flow-rate of 1 ml/min.

Retention time (t_R) data used	*Calculated molecular weight ($\times 10^3$)*			
	*17.0°C**	*20.0°C*,***	*25.0°C*	*30.0°C*
Measured t_R***	3.07	2.80	2.34	2.09
	(+3.74)		(−16.43)	(−25.36)
Compensated t_R§	2.84		2.67	2.73
	(+1.43)		(−4.64)	(−2.14)
Measured t_R	18.90	17.50	14.95	13.62
	(+8.00)		(−14.57)	(−22.17)
Compensated t_R	17.67		16.76	17.67
	(+0.97)		(−4.01)	(+0.97)
Measured t_R	244.27	233.00	204.83	192.72
	(+4.84)		(−12.09)	(−17.82)
Compensated t_R	231.80		223.66	229.83
	(+0.52)		(−4.01)	(−1.36)
Measured t_R	2987.78	2880.00	2590.25	2338.10
	(+3.74)		(−10.06)	(−18.82)
Compensated t_R	2877.18		2760.67	2809.85
	(−0.10)		(−4.14)	(−2.44)

* Solvent/pump head temperature.

** The calibration graph was established by fitting the retention data at 20.0°C in the cubic equation

$$\log \text{mol.wt.} = a(t_R)^3 + b(t_R)^2 + c(t_R) + d$$

where $a = -9.3380 \cdot 10^{-6}$, $b = -2.6850 \cdot 10^{-3}$, $c = -8.1416 \cdot 10^{-2}$, $d = 9.8298$.

*** Molecular weights were calculated by entering measured retention data into the above equation. Percentage errors are shown in parentheses.

§ Retention data were compensated by using the coefficient of cubic expansion, $\alpha = 1.103 \cdot 10^{-3}$, calculated from the following equation[10], and extrapolating to 30°C:

$$\rho(T) = 0.880[1 + 0.001085(25 - T)]$$

retention data and the calibration graph. The molecular weight was also calculated using the compensated retention time by taking thermal expansion into account.

RESULTS AND DISCUSSION

Table I shows the errors in molecular weight determination without and with solvent/pump head temperature compensation. It is significant that a 10°C deviation from the temperature at which the calibration graph was established (20°C) causes 19–25% error when a wide-molecular-weight range column such as Shodex 80M is used. On the other hand, the error can be reduced to only 2.5% by applying the simple compensation for retention time with the coefficient of cubic expansion.

These results suggest that the linear velocity or volumetric flow-rate of the mobile phase solvent dominates the retention time of a sample solute in GPC, and a major contribution to the variation of retention time is made by the thermal expansion of the solvent in GPC.

In order to confirm the above conclusion, the retention time variation was evaluated by changing the temperatures of both the solvent/pump head and the solvent/column while maintaining the temperature difference constant at 15°C. With this arrangement, as the solvent/pump-head temperature increases, the mass flow-rate from the solvent delivery system decreases, but the volumetric flow-rate increases by the same factor in the column system, and *vice versa*, and accordingly the volumetric flow-rate or the linear velocity in the column remains constant. It is remarkable that even though the solvent/pump head temperature was increased from 20 to 30°C and the column temperature from 35 to 45°C, the relative changes in the measured retention times for the four standard solutes were -0.098% for PS of mol.wt. $2.8 \cdot 10^3$, -0.106% for PS of mol.wt. $17.5 \cdot 10^3$, -0.079% for PS of mol.wt. $233 \cdot 10^3$ and -0.087% for PS of mol.wt. $2880 \cdot 10^3$.

CONCLUSION

As we have demonstrated, a 10°C change in the solvent/pump head temperature results in a 19–25% error in molecular weight determination while the column temperature is kept constant. A temperature variation of a few degrees is very likely to occur in an ordinary laboratory environment, because normally only the column is thermostated and the solvent/pump head is not. Contrary to expectation, good accuracy in GPC is not always achieved when the column is thermostated. On the contrary, the smaller is the variation of the temperature difference between the solvent/pump head and the solvent/column, the smaller the variations of the retention times become, even though the overall ambient temperature varies. In other words, temperature control of only the column system may cause poorer results than when no special temperature control is applied to the room and the column system.

REFERENCES

1 G. B. Cox, *J. Chromatogr. Sci.*, 15 (1977) 385–392.
2 Cs. Horváth and W. Melander, *J. Chromatogr. Sci.*, 15 (1977) 393–404.
3 C. W. Gehrke, K. C. Kuo, G. E. Davis, R. D. Suits, T. P. Waalkes and E. Borek, *J. Chromatogr.*, 150 (1978) 455–476.

4 H. Colin, J. C. Diez-Masa, G. Guichon, T. Czajkowska and I. Miedziak, *J. Chromatogr.*, 167 (1978) 41–65.
5 W. R. Sisco and R. K. Gilpin, *J. Chromatogr. Sci.*, 18 (1980) 41–45.
6 R. K. Gilpin and W. R. Sisco, *J. Chromatogr.*, 194 (1980) 285–295.
7 W. W. Yau, H. L. Shchan and J. P. Malone, *J. Polym. Sci.*, 6 (1968) 1349–1355.
8 D. D. Bly, H. J. Stoklosa and J. J. Kirkland and W. W. Yau, *Anal. Chem.*, 47 (1975) 1810–1813.
9 S. Mori and T. Suzuki, *Anal. Chem.*, 52 (1980) 1625–1629.
10 T. E. Hogen-Esch and J. Smid, *J. Am. Chem. Soc.*, 88 (1966) 318–324.

Journal of Chromatography, 454 (1988) 362–366
Elsevier Science Publishers B.V., Amsterdam — Printed in The Netherlands

CHROM. 20 808

Note

Dependence of R_F values of cobalt(III) complexes on the size of diamine chelate ligands on silica gel thin layers

GORDANA VUČKOVIĆ, M. J. MALINAR and M. B. ĆELAP*
Institute of Chemistry, Faculty of Science, University of Beograd, P.O. Box 550, 11001 Beograd (Yugoslavia)
(Received July 4th, 1988)

In a previous paper[1] we reported the dependence of the R_F values of cobalt(III) complexes, obtained by thin-layer chromatography (TLC) on silica gel, on the size of the five- and six-membered aminocarboxylato and diamine ligands. It was found that in the TLC separations with monocomponent solvent systems the R_F values of the complexes with aminocarboxylato ligands decrease with increasing chelate ring size. In contrast, the complexes which in addition to aminocarboxylato ligands contained oxalato ligands instead of nitro groups exhibited the reverse order. Finally, in TLC separations of complexes containing diamine ligands the R_F values of the complexes increased with increasing chelate ring size, except when elution was carried out with water, when the reverse order occurred. However, when TLC separations were carried out with multicomponent solvent systems no regularity was observed for any of the aforementioned series. In all instances a linear dependence was found between the number of five-membered rings substituted by six-membered rings and the R_M values of the complexes.

Continuing these investigations, in this study we examined complexes containing seven-membered diamine ligands and possible separation mechanisms.

EXPERIMENTAL

The complexes investigated were prepared according to procedures reported in the literature (Table I). TLC separations on silica gel 60 G (Merck, Darmstadt, F.R.G.) were carried out as described in an earlier paper[1] and the solubility of the complexes was determined as described in a subsequent paper[2].

RESULTS AND DISCUSSION

Twenty-one cationic and neutral cobalt(III) complexes were chromatographed on silica gel thin layers. In addition to the five-, six- or seven-membered diamine ligands, the investigated complexes also contained, except in one instance, glycinato, (*R*)-alaninato or nitro ligands (Table I). The chromatographic separations were performed with the use of ten monocomponent solvent systems (Table II). As can be seen from Table I, with the application of nine non-aqueous solvent systems the R_F values

0021-9673/88/$03.50

TABLE I

R_F VALUES OF THE INVESTIGATED COMPLEXES OBTAINED BY TLC

No.	*Isomer*	*Absolute configuration*	*Complex**	*Ref.*	$R_F \times 100$**									
					1	*2*	*3*	*4*	*5*	*6*	*7*	*8*	*9*	*10*
1	*cis*-(NO_2), *trans*-(NH_2)-		$[Co(NO_2)_2$gly en]	3	76	68	–	7	–	–	–	–	–	–
2			tn	4	72	71	–	12	–	–	–	–	–	–
3			tmd	5	68	73	–	21	–	–	–	–	–	–
4	*trans*-(NO_2)-		$[Co(NO_2)_2$gly en]	5	81	–	39	4	0	78	–	–	–	–
5			tn	4	72	–	52	11	4	91	–	–	–	–
6			tmd	5	60	–	66	22	7	95	–	–	–	–
7	*cis*-(NO_2)-	Λ-$(+)_{589}$-	$[Co(NO_2)_2$(*R*-ala)en]	6	87	63	59	21	0	84	–	–	–	–
8			tn	6	74	68	67	33	7	89	–	–	–	–
9			tmd	5	61	71	75	42	10	92	–	–	–	–
10	*cis*-(NO_2)-	Δ-$(-)_{589}$-	$[Co(NO_2)_2$(*R*-ala)en]	6	88	53	40	20	–	87	–	–	–	–
11			tn	6	79	60	53	29	–	90	–	–	–	–
12			tmd	5	67	65	63	43	–	93	–	–	–	–
13	*cis*-(NO_2)-		$[Co(NO_2)_2$ $en_2]^+$	7	49	–	–	–	–	–	76	12	–	–
14			tn_2	8	26	–	–	–	–	–	78	17	–	–
15			tmd_2	5	17	–	–	–	–	–	80	27	–	–
16	*trans*-(NO_2)-		$[Co(NO_2)_2en_2]^+$	7	45	24	–	–	–	25	79	18	5	57
17			tn_2	8	39	34	–	–	–	30	82	26	11	62
18			tmd_2	5	33	40	–	–	–	32	87	30	26	72
19			$[Coen_3]^{3+}$	9	56	–	–	–	–	–	–	–	–	–
20			tn_3	9	23	–	–	–	–	–	–	–	–	–
21			tmd_3	10	10	–	–	–	–	–	–	–	–	–

* glyH = glycine; *R*-alaH = (*R*)-alanine; en = 1,2-diaminoethane; tn = 1,3-diaminopropane; tmd = 1,4-diaminobutane.

** The compositions of the solvent systems 1–10 are given in Table II.

TABLE II

SOLVENTS USED FOR TLC

No.	*Solvent*	*Time of development (min)*
1	Distilled water	15
2	Methanol	15
3	Ethanol	40
4	Acetone	10
5	Acetylacetone	60
6	1,3-Propandiol	540
7	N,N-Dimethylformamide	10
8	Ethylene glycol monomethyl ether	55
9	Dimethyl sulphoxide	45
10	Glycerine	1080

of the complexes increased with increase in the chelate ring size. In contrast, with the use of water the reverse order was obtained.

In all instances a linear dependence was found between the chelate ring size and the R_M values of the complexes; with non-aqueous solvents this dependence was negative and with water it was positive (Figs. 1 and 2).

We attempted to correlate the results obtained with the solubility of the complexes in the solvent systems used. For this purpose we determined the solubility of three complexes in three solvent systems. As can be seen from Table III, in non-aqueous solvent systems an increase in solubility was followed by an increase in the R_F value, whereas in water this was not so.

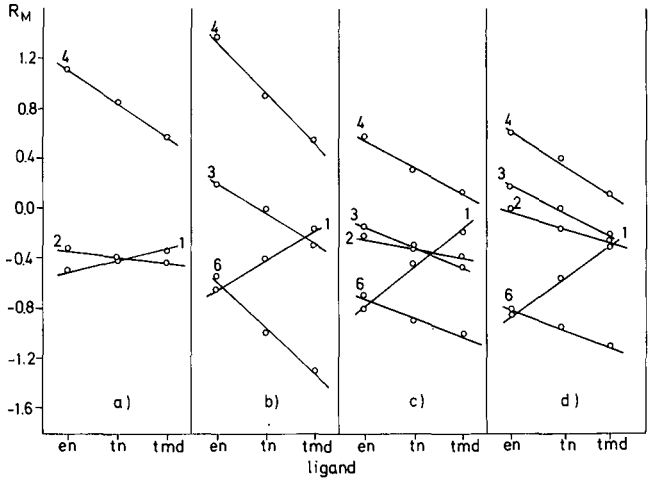

Fig. 1. Dependence of R_M values on the chelate ring size of the following complexes (see Table I): (a) 1–3; (b) 4–6; (c) 7–9; (d) 10–12. The numbers on the lines refer to the solvent systems used (see Table II).

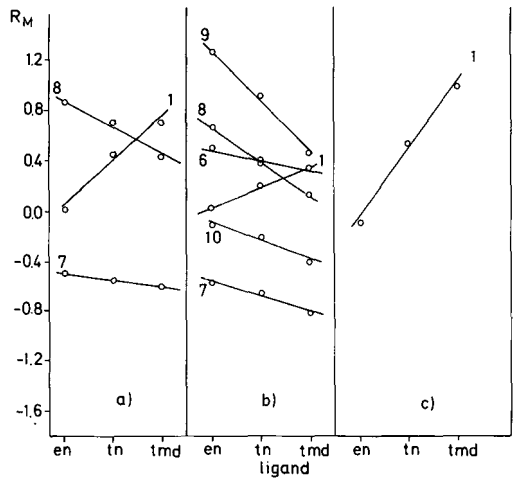

Fig. 2. Dependence of R_M values on the chelate ring size of the following complexes (see Table I): (a) 13–15; (b) 16–18; (c) 19–21. The numbers on the lines refer to the solvent systems used (see Table II).

It is known that when monocomponent solvent systems are used the R_F value of a complex depends on two factors: the strength of the adsorption of the dissolved substance to the adsorbent and the solubility of the substance in the solvent system used. The more strongly the complex is adsorbed the smaller its R_F value should be, whereas with increasing solubility of a complex its R_F value should increase.

As can be seen from Table III, in the chromatographic separations with water the solubility is not of major importance for the separation of the complexes, but rather the strength of their adsorption. The complex with 1,2-diaminobutane displays the lowest R_F value, as it forms the strongest hydrogen bonds. This is in agreement with the fact that in this series 1,4-diaminobutane is the strongest base (Table III).

In contrast, when TLC was carried out with non-aqueous solvent systems the other factor had the major influence, so that the complexes with ligands having larger chelate ring sizes displayed higher R_F values, on account of their higher solubility in the solvent system used.

TABLE III

SOLUBILITIES, R_F AND pK VALUES OF SOME OF THE INVESTIGATED COMPLEXES

*Complex**	*Solvent*						pK_1***	pK_2***
	Water		*Methanol*		*N,N-Dimethylformamide*			
	s**	$R_F \times 100$	s**	$R_F \times 100$	s**	$R_F \times 100$		
trans-$[Co(NO_2)_2en]^+$	0.067	45	0.002	24	0.007	79	7.00	10.09
trans-$[Co(NO_2)_2tn]^+$	0.447	39	0.007	34	0.033	82	8.64	10.62
trans-$[Co(NO_2)_2tmd]^+$	0.149	33	0.017	40	0.193	87	9.35	10.80

* Abbreviations as in Table I.
** s = solubility at 20°C (mol/dm^3).
*** Taken from ref. 11.

CONCLUSION

The regularities earlier established for cobalt(III) complexes containing five- and/or six-membered chelate rings appear to be valid also for complexes with seven-membered diamine rings. Hence a new possibility is offered for the determination of the composition of the corresponding complexes.

ACKNOWLEDGEMENTS

The authors are grateful to the Serbian Republic Research Fund for financial support and to Dr. Ružica Tasovac and Mrs. Zorica Lukanić for elemental microanalyses.

REFERENCES

1 M. B. Ćelap, Gordana Vučković, M. J. Malinar, T. J. Janjić and P. N. Radivojša, *J. Chromatogr.*, 196 (1980) 59.
2 G. Vučković, N. Juranić and M. B. Ćelap, *J. Chromatogr.*, 361 (1986) 217.
3 N. Matsuoka, J. Hidaka and Y. Shimura, *Bull. Chem. Soc. Jpn.*, 39 (1966) 1257.
4 M. B. Ćelap, M. J. Malinar and T. J. Janjić, *Rev. Chim. Miner.*, 13 (1976) 269.
5 M. J. Malinar and R. Herak, in preparation.
6 M. J. Malinar, R. Herak, M. B. Ćelap, N. Pavlović, S. Milić and D. Stojanov, *Glas. Hem. Druš. Beograd*, 46 (1981) 303.
7 Y. Shimura, *J. Am. Chem. Soc.*, 73 (1951) 5079.
8 M. B. Ćelap, M. J. Malinar and P. N. Radivojša, *Inorg. Chem.*, 14 (1975) 2965.
9 F. Woldbye, *Proc. R. Soc. London, Ser. A.*, 297 (1967) 79.
10 J. Fujita and H. Ogino, *Chem. Lett.*, (1974) 57.
11 C. R. Bertsch, W. C. Fernelius and B. P. Blode, *J. Phys. Chem.*, 62 (1958) 444.

Journal of Chromatography, 454 (1988) 367–371
Elsevier Science Publishers B.V., Amsterdam — Printed in The Netherlands

CHROM. 20 773

Note

Increasing the reliability of the identification of polymers by pyrolysis gas chromatography*

G. STOEV* and T. DENTSHEV
Bulgarian Academy of Sciences, Institute of Organic Chemistry, Sofia 1113 (Bulgaria)
(First received October 12th, 1987; revised manuscript received July 7th, 1988)

The interlaboratory reproducibility of gas chromatographic data for the identification of polymers by pyrolysis–gas chromatography (Py–GC) is unsatisfactory[1], although different means of improvement have been suggested. The method of hachured diagrams[2] can be applied only to certain polymer groups. The introduction of an internal standard in the pyrolysis products[3] eliminates this limitation but this method is unsuitable in Py–GC with capillary columns because of the large injection volume. The method of simultaneous pyrolysis of an unknown polymer with poly-α-methylstyrene, in which the retention times of the characteristic pyrolysis products are defined in relation to that of α-methylstyrene, can be applied in the identification of all polymers[4]. In this method, however, the relative retention times are defined exactly only for pyrolysis products that are chromatographed near to α-methylstyrene. The use of several polymers that generate standards covering the whole pyrogram could increase the precision of the relative retention times for all pyrolysis products. In this case, polymers that disintegrate into only one or two products should be used because of the risk of peak overlap with the pyrolysis products of the unknown polymer.

The properties of columns are very important for the reproducibility of GC data, and can be better specified with the g_p parameter for packed columns introduced by Van den Dool[5]. It has been established that this method can be applied to capillary columns[6]. Good reproducibility of the data from capillary columns with a fixed length and a fixed thickness of the film of the stationary phase is achieved when the value of g_p^5 varies within narrow limits, *i.e.*, $\pm 1\%$.

EXPERIMENTAL

As polymers that are pyrolysed to only one or two basic products in over 95% yield we selected poly(methyl methacrylate), poly-α-methyl methacrylate), poly-α-methylstyrene and polycarbonate. The polymers studied and the reference compounds were pyrolysed at 770°C for 5 s, using a Curie point pyrolyser directly connected to a capillary column[8] (Fig. 1). The capillary columns used (50 m × 0.3 mm I.D.) were

* Presented at the *6th Danube Symposium on Chromatography, Varna, October 12–17, 1987*. The majority of the papers presented at this symposium has been published in *J. Chromatogr.*, Vol. 446 (1988).

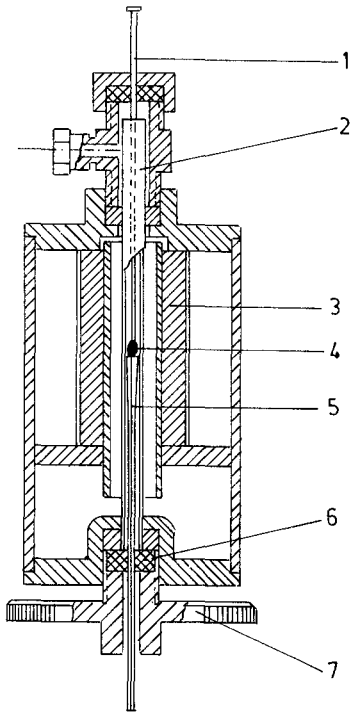

Fig. 1. Curie point pyrolyser directly connected to a capillary column: 1 = ferromagnetic wire; 2 = quartz tube; 3 = induction coil; 4 = sample; 5 = conical connecting capillary; 6 = additional gasket; 7 = connecting ring.

coated with PEG-20M or OV-101 (film thickness 0.20 – 0.26 μm) and the separation number was $TZ \geqslant 30$ (ref. 7). With these parameters the value of g_p is about 1.250 for PEG-20M, and about 1.000 for OV-101[6].

The flow-rate of the carrier gas (nitrogen) was adjusted to allow the C_{24} *n*-alkane to be chromatographed at 210 $\pm$ 2°C and 260 $\pm$ 2°C for PEG-20M and OV-101, respectively. *n*-C_{24} was added to pyridine at a level of 0.01 g in 10 ml. During pyrolysis *n*-C_{24} evaporates from the ferromagnetic wire and only a very small portion of it disintegrates under these conditions. The separation number for linalol–linalyl acetate and limonene–acetophenone must be less than 3 (ref. 6).

It was shown experimentally that the optimum separation of pyrolysis products is achieved with temperature programmes from 60 to 210°C at 2°C/min for the PEG-20M capillary column and from 35 to 260°C at 3°C/min for the OV-101 capillary column.

The experiments were performed with Pye Unicam 104 and Perkin-Elmer 910 gas chromatographs.

DISCUSSION

Methyl methacrylate has a relatively low molecular weight and a low polarity and is therefore chromatographed at the beginning of the pyrogram, which is why it

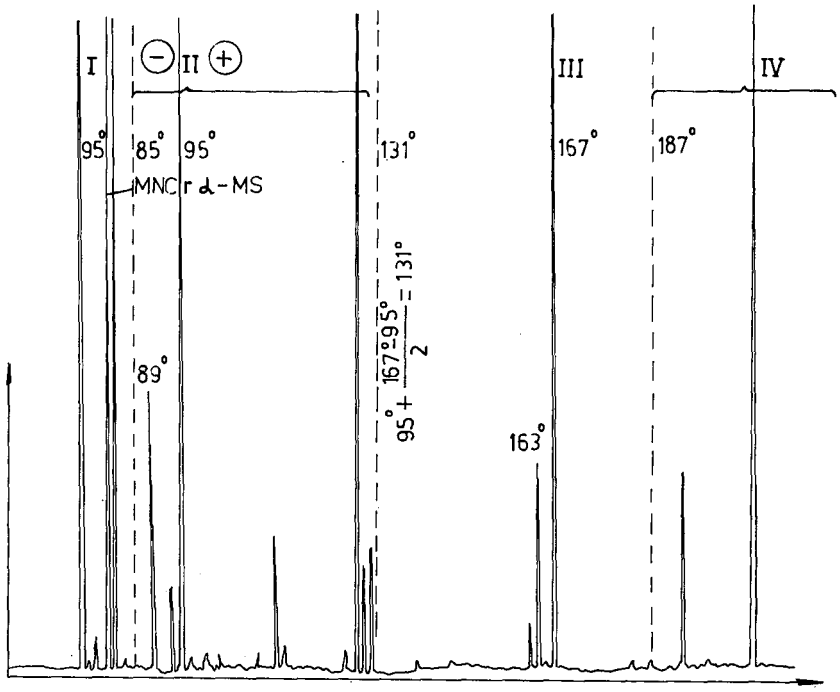

Fig. 2. Pyrogram of nylon-6,6, pyrolysed at 770°C for 5 s together with poly(methyl methacrylate), poly-α-methylstyrene and polycarbonate, obtained with a 50 m × 0.3 mm I.D. capillary column coated with PEG-20M (film thickness 0.23 μm), temperature programmed from 60 to 210°C at 2°C/min.

served as the first internal standard. α-Methylstyrene, because of its higher molecular weight, elutes later and is the second internal standard in the pyrogram. The polycarbonate pyrolysis products are chromatographed at higher temperatures and cover the second half of the pyrogram (Fig. 2).

These substances have an acidic character and from the form of their peaks we can estimate the absorption properties of the GC as regards this class of pyrolysis substances. In order to determine the response of the flame ionization detector to the internal standards so as to obtain peaks of comparable height, a solution of 0.02 g of poly(methyl methacrylate), 0.01 g of poly-α-methylstyrene and 0.5 g of polycarbonate in 10 ml of pyridine was injected on to the ferromagnetic wire with a microsyringe without contacting the polymer being studied. There is no need to evaporate all the pyridine because, owing to its basic properties, the form of its peak gives an indication of the behaviour of the GC system with respect to basic pyrolysis products.

In identifying polymers by Py–GC, the probability (P) of two polymers with a number of characteristic peaks, k, that seem identical, although in fact they are not, can be determined using the equation

$$P^{k}_{n,m} = \frac{(n - k)!}{n!m!}$$

The number of strips along the abscissa of the pyrogram, n, and along the ordinate, m,

TABLE I

VALUES OF THE CONFIDENCE INTERVAL OF THE MEAN $x = \bar{x} \pm 3\sigma$ OF THE RETENTION TEMPERATURES OF THE INTERNAL STANDARDS x

$\bar{x}$ = arithmetic mean; σ = standard deviation. Column, PEG-20M.

Compound (x)	$x = \bar{x} \pm 3\sigma$ (°C)
I. Methylmethacrylate	74.3 ± 1.4
Pyridine	83.0 ± 2.2
II. Methylstyrene	95.5 ± 1.3
III	167.4 ± 2.3
IV	208.0 ± 3.0

depend on the reproducibility of the GC data and are determined by the mean ($x \pm 3\sigma$) with 95% reliability. The values of n for the internal standards are given in Table I. On the basis of these data, the pyrograms are divided along the abscissa into strips from -3σ to $+ 3\sigma$ wide, using the largest value of the standard deviation for the internal standard IV:

$$\text{for a PEG-20M column } n = \frac{210 - 60}{3.0 \cdot 2} = 25$$

$$\text{for an OV-101 column } n = \frac{260 - 35}{3.6 \cdot 2} = 31$$

When calculating the strip width along the ordinate of the pyrogram, the precision of the measurement of the peak height must be taken into account. The strip width is determined from the reproducibility of the pyrolysis temperature and the homogeneity of the studied polymer. Our experience from studying different samples shows that 3σ may be up to 10% of the peak height. That is why the number of strips along the ordinate is $m = 5$ [100%/(2 · 10%)].

The probability of an coincidental overlap of a polymer with a defined number of characteristic pyrolysis products, *e.g.*, five, with another polymer having the same number of pyrolysis products in identification with a PEG-20M capillary column will be:

$$P^5_{25;5} = \frac{(25 - 5)!}{25!5!} = 1.31 \cdot 10^{-8} \; (k = 5, n = 25, m = 5)$$

and with an OV-101 column:

$$P^5_{31;5} = \frac{(31 - 5)!}{31!5!} = 1.26 \cdot 10^{-9} \; (k = 5, n = 31, m = 5)$$

The probability of coincidence of two different polymers when studied using a PEG-20M and an OV-101 capillary column is

$$P = P^5_{25;5} \cdot P^5_{31;5} = 1.65 \cdot 10^{-17}$$

There is another means of determining the probability of coincidental overlap, *i.e.*, by means of the relative retention time of the characteristic peaks. For this purpose, the pyrogram is divided into four sectors, the limits of which are defined as the arithmetic means of the retention temperatures of the internal standards (Fig. 2). For instance, the borderline between methyl methacrylate and α-methylstyrene will be at $75 + (95 - 75)/2 = 85°C$. Using this method of calculation, the relative retention time of a peak with a retention temperature of 89°C will be $(-)_{rel.}^{89} = (95 - 89)/(95 - 85) = 0.60$ and that for a peak with a retention temperature of 127°C will be $(+)_{rel.}^{127} = (127 - 95)/(131 - 95) = 0.89$.

This method of calculation is the difficult but offers enhanced precision. Thus, the maximum value of the interval $-3\sigma \pm 3\sigma$ of the relative retention times between sectors II and III is $2 \cdot 2.4°C$. The number of strips will be determined by $n = (210 - 60)/2.4 \cdot 2 = 31$, and the probability of a coincidental overlap is approximately $1.3 \cdot 10^{-8}$, *i.e.*, the identification is more reliable.

REFERENCES

1 B. B. Wheals, *J. Anal. Appl. Pyrol.*, 2 (1980/1981) 277.
2 V. R. Alishoev, V. G. Berezkin, A. A. Korolev and I. A. Tugorskii, *Fresenius Z. Anal Chem.*, 22 (1967) 151.
3 V. R. Alishoev and V. G. Berezkin, *Vysokomol. Soedin., Ser. A*, 13 (1971) 2777.
4 G. Stoev, *Dissertaton*, Higher Institute of Chemistry and Technology, Sofia, 1979.
5 H. van den Dool, *Ph.D. Thesis*, Rijksuniversiteit Groningen, Groningen, 1974.
6 G. Stoev, *Dokl. Bolg. Akad. Nauk*, 39, No. 12 (1986) 67.
7 G. Grob, Jr., G. Grob and K. Grob, *J. Chromatogr.*, 156 (1978) 1.
8 G. Stoev, *Dokl. Bolg. Akad. Nauk*, 32, No. 2 (1979) 179.

Journal of Chromatography, 454 (1988) 372–381
Elsevier Science Publishers B.V., Amsterdam — Printed in The Netherlands

CHROM. 20 825

Note

Direct coupling of a gas chromatograph to an ion trap detector

R. TIEBACH* and W. BLAAS
Max von Pettenkofer—Institut des Bundesgesundheitsamtes, Thielallee 88/92, Postfach 33 00 13, D-1000 Berlin 33 (F.R.G.)
(First received February 22nd, 1988; revised manuscript received May 26th, 1988)

The combination of capillary gas chromatography with mass spectrometry (GC–MS) is a powerful technique in trace analysis of complex samples. The two alternative interfacing methods described in the literature are direct coupling by positioning the GC capillary colum outlet in the evacuated ionization chamber of the mass spectrometer, or the use of a purged jet separator for the transfer of the GC eluate to the inlet capillary of the mass spectrometer[1,2]. In trace analysis the major advantage of the direct inlet system is the unsplit total analyte transfer into the mass spectrometer.

The ion trap detector ITD 700* is generally equipped with an open split interface. In an application note[3], the manufacturer proposed a direct inlet of the GC separation capillary into the analyzer block of the mass spectrometric detector. This construction was based on an early type of transfer line (Fig. 1, version I). To exchange GC capillary columns, the analyzer block of the ITD had to be cooled and the vacuum system was vented, the major disadvantage of most direct couplings in GC–MS equipment[4]. We installed our first direct connection by using the approved commercially available Finnigan transfer line (Fig. 1, version II). Although we have achieved excellent performance with the system, the disadvantages of turning off the instrument, remounting the main transfer line connections at the GC and MS sides and waiting about 24 h for appropriate and stable vacuum conditions to be re-established were still apparent. With our manipulation of the transfer line (Fig. 1, version III) we tried to overcome this time-wasting procedure. Results obtained and the performance of the new interface are discussed and three applications of the GC-ITD system are presented.

EXPERIMENTAL

Gas chromatography–mass spectrometry

All GC–MS analyses were performed on an Hewlett-Packard Model HP 5890A gas chromatograph directly coupled to a Finnigan ITD 700. For data processing, ITDS software revision 3.0 and the National Bureau of Standards (NBS) mass spectrum library were installed in an IBM AT2 data system. Samples were injected

* ITD 700 is a registered trademark of the Finnigan Corporation (Sunnyvale, CA, U.S.A.).

0021-9673/88/$03.50

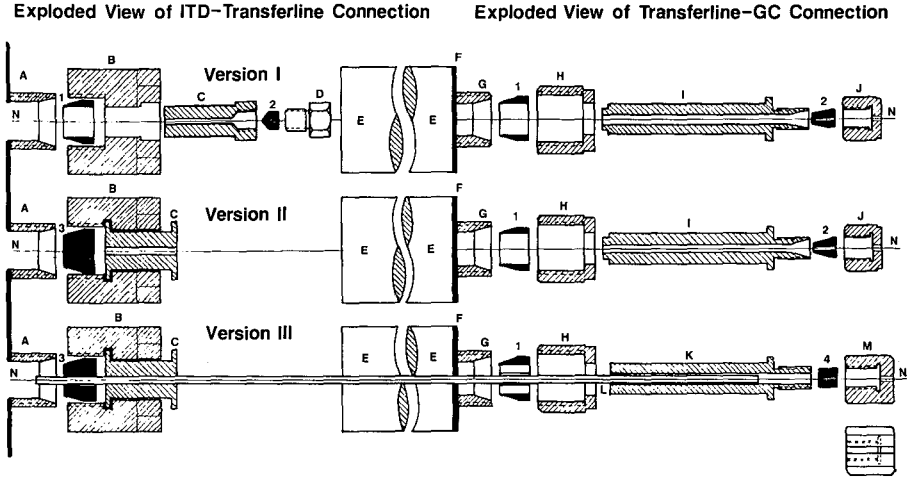

Fig. 1. Cross-sectional view of the GC–transfer line–ITD connections. For details see text. A = ITD manifold and Swagelok fitting, B = 7/8-in. nut, C = exit nozzle, D = 3/16- in. nut, E = heated transferline, F = GC oven wall, G = heated open split block, H = 1/2- in. nut, I = GC open split block adapter, J = 3/16-in. Swagelok nut, K = graphpack adapter, L = stainless-steel tubing, I.D. 0.5 mm, O.D. 0.75 mm, silver-soldered to graphpack adapter K, M = slit 7 mm hexnut, N = fused-silica capillary column, 1 = large-ring ferrule, 2 = small ferrule, 3 = large ferrule, 4 = graphpack brass-graphit ferrule.

manually on-column at the GC oven temperature. Retention gaps were installed in some experiments, and injected volumes never exceeded 1.0 μl. The pressure in the ITD analyzer was adjusted by the helium carrier gas flow regulator of the gas chromatograph so that the masses *m/z* 502 and 503 of the ITD calibrant perfluorotributylamine showed a good separation with a maximum peak height for *m/z* 502. The optimized flow setting obtained was then used as a pre-set value for all GC capillaries with identical lengths and internal diameters. Our experience has been that the film thickness of the stationary phase has little influence on the performance of the ITD.

Modification of the GC–ITD interface

To modify the GC–ITD coupling, the 7/8-in. nut of the transfer line was disconnected from the ITD manifold. At the GC side, the glass liner was removed from the heatable open split interface block. A 1.3-m section of stainless-steel tubing (0.5 mm I.D., 0.75 mm O.D.) was purged with a stream of pure oxygen and heated at the outside by means of a microburner flame. After cooling to ambient temperature, the tubing was washed with 100 ml each of *n*-hexane, dichloromethane, methanol and acetone. Sonic vibration was applied to support the cleaning effect of the successive washings. One end of the steel capillary was silver-soldered into a Graphpack* adapter. At this connection the inner surface of the tubing was smoothed with a 0.5-mm drilling tool. A 1/2-in. nut and ring ferrule were slid over the tubing onto the Graphpack adapter and the metal tubing was inserted through the transfer line from inside the GC oven. After tightening the nut and ferrule, the large ferrule was positioned

* Graphpack is a registered trademark of Gerstel (Mülheim, F.R.G.).

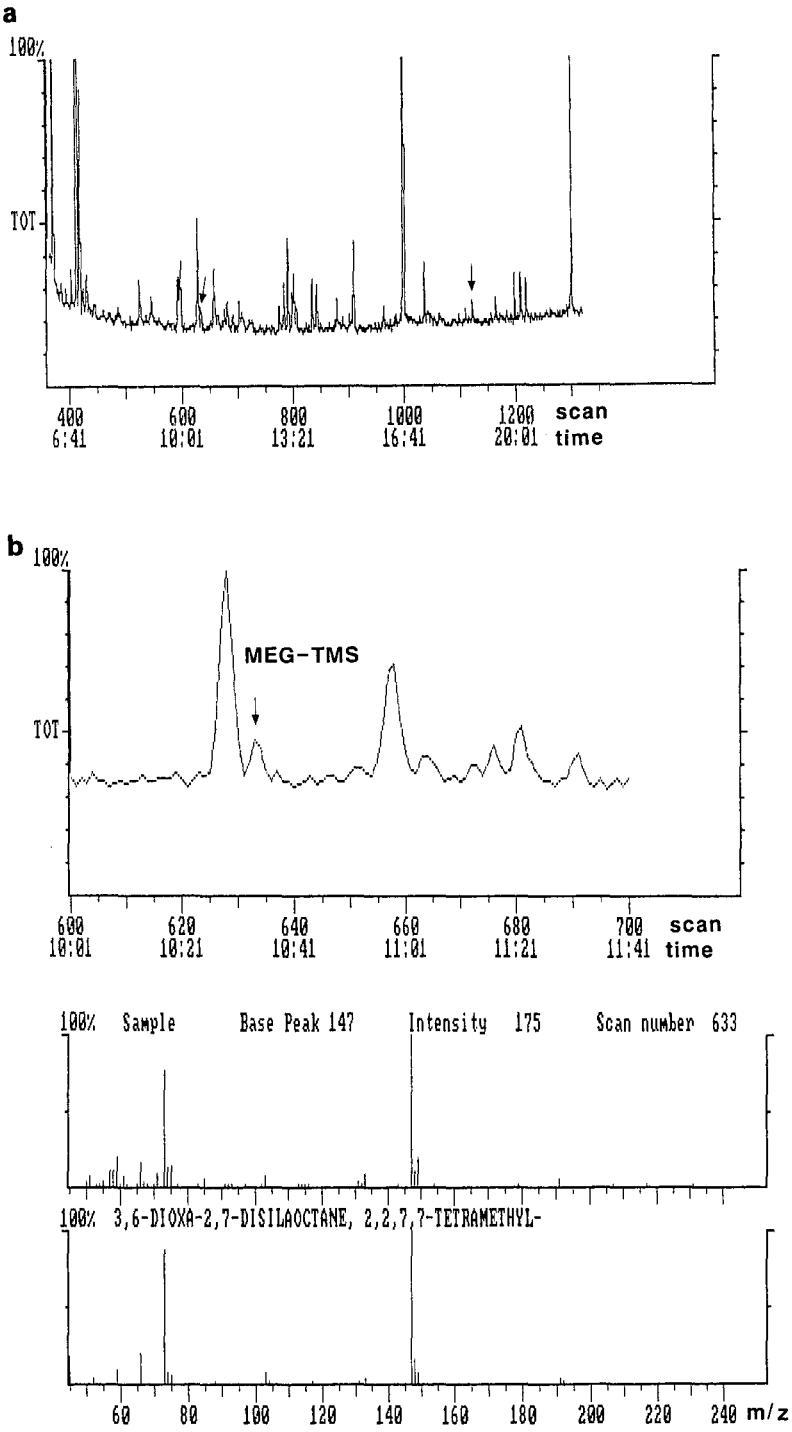
a
100%
TOT
400
6:41
600
10:01
800
13:21
1000
16:41
1200
20:01
scan
time
b
100%
MEG-TMS
TOT
600
10:01
620
10:21
640
10:41
660
11:01
680
11:21
700
11:41
scan
time
100% Sample Base Peak 147 Intensity 175 Scan number 633
100% 3,6-DIOXA-2,7-DISILAOCTANE, 2,2,7,7-TETRAMETHYL-
60
80
100
120
140
160
180
200
220
240
m/z

Fig. 2.

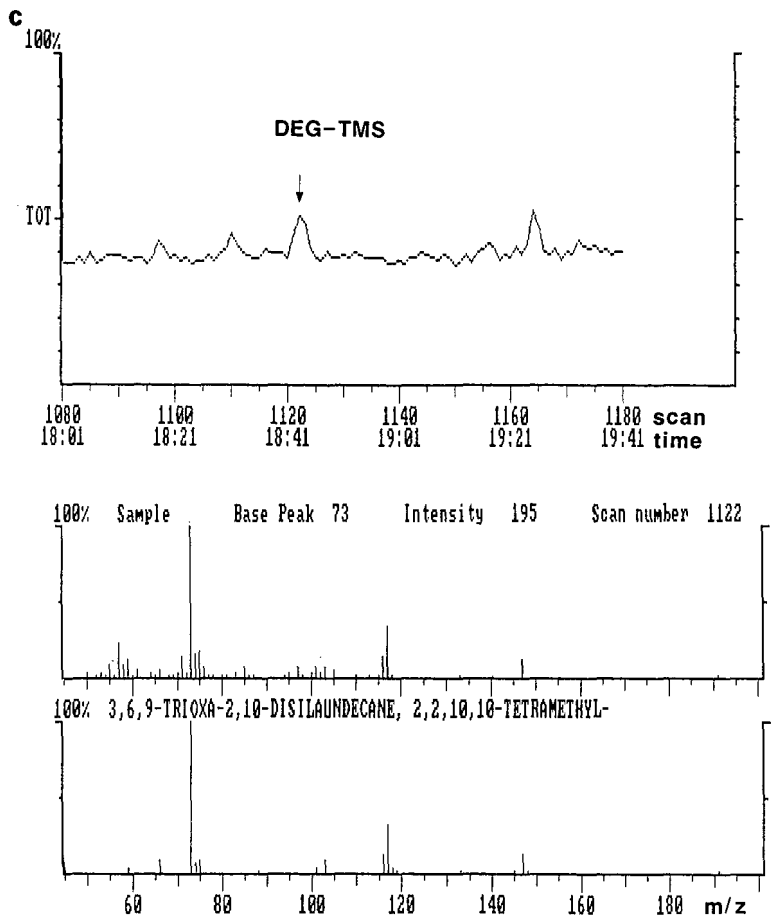

Fig. 2. Directly coupled GC–MS analysis of a diluted calibration standard in *n*-hexane, containing monoethylene glycol-TMS, diethylene glycol-TMS and the internal standards 1,4-butanediol-TMS and *n*-tetradecane. (a) Computer reconstructed total ion current (TIC) chromatogram; (b) TIC section, background-subtracted mass spectrum and NBS library reference spectrum identification for MEG-TMS peak, representing 574 fg monoethylene glycol; (c) TIC section, background-subtracted mass spectrum and NBS library reference spectrum identification for DEG-TMS peak, representing 636 fg diethylene glycol. GC: WCOT fused-silica capillary (60 m × 0.32 mm I.D.), film thickness 0.25 μm; coating SE-54 (SGE); temperature programme 70°C, 10 min; 10°C/min to 140°C, 2 min; 20°C/min to 250°C, 5 min. ITD: electron impact (EI) full scan acquisition, mass range *m/z* 50–250, 1 s per cycle.

onto the free end of the steel tubing in the 7/8-in. nut at the ITD side of the transfer line. The steel capillary should extend 5 mm beyond the large ferrule. This distance was marked with a scoring pencil. After withdrawing the tube from the open split interface block it was cut to the marked length. The exact measure (length of tubing + Graphpack adapter) was noted. After reinstallation, this part was finally sealed vacuum-tight inside the GC oven and at the ITD side. Both connections remained engaged in all further experiments, even during inspection and reassembly of the ion trap. After having fixed the fused-silica separation capillary to the injector, its free

end was marked with an ink pen at the point extending 5 mm beyond the exact length of the steel tubing plus the Graphpack adapter. A Graphpack ferrule was positioned at this mark and the capillary slid through the transfer line. The Graphpack connection was then tightly sealed with the slit hexnut. Replacement of GC capillary columns can now be achieved by simply disconnecting the Graphpack seal inside the GC oven, drawing back the used column and inserting the new one prepared with a Graphpack ferrule attached in the appropriate position as described above. After retightening the Graphpack connection and restabilization of ion trap parameters, the system is ready for GC–MS analysis.

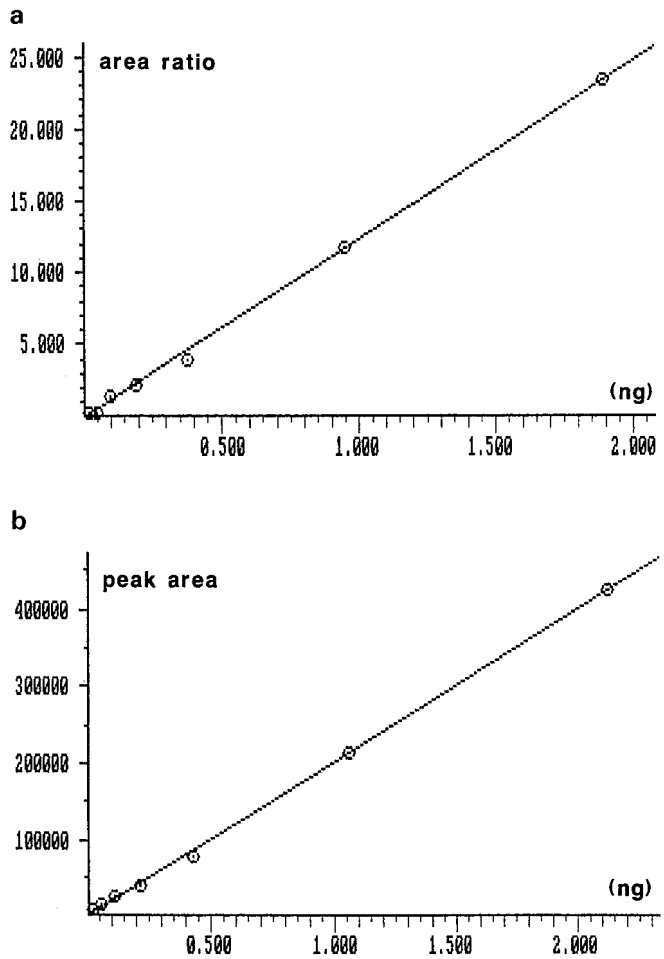

Fig. 3. Calibration plots for monoethylene glycol-TMS and diethylene glycol-TMS. Internal standard: *n*-tetradecane. (a) Peak area of MEG-TMS/peak area of *n*-tetradecane *vs.* corresponding amount of MEG injected (ng). (b) Peak area of DEG-TMS *vs.* corresponding amount of DEG injected (ng). For GC–MS conditions see Fig. 2., except for mass range *m/z* 50–300.

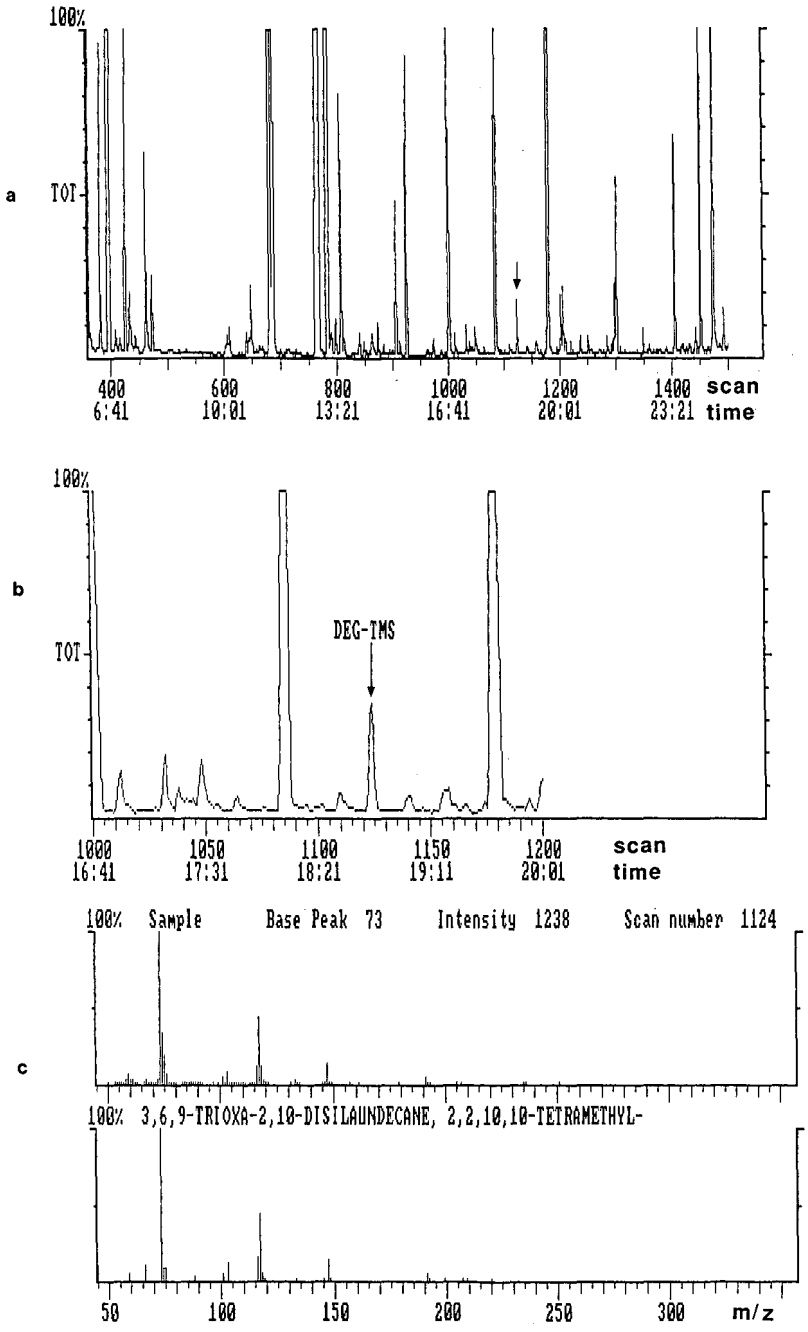

Fig. 4. Directly coupled GC–MS analysis of a white wine sample containing 1.189 mg/l (ppm) diethylene glycol. (a) Computer reconstructed TIC chromatogram of sample extract; (b) TIC section with DEG-TMS peak representing 297 pg diethylene glycol; (c) resulting mass spectrum and NBS library reference spectrum identification of DEG-TMS. For GC–MS conditions see Fig. 2, except for mass range *m/z* 50–300.

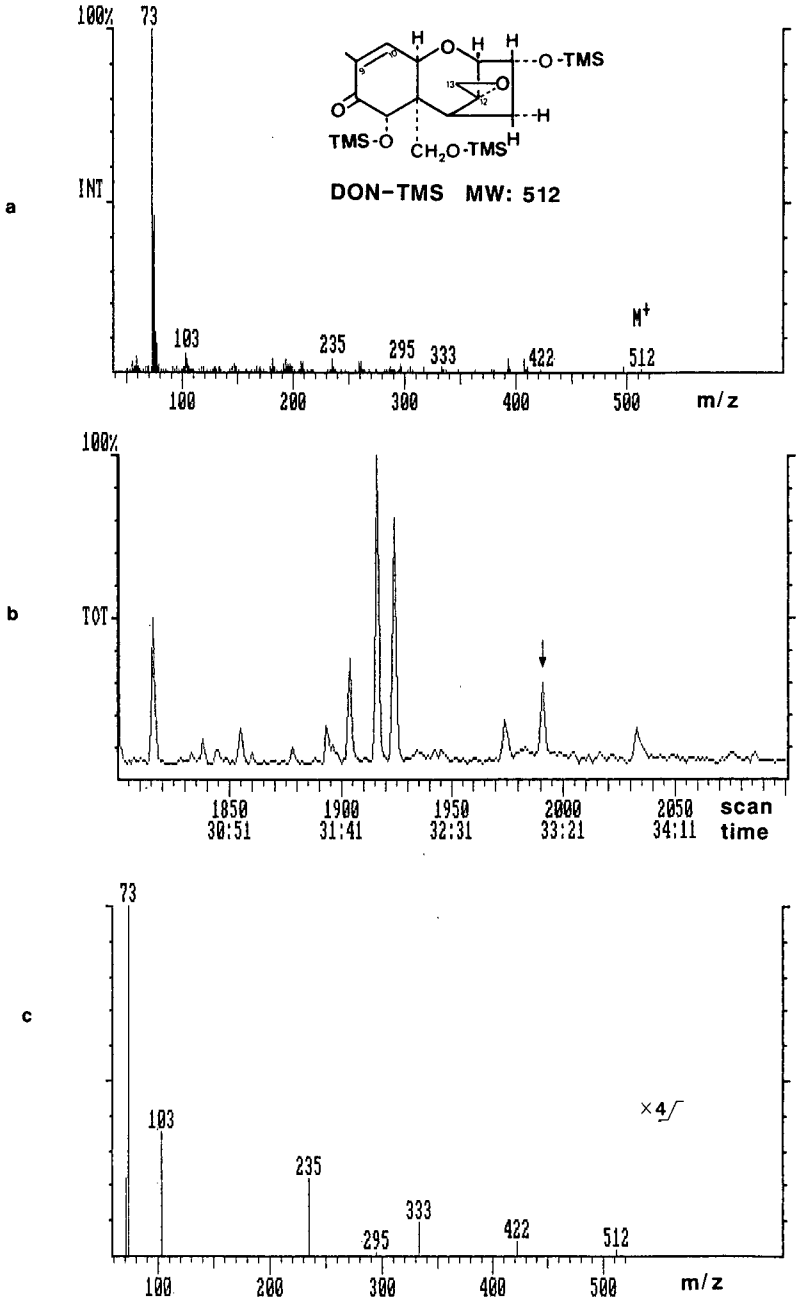

Fig. 5. Directly coupled GC–MS analysis of deoxynivalenol-TMS (DON-TMS). (a) Full scan reference mass spectrum of DON-TMS recorded from 600 pg DON standard. Designated ions are selected for measurements of samples in MID mode; (b) computer reconstructed MID chromatogram of a DON-contaminated wheat sample; (c) MID mass spectrum of DON-TMS peak representing 170 pg deoxynivalenol. GC: WCOT fused-silica capillary (60 m × 0.25 mm I.D.), film thickness 0.10 μm; coating DB-5 (J&W Scientific); 2-m retention gap, fused-silica megabore column, I.D. 0.53 mm (J&W Scientific); temperature-programme 80°C, 5 min; 4°C/min to 140°C, 2 min; 20°C/min to 260°C, 20 min. ITD: (a) EI full scan acquisition, mass range *m/z* 50–550, 1 s per cycle; (b) MID mode, selected ions for DON-TMS *m/z* 73, 103, 235, 295, 333, 422 and 512 (M^+).

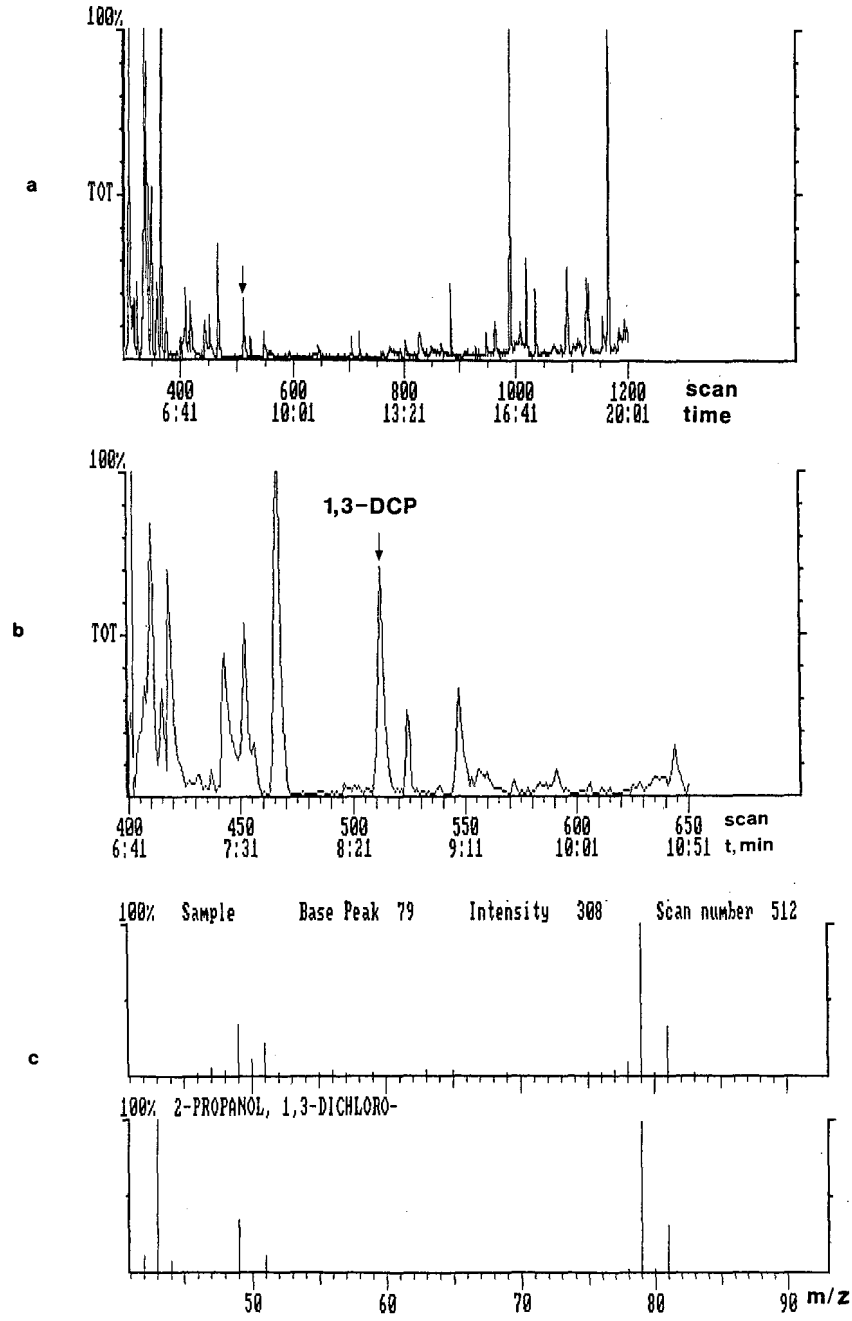

Fig. 6. Directly coupled GC–MS analysis of soy sauce containing 408 μg/kg (ppb) 1,3-dichloro-2-propanol (1,3-DCP). (a) Computer reconstructed TIC chromatogram of sample extract; (b) TIC section with peak representing 75 pg 1,3-DCP; (c) background-subtracted mass spectrum and NBS library reference spectrum identification. GC: WCOT fused-silica capillary (60 m × 0.25 mm I.D.), film thickness 0.25 μm; coating DB-5 (J&W Scientific); 2-m retention gap, fused-silica megabore column, I.D. 0.53 mm (J&W Scientific); temperature-programme 60°C, 8 min; 10°C/min to 200°C, 10 min. ITD: EI full scan acquisition, mass range *m/z* 46–90, 1 s per cycle.

RESULTS AND DISCUSSION

To demonstrate the increased sensitivity of our directly coupled GC–MS system, a calibration standard solution containing trimethylsilyl (TMS) derivatives of monoethylene glycol (MEG) and diethylene glycol (DEG), two compounds of increasing importance in wine control analysis, was diluted. From background-subtracted mass spectra of peaks detected with a signal-to-noise ratio $\geqslant 3/1$, both compounds, MEG–TMS and DEG–TMS, were identified by a full library fit search in rank 1. The amounts of derivatives injected corresponded to 574 fg free monoethylene glycol and 636 fg diethylene-glycol respectively. The total ion current, mass spectra and other information are shown in Fig. 2. In routine laboratory work, linear calibration plots for MEG amounts ranging from 18 pg to 1.89 ng and for DEG amounts from 21 pg to 2.12 ng were used in quantitation (Fig. 3.). The results of the analysis of a contaminated white wine containing 1.19 mg/l (ppm) diethylene glycol are presented in Fig. 4. On two other applications, GC–MS confirmation of GC results was required. In the first case, a wheat flour sample was shown to contain 575 μg/kg deoxynivalenol (DON, vomitoxin), a trichothecene mycotoxin frequently found in cereals[5]. To verify the contamination demonstrated by flame ionization detection (FID), we recorded full scan mass spectra of silylated DON reference material, selected characteristic fragment ions and examined the sample extract using the multiple ion detection (MID) mode. The Finnigan ITD software automatic quantitation procedure identified and calculated the contamination level to be 582 μg/kg (ppb), in excellent agreement with the GC–FID result (Fig. 5).

Another hazardous compound, 1,3-dichloro-2-propanol, in protein hydrolysates treated with hydrochloric acid was analyzed by Velisek *et al.*[6]. Following GC analysis with electron-capture detection (ECD), the contamination of a soy sauce sample was confirmed by using our GC–ITD system, as is demonstrated in Fig. 6. As little as 75 pg of the relatively low-molecular-weight compound (MW 128) were easily detected and identified.

CONCLUSION

Our modification of the Finnigan ion trap detector transfer line allows the rapid replacement of directly coupled fused-silica separation capillaries in GC–MS analysis without venting the vacuum system and time-wasting assembly. We have applied the direct coupling technique for more than 1 year now, and have obtained a remarkable increase in sensitivity of the GC–ITD combination, as is clearly demonstrated by the results described. In our opinion, the device presented could become an attractive alternative for those working in the field of trace analysis with the need to confirm analytical results by GC–MS.

ACKNOWLEDGEMENT

The authors thank Mr. W. Strauch for drawing the schematic diagram and for technical assistance.

REFERENCES

1 M.C. ten Noever de Brauw and C. Brunnée, *Fresenius' Z. Anal. Chem.*, 229 (1967) 321–335.
2 R. Kaiser, *Chromatographie in der Gasphase*, Bd. II, 2. Aufl., Bibliograph. Institut, Mannheim, 1966.
3 *How to Couple your Capillary Column Directly to the ITD*, Application note Finnigan, CA, 1985.
4 R.F. Arrendale, R.F. Severson and O.T. Chortyk, *Anal. Chem.*, 56 (1984) 1533–1537.
5 W. Blaas, M. Kellert, S. Steinmeyer, R. Tiebach and R. Weber, *Z. Lebensm.-Unters.-Forsch.*, 179 (1984) 104–108.
6 J. Velišek, J. Davidek, J. Hajšlová, V. Kubelka, G. Janiček and B. Mánková, *Z. Lebensm.-Unters.-Forsch.*, 167 (1978) 241–244.

Journal of Chromatography, 454 (1988) 382–386
Elsevier Science Publishers B.V., Amsterdam — Printed in The Netherlands

CHROM. 20 845

Note

New high-speed counter-current chromatograph equipped with a pair of separation columns connected in series

YOICHIRO ITO*
Laboratory of Technical Development, National Heart, Lung, and Blood Institute, National Institutes of Health, Bethesda, MD 20892 (U.S.A.)
and
F. EDWARD CHOU
Pharma-Tech Research Corporation, 6807 York Road, Baltimore, MD 21212 (U.S.A.)
(First received May 30th, 1988; revised manuscript received July 28th, 1988)

Recent advent of high-speed counter-current chromatography (HSCCC) has radically improved performance of counter-current chromatography in both separation time and partition efficiency[1–3]. The existing HSCCC centrifuge, however, has common problems in balancing the centrifuge system where a separation column is mounted on one side and a counterweight on the opposite side of the rotor. Because two-phase solvent systems applied to the separation column have a wide range in density, the weight of the counterbalance should be adjusted according to the solvent density and also to the volume of the stationary phase retained in the column. Failure to achieve proper balancing would produce excessive vibration of the centrifuge which often results in detrimental loss of the stationary phase from the column.

The present device conveniently eliminates the above problem by mounting a pair of identical multilayer coils symmetrically, one on each side of the rotary frame of the centrifuge. This provides an additional advantage of increased sample loading capacity for peforming preparative-scale separations.

PRINCIPLE AND DESIGN OF THE APPARATUS

The principle of the present device is diagrammatically illustrated in Fig. 1A where two identical columns are symmetrically arranged around the central axis of the centrifuge system. Each column undergoes synchronous planetary motion in such a way that it revolves around the central axis of the centrifuge and simultaneously rotates about its own axis at the same angular velocity (ω) as indicated by arrows. These two columns are equipped with a pair of flow tubes; both feed and return flow tubes enter the centrifuge system from the left side along the central axis and by forming an arch reach the right side of the first column. These flow tubes then exit the first column in the opposite side and again form an arch to return to the right side of the centrifuge through a straight path parallel to the centrifuge axis. On the right side of the centrifuge, they form a similar arch to reach the second column. With the above flow-tube arrangement, synchronous planetary motion of the column can maintain

0021-9673/88/$03.50

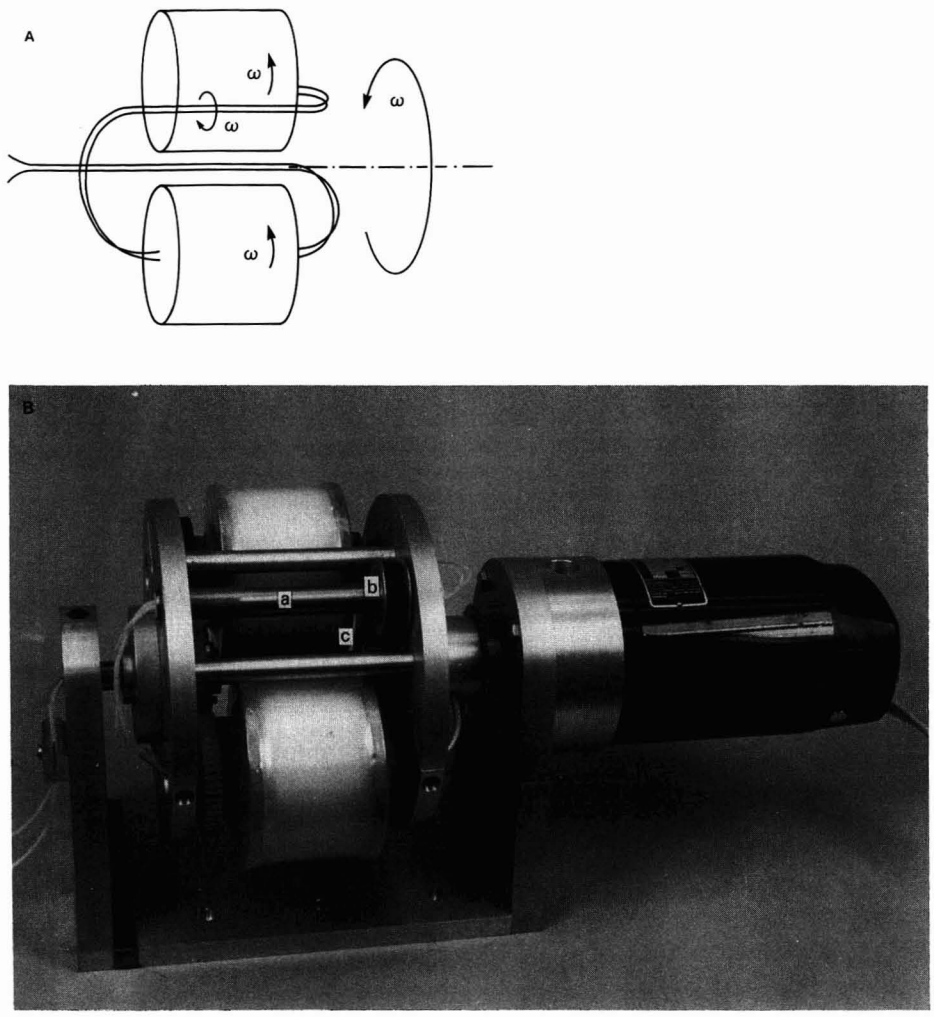

Fig. 1. (A) Design principle of the apparatus. (B) Photograph of the apparatus. Coupling the toothed pulley (b) on the rotary pipe (a) with a toothed belt to the identical stationary pulley (c) mounted on the central stationary shaft produces counter-rotation of the rotary pipe (a) to unwind the twist of the flow tubes caused by planetary motion of the column holders.

the integrity of the flow tubes without twisting, provided that the portion of the tubes connecting beween the two columns is counter-rotated ($-\omega$), either actively or passively, as indicated by the arrow.

Fig. 1B shows a photograph of our prototype based on the design principle described above. The motor drives the rotary frame around the central axis of the centrifuge. The rotary frame consists of a pair of aluminum discs rigidly bridged with multiple links and holds a pair of column holders in the symmetrical positions at a distance of 6.35 cm from the central axis of the centrifuge. Each column holder is equipped with a plastic planetary gear which interlocks with the identical stationary sun gear mounted around the central stationary shaft of the apparatus. This gear

arrangement produces the desired planetary motion of the column holder, *i.e.*, revolution around the central axis of the centrifuge and rotation about its own axis at the same angular velocity as in the existing HSCCC centrifuge.

The rotary frame of the present apparatus also holds a pair of identical rotary pipes, each equipped with a toothed pulley adjacent to the bearing, one rotary pipe (a) being used as a tube support and the other as a dummy to balance the centrifuge system. The pulley (b) on the rotary pipe (a) is coupled with a toothed belt to an identical stationary pulley (c) mounted around the central stationary shaft. This pulley coupling produces counter-rotation of the rotary pipe (a) to unwind the twist of the flow tubes caused by the planetary motion of the column holders. Consequently, the present design of the apparatus fulfills the mechanical requirements illustrated in Fig. 1A.

Both column holders can be removed from the rotary frame by loosening a pair of screws on each bearing block. Each separation column was prepared from a single piece of PTFE (polytetrafluoroethylene) tubing of 0.85 mm I.D. (Zeus Industrial Products, Raritan, NJ, U.S.A.) by winding it directly onto the holder hub and making multiple coiled layers with a capacity of about 45 ml. The β value (ratio of the rotational radius to the revolutional radius) of the multilayer coil ranged from 0.4 at the internal terminal to 0.75 at the external terminal. The layout of the flow tubes is schematically illustrated in Fig. 1A and summarized as follows: second column holder (upper-rear)–rotary pipe (a)–first column holder (lower-front) (one flow tube is connected to the column while the other bypasses it)–central stationary shaft-exit from the centrifuge system (clamped). As mentioned earlier, these flow tubes are free from twisting as the column holders undergo a synchronous planetary motion as indicated in Fig. 1A.

The apparatus can be operated up to the maximum speed of 2000 rpm with a Bodine speed controller. A Milton Roy metering pump was used to deliver the solvent while an LKB Uvicord S was used to monitor the absorbance of the effluent.

EXPERIMENTAL

All organic solvents, *n*-hexane, ethyl acetate and methanol, were glass-distilled chromatographic grade and purchased from Burdick and Jackson Labs. (Muskegon, MI, U.S.A.). A two-phase solvent system composed of *n*-hexane–ethyl acetate–methanol–water at a volume ratio of 3:7:5:5 was used in the present study. The solvent mixture was thoroughly equilibrated in a separatory funnel at room temperature and two phases separated shortly before use.

Test samples of indole-3-acetamide, indole-3-acetic acid, and indole-3-butyric acid were obtained from Sigma (St. Louis, MO, U.S.A.). The sample solution was prepared by dissolving a mixture containing 1 mg of each component in 1 ml of the above solvent system consisting of equal volumes of the two phases. The partition coefficient ($K = C_m/C_s$) for each component in this solvent system was 3.83 for indole-3-acetamide, 1.01 for indole-3-acetic acid, and 0.57 for indole-3-butyric acid.

The separation was initiated by filling the entire column with the upper non-aqueous phase followed by injection of sample solution through the sample port. Then the apparatus was rotated at 1600 rpm while the lower aqueous phase was introduced into the internal head terminal of the first column at a flow-rate of 1 ml/min. The effluent from the outlet of the second column was continuously mon-

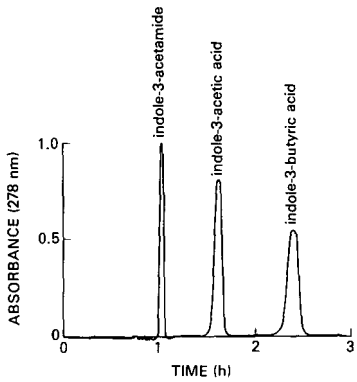

Fig. 2. Chromatogram of indole auxins obtained by the present method. Experimental conditions: solvent system: *n*-hexane–ethyl acetate–methanol–water (3:7:5:5); mobile phase: lower aqueous phase; elution mode: head to tail; flow-rate: 1 ml/min; sample size: 3 mg; revolution: 1600 rpm.

itored by the absorbance at 278 nm. After all peaks were eluted from the column, the apparatus was stopped and the column contents were collected into a graduated cylinder to measure the volume of the stationary phase retained in the column.

RESULTS AND DISCUSSION

Potential capability of the present apparatus was demonstrated by separation of indole plant hormones with a two-phase solvent system composed of *n*-hexane–ethyl acetate–methanol–water at a volume ratio of 3:7:5:5. Fig. 2 shows a UV trace of the chromatographic run where three components were well resolved in 3 h. From this chromatogram, partition efficiency was calculated according to the conventional gas chromatographic formula, $N = (4R/W)^2$, where N is the partition efficiency expressed in terms of theoretical plate number (TP); R, the retention time of the peak maximum; and W, the peak width expressed in the same unit as R. The results revealed high efficiencies ranging from 3000 TP (first peak) to 2400 TP (third peak), which double those obtained with the similar HSCCC centrifuge equipped with a single separation column[4]. The solvent front of the mobile phase emerged in 48 min (48 ml of elution), and retention of the stationary phase was 45%. The maximum pressure measured at the outlet of the pump was 105 p.s.i.

The above results clearly demonstrate high performance of the present HSCCC system. The symmetrical arrangement of paired identical separation columns on the centrifuge rotor ensures perfect balancing of the centrifuge system, regardless of the density of the applied solvents, once the separation column is equilibrated with the mobile phase*. This eliminates the necessity of tedious counterweight adjustment to

* During the pre-equilibrium period, the mobile phase gradually displaces the stationary phase starting from the first column to cause transient unbalance of the centrifuge system. This problem is common in all the centrifugal CCC systems. In the present semianalytical column with 45 ml capacity (90 ml total), a chloroform–acetic acid–water (2:2:1) system (density difference between the two phases is 0.24 g/cm^3) will cause, at a 70% retention level, the maximum unbalance of $0.24 \times 45 \times 0.3 = 3.2$ (g). In a larger column this unbalance will be increased proportionally to the column capacity. When a chloroform–water binary system (0.5 g/cm^3 in density difference) is applied, the increased density difference may be largely offset by the increase in stationary phase retention.

meet the density of the solvent system in the existing HSCCC system. Because of minimum vibration of the centrifuge system, the present system enables stable retention of the stationary phase in the rotating coil to yield higher peak resolution. Doubled column capacity in the present system further provides an important advantage for performing preparative-scale separations by increasing both the sample loading capacity and partition efficiency. We believe that the present new centrifuge design will greatly facilitate the use of the HSCCC technology in the near future.

REFERENCES

1 Y. Ito, *Adv. Chromatogr.*, 24 (1984) 181.
2 Y. Ito, *CRC Crit. Rev. Anal. Chem.*, 17 (1986) 65.
3 Y. Ito, J. Sandlin and W. G. Bowers, *J. Chromatogr.*, 244 (1982) 247.
4 Y. Ito and Y. W. Lee, *J. Chromatogr.*, 391 (1987) 290.

Journal of Chromatography, 454 (1988) 387–391
Elsevier Publishers B.V., Amsterdam — Printed in The Netherlands

CHROM. 20 784

Note

Isolation of virginiamycin-M_1 by droplet counter-current chromatography

KOICHI SAITO*, MASAKAZU HORIE, YOUJI HOSHINO and NORIHIDE NOSE
Saitama Institute of Public Health, 639-1, Kamiokubo, Urawa-shi, Saitama 338 (Japan)
YASUO SHIDA
Tokyo College of Pharmacy, 1432-1, Horinouchi, Hachioji-shi, Tokyo 192-03 (Japan)
and
HIROYUKI NAKAZAWA and MASAHIKO FUJITA
The National Institute of Public Health, 4-6-1, Shirokanedai, Minato-ku, Tokyo 108 (Japan)
(Received June 27th, 1988)

Droplet counter-currrent chromatography (DCCC) is a preparative separation technique based on the partitioning of a solute steady stream of droplets of mobile phase and the surrounding stationary phase. It is particularly useful for polar compounds and has been applied to the isolation of various types of natural products[1–3].

Virginiamycin (VGM), which is generally used as a feed additive for poultry, consists of factor M comprising M_1 and M_2 and factor S comprising S_1, S_2, S_3, S_4 and S_5. Since it is expected to have determined M_1, which is the main component of VGM, in rapid and simple routine analysis of VGM, the pure compound which is not commercially available, is required.

For the isolation of pure M_1 from crude VGM, Vanderhaeghe *et al.*[4] used silica gel open-column chromatography. However their method did not give sufficient separation of M_1 and M_2 from the crude VGM. The isolation and purification of M_1 from crude VGM by means of DCCC and, furthermore the correlation between the antibacterial activity of M_1 and VGM against Gram positive bacteria were investigated.

EXPERIMENTAL

Materials and apparatus

The crude VGM was obtained from Nihon Zenyaku Kogyo (Tokyo, Japan). All other reagents and solvents with high purity were obtained from Wako Pure Chemical Industries (Osaka, Japan) and were used without further purification. The silica gel pre-coated plate used for thin-layer chromatography (TLC) was Kieselgel 60 of 1 mm thickness and with a fluorescence indicator (Merck, Darmstadt, F.R.G.). The culture medium used for bioassay was antibiotic medium 11 (Difco, U.S.A.). All water used was distilled and deionized.

0021-9673/88/$03.50

The DCCC chromatograph used for separation of M_1 from crude VGM was supplied by Tokyo Rikakikai (Tokyo, Japan). The column consists of a hundred glass tubes (400 m × 3.4 mm I.D.) interconnected in series by capillary PTFE tubes. The samples were dissolved in a mixture of equivalent volumes of mobile and stationary phase and subsequently injected for DCCC using a 5-ml sample chamber. The mobile phase flow-rate was 24 ml/h and the eluate was collected in 5-ml fractions with a fraction collector (SF-160K; Toyo, Tokyo, Japan). The fractions eluted from the columns were monitored by an UV spectrophotometer (330; Hitachi, Japan) at 300 nm. The mixture of benzene–chloroform–methanol–water (26:14:24:6) used as the solvent system was allowed to equilibrate in a separatory funnel. Each column in DCCC had a lower layer of the stationary phase and an upper layer of the mobile phase.

For identification of M_1, an M-80 mass spectrometer (Hitachi, Japan) equipped with an M-003 data processing system was used. The ionization energies and trap currents were 70 eV and 60 μA, and the accelerating voltage was 3.0 kV for electron-impact mass spectrometry (EI-MS). For chemical ionization mass spectrometry (CI-MS), isobutane was used as the reagent gas.

An infrared absorption spectrophotometer (IR-435; Shimadzu Seisakusho, Japan) was also used for identification of M_1.

High-performance liquid chromatography (HPLC) was carried out using an LC-6A system (Shimadzu Seisakusho) equipped with an SPD-6A spectrophotometer set at a wavelength at 223 nm and a RF-530 fluorescence detector set at an excitation wavelength of 314 nm and an emission wavelength of 425 nm. A Kaseisorb LC ODS-300-5 reversed-phase column (250 mm × 4.6 mm I.D.; Tokyo Kasei Kogyo, Japan) was used. The mobile phase was acetonitrile–0.01% phosphoric acid solution (35:65) and chromatography was performed isocratically at ambient temperature at a flow-rate of 0.7 ml/min.

Isolation and purification of M_1

A 50-mg amount of crude VGM dissolved in the mixture of two phases was subjected to DCCC under the conditions described above. The chromatogram is shown in Fig. 1. Fractions of 450 to 750 ml eluted were evaporated at 40°C under reduced pressure. The residue was dissolved in an adequate volume of chloroform, and the mixture was spotted on a preparative TLC plate. Development was with the solvent system chloroform–methanol (95:5, v/v) in an equilibrated tank at room

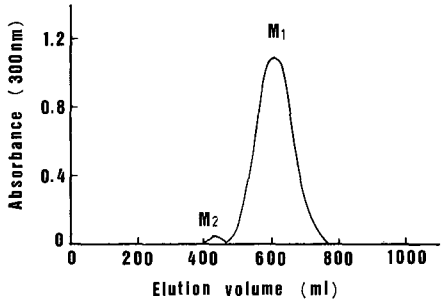

Fig. 1. Elution profile of virginiamycin-M_1 from DCCC.

temperature. The band of R_F 0.33 noted under UV light at 254 nm was scraped from the plate, and then dissolved in chloroform–methanol (9:1, v/v) and filtered to separate the sample substances from silica gel. The filtrate was evaporated to dryness at 40°C, and the residue was recrystallized twice from acetone. A 9.8-mg amount of pure M_1 as amorphous white crystals was obtained.

Determination of the partition coefficient and selection of the solvent system

To obtain the optimum partition coefficient (upper layer/lower layer), an 100-μg amount of crude VGM was added to 1 ml of the two-phase solvent mixture, and the mixture was shaken for 1 min. After separation, each layer (upper and lower) was pipetted out and subsequently subjected to HPLC with UV and fluorescence detection. M_1 was monitored by an UV detector, while VGM-S_1 (S_1), a main component of factor S, was monitored by the fluorescence detector. The partition coefficients of M_1 and S_1 were evaluated by measuring relative peak heights.

Microbiological assay

The antibacterial activity of VGM and M_1 was determined by a paper disk method with *Mirococcus luteus* ATCC 9341 having high sensitivity against VGM. The assay procedure was carried out according to the method of Katz *et al.*[5]. Each standard stock solution was prepared by dissolving VGM or M_1 in methanol to a concentration of 1000 μg/ml. A series of working standards of VGM or M_1 were prepared by diluting the stock solution in 50% methanol. Each filter-paper disk (10 mm in diameter) was impregnated by the aliquots (0.25, 0.5, 1.0, 2.5, 5.0, 10.0, 25.0 and 50.0 μg/ml of VGM or M_1). The disks were placed on the surface of an agar plate. After incubating for 16-18 h at 37°C, the diameter of the inhibition zone formed around the disk was measured with a vernier caliper.

RESULTS AND DISCUSSION

Selection of solvent system for DCCC and separation of M_1

The various solvent systems suitable for DCCC have been listed by Ogihara *et al.*[2]. Hostettmann[3] has also reported that TLC is a suitable method to find an appropriate solvent system. In this study, HPLC was utilized to determine the partition coefficient of M_1 in different solvent systems with high accuracy and rapidity.

Based on an examination using almost the same solvent systems, benzene–chloroform–methanol–water (26:14:24:6) was the most suitable solvent system for droplet formation with partition coefficients of 0.8 and 0.2 for M_1 and S_1, respectively.

The use of the upper layer as a mobile phase in the ascending mode of DCCC was expected for earlier elution of M_1. As shown in Fig. 1, the elution of M_1 in DCCC gave a chromatogram with good separation under the conditions described above. On the other hand, another component in factor M, M_2, was found in the 400 to 450 ml fraction of the eluate. Furthermore, these fractions were monitored by HPLC. Consequently, factor S components were found not to be present in the fraction of M_1.

On the other hand, although a slight amount of pigment derived from the crude VGM was found in the fraction of M_1, it was separated by employing TLC and recrystallization as described.

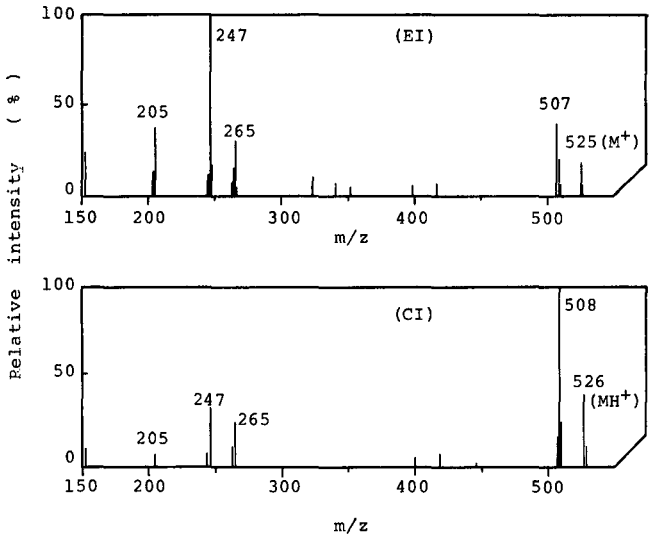

Fig. 2. Mass spectra of virginiamycin-M_1 measured by the EI and CI methods.

Confirmation of M_1

Fig. 2 shows the EI (A) and the CI mass spectrum (B) of the purified M_1. The parent peak at *m/z* 525 corresponds to the molecular weight of M_1 [M^+], while in the CI mass spectrum the peak at *m/z* 526 corresponds to the molecular weight of protonated M_1 [$M+H^+$]. The shift of the peak at *m/z* 507 in the EI mode is due to the loss of H_2O molecular ion from the parent peak, as is that of the peak at *m/z* 508 [$M+H-18^+$] in the CI mode. The other prominent fragmentation ions at *m/z* 265, 247 and 205, in Fig. 2 are typical ions of M_1. The molecular weight of M_1separated by open-column chromatography as reported by Vanderhaeghe *et al.*[4] was 555. This discrepancy may be due to insufficient purification of M_1 by column chromatography.

The IR spectral pattern of $M_1$was in good agreement with that reported by Vanderhaeghe *et al.*[4].

Correlation of the antibacterial activity between M_1 *and VGM*

Boon and Dewart[6] reported that the antibacterial activity of VGM depends on the synergism of factors M and S. The correlation between VGM and M_1 is therefore of interest. As shown in Fig. 3, the correlation between the inhibition zone of VGM

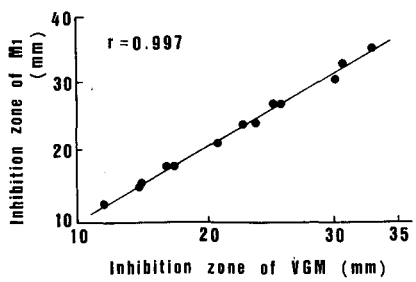

Fig. 3. Correlation between the antibacterial activity of VGM and M_1.

and that of M_1 exhibited a linear relationship with a correlation coefficient, r, of 0.993 ($n = 13$). Thus, from these results it is suggested that the amount of VGM in various samples can be determined by monitoring M_1 using HPLC.

CONCLUSION

Based on a study of the antibacterial activity of VGM and the main component, M_1, a good correlation, was found such that VGM could be determined by measuring M_1. DCCC has been used to obtain pure M_1 from crude VGM. From 50 mg of VGM, 9.8 mg of M_1 were obtained by using a two-phase system in DCCC.

ACKNOWLEDGEMENTS

We thank Nihon Zenyaku Kogyo for supplying the virginiamycin standard, and Dr. A. Tanaka for his help in the preparation of this paper.

REFERENCES

1 K. Okamoto, H. Yonezawa and N. Izumiya, *J. Chromatogr.*, 92 (1974) 147.
2 Y. Ogihara, O. Inoue, H. Otsuka, K. I. Kawai, T. Tanimura and S. Shibata, *J. Chromatogr.*, 128 (1976) 218.
3 K. Hostettmann, *J. Med. Plant Res.*, 39 (1980) 1.
4 H. Vanderhaeghe, P. Dijck, G. Parmentier and P. Somer, *Antibiot. Chemother.*, 7 (1957) 606.
5 S. Katz, J. Katz, J. Miller, R. Wang and R. Shapiro, *J. Assoc. Off. Anal. Chem.*, 67 (1984) 569.
6 B. Boon and R. Dewart, *Analyst (London)*, 99 (1974) 19.

Journal of Chromatography, 454 (1988) 392–397
Elsevier Science Publishers B.V., Amsterdam — Printed in The Netherlands

CHROM. 20 812

Note

Direct capillary trapping and gas chromatographic analysis of bromomethane and other highly volatile air pollutants

HEIKKI KALLIO*

*Department of Environmental Toxicology, University of California at Davis, Davis, CA 95616 (U.S.A.) and *Department of Chemistry and Biochemistry, Laboratory of Food Chemistry, University of Turku, SF-20500 Turku (Finland)*

and

TAKAYUKI SHIBAMOTO

Department of Environmental Toxicology, University of California at Davis, Davis, CA 95616 (U.S.A.)

(First received January 28th, 1988; revised manuscript received May 19th, 1988)

Bromomethane is still commonly used as a soil fumigant in green-houses and on strawberry cultivations, and as a methylating agent in warehouses and quarantine facilities. The analysis of the carry over residues of the fumigant in foodstuffs as well as the traces in ambient air have at least local interest[1].

Studies on *Klebsiella pneumoniae*[1], *Salmonella typhimurium*[1,2] and *Escherichia coli*[2] indicate a relatively low mutagenic efficiency of bromomethane. Tests on animals have suggested that bromomethane may cause disorders in the central nervous system. The LC-50 value (95% confidence) was 302 ppm in rats[3] and the oral LD-50 value was 214 mg/kg body weight when the subchronic oral toxicity in rats was investigated[4]. Danse *et al.*[4] also showed that a 3-month oral test caused carcinomas in the forestomach of a rat. Furthermore, it was found that bromomethane is a genotoxically active compound in the somatic cells of *Drosophila* larvae[5].

Trichloronitromethane (chloropicrin) is used as a lachrymatory factor in the bromomethane fumigants. Chloropicrin was found to be mutagenic to *E. coli* and *S. typhimurium*[2].

Krost *et al.*[6] developed a useful method for the analysis of bromomethane in air with capillary columns and electron-capture detection (ECD). The sample was collected in Tenax traps, desorbed thermally, cryofocused in a nickel capillary tubing and analysed after a second heat desorption step. The detection limit was found to be about 500 pg in 1 l of air. Attention had to be paid, however, especially to the breakthrough and recovery measurements. An obvious problem with a 0.5 mm I.D. capillary was the plugging of the tube with water. Some previously used air sampling methods like that of Noack *et al.*[7] and Brown and Purnell[8] are less sensitive, or less useful, in bromomethane analysis.

The aim of the present study was to develop a method to analyze highly volatile air pollutants like bromomethane with direct capillary trapping and fused-silica capillary columns.

0021-9673/88/$03.50

EXPERIMENTAL

Air pollutant trapping

Ambient air was sucked through a 35 cm × 0.32 mm (or 0.53 mm) deactivated fused-silica capillary tube with a pump. The centre part of the tubing (15 cm) was placed in a cold trap filled with solid carbon dioxide–acetone (−78°C) or liquid nitrogen (−196°C) during trapping. The volume of air passed through the capillary varied from 20 to 2000 ml.

In order to check for possible breakthrough of the volatiles, the following experiment was conducted. A 100-cm fused-silica capillary tube (0.53 mm I.D.) was coiled into two loops. The bottom halves of the loops (15 cm) were placed in the cold trap and the upper halves were kept at ambient temperature. One end of the tube was connected to a pump. The reference gas samples (*ca.* 1000 pg bromomethane and *ca.* 100 pg chloropicrin) were injected directly into the column chilled in solid carbon dioxide–acetone bath by using a 10-μl gas-tight syringe equipped with a 0.25 mm O.D. fused-silica capillary needle. An 100-ml volume of air was pumped in about 14 min by sucking through the sampling tube, then the tube was removed from the pump and cut into two pieces (each 50 cm). All the ends were sealed with SE-30 liquid phase material. The traps were kept chilled until analysis by gas chromatography (GC).

GC analysis of trapped samples

For the GC analysis an Hewlett-Packard 5890 chromatograph equipped with nickel-63 ECD was interfaced to an HP 3390A integrator. The outlet end of the sampling trap was connected to the on-column injector (J&W Scientific, Forsom, CA, U.S.A.) and the other end to the analytical column with a zero-dead-volume union. The trap was kept chilled all the time. A 60 m × 0.25 mm I.D. (film thickness 0.25 μm) bonded phase DB-1 or a 30 m × 0.32 mm I.D. (0.25 μm) bonded phase DB-1301 fused-silica capillary column (J&W Scientific) was used for GC analysis. When the connections were completed, the carrier gas (helium) was switched on for 1 min to purge oxygen from the column and the chilling trap was removed. The oven door was closed and the program was started.

Identification of the peaks on the gas chromatogram was performed by a co-injection method. The authentic reference gases were injected on-column before the cold trap was removed. The reference compounds were retained in the tubing with the trapped substances.

Threshold and linearity of detection

The linearity and detection threshold values of the ECD for bromomethane and chloropicrin were tested. Standard solutions of the analytes were made in hexane, and 1,2-dichloroethane (10^5 ng/ml) was added as an internal standard. Liquid samples, 0.3 μl, were introduced in the DB-1 column with on-column injection without cryofocusing. The contents of the analytes in hexane varied from 10 to 10^5 ng/ml and the amounts injected between 3 and $3 \cdot 10^4$ pg.

RESULTS

The cryosucking method was tested by collecting the impurities from laborato-

ry and ambient air and by analysing the electronegative volatiles (mainly halogenated compounds) by ECD. Fig. 1a shows a chromatogram of the laboratory air analysed with DB-1 liquid phase and Fig. 1b with DB-1301 liquid phase. The volume of the air samples trapped with liquid nitrogen in the deactivated capillary tube (0.32 mm I.D.) was in both cases 50 ml. Fluorotrichloromethane (Freon-11), di-, tri- and tetrachloromethanes and trichloroethylene were identified on the basis of co-injections with the reference compounds used in routine work in the laboratory. The relative and absolute amounts of the solvent traces varied all the time in the air, but the main peaks in the chromatograms were always present. Fig. 1a and b are not comparable to each other by quantitative means because the analyses were not carried out on the same day.

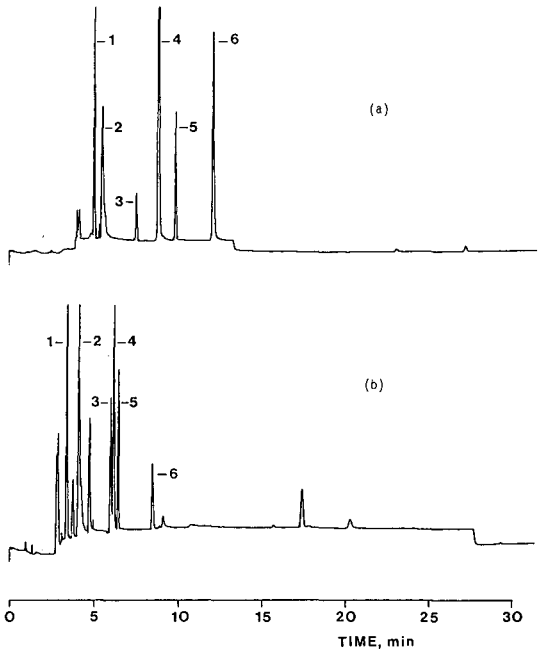

Fig. 1. Separation of some impurities in 50 ml of laboratory air collected by cryosucking in a capillary tube chilled in liquid nitrogen: 1 = fluorotrichloromethane (Freon 11); 2 = dichloromethane; 3 = trichloromethane; 4 = unknown; 5 = tetrachloromethane; 6 = trichloroethane. (a) 60 m × 0.25 mm DB-1 column, helium flow-rate 25 cm/s, isothermal 25°C. (b) 30 m × 0.32 mm DB-1301 column, helium flow-rate 21 cm/s, isothermal at 28°C. Detector temperature: 300°C.

An example of the breakthrough analysis of the volatiles is shown in Fig. 2a and b. No removal of water with a precondenser was done, which guaranteed a 100% introduction of all the volatiles in the air into the capillary tube. The compounds including bromomethane and chloropicrin were adsorbed in the first trapping loop (Fig. 2a). This was verified by GC analysis of the components in the second loop (breakthrough trap) shown in Fig. 2b.

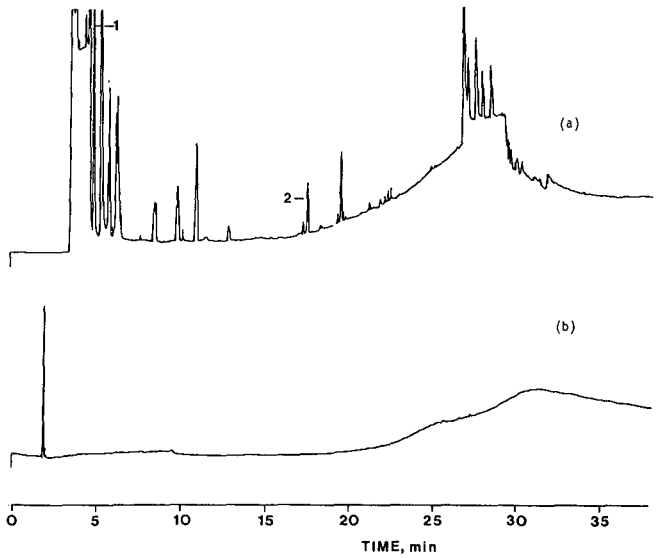

Fig. 2. Breakthrough test of the ambient air (100 ml) volatiles collected by cryosucking in capillary tube chilled in solid carbon dioxide–acetone. Bromomethane (1) and chloropicrin (2) co-injected in the tube at the beginning of the collection. (a) First trapping loop; (b) second trapping loop. Column: 60 m × 0.25 mm DB-1; isothermal at 29°C for 11 min, then programmed at 5°C/min to 100°C, finally held for 30 min. Detector temperature: 300°C.

The response curves for bromomethane and chloropicrin in hexane were determined by using 1,2-dichloroethane as an internal standard. Because of the varying ratio of the standard compound to the analyte in different samples, the correction factor was not constant. The lower the amount of the analyte, the higher was the correction factor. The relative responses of the compounds are presented in Fig. 3. Bromomethane had a far lower response than did chloropicrin; one bromine atom

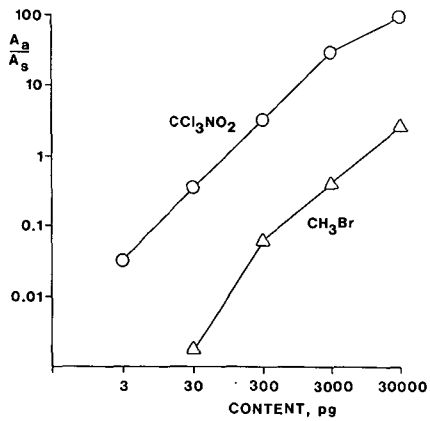

Fig. 3. Standard curves of bromomethane and chloropicrin analysed by a 60 m × 0.25 mm DB-1 column, isothermal at 60°C for 15 min, then programmed at 5°C/min to 100°C, finally held for 10 min. Internal standard: 1,2-dichloroethane, constant content $3 \cdot 10^4$ pg per injection. A_a = Area of the analyte peak; A_s = area of the internal standard peak.

against three chlorine atoms and one nitro group. The lowest point of the curve of bromomethane in Fig. 3 represents 30 pg of the compound and is close to the detection threshold value. The accurate value could not be determined due to some impurities in the redistilled hexane which were eluted at the same retention time as that of bromomethane, which was taken into account by subtracting the background. The threshold for chloropicrin was 3 pg.

DISCUSSION

The cryosucking of volatile samples in a capillary column or tubing for direct GC analysis is a very effective tool with many advantages and some limitations. The method developed may be compared with that of Kolb *et al.*[9], called "capillary head trapping", the principal differences being in the sample introduction.

Once the gaseous sample has been introduced into the capillary tube placed in the cold trap, no desorption steps using solvents or heat are needed. These operations might easily cause changes in the composition of the samples. Artifact formation is thus minimized with the capillary method proposed. Also the loss of volatiles is not a problem as long as the breakthrough during the sampling is verified to be zero (Fig. 2b). The collection should not be performed by compressing the air through a pump into a trap; only sucking is recommended. In this way the possibility of the collection of artifacts originating from the equipment can be minimized.

A piece of a capillary column or a whole column might be used as traps instead of the deactivated tubings. The use of liquid phase allows higher temperatures in the cold traps, also when volatiles with very low capacity factors are collected. When using the whole column as a trap, one connection in the column line can be avoided, which makes the procedure easier to operate. An obvious limitation is, however, the possible deterioration of the liquid phase due to sucking large amounts of air through the column. The polar phases, in particular, will be oxidized very rapidly, changing the selectivity and lowering the column efficiency.

When the sampling procedure is completed, the trap has to be inserted deeper into the coolant, to ensure that all the compounds retained are well chilled until analyzed. This is especially important with deactivated tubes without a liquid phase. The ends of the traps might be sealed with, for example, some viscous GC liquid phase like SE-30 or OV-1, which prevents the gas flow in the column during storage.

The connected capillary trap in the gas chromatograph has to be removed from the bath very slowly, starting from the injector side which was the outlet end of the tube when the sample was collected. In this way the most volatile compounds, like bromomethane, can be focused to a very short starting band. The problem of double peaks can easily be avoided and maximum column efficiency may be achieved even with thin film columns. Sampling traps should not be any longer than necessary to eliminate breakthrough of the compounds being analyzed.

The moisture content in the air might be a problem, when analyzing the very minor impurities, which exist at the level of ng/m^3 (ref. 10). During our ambient air experiments (temperature 32°C and relative humidity 48%), 1 l of air contained 16.2 mg of water. This amount blocked the megabore trapping capillary after about 0.5 l air was pumped through. With special movement of the trap in the coolant, maximum volume of air was aboyut 2 l. This indicates that, without removal of the water,

chloropicrin at concentrations of a few nanograms in 1 m^3 of air can be analyzed. In the case of bromomethane, the threshold level is about ten-fold when compared to chloropicrin.

In the case of the most volatile compounds, the main problem is not how to perform the collection nor how to remove the water. The problem appears usually when trace amounts of compounds with very low retentions have to be analyzed together with some major overlapping compounds. This is not, however, caused by the collection method, but a question of the efficiency and selectivity of the liquid phase.

The method as a whole is useful, because the only factor limiting the resolution is the column efficiency[11]. Therefore, the sensitivity in the case of bromomethane is about ten-fold that of the method of Krost *et al.*[6]. The cryosucking method may be used not only for air pollutant research, but also for food volatile analysis, both in the static and dynamic headspace procedures. In the case of foodstuffs with high water vapour pressure, such as sugar syrups, the maximum water loading capacity may be exceeded with as little as 20–30 ml volumes. Therefore, with liquid foodstuffs, a more accurate headspace introduction may often be possible with on-column injection by using a gas-tight syringe[12].

REFERENCES

1 P. G. N. Kramers, C. E. Voogd, A. G. A. C. Knaap and C. A. van der Heijden, *Mutat. Res.*, 155 (1985) 41.
2 M. Moriya, T. Ohta, K. Watanabe, T. Miyazava, K. Kato and Y. Shirasu, *Mutat. Res.*, 116 (1983) 185.
3 T. Honma, M. Miyagawa, M. Sato and H. Hasegawa, *Toxicol. Appl. Pharmacol.*, 81 (1985) 183.
4 L. H. J. C. Danse, F. L. van Velsen and C. A. van der Heijden, *Toxicol. Appl. Pharmacol.*, 72 (1984) 262.
5 A. J. Katz, *Proc. 16th Annual Meeting Environ. Mutagen Soc., Las Vegas, February 1985*, 1985, p. 13.
6 K. J. Krost, E. D. Pellizzari, S. G. Walburn and S. A. Hubbard, *Anal. Chem.*, 54 (1982) 810.
7 S. Noack, Ch. Reichmuth and F. El-Lakwah, *Fresenius' Z. Anal. Chem.*, 291 (1978) 121.
8 R. H. Brown and C. J. Purnell, *J. Chromatogr.*, 178 (1979) 79.
9 B. Kolb, B. Liebhardt and L. S. Ettre, *Chromatographia*, 21 (1986) 305.
10 H. B. Heath and G. Reineccius, *Flavor Chemistry and Technology*, Avi Publishing Company, Westport, CT, 1986, p. 6.
11 W. G. Jennings and M. Filsoof, *J. Agric. Food Chem.*, 25 (1977) 440.
12 H. Kallio, S. Rine, R. M. Pangborn and W. Jennings, *Food Chem.*, 24 (1987) 287.

Journal of Chromatography, 454 (1988) 398–405
Elsevier Science Publishers B.V., Amsterdam — Printed in The Netherlands

CHROM. 20 777

Note

Effect of differing thiols on the reversed-phase high-performance liquid chromatographic behaviour of *o*-phthaldialdehyde-thiol–amino acids

MELVIN R. EUERBY

Department of Pharmaceutical Chemistry, School of Pharmacy, University of London, 29–39 Brunswick Square, London WC1N 1AX (U.K.)

(First received May 16th, 1988; revised manuscript received June 28th, 1988)

Over the last decade increasing use has been made of the *o*-phthaldialdehyde (OPA)-thiol pre-column derivatisation of biologically important primary amino compounds[1–5], with special relevance to amino acids[1,2,4,6–10]. The resultant fluorescent derivatives are separated by reversed-phase high-performance liquid chromatography (HPLC) followed by fluorimetric detection and are believed to be N-alkyl-2-alkylthio substituted isoindole derivatives (Fig. 1).

To date, the thiols most commonly employed are mercaptoethanol[5–9], ethanethiol[2,10,11] and 3-mercaptopropionic acid[3,4,12] and their selection appears to be

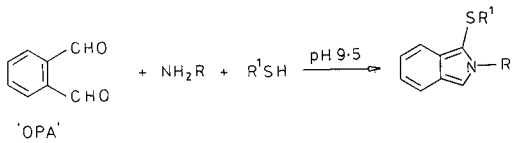

'OPA'

Amino acid	R=	Thiol	R^1 =
Lombricine	$CH(CO_2H)CH_2O\overset{\overset{O}{\|}}{P}(OH)OCH_2CH_2NH\overset{\overset{NH}{\|}}{C}NH_2$	Methanethiol	CH_3
		Ethanethiol	CH_2CH_3
Aspartic acid	$CH(CO_2H)CH_2CO_2H$		
		1-Propanethiol	$CH_2CH_2CH_3$
Serine	$CH(CO_2H)CH_2OH$		
		2-Mercaptoethanol	CH_2CH_2OH
Arginine	$CH(CO_2H)CH_2CH_2CH_2NH\overset{\overset{NH}{\|}}{C}NH_2$		
		3-Mercaptopropionic acid	$CH_2CH_2CO_2H$
		2-Mercaptoethane sulphonic acid	$CH_2CH_2\overset{\overset{O}{\|}}{S}(OH)OH$

Fig. 1. Proposed structures of the amino acid derivatives formed with OPA-thiols.

0021-9673/88/$03.50

determined solely by the stability of the resultant derivatives, rather than by other physicochemical properties which they may impart. Mercaptoethanol has been claimed to be less stable than either ethanethiol or 3-mercaptopropionic acid[12–14] but still remains the most widely used thiol. Recently, however, N-*tert.*-butyloxycarbonyl-L-cysteine, N-acetyl-L-cysteine and N-acetyl-D-penicillamine have been employed with OPA as the chiral derivatisation reagent for the chromatographic resolution of amino acids[15,16], amino compounds[16,17] and lombricine (a novel multifunctional amino acid derivative found in certain invertebrates)[18].

The retention times of the OPA-thiol–amino adducts can be altered by changing the organic modifier and by the addition of anions to the eluent[1,19]. It would be expected that the use of differing thiols would produce differing isoindoles with differing chromatographic properties; however, there are no reports in the literature which investigate this idea, with the exception of a paper describing the use of OPA and 2-aminoethanol or taurine to detect thiols in urine and marine sediment porewaters[19].

This article reports the findings of a study which compares the effects of a series of thiol homologues and two ionisable thiol derivatives with the commonly used mercaptoethanol on the retention times of aspartic acid, serine, arginine and lombricine (Fig. 1).

EXPERIMENTAL

Reagents and chemicals

All chemicals and solvents were of analytical or HPLC grade. Ultra-pure water was obtained by means of a Milli-Q system (Millipore). OPA, standard amino acids, mercaptoethanol, mercaptoethanesulphonic acid sodium salt were purchased from Sigma; methanethiol sodium salt, ethanethiol, propanethiol and 3-mercaptopropionic acid from Aldrich. Lombricine was prepared according to the method of Euerby *et al.*[20].

Chromatographic systems

HPLC apparatus and experimental conditions were as described for the assay of lombricine[21].

Pre-column derivatisaton procedure

The derivatisation reagents were prepared daily by dissolving 18.9 mg of OPA in 3.5 ml of methanol and 35 ml of borate buffer (pH 9.5 adjusted with 2 *M* sodium hydroxide). To 5.5 ml of this solution was added 200 nmol of the appropriate thiol, and the mixture stored at 4°C in the dark until use. The standard amino acid solutions (50 μl) were mixed with the derivatisation reagent (50 μl) and incubated for 5 min at ambient temperature in the dark before immediate injection onto the column.

RESULTS AND DISCUSSION

The reversed-phase gradient HPLC assay described previously[21] was used to investigate the effects of differing thiols on the retention times of aspartic acid, lombricine, serine and arginine. All the thiols investigated reacted with the amino acids

and OPA in alkaline conditions (pH 9.5) to give highly fluorescent derivatives which reached their maximum fluorescence within 5 min; all the derivatives formed were ammenable to reversed-phase HPLC on a 125 × 4.6 mm I.D. Spherisorb ODS II

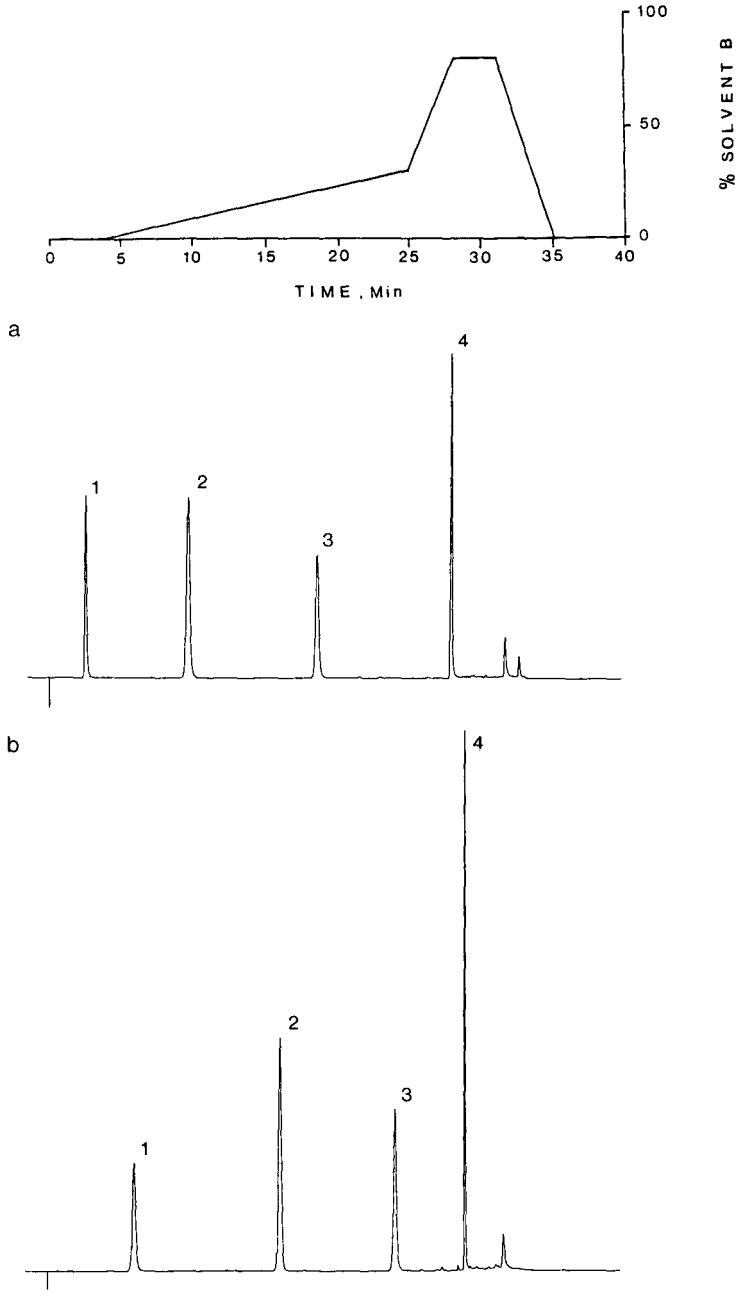

Fig. 1.

5-μm column (Fig. 2a–f). A series of four gradient runs were performed with the four amino acids for all the thiols. The derivatisation was performed prior to each injection and the reaction time was 5 min. Using peak heights, the average coefficient of variation was 1.5% and the average coefficient of variation for the retention time was 1.1%.

The partition coefficient values (log P) for mercaptoethanol and the thiol homologues methanethiol, ethanethiol and propanethiol were calculated from their hydrophobic fragmentation coefficients as described by Rekker[22] and were plotted against the retention times of the amino acids (Fig. 3 and Table I). It can be noted that there is a good relationship between the log P values of the thiols and retention

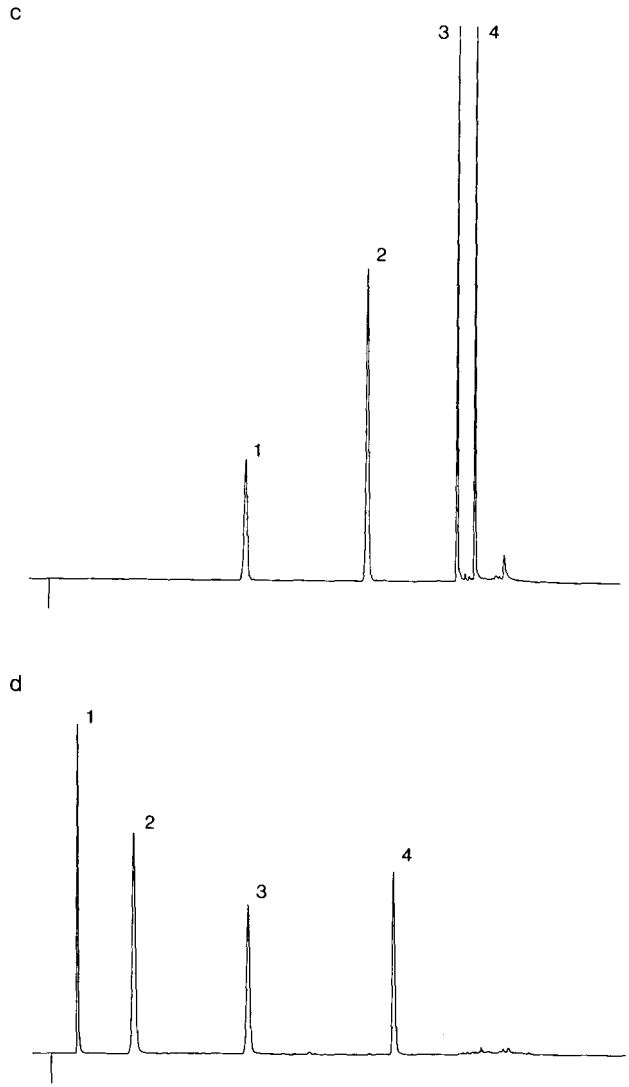

Fig. 1.

(*Continued on p. 402*)

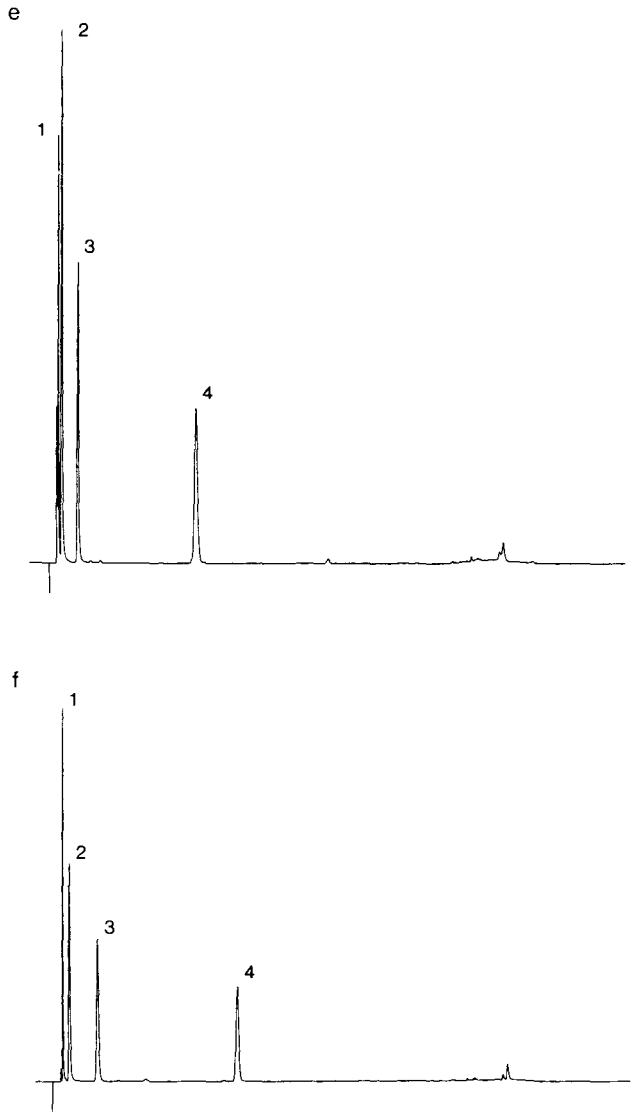

Fig. 2. HPLC of OPA–amino acid derivatives with differing thiols [(a) Methanethiol; (b) ethanethiol; (c) 1-propanethiol; (d) 2-mercaptoethanol; (e) 3-mercaptopropionic acid; (f) 2-mercaptoethanesulphonic acid] on a Spherisorb ODS II reversed-phase column (particle size 5 μm, 125 × 4.6 mm I.D.). Mobile phases: (A) 0.3 *M* sodium dihydrogenphosphate buffer (pH 7.2)–tetrahydrofuran–water (100:25:1875, v/v/v), (B) 0.3 *M* sodium dihydrogenphosphate buffer (pH 7.2)–acetonitrile–water (45:1100:855, v/v/v). Gradient: 0–4 min, 0% B; 4–25 min, 0–30% B; 25–28 min, 30–80% B; 28–31 min, 80% B; 31–35 min, 80–0% B; 35–40 min, 0% B. Flow-rate, 2 ml/min. Peaks: 1 = aspartic acid; 2 = lombricine; 3 = serine; 4 = arginine. Each peak corresponds to 50 pmol except for the serine and lombricine peaks which correspond to 30 and 75 pmol respectively. Fluorescence sensitivity employed was 0.2 R.F.U. Chromatographic conditions as in the Experimental section.

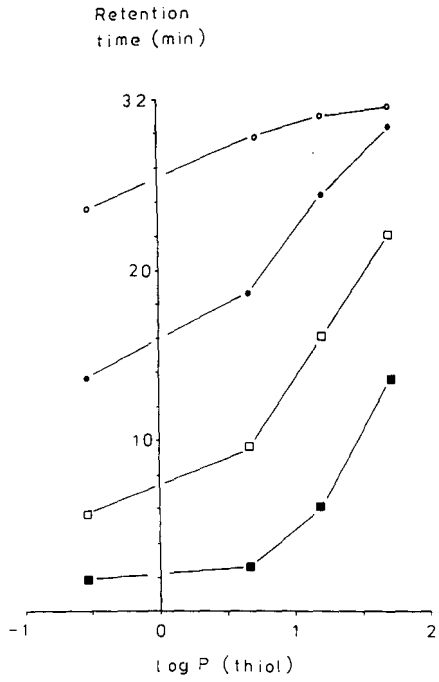

Fig. 3. The relationship of log P of the thiol (mercaptoethanol = −0.55; methanethiol = 0.66; ethanethiol = 1.18; propanethiol = 1.71) on the retention times of the resultant OPA-thiol–amino acid derivatives. Key to symbols: ○ = arginine; ● = serine; □ = lombricine; ■ = aspartic acid.

times, *i.e.* the more lypophilic the thiol the longer the retention time of the resultant derivative. The retention times for the derivatives of the thiol homologues and lombricine, which eluted on the linear gradient (4–25 min) part of the programme, were shown to be linearly related to the log P values of the thiols (regression analysis coefficient, r^2 = 0.9998). Whereas those of aspartic acid, serine and arginine showed no linearity owing to the fact that they eluted at differing gradients on the programme

TABLE I

EFFECT OF DIFFERING THIOLS ON THE RETENTION TIMES (min) OF AMINO ACIDS

Chromatographic conditions are as in the Experimental section.

Thiol	*Retention time (min)*			
	Aspartic acid	*Lombricine*	*Serine*	*Arginine*
Methanethiol	2.46	9.63	18.57	27.94
Ethanethiol	6.05	16.21	24.29	28.97
1-Propanethiol	13.60	22.00	28.32	29.58
2-Mercaptoethanol	1.80	5.64	13.60	23.70
3-Mercaptopropionic acid	0.52	0.76	1.90	10.12
2-Mercaptoethanesulphonic acid	0.60	1.04	3.24	12.80

TABLE II

EFFECT OF DIFFERING THIOLS ON THE SEPARATION FACTORS (α) OF AMINO ACIDS

Chromatographic conditions are as in the Experimental section.

Thiol	α		
	Aspartic acid/lombricine	*Lombricine/ serine*	*Serine/ arginine*
Methanethiol	3.91	1.93	1.50
Ethanethiol	2.68	1.50	1.19
1-Propanethiol	1.63	1.29	1.04
2-Mercaptoethanol	3.13	2.41	1.74
3-Mercaptopropionic acid	1.46	2.50	5.33
2-Mercaptoethanesulphonic acid	1.73	3.13	3.90

(*i.e.* the derivatives were experiencing differing rates of change of mobile composition). As expected, the ionisable thiol derivatives [3-mercaptopropionic acid (>99.5% ionised at pH 7.2) and mercaptoethanesulphonic acid] eluted faster than the lypophilic ones (*i.e.* methanethiol, ethanethiol and propanethiol); the polar thiol–mercaptoethanol derivative eluted between the ionic and lypophilic thiol derivatives.

There has recently been a report by Jinno and Tanigawa[23] describing the prediction of reversed-phase HPLC retention times of OPA-ethanethiol–amino acid derivatives. In the light of my findings it would be interesting to combine the thiol and amino acid hydrophobic parameters in Jinno and Tanigawa's[23] equations to, predict the retention times of a range of isoindoles. From Table II, it can be observed that changing the thiol employed in the pre-column derivatisation markedly effects the degree of separation achieved as a direct result of the shape of the gradient employed.

It appears, then, that by selecting a thiol of the appropriate log *P* value for use in the pre-column derivatisation reaction, it is possible to affect the retention time of the resultant derivative and also, depending on the gradient programme employed, the separation factors.

To conclude, the use of differing thiols in the OPA derivatisation of amino compounds provides a quick, convenient and complementary approach to optimising the assay of primary amino compounds.

ACKNOWLEDGEMENT

The C. W. Maplethorpe Trust is thanked for a research fellowship.

REFERENCES

1 P. Lindroth and K. Mopper, *Anal. Chem.*, 51 (1979) 1667.
2 J. D. Stuart, T. D. Wilson, D. W. Hill, F. H. Walters and S. Y. Feng, *J. Liq. Chromatogr.*, 2 (1979) 809.
3 R. Tawa, K. Koshide, S. Hirose and T. Fujimoto, *J. Chromatogr.*, 425 (1988) 143.
4 T. A. Graser, H. G. Godel, S. Albers, P. Földi and P. Fürst, *Anal. Biochem.*, 151 (1985) 142.
5 H. P. Fiedler and A. Plaga, *J. Chromatogr.*, 386 (1987) 229.
6 W. S. Gardner and W. H. Miller, III, *Anal. Biochem.*, 101 (1980) 61.
7 M. H. Joseph and P. Davies, *J. Chromatogr.*, 277 (1983) 125.

8 T. Hayashi, H. Tsuchiya and H. Naruse, *J. Chromatogr.*, 274 (1983) 318.
9 B. N. Jones and J. P. Gilligan, *J. Chromatogr.*, 266 (1983) 471.
10 M. H. Fernstrom and J. D. Fernstrom, *Life Sci.*, 29 (1981) 2119.
11 C. R. Krishnamurti, A. M. Heindze and G. Galzy, *J. Chromatogr.*, 315 (1984) 321.
12 P. Kucera and H. Umagat, *J. Chromatogr.*, 255 (1983) 563.
13 S. S. Simons, Jr. and D. F. Johnson, *Anal. Biochem.*, 90 (1978) 705.
14 S. S. Simons, Jr. and D. F. Johnson, *Anal. Biochem.*, 82 (1977) 250.
15 N. Nimura and T. Kinoshita, *J. Chromatogr.*, 352 (1986) 169.
16 R. H. Buck and H. Krumen, *J. Chromatogr.*, 387 (1987) 255.
17 N. Nimura, K. Iwaki and T. Kinoshita, *J. Chromatogr.*, 402 (1987) 387.
18 M. R. Euerby, L. Z. Partridge and P. Rajani, *J. Chromatogr.*, 447 (1988) 392.
19 K. Mopper and D. Delmas, *Anal. Chem.*, 56 (1984) 2557.
20 M. R. Euerby, L. Z. Partridge and W. A. Gibbons, *J. Chem. Res.*, submitted for publication.
21 M. R. Euerby, L. Z. Partridge and W. A. Gibbons, *J. Chromatogr.*, 445 (1988) 433.
22 R. F. Rekker, *The Hydrophobic Fragmental Constant*, Elsevier, Amsterdam 1977.
23 K. Jinno and E. Tanigawa, *Chromatographia*, 23 (1987) 675.

Journal of Chromatography, 454 (1988) 406–410
Elsevier Science Publishers B.V., Amsterdam — Printed in The Netherlands

CHROM. 20 750

Note

High-performance liquid chromatographic determination of macrosporin, altersolanol A, alterporriol A, B and C in fermentation of *Alternaria porri* (Ellis) Ciferri

R. SUEMITSU*, K. HORIUCHI, K. OHNISHI and S. YANAGAWASE
Department of Applied Chemistry, Faculty of Engineering, Doshisha University, Kamikyo-ku, Kyoto 602 (Japan)

(First received March 29th, 1988; revised manuscript received June 10th, 1988)

Macrosporin (Mac 1)[1], altersolanol A (As-A 2)[2], alterporriol A (Ap-A 3)[3], alterporriol B (Ap-B 3)[4] and alterporriol C (Ap-C 4)[5] have been found as metabolic pigments produced by *Alternaria porri* (Ellis) Ciferri, the causal fungus of black spot disease of stone-leek (Japanese name, negi). One of these pigments, As-A, inhibits elongation of the root in seeds of lettuce and stone-leek and shows antimicrobial activity against Gram-positive and -negative bacteria[6]. Also, Ap-A and Ap-B were found to be atropisomers of each other[3]. Cladofulvin[7] and asphodelin[8] have been reported as naturally occurring $\alpha\beta'$-bianthraquinone. The former is a metabolic product of *Cladosporium fulvum* and the latter is a component of *Aloe saponaria* HAW. Ap-C was found to be the second example of $\alpha\beta'$-bianthraquinone produced by fungi. Previously, we reported the high-performance liquid chromatographic (HPLC) determination of As-A, As-B and dactylariol, reduced anthraquinones produced during the fermentation period when *Alternaria porri* was cultured on Brian's medium T[9].

The structures of Ap-A, -B and -C show that they are modified bianthraquinones consisting of As-A and Mac (Fig. 1). So far as the biogenesis of Ap-A, -B and -C is concerned, two pathways can be considered, namely whether As-A and Mac are first metabolized and then bonded to alterporriols, or alterporriols are first metabolized and then their C–C linkages connecting the monomeric halves are cleaved to two halves of the molecules, As-A and Mac. This paper deals with the HPLC determina-

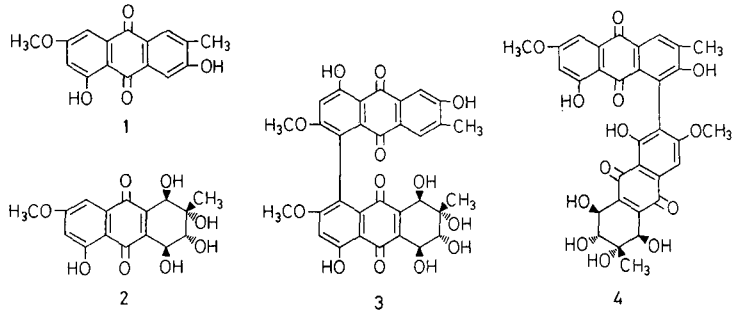

Fig. 1. Structures of pigments: 1 = macrosporin; 2 = altersolanol A; 3 = alterporriol A and B; 4 = alterporriol C.

0021-9673/88/$03.50

tion of Mac, As-A and Ap-A, -B and -C during the period of fermentation in order to explore their metabolic pathways.

EXPERIMENTAL

Material

Mac, As-A and Ap-A, -B and -C were isolated as metabolic pigments of *Alternaria porri* (Ellis) Ciferri (IFO 9762), which was isolated and donated by the Institute for Fermentation, Osaka, Japan (IFO).

High-performance liquid chromatography

HPLC was performed on a Shimadzu LC-6A liquid chromatograph equipped with a UV detector, operating at 254 nm for all assays. Three solvent systems were used for the resolution of five metabolic pigments, because their polarities in HPLC differed. For Ap-A, -B and -C, 0.05 *M* ammonium dihydrogen phosphate (adjusted to pH 2.5 with phosphoric acid)–acetonitrile (7:3) was used as the mobile phase. For As-A and Mac, the same components were used but in the ratios 4:1 and 1:1, respectively. The column used was a YMC A-312 (Yamamura Chemical Laboratories), commercially packed with reversed-phase octadecylsilica (5 μm) (150 mm × 6.0 mm I.D.), through which the above mobile phases were run at a flow-rate of 1.0 ml/min. Samples of 10 μl were injected on to the column.

Fermentation and extraction of pigments

A 2% sucrose solution of onion decoction was used as a culture medium. A number of 500-ml erlenmeyer flasks containing 200 ml of the medium were sterilized in an autoclave for 20 min at 2.3 bar and 120°C. The fungi, cultured on agar for 7–10 days, were inoculated into the flasks, which were then kept at 25°C. After fermentation for 1 day, 10 ml of the culture liquid were taken and extracted first with *n*-hexane to remove lipids and then with ethyl acetate (5 × 30 ml). After evaporation of the solvent, the coloured material obtained was denoted S-1 (1.1 mg). By a similar procedure, coloured material corresponding to fermentation periods of 2, 5, 7, 14, 21 and 28 days were obtained and denoted S-2 (2.1 mg) , S-3 (4.6 mg), S-4 (5.8 mg), S-5 (7.2 mg), S-6 (7.8 mg) and S-7 (8.7 mg), respectively, plus S-8 for blank (0.7 mg).

RESULTS AND DISCUSSION

Quantitative analysis of Mac, As-A and Ap-A, -B and -C during the fermentation period

As shown in Fig. 2, the retention times (t_R) were 6.4 min (As-A, $k' = 1.29$), 14 min (Mac, $k' = 5.13$), 22 min (Ap-B, $k' = 7.93$), 23 min (Ap-A, $k' = 8.31$) and 46 min (Ap-C, $k' = 17.61$). We used the internal standard method for quantitation and α-naphthol (t_R 26 min, $k' = 9.89$) was used as the internal standard for Ap-A, -B and -C, and benzoic acid (t_R 14 min, $k' = 3.96$) and naphthalene (t_R 19 min, $k' = 7.53$) for As-A and Mac, respectively. For example, methanolic solutions of As-A (1 mg/ml) (0.4, 0.6, 0.8, 1.0 and 1.2 ml) were placed into five sample vials and 1-ml portions of methanolic solutions of benzoic acid (1 mg/ml) were added. After the volumes had been adjusted to 10 ml with methanol, 10-μl portions of each were subjected to HPLC under the condition mentioned above. By plotting the peak-area ratios against sample weight a calibration graph for As-A was obtained. The calibration graph for Mac was

TABLE I

ANALYTICAL RESULTS FOR PIGMENTS

(A) Peak-area ratio to I.S.; (B) weight ratio to I.S.; (C) concentration (mg/ml).

Sample	*Macrosporin*			*Altersolanol A*			*Alterporriol A*			*Alterporriol B*			*Alterporriol C*		
	A	*B*	*C*	*A*	*B*	*C*	*A*	*B*	*C*	*A*	*B*	*C*	*A*	*B*	*C*
S-1	$1.08 \cdot 10^{-3}$	–	–	0.132	0.16	0.016	–	–	–	–	–	–	–	–	–
S-2	$2.52 \cdot 10^{-3}$	–	–	0.420	0.51	0.051	–	–	–	–	–	–	–	–	–
S-3	0.566	0.31	0.031	1.192	1.46	0.146	0,677	0.50	0.0050	0.741	0.35	0.0035	0.660	0.26	0.0026
S-4	0.141	0.06	0.006	1.023	1.25	0.125	0.234	0.17	0.0017	0.438	0.16	0.0016	0.524	0.21	0.0021
S-5	1.056	0.59	0.059	0.896	1.10	0.110	0.486	0.36	0.0036	0.519	0.21	0.0021	1.261	0.49	0.0049
S-6	1.591	0.91	0.091	0.635	0.78	0.078	1.063	0.79	0.0079	0.924	0.47	0.0047	1.537	0.60	0.0060
S-7	2.083	1.20	0.120	0.337	0.41	0.041	2.126	1.59	0.0159	1.855	1.07	0.0107	1.264	0.49	0.0049
S-8	–	–	–	–	–	–	–	–	–	–	–	–	–	–	–

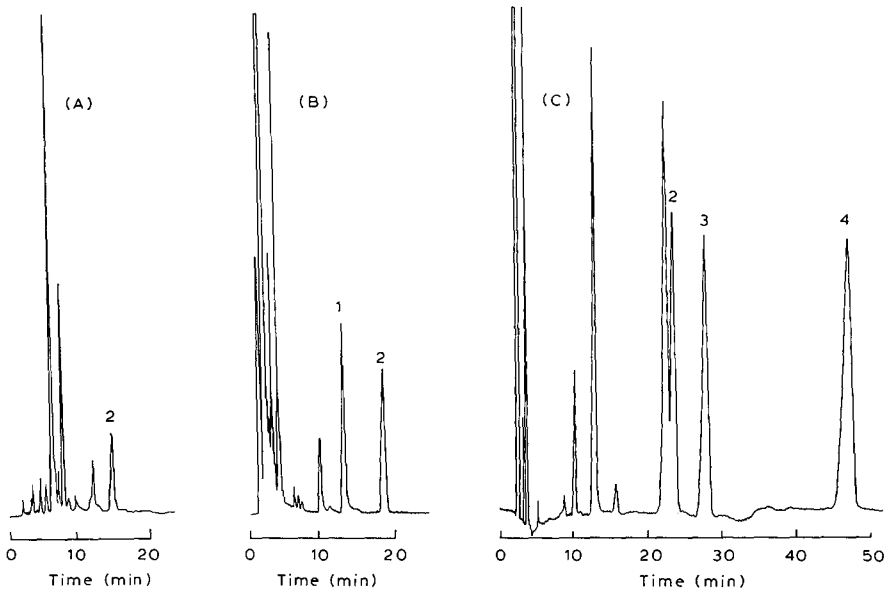

Fig. 2. Chromatograms of pigments and I.S. (A) 1 = Altersolanol A, 2 = benzoic acid; (B) 1 = macrosporin, 2 = naphthalene; (C) 1 = alterporriol B, 2 = alterporriol A, 3 = α-naphthol, 4 = alterporriol C.

obtained by using the same concentration as that of As-A, whereas for Ap-A, -B and -C the concentrations were reduced 10-fold. The limits of detection, based on a signal-to-noise ratio of 10, for Mac and As-A were 0.1 μg/ml and for Ap-A, -B and -C 1 μg/ml.

The concentrations of Mac, As-A and Ap-A, -B and -C were calculated from the detector responses (peak areas) by using the following linear equations for the calibration graphs obtained by using the method of least squares:

$$\text{Mac: } Y = (0.589X - 2.79 \cdot 10^{-2}) \cdot 0.1$$
$$\text{As-A: } Y = (1.232X - 6.70 \cdot 10^{-3}) \cdot 0.1$$
$$\text{Ap-A: } Y = (0.748X - 2.30 \cdot 10^{-3}) \cdot 0.01$$
$$\text{Ap-B: } Y = (0.647X - 1.26 \cdot 10^{-1}) \cdot 0.01$$
$$\text{Ap-C: } Y = (0.386X + 6.24 \cdot 10^{-3}) \cdot 0.01$$

where Y is the concentration of each pigment (mg/ml) and X is the ratio of peak area between each pigment and the internal standard (I.S.).

Extracts S-1 to S-8 were dissolved in methanol (10 ml) with the I.S. and then 10 μl of each were subjected to HPLC under the conditions given above. The results are shown in Table I and Fig. 3. Previously, we reported that As-A was not detected in the culture liquid of the onion decoction[2]. In this work, however, Aa-A was proved to be a metabolite by means of comparison of the retention time of the metabolite with that of an authentic sample.

As shown in Table I and Fig. 3, As-A and Mac were detected after fermentation for 1 day, whereas Ap-A, -B and -C were detected after 5 days. The content of As-A in

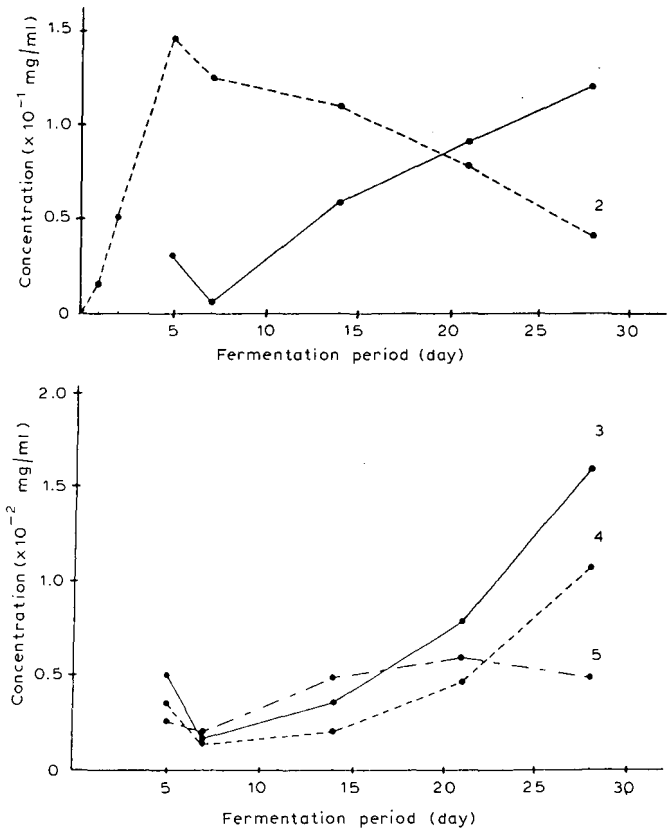

Fig. 3. Relationship between concentration of pigments and fermentation periods: 1 = macrosporin; 2 = altersolanol A; 3 = alterporriol A; 4 = alterporriol B; 5 = alterporriol C.

the culture liquid was found to increase continuously for 7 days and then gradually to decrease, whereas Mac and Ap-A, -B and -C were found to increase gradually for up to 28 days. Previously we reported[7] that in the early period of fermentation As-A is first formed, and then it is converted into As-B and dactylariol when *Alternaria porri* is cultured on Brian's medium T. The present results suggest that in the early period of fermentation As-A and Mac are first formed, and then these moieties are bonded to Ap-A, -B and -C when the fungus is cultured on onion decoction medium.

REFERENCES

1 R. Suemitsu, M. Nakajima and M. Hiura, *Agric. Biol. Chem.*, 25 (1961) 100.
2 R. Suemitsu and A. Nakamura, *Agric. Biol. Chem.*, 45 (1981) 2363.
3 R. Suemitsu, T. Yamamoto, T. Miyai and T. Ueshima, *Phytochemistry*, 26 (1987) 3221.
4 R. Suemitsu, T. Sano, M. Yamamoto, Y. Arimoto, F. Morimatsu and T. Nabeshima, *Agric. Biol. Chem.*, 48 (1984) 2611.
5 R. Suemitsu, T. Yamamoto, T. Ueshima and S. Yanagawase, *Phytochemistry*, 27 (1988) in press.
6 R. Suemitsu, Y. Yamada, T. Sano and K. Yamashita, *Agric. Biol. Chem.*, 48 (1984) 2383.
7 D. G. Davis and P. Hodge, *J. Chem. Soc., Perkin Trans. 1*, (1974) 2403.
8 A. Yagi, K. Makino and I. Nishioka, *Chem. Pharm. Bull.*, 26 (1978) 1111.
9 R. Suemitsu, Y. Yamada, T. Sano and M. Kitayama, *J. Chromatogr.*, 318 (1985) 139.

Journal of Chromatography, 454 (1988) 411–419
Elsevier Science Publishers B.V., Amsterdam — Printed in The Netherlands

CHROM. 20 804

Note

Application of ion chromatography to the analysis of chromium hydroxy salts

G. GRASSO*
Dipartimento di Ingegneria Chimica, Università di Napoli, Piazzale Tecchio, 80125 Naples (Italy)
and
G. BUFALO
Stazione Sperimentale per l'Industria delle Pelli e delle Materie Concianti, via Poggioreale 39, 80132 Naples (Italy)
(First received March 11th, 1988; revised manuscript received May 24th, 1988)

Basic (hydroxy) salts, *i.e.*, containing hydroxo groups, are widely used in industry, *e.g.*, in pigments, advanced ceramics, pharmaceuticals and tanning agents. Their exact composition, tested by quality control, is often desirable for property–structure correlations. This paper describes a general approach based on ion chromatography (IC) devoted to the complete analysis and indirect determination of the percentage basicity of similar commercial products (expressed as a percentage of equivalents of hydroxy groups present in combination with a coordinating metal). The conceptual approach is based on the overall mass balance of ionic species determined in this way in a compound or salt mixture.

This investigation relates to basic sulphatochromium salts and liquors, which are fundamental tanning media for the leather industry. Complications arising from Cr^{III} complexation by masking ligands used to regulate the tanning power, such as acetate or oxalate, make the direct injection of non-pretreated samples useless owing to the high stability of organochromium complexes. These limitations were overcome by adopting a ligand substitution technique involving 2,6-pyridinecarboxylic acid (PDCA) as powerful chelating[1–4] and releasing tridentate agent:

$$CrL_n + 2PDCA \rightleftharpoons Cr(PDCA)_2 + nL$$

Although this pretreatment was developed specifically for use with chromium complexes, it would appear to be of general relevance and to be applicable to the IC analysis of many other strongly complexed anions.

EXPERIMENTAL

Reagents and samples

All chemicals and reagents were of analytical-reagent grade. Deionized water was used throughout.

0021-9673/88/$03.50

Chromium salts masked with acetate, formate, oxalate and phthalate were prepared by mixing and boiling potassium disulphatochromate(III) [$KCr(SO_4)_2 \cdot 12H_2O$; chrome alum] with stoichiometric amounts of sodium salts of the organic acids. The molar ratios of chromium to complexing agents were 1:0.5 for monodentate and 1:0.25 for bidentate organic acids, the optimum masking effect being limited to 0.25–0.5 equiv. of the salts of the organic acid per chromium atom[5]. A mixed salt containing sodium chloride in a 1:0.5 molar ratio was also prepared in order to simulate recycled tanning liquors.

Apparatus and chromatographic conditions

A Dionex 2000i ion chromatograph equipped with a conductivity detector was used. The IC system was linked to a Shimadzu Chromatopac C-R3A digital integrator. The sample loop size was 50 μl.

The conditions for IC anion analyses were as follows: HPIC-AS4A analytical column with an HPIC-AG4A guard column and AFS-1 anion fibre suppressor (Dionex); eluent, 16 m*M* sodium hydrogen carbonate–18 m*M* sodium carbonate for general purposes and 6 m*M* sodium tetraborate for acetate and formate; flow-rate, 1.6 ml/min; suppressor regenerant, 0.0125 *M* sulphuric acid. The conditions for IC analyses of alkali metals (sodium and potassium) were as follows: HPIC-CS3 analytical column with an HPIC-CG3 guard column and a CMMS micromembrane suppressor (Dionex); eluent, 25 m*M* hydrochloric acid–0.25 m*M* 2,3-diaminopropionic acid; flow-rate, 1.0 ml/min; regenerant of CMMS, 0.1 *M* tetrabutylammonium hydroxide.

The ionic species investigated were identified and quantitated by comparison with mixtures of standards and by means of calibration graphs. Chromatograms obtained from typical standard mixtures of anions are presented in Fig. 1, showing the efficient separation of the six anions considered. The retention times of sodium and potassium under the above conditions were 3.1 and 4.8 min, respectively, for concentrations of 2–10 mg/l (selectivity, $\alpha = 2.03$), thus allowing a clear separation of the two very narrow peaks.

Analytical procedure

The analysis of chromium salts was carried out by dissolving 10 g of the solid in water to give 100 ml of solution (boiling for 20 min to mask) and diluting the resulting solutions to volume in water to obtain 0.15% solutions. Aliquots of 3 ml of these solutions were diluted to 50 ml and chromatographed (50-μl injections). The masked salts were pretreated by adding 30–35 ml of 0.4% PDCA solution to 3-ml aliquots and boiling under reflux for 1 h before the final dilution to 50 ml (*ca.* 0.25% PDCA, final solution concentration). Between successive injections it was essential to wait 20 min for complete elution of PDCA from the HPIC-AS4A anionic column.

Chromium when strongly complexed is not quantitatively recovered and detected by the usual IC procedures, and therefore it was determined by titrimetry. Aliquots (5 ml) of the 0.15% chromium salt solutions were first oxidized with hydrogen peroxide, then the iodine released from excess of potassium iodide was titrated with 0.05 *M* sodium thiosulphate standard solution. The well known high accuracy and precision of the iodimetric method (see the standard deviations in Table I) was also required in order to minimize errors in calculating the molar ratios to chromium of the analytes involved in the basicity studies.

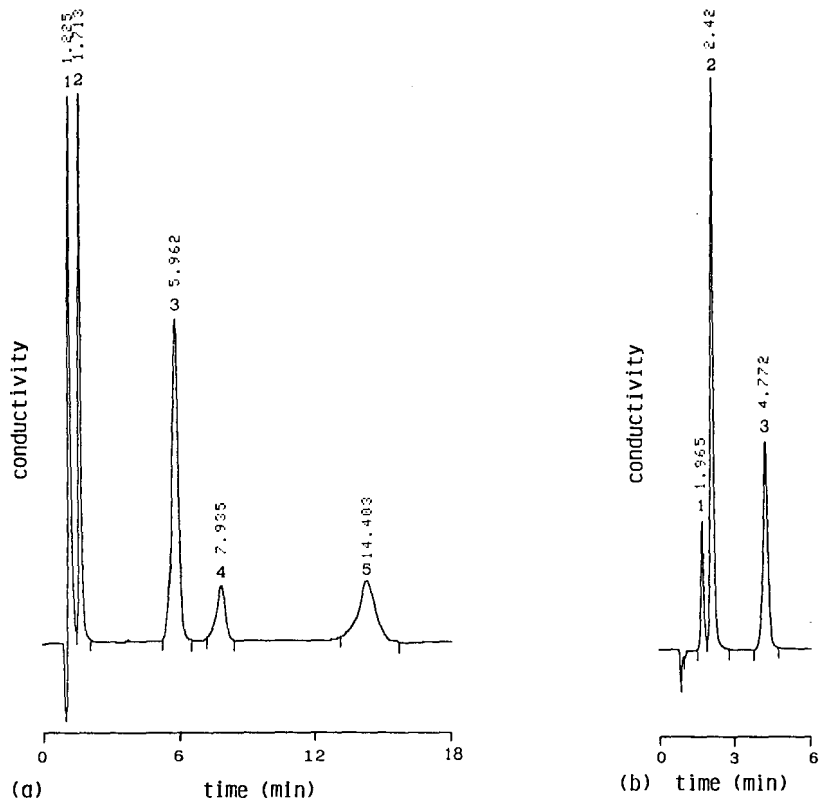

Fig. 1. Chromatograms of standard mixtures of anions. (a) Eluent, 16 m*M* $NaHCO_3$–18 m*M* Na_2CO_3. Peaks: 1 = acetate (8.0 mg/l); 2 = chloride (2.5 mg/l); 3 = sulphate (6.0 mg/l); 4 = oxalate (2.3 mg/l); 5 = phthalate (20.0 mg/l). (b) Eluent 6 m*M* $Na_2B_4O_7$. Peaks: 1 = acetate (6.0 mg/l); 2 = formate (8.5 mg/l); 3 = chloride (3.0 mg/l).

Basicity calculation

The basicity of chromium salts was obtained from their percentage compositions determined by IC, *i.e.*, starting from the simplest (empirical) formulae written in terms of molar ratios n_i' and m_j' to chromium of the overall cations M_i and anions L_j present in the samples:

$$\sum_i (M_i)_{n_i'} Cr(OH)_x \sum_j (L_j)_{m_j'}$$

The percentage basicity (%*B*) related to chromium was therefore calculated from the overall mass balance of ionic species and their valencies (oxidation numbers) v_i and v_j:

$$\%B = (x/3) \cdot 100 = \left(\sum_i n_i' v_i + 3 - \sum_j m_j' v_j \right) \cdot 100/3 \qquad (1)$$

TABLE I

CONCENTRATIONS OF THE IONIC SPECIES CONSTITUTING THE SYNTHETIC CHROMIUM SALTS INVESTIGATED AND PRECISION OF THE IC MEASUREMENTS

Precision expressed as relative standard deviation (R.S.D., %) of the mean value $\bar{x}$ or coefficient of variation (C.V., %): RSD = C.V. = (S.D./$\bar{x}$) · 100. Results based on three determinations for each sample.

Parameter	*Constituent*								
	Na^+	K^+	Cr^{3+}	$HCOO^-$	CH_3COO^-	Cl^-	SO_4^{2-}	$C_2O_4^{2-}$	*Phthalate*
Concentration (g per 100 g)	1.0–2.1	7.1–7.4	9.5–9.8	4.2	5.4	3.3	35.4–36.3	4.1	7.6
R.S.D. (%)	2.1	1.9	1.0*	1.4	1.7	1.5	1.6	1.7	2.3

* Titrimetric (iodimetric).

The influence of the experimental errors of the individual determinations on the precision of the final result, *i.e.*, the absolute uncertainty in the calculated value of $\%B$, was calculated using propagation errors theory[6]. The standard deviations (S.D.) of the molar ratios in eqn. 1 were calculated from the S.D. of the molar composition of each ionic species and of the chromium.

RESULTS AND DISCUSSION

Table I gives typical analytes that constitute basic chromium salts or liquors, their concentrations in the investigated synthetic samples and the precision of the IC measurements (chromium was determined by oxidimetry).

Sodium, potassium, formate, acetate and chlorine were quantitatively evaluated using the heights of their narrow peaks and sulphate, oxalate and phthalate using the areas of their broader peaks. The average precision of the PDCA pretreatment and of the chromatographic procedure as indicated by the reported relative standard deviations (R.S.D.), was found to be *ca.* 2%, ranging from 1.4% (formate) to 2.3% (phthalate). The reproducibility obtained seems satisfactory and might be due to the high quality of the pump delivery system.

The recovery of the masking ligands released by the PDCA pretreatment was also found to be almost complete (Table II). The relative errors of the compositions found ranged from 1.5% for formate to 2.4% for oxalate, showing the good accuracy of the PDCA pretreatment. The results obtained therefore demonstrate the reliability of the IC method and of the proposed sample pretreatment in the analysis of ionic species in basic sulphatochromium compounds.

The amounts of PDCA and the pretreatment (boiling) time were previously assessed by performing recovery studies based on stressed limiting conditions, *i.e.*, using as a reference masked salt the very stable chromium(III)–oxalate 1:2 complex (with the strongest chelating effect of the masking ligands considered). The high molar ratio of complexation in the standard complex (1:2) exceeded 10-fold the common values of commercial oxalate-masked salts (1:0.25), thus ensuring the effectiveness of the pretreatment parameters optimized with respect to routine analyses with wide confidence margins.

Fig. 2 shows the results of the investigation to establish the optimum complexation conditions of the Cr^{III} reference salt with PDCA which accounts for both the amount (0.25%, final solution concentration) and the time (1 h) recommended for

TABLE II

ACCURACY OF THE PDCA PRETREATMENT FOR THE SYNTHETIC CHROMIUM SALTS INVESTIGATED

Masking ligand	*Expected (g per 100 g)*	*Found ± S.D. (g per 100 g)*	*Recovery (%)*	*Relative error (%)*
$HCOO^-$	4.15	4.09 ± 0.06	98.5	1.5
CH_3COO^-	5.46	5.36 ± 0.09	98.0	2.0
$C_2O_4^{2-}$	4.13	4.03 ± 0.07	97.6	2.4
Phthalate	7.56	7.40 ± 0.17	97.9	2.1

TABLE III

COMPOSITION AND PERCENTAGE BASICITY CALCULATIONS WITH PRECISION AND ACCURACY

Sample	*Constituents*	*Molar ratio*	*Expected*		*Found**			*%B (% basicity units)*			
			g per 100 g	*mol/kg*	*g per 100 g*	*mol/kg*	*S.D. (mol/kg)***	*Expected*	*Found*	*S.D.****	*Absolute error*
Chrome alum	K^+	1	7.83	2.002	8.0	2.05	0.04				
	Cr^{3+}	1	10.41	2.002	10.4	2.00	0.02				
	SO_4^{2-}	2	38.48	4.004	39.0	4.06	0.06				
	$KCr(SO_4)_2 \cdot 12H_2O$							0.0	−1.2	2.2	1.2
33% basic sulphate	Na^+	1	7.86	3.421	7.4	3.21	0.07				
	K^+	—	—	—	0.66	0.17	0.004				
	Cr^{3+}	1	17.79	3.421	17.5	3.36	0.04				
	SO_4^{2-}	1.5	49.29	5.131	48.6	5.06	0.08				
	$(Na,K)CrOH(SO_4)_{3/2}$							33.3	32.7	2.1	0.6
Masked 33% basic sulphate	Na^+	1.5	10.58	4.602	10.3	4.48	0.08				
	K^+	—	—	—	0.61	0.15	0.003				
	Cr^{3+}	1	15.96	3.069	16.2	3.12	0.03				
	SO_4^{2-}	1.5	44.22	4.602	44.8	4.66	0.07				
	$C_2O_4^{2-}$	0.25	6.76	0.767	6.6	0.75	0.01				
	$(Na,K)CrOH(SO_4)_{3/2} \cdot \frac{1}{4}Na_2C_2O_4$							33.3	34.3	2.3	1.0

* Results based on three determinations for each sample.

** S.D. of the molar ratio of the species i (or j) was calculated from these values by means of the equation $s_i' = (n_i/n_{Cr})[(s_i/n_i)^2 + (s_{Cr}/n_{Cr})^2]^{1/2}$, where s_i' = S.D. of the molar composition n_i of the species i (or j) and s_{Cr} = S.D. of the molar composition n_{Cr} of the chromium.

*** S.D. of $\%B = s_B = \left[\sum_i (s_i')^2 + \sum_j (s_j')^2\right]^{1/2} \cdot 100/3$, where s_i' and s_j' are the S.D.s of the molar ratios of species i and j.

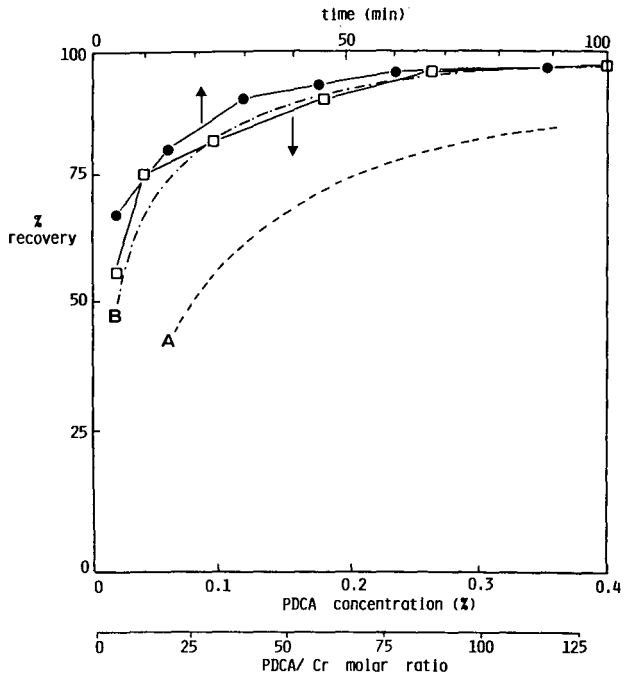

Fig. 2. Effect of the amount of PDCA and pretreatment (boiling) time on the recovery of oxalate from the Cr–oxalate 1:2 complex. Lower scale, boiling time fixed at 1 h; upper scale, amount of PDCA fixed at 0.25% (final solution concentration). A and B are recoveries provided by eqn. 3 with different hypothesis, B taking into account the influence of pH.

completing the masking ligand substitution with PDCA. Under the reaction conditions used (boiling for 1 h), the oxalate recovery was about 50% for PDCA:Cr molar ratios of the same order of magnitude as the stoichiometric ratio required for chelation (2:1), approaching a limiting value of 97.5% when the molar ratios were increased to 50–60 times the initial values. Hence from a practical point of view a large excess of PDCA is necessary to complete the substitution of the oxalate chelating ligand as rapidly as possible.

Completeness of the ligand substitution reactions is regulated by both thermodynamic (*i.e.*, ratios of the respctive conditional formation constants) and kinetic factors, the ligand exchange kinetics of Cr^{III} being very slow. The effect of the kinetic factors is illustrated in the top experimental graph in Fig. 2, showing that equilibrium conditions are reached after boiling for *ca.* 1 h.

Thermodynamic factors require much more discussion. In this respect it is useful to compare the experimental recovery curve (at constant time) shown in the Fig. 2 with the theoretical plots obtained by equilibrium calculations. When two ligands are present, which complex is formed depends on the ratio of the overall equilibrium constats and the ratio of the ligand concentrations. For the system Cr–oxalate–PDCA the equilibrium constant K of the reaction

$$Cr(Ox)_2^- + 2PDCA^{2-} \rightleftharpoons Cr(PDCA)_2^- + 2Ox^{2-} \quad (2)$$

is $K = {}_{PDCA}\beta_2/{}_{Ox}\beta_2 = 4.36 \cdot 10^7/3.23 \cdot 10^{10} = 1.35 \cdot 10^{-3}$, ${}_{Ox}\beta_2$ and ${}_{PDCA}\beta_2$ being the overall formation constants of the oxalate[7] and the PDCA[1] 1:2 complexes, respectively (${}_{Ox}\beta_2 = {}_{Ox}K_1 \cdot {}_{Ox}K_2 = 2.18 \cdot 10^5 \cdot 1.48 \cdot 10^5$). Thus the [$PDCA^{2-}$] equilibrium concentration will be

$$[PDCA^{2-}] = \left[\frac{c\alpha(c2\alpha)^2}{Kc(1-\alpha)}\right]^{1/2} \tag{3}$$

$$= c' - c2\alpha \approx c'$$

where c is the initial molar concentration of chromium, c' is the total concentration of $PDCA^{2-}$ (free and combined) and α is the recovery. Substituting in eqn. 3 the experimental value of c ($1.8 \cdot 10^{-4}$ mol/l), one can obtain the plot of α% *versus* [$PDCA^{2-}$] or PDCA% (dashed line in Fig. 2). The theoretical results so obtained appear to be inconsistent with the experimental results (bottom experimental graph in Fig. 2). A much better theoretical model can be obtained by taking in account that the oxalate ligand is derived from a weak acid, *i.e.*, the species Ox^{2-} is subtracted from the complexation equilibrium by the hydrolysis reaction. Therefore, making use of the dissociation constants of oxalic acid ($pK_{a_1} = 1.25$, $pK_{a_2} = 4.28$) we obtain the following generalized form of the ${}_{Ox}K_1'$ conditional formation constant, showing pH dependence[8]: ${}_{Ox}K_1' = {}_{Ox}K_1/(1 + [H^+]K_{a_2} + [H^+]^2K_{a_1} \cdot K_{a_2})$.

Our recovery experiments were carried out at pH 3.5 in order to give a maximum yield of the $Cr(PDCA)_2^-$ complex[1]. At pH 3.5, ${}_{Ox}K_1' = 3.09 \cdot 10^4$. From this value one can calculate the value of the effective or conditional constant of eqn. 2 at the considered pH: $K' = {}_{PDCA}\beta_2/{}_{Ox}\beta_2' = {}_{PDCA}\beta_2/{}_{Ox}K_1' \cdot {}_{Ox}K_2 = 9.54 \cdot 10^{-3}$. Substitution of this K' value in eqn. 3 allows a new plot of α% *versus* [$PDCA^-$] and also PDCA% to be drawn (dotted and dashed line in Fig. 2), which agrees very satisfactorily with the experimental trend. The high yields of the oxalate recovery shown in Fig. 2 account for the good recoveries of the other masking ligands (Table II) whose formation constants are 100 times lower (the pK_1 values of the first formation constants of the Cr–formate and the Cr–acetate complexes are *ca.* 3).

From the R.S.D. values in Table I it would possible to calculate the S.D.s of the molar ratios of the analytes that constitute typical basic salt formulations of approximately known composition. Therefore, this would allow to the precision to be obtained when calculating their basicity from eqn. 1. At compositions of the same order of magnitude as those shown in Table I, a precision of *ca.* 2% basicity units was obtained for oxy salts composed of three or four ionic species (Na^+ or K^+, Cr^{3+}, SO_4^{2-} and masking anion).

Table III summarizes the experimental data for chrome alum, 33% basic sodium sulphate (commercial grade, 26% Cr_2O_3) and the same 33% basic salt masked with sodium oxalate with a $Cr:C_2O_4^{2-}$ molar ratio of 1:0.25. The S.D. values of the percentage basicity range from 2.1 to 2.3 percentage basicity units and the absolute errors range from 0.6 to 1.2 percentage basicity units. In the samples examined basicity can therefore be determined with satisfactory precision and accuracy for composition quality control. In contrast, the classical alkalimetric methods give large errors in the presence of masking agents.

ACKNOWLEDGEMENT

We are grateful to the Director of the Stazione Sperimentale for permission to publish this work.

REFERENCES

1 E. Chiacchierini, G. D'Ascenzo, G. De Angelis, A. Magri and V. Petrone, *Ann. Chim. (Rome)*, 67 (1977) 195.
2 D. R. Marks, *Ph.D. Thesis*, Memphis State University, Memphis, TN, 1977.
3 K. Wieghardt, U. Quilitzsch and J. Weiss, *Inorg. Chim. Acta*, 89 (1984) 43.
4 *Application Note No.* 26, Dionex, Sunnyvale, CA, 1986.
5 K. H. Gustavson, *The Chemistry of Tanning Processes*, Academic Press, New York, 1956, p. 78.
6 I. M. Kolthoff, E. B. Sandell, E. J. Meehan and S. Bruckenstein, *Quantitative Chemical Analysis*, Macmillan, London, 1969, pp. 398–399.
7 L. G. Sillén and A. E. Martell, *Stability Constants of Metal–Ion Complexes*, Chemical Society, London, 1964.
8 I. M. Kolthoff, E. B. Sandell, E. J. Meehan and S. Bruckenstein, *Quantitative Chemical Analysis*, Macmillan, London, 1969, p. 120.

Journal of Chromatography, 454 (1988) 420–424
Elsevier Science Publishers B.V., Amsterdam — Printed in The Netherlands

CHROM. 20 821

Note

Silicic acid column chromatography of phosphonolipids

X. Some phosphono analogues of 1-O-alkylethylene glycol

MICHAEL C. MOSCHIDIS
SANCORIN LABS, 3 Spetson Street, Dafni 17237, Athens (Greece)
(Received July 15th, 1988)

The silicic acid column chromatographic properties of the 1-O-alkylethylene glycol phosphono analogues of lecithin and cephalin have been examined[1]. The synthesis of 1-O-alkylethylene glycol phosphonic acid analogues of lecithin and cephalin was subsequently reported[2]. In this note the silicic acid column chromatographic properties of the latter phosphonolipids are examined and comparisons drawn with those of other phosphonolipids and phospholipids.

In particular, the column chromatographic behaviour has been studied, in two separate experiments, of (a) 1-O-dodecylethylene glycol-2-(2-trimethylammonioethyl)-phosphonate and 1-O-dodecylethylene glycol-2-(2-aminoethyl)phosphonate in the presence of their phosphoryl analogues and (b) the above two phosphonolipids in the presence of cardiolipin, cephalin and the phosphono analogues of cephalin and lecithin. Collected fractions were analysed by thin-layer chromatography (TLC) and IR spectroscopy to confirm species identification.

EXPERIMENTAL

Instrumentation

IR spectra were recorded on a Perkin-Elmer 197 double-beam IR spectrophotometer. A glass column (35 cm × 1.6 cm I.D.) was employed for the separations.

Reagents

Solvents for column chromatography and TLC were of analytical reagent grade (Merck, Darmstadt, F.R.G.) and were distilled before use. TLC was conducted on 20 cm × 20 cm chromatographic plates with a 0.25-mm layer of silica gel G or 60 F_{254} (Merck).

Standards

All phosphonolipids employed in these experiments were synthetic compounds. Cardiolipin and cephalin were obtained from Koch-Light (Colnbrook, U.K.), ethylene glycol monododecyl ether from Lancaster Synthesis (U.K.) and silicic acid for column chromatography from Sigma Chemical (St. Louis, MO, U.S.A.).

0021-9673/88/$03.50

TABLE I

ELUTION OF THE CHROMATOGRAPHIC COLUMN

Column: 35 × 1.6 cm I.D. loaded with 11.0 g of silicic acid to a height of 10.0 cm and a total volume of 26 ml. Flow-rate: 1.0–1.6 ml/min. Fractions of *ca.* 5.0 ml were collected.

Methanol–chloroform	*No. of column volumes*	*Total volume of solvent (ml)*	*Fractions collected*
0:100	2	50	1–9
1:99	2	50	10–19
5:95	3	75	20–36
10:90	3	75	37–53
20:80	5	130	54–81
40:60	9	225	82–127

Procedure

The procedure was similar to that described earlier[3]. Column elution was effected with methanol–chloroform mixtures as indicated in Tables I and II. IR spectra of the various pilot fractions were recorded as chloroform solutions or KBr discs.

TLC was performed on silica gel G or 60 F_{254} plates (Merck). The chromatograms were developed in two chambers of dimensions 20.5 × 8 cm (Desaga) and each analysis usually took 45 min. The plates were developed in chloroform–methanol–water (65:25:4) (system A) and methanol–water (2:1) (system B). Visualization was effected with molybdenum blue, iodine vapour, UV irradiation and the Stillway-Harmon procedure[4]. Standards were also spotted on the plates to aid in the detection of the developed spots.

RESULTS AND DISCUSSION

As mentioned above, column elution was effected with methanol–chloroform mixtures and the fractionation pattern of the lipids is depicted in Figs. 1 and 2.

Fractions were identified by TLC abd IR spectroscopy as indicated in Tables III and IV. With the solvents used, (a) 100% and (b) 99.9% of the lipids applied to the column could be recovered.

From the experimental data, 1-O-alkylethylene glycol-2-(2-aminoethyl)phosphonate is eluted with methanol–chloroform (20:80) and towards the end of the

TABLE II

CHROMATOGRAPHIC CONDITIONS

The column (35 cm × 1.6 cm I.D.) was packed with 12.0 g of silicic acid to a height of 10.5 cm and a total volume of 27 ml. Flow-rate: 1.0–1.5 ml/min. Fractions of *ca.* 5.0 ml were collected.

Methanol–chloroform	*No. of column volumes*	*Total volume of solvent (ml)*	*Fractions collected*
5:95	3	75	1–18
20:80	5	140	19–48
40:60	9	225	49–95

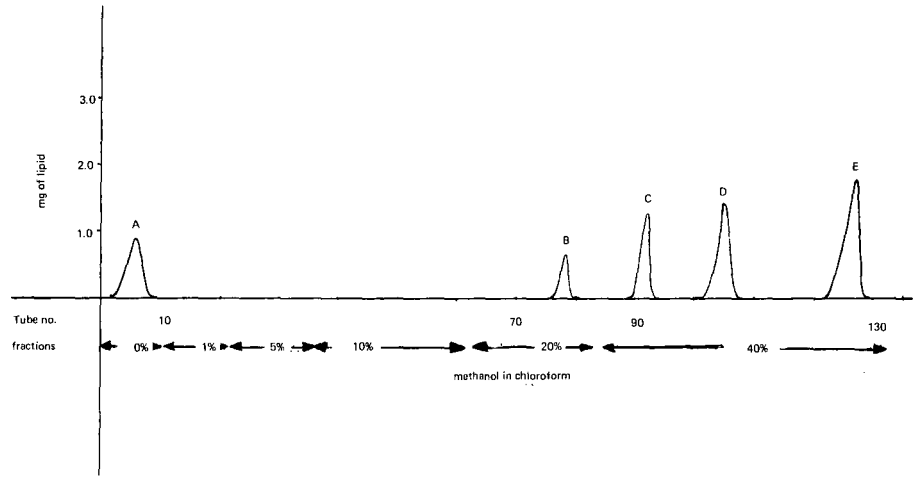

Fig. 1. Chromatography of ethylene glycol phosphono- and phospholipids on a column of silicic acid with methanol–chloroform as the eluent. Composition of the lipids: A = 1-O-dodecylethylene glycol, 2.8 mg; B = 1-O-alkylethylene glycol-2-(2-aminoethyl)phosphonate, 1.7 mg; C = 1-O-alkylethylene glycol-2-phosphorylethanolamine, 3.2 mg; D = 1-O-alkylethylene glycol-2-(2-trimethylammonioethyl)phosphonate, 3.8 mg; E = 1-O-alkylethylene glycol-2-phosphorylcholine, 5.3 mg. The lipids were applied to the column in 3.0 ml of chloroform.

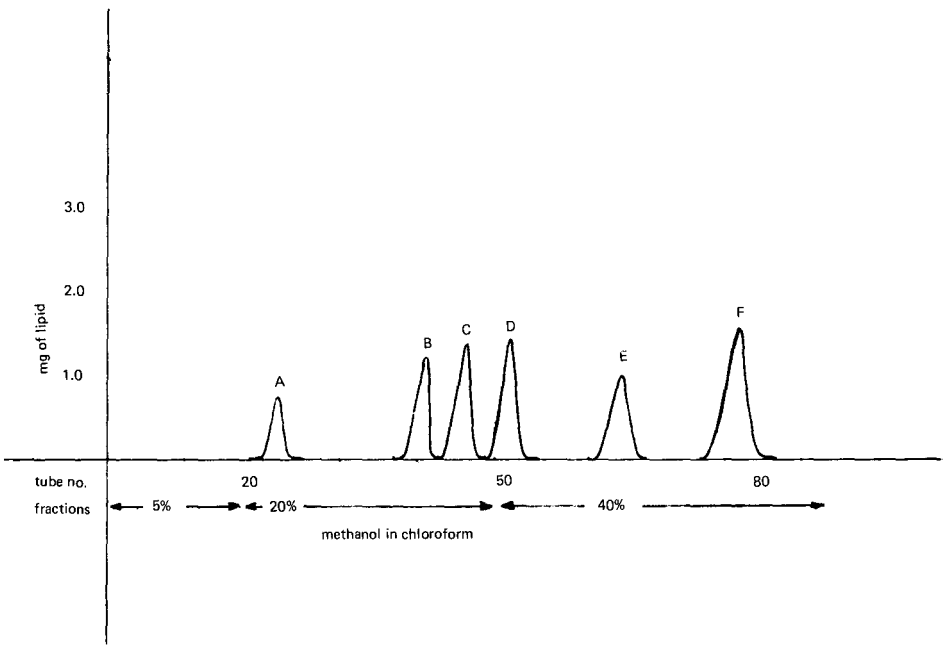

Fig. 2. Chromatography of phosphono- and phospholipids on a column of silicic acid with methanol–chloroform as the eluent. Composition of the lipids: A = cardiolipin, 2.3 mg; B = 1-O-alkylethylene glycol-2-(2-aminoethyl)phosphonate, 2.8 mg; C = phosphono analogue of cephalin, 3.4 mg; D = cephalin, 4.6 mg; E = 1-O-alkylethylene glycol-2-(2-trimethylammonioethyl)phosphonate, 3.2 mg; F = phosphono analogue of lecithin, 5.1 mg. The lipids were applied to the column in 4.0 ml of chloroform.

TABLE III

COMPOSITION OF FRACTIONS OBTAINED BY CHROMATOGRAPHY OF LIPIDS ON SILICIC ACID

A 16.8-mg amount of lipids was applied to the column. The total recovery was 100%.

Solvent	*Fractions collected*	*TLC R_F value*		*Component identified by IR spectra*
		System A	*System B*	
Chloroform	4–9	0.94	0.85	1-O-Alkylethylene glycol
Methanol–chloroform (20:80)	77–80	0.75	0.92	1-O-Alkylethylene glycol-2-(2-aminoethyl)phosphonate
	90–93	0.73	0.00	1-O-Alkylethylene glycol-2-phosphorylethanolamine
Methanol–chloroform (40:60)	102–107	0.44	0.86	1-O-Alkylethyleneglycol-2-(2-trimethylammonioethyl)phosphonate
	123–129	0.42	0.00	1-O-Alkylethylene glycol-2-phosphorylcholine

elution process, whilst the corresponding lecithin phosphono analogue is eluted in the initial stages of the elution with methanol–chloroform (40:60). From the results of the second experiment, there is good separation of the 1-O-alkylethylene glycol phosphonolipids from the corresponding glycero phosphonolipids which are eluted in their respective fractions following the ethylene glycol phosphonolipids.

When compared, however, with the 1-O-acylethylene glycol phosphonolipids, considerable overlapping is noted in some instances, as , *e.g.*, for the 1-O-alkylethyleneglycol phosphono analogue of cephalin with the 1-O-acylethyl glycol analogue of cephalin: for the 1-O-acylethylene glycol phosphono analogue of lecithin with the 1-O-alkylethylene glycol phosphono analogue of cephalin and finally for the 1-O-alkylethylene glycol phosphono analogue of lecithin with the phosphono analogue of lecithin proper.

TABLE IV

COMPOSITION OF FRACTIONS OBTAINED BY CHROMATOGRAPHY OF LIPIDS ON SILICIC ACID

A 21.4-mg amount of lipids was applied to the column. The total recovery was 99.9%.

Solvent: methanol–chloroform	*Fractions collected*	*TLC R_F value*		*Component identified by IR spectra*
		System A	*System B*	
5:95	–	–	–	–
20:80	21–23	0.68	0.00	Cardiolipin
	38–42	0.75	0.92	1-O-Alkylethylene glycol-2-(2-aminoethyl)phosphonate
	45–47	0.72		
	45–47	0.72	0.89	Phisphono analogue of cephalin
40:60	49–52	0.73	0.00	Cephalin
	66–69	0.44	0.86	1-O-Alkylethylene glycol-2-(2-trimethylammonioethyl)phosphonate
	78–84	0.43	0.82	Phosphono analogue of lecithin

Problems will be experienced when attempting to differentiate these phosphonolipids from a multi-component system, which can be resolved only by conducting additional research along these lines.

REFERENCES

1 M. C. Moschidis, *J. Chromatogr.*, 351 (1986) 376.
2 M. C. Moschidis, *Chem. Phys. Lipids*, 43 (1987) 39.
3 M. C. Moschidis, *J. Chromatogr.*, 270 (1983) 344.
4 L. W. Stillway and S. J. Harmon, *J. Lipid Res.*, 21 (1980) 1141.

Journal of Chromatography, 454 (1988) 425–431
Elsevier Science Publishers B.V., Amsterdam — Printed in The Netherlands

CHROM. 20 846

Note

Two-dimensional thin-layer chromatographic separation of phospholipid molecular species using plates with both reversed-phase and argentation zones

DONALD A. KENNERLY

Department of Internal Medicine, University of Texas Health Science Center at Dallas, 5323 Harry Hines Boulevard, Dallas, TX 75235 (U.S.A.)

(First received April 13th, 1988; revised manuscript received July 27th, 1988)

Reversed-phase high-performance liquid chromatography (HPLC) has been used by a variety of investigators seeking to separate molecular species of glycerol-based lipids. This approach achieves fairly good separation of intact phospholipids[1,2], derivatives of 1,2-diglycerides[3–5] or derivatives of phosphatidic acid (PA)[6]. Several aspects of this technique limit application to studies of cellular lipid metabolism: (1) chromatographing each sample separately is time consuming since each sample requires 40–120 min, (2) HPLC equipment and solvents are costly and (3) adjacent peaks, incompletely resolved by HPLC, are often metabolically unrelated since very different fatty acids may have similar hydrophobicities[1–6].

Separating related subclasses of molecular species of diacyl forms of phospholipids using argentation thin-layer chromatography (TLC) of a derivative of PA was recently reported by this laboratory[7]. This technique permitted good separation of nine bands consisting of subclasses of molecular species based on the number and distribution of double bonds present in the esterified fatty acids. The compounds grouped within a single chromatographic subclass tended to have similar structures (16:0/20:4, 18:0/20:4 and 20:0/20:4 for example). Although this technique has proven valuable in assessing the validity of existing concepts of the origin of 1,2-diacylglycerol (DAG)[8], more complete resolution of molecular species would be highly desirable, particularly if the attractive characteristics of a TLC-based separation (ease of analysis of multiple samples and modest cost) could be retained.

The current studies describe a two-dimensional TLC analysis employing both argentation and reversed-phase chromatography on a single plate consisting of two distinct and differentially modified zones. Combining argentation and reversed-phase chromatography on a single TLC plate was initially described by Bergelson *et al.*[9] who used this technique for the separation of fatty acids with a variety of unusual isomeric forms. These studies did not use a bonded reversed-phase adsorbant, but rather impregnated the plates with dodecane, applied the sample, performed the reversed-phase separation, introduced silver nitrate into the plate and after drying it, then performed the argentation-based separation. Because argentation chromatography depends primarily on the degree of unsaturation of fatty acids, the application of both reversed-phase and argentation TLC on a single plate resulted in good resolu-

0021-9673/88/$03.50

tion of a sample containing a variety of fatty acid methyl esters. Unfortunately, our attempts to adapt this technique to the more challenging separation of molecular species of derivatives of DAG resulted in inadequate separation (data not shown). Additionally, the use of dodecane impregnation (as opposed to a bonded reversed-phase adsorbant) imposed serious limitations on the application of this approach because plates could not be fully prepared prior to TLC since the solvents for argentation TLC displace the impregnated dodecane while those for reversed-phase TLC similarly displace impregnated silver nitrate. Thus, so long as neither modification involved covalent coupling, impregnation with the second was necessary after development in the first dimension. As described subsequently, this limitation was overcome by designing a two-dimensional TLC plate that can be used "as is" for both argentation and reversed-phase TLC without further modification during the chromatographic development.

EXPERIMENTAL

Materials and their sources: unlabeled phospholipids (Serdary, Port Huron, MI, U.S.A.); *Clostridium welchii* phospholipase C (Sigma, St. Louis, MO, U.S.A.); authentic 1,2-diacylglycerols (Nuchek Prep, Elysian, MN, U.S.A.); [γ-^{32}P]ATP (ICN, Irvine, CA, U.S.A.); octadecyltrichlorosilane and silver nitrate (Aldrich, Milwaukee, WI, U.S.A.); XAR film for autoradiography (Kodak, Rochester, NY, U.S.A.); plastic backed silica gel TLC plates (Polygram Sil G 20 × 20 cm; Brinkmann, Westbury, NY, U.S.A.); organic solvents (Burdick & Jackson, Muskegon, MI, U.S.A.); all other chemicals (Sigma, St. Louis, MO, U.S.A.).

Phospholipids were converted to DAG using *Cl. Welchii* phospholipase C as described previously[10]. Authentic or phospholipid-derived DAG was labeled by radioactive phosphorylation using [γ-^{32}P]ATP and *Escherichia coli* DAG kinase as described in detail previously[7,8,11]. The resultant labeled phosphatidic acid ([^{32}P]PA) was converted to a more hydrophobic derivative (dimethyl-PA or DMPA) by methylation of its phosphoric acid hydroxyl groups using diazomethane and the DMPA purified by TLC[7,8].

TLC plates containing both argentation and reversed-phase zones were formed by derivatization of part of the silica gel plate with octadecylsilane (ODS) and impregnating the remainder with silver nitrate. Commercially prepared plates containing a 17-cm reversed-phase zone with a 3-cm band of silica gel can be purchased (KC18-F; Whatman, Clifton, NJ, U.S.A.) but despite considerable effort, separations on the reversed-phase portion of the commercially prepared plate were never adequate. The smearing and resultant poor resolution may in part have been due to insufficient reversed-phase derivatization of the silica gel (*vide infra*).

Fig. 1 illustrates our approach to derivatizing silica gel plates and the two-dimensional TLC employed in the subsequent studies. Silica gel plates were washed by development in chloroform–methanol (1:1) to 1 cm from the top, dried and heated to 110°C for 1 h. In a significant modification of a previous method[12], a portion of the silica gel plate was converted to a covalently linked ODS reversed-phase adsorbant by dipping the plate (with the solvent front of the chloroform–methanol wash on the left) into a dipping tank containing 5% (v/v) octadecyltrichlorosilane in dry toluene to a line 16 cm from the bottom. The plate was placed in a tank with a saturated

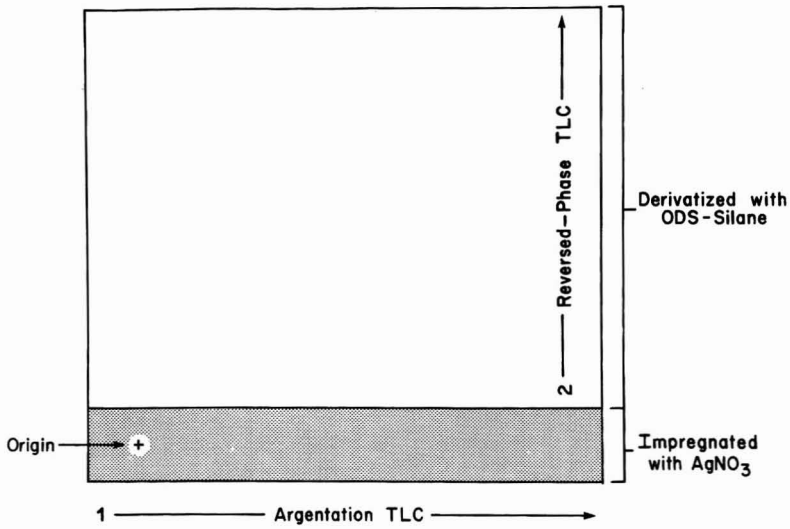

Fig. 1. Sequential use of both argentation and reversed-phase chromatography on a single TLC plate. The hatched area in this schematic representation represents the 4-cm portion of the plate impregnated with silver nitrate while the remainder is the portion covalently derivatized with ODS for reversed-phase chromatography as described in detail in the next. After activation, a sample was spotted at the origin. Sequential developments in the argentation TLC (arrow number 1) were accomplished using chloroform–methanol mixtures (95:5 to 5 cm above the origin followed by 98.75:1.25 to the top). After drying and turning the plate 90°, all compounds were chromatographed to the junction with the reversed-phase portion of the plate by developing in acetonitrile to 6 cm from the bottom. Reversed-phase TLC was then accomplished by developing twice using acetonitrile–tetrahydrofuran (4:1) (arrow number 2).

toluene atmosphere and after 5–10 min it was redipped in the octadecyltrichlorosilane solution, removed and allowed to react for 5–10 min more. The plates obtained by dipping only once did not produce sufficient reversed-phase separations due to band broadening (data not shown) probably as the result of inadequate reversed-phase derivatization. The plate was washed by successively dipping it into dry toluene and light petroleum (b.p. 35–60°C) and the remaining chlorosilane groups converted to methyl ethers by dipping the plate into dry methanol. After drying, the remaining 4 cm of underivatized silica gel was impregnated by dipping the plate (now with the solvent front from the chloroform–methanol wash on the right) into an aqueous solution of 5% (w/v) silver nitrate and activated as described in detail previously[7]. In experiments in which separated lipids were eluted and their fatty acid methyl esters examined by gas chromatography (GC), the derivatized plates were washed by sequential development with chloroform and diethyl ether.

Using these new plates, molecular species of [^{32}P]DMPA derivatives of DAG were separated by the sequential use of argentation TLC and reversed-phase TLC. As illustrated in Fig. 1, the lipid sample was applied in a spot 1.5 cm from each edge within the strip of the plate impregnated with silver nitrate and developed first with chloroform–methanol (95:5) to 5 cm above the origin and after brief drying, developed again in the same direction with chloroform–methanol (98.75:1.25) to the top of the plate. After drying, the plate was rotated 90° so that the silver nitrate impregnated strip was at the bottom and the labeled DMPA sample moved to the junction of the

reversed-phase zone by developing with acetonitrile to 6 cm from the bottom of the plate (2 cm above the silver nitrate and reversed-phase junction). Reversed-phase separation (based on the hydrophobicity of the relevant compounds) was accomplished by twice developing the chromatogram to the top of the plate using acetonitrile–tetrahydrofuran (4:1). After drying, the plates were autoradiographed for 3–8 h. In selected experiments in which separated lipids were subjected to further analysis, radioactive areas identified by autoradiography were removed from the plate and extracted using heptane–ethyl acetate (1:1) prior to alkaline methanolysis and GC of the fatty acid methyl esters[8].

Separation of molecular species of [^{32}P]DMPA formed by radioactive phosphorylation of DAG (derived from porcine liver phosphatidylcholine by phospholipase C hydrolysis) and methylation of the resultant [^{32}P]PA (using diazomethane) is illustrated in Fig. 2. All major and most minor molecular species of this lipid were resolved. The multiple forms of pentaenoic and hexaenoic molecular species were not characterized due to their modest representation in the lipids examined, but multiple

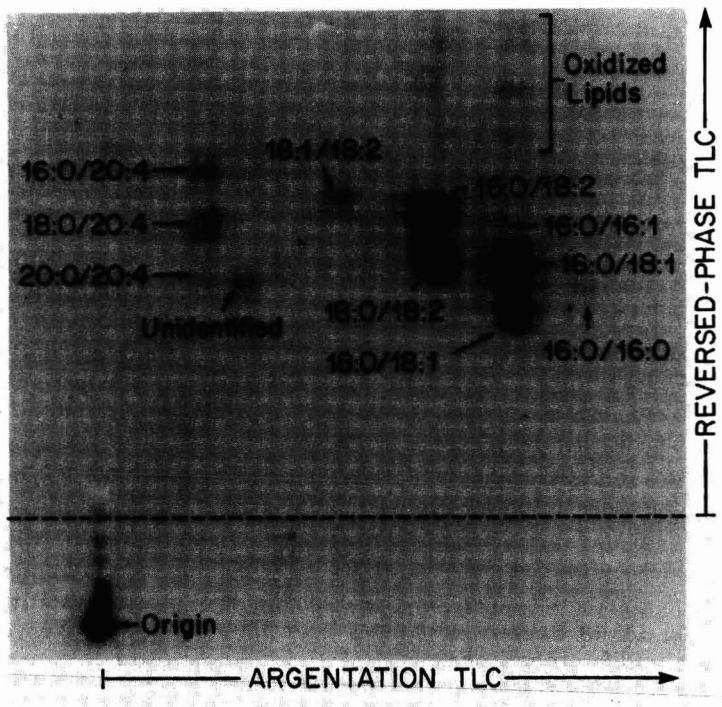

Fig. 2. Separation of molecular species of [^{32}P]DMPA. Porcine liver phosphatidylcholine was converted to DAG using *C. welchii* phospholipase C, purified and intensely radioactively phosphorylated using [γ-^{32}P]ATP and *E. Coli* DAG kinase[11]. The resultant [^{32}P]PA was purified and methylated (using diazomethane) to form [^{32}P]DMPA and 500 000 cpm of the latter was spotted at the origin, developed as illustrated in Fig. 1 and autoradiographed for 3 h. The junction of the argentation and reversed-phase phase zones is indicated by a dashed line and the relevant portion of the autoradiograph illustrated. Radioactive areas were removed and following elution, the lipids were either quantitated by liquid scintillation counting or characterized by GC of the fatty acid methyl esters formed by alkaline methanolysis. The identity of the labeled spots is indicated.

bands were observed when the authoradiographs were exposed for longer periods (data not shown). R_F values were quite reproducible from plate to plate and from day to day (± 5–10%; data not shown). The quantitative molecular species distribution of porcine liver phosphatidylcholine obtained using this method (Fig. 2) was similar to a previously published estimate that employed HPLC[2].

RESULTS AND DISCUSSION

These studies sought to develop an appropriate TLC matrix for two-dimensional TLC separation of structurally similar molecular species of radioactively labeled DMPA derived indirectly from phospholipids or DAG. Assessing the metabolic source and fate of DAG in mast cells by determining the molecular species "fingerprint" of DAG and comparing it to that of potential precursors and metabolic products is a major goal of our laboratory. Several previous studies using reversed-phase HPLC alone have had varying degrees of success in resolving molecular species of neutral glycerides or phospholipids[1–6]. In our experience, reversed-phase HPLC alone was not found to be sufficient for the separation of even the major molecular species of labeled DMPA derived from egg phosphatidylcholine[8] and additionally was found to be quite cumbersome. In that study, excellent separation of molecular species was accomplished by further subjecting HPLC-derived peaks to silver nitrate TLC[8] suggesting that complete molecular species analysis of DAG derivatives might be possible using argentation and reversed-phase TLC. The two-dimensional TLC described in the current study (using plates designed to take advantage of both reversed-phase and argentation chromatography) provide sufficiently good resolution of molecular species to generate a "fingerprint" that will permit more accurate prediction of the role of different pathways proposed to be involved in DAG formation and removal during cellular stimulation.

Compared to reversed-phase HPLC, this combined reversed-phase and argentation TLC separation of molecular species of a DMPA (which can be formed from either DAG or PA) has a number of advantages: (1) molecular species are well separated and compounds that are spatially close are structurally related so that an error in identifying a compound would be a conservative one (reversed-phase HPLC causes dissimilar compounds to often have very similar retention times[1–5]); (2) the current TLC-based method requires only simple techniques and relatively inexpensive materials and equipment; (3) multiple analyses require less time (6 h to run 25 samples in a single large TLC tank compared with 16–50 h for 25 sequential 40–120 min HPLC runs); (4) autoradiographic detection followed by liquid scintillation counting of labeled compounds is more sensitive than direct scintillation spectromery of HPLC effluent.

Certain aspects of the current technique limit its application. First, custom derivatization of the silica plates is labor intensive. Treating and activating 25–50 plates requires 4–6 h of attention during an 8–10 h period. Second, the 18:1/18:1 molecular species significantly overlaps the 18:0/18:2 spot as does the 16:1/18:1 with the 16:0/18:2 (determined by GC analysis of the latter) although the cellular presence of each of the former represent modest fractions of each of the latter. Third, the use of tritium labeled compounds is complicated by the fact tritiated lipids migrate significantly differently than do unlabeled compounds in argentation chromatographic

analysis[13]. Thus, identification of labeled areas by non-destructive staining of unlabeled standard compounds added to the samples prior to chromatography does not accurately identify the location of corresponding tritiated compounds which are best determined by fluorography. This differential migration of tritiated compounds can be used to advantage insofar as it permits enrichment of radioactive specific activity of tritiated synthetic products.

Chromatographic analysis of 1-alkyl and 1-alkenyl lipids is important in a variety of cells in which choline and ethanolamine phospholipids are enriched in ether-containing species. When 1-alkyl and 1-alkenyl molecular species were compared to their diacyl counterparts, a 2–8% change in R_F was observed for both the reversed-phase and argentation chromatographic steps (data not shown). As a result, utilizing the TLC described in this paper to resolve molecular species of phospholipids with a significant ether content requires prior separation of the labeled DMPA into 1-acyl, 1-alkyl and 1-alkenyl subclasses as has been described previously[14,15].

One refinement not routinely utilized is the use of parallel lanes containing authentic standards to enhance identification of relevant sample spots. By making a slightly wider silver nitrate impregnated band (5 cm), a lane for a sample containing authentic standards can be run in parallel with the principal sample (in the orientation of Fig. 1, standards were applied below the sample). This standard-containing lane is cut off prior to development in the second dimension. Appropriate authentic standards can similarly be employed to help identify compounds separated in the second dimension by spotting them to the right (orientation of Fig. 1) of the anticipated migration of the compound with the highest R_F value in the first dimension.

In addition to using these plates (containing both reversed-phase and argentation zones) for molecular species analysis of fatty acid containing lipids, this technique holds promise for a variety of other types of separations. Although no data exist in this regard, this method might prove to be quite useful for separating arachidonic acid metabolites, natural and synthetic steroids and the products of a variety of synthetic reactions in which the products have modest differences in hydrophobicity and degree of unsaturation.

ACKNOWLEDGEMENTS

I wish to thank Mr. James Elson for his expert technical assistance in these experiments. This research was supported a grant from the NIH (R01-22277) at a time when the author was a Pfizer Scholar and an Asthma and Allergy Developing Investigator in Immunopharmacology.

REFERENCES

1 G. M. Patton, J. M. Fasulo and S. J. Robins, *J. Lipid Res.*, 23 (1982) 190.
2 M. Smith and F. Jungalwala, *J. Lipid Res.*, 22 (1981) 697.
3 M. L. Blank, M. Robinson, V. Fitzgerald and F. Snyder, *J. Chromatogr.*, 298 (1984) 473.
4 S. Pind, A. Kuksis, J. J. Myher and L. Marai, *Can. J. Biochem. Cell Biol.*, 62 (1984) 301.
5 J. Krüger, H. Rabe, G. Reichmann and B. Rüstow, *J. Chromatogr.*, 307 (1984) 387.
6 J. Y.-K. Hsieh, D. K. Welch and J. G. Turcotte, *J. Chromatogr.*, 208 (1981) 398.
7 D. A. Kennerly, *J. Chromatogr.*, 363 (1986) 462.
8 D. A. Kennerly, *J. Biol. Chem.*, 262 (1987) 16305.

9 L. D. Bergelson, E. V. Dyatlovitskaya and V. V. Voronkova, *J. Chromatogr.*, 15 (1964) 191.
10 M. Rodbell, *J. Biol. Chem.*, 241 (1966) 130.
11 D. A. Kennerly, C. W. Parker and T. J. Sullivan, *Anal. Biochem.*, 98 (1979) 123.
12 R. K. Gilpin and W. R. Sisco, *J. Chromatogr.*, 124 (1976) 257.
13 D. S. Sgoutas and F. A. Kummerow, *J. Chromatogr.*, 16 (1964) 448.
14 O. Renkonen, *Biochim. Biophys. Acta*, 152 (1968) 114.
15 Y. Nakagawa and L. A. Horrocks, *J. Lipid Res.*, 24 (1983) 1268.

Journal of Chromatography, 454 (1988) 432–437
Elsevier Science Publishers B.V., Amsterdam — Printed in The Netherlands

CHROM. 20 809

Note

In situ mineralization and determination of phosphorus in phospholipids on silica gel sintered thin-layer chromatographic plates

TAKASHI TERABAYASHI*, TADAO OGAWA and YASUHIRO KAWANISHI
Laboratory of Biochemistry, Department of Chemistry, Kitasato University, 1-15-1 Kitasato, Sagamihara, Kanagawa 228 (Japan)
and
JUKICHI ISHII
Iatron Laboratories, Inc., 1-11-4 Higashi-Kanda, Chiyoda-ku, Tokyo 101 (Japan)
(First received June 9th, 1988; revised manuscript received July 11th, 1988)

Thin-layer chromatography (TLC) has been used as a simple technique for qualitative and quantitative analyses of lipids. Phospholipids separated by TLC have been determined by colorimetric methods after extraction from the scraped spots[1], by densitometry after visualization using colour reagents or charring reagents[2] or by hydrogen flame ionization detection (FID)[3]. The scraping method is generally accepted but tedious. Most densitometric methods and the FID method are not based on phosphorus determination. Dittmer–Lester reagent[4], a specific reagent for phospholipid detection, is not suitable for densitometry because of the blotchy and grainy sample spots obtained[2].

We therefore designed a method for the determination of lipid phosphorus directly on a TLC plate. Phospholipids were separated on a silica gel sintered TLC plate and mineralized directly on it. The phosphoric acid liberated was determined by densitometry after visualization with Brilliant Green. The determination of amino nitrogen by the ninhydrin method prior to the mineralization procedure did not interfere with the determination of phosphorus by this method. The nitrogen to phosphorus ratio in phosphatidylethanolamine was easily determined on the same silica gel sintered TLC plate after development.

EXPERIMENTAL

Reagents and standard samples

Brilliant Green (BG) was obtained from Wako (Tokyo, Japan). Other reagents were of analytical-reagent grade. Phosphatidylethanolamine (PE), phosphatidylcholine (PC) and sphingomyelin (SM) were prepared from egg yolk[5]. The purity of each lipid was over 98% by high-performance (HP) TLC (silica gel 60, Merck). The determination of lipid phosphorus was performed essentially by the method of Bartlett[6].

TLC plates

Silica gel sintered TLC plates (10 × 10 cm) (Iatron Labs., Tokyo, Japan) were

0021-9673/88/$03.50

prepared with uniform-sized particles of silica gel (15 μm) to obtain well defined sample spots with good resolution. The plates were cleaned by immersion in fuming nitric acid overnight at room temperature, rinsed with distilled water and activated at 100°C for 30 min before use.

Solvent systems

The following solvent systems were used: (1) ethyl acetate–n-propanol–chloroform–methanol–water–glacial acetic acid (25:25:25:10:6:0.5, v/v), (2) chloroform–methanol–water–glacial acetic acid (45:15:2:0.2, v/v) and (3) chloroform–methanol–water–28% ammonia (45:15:2:0.1, v/v).

In one-dimensional TLC, the plate was developed 5 cm from the origin with solvent system 2. After drying *in vacuo*, the plate was further developed to the top with solvent system 1. In two-dimensional TLC, the plate was developed in the first direction in the same manner as in one-dimensional TLC, then thoroughly dried *in vacuo* and run in the second direction with solvent system 3.

Spray reagents

Two spray reagents, A and B[7], were used for visualization with Brilliant Green. A was a mixture of 5 ml of 1% aqueous ammonium molybdate solution, 5 ml of 25% hydrochloric acid and 90 ml of acetone. B was a mixture of solutions 1 and 2. Solution 1 was prepared by dissolving 2 g of BG in 350 ml of water and solution 2 by dissolving 4 g of ammonium molybdate in 40 ml of water with heating followed by cooling, addition of 50 ml of 10 *M* hydrochloric acid and dilution to 100 ml with water. Solutions 1 (350 ml) and 2 (100 ml) were mixed, left for 3 h and filtered into a brown bottle. The solutions were stored at room temperature and were stable for 5 weeks.

Procedures

A 1-μl volume of lipid solution [10–100 ng/μl of lipid in chloroform–methanol (9:1)] was spotted on the TLC plate with a Hamilton 7002N microsyringe and developed with the solvent systems described above. The dried TLC plate was sprayed with 60% perchloric acid, covered with a glass plate and heated at 130°C for 90 min on an aluminium block heater. The TLC plate was further heated at 130°C for 5 min without the cover plate to remove perchloric acid. The cooled plate was sprayed with reagent A and heated at 85°C for 3 min. After cooling, the plate was sprayed with reagent B. As soon as green spots had appeared on an orange background, the TLC plate was covered with a glass plate to keep the concentration of hydrochloric acid constant. After 30 min, the coloured spots were scanned with a Shimadzu CS-910 dual-wavelength TLC scanner (sample, 620 nm; reference, 400 nm; reflection mode). The extinction profiles were recorded with a Hewlett-Packarsd 3390A integrator.

RESULTS AND DISCUSSION

The advantage of the silica gel sintered TLC plate is its durability to treatment with strong acids at high temperatures. The silica gel thin layer did not crumble even after the mineralization procedures. After the analysis, the plate could be used repeatedly by applying the cleaning procedure described above.

Fig. 1 is a two-dimensional thin-layer chromatogram of egg yolk phospholipids. The chromatogram shows well resolved and defined spots. As the adsorptive activity of the sintered TLC plate was less than that of the usual HPTLC plate, the solvent system was modified to reduce the proportions of polar solvents such as methanol and water. The addition of a small amount of glacial acetic acid contributed to a better definition of the sample spots.

The most popular method for determining organic phosphorus is colorimetric measurement of the blue colour developed by reducing phosphomolybdic acid. However, on spraying with reducing reagents such as 1-amino-2-naphthol-4-sulphonic acid reagent, L-ascorbic acid solution and amidol reagent, the background of the chromatogram developed the same blue colour as the sample spots, which then could not easily be distinguished from the background. The examination of other dyes showed BG to be optimal. BG is both an acid–base and a redox indicator, and an analogue of Malachite Green, which has been used for qualitative and quantitative analyses of lipid phosphorus[8,9]. The mechanism of the coloration of BG was elucidated by Trujillo *et al.*[10]. After the visualization procedure, green spots appeared on an orange background. The absorption maxima were 620 nm for the sample spot and 400 nm for the background. The developed colour is stable for about 40 min from 20 min after the colour development. After 60 min, the background intensity increases with increase in both the colour intensity of sample spots and its coefficient of var-

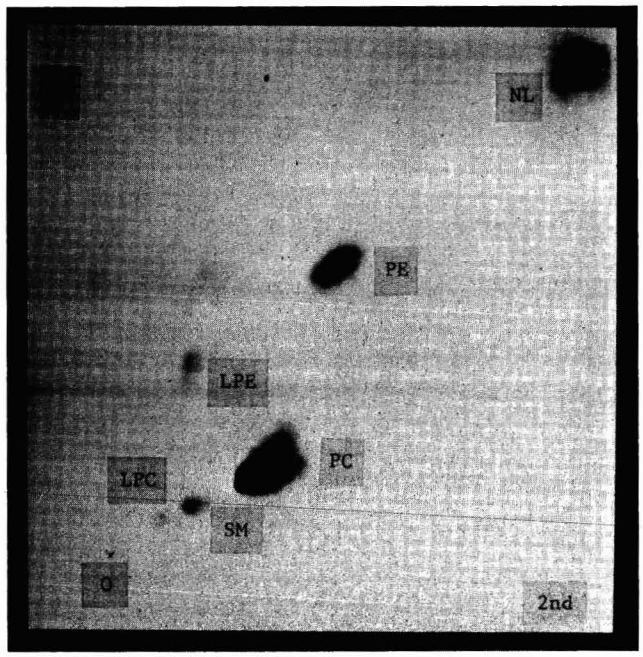

Fig. 1. Two-dimensional thin-layer chromatogram of phospholipids using the silica gel sintered TLC plate. Egg yolk phospholipid fraction (200 ng of total lipid phosphorus) was developed. PE = phosphatidylethanolamine; LPE = lysophosphatidylethanolamine; PC = phosphatidylcholine; LPC = lysophosphatidylcholine; SM = sphingomyelin. Phospholipids were visualized with 50% sulphuric acid. Chromatographic conditions as in text.

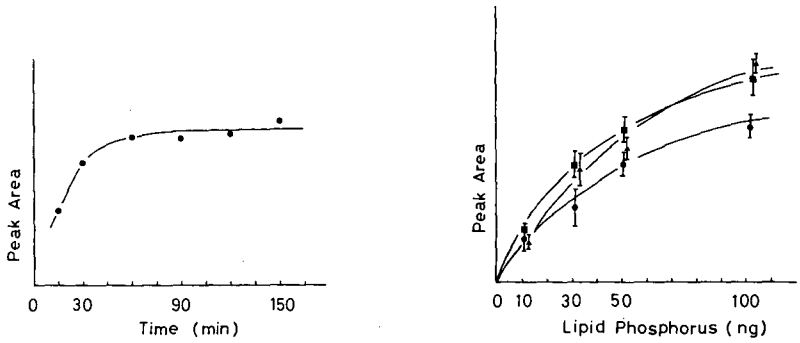

Fig. 2. Effect of time of heating on the mineralization. PE (100 ng of lipid phosphorus) was mineralized at 130°C and visualized with BG.

Fig. 3. Calibration graphs in the range 10–100 ng of lipid phosphorus for (▲) PE, (■) PC and (●) SM. Phospholipids were separated by one-dimensional TLC, followed by mineralization and visualization with BG. Abbreviations as in text.

iation (C.V.) value. Therefore, densitometric scanning between 20 and 60 min after colour development is to be preferred.

The effect of the time of heating on the mineralization performance of the organic phosphorus compound was investigated (Fig. 2). Although the colour density reached a plateau at around 60 min, a time of 90 min was adopted to ensure complete mineralization. In the TLC scraping method, phospholipids were mineralized at 180°C[1]. On the sintered TLC plate, phospholipids were mineralized sufficiently at 130°C. Fig. 3 shows the calibration graphs for PE, PC and SM, determined after one-dimensional TLC. The colour development was saturated at around 100 ng of phosphorus. In the range 10–100 ng of phosphorus, the coefficient of variation of the peak area for each phospholipid was 5–15%. Unfortunately, the individual calibration graphs were not the same for all phospholipids on a phosphorus basis. Macala *et al.*[11] reported that the densitometric responses were affected by diffusion of the sample spots during development. In this method, the spot grew broarder not only

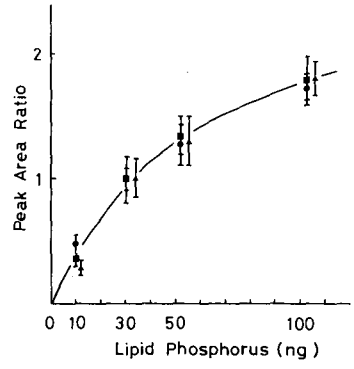

Fig. 4. Modified calibration graphs for (▲) PE, (■) PC and (●) SM. In place of the colour response itself, ratios of the response at each amount of lipid phosphorus amount to that of a fixed amount (30 ng) were plotted. Abbreviations as in text.

TABLE I

MAJOR PHOSPHOLIPID COMPOSITION OF EGG YOLK

Phospholipid	*Lipid phosphorus* (ng)*	*wt. %*	
		*Present method***	*Reference****
PC	53.3 ± 2.50	75.9 ± 2.1	80.7
PE	18.0 ± 0.82	20.2 ± 2.0	16.5
SM	3.1 ± 0.14	3.8 ± 0.15	2.8

* Values are means ± standard deviations of three determinations. Amounts of phosphorus in PC and PE were determined after the development of egg yolk phospholipid fraction (80.8 ng of total lipid phosphorus). For SM, the amount of sample was increased 3-fold and the value of phosphorus in SM was divided by three.

** Lipid composition represented as weight percentage for comparison with reference values. The molecular weight of each lipid was calculated by assuming that each lipid contained only stearic acid.

*** Amount of PE, PC and SM were taken from ref. 12 and calculated as weight percentage of major components.

during development but also in the mineralization. To correct for these influences, the ratios of the responses of varying amounts of phosphorus to the response at 30 ng were plotted (Fig. 4). For all the phospholipids investigated the relationship between this ratio and the amount of phosphorus agreed well. Therefore, an external standard mixture consisting of phospholipids, all of which contained 30 ng of phosphorus, was developed alongside unknown samples.

The phospholipid composition of egg yolk was measured very easily by this method. The results obtained are in close agreement with literature values[12] (Table I). A further advantage of this method is that the determination of other constituents such as the amino group prior to the mineralization procedure did not interfere with the subsequent determination of phosphorus. The amount of nitrogen in PE was

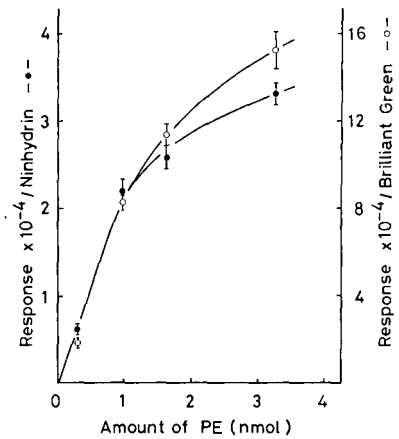

Fig. 5. Calibration graphs for PE in the range 0.3–3 nmol. After development, PE was determined by the ninhydrin method, followed by mineralization and determination by this method on the same plate. Chromatographic conditions and abbreviations as in text.

determined after development on the sintered TLC plate by the ninhydrin method. After the densitometry (570 nm), the same plate was submitted to mineralization and applied to the phosphorus determination (Fig. 5). The nitrogen:phosphorus ratio for PE was 1.06 ± 0.19 at 1 nmol, which is very close to the theoretical value of 1.00.

ACKNOWLEDGEMENT

We thank Mr. Tamotsu Kotake (Kitasato University) for technical assistance.

REFERENCES

1 Y. H. Itoh, T. Itoh and H. Kaneko, *Anal. Biochem.*, 154 (1986) 200–204.
2 J. Sherman and S. Bennett, *J. Liq. Chromatogr.*, 6 (1983) 1193–1211.
3 T. Terabayashi, T. Ogawa, Y. Kawanishi, M. Tanaka, K. Takase and J. Ishii, *J. Chromatogr.*, 367 (1986) 280–285.
4 J. C. Dittmer and R. L. Lester, *J. Lipid Res.*, 5 (1964) 126–127.
5 A. R. Johnson and J. B. Davenport, *Biochemistry and Methodology of Lipids*, Wiley-Interscience, Toronto, 1971, p. 155.
6 G. R. Bartlett, *J. Biol. Chem.*, 234 (1959) 466–468.
7 F. Jungnickel, *J. Chromatogr.*, 31 (1967) 617–618.
8 H. H. Hess and J. E. Derr, *Anal. Biochem.*, 63 (1975) 607–613.
9 M. Goppelt and K. Resch, *Anal. Biochem.*, 140 (1984) 152–156.
10 A. Trujillo, S. W. Kang and H. Freiser, *Anal. Chim. Acta*, 182 (1986) 71–81.
11 L. J. Macala, R. K. Yu and S. Ando, *J. Lipid Res.*, 24 (1983) 1243–1250.
12 F. D. Gunstone, J. L. Harwood and F. B. Padley, *The Lipid Handbook*, Chapman & Hall, London, 1986, p. 166.

Journal of Chromatography, 454 (1988) 438–443
Elsevier Science Publishers B.V., Amsterdam — Printed in The Netherlands

CHROM. 20 830

Note

Purification of long-chain, saturated, free fatty acids

KENNETH J. LONGMUIR* and SHERRY HAYNES
Department of Physiology and Biophysics, California College of Medicine, University of California, Irvine, CA 92717 (U.S.A.)
(First received February 18th, 1988; revised manuscript received July 25th, 1988)

Saturated, radiolabeled, free fatty acids (FFAs) are often contaminated with fatty acids which are desaturated or of different chain length. To remove these materials, most purification schemes require conversion of the FFAs to the methyl ester, followed by various thin-layer chromatography (TLC) or column liquid chromatography (LC) separations[1]. We wished to avoid the esterification step since our intention was to synthesize the fatty acyl coenzyme A thioester from the free acid[2]. More recently, methods have been reported for the separation of FFAs by high-performance liquid chromatography (HPLC)[3,4]. However, purification of highly radiolabeled material by HPLC requires extensive clean-up of equipment normally used for analytical work. Also, critical pairs of FFAs may not be completely resolved[1].

The two-step procedure reported here offers a practical alternative to an HPLC purification of highly radiolabeled, saturated, FFAs. Unsaturated FFAs were easily eliminated by treatment with osmium tetroxide followed by silica gel column chromatography. Saturated FFAs of different chain lengths were then purified and recovered in high yield by preparative TLC using C_2 reversed-phase plates.

EXPERIMENTAL

Various lots of radiolabeled [1-^{14}C]palmitic acid and [1-^{14}C]stearic acid, 50–60 μCi/μmol, were obtained from ICN (Irvine, CA, U.S.A.), Amersham (Arlington Heights, IL, U.S.A.), and New England Nuclear (Boston, MA, U.S.A.). Stock solutions were prepared in acetone–1 *M* hydrochloric acid (100:1). (The inclusion of hydrochloric acid was essential for avoiding loss of material due to adherence of FFAs to glass tubes and pipets.) Unlabeled FFAs were obtained from Sigma (St. Louis, MO, U.S.A.). Osmium tetroxide was obtained from Ted Pella (Redding, CA, U.S.A.). All solvents were glass-distilled from Baxter, Burdick & Jackson (Irvine, CA, U.S.A.). Silica gel 60 (250 μm thick), RP-2 (250 μm thick), and RP-18 (200 μm thick) TLC plates were obtained from EM Science (Cherry Hill, NJ, U.S.A.). Silica gel for column chromatography (SilicAR CC-7) was obtained from Mallinckrodt (Paris, KY, U.S.A.). Silver nitrate TLC plates were prepared by briefly immersing silica gel 60 plates into 15% silver nitrate in acetonitrile[5]. All plates were activated for 1 h at 70°C prior to use.

0021-9673/88/$03.50

Osmium tetroxide treatment and column chromatography

In a typical preparation, 10 μCi (approximately 50 μg) of radiolabeled FFA was placed in a test tube, the solvents evaporated, and the sample dried 1 h over phosphorus pentoxide *in vacuo*. To the residue was added 200 μl of osmium tetroxide in carbon tetrachloride (50 mg/ml). After 1 h at room temperature, the solvent was evaporated, and 2 ml of 1 *M* hydrochloric acid were added. The FFAs were extracted three times into 2.0 ml of diethyl ether.

The ether was evaporated, the residue dissolved in hexane–diethyl ether (90:10, v/v), and loaded onto a column of 5 g of activated silica gel. The column was flushed with 25 ml hexane–diethyl ether (90:10), and the product eluted with 50 ml hexane–diethyl ether (75:25), followed by 25 ml hexane–diethyl ether (50:50). The products were collected into 10-ml fractions. The solvents were evaporated, the residues redissolved in acetone–1 *M* hydrochloric acid (100:1), and the radioactivity determined. The two or three fractions containing the largest quantities of radioactivity were combined.

Reversed-phase TLC

RP-2 reversed-phase TLC plates were pre-run in dioxane–0.001 *M* hydrochloric acid (7:3). FFAs were streaked onto the plates using acetone–1 *M* hydrochloric acid (100:1). Plates were run in dioxane–0.001 *M* hydrochloric acid (7:3). Radiolabeled fatty acids were visualized by autoradiography (Kodak XAR-5 film). After scraping the gel from the plate, the product was extracted three times into 3 ml acetone–1 *M* hydrochloric acid (100:1).

Analytical methods

Radioactivity was determined by liquid scintillation counting in Triton–toluene scintillant[6]. One-dimensional TLC analysis of FFAs was carried out on silica gel 60 TLC plates with a solvent system of hexane–diethyl ether–acetic acid (10:10:0.5). Fatty acid methyl esters were prepared using boron trifluoride, 12% in methanol[7], and extracted into hexane. Fatty acid methyl esters were analyzed on silver nitrate TLC plates by running plates twice in toluene at $-20°C$[5]. Fatty acid methyl esters were also analyzed by reversed-phase TLC on RP-18 plates by running twice in acetonitrile at room temperature[8]. Radiolabeled products were visualized by autoradiography. NMR analysis was carried out on a Bruker MSL-300 spectrometer ([^{2}H]chloroform solvent). Gas–liquid chromatography (GLC) was carried out on a Varian Model 3700 chromatograph with a 6 ft. $\times$ $\frac{1}{8}$ in. I.D. stainless-steel column of 10% SP-2330 (Supelco, Bellefonte, PA, U.S.A.) operating at 185°C.

RESULTS AND DISCUSSION

Removal of unsaturated fatty acids and other contaminants

The thin-layer chromatogram in Fig. 1 illustrates some of the contamination problems that were encountered with commercially-available, radiolabeled, palmitic and stearic acids (lane 1). To remove the unwanted materials, FFAs were first treated with osmium tetroxide, which reacted with unsaturated sites to form osmate esters. Osmium treatment of unsaturated fatty acid reduced its mobility on TLC, as seen most clearly with the stearic acid sample (lane 2). Subsequent silica gel column chro-

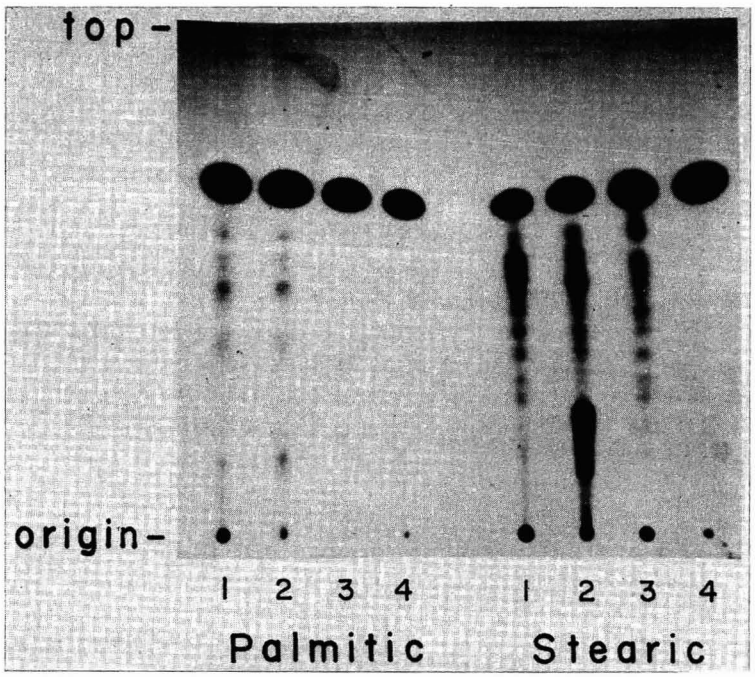

Fig. 1. TLC of radiolabeled palmitic and stearic acids on silica gel 60 TLC plates (hexane–diethyl ether–acetic acid, 10:10:0.5). Approximately 100 000 cpm ^{14}C per sample. (1) Untreated FFAs. (2) FFAs following treatment with osmium tetroxide. (3) FFAs after column chromatography only. (4) FFAs following treatment with osmium tetroxide and column chromatography.

matography successfully removed all contaminating material (lane 4). Recoveries of saturated FFAs following osmium treatment and column chromatography were on the order of 75–90% (Table I). Most of the loss occurred during column chromatography, due to the small quantities of fatty acid (<50 μg) used for these experiments.

To confirm that unsaturated contaminants were eliminated, the FFAs were converted to methyl esters and analyzed by silver nitrate TLC. As seen in Fig. 2, the osmium tetroxide and column chromatography treatments efficiently removed unsaturated fatty acids.

TABLE I

RECOVERIES OF FREE FATTY ACIDS AFTER VARIOUS PURIFICATION STEPS

Treatment	*Recovery (%)*	
	[^{14}C]Palmitic acid	*[^{14}C]Stearic acid*
Osmium tetroxide only	97	97
Column chromatography only	86	79
Osmium tetroxide plus column chromatography	87	74
Preparative reversed-phase TLC (RP-2 plate)	93	94

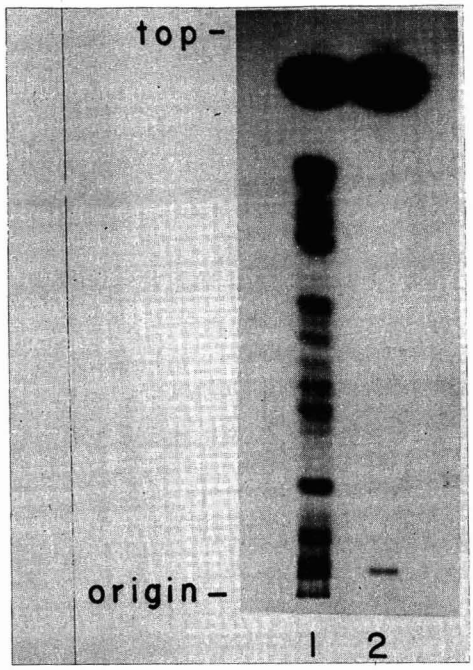

Fig. 2. Silver nitrate chromatography of purified, [^{14}C]stearic acid methyl ester. Stearic acids were converted to methyl esters, and approximately 100 000 cpm of material applied to a silica gel 60 plate impregnated with silver nitrate. Lane 1: untreated stearic acid. Lane 2: stearic acid following treatment with osmium tetroxide and column chromatography. (Material near the origin in lane 2 is a small quantity of free acid.)

Separation of saturated FFAs by chain length

Saturated FFAs were separated by preparative TLC on C_2 reversed-phase plates (silanized with dichlorodimethylsilane). Fig. 3 illustrates the separation of palmitic and stearic acids (after removal of unsaturated contaminants). Preparative TLC was successful when carried out with a solvent system of dioxane–dilute hydrochloric acid. Use of dioxane–water–formic acid mixtures, as reported elsewhere[9], were unsuccessful due to delamination of the reversed-phase material from the glass plate.

Recoveries of palmitic and stearic acids from the reversed-phase plates were excellent using a solvent system of acetone–1 *M* hydrochloric acid (100:1) (Table I). NMR analysis of the fatty acid revealed no detectable contamination from the silanized material.

To confirm that saturated free acids were successfully resolved by preparative TLC, the radiolabeled palmitic and stearic acids were converted to methyl esters and analyzed by reversed-phase TLC using RP-18 plates (data not shown). Neither the stearic nor palmitic acid samples contained saturated fatty acids of different chain length.

The capacity of the RP-2 plates (250 μm thickness) was determined for both palmitic and stearic acids by adding increasing amounts of unlabeled FFA to radiolabeled samples (data not shown). The maximum amounts of palmitic and stearic acids that could be streaked onto the plate without overloading were 200 μg/cm of

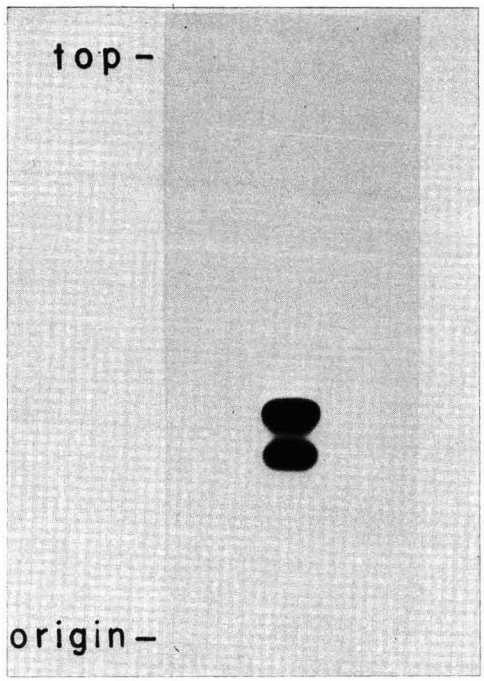

Fig. 3. Reversed-phase TLC of radiolabeled palmitic and stearic acids (following purification with osmium tetroxide and column chromatography). Approximately 100 000 cpm ^{14}C were applied to an RP-2 plate and run in dioxane–0.001 *M* hydrochloric acid (7:3). Upper band: palmitic acid. Lower band: stearic acid.

palmitic acid and 50 μg/cm of stearic acid. When larger quantities of material were applied, excessive spreading of the sample occurred during chromatography.

To confirm the advantages of these methods, fatty acid purity was also assessed on the basis of mass by GLC analysis with flame ionization detection. For these experiments, 200 μg of a mixture of palmitic, myristic, stearic, palmitoleic, and oleic acids (5:1:1:1:1) were prepared and the palmitic acid isolated using the purification procedures described above. (0.05 μCi of [1-^{14}C]palmitic acid was included to locate product.) Fig. 4A shows the GLC of the untreated mixture. Fig. 4B shows the saturated fatty acid fraction obtained after osmium tetroxide treatment and column chromatography. Following the osmium and column chromatography treatments, the palmitic acid was separated from the other saturated free acids by preparative reversed-phase TLC. As seen in Fig. 4C, contaminating fatty acids were below the level of detection.

Advantages of the method

Osmium tetroxide treatment followed by rapid column chromatography of FFAs required only a few hours to complete. The method was clearly faster than the time required to perform a more common approach of esterification, preparative silver nitrate TLC, and hydrolysis back to the free acid.

In our experience, saturated fatty acid contaminants in commercially-available samples differ by multiples of two carbon atoms. These free acids of undesired chain

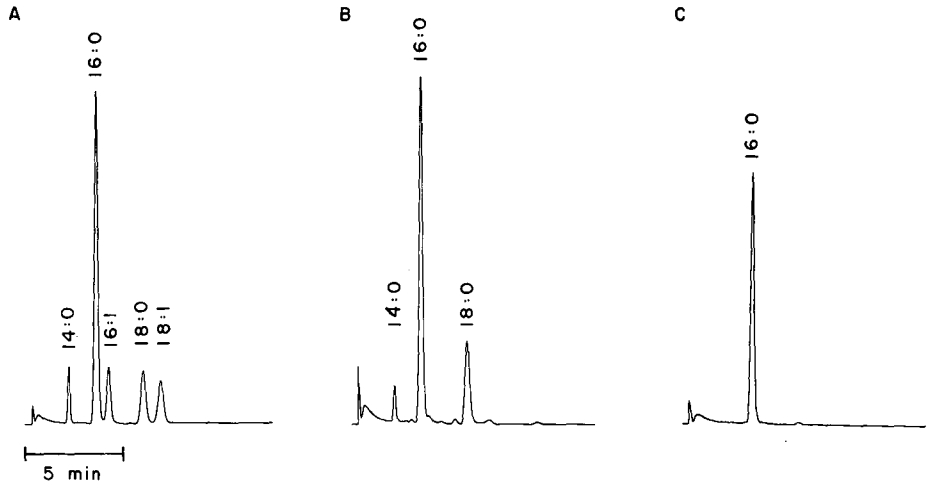

Fig. 4. GLC of a mixture of saturated and unsaturated fatty acids before and after purification steps to obtain palmitic acid. Palmitic, myristic, stearic, palmitoleic, and oleic acids were prepared in a ratio of 5:1:1:1:1. Approximately 200 μg of the mixture were treated with osmium tetroxide and the saturated fatty acids isolated by column chromatography. The palmitic acid fraction was then isolated by reversed-phase TLC. FFAs were converted to methyl esters prior to GLC analysis. (A) Fatty acid mixture before treatment. (B) Saturated fatty acids recovered after treatment with osmium tetroxide and isolation by column chromatography. (C) Palmitic acid fraction recovered after purification by preparative TLC.

length were easily separated by reversed-phase TLC. While a higher resolution can probably be achieved using preparative HPLC, radiochemical decontamination of HPLC equipment can be tedious, particularly when such equipment is usually used for analytical work. TLC offers the more convenient approach to purifying radiolabeled material on a preparative scale.

ACKNOWLEDGEMENTS

This work was supported by grants from the National Heart, Lung, and Blood Institute (HL-34624) and the American Lung Association of California.

REFERENCES

1 W. W. Christie, *Lipid Analysis*, Pergamon, Oxford, 2nd ed., 1982, p. 73–79.
2 J. E. Bishop and A. K. Hajra, *Anal. Biochem.*, 106 (1980) 344–350.
3 M. Van Rollins, M. I. Aveldano, H. W. Sprecher and L. A. Horrocks, *Methods Enzymol.*, 86 (1982) 518–530.
4 A. K. Batta, V. Dayal, R. W. Colman, A. K. Sinha, S. Shefer and G. Salen, *J. Chromatogr.*, 284 (1984) 257–260.
5 E. P. Gelman and J. E. Cronan, *J. Bacteriol.*, 112 (1972) 381–387.
6 J. E. Bleasdale, P. C. Wallis, P. C. MacDonald and J. M. Johnston, *Biochim. Biophys. Acta*, 575 (1979) 135–147.
7 L. D. Metcalfe and A. A. Schmitz, *Anal. Chem.*, 33 (1961) 363–364.
8 K. J. Longmuir, C. Resele-Tiden and M. E. Rossi, *J. Lipid Res.*, 29 (1988) 1065–1077.
9 D. Heusser, *J. Chromatogr.*, 33 (1968) 62–69.

Journal of Chromatography, 454 (1988) 444–449
Elsevier Science Publishers B.V., Amsterdam — Printed in The Netherlands

CHROM. 20 865

Note

Determination of carbohydrate composition of soil hydrolysates by high-performance liquid chromatography*

D. A. ANGERS* and P. NADEAU
Agriculture Canada, Research Station, 2560 Hochelaga Blvd., Sainte-Foy, Québec G1V 2J3 (Canada)
and
G. R. MEHUYS
Department of Renewable Resources, Macdonald College of McGill University, Sainte-Anne-de-Bellevue, Québec H9X 1C0 (Canada)
(First received June 21st, 1988; revised manuscript received July 28th, 1988)

Carbohydrates represent 5–25% of the organic matter in soils[1]. Their importance in relation to soil aggregation and to other soil processes is well recognized[1]. Carbohydrates are present in soil in many forms, ranging from plant debris and faunal remains to products of chemical, biochemical and microbial synthesis and decomposition.

Paper and gas chromatography, as well as colorimetric procedures, have been used previously to identify and quantitate the monosaccharide components of soil carbohydrates. Gas–liquid chromatography of alditol acetate derivatives has been the most widely used method[1–3]. However, the extensive sample preparation procedures required and the sensitive chromatographic operating parameters are disadvantages of this method. Conversely, high-performance liquid chromatography (HPLC) offers advantages such as speed and minimum sample purification without the need for derivatization.

Six to eight neutral sugars are usually present in soil hydrolysates. The five major ones, representing more than 90% of total neutral sugars, are hexoses (glucose, galactose and mannose) and pentoses (xylose and arabinose). Rhamnose, fucose and ribose are also found but in lesser amounts (<5%). Recently, a resin-based carbohydrate analysis column from Bio-Rad Labs. has been used for the analysis of wood and wood pulp hydrolysates. This column was found appropriate for the separation and quantification of the five sugars (glucose, galactose, mannose, arabinose and xylose) found in this material[4].

In this paper we present the results of the application of HPLC of underivatized sugars to the study of carbohydrates in hydrolysates of five soils differing in their organic matter content.

* Contribution No. 342 of the Agriculture Canada Research Station, Sainte-Foy.

0021-9673/88/$03.50

MATERIALS AND METHODS

Preparation of samples

Five surface soils from different regions of Québec, Canada were used for the determinations. They cover a range of organic carbon contents from 12 to 86 g kg^{-1}. Between 1.0 and 2.0 g of dry (40°C) finely ground soil was hydrolysed for 24 h at 80°C in 10 ml 1.5 *M* sulfuric acid in sealed tubes. The suspension was then filtered, washed with distilled water and adjusted to a final volume of 25 ml. A 10-ml aliquot was neutralized to pH 7 by adding solid barium carbonate. To remove the barium sulfate precipitate, the suspension was shaken, centrifuged (3000 *g*) and filtered (Whatman 42). The clear sugar solution obtained was stored at 4°C until analysis.

Liquid chromatography

HPLC analyses were performed using a Waters system consisting of a Model 510 pump, Model U6K sample injector, Model 840 system controller and Model 410 refractive index detector. The column was an Aminex HPX-87P carbohydrate analysis column (300 × 7.8 mm) (Bio-Rad Labs.). Cation and anion microguard columns were placed in front of the analytical column. The separation was performed isocratically using demineralized water at a flow-rate of 0.6 ml min^{-1}. The column was maintained at 85°C. The injection volumes depended on the sugar content and were usually 75 or 100 µl. Before injection, all samples were centrifuged (13 000 *g*) to eliminate particles in suspension. Detector response factors were determined from a standard solution of five sugars.

Confirmation of peak identities

Separation of samples was also performed on two other types of columns with different selectivities. A cationic resin in the calcium form (Sugar Pak I, Waters, 300 × 6.5 mm) was eluted with water containing 50 mg l^{-1} EDTA-$Ca^{2+}Na_2^+$ at a flow-rate of 0.5 ml min^{-1}. This column was maintained at 90°C during the separations. The second column was a Carbohydrate Analysis Column (Waters, 300 × 3.9 mm, amino-bonded silica); this column was kept at 25°C during the separations, using acetonitrile–water (80:20) as eluent at a flow-rate of 2.0 ml min^{-1}.

Carbon content of the soil samples was measured by dry combustion using a LECO C determinator and assumed to be total organic carbon because carbonates were absent from the soil samples.

RESULTS AND DISCUSSION

The chromatographic separation of a standard solution of five sugars on the Bio-Rad column Aminex HPX-87P is presented in Fig. 1A. The following elution times were obtained: glucose (13.3), xylose (14.4), galactose (15.1), arabinose (16.4) and mannose (16.9 min). The individual sugars are well resolved and can be quantitated individually. Fig. 1B and C show the separation of sugars obtained from two samples of soil hydrolysates widely different in organic matter content. In both cases, the sugars from the samples had retention times identical to those of the standards.

Confirmation of the identities of sugars from the samples was obtained by using

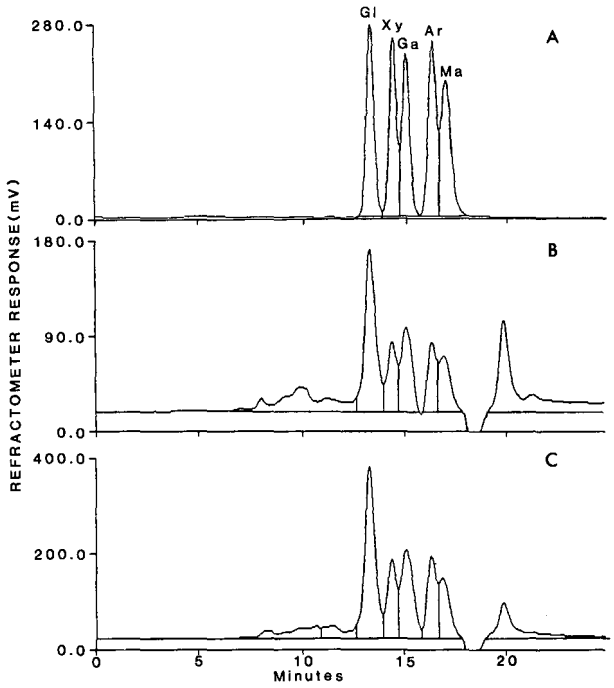

Fig. 1. Chromatographic separation on HPX-87P column (Bio-Rad Labs.) of the sugars glucose (Gl), xylose (Xy), galactose (Ga), arabinose (Ar) and mannose (Ma). (A) Separation of a standard solution containing 10 μg of each of the standard sugars. (B) Separation of sugars from a soil hydrolysate from Yamaska loam. (C) Separation of sugars from a soil hydrolysate from Normandin clay.

two other chromatographic systems offering different selectivities. Contrary to the HPX-87P column, sugars could not be individually resolved on the Sugar Pak column (Fig. 2). Only three peaks were obtained from the five component sugars (Fig. 2A). Glucose eluted in the first peak; galactose, mannose and xylose co-eluted in the second peak, and arabinose in the last peak. When soil samples were chromatographed on the same column (Fig. 2C), peaks corresponding directly to the elution times of the standard sugars were present, thus suggesting the presence of these sugars in the samples. With the Carbohydrate Analysis Column, the retention times for glucose and mannose were too close to each other (Fig. 3A) for them to appear as individual peaks. When soil samples were analyzed on this column (Fig. 3B and C), peaks corresponding to the elution times of the sugars of the standard were present. As a direct correspondence between the elution times of sugars from soil samples and those from the calibration solution was obtained with all three chromatographic systems, we are confident with the results of the identification of the sugars in our samples.

The method presented in this paper was intended first to separate five major soil sugars. Small amounts of rhamnose (<6%), fucose (<3%) and ribose (<2%) can also be detected in soil hydrolysates. Chromatography of standards on the HPX-87P column containing these minor sugars showed that rhamnose co-eluted with galactose and that fucose co-eluted with arabinose. Separation of these minor constituents was therefore not possible.

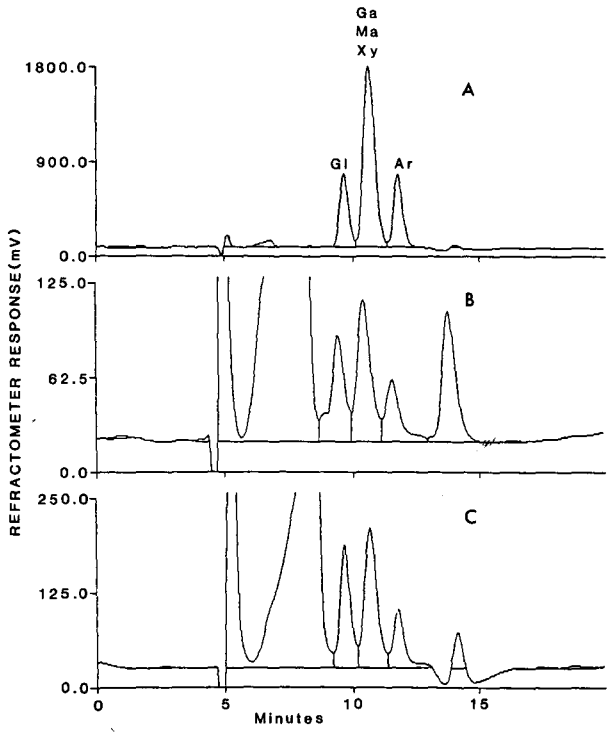

Fig. 2. Chromatographic separation of sugars on Sugar Pak column (Waters). (A) Separation of a standard solution containing 10 μg of each of the standard sugars. (B) Separation of sugars from a soil hydrolysate from Yamaska loam. (C) Separation of sugars from a soil hydrolysate from Normandin clay.

The carbon content and concentration of each sugar component for the five soil types are presented in Table I. As expected, large differences in sugar content were found for soils differing in carbon content. Total sugars accounted for nearly 20% of organic carbon, in accordance with published results[1]. The relative proportions of each sugar relative to total sugars are also in agreement with previously published data[1]. However, galactose was present in slightly larger concentration than is usually reported. This can be explained by the co-elution of rhamnose with galactose.

The chromatographic separations were made on samples obtained by using a partial hydrolysis of soil. A "total hydrolysis" procedure[1] was also assayed for comparison. This method involves a pretreatment in concentrated (72%) sulfuric acid prior to the hot dilute (0.5 *M*) acid hydrolysis. Total hydrolysis of the five soil samples resulted in an increase in total monosaccharides (Table II). Most of the effect could be attributed to a large increase in the concentration of glucose (2–3 fold) and xylose (1.3-fold) with little or no consistent changes in the content of the other sugars. This confirms that the pretreatment with concentrated sulfuric acid resulted in the hydrolysis of cellulose and the consequent release of large amounts of glucose[1].

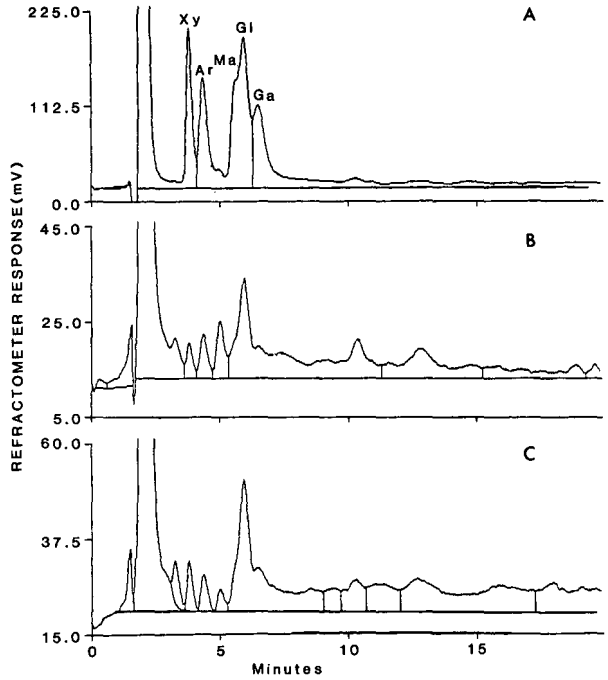

Fig. 3. Chromatographic separation of sugars on Carbohydrate Analysis Column (Waters). (A) Separation of a standard solution containing 10 μg of each of the standard sugars. (B) Separation of sugars from a soil hydrolysate from Yamaska loam. (C) Separation of sugars from a soil hydrolysate from Normandin clay.

CONCLUSION

Our results clearly demonstrate the applicability of the HPLC separation techniques to the analyses of sugars from soil hydrolysates. This method combines rapid analysis times and ease of sample preparation. No derivatization is necessary and sample prepurification is brief. The Bio-Rad HPX-87P column permits appropriate

TABLE I

CARBON CONTENT AND SUGAR CONCENTRATION IN HYDROLYSATES OF FIVE SOIL SAMPLES

Coefficient of variation varied between 2 and 10% with an average of 5%.

Soil	*Carbon* ($g\ kg^{-1}$)	*Sugars* ($mg\ kg^{-1}$)					
		Glucose	*Galactose*	*Mannose*	*Arabinose*	*Xylose*	*Total*
St-Nicolas clay loam	12	1037	645	299	222	367	2570
Yamaska loam	21	1507	1077	599	574	580	4337
Kamouraska clay	24	1651	1244	593	660	703	4851
Soulanges sandy loam	41	1807	1399	630	722	1005	5563
Normandin clay	86	3417	2744	1435	1615	1448	10659

TABLE II

SUGAR CONCENTRATION IN TOTAL HYDROLYSATES OF FIVE SOIL SAMPLES

Coefficient of variation varied between 2 and 10% with an average of 5%.

Soil	*Sugars ($\overline{mg\ kg^{-1}}$)*					
	Glucose	*Galactose*	*Mannose*	*Arabinose*	*Xylose*	*Total*
St-Nicolas loam	2695	614	127	425	543	4404
Yamaska loam	3763	978	703	360	815	6619
Kamouraska clay	3946	1207	360	736	973	7222
Soulanges sandy loam	5697	1339	268	872	1442	9638
Normandin clay	8863	3115	1253	2145	1933	17309

separation and quantitation of the most important sugars present in soil samples. However, analysis of minor sugars (rhamnose and fucose particularly) is not easily achieved due to their co-elution with the major sugars. Nevertheless, this method has a considerable potential for simplifying comparison studies of soils containing various amounts of carbohydrates.

ACKNOWLEDGEMENTS

The authors wish to thank Dr. M. Schnitzer for helpful comments and revision of the manuscript.

REFERENCES

1 M. V. Cheshire, *The Nature and Origin of Soil Carbohydrates*, Academic Press, New York, 1979, 216 pp.
2 J. M. Oades, *J. Chromatogr.*, 28 (1967) 246–252.
3 M. Spiteller, *Z. Pflanzenernaehr. Bodenkde.*, 143 (1980) 720–729.
4 F. E. Wentz, A. D. Marcy and M. J. Gray, *J. Chromatogr. Sci.*, 20 (1982) 349–352.

Journal of Chromatography, 454 (1988) 450–454
Elsevier Science Publishers B.V., Amsterdam — Printed in The Netherlands

CHROM. 20 860

Note

Chiral high-performance liquid chromatographic analysis of phenoxy herbicide mixtures

B. BLESSINGTON* and N. CRABB
Department of Pharmaceutical Chemistry, Bradford University, Bradford, West Yorkshire, BD7 1DP (U.K.)

(First received July 4th, 1988; revised manuscript received July 26th, 1988)

2-(4-Chloro-2-methylphenoxy)propanoic acid (CMPP) is a member of the phenoxy herbicide group; its annual U.K. and world production have been estimated at 3500 and 20 000 tons, respectively[1]. It has been recognised that its herbicidal activity is stereoselective, since only the (+)-enantiomer has appreciable activity[2]. Recent developments have led to the marketing of this agent in optically pure form by BASF (trade name Duplosan). Within the next two years The Netherlands and Switzerland will restrict the scale of CMPP to the active enantiomer only. Other countries are considering similar legislation. Such developments require assay methods for quality control and regulatory purposes.

We have previously reported the direct chiral separation of CMPP using an α_1-acid glycoprotein (Enantiopac) chiral stationary phase (CSP)[3]. The same enantiomers could also be separated, after conversion to their diphenylamides, using a Pirkle ionic CSP [with N-(3,5-dinitrobenzoyl)-(*R*)-(−)phenylglycine as chiral ligand]. We now wish to report preliminary work on the analysis of mixed-herbicide formulations. Such formulations arise because different phenoxy herbicides have different specificities, so much broader herbicidal action will result from the use of mixed formulations. Typical blends include CMPP, the related chiral 2-(2,4-dichlorophenoxy)-propanoic acid (2,4-DP) and the non-chiral 4-chloro-2-methylphenoxyacetic acid (MCPA).

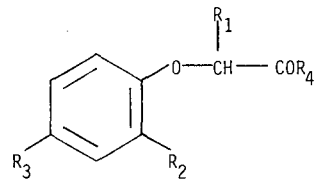

	R_1	R_2	R_3
CMPP	CH_3	CH_3	Cl
2,4-DP	CH_3	Cl	Cl
MCPA	H	CH_3	Cl

R_4 = OH (free acids) or $N(C_6H_5)_2$ (diphenylamide derivatives)

EXPERIMENTAL

Materials

Herbicide samples were gifts from A. H. Marks Co. (Bradford, U.K.) and May & Baker (Dagenham, U.K.), γ-Aminopropyl silica (5 μm) was purchased as Spherisorb NH_2 from Jones Chromatography and packed into a 30 cm × 4.6 mm I.D. column. N-(3,5-Dinitrobenzoyl)-(*R*)-(−)-phenylglycine was purchased from Sigma. The 10-cm Enantiopac column was purchased from LKB (Bromma, Sweden). All solvents used were HPLC grade, other materials were of laboratory grade and used as purchased.

Equipment

The Pye Unicam HPLC system used consisted of a PU 4010 pump, PU 4020 UV detector, PU 4047 column module and a DP 88 computing integrator.

Storage and testing of Enantiopac column

The Enantiopac column was stored in propan-2-ol–water (50:50, v/v) at a temperature of 10°C. Prior to each use the column was equilibrated in a mobile phase of propan-2-ol–0.1 *M* sodium chloride in phosphate buffer (10 m*M*, pH 6) (8:92, v/v) and tested by the injection of 20 μl disopyramide (0.1 mg/ml) in the mobile phase. Baseline resolution for this reference racemate was always obtained during our study.

Preparation, testing and storage of Pirkle column

Preparation of the Pirkle CSP, from a prepacked 30-cm γ-aminopropyl silica column and a solution of N-(3,5-dinitrobenzoyl)-(*R*)-(−)-phenylglycine was in accordance with the *in situ* method described by Pirkle *et al.*[4]. The final stage of preparation involved equilibration in a mobile phase of propan-2-ol–hexane (10:90, v/v). On achieving a stable baseline the column was tested using phensuximide as the test racemate. On injection of 20 μl of a 1-mg/ml solution, clear separation (but not to baseline) of the enantiomes was considered satisfactory.

Preparation of herbicide derivatives

Diphenylamide derivatives of the herbicides were prepared in the following manner. A 2-mg amount of the herbicide was weighed into a quickfit centrifuge tube. Thionyl chloride (1 drop) was added and the tube was stoppered and heated over a steam bath for 10 min. The contents were then evaporated to dryness under reduced pressure and reconstituted in 1 ml of a solution of 2 mg/ml diphenylamine in chloroform. The tube was shaken regularly over a period of 10 min prior to reducing to dryness. The residue was dissolved in 10 ml of propan-2-ol–hexane (10:90, v/v) and this solution was diluted 10-fold prior to HPLC analysis on the Pirkle column.

Herbicidal agents were extracted from commercial blends by first acidifying the solution and then extracting the acidic herbicides into chloroform. After evaporating the chloroform layer to dryness, under reduced pressure, derivatisation was accomplished as described above.

RESULTS AND DISCUSSION

Examination of individual compounds on the Enantiopac column revealed good separation for CMPP, as previously reported, but only poor separation for 2,4-DP. Systematically varying the pH and propan-2-ol content of the mobile phase failed to yield useful separation of 2,4-DP (see Table I). This must reflect the strict specificity of the binding sites of the α_1-acid glycoprotein and means that Enantiopac separations cannot be considered as group separation systems. A further disadvantage with the Enantiopac column became apparent when MCPA was run under conditions optimised for CMPP because 2,4-DP gave poor, but evident separation. However, the retention time of MCPA corresponded to that of the (−)-enantiomer of CMPP.

These are serious limitations of the Enantiopac method. Taken in conjunction with the cost, erratic behaviour and short lifetime of these columns[5,6] they render the Enantiopac system unreliable for routine chiral analysis of phenoxy herbicides.

In contrast the ionic Pirkle column performed well when used to assay mixed phenoxy herbicides as their diphenylamide derivatives. Clear separation of the CMPP amide enantiomers (as previously reported[3]), 2,4-DP amide enantiomers and the non-interfering elution of MCPA amide was obtained (see Table II). For both chiral herbicides the derivatisation step was validated. Racemic materials gave virtually 50:50 response ratios for the enantiomeric amides whilst the purest samples of (+)-CMPP and (+)-2,4-DP available to us gave 0% and 3% of the (−)-enantiomers respectively (as calculated from integrated peak areas), so excluding significant racemisation. Further work is in hand to judge the exact extent of racemisation during these reactions and to formalise and validate conditions in a detailed assay method.

TABLE I

THE CHROMATOGRAPHIC EXAMINATION OF (±)-CMPP AND (±)-2,4-DP ON AN α_1-ACID GLYCOPROTEIN (ENANTIOPAC) CSP

Mobile phase: 0.1 *M* sodium chloride in phosphate buffer (10 m*M*); variable pH and Propan-2-ol concentration. Flow-rate: 0.2 ml/min. Detection: 240 nm. t_R = Retention time of first eluted enantiomer; k' = capacity factor; α = separation factor; R_s = resolution.

Mobile phase variable		*Solute*	t_R *(min)*	k'	α	R_s
Propan-2-ol in mobile phase (%)	*pH*					
8	6	(±)-CMPP	31	6.4	1.16	1.06
		(±)-2,4-DP	25	4.8	1.00	0.00
6	6	(±)-CMPP	36	6.9	1.21	1.35
		(±)-2,4-DP	30	5.6	1.00	0.00
4	6	(±)-CMPP	40	7.5	1.25	1.60
		(±)-2,4-DP	30	5.4	1.09	0.33
6	9	(±)-CMPP	34	6.8	1.21	1.34
		(±)-2,4-DP	27	5.2	1.00	0.00
6	4	(±)-CMPP	36	6.9	1.22	1.33
		(±)-2,4-DP	28	5.1	1.00	0.00

TABLE II

THE CHROMATOGRAPHIC BEHAVIOUR OF PHENOXY HERBICIDES AS DIPHENYLAMIDE DERIVATIVES ON A PIRKLE IONIC TYPE CSP

Mobile phase: propan-2-ol–hexane (10:90, v/v); flow-rate: 1.0 ml/min; detection: 240 nm.

Solute	t_R *(min)*	k'	α	R_s	*(+)-Enantiomer (%)*	*(−)-Enantiomer (%)*
(±)-CMPP	8.2	2.00	1.10	1.20	50.8	49.2
(±)-2,4-DP	9.2	2.37	1.11	1.14	49.3	50.7
(+)-CMPP	8.2	2.00	–	–	100.0	0.0
(+)-2,4-DP	9.2	2.37	–	–	97.0	3.0
MCPA	12.1	3.41	–	–	–	–

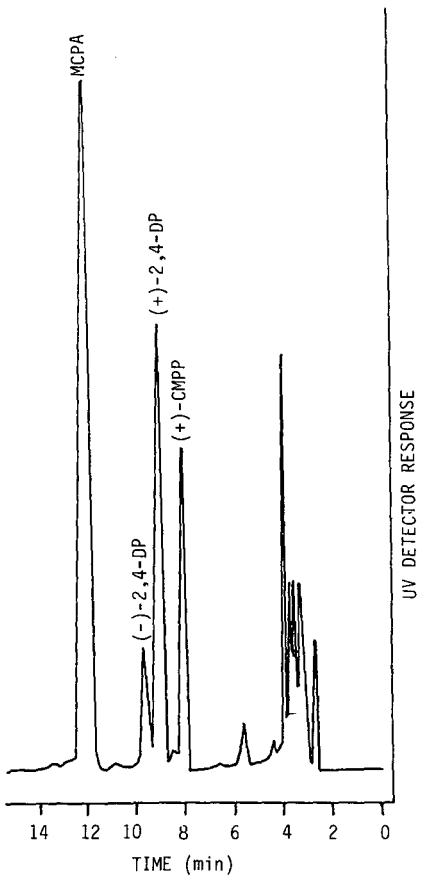

Fig. 1. The analysis of (+)-CMPP, (+)-2,4-DP and MCPA in a commercial mixed formulation using a Pirkle ionic CSP. The 2,4-DP in this non-compliant sample contains 20% of the (−)-enantiomer. Less than 5% of the (−)-CMPP isomer was found. Mobile phase: propan-2-ol–hexane (10:90, v/v); flow-rate: 1 ml/min; detection: 240 nm.

The technique was used to determine the optical purity of (+)-CMPP and (+)-2,4-DP in commercial mixed-herbicide formulations. Fig. 1 shows the chromatogram obtained for a non-compliant sample. Here the CMPP assay was acceptable but the 2,4-DP contained an unacceptably high level (20%) of the (−)-enantiomer. Peaks were identified by comparison with the retention times of authentic (+)-CMPP, (+)-2,4-DP and MCPA as well as the actual materials used in the manufacture of the commercial sample. It is important to note that the analysis of such formulations cannot be accomplished by polarimetric methods alone, chromatographic resolution is required. The low cost of Pirkle columns compared to Enantiopac columns is a notable feature. Moreover the Pirkle system seems to be considerably more robust. Both columns, however, are more temperamental than typical GC and reversed-phase HPLC systems. The requirement to derivatise the herbicides in order to obtain separations on Pirkle columns is a major limitation. The method must be compared with derivatisation methods to yield diastereomers which can then be separated by non-chiral GC and HPLC methods (details of such separations are in press).

CONCLUSIONS

The Pirkle ionic CSP can be used for the analysis of commercial blends of CMPP, 2,4-DP and MCPA herbicides. The method requires conversion of the free acids to diphenylamides prior to HPLC.

In contrast, the separation of such herbicides by direct analysis on an α_1-acid glycoprotein column (Enantiopac) cannot, in our hands, provide an effective analysis. Good separation of CMPP alone can be obtained. The chiral specificity of the Enantiopac column is such that minor substrate structural modification markedly alters the separation obtainable. Interference with the non-chiral MCPA was also found.

REFERENCES

1 Commercial Sales Department, A. H. Marks Co., Bradford, personal communications.
2 H. Luers, *The Agronomist, No. 1*, BASF, Hadleigh, 1988, pp. 6-7.
3 B. Blessington, N. Crabb and J. O'Sullivan, *J. Chromatogr.*, 396 (1987) 177–182.
4 W. H. Pirkle, J. Finn, J. Schreiner and B. Hamper, *J. Am. Chem. Soc.*, 103 (1981) 3964–3966.
5 *Practical Workshop Sessions, Bradford Analytical Course in Chiral Separations in HPLC*, Bradford University, Bradford, March 1988.
6 *Workshop Discussion Sessions, Chromatographic Society International Symposium on Biomedical Applications of Liquid Chromatography*, Bradford, March 1988.

Author Index